



SALAZAR RESOURCES LTD.

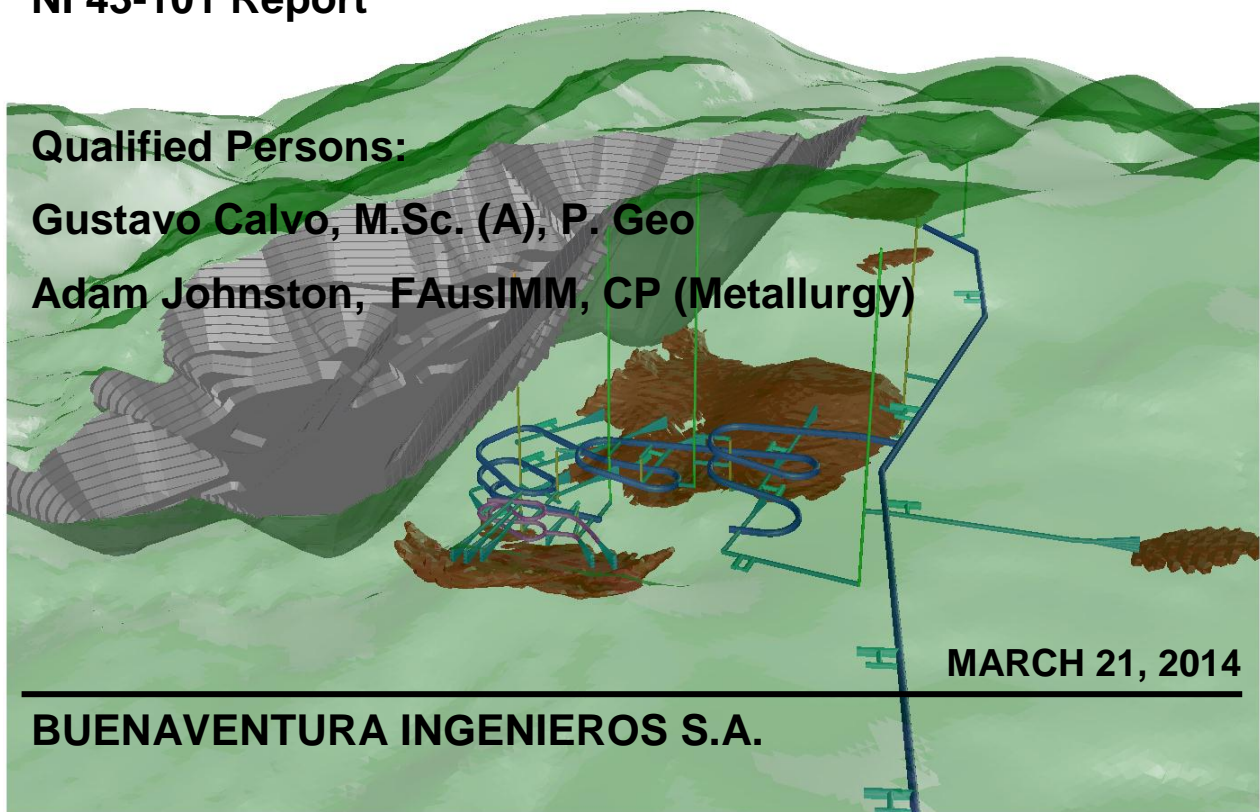
**CURIPAMBA PROJECT - EL DOMO DEPOSIT
PRELIMINARY ECONOMIC ASSESSMENT
CENTRAL ECUADOR**

NI 43-101 Report

Qualified Persons:

Gustavo Calvo, M.Sc. (A), P. Geo

Adam Johnston, FAusIMM, CP (Metallurgy)



BUENAVENTURA INGENIEROS S.A.

TABLE OF CONTENTS

	PAGE
1. SUMMARY	1
Executive Summary	1
Technical Summary.....	8
2. INTRODUCTION	16
Sources of Information	16
Units and Currency	19
3. RELIANCE ON OTHER EXPERTS.....	19
4. PROPERTY DESCRIPTION AND LOCATION	21
Mineral Tenure	22
5. ACCESSIBILITY, CLIMATE, LOCAL RESOURCES, PHYSIOGRAPHY AND INFRASTRUCTURE	31
Accessibility	31
Climate.....	33
Local Resources	33
Infrastructure	33
Physiography	33
6. HISTORY.....	35
7. GEOLOGICAL SETTING AND MINERALIZATION.....	39
Regional Geology.....	40
Local Geology	45
Property Geology	46
Hydrothermal Alteration.....	65
Cu-Au-Zn-Ag-Pb Mineralization.....	68
Ore Mineralogy.....	73
8. DEPOSIT TYPES	81
9. EXPLORATION	96
Exploration Guides	102
Other deposit types	104
10. DRILLING.....	106
11. SAMPLE PREPARATION, ANALYSIS AND SECURITY	117
12. DATA VERIFICATION	120
Database Verification	121
Salazar Quality Assurance and Quality Control (QA/QC)	123

BISA Verification Sampling.....	132
13. MINERAL PROCESSING AND METALLURGICAL TESTING.....	162
Metallurgical Samples	162
Representativity of the 2013 Block Model.....	163
Metallurgical Testing	166
Results	179
14. MINERAL RESOURCES ESTIMATE	180
General Statement	180
Compositing	197
Treatment Of High GradeS.....	197
Variography.....	203
Block Model	204
Estimation Parameters	206
Block Model Validation	214
Asumptions Used In Resource Modelling	223
Mineral Resource Estimate and Classification.....	223
15. MINERAL RESERVE ESTIMATE.....	232
16. MINING METHODS.....	233
Open Pit.....	233
Underground Mine	251
17. RECOVERY METHODS	267
18. PROJECT INFRASTRUCTURE	269
General Characterization of Alternatives	269
Hydrological Evaluation.....	272
Locations of Tailings Dam Alternatives.....	272
Alternative Locations for Waste Rock Dumps.....	274
Alternatives for Topsoil Deposits	275
Alternatives for the Location of Facilities	276
Alternative Locations for Tailings Dams.....	277
Electrical Power Supply.....	278
Water Supply.....	278
Road Access	279
Assumptions	281
19. MARKET STUDIES AND CONTRACTS.....	282
20. ENVIRONMENTAL STUDIES, PERMITTING, AND SOCIAL OR COMMUNITY IMPACT	283
.....	283

21. CAPITAL AND OPERATING COSTS	284
Estimate of Operating and Capital Expenditures	284
Contingencies	284
Open Pit Operation	284
Underground Operation.....	286
22. ECONOMIC ANALYSIS	288
Revenue Assumptions	288
Depreciation	291
Taxes and Other Expenses	292
Discount Rate.....	292
Financing Scheme	293
Parameters of Financial Analysis	293
Profit and Losses Statement	293
Cash Flow and Financial Indicators.....	294
Sensitivity Analysis.....	297
23. ADJACENT PROPERTIES.....	299
24. OTHER RELEVANT DATA AND INFORMATION	300
25. INTERPRETATION AND CONCLUSIONS	301
26. RECOMMENDATIONS	304
27. REFERENCES.....	307
28. DATE AND SIGNATURE PAGE.....	312
29. CERTIFICATE OF QUALIFIED PERSON	313
30. APPENDIX 1	315
Photographs.....	315

LIST OF TABLES

	PAGE
Table 1.1 Proposed Program and Budget	7
Table 1.2 Metallurgical Balance Sheet — Recoveries and Grades.....	10
Table 1.3 El Domo Mineral Resource Estimate - December 15, 2013.....	11
Table 1.4 Infrastructure Alternatives.....	13
Table 1.5 Initial Capital Cost and Sustaining Cost (CAPEX) with 25% Contingency.....	14
Table 1.6 Operating Costs (OPEX) with 20% Contingency	14
Table 2.1 Previous Studies	17
Table 4.1 Property Status, Salazar Resources Ltd — Curipamba Project	22
Table 4.2 Ecuador Mining Law 2013 – Summary	25
Table 4.3 Permit status, Salazar Resources Ltd — Curipamba Project.....	28
Table 7.1 Correlation of Lithostratigraphic Units in the Curipamba Project	45
Table 7.2 Correlation of Lithological Units — El Domo	49
Table 7.3 Summary of the Hydrothermal Alteration In The El Domo Deposit.....	65
Table 7.4 Location of Petrographic Samples	74
Table 7.5 Ore Assemblages in The El Domo Deposit.....	75
Table 8.1 Geological and Economic Data of the VMS Deposits of the Ecuadorian Andes....	93
Table 9.1 Summary of Exploration Work, Salazar Resources Ltd. – Curipamba Project	97
Table 9.2 Curipamba Prospects, Others than the El Domo	98
Table 9.3 Prospects other than VMS near the Curipamba Area	105
Table 10.1 Drilling Summary, Salazar Resources Ltd — Curipamba Project.....	106
Table 10.2 Phase I Drill Holes, Salazar Resources Ltd — Curipamba Project.....	108
Table 10.3 Phase II Drill Holes, Salazar Resources Ltd — Curipamba Project.....	109
Table 10.4 Phase III Drill Holes, Salazar Resources Ltd — Curipamba Project.....	110
Table 10.5 Phase IV Drill Holes, Salazar Resources Ltd — Curipamba Project	112
Table 10.6 Drill Holes Used on the Resource Estimate — BISA 2013.....	114
Table 10.7 Mineralized Intercepts from the Main Ore Zone in El Domo — BISA 2013	114
Table 12.1 Sampling and Analytical Labs.....	121
Table 12.2 Drill Holes with <75% Core Recovery in the Mineralized Zone	122
Table 12.3 Reference Materials Expected Values and Ranges	124
Table 12.4 Reference Materials CU-152 and CU-16	125
Table 12.5 Reference Materials PB-130 and PB-140	126
Table 12.6 Blanks BL-115 and BK Summary	129
Table 12.7 Cu and Zn Assays for Blanks BL115 and BK — Inspectorate.....	129

Table 12.8 Verification Sampling 1 — BISA 2013	132
Table 12.10 Verification Sampling 1 by Types — BISA 2013	133
Table 12.11 Preparation Methods — ALS Global	133
Table 12.12 Analytical Methods — ALS Global	133
Table 12.13 External Control Sampling — Acme Labs	134
Table 12.14 Analytical Methods — Acme Labs	134
Table 12.15 Analytical Results for Reference Material CU 152 — ALS Global	135
Table 12.16 Analytical Results for Reference Material CU 152 — Acme Labs	135
Table 12.17 Reference Material CU 152 — Results Summary	135
Table 12.18 Analytical Results for Reference Material PB 140 — ALS Global	136
Table 12.19 Analytical Results for Reference Material PB 140 — Acme Labs	136
Table 12.20 Reference Material PB 140 — Results Summary	137
Table 12.21 Twin Samples Summary	138
Table 12.22 Duplicate Samples — BISA 2013	139
Table 12.23 Coarse Reject Duplicate Results	140
Table 12.24 Pulp Duplicate Results	142
Table 12.25 Summary of Failed Pulp Duplicate Samples	144
Table 12.26 Blank Sample Results — ALS Global	144
Table 12.27 Blank Sample Results — Acme Global	144
Table 12.28 Summary of Verification Sampling 2 — BISA 2013	147
Table 12.29 Summary of Samples by Analytical Laboratory	147
Table 12.30 QA/QC Sample Verification Sampling 2	147
Table 12.31 Samples Discarded with Errors	148
Table 12.32 Analytical Results for Reference Material CU 145	149
Table 12.33 Analytical Results for Reference Material CU 163	149
Table 12.34 Reference Material Copper 163 Results Summary	150
Table 12.35 Coarse Reject Duplicate Results of Verification Sampling 2	151
Table 12.36 Summary of Failed Samples in Coarse Reject Duplicates	153
Table 12.37 Summary of Failed Samples - Pulp Duplicates	155
Table 12.38 Summary of Failed Samples by Laboratory - Pulp Duplicates	155
Table 12.39 Summary of Failed Samples as a Function of the Thresholds Used for the Deterministic Model	155
Table 12.41 Results for Internal Duplicates of Pulp Samples	156
Table 12.42 Analytical Results for Blank BK	159
Table 13.1 Flotation Test Results – Inspectorate 2008	166
Table 13.2 Head Assays — G&T 2010	166

Table 13.3 Chemical Analysis of Head Composites	167
Table 13.4 CPO-001 – Reagents and Dosages	169
Table 13.5 CPO-001 – Results of Flotation Test	171
Table 13.6 CPO-002 – Reagents and Dosages	172
Table 13.7 CPO-002 – Results of Flotation Test	173
Table 13.8 CPO-003 – Reagents and Dosages	175
Table 13.9 CPO-003 – Results of Flotation Test	177
Table 13.10 Chemical Analyses of Copper and Zinc Concentrates	178
Table 13.11 Metallurgical Balance Projection – Recoveries and Grades.....	179
Table 14.1 El Domo Mineral Resource Estimate - December 15, 2013.....	180
Table 14.2 Metal Unit Values for NSR Calculation	181
Table 14.3 Summary of Drilling Campaigns at El Domo.....	181
Table 14.4 Drill Holes Used in the Resource Declarations for El Domo.....	182
Table 14.5 Mineral Resource Estimate by RPA in 2010 and 2011	183
Table 14.6 Parameters Used in the Lithological Modelling	184
Table 14.7 Correspondence between Modelled and Logged Lithological Units	188
Table 14.8 Estimation Domains Defined for Copper (%)	193
Table 14.9 Estimation Domains Defined for Zinc (%)	194
Table 14.10 Estimation Domains Defined for Lead (%)	194
Table 14.11 Estimation Domains Defined for Gold (g/t).....	195
Table 14.12 Estimation Domains Defined for Silver (g/t)	195
Table 14.13 Estimation Domains Defined for Specific Gravity	196
Table 14.14 Parameters for Calculation of Experimental Correlograms	203
Table 14.15 Limits of Block Models.....	205
Table 14.16 Interpolation Plan for Copper (%)	208
Table 14.17 Interpolation Plan for Zinc (%)	209
Table 14.18 Interpolation Plan for Lead (%)	210
Table 14.19 Interpolation Plan for Gold (g/t).....	211
Table 14.20 Interpolation Plan for Silver (g/t)	212
Table 14.21 Interpolation Plan for Specific gravity.....	213
Table 14.22 El Domo Mineral Resource Estimate - December 15, 2013.....	224
Table 16.1 Mining Block Parameters.....	234
Table 16.2 Mining Block Cost Parameters	235
Table 16.3 Mining Block Design Parameters.....	235
Table 16.4 Optimization Results.....	235
Table 16.5 Metal Prices for Sensitivity Analysis	236

Table 16.6 Sensitivity Analysis	237
Table 16.7 Open Pit Design Parameters	238
Table 16.8 Base Case — Resources with Mining Potential	241
Table 16.9 Diluted Mining Plan	242
Table 16.10 Mineral Production Plan for Processing	243
Table 16.11 Mining Equipment Fleet	245
Table 16.12 Waste Rock Dump Design Parameters	246
Table 16.13 Uptime Per Day	248
Table 16.14 Resources By Mineral Type	252
Table 16.15 Underground Development — Advance Rates	253
Table 16.16 Underground Resources With Mining Potential	255
Table 16.17 Underground Development Program	257
Table 16.18 Underground Production Program by Mineral Type	258
Table 16.19 Underground Production Program	259
Table 16.20 Underground Mine Equipment Fleet	261
Table 16.21 Underground Infrastructure	265
Table 18.1 Size and Volume of Tailings Dams Alternatives	273
Table 18.2 Volume and Geometry of Waste Rock Dumps Alternatives	274
Table 18.3 Volume and Geometry of Topsoil Deposit Alternatives	275
Table 18.4 Parameters for the Assessment of Location of Facilities	276
Table 18.5 Parameters for Assessing Location of the Processing Plant	277
Table 18.6 Estimated Electrical Power Peak Demand	278
Table 18.7 Parameters for Evaluating Access Alternatives	279
Table 21.1 Pre-Production Investment and Sustaining Capital Expenditures	284
Table 21.2 Open Pit Operating Costs (2,000 tpd)	285
Table 21.3 Underground Pre-Production Investment and Sustaining Capital Costs	286
Table 21.4 Underground Operating Costs (1,000 tpd)	287
Table 22.1 Metal Unit Values Used for NSR Calculation	288
Table 22.2 Smelting Treatment and Charges for Refining Copper	289
Table 22.3 Smelting Treatment and Charges for Refining Zinc	290
Table 22.4 Smelting Treatment and Charges for Refining Lead	291
Table 22.5 Profit and Losses Statement	296
Table 22.6 Range of Sensitivity of Economic Parameters	298
Table 26.1 Proposed Program and Budget	306

LIST OF FIGURES

	PAGE
Figure 1.1 NPV Sensitivity.....	15
Figure 4.1 Location Map	21
Figure 4.2 Exploration Claims Map	27
Figure 5.1 Project Accessibility Map.....	32
Figure 5.2 Electrical Grid Map of Ecuador.....	34
Figure 7.1 Regional Geology — The Macuchi Terrane and Location of VMS Deposits	43
Figure 7.2 Curipamba Project — Location of The El Domo Deposit and Nearby Prospects .	47
Figure 7.3 Geology of the El Domo Deposit and Exploration Drilling	48
Figure 7.4 Stratigraphic Column of the El Domo Deposit.....	52
Figure 7.5 Central E-W Cross-Section of the El Domo Deposit Based on the 3D Model	54
Figure 7.6 Structural Setting of the El Domo Deposit	63
Figure 8.1 Genetic Model for Massive Sulphide at Curipamba. The Sketch Shows the Zone Before Intrusion of the Late Andesite and Rhyolite.....	89
Figure 9.1 Areas where Geophysical Exploration has been Performed — IP Anomalies are Shown.....	101
Figure 10.1 El Domo Drilling Map — Las Naves Area	107
Figure 11.1 Photographic Procedure for Core Boxes	118
Figure 11.2 Sample Cutting with a Diamond Saw	119
Figure 12.1 Statistical Control Chart for CU-152 For Gold, Silver, And Copper	125
Figure 12.2 Statistical Control Chart for CU-163 For Gold, Silver, And Copper	126
Figure 12.3 Statistical Control Chart for PB-130 for Silver, Copper, Lead and Zinc	127
Figure 12.4 Statistical Control Chart for PB-140 for Silver, Copper, Lead And Zinc.....	127
Figure 12.5 Statistical Control Chart for Blank BL115.....	130
Figure 12.6 Statistical Control Chart for Blank BK	131
Figure 12.7 Statistical Control Charts for Reference Material CU 152	136
Figure 12.8 Statistical Control Charts for Reference Material PB 140	137
Figure 12.9 Twin Samples Max-Min Charts for Gold, Silver, Copper, Lead, and Zinc.....	139
Figure 12.10 Coarse Reject Duplicate Max-Min Charts for Gold, Silver, Copper, Lead, and Zinc	141
Figure 12.11 Pulp Duplicates Max-Min Charts for Gold, Silver, Copper, Lead, and Zinc	143
Figure 12.12 Statistical Charts for Blank BK.....	146
Figure 12.13 Statistical Control Charts for Reference Material CU 145	149
Figure 12.14 Statistical Control Charts for Reference Material CU 163	150

Figure 12.15 Coarse Reject Duplicate Max-Min Charts for Gold, Silver, Copper, Lead, And Zinc.....	152
Figure 12.16 Pulp Duplicate Max-Min Charts for Gold, Silver, Copper, Lead, And Zinc.....	154
Figure 12.17 Internal Duplicates of Coarse Rejects Max-Min Chart for Gold, Silver, Copper, Lead, And Zinc.....	157
Figure 12.18 Internal Duplicates of Pulp Samples Max-Min Chart for Gold, Silver, Copper, Lead, And Zinc.....	158
Figure 12.19 Statistical Control Charts for Blank BK	160
Figure 13.1 Distribution of Tonnes and Metal Contents.....	163
Figure 13.2 Comparison of 2011 and 2013 Block Models	164
Figure 13.3 Tests Diagram for Composites CPO-001 and CPO-002.....	170
Figure 13.4 Tests Diagram for Composite CPO-003	176
Figure 14.1 Lithological Model in Section 9588300N and Section 69505E	185
Figure 14.2 Lithological Model in Plan View at the 830 m Level	186
Figure 14.3 3D View of the VMS Solid with the Mineralized Intersects.....	187
Figure 14.4 Normal Probability Plot for Cu (%) in the VMS Unit	189
Figure 14.5 Generation of the Deterministic Model for Cu (%) with a 0.3% Cu Threshold ..	190
Figure 14.6 Deterministic Model for Cu in Section 9855300N	190
Figure 14.7 Deterministic Models and Normal Probability Plots for Zn, Au, and Pb.....	191
Figure 14.8 Cross-Section of El Domo showing Two Structural Domains.....	192
Figure 14.9 Probabilistic Diagram Of Specific Gravity By Estimation Domains.....	197
Figure 14.10 Analysis of Run-Length Composites for Cu GU01	198
Figure 14.11 Analysis of Run-Length Composites for Zn GU01	199
Figure 14.12 Analysis of Run-Length Composites for Pb GU01	200
Figure 14.13 Analysis of Run-Length Composites for Au GU01	201
Figure 14.14 Analysis of Run-Length Composites for Ag GU01	202
Figure 14.15 Correlogram of Cu GU02 in the Azimuth 90° and Dip 0°	204
Figure 14.16 Estimates of Copper (%) in Section 9588300N, Highlighting the VMS Unit ...	214
Figure 14.17 Estimates for Copper (%) in Section 830 m, Highlighting the VMS Unit.....	215
Figure 14.18 Estimates for Zinc (%) in Section 9588300N, Highlighting the VMS Unit	215
Figure 14.19 Estimates for Zinc (%) at Level 830 m, Highlighting the VMS Unit.....	216
Figure 14.20 Estimates of Gold (g/t) in Section 9588300N, Highlighting the VMS Unit.....	216
Figure 14.21 Estimates of Gold (g/t) at Level 830 m, Highlighting the VMS Unit	217
Figure 14.22 Validation Outline for GU01CU.....	218
Figure 14.23 Validation Outline for GU01ZN	219
Figure 14.24 Validation Outline for GU01PB	220

Figure 14.25 Validation Outline for GUAU01	221
Figure 14.26 Validation Outline for GUAG01	222
Figure 14.27 Resource Classification Matrix for the VMS and Grainstone.....	226
Figure 14.28 Resource Classification Matrix for the Breccia and Gypsum.....	228
Figure 14.29 Resource Classification in Plan View.....	229
Figure 14.30 Mineral Resources Estimates from 2010 to 2013	230
Figure 14.31 Grade-Tonnage Curves for the Mineralized Units - El Domo Deposit	231
Figure 16.1 Open PIT Optimal Cone	236
Figure 16.2 Sensitivity of Open Pit Optimization.....	237
Figure 16.3 3D Open Pit View	239
Figure 16.4 Pit Design in Plan View	239
Figure 16.5 Annual Mining Plan	244
Figure 16.6 Waste Rock Dump Final Boundary.....	247
Figure 16.7 Underground Mineralized lenses	251
Figure 16.8 Chambers and Pillars — Cross Section.....	253
Figure 16.9 Underground Mine Design.....	255
Figure 16.10 Underground Production Program by Mineral Type.....	259
Figure 16.11 Underground Production Program by Type of Work	260
Figure 16.12 Chamber-and-Pillar Mining Method Layout.....	263
Figure 16.13 Underground Mining Areas.....	264
Figure 16.14 Central and Southern Underground Mining Zones.....	264
Figure 17.1 Process Flow Diagram	268
Figure 18.1 Alternative Locations of Main Structures	271
Figure 18.2 Project Access Roads	280
Figure 21.1 Open Pit — Distribution of Operating Costs	285
Figure 21.2 Underground — Distribution of Operating Costs.....	287
Figure 22.1 Life of the Project EBITDA, OPEX, and Operating Margin.....	294
Figure 22.2 Life of the Project OPEX, Depreciation, and Pre-Tax Profits	294
Figure 22.3 Cash Flow After Taxes	295
Figure 22.4 Project Sensitivity to Metal Prices.....	297
Figure 22.5 Sensitivity of NPV to Revenue, OPEX and CAPEX	298

1. SUMMARY

EXECUTIVE SUMMARY

Buenaventura Ingenieros S.A. (BISA) was retained by Mr. Fredy Salazar, President and CEO of Salazar Resources Limited. (Salazar), to prepare an independent Preliminary Economic Assessment (PEA) on the El Domo Deposit, the most advanced deposit in the Curipamba project located near Ventanas, Ecuador. The purpose of this report is to provide sufficient information for shareholders, investors, and stakeholders about the geology, mineral resource, evaluation of mining methods, conduct preliminary metallurgical testing, evaluation of infrastructure alternatives, preliminary capital expenditures and operation costs, and economic analysis. This Technical Report conforms to National Instrument 43-101 Standards of Disclosure for Mineral Projects (NI 43-101).

Salazar is a TSX Venture Exchange listed (TSX.V:SRL | FSE:CCG) mineral resource company engaged in mineral exploration and development in Ecuador. Deposit types being explored by Salazar in Ecuador include Epithermal Au-Ag and Porphyry Cu-Mo-Au. The target on the Curipamba Property is gold-rich volcanogenic massive sulphide (VMS) deposits.

CONCLUSIONS

BISA offers the following conclusions and recommendations:

- The El Domo deposit is the largest known Au-rich, Cu-Zn-Ag-Pb volcanogenic massive sulphide (VMS) deposit emplaced within the Macuchi Terrane, a juvenile island magmatic arc of Paleocene–Eocene age. It formed in an intra-magmatic arc third-order basin in a setting similar to that of other Andean deposits. Somewhat similar global equivalents are the bimodal-felsic deposits of the Hokuroko basin (Japan) and the VMS deposits of Tasmania.
- The massive sulphide mineralization occurs in the Macuchi Formation as stratabound orebodies, mainly in the contact between a rhyodacitic dome and the overlying mafic, glass-rich, mass flows. The overlying rocks host semi-massive to disseminated mineralization. The mineralization is replacive on both the glassy carapace of the rhyodacite and the volcanoclastic rocks. This replacement took place only a few metres below the seafloor.
- The massive polymetallic sulphides consist primarily of pyrite, sphalerite, chalcopyrite, and less abundant galena, bornite, and tennantite; silver is concentrated in discrete phases such as stromeyerite and proustite.
- The orebody has marked lateral and vertical zoning with a lower Cu-rich zone and an external Zn-Pb-barite zone. The copper-rich zone replaced the external zone, with most of the gold and silver concentrated along this replacement zone.
- The area has good exploration potential for VMS deposits. The optimal target should be the contact of the rhyodacite domes with mafic, glass-rich rocks, or the outer carapace of domes capped by massive andesite-basalt.
- BISA believes that the procedures and protocols used by Salazar for its drilling, logging, sampling, preparation, and sample analysis program comply with international practices in the mining industry.
- The independent QA/QC verification carried out by BISA concludes that the duplicates of coarse rejects from preparation demonstrate acceptable precision and reproducibility of the original results. In contrast, the pulp duplicate precision is relatively low, with failures of over 10% for all the elements analysed (especially Au, Pb, and Cu) in both the ALS Global and Inspectorate laboratories.
- The blank samples used are adequate for Au, Ag, and Pb, but in the case of Cu and Zn, the values are much higher than the lower analytical limits of detection established in the laboratories used by Salazar.
- The metallurgical tests indicate that the recovery of pay metals to concentrates by froth flotation of feed from the El Domo deposit is technically feasible.

- It may be possible to improve Cu-Zn separation. Mineralogical results indicate that significant amounts of free sphalerite are present in the copper concentrate. This means that the selectivity of copper and zinc separation may be improved, compared to the results of the first phase of testing reported in the PEA.
- Mineral Resources were estimated based on a 3D geological interpretation for a VMS deposit; four mineralized units have been considered for mineral resource estimation (VMS, Grainstone, Breccia, and Gypsum). The cutoff value applied is US\$30 NSR per tonne.
- Indicated Mineral Resources have been estimated at 6.080 million tonnes at an average grade of 2.33% Cu, 3.06% Zn, 0.28% Pb, 2.99 g/t Au, and 55.81 g/t Ag, containing 312.95 million pounds Cu, 409.56 million pounds Zn, 37.76 million pounds Pb, 584,457 ounces Au, and 10.91 million ounces Ag. The current Indicated Mineral Resource estimate shows the following increases relative to the 2011 Indicated Resource estimate: a 7% increase in contained copper, a 34.4% increase in contained zinc, a 17.4% increase in contained gold, and a 26.8% increase in contained silver.
- The Inferred Mineral Resource is 3.882 million tonnes at an average grade of 1.56% Cu, 2.19% Zn, 0.16% Pb, 2.03 g/t Au, and 42.92 g/t Ag, containing 133.46 million pounds Cu, 187.39 million pounds Zn, 13.96 million pounds Pb, 253,607 ounces Au, and 5.36 million ounces Ag. The current Inferred Mineral Resource estimate shows the following increases compared to the 2011 Indicated Resource estimate: a 118.1% increase in contained copper, a 108.0% increase in contained zinc, a 125.2% increase in contained gold, and a 118.7% increase in contained silver.
- Two structural domains have been established in the El Domo deposit: the Eastern Sector (El Domo hill) and the Western Sector, where most of the deposit is located. In the Eastern Sector, the VMS lenses lie at a greater depth underneath the andesitic dome. The eastern continuity of the lenses needs to be confirmed by a drilling program.
- The mining methods study considers two scenarios: open pit mining for the western domain of the deposit and underground mining for the eastern domain.
- The economic and financial assessment considers a total 14-year life of mine: nine years of surface mining, with production of 2,000 tpd, followed by five years of underground mining with a production of 1,000 tpd.
- The mining production, considering the mine plans for both scenarios (open pit and underground) and the reported metallurgical ore types, are: zinc mineral type 1.74 Mt;

mixed mineral Cu/Zn type 3.00 Mt; and copper mineral type 2.18 Mt. The mining scenario also includes 46 Mt of waste rock and 0.98 Mt of low-grade material.

- A preliminary evaluation of infrastructure alternatives have been carried out: seven alternatives for tailings dams, five areas for the waste rock dumps, two deposits for topsoil, three alternative locations for the processing plant, four alternatives for facilities, three alternatives for the water adduction line, two alternatives for the water pipeline, five alternatives for the tailings transport system, three alternatives for the power supply system, and three alternatives for access to the mine. No major drawbacks are noted, and some work will have to be done to ensure the services required for the project.
- The preliminary estimates of pre-production capital investment total US\$110.3 million, an amount consistent with the current costs of mining and construction equipment. Operating through a mining contractor has been considered; this option reduces CAPEX but increases the operating cost. The mode of operation will be analysed in more detail in the pre-feasibility stage.
- The after-taxes financial evaluation of the project gives the following results:
 - Net Present Value (10% discount rate): US\$86.72 million
 - Internal Rate of Return: 30%
 - Payback Period: 2 years

RECOMMENDATIONS

BISA proposes the following recommendations:

- A systematic directional survey location program should be implemented for all future drilling.
- To provide consistency in the methods, one laboratory of the two currently used should be used as the primary laboratory for all analyses, and that the second laboratory should be used for external checking of the assays.
- The QA/QC program should be modified to include: establishment of a protocol for non-compliant results and a formal reporting system for QA/QC results; insertion of twin samples, coarse and fine duplicates, certified standards, and blanks in future programs; use of certified reference materials representative of the deposit; and preparation of adequate blanks.
- In future, the original stored pulp samples should not be used due to the low precision reported in the QA/QC programs of RPA and BISA. Any verification or validation must be done with existing samples of coarse rejects.
- Improving storage conditions of the reject samples in Quito, Ecuador. The samples should be stored in an orderly fashion, in a suitable environment.
- A detailed petrographic and mineragraphic study is strongly recommended to support metallurgical testing and aid in defining geometallurgical domains.
- Future exploration should focus on zones of mafic volcanoclastic flows with evidence of underlying felsic volcanics. Stream sediment geochemistry is crucial for finding new anomalies. Geophysical surveys are also key techniques. However, the mineralization is poorly magnetic and the sphalerite is generally poor in iron. Negative magnetometric anomalies may be useful for defining hydrothermal systems and feeder zones. Helicopter-borne Versatile Time-Domain Electromagnetic (VTEM) and similar EM techniques can be useful to find Cu-pyrite-rich ores; targeting the sphalerite-rich zones can be trickier, but again VTEM has given good results in pyrite-poor orebodies. Ground EM and further drilling should be carried out in areas with the best combination of geology and airborne anomalies.
- Additional metallurgical testing should be carried out to optimize the process performance for the selective recovery of Cu, Zn, and Pb and to reduce reagent consumption.
- Geo-metallurgical mapping should be performed to identify areas with high clay contents that may interfere with the recovery processes.
- Study the use of specific reagents for Au and Ag to increase their recovery to the copper concentrate.

- Study the use of a Cu/Pb separation train to clean the copper concentrate and produce a lead concentrate as another commercial product.
- Closed-cycle flotation tests are needed in order to confirm the recoveries and grades obtained.
- Conduct flotation tests with water drawn from the project's area of influence to assess its effect on the recovery of Cu and Zn.
- Salazar should acquire systematic SG measurements of full sample lengths from all lithology units, thus providing direct information relating density to grade.
- Salazar should continue the investigation and interpretation of grade directional trends and further variography evaluation.
- An infill drilling program should be completed to upgrade the start-pit resources to the measured category as a requirement for the pre-feasibility.

A drilling program to define the nature and continuity of the VMS mineralization under the El Domo andesite is also recommended.

- It is advisable to promptly undertake a topographic survey of the project area, with greater accuracy in areas required for the facilities.
- Hydrological and geotechnical studies should be undertaken in areas slated for the pits, waste dumps, processing plant, and in general in all areas requiring heavy structures. The geotechnical investigation is a priority in order to define the pit profiles and volumes of mineral and waste material that must be removed.
- In the next project stage, the technical options identified in this conceptual study should be analysed in greater detail. Trade-off studies should be developed in the prefeasibility stage to set the basis for a subsequent feasibility study.
- Although the financial projection results are positive, the high cost of pre-stripping presents a significant outlay and risk. Therefore, the underground alternative could be reconsidered. The pit profiles are provisional and may change, as there are no geotechnical studies available. The pre-stripping volumes could vary, changing the economic and financial parameters presented in this report.
- A pre-feasibility stage work program should consist of several studies that include: infill drilling, additional metallurgical testing, resource model update and reserve estimates, processing plant engineering, infrastructure and project engineering. The work program and estimated budget for a prefeasibility study are summarized in Table 1.1.

TABLE 1.1 PROPOSED PROGRAM AND BUDGET

Pre-Feasibility Program	Proposed Cost US\$
Project Management	200,000
Staff relocation	20,000
Communications- telephone/fax/radio/hardware/software	15,000
Community Engagement	170,000
Environmental compliance	160,000
Land Acquisition	800,000
Mining Concessions	500,000
Road Maintenance	20,000
Transportation - Vehicles	50,000
Shipping - Couriers, Freight	20,000
Field Costs	500,000
Underground Development (300m)	600,000
GEOLOGY	
Geological Model Update	20,000
Structural Study	30,000
Ore mineralogy	35,000
QA/QC Program	10,000
Resource Model Update	95,000
Infill Diamond Drilling	
Drilling 6,055m@150US\$/m	908,250
Logging and Sampling	185,000
Supplies and Core Boxes	55,000
Preparation and Assaying 4,000 Samples	280,000
MINING	
Geotechnical / Geomechanical Evaluation	300,000
Open Pit Studies	120,000
METALLURGICAL TESTING AND PROCESS	
Metallurgical and process studies	500,000
INFRASTRUCTURE	
Geotechnical and Hydrogeological Studies	420,000
ECONOMIC EVALUATION	
Financial Study	40,000
Sub-total	6,053,250
Contingencies - 10%	605,325
Total	6,658,575

TECHNICAL SUMMARY

GEOLOGY

The Curipamba Property is located in western central Ecuador, within the Macuchi Terrane, a predominantly juvenile island magmatic arc of Paleocene–Eocene age. In the area, the geology includes a basal rhyodacite unit overlain by two interfingering volcanoclastic sequences, one mafic and the other felsic, and two coherent younger lithofacies, one andesitic and another rhyolitic, which intruded the sequence in both the north and south of the property.

The VMS deposit of El Domo is located in the contact between a rhyodacitic dome and overlying glass-rich volcanoclastic flows deposited in a third-order, likely pull apart, basin. The main mineralization forms a large massive sulphide lens with clear mineralogical zonation, with an internal chalcopyrite-rich zone and an external sphalerite-galena-barite one separated by a polymetallic ore of intermediate characteristics. Most of the gold and silver are located in the polymetallic ore. The gold occurs dominantly as invisible grains whereas the silver appears as discrete phases such as stromeyerite and proustite. The deposit is interpreted as having formed via the replacement of glassy permeable felsic and mafic rocks along the contact due to the mixing of deep magmatic-hydrothermal fluids and seawater.

The immediate area has great potential for VMS exploration, which should focus on the contact between felsic domes and overlying mafic volcanic and volcanoclastic rocks.

MINERAL PROCESSING

BISA commissioned Transmin MC E.I.R.L. (Transmin) of Lima, Peru to design and supervise the metallurgical testing. Transmin was also responsible for reviewing the previous metallurgical studies conducted at the El Domo project. Three metallurgical testing programs have been completed on composite samples from the El Domo deposit. The first program was performed by Inspectorate Services Peru S.A.C (Inspectorate) in 2008. The second test program was carried out by G&T Metallurgical Services Ltd (G&T) in 2010. Finally, the third metallurgical test program was conducted by the SGS del Peru S.A.C. (SGS) laboratory in 2013 under the supervision of Transmin. All the programs were conducted at a laboratory scale on composite samples from El Domo drill cores.

The samples and composites used in the 2013 test program were selected from the block model produced by Roscoe Postle Associates Inc. (RPA) in 2011. In early November of

2013, BISA generated a new block model, making it necessary to check the representivity of the samples used in the study.

The new zones in the 2013 Block Model are not substantially different to what was tested with respect to oxidation and rock competence, and no differences were found in the contents of the metals of interest. Therefore, for a preliminary economic assessment (PEA), it would be justifiable to assume that the 2013 mineral resource will have a similar recovery and concentrate grade as the samples collected for the 2011 resource base.

The first program yielded poor recovery results for metals such as Cu, Zn, Au, and Ag. The second program by G&T achieved satisfactory zinc and copper concentrate grades, but recoveries were low. In the third program, the tests were carried out on three composite samples representative of the existing types of mineralization (zinc mineral, mixed mineral Cu/Zn, and copper mineral). The tests focused on the flotation of the copper and zinc concentrates separately. The flotation tests used industry-standard methods and reagents for the production of copper and zinc concentrates by differential flotation techniques.

Based on the results from the 2013 flotation testing program, an estimate was made of the recoveries and grades of the Cu and Zn concentrates that would be produced in an efficiently operated industrial plant with ore similar to the composites studied. The estimate results are presented in Table 1.2.

TABLE 1.2 METALLURGICAL BALANCE SHEET — RECOVERIES AND GRADES

Composite ID	Products	Weight, %	Assays					Distribution				
			Cu, %	Zn, %	Pb, %	Au, g/t	Ag, g/t	Cu, %	Zn, %	Pb, %	Au, %	Ag, %
CPO-001 Zinc Mineral	Concentrate Cu	2.46	19.7	17	1.31	8.18	748	58.2	8.24	7.67	6.16	22.6
	Concentrate Pb	0.61	17.7	17	47.3	21.8	1,995	6.47	0.92	69	4.11	15.1
	Concentrate Zn	9.49	1.73	45.5	0.31	14	286	19.7	85.4	6.9	40.8	33.4
	Final Tail	87.4	0.15	0.31	0.08	1.83	26.9	15.5	5.39	16.4	49	28.9
	Head Calculated	100	0.89	5.11	0.42	3.26	81.2	100	100	100	100	100
CPO-002 Mixed Mineral Cu / Zn	Concentrate Cu	7.62	21	8.51	0.94	8.77	230	75	29.8	49.6	29.3	40.8
	Concentrate Zn	2.59	6.28	42	0.86	19.4	371	7.62	50	15.4	22	22.4
	Final Tail	89.8	0.41	0.49	0.06	1.24	17.6	17.4	20.2	35	48.7	36.8
	Head Calculated	100	2.13	2.17	0.14	2.28	42.9	100	100	100	100	100
CPO-003 Copper Mineral	Concentrate Cu	13.9	24.2	2.34	0.09	3.69	53.1	89.7	80.9	43.4	24.4	39.7
	Final Tail	86.1	0.45	0.09	0.02	1.84	13	10.3	19.1	56.6	75.6	60.3
	Head Calculated	100	3.75	0.4	0.03	2.1	18.6	100	100	100	100	100

Based on the results of these metallurgical tests, a possible scenario for processing the ore from the El Domo deposit has been outlined. This process is preliminary and could be subject to changes based on the results of more detailed metallurgical studies during the next project phase.

MINERAL RESOURCES

The Mineral Resource update considers a total of 31,770 m of core corresponding to four drilling campaigns carried out from 2007 to 2012 in a drill-hole grid of about 50 m x 50 m.

The Mineral Resource update for the El Domo deposit includes: the database review, geological modelling, exploratory data analysis, mineral resource estimation, and resource classification. The mineral resource estimate is based on a Net Smelter Return (NSR) cutoff value of US\$30 per tonne. The NSR was calculated using the following assumptions: metal prices, metallurgical recovery factors, and common industry values for smelter terms. Four mineralized units with estimates above the cutoff value have been considered as mineral resources: volcanogenic massive sulphides (VMS), polymictic volcanoclastic breccia with massive sulphide clasts (Grainstone), stockwork quartz-pyrite (Breccia), and stockwork anhydrite-gypsum (Gypsum).

The resource estimate completed by BISA is given in Table 1.3.

TABLE 1.3 EL DOMO MINERAL RESOURCE ESTIMATE - DECEMBER 15, 2013

Unit	Category	Tonnes (Mt)	Copper (%)	Zinc (%)	Lead (%)	Gold (g/t)	Silver (g/t)
VMS	Indicated	5.468	2.52	3.27	0.30	3.23	59.19
Grainstone	Indicated	0.216	0.92	1.01	0.12	1.09	27.91
Breccia	Indicated	0.345	0.49	1.33	0.13	0.76	26.91
Gypsum	Indicated	0.051	0.94	0.39	0.03	0.34	7.40
Total Indicated		6.080	2.33	3.06	0.28	2.99	55.81
VMS	Inferred	3.093	1.75	2.59	0.19	2.38	49.45
Grainstone	Inferred	0.170	0.96	0.69	0.10	1.00	19.24
Breccia	Inferred	0.370	0.53	0.83	0.07	0.78	24.89
Gypsum	Inferred	0.249	1.13	0.26	0.01	0.27	4.80
Total Inferred		3.882	1.56	2.19	0.16	2.03	42.92

Notes:

- CIM definitions were followed for mineral resources
- The Mineral Resource Estimate is based on 3D geological modelling of the volcanogenic massive sulphide deposit (VMS). Four mineralized units with an NSR cutoff of US\$30 per tonne were considered as mineral resource
- Metal prices used are US\$2.95/lb Cu, US\$0.91/lb Zn, US\$0.91/lb Pb, US\$1,200/oz Au, and US\$20.00/oz Ag
- Metallurgical recovery factors assumed were based on three mineral types defined by the metal ratio Cu/(Zn+Pb):
 - Zinc Mineral (Cu/(Pb+Zn)<0.3): 15% Cu, 90% Zn, 40% Pb, 50% Au and 65% Ag
 - Mixed Cu/Zn Mineral (0.3≤Cu/(Pb+Zn)≤3.0): 75% Cu, 50% Zn, 0% Pb, 55% Au and 65% Ag
 - Copper Mineral (Cu/(Pb+Zn)>3.0): 90% Cu, 0% Zn, 0% Pb, 30% Au and 40% Ag
- Common industry values for smelter terms were assumed
- Bulk density was estimated based on specific gravity determinations for each lithological unit

Currently, there are neither Measured Mineral Resources nor Mineral Reserves estimated for the El Domo Deposit.

MINING METHODS

The El Domo VMS deposit has been divided into two structural domains: Western Sector and the Eastern Sector where the potentially minable resources are located. The mineralization of the Western Sector has been evaluated for mining by open pit methods as the mineral lenses are close to the surface. In the case of the Eastern Sector, the mineralization occurs deeper, underneath the andesite dome, and it has been assessed for mining by underground methods (chamber-and-pillar) because of the depth and a good rock competence.

The open pit design was based on a 2,000 tpd case. At this production rate, the life of mine is nine years with one year of pre-stripping. This mining plan fulfills Ecuadorian standards for medium-scale mining.

Production from the diluted open pit mining plan amounts to a total of 6,213,029 tonnes at an operative cutoff of 1% Cu (equivalent) which is approximately US\$ 30 NSR, distributed as follow: 1,279,094 tonnes of copper mineral, 2,447,666 tonnes of mixed Cu/Zn mineral, 1,508,021 tonnes of zinc mineral, and 978,248 tonnes of the low grade stockpile. Additionally, 46,220,572 tonnes of waste rock have been considered for a stripping ratio of 7.44.

The underground potentially minable mineral resources were calculated considering the mineral accessibility and applying a NSR cutoff value of US\$40 per tonne. The underground operation was designed for a medium-scale production of 1,000 tpd with an expected life of mine of five years. Based on production requirements, it was estimated that approximately 9,000 metres of underground development would be necessary, including both horizontal and vertical workings. A total production of 1,751,024 tonnes has been estimated: 903,023 tonnes of copper mineral, 619,703 tonnes of mixed Cu/Zn mineral, and 228,478 tonnes of zinc mineral.

INFRASTRUCTURE

The objective of the infrastructure conceptual study is to evaluate different alternatives for laying out the surface structures in order to minimize operational costs. The structures evaluated are: tailings dams, waste rock dumps, a topsoil bank, processing plant platform, facilities platform, water supply, electrical supply, and alternative accesses to the mine.

The local hydrological analysis is based on rainfall information from the INAMHI (National Institute of Meteorology and Hydrography) provided by Salazar.

BISA observed various alternatives for the El Domo PEA. The optimal alternative to be developed in the next project phase should consider the best options in engineering, economic, social, and environmental terms.

A reconnaissance of the area took into account the geomorphology, basin shape, stream gradients, topography, availability of borrow materials, surface water runoff, and geological/geotechnical risks, as well as proximity to the mineral deposit.

The surface structures evaluated are:

- Seven alternatives for the location of the tailings dams
- Five alternatives for the waste rock dumps
- Two top soil deposits alternatives
- Three alternatives for the processing plant
- Four facilities alternatives
- Three alternatives for the electrical power supply
- Water supply
- Component systems (uptake, desander, storage pond, drive line, repumping stations, and storage tank for untreated and drinking water)
- Solid waste landfill
- Domestic wastewater treatment plant (WWTP)
- Road access (Las Naves – mine, mine – El Congreso, El Congreso – main road, and Echeandía – main road).

The investment costs for the recommended structural alternatives mentioned have been evaluated and presented in a balance sheet. Table 1.4 summarizes the recommended alternatives as well as the initial investment costs, sustaining costs and total investment for each alternative.

TABLE 1.4 INFRASTRUCTURE ALTERNATIVES

Recommended Alternatives	Initial Investment (US\$M)	Investment During Operations	Total Investment (US\$M)
Tailings Impoundment - Alternative 1	12.1	87.85	99.95
Waste Rock Dump – Alternative 1A	0.59		0.59
Top Soil Dump – Alternative 1	0.66		0.66
Access: Las Naves-Naves Chico-Mine	8.72	11.38	20.1
Mine Facilities - Alternative 3	7.66		7.66
Processing Plant – Alternative 2 (*)	9.89		9.89
Water supply and tailings transport – Discharge Line and Water Pipe – Alternative 1	3.17		3.17
Tailings transport	0.49		0.49
PTAP, PTARD, PTARI, Landfill, S.C.I	1.96		1.96
Electrical supply	2.79		2.79
Total Investment Cost	48.03	99.23	147.26

(*)For Capital Cost Estimate purposes, the "Processing Plant — Alternative 2" is included in the Processing Plant cost instead of infrastructure capital costs..

CAPITAL AND OPERATING COSTS

The capital cost (CAPEX) and operating cost (OPEX) were estimated using cost data from similar projects and staff experience as a reference. A 25% contingency rate was considered for capital costs and 20% for operating costs. Table 1.5 and Table 1.6 show the results with the contingency used.

TABLE 1.5 INITIAL CAPITAL COST AND SUSTAINING COST (CAPEX) WITH 25% CONTINGENCY

CAPEX	Open Pit			Underground Mine		
	Initial	Sustaining	Total	Initial	Sustaining	Total
Mine	19,513,886	554,115	20,068,001	11,832,708	3,001,850	14,834,558
Processing plant	43,890,000	0	43,890,000			
Infrastructure	38,130,792	88,269,650	126,400,442			
Others	8,750,000	17,000,000	25,750,000	4,000,000	562,500	4,562,500
Total	110,284,678	105,823,765	216,108,443	15,832,708	3,564,350	19,397,058

TABLE 1.6 OPERATING COSTS (OPEX) WITH 20% CONTINGENCY

Operating costs	Open Pit	Underground Mine
	US\$	US\$
Mine	182,104,016	67,083,461
Processing	93,195,428	26,268,065
Administration	15,532,571	4,378,011
Others	13,024,067	
Total	303,856,082	97,729,537

ECONOMIC ANALYSIS

The after-taxes financial evaluation of the El Domo project yields good economic indicators: a positive cash flow of US\$ 202.6 million, and the net present value (10% discounted rate) of US\$ 86.72 million with an internal rate of return of 30%; and a capital repayment period (payback) after start of production of two years.

Figure 1.1 shows the sensitivity of the NPV to changes in revenue, OPEX, and CAPEX. Change in revenue (price of metals and production rate) is the most critical factor.

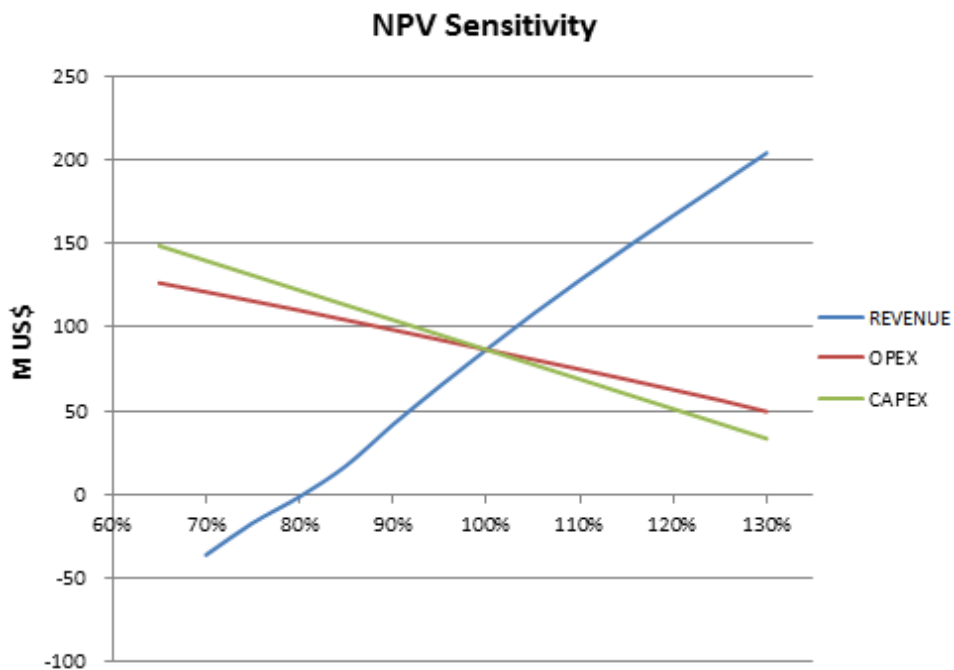


FIGURE 1.1 NPV SENSITIVITY

2. INTRODUCTION

Buenaventura Ingenieros, S.A. (BISA) was retained by Fredy Salazar, President and CEO of Salazar Resources Ltd (Salazar), to prepare an independent Preliminary Economic Assessment (PEA) on the Curipamba Project (the Project) located in the cantons of Las Naves, Echeandía, and Ventanas (provinces of Bolívar and Los Ríos, Central Ecuador. The purpose is to provide an updated Mineral Resource estimate of the El Domo deposit, conduct metallurgical testing, evaluate underground and open pit mining alternatives, conceptual infrastructure, cost estimates, and preliminary financial modelling. This Technical Report conforms to National Instrument 43-101 Standards of Disclosure for Mineral Projects (NI 43-101).

Salazar is a Toronto Stock Exchange (TSX) listed (TSX-V: SRL) mineral resource company engaged in mineral exploration and development in Ecuador. This report deals with the gold-rich Cu-Zn-Pb-Ag volcanogenic massive sulphide (VMS) deposits being explored on the Curipamba Project, east of Ventanas (Central Ecuador). The El Domo deposit is at the most advanced stage in the Curipamba project and is the subject of the current PEA study.

SOURCES OF INFORMATION

Gustavo Calvo (P. Geo., Director of Geology, BISA), Ricardo Arrarte (Project Manager, BISA), Erick Contreras (Geologist, BISA), Luis Miguel La Torre (Principal Metallurgist, Transmin), and Fernando Tornos (Consulting Geologist, BISA) first visited the Curipamba site and the Salazar office in Ventanas on April 22–27 of 2013 accompanied by Francisco Soria (Chief Geologist, Salazar), Carlos Aguila (Senior Geologist, Salazar), and Diego Bastida (Geologist, Salazar), with whom technical discussions were held. During this visit, BISA viewed the sampling facility, inspected the core boxes and logging records, checked the logging and sampling procedures and the bulk density determination methodology, and reviewed plans and sections as well as the available geological reports. Drilling platforms and a number of mineral showings were also visited at the El Domo site. QA/QC verification sampling of twin core samples, coarse rejects, and pulp samples were also undertaken during the visit. BISA has not conducted detailed land status evaluations, and has relied upon previous qualified reports, public documents and statements by Salazar regarding property status and legal title to the Project.

The documentation reviewed, and other sources of information, is listed in Table 2.1 and at the end of this report in Section 27 References.

TABLE 2.1 PREVIOUS STUDIES

Author	Work
BGS-CODIGEM	1/100000 mapping
Beate (2007)	1/25000 mapping. Preliminary petrographic study.
Deep Search Exploration Technologies Inc. (2006)	First NI 43-101 report with preliminary information. Systematic rock sampling and analysis. Definition of an exploration model similar to Eskay Creek.
Pratt (2008)	Detailed 1/3000 mapping and cross-sections of Las Naves area. Vulcanological interpretation. He was the first to document and describe the deposit as a volcano-sedimentary massive sulphide, establishing the area's lithostratigraphy.
Schandl (2009)	Petrographic study of 17 samples, including characterization by ETEC microprobe.
Franklin (2009)	Geological interpretation, selective logging, petrochemical study, and interpretation of regional geochemical data. Identified a presumed marker unit in hanging wall of the mineralization and predicted the location of the presumed feeder systems to other VMS deposits.
Buckle (2009)	NI 43-101 Report synthesizing previous information.
Franklin (2010)	Logging of new core, reinterpretation of the drillcore geochemistry, and new ideas for exploration.
Mayor (2010)	1/7500 structural study and study of the tectonic setting of the mineralization.
Valliant W, Peltz P, Cook B (2010)	Technical Report on the Curipamba Project, Central Ecuador NI 43-101 Report, Scott Wilson Roscoe Postle Associates INBc
Lavigne and McMonnies (2011)	NI 43-101 report synthesizing all the previous work.
Vallejo (2013)	1/2000 mapping – logging of new drillcore. Geochemistry of igneous rocks. Whole rock analyses of 20 samples and 1 Ar-Ar dating.

GLOSSARY AND ABBREVIATION OF TERMS

°C	degree Celsius	km	kilometre
°F	degree Fahrenheit	km/h	kilometre per hour
µm	micron (micrometre)	kPa	kilopascal
µg	microgram	kv	kilovolt
A	ampere	kw	kilowatt
a	annum	kwh	kilowatt-hour
bbl	barrels	L	litre
Btu	British thermal units	lb	pound
C\$	Canadian dollars	L/s	litres per second
cal	calorie	m	metre
cfm	cubic feet per minute	M	mega (million)
cm	centimetre	m ²	square metre
cm ²	square centimetre	m ³	cubic metre
d	day	masl	metres above sea level
dia.	diameter	mph	miles per hour
dmt	dry metric tonne	m ³ /h	cubic metres per hour
dwt	dead-weight ton	m ³ /t	cubic metres per tonne
ft	foot	m ³ /h	cubic metres per hour
ft/s	foot per second	oz/t	ounce per short ton
ft ²	square foot	oz	Troy ounce (31.1035g)
ft ³	cubic foot	ppm	part per million
g	gram	psia	pound per square inch absolute
G	giga (billion)	psig	pound per square inch gauge
Gal	Imperial gallon	RL	relative elevation
g/L	gram per litre	s	second
g/t	gram per tonne	st	short ton
gpm	Imperial gallons per minute	stpa	short ton per year
g/ft ³	grain per cubic foot	stpd	short ton per day
g/m ³	grain per cubic metre	t	metric tonne
hr	hour	tpy	metric tonne per year
ha	hectare	tpd	metric tonne per day
hp	horsepower	US\$	United States dollar
in	inch	US\$/lb	United States dollar per pound
in ²	square inch	US\$/oz	United States dollar per troy ounce
J	joule	USg	United States gallon
k	kilo (thousand)	USgpm	United States gallon per minute
kcal	kilocalorie	V	volt
kg	kilogram	W	watt
kg/t	kilogram per tonne	yd ³	cubic yard

UNITS AND CURRENCY

Unless otherwise stated all units used in this report are metric. Copper, lead and zinc values are reported in percent unless some other unit is specifically stated. Gold and silver values are reported in grams per metric tonne (g/t) unless some other unit is specifically stated. The US\$ is used throughout the report.

3. RELIANCE ON OTHER EXPERTS

This report has been prepared by Buenaventura Ingenieros S.A. (BISA) for Salazar Resources Ltd (Salazar). The information, conclusions, opinions, and estimates contained herein are based on:

- Information available to BISA at the time of preparation of this report
- Assumptions, conditions, and qualifications as set forth in this report
- Data, reports, and other information supplied by Salazar and other third-party sources

For the purpose of this report, BISA has relied on land tenure, permitting, and ownership information provided by Salazar. BISA has not researched property title or mineral rights for the Curipamba Project and expresses no opinion as to the ownership status of the property.

BISA has relied on Salazar for guidance on applicable taxes, royalties, and other government levies or interests applicable to revenue or income from the Project. Except for the purposes legislated under provincial securities laws, any use of this report by any third party are at that party's sole risk.

The authors have relied upon geological information and opinions provided by Dr Fernando Tornos, a well-known expert in volcanogenic massive sulphide (VMS) deposits. Dr Tornos is not a Qualified Person as defined by NI 43-101. Dr Tornos received his PhD in January 1990 from the Universidad Complutense de Madrid (UCM) in Spain, and is currently a Senior Researcher at the Consejo Superior de Investigaciones Científicas (CSIC, Spain), fellow of the Society of Economic Geologists (SEG), and former President of the Society for Geology Applied to Mineral Deposits (SGA). Dr Tornos' contribution to this report includes chapters 7, 8, 9, and 23. Work done by Dr Tornos comprises the following:

- Re-logging the cores of drill holes 07-15, 10-64, 10-68, 11-98, 11-106, 11-123, 11-163, 11-187, and 12-196 with special attention to the lithofacies of the volcanic rocks, the mineralization, and the hydrothermal alteration
- Construction of a lithostratigraphic column of the Curipamba district
- Lithofacies characterization of the volcanic and subvolcanic rocks
- Modelling of the massive sulphide mineralization, its controls and genesis
- Petrographic study of 20 selected samples from the massive sulphides, including XRD analyses and SEM characterization
- Critical review and synthesis of previous reports

4. PROPERTY DESCRIPTION AND LOCATION

The Curipamba Project is located in the foothills of the Cordillera Occidental of the Ecuadorian Andes and covers the provinces of Bolívar and Los Ríos. The Project is a contiguous area comprising seven concessions that cover 30,327.18 ha, located immediately east of Ventanas and 350 km southwest of Quito (Figure 4.1).



FIGURE 4.1 LOCATION MAP

MINERAL TENURE

The concessions block measures 26 km north-south and 14 km east-west and comprises, from north to south: Las Naves 1, Las Naves 2, Las Naves 5, Las Naves, Las Naves 3, Jordan 1, and Jordan 2 (Table 4.1 and Figure 4.1). The property is located on UTM PDSA 56 zone 17 South Coordinates at 681,000E, 9,842,000N and 702,000E and 9,869,000N.

TABLE 4.1 PROPERTY STATUS, SALAZAR RESOURCES LTD — CURIPAMBA PROJECT

Concession	Area (ha)	Recording Date	Expiry date	Fees required US\$/Year(2013)	Status
JORDAN 1	4,900	26/10/2006	26/10/2036	77,910	Good standing
JORDAN 2	4,627.18	11/04/2006	11/04/2036	73,572	Good standing
LAS NAVES	1,460	18/02/2003	18/02/2033	23,214	Good standing
LAS NAVES 1	4,900	19/08/2005	19/08/2035	38,955	Good standing
LAS NAVES 2	4,900	19/08/2005	19/08/2035	77,910	Good standing
LAS NAVES 3	4,840	19/08/2005	19/08/2035	76,956	Good standing
LAS NAVES 5	4,700	03/02/2006	03/02/2036	37,365	Good standing
TOTAL	30,327.18			405,882	

Third-party properties surrounding the Curipamba Project are shown in Figure 4.2. The location of a kaolin mine on a separate block not owned by Salazar is also shown in Figure 4.2; the kaolin deposit is surrounded by the Jordan 2 concession.

In Ecuador, exploration and mining activities are broken down into four phases:

- Initial exploration, 4 years maximum
- Advanced exploration, 4 years maximum
- Economic evaluation, 2 years maximum
- Exploitation, 25 years, renewable

According to Ecuadorian Mining Law published on January 29 of 2009, exploitation concessions have a term of 25 years and may be approved for renewal for successive 25-year periods provided that the registered concession holder gives notice and files a work and investment plan before the expiry date. A number of permits, as outlined in the Mining Law, are required prior to initiation of exploration activities, including an Environmental Impact Assessment (EIA), an archaeological/cultural heritage permit, and a water use permit. The permit status of the Salazar concessions is summarized in Table 4.3.

The Mining Law requires that the company pay per annual property maintenance 2.5% of the minimum salary per hectare. The minimum salary in Ecuador for 2013 was US\$318 and for 2014 it is US\$340, and it is updated every year. As an alternative to this payment, the company can pay US\$7.95 per hectare per year for the initial four-year exploration phase. In the second four-year period (i.e. advanced exploration), the rate increases to 5%, or US\$15.9 per hectare per year. In the exploitation phase, the fee is 10% of the minimum salary or US\$31.8 per hectare yearly, on a maximum of 5,000 ha (US\$159,000). Salazar concessions Jordan 1, Jordan 2, Las Naves, Las Naves 2, and Las Naves 3 are advanced explorations, and Las Naves 1 and Las Naves 5 are initial explorations.

There is no maximum number of concessions for each concessionaire, but there is a limit of 5,000 ha per concessionaire in the exploitation phase. Mining royalties have been set at a minimum of 5% and a maximum of 8% mineral sales. No back-in rights are applicable. The base sales price for minerals is open to “negotiation” where mining is conducted pursuant to an exploitation contract. The following taxes are applicable to mining activities:

- 22% income tax
- 15% profit sharing (3% workers and 12% social projects)
- 70% of windfall revenue (basis for application not yet determined)
- 12% VAT. VAT on exportation activities is not subject to refund in case of export
- Accelerated depreciation subject to special approval

On July 16 of 2013, the Fundamental Bill of Amendment to the Mining Act, to the Amended Tax Fairness Act and to the Fundamental Internal Taxation Act (the Bill) takes effect. The Bill includes major amendments (Table 4.2), in particular the following:

- The creation and promotion of medium-scale mining, a non-existent category in the previous Mining Act (MA)
- New norms for regulating and sanctioning illegal mining, aiming to eradicate it
- The rationalization of permits and authorizations for mining, making these processes swifter and more straightforward
- The modification of the windfall profits tax in an attempt to overcome a current obstacle in the negotiation of exploitation contracts with private companies

Together with the creation of the category of medium-scale mining, one of the most important changes is the increase in production volumes permitted for what is called small-scale mining.

- The production ranges for medium-scale mining for metal minerals are 301–1,000 tonnes per day in underground mining, 1,001–2,000 tonnes per day in open pit mining, and 1,501–3,000 m³ per day in alluvial mining.
- The production ranges for small-scale mining for metal minerals are up to 300 tonnes in underground mining, up to 1,000 tonnes in open pit mining, and up to 1,500 m³ in alluvial mining.

TABLE 4.2 ECUADOR MINING LAW 2013 – SUMMARY

MID-SIZE MINING	LARGE PROJECTS
Underground Mining between 300 – 1,000 t/day Open Pit Mining between 1,000 – 2,000 t/day	> 1,000 t/day for Underground mining > 2,000 t/day for Open Pit mining
Mining concessions granted up to 10 years: 4 years early exploration (US\$ 8.5/Ha) + 4 years advanced exploration (US\$17.0/Ha) + 2 years feasibility study (US\$17.0/Ha)	Mining concessions granted up to 10 years: 4 years early exploration (US\$ 8.5/Ha) + 4 years advanced exploration (US\$17.0/Ha) + 2 years feasibility study (US\$17.0/Ha)
Ruled by mining law, no negotiation with government. Once the mine starts operations, the annual payment jumps to US\$17.0/Ha up to 25 years (renewable)	Negotiation with the government to obtain operational permit. Once the mine becomes operations, the annual payment jumps to US\$21.9/Ha up to 25 years (renewable)
Fixed Royalty of 3% on NSR for Small Mining Fixed Royalty of 4% on NSR for Mid-Size Mining	Royalty between 5-8% on NSR
No windfall taxes	Windfall tax applicable once original investment has been repaid
1% taxes on the sale or indirect transfer of shares of a mining company	1% taxes on the sale or indirect transfer of shares of a mining company
Total tax burden ~ 50% (includes Royalty, VAT, Profit Sharing and Corporate Taxes). No windfall taxes	Total tax burden ~ 50% (includes Royalty, VAT, Profit Sharing and Corporate Taxes)

Capping Royalties: For Mid-Sized Mining a Fixed Royalty of 4% on NSR have been established. In the case of large projects, concessionaires will have to pay a minimum royalty of 5% on the sale of the principal mineral or secondary minerals and , for gold, copper or silver, no higher than 8%. In other words, a range is set for royalties, thus creating more investor certainty.

Permits: One of the main obstacles faced by the mining industry in Ecuador has been obtaining an Environmental Licence to operate. The current process of approving Environmental Impact Studies and granting an Environmental Licence can take from 12 to 18 months, which not only has a negative impact on business planning but also encroaches on the limited exploration period granted to mining concessionaires.

As for the amendments to environmental permits made by the Bill, the main changes — and our comments — are as follows:

- a) For artisanal mining, environmental fact sheets will need to be approved, while, for small-scale mining, the Environmental Licence will allow concessionaires to perform exploration and exploitation activities at the same time (Art. 13 of the Bill).
- b) With regard to medium-scale and large-scale mining, environmental fact sheets will need to be approved for the initial exploration stage. This is a different and much simpler category than the environmental impact studies currently required for each stage of the mining concession (initial exploration, advanced exploration, exploitation, etc.). Said amendment is very reasonable as the environmental impact is minimal in the initial exploration stage (Art. 13 of the Bill).
- c) In medium-scale and large-scale mining, an environmental declaration, instead of the current Bill needed; as mentioned above, this is a different and much simpler concept (Art. 13 of the Bill).
- d) When a concessionair has completed all the requirements for the approval of the environmental licence, it must be granted within six months of the presentation of the required documentation. Should the competent authority fail to respond within said timeframe, this shall be taken as tacit agreement to the commencement of mining activities. In other words, the Bill establishes positive administrative silence for the approval of environmental licences (Art. 13 of the Bill).
- e) The amendments proposed in the Bill will clearly entail modifications to the Environmental Regulations for Mining Activities, which will have to incorporate a transitional regime for activities currently in the process of obtaining a licence (Art. 13 of the Bill). They are positive for the industry as they eliminate of useless red tape that used to hamper the start of mining activities. It also circumvents undue interference by local governments in the management and control of non-renewable natural resources, which, by order of the Constitution, is the exclusive jurisdiction of the Central State.

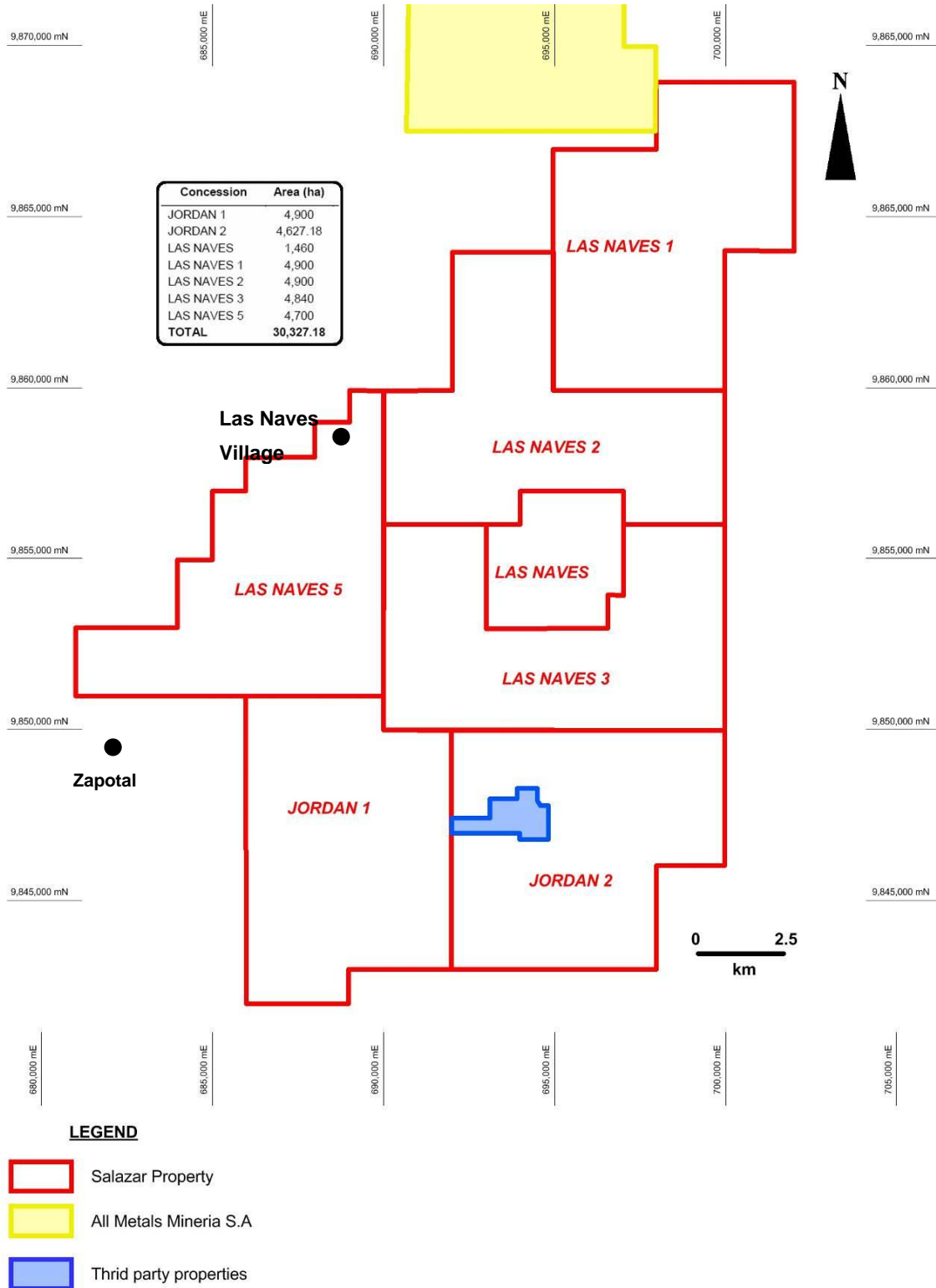


FIGURE 4.2 EXPLORATION CLAIMS MAP

TABLE 4.3 PERMIT STATUS, SALAZAR RESOURCES LTD — CURIPAMBA PROJECT

No.	Date	Document Type	Document	Authorized Company	Status
1	16/11/2007	Survey	Approval of EIA for exploration for the following concessions: Las Naves; Las Naves 1, 2, 3, 4, and 5; Jordan; Jordan 1, 2, 3, and 4.	Subsecretary of Environmental Protection; Ministry of Mines and Petroleum	APPROVED
2	07/06/2009	Certificate	Certificate of Intersection of the National System Protected Areas	Ministry of the Environment	OK, no conflict with protected areas
3	02/10/2009	Survey	Update of EIA, for Exploration, on 15/12/2009, Official registry date	Ministry of the Environment	APPROVED
4	14/01/2010	Permits	Water permit for use of water for exploration, Request No. 1	National Secretary of Water	APPROVED
5	28/10/2010	Permit	Water permit for use of water for exploration, Request No. 2	National Secretary of Water	APPROVED
6	30/03/2010		Patent payments	Ministry of Natural and Non-Renewable Resources	COMPLETED
7		Substitution of Mining Titles and patent payments	Substitution of mining titles for 25 years for concessions	Ministry of Natural and Non-Renewable Resources	GRANTED
07-ene	27/04/2010		Jordan 1, Code 700918	Ministry of Natural and Non-Renewable Resources	GRANTED
07-feb	15/03/2010		Jordan 2, Code 200652	Ministry of Natural and Non-Renewable Resources	GRANTED
07-mar	15/03/2010		Las Naves, Code 200508	Ministry of Natural and Non-Renewable Resources	GRANTED
07-abr	15/03/2010		Las Naves 1, Code 200627	Ministry of Natural and Non-Renewable Resources	GRANTED
07-may	15/03/2010		Las Naves 2, Code 200628	Ministry of Natural and Non-Renewable Resources	GRANTED
07-jun	15/03/2010		Las Naves 3, Code 200629	Ministry of Natural and Non-Renewable Resources	GRANTED
07-jul	27/04/2010		Las Naves 5, Code 700885	Ministry of Natural and Non-Renewable Resources	GRANTED
8	April - May 2010	Socialization Interministry Commission	Socialization and presentation of Curipamba Sur by Ecuadorian State Authorities. (1) Echeandía 26/04/2010; (2) El Congreso 27/04/2010; (3) San Luis de Pambil 28/04/2010; (4) Las Naves 29/04/2010; and (5) Jerusalem 12/05/2010	Ministry of Natural and Non-Renewable Resources, National Secretary of Water, Ministry of the Environment, Subsecretary of the Communities	COMPLETED
9	03/06/2010	Permit	Final Authorization for restart of activities Advanced Exploration Phase	Ministry of Natural and Non-Renewable Resources	GRANTED
10		Certificates	Fulfillment of Art. 26 of the New Mining Law*		

10-ene	09/04/2010	Certificate		National Office of Civil Aviation	GRANTED
10-feb	07/05/2010	Certificate		Ministry of Defense	GRANTED
10-mar	02/06/2010	Certificate		Superintendence of Telecommunications	GRANTED
10-abr	10/06/2010	Certificate		National Office of Hydrocarbons	GRANTED
10-may	28/05/2010	Certificate		Ministry of Transportation and Public Works	GRANTED
10-jun	21/06/2010	Certificate		National Institute of Cultural Heritage	GRANTED
10-jul	16/06/2010	Certificate		Ministry of Electricity and Non-Renewable Resources	GRANTED
11	13/05/2011	License	ENVIRONMENTAL LICENCE: Environmental Auditing of EIA 2010 for Curipamba Sur 3 (Concessions Las Naves 1 and Las Naves 2).	Ministry of the Environment	GRANTED
12	13/05/2011	License	ENVIRONMENTAL LICENCE: Environmental Auditing of EIA 2010 for Curipamba Sur 2 (Concessions Las Naves 5 and Jordan 1)	Ministry of the Environment	GRANTED
13	12/05/2011	License	ENVIRONMENTAL LICENCE: Environmental Auditing of EIA 2010 for Curipamba Sur 1 (Concessions Las Naves, Las Naves 3 and Jordan 2).	Ministry of the Environment	GRANTED
14	30/03/2011	Reports	Annual Exploration Reports of the Curipamba Concessions: Las Naves, Las Naves 1, Las Naves 2, Las Naves 3, Las Naves 5, Jordan 1, and Jordan 2	ARCOM (Regulatory and Mining Control Agency)	APPROVED
15	30/03/2011		PATENT PAYMENTS	Ministry of Natural and Non-Renewable Resources	COMPLETED
16	15/11/2011	Regulation	Mining Occupational Safety and Security Internal Regulation	Ministry of Labour Relations	APPROVED
17	28/11/2011	Regulation	Internal Work Rules	Ministry of Labour Relations	APPROVED
18	26/03/2012	Reports	Annual Exploration Reports of the Curipamba Concessions: Las Naves, Las Naves 1, Las Naves 2, Las Naves 3, Las Naves 5, Jordan 1, and Jordan 2	ARCOM (Regulatory and Mining Control Agency)	APPROVED

19	26/03/2012		PATENT PAYMENTS	Ministry of Natural and Non-Renewable Resources	COMPLETED
20	03/07/2013		Environmental Auditing of EIA 2011 for Curipamba Sur 1 (Concessions Las Naves, Las Naves 3, and Jordan 2)	Ministry of the Environment	APPROVED
21	10/09/2013		Environmental Auditing of EIA 2011 for Curipamba Sur 2 (Concessions Las Naves 5 and Jordan 1)	Ministry of the Environment	APPROVED
22	24/04/2013		Environmental Auditing of EIA 2011 for Curipamba Sur 3 (Concessions Las Naves 1 and Las Naves 2)	Ministry of the Environment	APPROVED
23	27/03/2013	Reports	Annual Exploration Reports of the Curipamba Concessions: Las Naves, Las Naves 1, Las Naves 2, Las Naves 3, Las Naves 5, Jordan 1, and Jordan 2	ARCOM (Regulatory and Mining Control Agency)	APPROVED
24	27/03/2013		PATENT PAYMENTS	Ministry of Natural and Non-Renewable Resources	COMPLETED
25	10/10/2013	Presented	Environmental Auditing of EIA 2012 for Curipamba Sur 1 (Concessions Las Naves, Las Naves 3, and Jordan 2)	Ministry of the Environment	IN PROCESS
26	25/10/2013	Presented	Environmental Auditing of EIA 2012 for Curipamba Sur 2 (Concessions Las Naves 5 and Jordan 1)	Ministry of the Environment	IN PROCESS
22	22/10/2013	Presented	Environmental Auditing of EIA 2011 for Curipamba Sur 3 (Concessions Las Naves 1 and Las Naves 2)	Ministry of the Environment	IN PROCESS

*According to the new Mining Law, EIA, and the Environmental Auditing, the total project area must not exceed 15,000 hectares. Therefore, Curipamba Sur has been divided into 3 projects for the auditing: Curipamba Sur 1, Curipamba Sur 2, and Curipamba Sur 3 (30,327.18 hectares in 7 concessions).

Reports of the Surface Water Quality Monitoring are presented to both The Ministry of the Environment and SENAGUA (National Water Secretariat) on a biannual basis. This provision came into force after receiving the environmental licence for the Curipamba project.

Progress reports on the implementation of the Environmental Management Plan have been submitted to the Ministry of the Environment on a quarterly basis. This provision came into force after receiving the environmental licence for the Curipamba project.

5. ACCESSIBILITY, CLIMATE, LOCAL RESOURCES, PHYSIOGRAPHY AND INFRASTRUCTURE

ACCESSIBILITY

The Curipamba Project is located in the Western Mountain Range (Cordillera Occidental) adjacent to the western coastal flatlands. Access to the area is excellent along paved roads, which branch off at Ventanas and Zapotal from the main coastal highway that connects Quito and Guayaquil (Figure 5.1). The international airport in Guayaquil can be reached in 2.5 hours by road. Salazar maintains a drill core logging, sampling, and secure storage warehouse in the town of Ventanas, on the main highway between the cities of Quevedo and Guayaquil. Ventanas is about a 30-minute drive from the town of Las Naves. Access inside the property is along year-round gravel roads (former logging roads) that connect the Salazar exploration office in Las Naves with the field camp at El Congreso. Secondary roads and trails cross much of the central portion of the Project area (Figure 5.1). Most of the zones of mineral exploration interest are accessible by secondary dirt roads and a short hike on foot. In the northern part of the property, a few areas require mule access.

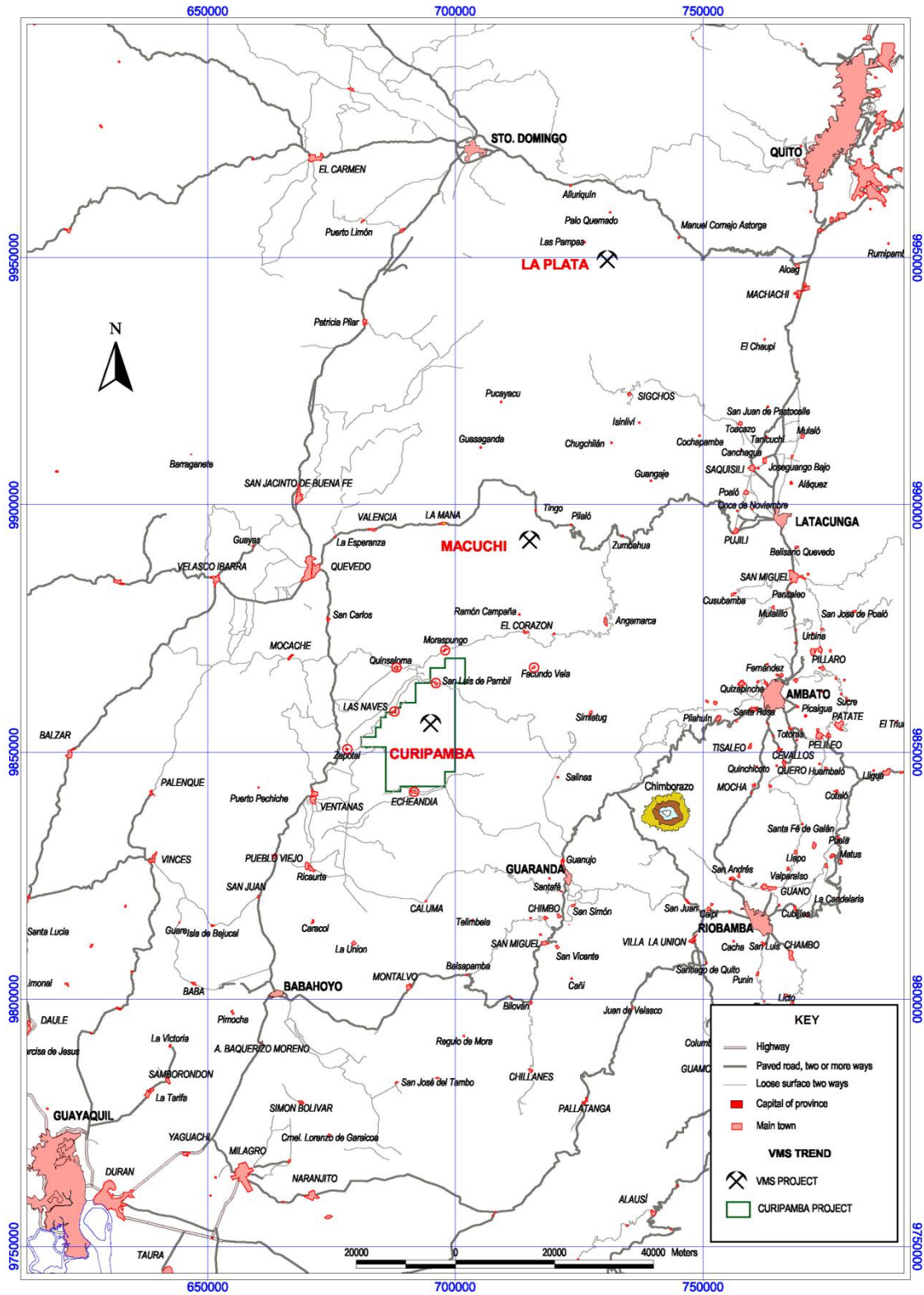


FIGURE 5.1 PROJECT ACCESSIBILITY MAP

CLIMATE

The climate at Curipamba is tropical, humid, and hot most of the year, with lush forest in the Curipamba Concession. The wet season is from December to May, with an average annual rainfall between 2,200 and 2,500 mm, and the dry season is from June to November. The climate has little effect on the operating season and exploration activities can be carried out year-round.

LOCAL RESOURCES

The Curipamba area is near the towns of Ventanas, Quevedo, and Babahoyo and the city of Guayaquil, where supplies and labour can be easily obtained. The Property is well forested, with thick grass covering areas that have been cleared for raising livestock. In areas with cattle, there are numerous ticks in the vegetation. Crops include banana, coffee, cacao, and oranges. The population is dedicated to agriculture and trade. There are no large gold or base metal mines operating in this part of Ecuador. Therefore contractors, skilled labour, heavy mining equipment, and so on, would have to be acquired elsewhere.

INFRASTRUCTURE

There is no infrastructure in the Project area apart from good road access. The national power grid is within 20 km of the Naves Central (El Domo) area in the Echeandía Canton (Figure 5.2).

PHYSIOGRAPHY

The Project area is located where the Andes meet the coastal flatlands. The physiography is characterized by floodplains to the west and moderate to steep-sloped hills to the east, with elevations ranging from 100 masl to 1,000 masl in less than seven kilometres of horizontal distance.

Drainage is dominated by the strong, west-flowing Suquibí and Runayacu (also called Oncebí) rivers. All streams and rivers drain into the Pacific Ocean and have deeply incised the mountain-sides to form the east-west elongated Las Naves hill. Towards the south, a parallel-elongated hill separates the Runayacu River from the Chazo Juan and Echeandía river system.

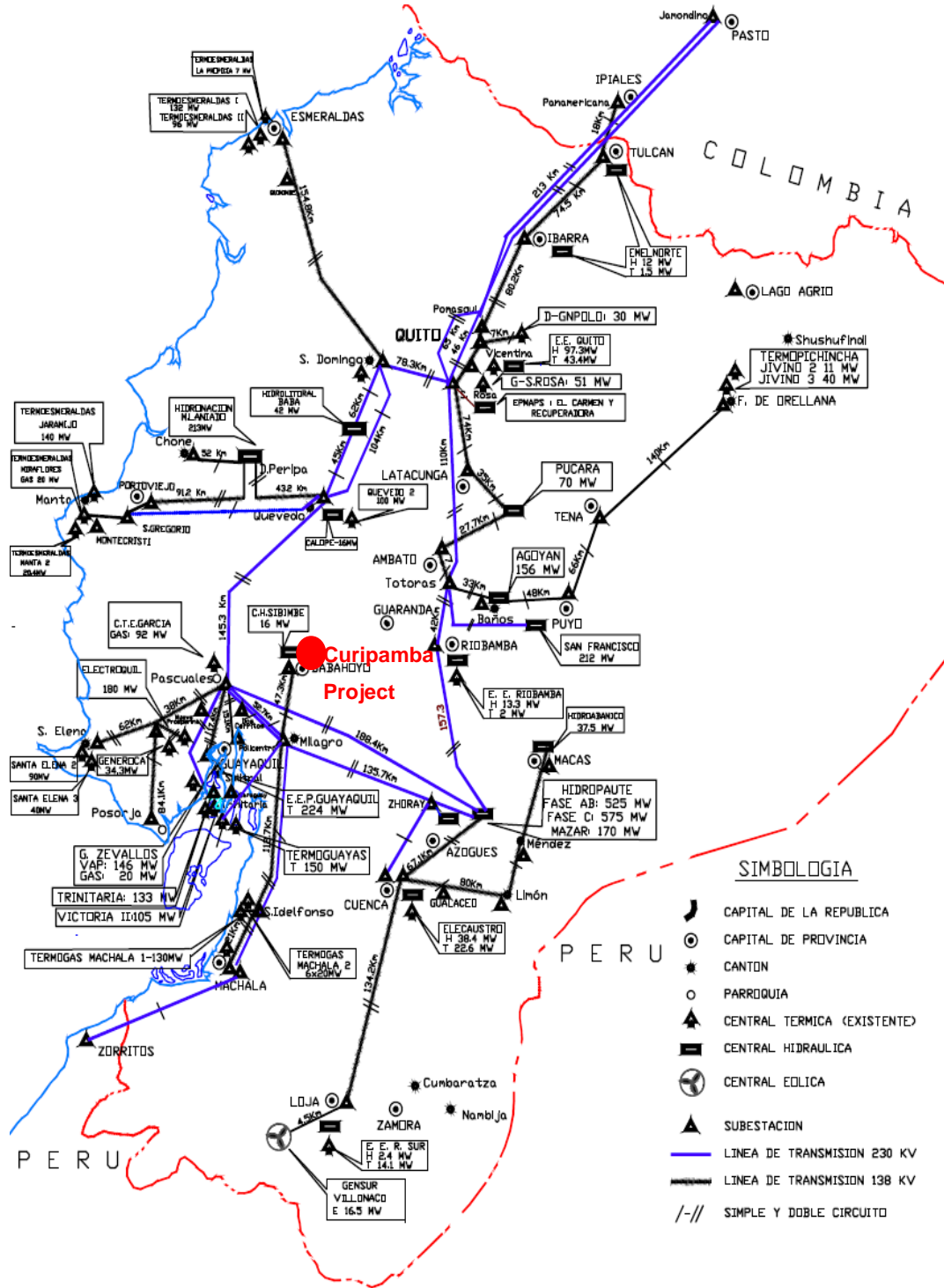


FIGURE 5.2 ELECTRICAL GRID MAP OF ECUADOR

6. HISTORY

This description of the property history was taken, for the most part, from Lahti (2006), Valliant et al (2010) and Lavigne and McMonnies (2011).

- In 1991, RTZ Mining PLC Inc. (RTZ) conducted a semi-detailed stream sediment reconnaissance survey in the Ecuadorian Western Andes near the Curipamba Project, collecting 548 samples. This information was in the public domain in 2004 when Amlatminas (now Curimining) purchased the information from the Ecuadorian government. Although more than thirty elements were analysed, only the two most important elements from an economic standpoint (gold, copper, and the pathfinder element arsenic) were plotted on a map that also included the drainage and an outline of the Curipamba Property. All results were plotted, including those outside of the Curipamba Property. A number of anomalous areas were indicated, but none corresponded to what are now the best-known mineralized occurrences on the Curipamba Property. The best copper anomalies are found on the claims north of the Suquibí River in the northern part of the property. In the southern two-thirds of the Curipamba Property, there is no significant copper enrichment, including the ground with gold-bearing outcrops. Only scattered samples with gold concentrations ranging from 21 ppb to 200 ppb were indicated in the bottom two-thirds of the Curipamba Project.
- The concession for Las Naves was obtained from the Ecuadorian state in February of 2003 by Mr Leiva Iván Santillán. He transferred the properties to Amlatminas (owned by Fredy Salazar) in 2005.
- In 2004, Fredy Salazar and Acosta Geovani staked the 16 claims comprising the original Curipamba Property. In September of 2006, the Curipamba claims were transferred to Curimining S.A. (owned by Fredy Salazar and Pablo Acosta). Mr Salazar and Mr Acosta subsequently agreed to sell their shares in Curimining to Consolidated Kookaburra. Prior to being transferred to Curimining, the claims were held by Mr. Salazar and Mr. Acosta as Amlatminas, a private Ecuadorian company owned by Mr. Salazar through which exploration activities on the Curipamba property were conducted.

- On March 13 of 2006, Newmont Mining Corporation (Newmont) was granted a three-month exclusive access to the Curipamba Property and agreed to possible Joint Venture (JV) terms in a Letter of Intent. Newmont conducted a semi-detailed Bulk Leachable Extractable Gold (BLEG) stream sediment survey on the property, collecting 225 samples. The Newmont BLEG stream sediment survey identified significant gold concentrations in streams draining mineralized areas; however, Newmont did not reach a final agreement and does not retain any interest in the property. According to Lahti (2006), the BLEG method provided a good indication of epithermal gold mineralization, as suggested by the distribution of stream sediment arsenic, silver, and mercury. The method identifies the claims above the Umbe River as having potential for gold and copper mineralization. Similarly, the BLEG survey identifies the southern two-thirds of the Curipamba Property as being enriched in gold, silver, arsenic and, to a much lesser degree, copper. The enrichment in BLEG arsenic, silver, mercury, and molybdenum gives a strong epithermal signature over and adjacent to the gold-silver mineralization at Sesmo Sur, Las Naves Central, Roble, Caracol, and Piedras Blancas (Lahti, 2006).

- In April of 2007, Salazar hired the company Geofísica Consultores of Peru to carry out induced polarization and magnetometer studies in the principal stream's sediments, rocks, and soil anomalies. As a result of this work, 13 IP geophysical anomalies (chargeability and resistivity) were identified in the El Domo deposit and in the surrounding area.

- From late 2007 to April of 2008, Phase I drilling with 51 diamond drill holes (DDH) totaling 10,003 m was completed to test 11 target areas (Buckle, 2009). Drill hole CURI-39 intersected the El Domo mineralization in February of 2008, cutting 12.22 m of massive sulphides (12.22 m at 1.20% Cu, 4.54% Zn, 3.62 g/t Au, and 51.89 g/t Ag).

- On April 18 of 2008, Ecuador's Constitutional Assembly passed a Constituent Mandate Resolution (the "Mining Mandate") that provided, among other provisions, for the suspension of mineral exploration activities for 180 days or until a new Mining Law was approved. In January of 2009, the new Mining Law was passed into law. The new Mining Law states that each company must negotiate an exploitation contract with the government.

- In April and May of 2008, Salazar hired Dr Warren Pratt of Specialized Geological Mapping Ltd to map the El Domo prospect (Las Naves), log drill cores, and determine the volcanic lithostratigraphy (Pratt, 2008).
- In March of 2009, Dr Pratt returned to conduct geological mapping and core logging at the Sesmo Sur prospect, about seven kilometres south of El Domo (Las Naves). The main goal of the visit was to map Sesmo Sur and make geological sections based on the mapping and core logging. The plan was also to create a lithostratigraphic column that would allow correlation with the massive sulphide horizon at El Domo (Pratt, 2009).
- In July of 2009, Salazar hired Dr Jim Franklin of Franklin Geosciences Ltd to review the geological attributes of the newly discovered VMS deposit and occurrences on the Curipamba Project. The objectives of the visit were to examine the overall setting of the occurrences, review selected drill holes to provide comments on the lithologies and principal controls on the occurrences, and to provide suggestions for further work to constrain the controls on mineralization (Franklin, 2009).
- Subsequent to January 29 of 2009, the new mining regulations were implemented.
- From March to May of 2010, Salazar was re-issued title (replacing titles according to the new mining law) to its mining properties of the Curipamba Project by the Ministry of Non-Renewable Natural Resources, and Salazar has complied with all legal requirements and regulations and with the corresponding legal process.
- On June 3 of 2010, Salazar received official notice from the Minister of Mines and Petroleum of Ecuador authorizing the restart of field operations. The notice granted Salazar the right to continue its exploration program in five properties within the Curipamba Project (Las Naves, Las Naves 2, Las Naves 3, Jordan 1, and Jordan2) in Central West Ecuador, subject to receipt of certain permits. On January 14 of 2010, Salazar received its water permit and filed an updated environmental impact assessment.
- From June 4 to September 23 of 2010, the Phase II drilling program was carried out at El Domo, with 20 drill holes completed for a total of 3,241.38 metres.

- In August of 2010, Salazar commissioned Scott Wilson Roscoe Postle Associates (Scott Wilson RPA), the predecessor to RPA, to undertake a resource estimate of the El Domo deposit. Scott Wilson RPA submitted the NI 43-101 Technical Report on the Curipamba Project to Salazar on October 8 of 2010 (Valliant et al. 2010).
- From September 2010 to August of 2011, the Phase III drilling program was carried out on the El Domo target, with 84 drill holes (DDH) completed for a total of 15,582.85 metres.
- In November of 2010, Dr Franklin made his second visit to the project to review the geology, drill cores, and provide new directions for geological exploration.
- In 2011, Roscoe Postle Associates Inc. (RPA) completed a new resource modelling of El Domo, adding the Phase III drilling results. RPA submitted the NI 43-101 Technical Report on the Curipamba Project to Salazar on November 7 of 2011 (Lavigne and McMonnies, 2011).
- From August of 2011 to April of 2012, the Phase IV drilling program was carried out on the El Domo target, with 51 drill holes (DDH) completed for a total of 10,248.77 metres.
- In April of 2013, Salazar commissioned Buenaventura Ingenieros S.A. (BISA) to complete a Preliminary Economic Assessment (PEA) of the El Domo deposit. A new resource estimation that includes Phase IV drilling results, preliminary mining and engineering designs, and preliminary metallurgical testing are contained in the respective sections of this report.

7. GEOLOGICAL SETTING AND MINERALIZATION

The Curipamba Project is located in western central Ecuador, in the province of Bolívar near the town of Ventanas; it is part of the western and lowermost foothills of the northern Cordillera Occidental of the Andes, near the boundary with the western coastal plain (Figure 4.1). Geologically, it is located in the central equatorial Andes, within the Macuchi Terrane, a predominantly juvenile island magmatic arc of Paleocene–Eocene age adjacent to the Amazonian Craton (Figure 7.1).

The El Domo deposit is part of the Las Naves Central area of the Curipamba Project and up to now it is the best-developed and best-known part of the project. The property comprises newly recognized volcanogenic massive sulphide (VMS) mineralization rich in copper, zinc, silver, and gold in an area of circa 2 x 3 km². The project also includes several other prospects and geochemical anomalies such as Sesmo, El Gallo, Roble, Cade, Caracol, and Roble Este (Figure 7.2), which are described briefly in Chapter 9 of this report.

The first drill hole intersection of the massive sulphides was obtained in February of 2008 (CURI-39) when drilling a geophysical (but not geochemical) anomaly in the El Domo area, with a strong chargeability response. The drilled target is one of a group of thirteen geophysical anomalies striking NW-SE and curving to a NNE strike (Pratt 2008) identified in an area approximately 2 km x 1 km. Drill hole CURI-39 reported grades of 4.54% Zn, 1.20 % Cu, 3.62 g/t Au, and 51.75 g/t Ag over 12.4 metres. The early exploration models of Salazar Resources were of VMS deposits, first similar to Eskay Creek and afterwards of the Kuroko type. However, Newmont interpreted this deposit as being epithermal.

The geology of the area is dominated by a submarine mafic volcanic sequence (Macuchi Group, Paleogene–Eocene) with potential for volcanic-hosted massive sulphide deposits (VMS) that is intruded by likely younger subvolcanic calc-alkaline plutonism also having potential for the formation of porphyry and epithermal styles of mineralization. The Macuchi Group hosts several massive sulphide deposits mined in recent years (Table 8.1 and Figure 7.1).

The dominant mineralization consists of a large sub-horizontal lens of massive sulphides at least 800 m long (N-S) and 350–500 m wide that is part of a larger zone of mineralization

that has been partially dismembered by later intrusions. Estimated tonnages and grades are 6.080 Mt at 2.33% Cu, 3.06% Zn, 2.99 g/t Au, 55.81 g/t Ag, and 0.28% Pb for indicated resources; inferred resources are 3.882 Mt with 1.56% Cu, 2.19% Zn, 2.03 g/t Au, 42.92 g/t Ag, and 0.16% Pb (Table 14.1). These mineral grades are similar to those reported at the nearby La Plata and Macuchi deposits, which are hosted by the same sequence (Table 8.1). However, the tonnage at El Domo is significantly larger, making this the largest VMS deposit in the Central Andes of Ecuador.

The only operating mine in the study area is a small kaolin deposit. There are no other mines nearby, but within the property there are some minor prospects with small workings.

REGIONAL GEOLOGY

The Andes of Ecuador comprise two mountain chains, the Cordillera Central and the Cordillera Oriental, separated by a central inter-Andean depression basin. To the west, the Cordillera Occidental predominantly consists of fault-bounded Cretaceous–Tertiary volcanic oceanic and island arc terranes (Litherland and Aspden 1992; Kerr et al. 2002; Spikings et al. 2005). Here, strike-slip fault displacement along approximately north-south trending faults has resulted in a complicated assemblage of tectono-stratigraphic units that juxtaposes volcanosedimentary successions of similar lithologies but different ages. These terranes, of dominant oceanic affinity, have traditionally been interpreted as being successively accreted without obduction west of the Amazon craton to a long-lived continental margin from the Late Jurassic to the Eocene. Superimposed on them are four magmatic arcs also related to the subduction of the Farallon/Nazca plate beneath the continent.

The largest and youngest units are the Pallatanga and the Macuchi terranes (Figure 7.1), thought to be accreted during the Eocene. The Macuchi Terrane, which hosts the Curipamba Project, is several hundred kilometres long and tens of kilometres wide. It has been classically interpreted as an allochthonous terrane accreted to the Pallatanga continental margin during the Late Eocene in response to the closure of a back-arc basin (Spikings et al. 2001; Hughes and Pilatasig 2002; Kerr et al. 2002). However, recent work suggests that the Pallatanga Terrane represents the oceanic basement of the Western Cordillera, being a dismembered terrane from the Caribbean plateau (Luzieux et al. 2006; Vallejo et al. 2006; Spikings et al. 2005; Vallejo et al. 2009). In addition, there are doubts about the exact nature of the Macuchi Terrane. The presence of detrital zircon of Cambrian age inherited from the

nearby basement suggests that the Macuchi Terrane is perhaps a forearc basin that formed near its present position and close to an eroding basement like that in the Eastern Cordillera.

The Pallatanga Group, of likely Coniacian age (Late Cretaceous), comprises discontinuous tectonic slices striking NNE-SSW along the eastern border of the Western Cordillera (Reynaud et al. 1999). It consists of an oceanic plateau sequence comprising submarine basalt, locally as pillow lavas and hyaloclastite breccia as well as underlying microgabbro. This volcanic sequence is overlain by marine turbidites derived from an unknown basaltic to andesitic volcanic source, and a tectonic *mélange* with slivers of ophiolite (Hughes and Pilatasig 2002), all of them interpreted as related to a mantle plume (Vallejo et al. 2006); no subaerial rocks are reported here. Vallejo et al. (2013) have obtained a U-Pb zircon age of 88 ± 2 Ma for igneous rocks of this group.

The Macuchi Terrane, cropping out on the western flank of the Cordillera Occidental (between 0° and $2^\circ 30'S$), contains an intra-oceanic island arc volcanic sequence included in the Macuchi Group. As a whole, it is interpreted as an oceanic plateau sequence. The Macuchi Group comprises predominantly submarine volcanic and volcanoclastic rocks with subordinate sedimentary rocks (BGS-CODIGEM 1993; McCourt et al. 1997). More than 80% of the sequence is dominated by volcanoclastic and epiclastic rocks, including lithic-rich sandstone and breccia with more accessory siltstone and chemical sediments, mostly chert grouped in a turbidite-like sequence. The sequence also includes domes and flows of basalt to basaltic andesite, with abundant pillow lavas/breccias and hyaloclastic textures as well as their sub-volcanic equivalents (dykes) of micro-porphyrific basalt and diabase. Most of these rocks show pervasive hydrothermal-submarine alteration with chlorite-epidote (Aguirre and Atherton 1987). The non-volcanic sedimentary fraction is dominated by scarce calcarenite and recrystallized limestone fringing a presumed reef system (Hughes and Pilatasig 2002). This sequence has an estimated minimum thickness of 2.0 to 2.5 km (Aguirre and Atherton 1987). It seems that the Macuchi Terrane is more abundant in basalt than the Pallatanga Terrane, which is interpreted as due to a more primitive nature of the Macuchi magmatic arc in comparison to the Pallatanga Terrane.

In detail, Chiaradia and Fontboté (2001) have distinguished two major units within the Macuchi Group. The Basal Macuchi includes primitive basalt, mostly as submarine lava flows, interbedded with mudstone. The Main Macuchi is predominantly volcanoclastic, less primitive, basaltic andesite to andesite, and formed in a younger arc. Although most works emphasize the almost exclusive predominance of mafic rocks, the Macuchi Group also

includes several felsic, dacitic to rhyolitic, domes that seem to be directly related to the already known massive sulphide orebodies (Chiaradia and Fontboté 2001; Vallejo 2013), suggesting that the magmatism is bimodal. The orebodies always occur in the footwall of the known VMS, suggesting a direct relationship between the scarce rhyodacite and the mineralization (Pratt 2008; Chiaradia et al. 2008).

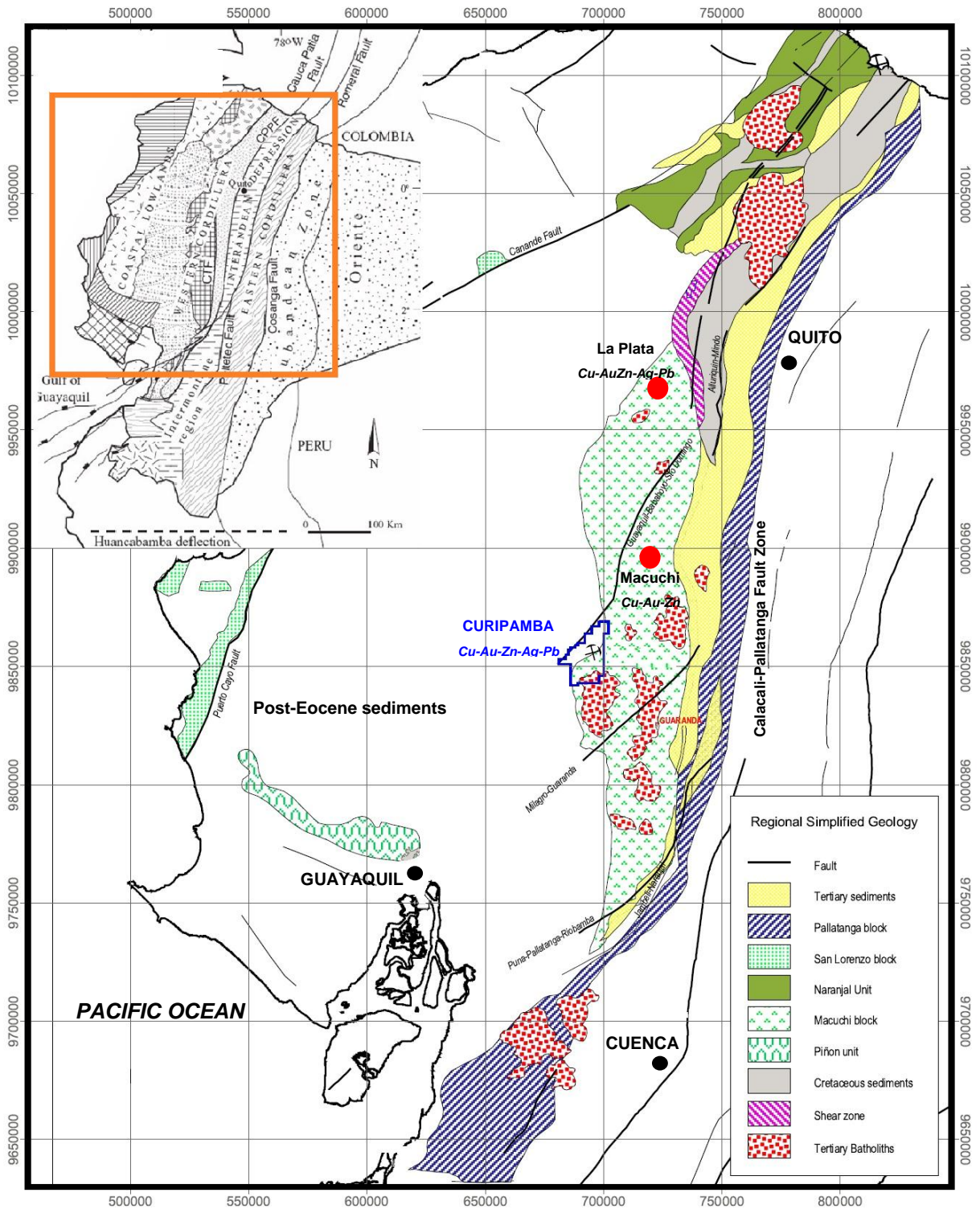


FIGURE 7.1 REGIONAL GEOLOGY — THE MACUCHI TERRANE AND LOCATION OF VMS DEPOSITS

Whole-rock and trace-element geochemical studies show that the basalt to basaltic andesite have MORB-like tholeiitic affinities and primitive arc lavas with locally depleted LREE (Kerr et al. 2002), whereas the felsic rocks are calc-alkaline (Hughes and Pilatasig 2002; Chiaradia and Fontboté 2001; Chiaradia et al. 2008; Vallejo 2013). Although most of the sequence can be accounted for by fractional crystallization of a primitive melt, the most likely derivation of the felsic rocks is the partial melting of a continental crust, as determined by Chiaradia and Fontboté (2001) on the basis of lead isotope geochemistry. This suggests that crustal contamination was likely during the magmatic evolution, which is consistent with the sub-autochthonous nature of the Macuchi Terrane.

Radiometric and biostratigraphic dating (Vallejo 2013; Egüez 1986) indicate a Paleocene to Late Eocene age for the Macuchi Group. The age of the sedimentary rocks was determined from Middle Eocene foraminifera and Late Eocene radiolaria from a typical terrane section (Egüez 1986). Additionally, andesite sills have been dated by K/Ar to circa 42 and 36 Ma. Finally, an Ar-Ar age of 41.5 ± 0.4 Ma has been obtained from the volcanoclastic mafic rocks in the El Domo deposit (Vallejo 2013).

The southern Macuchi Group hosts abundant discordant intrusive rocks of intermediate to felsic composition, mostly large medium- to coarse-grained tonalite and granodiorite plutons rich in hornblende and biotite. There are also abundant porphyritic to micro-tonalite dykes and stocks along the major faults. Franklin (2009) has highlighted the importance of these intrusive rocks in generating magmatic-hydrothermal systems, but up to now there are no accurate geochronology nor geochemical studies supporting such a hypothesis. Contact metamorphic aureoles are well developed and range in age from 35 to 14 Ma; in other words, it seems as though these intrusive rocks are younger than the volcanic rocks of the Macuchi Group and belong to a Middle to Late Tertiary magmatic arc unrelated to the predominantly primitive mafic volcanism of the Macuchi Group.

The Macuchi Group is in tectonic contact to the east through the Toachi Fault and its southern extension the Chimbo Lineament (Vallejo et al., 2009) with the siliciclastic Angamarca Group (Paleocene–Eocene) and the Pallatanga terrane (Hughes and Bermudez 1997; McCourt et al. 1997). Their eastern limit is another major and complex suture zone, the Calacali–Pallatanga Fault Zone. This fault zone and its northern and southern extensions are likely the eastern boundary of the North Andean Block (Ramos 2009). To the west, the Macuchi Group hides below the alluvial fan deposits of the coastal zone.

LOCAL GEOLOGY

Regionally, the Macuchi Group rocks consist mainly of basalt, andesite, and rhyodacite, both coherent and volcanoclastic. Very likely, they belong to the Main Macuchi unit. The volcanic rocks include a wide variety of well-preserved lithofacies interpreted in very different ways by geologists studying the property (Table 7.1).

TABLE 7.1 CORRELATION OF LITHOSTRATIGRAPHIC UNITS IN THE CURIPAMBA PROJECT

This study	Pratt (2008)	Franklin (2009)	Vallejo (2013)
Topsoil/cover			Quaternary deposits
Rhyolite Dome II	----- Not described -----		
Andesite Dome	Andesite	Andesite	Porphyritic andesite
Basalt		Basalt	Mafic Unit
Crystal-Rich Volcanoclastic Breccia	Upper Tuffaceous Unit (UTU)	Epiclastic Unit	Volcanoclastic Unit
Polymictic Volcanoclastic Breccia	Massive Sulphide Unit (MSU), including Grainstone	Debris flow or Breccia Unit including Grainstone	Polymictic Breccia
Semi-Massive Sulphides			
Massive Sulphides		Massive Sulphides	Massive Sulphides
Rhyodacite	Lower Acid Unit (LAU)	Hydroclastic breccia units and massive flows or a flow-dome complex	Felsic Unit
Stockwork Q-py		Stockwork	Stockwork
Stockwork anhydrite/gypsum		Anhydrite	

The rocks of the Macuchi Group show only subtle diagenesis, no metamorphism, and are virtually undisturbed, with almost no tectonic fabrics. Most of the primary features in both the volcanic rocks and massive sulphides are well preserved. Schandl (2009) describes sub-greenschist facies metamorphism, but no assemblages have been found other than submarine hydrothermal alteration with no growth of metamorphic minerals. Furthermore, the rocks have no cleavage and the fabric is likely primary.

The youngest sequence in the study area includes undifferentiated Plio–Pleistocene andesite and dacite volcanic flows, included in the Lourdes, Sagoatoa, Puñalica, and Quilotoa volcanics reported in the 1:100,000 geological maps of Ecuador. The first group includes felsic quartz- and feldspar-phyric volcanic rocks with widespread hydrothermal alteration and intense weathering. The second and third groups of volcanic rocks include pyroxene-bearing coherent and clastic andesite considered remnants of partially eroded pre-Quaternary volcanics.

PROPERTY GEOLOGY

As mentioned above, the Curipamba Project includes predominantly volcanic and volcanoclastic rocks assigned to the Macuchi Group of Middle Paleocene–Eocene age (Hughes and Pilatasig 2002; Vallejo 2007; McCourt et al. 1997) on a regional scale and at the project site (Pratt 2008). They are overlain by Late Tertiary–Holocene volcanic rocks and Holocene alluvial deposits that are the dominant outcropping rocks; most of the Curipamba Project is covered by five to six metres of volcanic ash from eruptions of the Quilotoa Volcano.

The area geology is relatively simple since there is a uniform and well-defined stratigraphy (Figure 7.2 to Figure 7.4). In brief, it includes a basal rhyodacite unit overlain by two interfingering volcanoclastic sequences, one mafic and another felsic, and two coherent younger lithofacies, one andesitic and the other rhyolitic, which intruded the sequence in both the north and south of the property. The massive sulphides are located in the contact between the rhyodacite and the volcanoclastic rocks but also within the mafic volcanoclastics. These latter rocks, termed “Grainstone” or “Grainstone Breccia”, are interpreted as a marker unit in the immediate hanging wall of the massive sulphides (Franklin 2009) that may be used to guide exploration for additional camp-wide resources. Figure 7.2 is a geological map of the Las Naves/El Domo area (Pratt 2008).

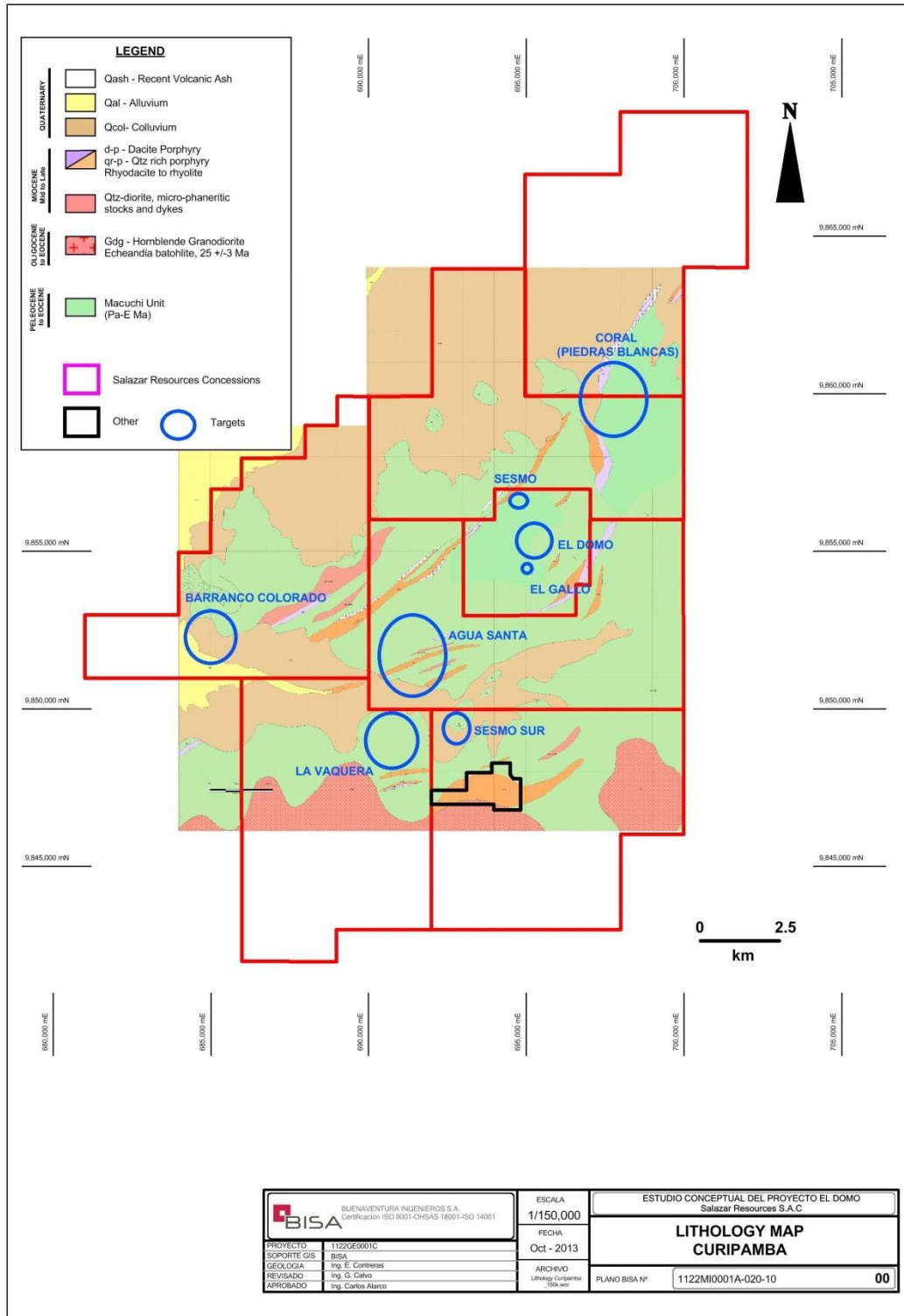


FIGURE 7.2 CURIPAMBA PROJECT — LOCATION OF THE EL DOMO DEPOSIT AND NEARBY PROSPECTS

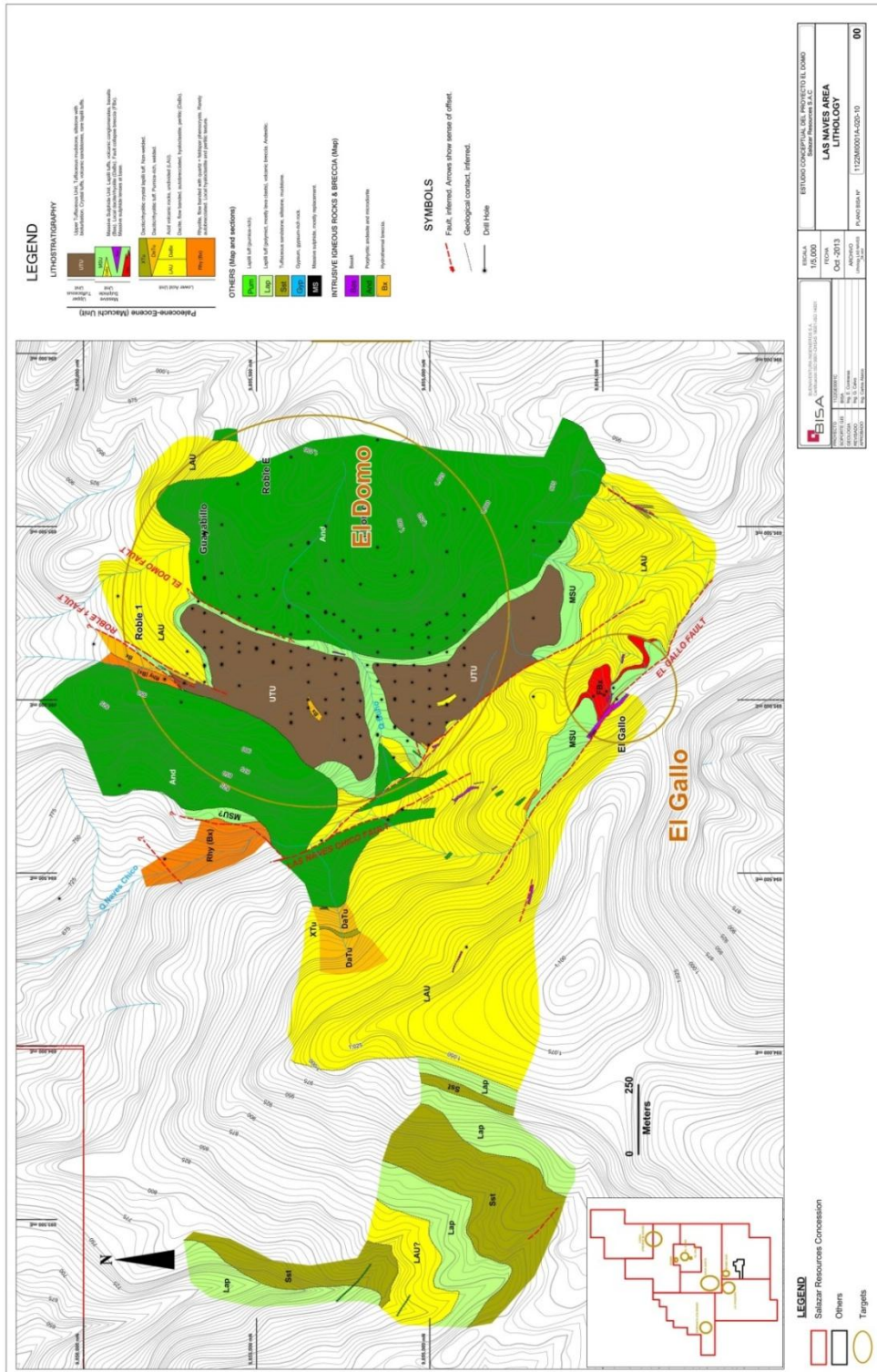


FIGURE 7.3 GEOLOGY OF THE EL DOMO DEPOSIT AND EXPLORATION DRILLING

TABLE 7.2 CORRELATION OF LITHOLOGICAL UNITS — EL DOMO

Rhyolite II	RHY			Rhyolite dome complex dominated by in-situ and transported hyaloclastite (including non-welded pumice) and a small proportion of coherent rocks. Virtually unaltered and likely post-mineralization.
Andesite	AND	Andesite	AND	Andesitic dome dominated by coherent facies with little hyaloclastite. It is not affected by ore-forming-related alteration and is assumed to be post-mineralization.
Mafic dykes	B	Basalt	B	Dykes of basalt/andesite
Felsic dykes	RHY			Dykes of rhyolite
Crystal-rich volcanoclastic breccia	BVX	Tuff	T	Mass flow dominated by fragments of plagioclase-rich dacite that could be derived from non-welded pumice. Includes several units with graded bedding, erosional bases and tops dominated by crystal-rich sandstone and green and red mudstone. Lack of hydrothermal alteration.
Basalt	B	Basalt	B	Subvolcanic sills of basalt intruded in wet sediments.
Polymictic volcanoclastic breccia	BVP	Tuff	T	Complex volcanoclastic unit with alternating polymictic breccias with heterometric fragments of variegated origin with mafic glass-rich breccia and sandstone. Minor layers of black mudstone.
Semi-massive sulphides	SMS	Grainstone	GR	Semi-massive to disseminated mineralization replacing the polymictic volcanoclastic breccia.
		Volcanogenic massive sulphides	VMS	
Massive sulphides	VMS	Volcanogenic massive sulphides	VMS	Massive sulphides showing pronounced lateral and vertical zonation (Cu->Zn + Pb) replacing the uppermost rhyodacite and the footwall of the polymictic volcanoclastic breccia.
Rhyodacite	RD	Rhyolite	RHY	Dome complex of rhyodacite with coherent and brecciated facies, including dominant in-situ hyaloclastite. Coherent facies with local flow banding that dominates in the deep zones.
Stockwork quartz-pyrite	SS	Breccia	BXH	Ore-related stockwork hosted by a zone of quartz-sericite-alteration of the rhyodacite.
Stockwork anhydrite-gypsum	SY	Gypsum	GY	Outer shell of stockwork and stratabound masses within the rhyodacite.
Other lithologic terms used in previous reports	RD	Rhyolite		Rhyolite flows/rhyolitic breccia
	RD	Rhyolite		Autobrecciated dacite
	RD	Rhyolite		Rhyolitic tuff
	???	Hydrothermal breccia		Hydrothermal breccias of different setting and significance
	MF	Tuff		Andesitic tuff/crystal tuff/fine-grained tuff
	MF	Tuff		Volcanic breccia/polymictic breccia

The massive sulphides are related to a major zone of hydrothermal alteration, which includes extensive sericitization-silicification in the rhyodacitic footwall and widespread silicification-chloritization-argillitization in the overlying mafic volcanoclastic rocks. The rhyodacite shows a rather well-developed sulphide-rich stockwork zone and abundant vein-like gypsum replacing earlier anhydrite.

In the mineralized area, the strata are almost flat-lying. They seem to occupy a gentle syncline with a vertical axis and a relatively flat, or gently dipping, core but with steep limbs adjacent to the intrusions. Figure 7.4 shows a lithostratigraphic column of the studied sequence highlighting the key features of the main lithologies.

LOWER FELSIC UNIT (LFU)

This unit, defined by Pratt (2008) as the Lower Acid Unit (Table 7.2), includes a suite of felsic volcanic rocks (rhyolite and overlying dacite) with variegated textures and hydrothermal alteration. It forms the footwall of the orebody and is likely the oldest exposed rock in the area; however, Franklin (2010) has proposed that the Lower Felsic Unit is most likely underlain by mafic flows and volcanoclastic rocks. Its lateral extension is also unknown since it is covered by the younger lithologies. As estimated from drill core logging, the minimum thickness of this unit is between 150–200 metres.

The Lower Felsic Unit is mainly composed of two distinct lithologies with transitional boundaries, the coherent (Photos 1–3) and the fragmental rhyodacite (Photos 4, 5, and 7); the former is more abundant in the footwall. The coherent rhyodacite is whitish to light cream, massive or showing rather continuous, sometimes convoluted, flow banding. It is almost aphyric, but locally there is randomly distributed free quartz (1–5%) in (usually) reabsorbed, 1–5 mm phenocrysts and sub-euhedral to euhedral oligoclase-albite 1–3 mm phenocrysts in a cryptocrystalline groundmass of plagioclase and glass microlites. This groundmass shows widespread devitrification with abundant perlitic textures.

The fragmental rhyodacite has a non-coherent texture and is typically overlies the massive facies, but there are abundant zones of coherent facies within the fragmental one and vice versa. The rocks include pseudo-brecciated zones with only poorly defined fragments highlighted by the devitrification and the subsequent hydrothermal alteration (autobreccia). More common is the hyaloclastite, which has angular to sub-angular fragments, sometimes curvilinear and chilled, with a generalized jigsaw pattern in a darker and originally glassy groundmass of similar composition and ranging in size from a few centimetres to several metres in diameter. The hyaloclastite sometimes grades into a transported hyaloclastite that includes more rounded and heterogeneous fragments, mostly of the same composition but a different texture. It includes fragments with flow banding, massive or even minor fine-grained basalt or basaltic andesite that could represent magmatically eroded dykes or even fragments incorporated into the transported breccia. These rocks are usually poorer in quartz than the coherent facies, probably related to quenching. Pratt (2008) has described the presence of peperitic textures; however, they are unlikely since there are no fine-grained siliciclastic sediments within the unit.

This unit has been interpreted in different ways, mostly as a rhyolitic dome or flow-dome submarine complex overlain by dacitic flows or hyaloclastite (Pratt 2008; Franklin 2009) with

a significant proportion of hydroclastic breccia and even tuffs; the stratiform character and the absence of cross-cutting dykes have been noted as arguments for a lava flow.

There are few geochemical data available for this unit. Vallejo (2013) reports that the Lower Felsic Unit consists of high silica (65–78%) calc-alkaline to transitional dacite to rhyolite with a chemistry compatible with that of magmatic arcs as based on the immobile element geochemistry. The high Zr (100–155 µg/g) and Y (13–23 µg/g) contents are compatible with high-temperature magmas derived from the partial melting of hydrated crust (Barrie et al. 1993). As Vallejo (2013) states, all the felsic rocks of the Lower Unit can be ascribed to the same magmatic unit. It is a chemically homogeneous rock but texturally very heterogeneous — which is sometimes difficult to interpret due to major hydrothermal alteration.

On the whole, this unit is interpreted as a large submarine felsic (crypto-)dome complex that includes most of the intrusive and extrusive lithofacies commonly present in these complexes: massive coherent rocks (including dykes), autobreccias, and both in-situ and transported hyaloclastite, reflecting the growth of these domes in pulses; no clear flows have been observed. These rocks irregularly alternate within the drill core, reflecting the complex dynamic growth of these systems. The presence of transported hyaloclastite (characterized by rounded non-jigsaw breccia textures with texturally different fragments, and sometimes exotic ones) confirms that at least some of the dome erupted into the seafloor, and mass flows formed during dome growth. As Pratt (2008) has noted, felsic flows are uncommon in the seafloor due to the high viscosity of the high-silica melts — when present, they are highly brecciated rocks very different to hyaloclastite. In agreement with (Pratt 2008), BISA believes that most of the brecciation is hydro-magmatic and not hydrothermal. In addition, no evidence has been found of the diatreme reported by Beate (2007). Thus, there is no clear evidence of hydrothermal breccia formation and most of the fragmental rocks can be interpreted as hyaloclastite.

There is no unambiguous evidence of the depth of formation of the dome, but at least some of it emerged onto the seafloor. In fact, these domes can form at any depth, from some tens to thousands of metres. In a regional context, these rocks reflect an event of major submarine felsic volcanism that slightly pre-dated the formation of the overlying massive sulphides. However, not all the felsic rocks are located within the Lower Felsic Unit, and there is some dacite within the Hanging Wall Unit and likely late rhyolite domes.

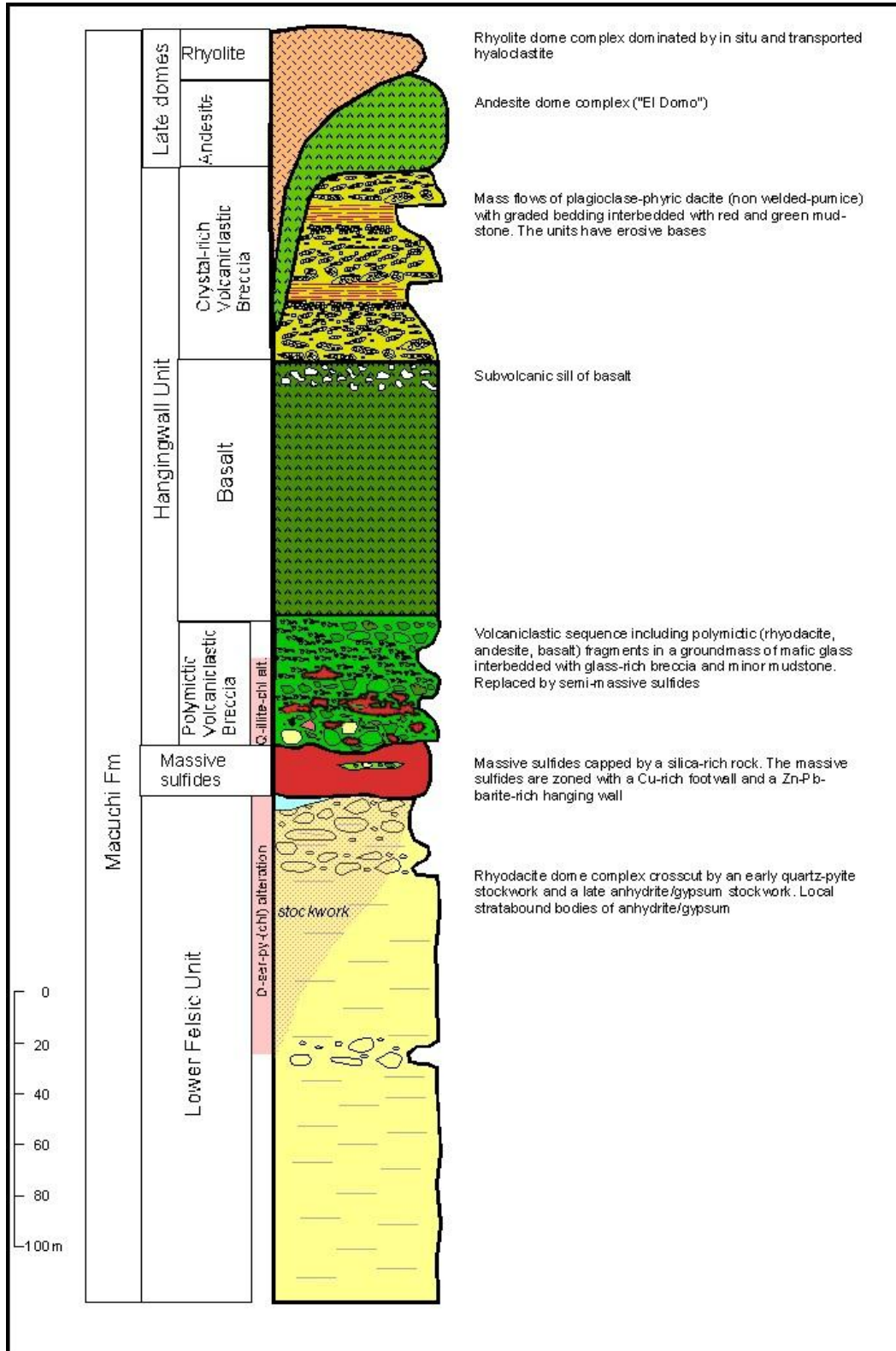


FIGURE 7.4 STRATIGRAPHIC COLUMN OF THE EL DOMO DEPOSIT

MASSIVE SULPHIDE UNIT (MSU)

This unit hosts the bulk of the volcano-sedimentary massive sulphides (>70% of Cu, Au, Zn, and Ag) although some of the mineralization is also hosted in the overlying Hanging Wall Unit as disseminated to semi-massive sulphides and as a stockwork and hydrothermal breccias in the Lower Felsic Unit. Since this unit is exclusively formed of ore, it is described in more detail below. Its thickness ranges between 20 cm and 25 m and strictly follows the contact between the Lower Felsic Unit and the Hanging Wall Unit. The upper contact of the massive sulphides is marked by a rather continuous layer, several metres thick, of white to grey fine-grained silica. Despite being rather massive, the chert sometimes shows crude banding. No clear replacement textures have been found, but it is worth noting that this horizon is usually bounded by abundant clay.

HANGING WALL UNIT (HWU)

This unit occupies the immediate hanging wall of the Massive Sulphide Unit, and also hosts discontinuous lenses of massive, semi-massive, and disseminated mineralization described below. The pre-mineralization/alteration features are described here since BISA considers that the mineralization replaced the volcanoclastic rocks (see Chapter 8.2.1).

The Hanging Wall Unit includes volcanoclastic and epiclastic rocks with fragmental texture. Two major subunits can be clearly differentiated: the Polymictic Volcanoclastic Breccia usually occurs in the sequence footwall and has irregular hydrothermal alteration and mineralization; therefore, it was included in the Massive Sulphide Unit (MSU) by Pratt (2008). The Crystal-Rich Volcanoclastic Breccia shows no hydrothermal alteration or mineralization and is usually located above the Polymictic Breccia; however, it is sometimes interfingering with it. Despite being broadly coeval, the sources and emplacement mechanisms of these two volcanoclastic units are very different.

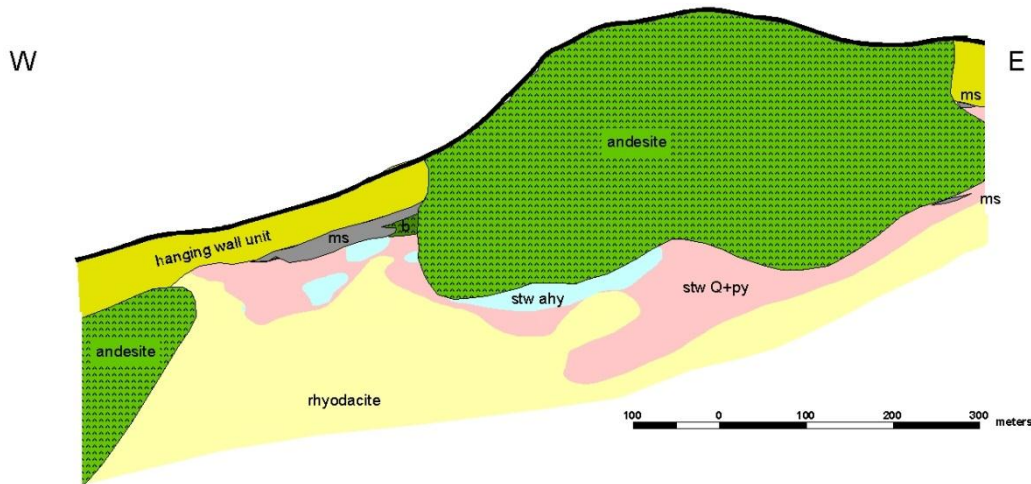


Figure 7.5 Central E-W Cross-Section of the El Domo Deposit Based on the 3D Model

POLYMICITIC VOLCANICLASTIC BRECCIA

This unit is dominated by clast-supported, chaotic, and unsorted coarse breccia with more accessory fine-grained breccia, sandstone, siltstone, and shale. Total unit thickness is circa 50 metres. These rocks are brown to green and show conspicuous meteoric degradation in the drill core.

In the coarse breccia, the fragments are usually angular to sub-angular and range from a few millimetres to some five centimetres in size; they are dominated by irregularly devitrified dark glass with abundant perlitic structures and curvilinear edges suggesting minor reworking. However, the breccia includes abundant non-glassy fragments with: (1) rounded fine-grained porphyritic andesite with variable proportions of plagioclase phenocrysts, typical of the Macuchi Group, likely rocks similar to the Andesitic Dome; (2) volcanoclastic sandstone, quartz, and feldspar-rich phyric rhyodacite with flow banding similar to that of the Lower Felsic Unit; (3) almost aphyric rhyolite with flow banding; (4) dark-grey, vesicular magnetic glassy aphyric basalt with some pyrite; (5) red jasper; (6) silicified organic-matter-rich black sediments; (7) siliciclastic sediments; (8) rare diorite; and (9) pink quartz-feldspar porphyry (Pratt 2008; Vallejo 2013). The groundmass is primarily composed of glass.

The breccias occur as large units some 6–10 m thick and show no obvious sorting or lamination except for some crude grain sorting locally (Photos 36–38). At the unit scale, the

proportion of felsic fragments and glass seems to decrease upwards, with the hanging wall of the sequence being more monomictic and enriched in andesite (Pratt 2008). In the lower part of the unit, the proportion of lithic clasts is less than 5%. Glass is especially abundant in the first 1–5 m above the massive sulphides; here, Buckle (2009) reports clasts with different styles of alteration alternating with fresh glass-rich clasts, suggesting that the hydrothermal alteration pre-dated their erosion and deposition. They include clasts with epidote + pyrite, silicified clasts, interpreted massive sulphide clasts, and very rare amethyst clasts. In the lower part, this breccia alternates with characteristic layers of fine-grained breccia made up of clasts of mafic glass, some 2 mm–1 cm in size, supported by a major portion of groundmass of the same composition.

The breccias are interbedded with 5–20 cm-thick layers of volcanoclastic sandstone, dark siltstone, and shale resembling a turbidite in some places. The sandstone has abundant sedimentary structures including graded, parallel, and cross-bedding, erosional structures, load casts, and syn-sedimentary micro-faulting. These rocks are very immature and are dominated by angular, fine-grained but inequigranular quartz clasts and sometimes abundant plagioclase with interstitial sericite. There are also sporadic intervals of 20–40 cm of mafic glass with features indicating a primary origin and minor reworking (i.e. pyroclastic). These are the only likely true pyroclastic rocks found in the area.

The siltstone occurs as centimetre-to-metre layers capping the sandstone units and grading into fine-grained and darker mudstone. In the contact between sandstone-siltstone or sandstone-mudstone, there are abundant dewatering textures such as sand dykes that are likely related to sedimentation in a tectonically unstable environment. However, lateral facies changes seem to be common and it has not been possible to define a homogeneous section for this unit.

All the previous studies note lenses and fragments of massive sulphides in this breccia. In fact, Vallejo (2013) describes three different breccia units, those within the massive sulphides, those being replaced by the sulphides with the formation of pseudoclasts, and breccia with reworked massive sulphides in the hanging wall. However, all the presumed massive sulphides observed in the drill core seem to be replacement, and the true fragmental massive sulphides are only noted in outcrop at the El Gallo prospect (Pratt, 2008; Vallejo, pers. comm.) in a sedimentary (fault scarp?) breccia with unclear relationships with this unit. These rocks show typical submarine alteration with widespread devitrification to chlorite, magnetite, and epidote. As discussed below, this alteration is independent and predates the

ore-related alteration with quartz (chalcedony), illite, carbonate, and pyrite, which seems to be synchronous with the formation of the 'pseudo-clasts' of massive sulphides by replacement.

The mafic component of this unit was geochemically studied by Vallejo (2013). These rocks have 45–48% SiO₂, are sub-alkaline to tholeiitic, and have flat normalized REE patterns typical of primitive mafic rocks. Ar-Ar dating of hornblende from this unit has yielded a plateau age of 41.5±0.4 that is indistinguishable from the total fusion and inverse isochron ages and consistent with other radiometric and biostratigraphic ages of the Macuchi Group (Chiaradia et al. 2008; Vallejo et al. 2009).

Franklin (2009) has noted a distinctive hard, emerald-green breccia marker level (grainstone) that has been found in most drill holes and several outcrops, which should mark the hanging wall of the orebody and serve as a marker horizon. This breccia is locally bedded, fragment-supported (0.5–1.5 mm), smectite-rich, and commonly mineralized. According to Franklin (2009), it is continuous throughout the mineralized area. However, the term “grainstone” is restricted to carbonate rocks (Dunham 1962) and should therefore be avoided here, so perhaps a term such as "green volcanoclastic breccia" should be used.

Previous works have interpreted these rocks as graded lapilli tuff and mudstone debris avalanches produced by explosive submarine eruptions (Pratt 2008) or related to the hydrothermal brecciation of early mafic volcanism and further slumping near a fault scarp (Franklin 2009). Possible ore fragments in one of the breccias led Vallejo (2007) to conclude that this unit formed after the mineralization and was deposited in a depression. In his model, the breccia is related to the collapse of andesitic domes and its volcanoclastic cover, possibly contemporaneous with pyroclastic volcanism that includes the intercalated and overlying tuffs and lapilli.

As discussed in more detail below, our interpretation is that the Polymictic Volcanoclastic Breccia is not a primary pyroclastic unit but a volcanoclastic one broadly synchronous with the mineralization. The fragmental rocks derive from the erosion and re-sedimentation of earlier poorly consolidated juvenile pyroclastic volcanic rocks in the flanks of a submarine volcano. During the avalanche, the mass flow incorporated many clasts of varied origin that predominate in the upper part of the sequence. The lack of volcanic ash suggests that the eruptions took place at rather considerable depths.

Within the Polymictic Volcaniclastic Breccia and the Massive Sulphide Unit, there is a massive basalt-andesite rock (25–150 m thick) previously interpreted as a lava flow (Pratt 2008; Buckle 2009). This presumed lava flow has irregular tops and includes hyaloclastic margins and local peperites; Pratt (2008) describes chilled margin pillows, but Vallejo (2013) believes these structures could be interpreted as a hyaloclastite. The few observed examples suggest that this rock is a high-level sill intruded into wet mud, which is consistent with the crosscutting relationships with the stratigraphy. The hanging wall is made up of 20–30 cm of peperite with droplets of basalt in shale and is underlain by a vesicle-rich zone (Photo 42). The footwall includes a breccia with 0.5–1 cm basalt fragments in a shale groundmass. The contact with the massive sulphides has not been observed.

This rock is dark, predominantly aphyric, and contains only some plagioclase, pyroxene, and olivine phenocrysts in a cryptocrystalline groundmass of euhedral plagioclase, clinopyroxene, and magnetite. The rock is affected by submarine metasomatism with widespread replacement by chlorite, iron oxides, calcite, pumpellyite, pyrite, and quartz. It has abundant vesicles infilled with zeolites, quartz, epidote, or calcite.

Pratt (2008) is of the opinion that this basalt was the original source of the mafic clasts in the underlying Polymictic Volcaniclastic Breccia. He notes that the lava flow is overlain by breccia with basalt fragments and that there is a noticeable upward decline in basalt clasts within the breccia; furthermore, other drill holes in which basalt is absent show far fewer basalt clasts. The basaltic unit seems to thicken towards the north, but locally it pinches out in the breccia.

CRYSTAL-RICH VOLCANICLASTIC BRECCIA

As mentioned above, this unit is usually located above the Polymictic Volcaniclastic Breccia although they sometimes interfinger close to their contact. The minimum total thickness is near 75 m. These rocks are responsible for most of the gentle undulating topography in the project site. This unit comprises several sub-units (up to 15 m thick) that include three different rocks, not always present.

The base is formed by the chaotic accumulation of coarse-grained, highly heterometric (1–10 cm) fragments of feldspar-rich dacite, 2–5 m in thickness (Photo 45). The rock shows abundant (50–95%) 2–5 mm phenocrysts of feldspar and only seldom quartz supported by a highly foliated groundmass of glass, altered to sericite and chlorite; there are minor amounts of pyroxene and clinoamphibole. These fragments are sometimes poorly defined due to re-

equilibration between them or with a groundmass of similar composition. These rocks are highly monolithic and only some fragments of medium-grained dacite and jasper with disseminated pyrite have been found. The abnormal abundance of plagioclase suggests these rocks are the product of the compaction of vesicle-rich rocks even though there is no evidence of welding; however, some putative pumice tubes have been found.

These rocks grade into 5–7 m of volcanoclastic sandstone with abundant millimetric-sized broken plagioclase crystals, 1–3 mm flattened glass defining a lamination and perhaps some minor intercalations of chemical sediments; there is widespread normal and graded bedding, syn-sedimentary slumping, and faulting. Capping the sequence or interbedded with the sandstone there is 2–3 m of green and red siltstone with local millimetric sedimentary layering and locally graded bedding. These sediments incorporate 5–10 cm fragments of flattened clasts here interpreted as pumice fragments that floated after the eruption and later sank into the fine-grained sediments. These sediments are ripped off and incorporated as rafts in the base of the next unit (Photos 43 and 44). Here, the erosion of the underlying sediments produced major disruption and folding, sometimes incorporating soft clasts with convoluted layering.

Overall, the Crystal-Rich Volcanoclastic Breccia is interpreted as a succession of large, high-energy mass flows composed of three classic units with normal grading and an erosional base, which episodically flowed into the basin with a turbidite-like mechanism. The relationships between individual subunits suggest that there was significant erosion and ripening of the already settled sediments when the next one flooded into the basin. Some studies (Pratt 2008) report widespread bioturbation that BISA has not observed. Pumice fragments within the siltstone indicate that these mass flows were synchronous with submarine explosive volcanism. No texturally equivalent rocks have been found in the area and likely these rocks are exotic flows that came from several kilometres away into the basin. Despite being originally porous and reactive rocks, they do not show noticeable hydrothermal alteration other than the diagenetic transformation of glass into chlorite, suggesting that they postdated the ore-forming process and related hydrothermal alteration

The Polymictic Volcanoclastic Breccia and the Crystal-Rich Volcanoclastic Breccia represent two almost synchronous types of volcanism coeval with basin formation and massive sulphide precipitation. Both rocks seem to be exotic to the basin, but more geochemistry is definitely needed to understand the precise relationships with the local sequence and the ore-forming process.

BASALTIC ROCKS

Within the Polymictic Volcaniclastic Breccia and the Massive Sulphide Unit, there is a massive basalt-andesite coherent rock (some 15 m thick) that has been previously interpreted as a lava flow (Pratt 2008; Buckle 2009). This presumed lava flow has irregular tops and includes brecciated margins and local peperites. Pratt (2008) describes chilled margin pillows, but Vallejo (2013) believes these structures could be interpreted as a hyaloclastite. The few observed examples suggest that this rock is a high-level sill intruded into wet mud, which is consistent with the crosscutting relationships with the stratigraphy. The hanging wall is made up of 20–30 cm of peperite with droplets of basalt in shale and is underlain by a vesicle-rich zone (Photo 42). The footwall includes a breccia with 0.5–1 cm basalt fragments in a shale groundmass. The contact with the massive sulphides has not been observed.

This rock is dark, mainly aphyric, and with only some plagioclase, pyroxene, and olivine phenocrysts in a cryptocrystalline groundmass made up of euhedral plagioclase, clinopyroxene, and magnetite; the rock is affected by submarine metasomatism with widespread replacement by chlorite, iron oxides, calcite, pumpellyite, pyrite, and quartz. It has abundant vesicles infilled with zeolites, quartz, epidote, or calcite.

Pratt (2008) considers that this basalt was the original source of the mafic clasts in the underlying Polymictic Volcaniclastic Breccia. He observes that the lava flow is overlain by breccia with basalt fragments and there is a noticeable upward decline in basalt clasts within the breccia. Furthermore, other drill holes in which basalt is absent show far fewer basalt clasts. The basaltic unit seems to thicken towards the north, but locally it pinches out in the breccia.

ANDESITE DOME

The project area is named due to the presence of an andesitic dome-like structure east of the orebody. It is dominated by highly homogeneous massive or coherent facies showing only local magmatic foliation. The rock has widespread brecciation, including autobreccias, hyaloclastite, and transported hyaloclastite (Photo 50) all around the dome that are not concentrated in the external zones. These features indicate that it is an extrusive dome and grew from different pulses of upflowing magma. In fact, Pratt (2008) describes the presence of at least two intrusive events. The edge is marked by fine-grained and phenocryst-poor

facies with local bleaching. Pratt (2008) also described peperite textures not observed by our geologists.

This rock is made up of an irregularly devitrified green glassy groundmass with isolated small feldspar and pyroxene (?) phenocrysts (1–3 mm). There are rare quartz phenocrysts (or xenocrysts) and small mafic clots and xenoliths. This rock has rather abundant amygdales, locally streaked out in a weak flow foliation infilled with stilbite and calcite. It shows minor seafloor hydrothermal alteration, with replacement of the glassy groundmass by chlorite, epidote, minor illite, and magnetite. The andesite is generally non-magnetic, and has 56–68% SiO₂. Geochemically, it corresponds to tholeiitic basalt-andesite to andesite with a typical island arc signature (Vallejo 2013).

The El Domo intrusion has steep contacts marked by chilled margins and breccia bodies. When crosscutting the massive sulphides, they show evidence of cataclasis and local recrystallization to coarse-grained sulphides. However, most of the observed contacts of the andesite with the host rocks are faulted and locally sheared, with the formation of metre-thick shear zones that can include fragments of massive sulphide. This is somewhat similar, but at a significantly smaller scale, to what is observed in the La Plata deposit (see Chapter 8).

Pratt (2008) stresses that the andesite does not form well-defined stocks, but seems to be sheet-like stocks that pinch out upwards and towards the north. Vallejo (2013) interprets it as several coalescent sub-volcanic andesite bodies that perhaps extruded onto the seafloor, as evidenced by the local presence of transported hyaloclastite.

RHYOLITE DOMES

The geological mapping (Figure 7.3) shows that the El Domo sector includes some dome-like bodies of rhyolite that seem to crosscut previous lithologies. In the drill core, this rhyolite is mainly aphyric with only 1–2 mm quartz crystals in an irregularly devitrified, spherulite-rich, glassy groundmass. It has extremely variegated, well-preserved structures, including coherent facies with flow banding, hyaloclastite, and transported hyaloclastite with abundant pumice fragments, with the fragmental rocks close to the edge of the body (Photos 47–49). The lithofacies are very irregularly distributed, suggesting an evolving polyphase extrusive felsic dome, but the fragmental ones clearly dominate over the coherent facies. The rock shows only minor, irregular chloritization, indicating that it postdates the mineralization.

This rock is perhaps equivalent to the submarine volcanic crypto-dome of glassy dacite that crosscuts the Crystal-Rich Volcaniclastic Breccia described by Pratt (2008).

MAFIC AND FELSIC DYKES

All the described rocks are crosscut by abundant high-level mafic and felsic dykes that are interpreted as the feeder dykes of the basaltic sill and the late andesite and rhyolite domes. However, the basaltic dykes are massive and sometimes crosscut the whole sequence, even the basaltic sill. The basalt comprises a black, dominantly aphyric rock with scattered olivine, Ti-augite, and plagioclase phenocrysts, and up to 5% magnetite in the groundmass (Pratt 2008). It is sometimes rich in vesicles and has abundant amygdales of chalcedony, chlorite, and/or calcite. Porphyritic andesite dykes are widespread in the area along sub-vertical NE-SW and mostly dominant NNW-SSE structures; they are best seen in the Lower Felsic Unit.

The felsic dykes are mainly glassy rhyolite with widespread devitrification and likely peperitic margins suggesting subvolcanic intrusion into wet sediments (Mayor 2010); they probably correspond to the feeder zones of the rhyolite domes. These dykes are only up to a few metres thick and do not have major hydrothermal alteration except for minor chloritization (+pyrite), so they also postdated the ore-forming event.

GRANODIORITE-DIORITE

Pratt (2008) has described a major granodiorite batholith west of the El Domo area that appears to have caused significant contact metamorphism of the host rocks. Major bodies of coarse-grained diorite also occur within the project area. Franklin (2009) interprets these rocks as being the possible subvolcanic roots of the mafic rocks and the sources of heat, metals, or fluids leading to the mineralization. However, and as noted in the chapter on Regional Geology, they likely postdate the volcanic rocks.

QUATERNARY DEPOSITS

The project area is located on the westernmost slopes of the Andes, with very active sedimentation. Most of the volcanic rocks are covered by colluviums (up to 10 m thick) dissected by alluvial deposits. The colluvial deposits are thicker and more abundant at the break of slope. They include multi-event, gravity-driven, matrix-supported deposits from local as well as distal sources. Boulders of all sizes (up to 10–20 cm in diameter) are embedded in a clay-rich matrix. The boulder lithology is polymictic, although those from the Macuchi Group, with typical regional propylitic alteration, tend to dominate.

TECTONIC SETTING

The tectonic setting in which this magmatic-hydrothermal event took place is probably related to the oblique Eocene deformation. Here, the oblique subduction of the Farallon/Nazca plate beneath the continent produced major NNE dextral strike-slip deformation and related extensional structures that channelized the ascent of mafic magmas through an overthickened basement, with local partial melting of the continental crust and contamination.

In detail, the area geology is consistent with the mineralization and the host rocks being located in a NNE-SSW trending graben at least 6 km² in extent. The structural framework and orientation of the faults is consistent with a fracture pattern associated with right lateral strike-slip faults and synchronous opening of pull-apart or transtensional basins. Major deformation was accommodated by the NNE-SSW faults (which have a significant offset), with the NNW-SSE structures being extensional faults with only minor displacement (Figure 7.6). As interpreted by Mayor (2010), the graben is bounded by the steeply dipping Roble 1 and El Domo faults. It is truncated at the southwestern boundary, against footwall rocks, by the NW-SE trending Naves Chico Fault Zone and at the northeastern boundary by an unnamed fault. The western edge is defined by the Cade and Cade Sur anomalies and a string of unnamed and untested prospects hosted in breccia. Detailed geophysics show the importance of these lineaments, with the magnetic anomalies located along these NNE-SSW structures, while the IP anomalies seem to correlate mostly with the NNW-SSE steeply dipping faults. The structure itself is crosscut by NNE-SSW extensional faults with little displacement that predominate in the area and control drainage.

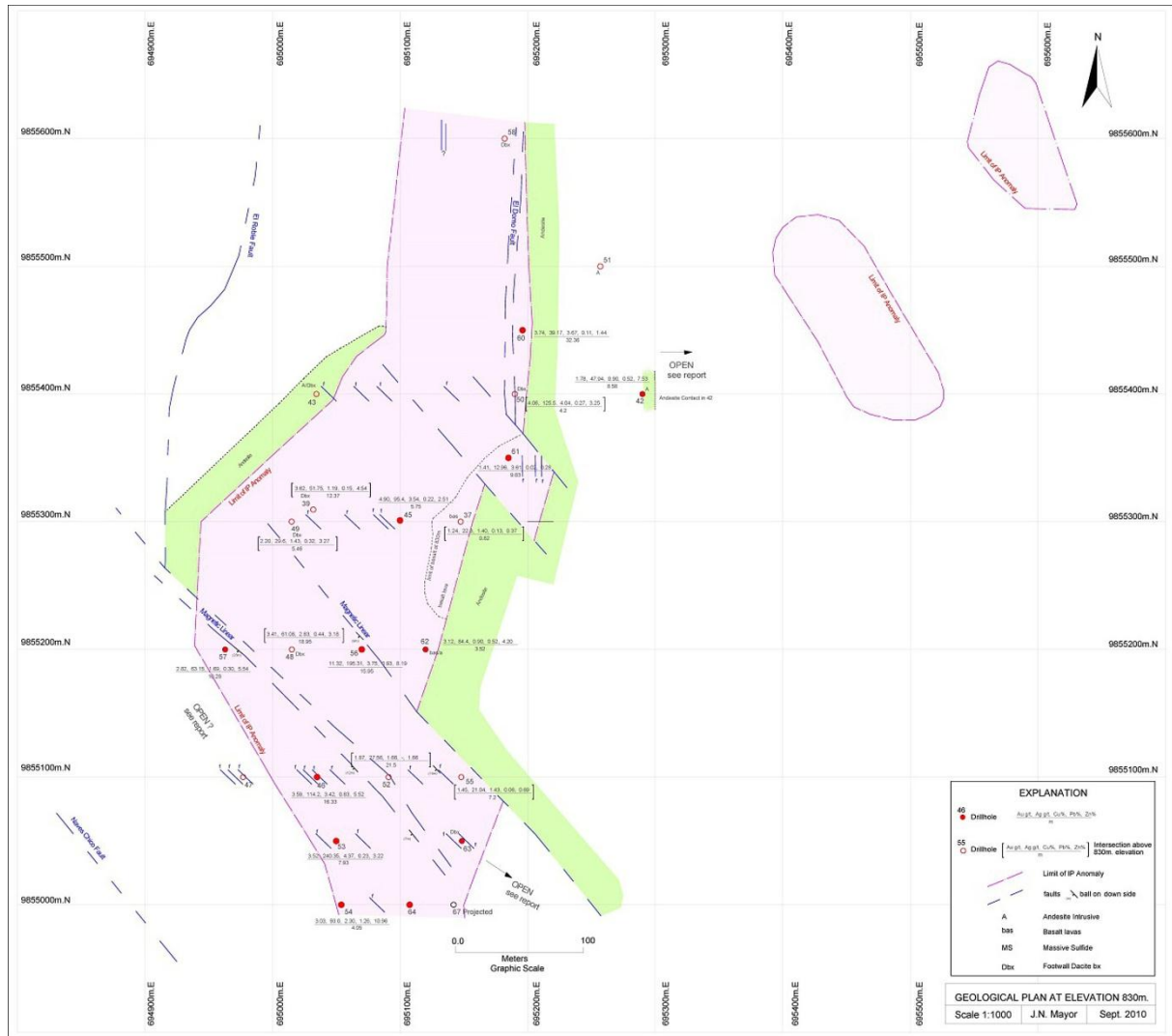


FIGURE 7.6 STRUCTURAL SETTING OF THE EL DOMO DEPOSIT

The massive sulphides are located in a syncline-like structure with a relatively flat or gently dipping (up to 12°SE) core but steeper limbs. The rocks have a general NNE-SSW trend similar to that of the whole Macuchi Group at a regional scale (N30°E) and coinciding with the regional structural lineaments. The eastern margin of this syncline is marked by the El Domo andesite intrusion, the west side by another major andesite intrusion, and the northern part of the camp by another rhyolitic (crypto-) dome (Figure 7.4).

Faulting is widespread in the drill core and ranges from zones of intensely broken core indicating brittle faulting and cracking to distinct fault breccia and gouge with features of brittle-ductile shearing in the rocks with strong argillic alteration. Locally, these latter structures define major shear zones with up to 10 m of hydrothermally altered rocks (including brecciated and sheared fragments of massive sulphides) showing tectonic cleavage and, therefore, indicative of brittle-ductile behaviour. Furthermore, Pratt (2008)

describes the injection of ductile sericite/illite and gypsum into the fault zones and forming significant amounts of the fault gouge. However, this deformation is much more subtle than in other nearby massive sulphides. These rocks appear less deformed than La Plata, where there are several large mineralized shear zones with abundant massive sulphide fragments carrying a significant part of the Au-rich ore (Chiaradia et al. 2008).

The extensional NNW-SSE faults have had a complex history and are probably the channelways of the magmatic and hydrothermal activity. They have channelized the major basaltic-andesitic and rhyolitic dykes as well as likely hydrothermal breccias; they also seem to control the pathways for the feeder systems for the massive sulphide mineralization. The El Domo intrusion has also been channelized by one of the structures (El Domo Fault) limiting the graben. In fact, it is associated with zones of mineralized breccias, something that Pratt (2008) has interpreted as indicative of the El Domo being a zone of major upflow of hydrothermal fluids, that is, the structure that channelized most of the fluids forming the massive sulphides.

As described in Chapter 7, the combined effect of faulting and intrusion has somewhat disturbed the area's geology. Near the faults bounding the structure at the southeastern and northwestern zones, the sequence is tilted and faulted. Close to the contacts with both andesite units, the massive sulphides become sub-vertical, faulted, and broken-up. All these features are interpreted as related to the andesite intrusion and its rheological differences with the host rocks. The history of these faults is therefore likely to be very long and complex with several reactivation events (Pratt 2008).

This graben probably formed by Eocene transpressional deformation and controlled the deposition of the volcanosedimentary rocks of the Hanging Wall Unit. The geological data suggest that the El Domo deposit formed in a third-order basin within a larger intra-magmatic arc basin. There are no geophysical or geological data supporting the presence of a caldera. However, the structure and composition of the volcanoclastic rocks (as well as the intrusion of late bimodal domes) are typical of caldera settings. Furthermore, most magmatic-hydrothermal-related VMS deposits are associated with calderas, which strongly suggests that there was one at El Domo, probably dismantled due to further erosion.

The extensional faults that postdate the ore-forming event remobilized some of the ore (see Chapter 8), and form N-S trending grabens likely related to post-collisional transform faults of

post-Eocene to Quaternary age. Late dextral reactivation has also been observed in many of the faults, likely related with the modern reactivation of the Chimbo-Toachi Shear Zone.

HYDROTHERMAL ALTERATION

The formation of the El Domo VMS deposit is accompanied by major stratabound hydrothermal alteration mainly controlled by the fluid-rock ratio and the composition of the protolith. Overall, the area is affected by a large hydrothermal halo related to the ore-forming process. The Footwall Felsic Unit has been affected by quartz-sericite alteration, whereas the Polymictic Volcaniclastic Breccia is irregularly altered to an assemblage including chlorite, phyllosilicates, and quartz. The other rocks in the area are virtually unaltered and only the igneous rocks show subtle seafloor hydrothermal alteration.

TABLE 7.3 SUMMARY OF THE HYDROTHERMAL ALTERATION IN THE EL DOMO DEPOSIT

Polymictic Volcaniclastic Breccias	Argillic	Dominated by replacement of the mafic glass by clay and phyllosilicates, primarily nontronite, smectite, illite, carbonate, and chlorite, with variable amounts of quartz and pyrite and lesser amounts of magnetite; the fragments of felsic volcanic rocks are replaced by K feldspar. Lenses and veinlets of gypsum. Pronounced Mn anomaly.
	Semi-massive sulphides	Disseminated mineralization in the most altered zones and preferentially replacing mafic fragments and groundmass.
Massive sulfides	Chert	Continuous chert layer bounded by a zone of argillic alteration
	Barite cap	Zone of coarse-grained massive barite with disseminated sulphides.
	Massive sulphides	Showing pronounced lateral and vertical zonation (Cu->Zn + Pb) replacing the uppermost rhyodacite and the footwall of the Polymictic Volcaniclastic Breccia.
Lower Felsic Unit	Hematization	Irregular zone of hematite staining external to the hydrothermal zone.
	Propylitic	External and irregular, poorly defined aureole of chlorite – smectite – quartz – pyrite assemblage.
	Sericite	Pervasive replacement of feldspar and irregular of groundmass by sericite (illite).
	Quartz-sericite	Pervasive replacement by silica and sericite (illite).
	Quartz-pyrite-sericite	Internal alteration zone, texturally destructive.
	Stockwork of quartz - pyrite	Stockwork zone in the quartz-pyrite-sericite zone.
	Stockwork anhydrite-gypsum	Semi-continuous stratabound zone of massive anhydrite-gypsum veins.

The Footwall Felsic Unit shows widespread and pervasive (but only locally texturally destructive) hydrothermal alteration with intensity in direct relationship with the thickness of the massive sulphides. Vallejo (2013) reports that the alteration is circa 2 x 2 km² in extent; the most intense hydrothermal alteration and veining seems to be located beneath the central part of the orebody regardless of the rhyodacite structure. The alteration consists of an irregularly distributed association of sericite-illite, quartz, pyrite, and sometimes carbonate with loss of the mafic minerals; accessory chlorite replaces these minerals or is disseminated in the altered rocks. The pink to greenish volcanic rocks are bleached into a white rock with the glassy groundmass almost completely replaced by quartz, sericite, and pyrite, and the feldspar phenocrysts replaced by sericite. The rock is demagnetized likely due to sulphidization of the magnetite. There is an irregular and likely more external zone made up of chlorite + smectite + quartz.

The deep parts and the zones with higher fluid flux (that is, the orebody footwall, the feeder zones, and the most permeable breccia zones) are silica-enriched. Pratt (2008) defines a zoned halo with the internal quartz-sericite zone grading into an outer zone of light-grey illite, and finally into a light-green smectite (montmorillonite?) alteration. Both zones lack significant amounts of quartz and pyrite. However, in the internal zone, the hydrothermal alteration is accompanied by the growth of variable but significant amounts of pyrite that is never higher than 10%; locally, it mimics the flow banding or is disseminated in the groundmass. However, most of it is found in the stockwork veins with other sulphides and quartz, as described below.

Eight kilometres south of El Domo there is a kaolin mine, suggesting that the phyllic alteration is widespread and perhaps not always related to the VMS deposits.

A characteristic feature of El Domo is large amounts of gypsum — and probably its high-temperature precursor, anhydrite. The calcium sulphates ± pyrite form thick veins and stratabound bodies that are up to 5 m thick, mostly in a semi-continuous stratabound zone beneath the massive sulphides (Schandl 2009) (Photos 10 & 11). These sulphates likely reflect the fluid-mixing zone of the deep Ca-rich fluids with seawater. The gypsum shows frequent evidence of ductile disturbance and likely injection along faults.

Pratt (2008) has described local hematization within the Lower Acid Unit that could be an early hydrothermal alteration. In fact, widespread hematite alteration is described in the

hanging wall of the La Plata massive sulphides (Chiaradia et al. 2008), but here it is much less significant.

Geochemically, the silica-sericite alteration is marked by the removal of Na and Ca during the destruction of plagioclase and the input of silica, iron, minor magnesium, and perhaps potassium. This alteration is broadly similar to that found in many stockwork or feeder zones of VMS deposits; however, it seems as if the fluids were low in Fe-Mg, inhibiting the formation of widespread chlorite, the most typical mineral in the internal zones of the feeder zones. Geophysically, these alteration zones correspond to magnetic lows and variable resistivities that mark the silica- and phyllosilicate-rich zones, respectively.

The massive sulphides are overlain by a zone of somewhat different hydrothermal alteration, which suggests a strong control of the protolith composition on the hydrothermal assemblage. The immediate hanging wall, in the Polymictic Volcaniclastic Breccia, is dominated by major, white to grey, fine-grained stratabound silicification. This is especially prominent just above the massive sulphides, where there is a rather continuous layer of chert bounded by clay, forming a metre-thick pervasive and texturally destructive argillic alteration.

The polymictic breccia overlying the massive sulphide horizon hosts an irregular and pervasive but texturally non-destructive stratabound hydrothermal alteration that is more subtle than in the footwall rocks; it can be traced up to 100 m above the deposit. It is especially intense in the footwall and above the massive sulphides and seems to be mainly controlled by the glassy, fine- to medium-grained volcaniclastic mafic rocks. This circumstance indicates a major control of the lithology, which very likely reflects the most permeable or reactive zones as in many VMS deposits (see Tornos et al. in press). The other rocks in the Polymictic Breccia Unit show less intense alteration.

This alteration is dominated by the replacement of the glass by clay and phyllosilicates, primarily nontronite, smectite, illite, carbonate, and chlorite with variable amounts of quartz and pyrite and lesser amounts of magnetite; the fragments of felsic volcanic rocks are replaced by K-feldspar (Photos 38–41). All these hydrothermally altered rocks also host lenses and veinlets of gypsum.

This alteration has produced major Mn enrichment (typical in hydrothermal alteration distal to VMS deposits) accompanied by an increase in Mg and depletion in Na (Franklin 2010). Similarly, Vallejo (2013) reports that there is a large geochemical halo around the orebody

with a noticeable modification of the original Ba/Sr values up to 30 m above and 40 m below the orebody.

This alteration hosts abundant mineralization, both as disseminations and selective replacement of clasts and as massive sulphides. Pratt (2008) has predicted that these hydrothermally altered rocks are unlikely to produce any significant IP/resistivity response.

The hydrothermal alteration is synchronous with the massive sulphide formation, as evidenced by the lack of sericitization and silicification of the crosscutting felsic and mafic dykes. However, the igneous rocks that crosscut the ore-related alteration show widespread seafloor hydrothermal alteration, including chlorite-epidote assemblages. Locally, the basalt and the andesite have vesicles and fractures with zeolites.

The altered rocks of the Footwall and the Hanging Wall Units both show an external zone of propylitic hydrothermal alteration, which is classically interpreted as due to the circulation of hot fluids equilibrated with seawater. Alteration minerals include smectite, chlorite, pyrite, calcite, and locally quartz-epidote.

Previous studies have highlighted the presence of breccia rocks in the El Domo deposit. Beate (2007) has reported diatreme breccias, whereas Pratt (2008) described hydrothermal breccias and pebble dykes up to several metres wide crosscutting the Lower Felsic Unit. However, most of the breccias we have found in the footwall rocks seem to be stratabound in-situ and transported hyaloclastite. Pratt (2008) describes different types of hydrothermal breccias emplaced in different episodes. The most significant ones are synchronous with the hydrothermal alteration and seem to be restricted to zones of major fluid flow within the Lower Felsic Unit; these breccias are rich in sericite and fine-grained pyrite. However, hydrothermal breccias are also common along the NNE-SSW faults, where breccias of equivalent composition with quartz, sericite, and pyrite and likely remobilizing the previous mineralization sometimes occur in the tectonic contact with the post-ore andesite.

CU-AU-ZN-AG-PB MINERALIZATION

The main orebody at El Domo (Main Ore Zone) forms a single, large, sub-horizontal stratabound 550 x 200 m, N-S crescent-shaped massive sulphide sheet some 10–35 m in thickness in the contact between the Lower Felsic Unit and the Polymictic Volcaniclastic Breccia (see Figure 7.5). The northern part dips shallowly to the east, and the southern part

dips shallowly to the west. Above this stratabound body there are some smaller lenses of massive sulphides and disseminated mineralization hosted by the Polymictic Volcaniclastic Breccia described below. The Main Ore Zone occurs at depths between 40–100 m, but in the eastern area (near the Andesite Dome) the ore zone is deeper. The massive, semi-massive, and disseminated sulphides (Types 2 and 3) are included by Pratt (2008) in the Massive Sulphide Unit; however, the mineralization seems to be dominantly replacement and it crosscuts lithologic boundaries so it does not have a true sedimentary significance.

The massive sulphide lens appears to be entirely absent in some places; in fact, Pratt (2008) reports the local fine-grained volcaniclastic sediments directly overlying the Lower Felsic Unit with no mineralization or hydrothermal alteration. In other places, the massive sulphides are only 20 cm thick, which can have profound implications on the resource evaluation (Pratt 2008).

MAIN ORE ZONE

The Main Ore Zone is a large, massive sulphide lens with the classic zonation of VMS deposits. It includes a large, stratabound core zone of pyrite + chalcopyrite, an intermediate zone of polymetallic (Zn-Cu) ore, and a sphalerite-galena-(barite) zone in the hanging wall and edge of the deposit (Upper Polymetallic Zone). The latter sometimes grades upwards into massive barite. The contact between zones is very irregular and gradation between the assemblages takes place within only a few metres.

The silica-rich rock forms a discontinuous layer (0.2–3 m thick) of fine-grained whitish to grey silica with local inherited banding and colloform textures (Photos 34 & 35). Pratt (2008) describes botryoidal texture with convex-upwards surfaces that he interprets as the only convincing exhalative textures in the deposit. This rock could be a chemical exhalite similar to that found elsewhere capping exhalative ore deposits (Spry et al. 2000; Peter and Goodfellow 1996). However, in detail it shows replacement textures on the Volcaniclastic Polymictic Breccia, suggesting that it forms an external metasomatic aureole to the massive sulphides. Similar cherts have been reported from La Plata (Chiaradia et al. 2008).

The barite zone forms a discontinuous layer between the silica-rich rocks and the Upper Polymetallic Zone of the massive sulphides. It is dominated by massive to bladed coarse-grained barite with some interstitial sulphides, quartz, clay, and carbonates. The massive sulphides prograde on the barite, replacing it but leaving abundant interstitial barite as well as variable amounts of carbonates (sometimes very abundant), quartz, and clays. This

Upper Polymetallic Zone is characterized by an abundance of coarse-grained sphalerite with irregularly distributed chalcopyrite and minor amounts of pyrite, bornite, galena, and tennantite. Both gold and silver seem to be preferentially concentrated in this zone. The lower part of the massive sulphide lens is characterized by abundant pyrite and chalcopyrite (Cu-rich ore).

The contact between the lowermost massive sulphides and the stockwork is gradational, with a gradual increase in fragments of pervasively altered rhyodacite that are first supported and replaced by sulphides and later occur as the groundmass of breccias or as thin veinlets along with quartz. These latter rocks are interpreted as being the stockwork or feeder zone and are described below.

SEMI-MASSIVE SULPHIDES AND DISSEMINATED MINERALIZATION

Overlying the massive sulphides of the Main Ore Zone and within the Polymictic Volcaniclastic Breccia there are at least three, up to 10 m-thick, lenses of massive sulphides and abundant disseminated to semi-massive mineralization separated from the Main Ore Zone by hydrothermally altered breccia and mudstone (Franklin 2009). This mineralization is enclosed in an aureole of hydrothermal alteration and seems to be restricted to the lower Volcaniclastic Polymictic Breccia, where stratabound zones of mineralized/altered rocks alternate with others showing minor mineralization and lacking hydrothermal alteration. The drill core shows that the hydrothermal alteration is limited and controlled by layers of mudstone. It likely formed impervious levels that channelized fluid flow below them and focused the stratabound mineralization and related alteration. In detail, most of the ore here occurs in the glass-rich units, and the coarse polymictic breccia and the siltstone are seldom mineralized. Franklin (2009) has described two mineralized units capped by a breccia that is a marker horizon useful for exploration. In previous reports and in the BISA's resource estimate, this mineralization has been termed "Grainstone".

The massive sulphides here show a zonation similar to that described above, with an upper Zn-Cu-Ag-Au enrichment and a Cu-enriched footwall. They also include a silica-rich aureole that sometimes hosts bands of fine-grained sulphides. Franklin (2009) has described quartz-pyrite-chalcopyrite stringer mineralization underlying these lenses.

A significant part of the ore here occurs disseminated or as isolated patches (fragmental ore). It forms aggregates of massive sulphides a few millimetres to 1 metre in diameter that several previous reports describe as clasts (Photos 33–35 and 38–40). However, there is

considerable evidence that these 'pseudo-fragments' are a product of the selective replacement of the host rock synchronously with the hydrothermal alteration. These 'pseudo-fragments' are more abundant in the base of the mass flow units and are sometimes preferentially enriched along certain layers (the mafic glass-rich ones). In detail, some of the clasts of the breccia (jasper, porphyritic dacite, and especially the glassy andesite) show a rim of sulphides.

These sulphide aggregates can have a margin of chalcopyrite or pyrite and a core of sphalerite, but most of the major ones are made up of massive sphalerite. In detail, the sulphide aggregates are larger than the accompanying clasts, have irregular morphologies with abundant embayments, and replacement contacts with the silicate groundmass. The groundmass and the fine-grained sediments, when composed of volcanic glass, show abundant, fine-grained disseminated sulphides, predominantly framboidal pyrite and sphalerite accompanied by barite and gypsum. There is some evidence of open-space filling by laminated sulphides (Lavigne J. & McMonnies E., 2011).

However, Vallejo (2013) describes that, in some outcrops (El Gallo, see Chapter 8), there are breccias with up to 80-cm-long, angular to sub-angular massive sulphide fragments in an unaltered groundmass that could well correspond to fragmented and eroded massive sulphides that were exposed at the surface, eroded, and resedimented into the mass flows. Although most of the mineralization occurs in the rhyodacite and the Polymictic Breccia, the basalt is also mineralized. Sulphides (mainly pyrite, sphalerite, and chalcopyrite) fill some of vesicles, indicating again that the mineralization was early and before diagenesis. Locally, the basalt groundmass is replaced by disseminated sulphides (Pratt 2008).

STOCKWORK MINERALIZATION

Beneath the Main Ore Zone, there is a stringer or stockwork low-grade mineralization hosted by a large zone of hydrothermal alteration within the rhyodacite (see Section 7.5). The contact with the overlying massive sulphides is a zone several metres thick of quartz and pyrite. This stockwork zone is large in volume but generally low grade.

The dominant stockwork is formed by irregular veinlets, several millimetres to 5 cm thick (Photos 6–9). The distribution and morphology of the veins (as well as of the enclosing alteration zone) does not show any obvious structural control, suggesting that it developed by hydrothermal overpressure.

The uppermost part of the stockwork zone is formed by sulphide-supported breccias. Inside the stockwork, there are large breccia zones, both hydrothermal and hyaloclastic. These zones have preferential veining, with the quartz-sulphide veins being channelized through the clast rims, highlighting the fragmental nature of the rocks. The veins are thicker and more irregular than in the coherent rocks. The groundmass is preferentially altered and replaced by disseminated sulphides.

Hydrothermal breccias are fairly common (Pratt 2008), with heterometric, sometimes jigsaw fragments, supported by quartz and pyrite. However, not all the breccia rocks are mineralized and the stockwork also crosscuts massive rhyodacite. A significant part of the sulphides are disseminated in the most altered zones. Locally, the sulphides have replaced some flow bands in the coherent rocks, giving the mineralization a stratiform appearance, suggesting that fluid pressure controlled the formation of the stockwork zone.

The veins are usually massive and sometimes have a narrow dark rim of very fine-grained pyrite, with the core infilled by coarse-grained quartz and sulphides, mainly pyrite with some chalcopryrite, minor sphalerite and accessory galena; however, there are some early veins of massive sphalerite. Barite, anhydrite, and sericite are locally present. Pratt (2008) interprets the sinuous and irregular morphology of the stockwork as due to its high level of emplacement, probably close to the seafloor. Only locally are there voids indicative of open-space filling with geopetal structures infilled with barite and chalcedony.

BISA's geologists found no evidence of chimneys or venting of hydrothermal fluids on the seafloor except some hydrothermal conduits within the massive sulphides. The contact of the stockwork with the massive sulphides is gradual, suggesting that the system was controlled by diffuse flow.

These quartz-sulphide veins are crosscut by massive veins of medium- to coarse-grained gypsum with disseminated pyrite several millimetres to 1 metre thick. The gypsum likely replaced former anhydrite. Some of the sulfates also occur as massive replacements. The anhydrite/gypsum preferentially replaced the hyaloclastite and the most altered rocks, sometimes mimicking the original texture. These veins are mainly located near the stockwork-massive sulphide interface or form an external aureole to the quartz-sericite-pyrite alteration, which is consistent with the anhydrite being the product of fluid mixing between a hot (>300°C), reduced hydrothermal fluid and seawater.

Pratt (2008) describes mineralization in breccia in early high-angle NNE-SSW structures, 1 to 2 m wide, which acted as partially brecciated "pebble dykes" that could correspond to deep feeder zones beneath the stockwork zone. These hydrothermal breccias can be easily distinguished from the host rock and contain angular and rounded silicified clasts.

ORE MINERALOGY

A brief preliminary mineralogical study has been carried on 17 samples from the Main Ore Zone and the disseminated ore in the Volcaniclastic Polymictic Breccia (Table 7.4). These rocks are not representative of the whole of the orebody and were collected for a preliminary mineralogical characterization. The data obtained are somewhat different from previous studies, suggesting that there is an urgent need for a more systematic and definitive mineralogical study. A more detailed mineralogical characterization is needed to orient the metallurgical tests.

The observed massive sulphides can be grouped into six different ore assemblages (Table 7.5): (1) **Assemblage A**: a pyrite-chalcopyrite assemblage that corresponds to the lower copper-rich zone (6 samples); (2) **Assemblage B**: dominated by iron-poor sphalerite with minor galena and barite (1 sample); (3) **Assemblage C**: a complex, fine-grained assemblage dominated by iron-rich sphalerite, chalcopyrite, and tennantite that contains most of the silver-bearing minerals (4 samples); (4) **Assemblage D**: a late Cu-rich assemblage formed either by massive chalcopyrite or by a bornite \pm tennantite \pm sphalerite assemblage (3 samples); (5) **Assemblage E**: a barite-sphalerite assemblage (1 sample). The latter four assemblages correspond to the Polymetallic Upper Ore Zone and seem to be heavily intermixed. There is also an assemblage product of the supergene alteration (**Assemblage F**) with covellite and chalcocite replacing the pyrite-chalcopyrite mineralization. Finally, there are two samples from the disseminated ore. Selected photographs are included in Appendix I. This classification broadly coincides with that defined in this report for the metallurgical tests, a high-grade copper mineral ($Cu/(Zn+Pb) > 3$; Assemblage A), a mixed Cu/Zn mineral ($3 > Cu/(Zn+Pb) > 0.33$; Assemblages C and D), and a Zn-Pb mineral ($Cu/(Zn+Pb) < 0.33$; Assemblages B and E).

TABLE 7.4 LOCATION OF PETROGRAPHIC SAMPLES

Sample	Location	Classification
DOM-04	Drill hole 11-106 (49.94 m). Mineralization sphalerite	Massive sulphide. Assemblage B replaced by Assemblages C and D
DOM-06a		Massive sulphide Assemblage A
DOM-11	Drill hole 10-64 (54.70 m) Mineralization replacing mass flow	Massive sulphide Assemblage A
DOM-21	Drill hole 10-68 (88.40 m). Sphalerite near contact	Massive sulphide Assemblage B replaced by Assemblage C
DOM-22	Drill hole 10-68 (92.00 m). Sphalerite near contact with chert	Massive sulphide Assemblage B replaced by Assemblage C
DOM-23	Drill hole 10-68 (92.36 m). Sphalerite near host rock contact	Massive sulphide Assemblage B replaced by Assemblage C
DOM-24	Drill hole 10-68 (96.15 m). Massive sulphide	Massive sulphide Assemblage A
DOM-25	Drill hole 10-68 (98.00 m). Massive sulphide	Massive sulphide Assemblage A
DOM-27	Drill hole 11-123 (69.30 m). Mineralization sphalerite-chalcopyrite	Massive sulphide Assemblage B with incipient replacement by C
DOM-28	Drill hole 11-123 (77.10 m). Mineralization sphalerite-chalcopyrite-barite	Massive sulphide Assemblage A replaced by B
DOM-29	Drill hole 11-123 (72.40 m). Mineralization sphalerite + chalcopyrite	Massive sulphide Assemblage B replaced by Assemblage C
DOM-67	Drill hole 161 (262.10 m). Massive sulphide	Massive sulphide Assemblage D
DOM-68	Drill hole 56 (70.90 m). Massive sulphide	Massive sulphide Assemblage A
DOM-69	Drill hole 60 (131.20 m). Massive sulphide	Massive sulphide Assemblage A
DOM-70	Drill hole 73 (58.00 m). Massive sulphide	Massive sulphide Assemblage D
DOM-72	Outcrop of massive sulphides	Massive sulphide Assemblage A

TABLE 7.5 ORE ASSEMBLAGES IN THE EL DOMO DEPOSIT

<i>Assemblage</i>	<i>Denomination</i>	<i>Zone</i>	<i>Paragenesis</i>	<i>Comments</i>
A	Copper mineralization I	Lower Cu-rich Zone	py I + cp I + (sph + gn)	Coarse-grained porous pyrite and massive chalcopyrite
B	Zinc mineralization	Upper Polymetallic Zone	sph I + ba + (gn)	Coarse-grained low-Fe sphalerite
C	Polymetallic mineralization (Zn-Cu-Ag-Au)		sph II + tenn + cp II + (str + proust + gn)	Fine-grained and mineralogically complex assemblage dominated by Fe-rich sphalerite
D	Copper mineralization II		cp III + (gn) (1) bn + sph III + tenn + (py II + gn + cp IV + str) (2)	Coarse-grained late Cu-rich assemblage dominated by chalcopyrite and bornite + tennantite
E	Barite mineralization	Barite cap	ba + sph (+gn)	Coarse-grained barite with accessory sulphides
F	Supergene alteration		cv + cc + goe	Only present at very shallow depths

ba: barite; cp: chalcopyrite; cc: chalcocite; cv: covellite; gn: galena; proust: proustite; py: pyrite; sph: sphalerite; str: stromeyerite; tenn: tennantite

The pyrite + chalcopyrite Assemblage A is rather heterogeneous and characterized by early, coarse-grained pyrite (Photos 12 & 13). The earliest one (30–60 µm) shows abundant primary textures, including zoned crystals, colloform, botryoidal, and radiating growths and framboidal grains. It evolves into coarse-grained (< 2 mm) structureless highly porous pyrite with few inclusions interpreted as related to the diagenetic maturation of the early pyrite; in fact, there are common inherited textures in these grains, including botryoidal and euhedral growth zones. The pyrite is brecciated and later cemented, supported and replaced by fine- to coarse-grained massive chalcopyrite (<200 µm) almost inclusion-free that locally forms the bulk of the sample with only some inherited and corroded grains of pyrite inside. Locally, the assemblage is dominated by pyrite chalcopyrite with only residual grains of anhedral pyrite. Only some Fe-poor sphalerite and galena in small grains (10–20 µm) at the edge of the pyrite crystals and tennantite (<30 µm) are found here. In one sample, the proportion and size (2 mm) of the sphalerite grains is high, suggesting that it may have been adjacent to the boundary zone. This sphalerite coexists with abundant chalcopyrite (8–10 µm) and tennantite (2–10 µm). Pyrrhotite and arsenopyrite are minor phases in this assemblage.

Intergrown minerals within the sulphides include undeformed barite (up to 20%), carbonates (<30%), and quartz (<10%), the latter in zoned crystals, with minor amount of clays.

The other three primary sulphide-rich assemblages grouped in the Upper Polymetallic Zone are distinguished by the abundance and type of copper sulphide present, with only small amounts in the sphalerite-rich assemblage (Assemblage B), the abundance of fine-grained tennantite (Assemblage C), and the presence of coarse-grained chalcopyrite and bornite (Assemblage D).

In Assemblage B, iron-poor sphalerite dominates (Photos 15 & 16). This early sphalerite (sph I) forms colloform to massive coarse-grained aggregates with few inclusions of framboidal and colloform (10–100 µm) to euhedral porous pyrite, which seems to be the first mineral to precipitate in a similar fashion to that described in the pyrite + chalcopyrite ore. There is evidence of replacement of Assemblage A by sphalerite (Photo 14). There are large crystals of honey-coloured sphalerite replaced by a later fine-grained but also Fe-poor one. This abundant sphalerite I is intergrown with barite, quartz, carbonates, and clays and is associated with medium-sized sometimes skeletal galena; locally, there is some ilmenite replaced by rutile that is likely inherited from the volcanic protolith.

Both Assemblages A and B are clearly replaced by the later Assemblage C, which is the most complex, fine grained-assemblage of the mineralization (Photos 17–31). This assemblage defines the onset of the late, likely high-temperature, Cu-rich replacement. It is dominated by Fe-rich sphalerite characteristically associated with Cu, As, and Ag-bearing sulphides, including chalcopyrite as well tennantite with minor amounts of inherited (?) galena, pyrite, stromeyerite, and proustite (all in grains of 20–100 µm). Textures of this assemblage are mainly interlocked with complex intergrowths of these fine-grained minerals. There are local bands of intergrown fine-grained (2–5 µm) chalcopyrite, sphalerite, tennantite, and stromeyerite. They sometimes define conduits or flow paths with concentrically arranged crystals of Cu-Fe-bearing sulphides within the sphalerite. Franklin (2009) reports boulangerite, probably associated to this event. The proportion of pyrite in this assemblage is strikingly low and is only abundant in the interphase with the footwall pyrite + chalcopyrite assemblage.

The proportion of chalcopyrite increases gradually to the almost complete replacement of the sphalerite and later of the other sulphides, forming Assemblage D, a second Cu-rich assemblage product of the final replacement of the Zn-rich Assemblage B, and the intermediate polymetallic Assemblage C. This copper-rich ore includes two associations, a chalcopyrite-rich one and a bornite-rich one with unknown relationships between them — but they seem to be coetaneous. The first assemblage is made up of almost massive

chalcopyrite (30 μm –1 mm) with only minor inclusions (<10 μm) of tennantite, sphalerite, galena, and stromeyerite. Despite this profuse replacement, there is little chalcopyrite disease in the sphalerite.

Pyrite is not abundant in this assemblage and occurs as an early accessory, likely inherited, phase. The galena (20–60 μm) has a rather erratic location. It is associated with the sphalerite I as inclusions in the chalcopyrite or as a late phase crosscutting everything with fine-grained pyrite. It contains inclusions of, and can be partly replaced by, tennantite.

The bornite-rich assemblage has not been described in previous reports and its distribution is unknown. However, it is included in more than 15% of the studied samples. The assemblage includes Fe-rich sphalerite II and bornite (40 μm –3mm) with tennantite (10–100 μm), stromeyerite, proustite (30–150 μm), pyrite, chalcopyrite (20–40 μm), and galena (50–300 μm). Locally, there are complex concentric growths of sphalerite-tennantite-bornite-chalcopyrite that are interpreted as hydrothermal conduits formed synchronously with the replacement. Interestingly, the sphalerite has minute inclusions of possible chalcocite (2–4 μm). As discussed below, the presence of both hypogene chalcocite and bornite could represent a high sulphidation assemblage similar to that described in La Plata (Chiaradia and Fontboté 2000).

The disseminated ore has a mineralogy similar to that of the sphalerite + chalcopyrite ore, with the sulphides and barite replacing the hydrothermally altered host rock. Here, there is an early framboidal pyrite replaced by sphalerite I, galena, and pyrite and later Fe-rich sphalerite, chalcopyrite, and tennantite in a sequence similar to that of Assemblage C. Most of the ‘fragments’ are made up of almost massive chalcopyrite with tennantite.

Chalcopyrite stained to an unusual purplish-blue colour has been reported — EPMA analysis suggests that this unusual chalcopyrite contains 2.2 wt% - 3.7 wt% Br. Our study has found no chalcopyrite with these features.

The barite forms blade-like aggregates or massive euhedral aggregates with interstitial sulphides (Assemblage E) that are gradually replaced by them, mostly sphalerite and galena (Assemblage B). Hydrothermal quartz and carbonates are uncommon within the massive sulphides, but sometimes form almost monomineral aggregates. Sericite, clays, and anhydrite are rare.

Whole-rock analyses of the intervals where the samples were taken show that Assemblages C and D carry most of the gold and silver. The content in precious metals is small in the pyrite + chalcopyrite ore (Assemblage A) and the Zn-rich ore (Assemblage B).

Some of the studied samples of Assemblage C are enriched in Ag, with up to 769 g/t. Preliminary reports suggest that the tennantite, bornite, and galena are relatively Ag-poor (<0.5% Ag), but these contents could account for the observed ore grades. The SIMS data of Lavigne and McMonnies (2011) reveal that, of the studied minerals, bornite and tennantite have the highest Ag contents (3,000–3,500 g/t). This means that only samples containing more than 20% of these minerals could have the recorded high Ag grades (>700 g/t), which seldom occurs. Therefore, the most likely interpretation is that there are other major but undetected silver carriers. Our results indicate that this could be the stromeyerite (CuAgS) and proustite (Ag₃AsS₃) (which are rather abundant in Assemblage C) or any other undetected silver sulphosalts. Again, more analyses are needed to clarify this critical issue.

Despite the high gold grades in these rocks, no free gold is noted in our study. This may be due to non-representative sampling, a high nugget effect, or that the gold is invisible and occurs as minute inclusions (<1 µm) or solid solution in some phases. Schandl (2009) has found free gold within the sphalerite + chalcopyrite mineralization (Assemblage C?), where it occurs as minute (5 µm–50 µm) inclusions in sphalerite and in fractures generated synchronously with the replacement by chalcopyrite. Small gold grains also occur in the rim of some galena crystals or intergrown with chalcopyrite. Two small grains of gold were also identified in a late carbonate veinlet that crosscuts the sphalerite.

The SIMS data (Lavigne and McMonnies 2011) suggest that around 61% of the gold occurs as free grains, as electrum (Au₈₈Ag₁₂ - Au₉₈Ag₂). The remaining gold is interpreted as being invisible, in 0.1–0.2 µm sized grains mainly hosted by the pyrite. However, there is a strong relationship of the gold contents with the pyrite-poor sphalerite-chalcopyrite ore rich in tennantite, whereas there is almost no gold in the pyrite-rich samples. Again, the good correlation with the As suggests that it could be related with the tennantite, but more specific analyses are needed.

On the whole, the mineralization shows pristine evidence of a large ore-refining process as defined by Large (1992), with the gradual replacement of the assemblages formed at low temperature, or due to fluid mixing (barite + sphalerite) in the external zone of the ore-forming system, by others that precipitate at higher temperatures or higher deep/shallow fluid

ratios, like the copper sulphides. This forms well-defined ore zoning that is described elsewhere in volcanogenic massive sulphides (Large 1992; Lydon 1988a; Lydon 1988b). It is worth noting that these refining processes can occur in any style of VMS mineralization regardless of their exhalative or replacive origin (Tornos et al. in press).

These ore minerals show rather primitive and immature textures, with large variations in grain size and abundant early/diagenetic textures, which is consistent with the low degree of deformation/metamorphism. However, and probably related to the specific environment of formation (by replacement), the ores are relatively coarse-grained. The grain size is very irregular and the sulphides show complex and intricate intergrowths, especially in Assemblage C. It is possible to distinguish abundant primary textures. The sulphides include in-situ brecciated zones that could have formed by hydrothermal overpressure, by inheritance from the replaced rocks or, as noted by Franklin (2009), by some form of collapse related to anhydrite dissolution. The three types of formation probably coexist, in fact. There are also some conduits with rings of chalcopyrite or tennantite with inward-growing crystals and a sphalerite-filled internal cavity. These structures are similar to the conduit zones reported by Tesalina et al. (1998) and Herrington et al. (1998) in the fossil VMS deposits of the Urals. Some have been attributed to tubeworms, but our study has found no evidence of biogenic activity.

The relatively low Sb, Hg, and Bi contents when compared to As are rather uncommon in these systems. Tennantite is widespread in the deposit, especially in the replacement zone of the Zn-rich Assemblage B by the Cu-rich Assemblage D. The As-Ag-Au association is mainly located in the transition zones between Assemblages B and D, where copper mineralization gradually replaced Zn-Pb mineralization. Despite the replacement of sphalerite by chalcopyrite, this replacement is fairly common in massive sulphides elsewhere, there is little evidence of its association with the input of As-Ag-Au in the system.

The Fe-poor sphalerite is highly enriched in Cd, which could affect the concentrate either positively or negatively. Previous analyses suggest that the ore is poor in Ga and In.

Covellite is fairly abundant in the surface exposures, where it occurs as veins or rimming sphalerite, pyrite, and chalcopyrite. It has not been observed in the drillcore samples, indicating that it is a late and supergene phase, not primary as described in La Plata by Chiaradia et al. (2008). Marcasite, goethite, chalcocite, and chalcocyanite have also been observed as supergene phases.

METALLURGICAL IMPLICATIONS

The petrographic study suggests some general guidelines on the geometallurgy of the El Domo deposit.

The lower Cu-rich zone should show textures and grain sizes that would allow for significantly better liberation than in many other massive sulphides that yield economic recoveries. The Upper Polymetallic Ore may be more difficult to liberate. Although the iron-poor, sphalerite-rich Assemblage B and the copper-rich Assemblage D are coarse-grained and have textures that suggest easy liberation, Assemblage C is more complex. In this assemblage, the different sulphides are fine-grained (up to 20 µm) and intergrown. However, the proportion of this assemblage in the whole deposit is likely rather low.

Most of the silver and gold seem to be related to the early stages of these latter copper-rich assemblages near the contact with the earlier sphalerite. Both precious metals seem to be spatially related with the tennantite-rich rocks, suggesting that the concentrate carrying the precious metals will contain arsenic.

The studied samples do not show any mineralogical modifications of the sulphides that could be due to long-term storage. Furthermore, the supergene alteration is restricted to the mineralization cropping out at the surface.

8. DEPOSIT TYPES

Most of the economic metallic mineralization at El Domo occurs as stratabound massive sulphides. However, other mineralization styles have been identified in the project area, including:

1. A stockwork zone hosted by the Lower Felsic Unit and beneath the massive sulphides, with veins and disseminations of pyrite, chalcopyrite, and sphalerite. Except in minor places (e.g. close to the immediate footwall of the massive sulphides), this mineralization is of low grade and tonnage.
2. Stratabound massive sulphides in the contact between the Lower Felsic Unit and the Polymictic Volcaniclastic Breccia (Main Ore Zone). It includes more than 90% of the indicated and inferred sources and more than 90% of the total metal content.
3. Semi-massive to disseminated ore as stratabound lenses within the Polymictic Volcaniclastic Breccia. Despite its relatively high grade (0.92% Cu, 1% Zn, 1.1 g/t Au, 0.12% Pb, and 28 g/t Ag), this type of mineralization is only a small part (<4%) of the total tonnage.
4. Possible fossil fault scarp collapse breccias with transported massive sulphide blocks, perhaps located near the hanging wall of the Volcaniclastic Polymictic Breccia (El Gallo).
5. Local remobilization along faults — with local high grades in Zn-Cu and precious metals. These orebodies are small and of no interest for bulk mining. They include dismembered massive sulphide boulders, commonly located at the contacts of the andesite stocks and dykes (Sesmo).
6. Hydrothermal quartz-rich breccias with gold, silver sulphosalts, chalcopyrite, galena, sphalerite, barite, and elevated concentrations of antimony, arsenic, bismuth, and mercury (Caracol).
7. Disseminated chalcopyrite (porphyry-like mineralization?) in granodiorite intrusive stocks.

The main mineralization at El Domo shares most of the features of classic volcanic-hosted massive sulphide deposits (Franklin et al. 2005; Franklin et al. 1981; Large 1992; Large et al. 2001; Lydon 1996; Lydon 1988a; Lydon 1988b). Key diagnostic features of this style of mineralization include the spatial and chronologic relationship with submarine felsic/mafic volcanism, an underlying stockwork or feeder zone related to major hydrothermal alteration (usually more prominent in the footwall than in the hanging wall), and massive or semi-

massive ore formed on or near the seafloor, usually rich in pyrite and economic grades of Cu, Zn and Pb, as well as Au and Ag. VMS deposits are major sources of Zn, Cu, Pb, Ag, and Au, and significant sources for Co, Sn, Se, In, Bi, Te, Tl, Ga, and Ge. There are over 800 VMS deposits known worldwide, up to 56 of which are considered world class (>32 Mt). Most are grouped into a few provinces of Archean to Present age: the Abitibi Belt, Bathurst District, Urals, Skellefte, Iberian Pyrite Belt, and Tasmania (Large and Blundell 2000). As discussed below, the Mesozoic–Cenozoic Andean Belt is now considered a major province. Most of these deposits formed in extensional-transpressional tectonic settings, including both oceanic seafloor spreading and arc environments. Most ancient VMS deposits still preserved in the geological record formed mainly in oceanic and continental nascent-arc, rifted-arc, and back-arc settings. The crustal composition exerts a major control on the ore contents of VMS deposits, with Cu-Au-(Zn) deposits forming mainly on the primitive crust and Zn-Cu-Pb-Ag deposits on continental crust (Barrie and Hannington 1999). The immediate host rock and the depositional environment play a critical role in the style of mineralization (Tornos et al. in press). Most VMS provinces form in extensional settings such as volcanic calderas or pull-apart basins, which favour the focused upflow of melts and fluids, the formation of domes and glass-rich mass flows, and establish anoxic bottoms.

At El Domo, the mineral assemblage and the ore grades indicate that it is a classic polymetallic, Au-rich deposit. However, its classification based on the host-rock composition is not straightforward. This is mainly due to the unusual volcanic setting, with felsic domes in an overall mafic sequence and few siliciclastic rocks. The Zn:Cu:Pb ratios, high Au-Ag contents, immediate geological setting, and Pb-isotope ratios (Chiaradia and Fontboté 2001) suggest it belongs to the bimodal felsic style of mineralization of Barrie and Hannington (1999), with the best-known examples found in the Hokuroko basin and the Cambrian deposits in Tasmania. These sequences are characterized by bimodal sequences with a scant proportion of fine-grained siliciclastic rocks. They are typical of island intra-arc settings with a paucity of sediments. Although the sequence is largely mafic with only a few felsic volcanic rocks, the clear relationship of the orebodies with felsic volcanic rocks suggests that they belong to the bimodal felsic group. Pratt (2008) was the first to document and describe the Kuroko-type VMS environment in the Curipamba concessions.

However, the general geological environment (formed in an immature intra-island arc setting) and the dominance of mafic juvenile rocks suggest it could belong to the bimodal-mafic-type. Nevertheless, in detail, the mineralization includes different pre-zones and mineral assemblages as described below.

An important feature at El Domo is that it is a virtually undisturbed ore system with little recrystallization, metamorphism, and deformation. This is rather uncommon in VMS deposits and only certain deposits in Turkey, Japan, Peru and, obviously, present-day systems are so pristine.

STYLE OF MINERALIZATION

The volcanogenic massive sulphides occur in specific geological environments where they can accumulate and be preserved. Recent studies have shown that the largest VMS deposits formed as replacements of volcanic or volcanoclastic rocks below the seafloor, with exhalative ones less common in the geological record (Tornos et al. in press). The Curipamba massive sulphides have been interpreted by Franklin (2009) as having formed at least partially in submarine mounds, similar to those found currently in the oceanic floor, including a massive mound and a brecciated apron. However, other studies emphasize that most, if not all, of the Curipamba massive sulphides formed by replacement of volcanoclastic rocks, mainly the highly permeable and reactive Polymictic Volcanoclastic Breccia at the contact with the underlying Footwall Rhyodacite (Pratt 2008; Vallejo 2013). As Pratt (2008) states, there is little evidence of the formation of chimneys, sedimentary mound breccias, or sulphide-rich sediments.

The main arguments for the exhalative genesis include the location on seafloor depressions (Pratt 2008), a possible exhalite zone, breccia zones related with anhydrite dissolution, and centimetre-sized tubes interpreted as tubeworm relicts within the massive sulphides (Pratt 2008). However, our interpretation is that they are hydrothermal conduits similar to those described by Herrington et al. (1998) in the VMS deposits of the Urals.

No structures evidencing exhalation on the seafloor have been found. Most of the massive sulphides seem to have formed by the stratabound replacement of the Polymictic Volcanoclastic Breccia, especially of the fine-grained mafic glass-rich units. The sulphides preferentially replaced the glass-rich groundmass of the breccia and, later, the larger clasts gave rise to semi-massive to massive sulphides sometimes having gradual but narrow contacts with the altered breccia. Most of the transported clasts described by Pratt (2008) are here interpreted as small aggregates of replacement massive sulphides. They are larger than adjacent clasts and some are zoned, with an internal zone of pyrite and an external one of chalcopyrite. They always have irregular and sometimes amoeboidal contacts incompatible with erosion and transport in an aqueous setting. Some of these pseudoclasts are also a

product of the selective replacement of breccia fragments — some inheriting a core of highly altered volcanic rock surrounded by the sulphides.

Several pieces of evidence indicate that the replacement took place during early diagenesis, before compaction and synchronously with the devitrification of the glass. They include the selective replacement of perlite and the mimic replacement of glass fragments by sulphides. However, the massive sulphides show only subtle structures, mostly remnants of breccias and banding interpreted here as inherited from the protolith. No sedimentary banding or brecciation has been found, which is probably related with the hydrothermal refining.

A rather continuous chert layer above the main lens of massive sulphides probably marks a zone of steep thermal gradients and major fluid mixing of the hydrothermal fluid and seawater. This zone, prograding with the hydrothermal system, could prevent oxidation during the late influx of cold and oxidizing seawater in the waning states of hydrothermal activity. This horizon has been interpreted as an exhalite deposited on the seafloor; however, the contacts are also replacive and likely correspond to a level of extensive silicification.

The massive sulphides are enclosed in an aureole of hydrothermal alteration. These rocks include disseminated as well as semi-massive sulphides, always including an aureole of hydrothermal alteration. Despite being a rock that is usually host to replacement massive sulphides elsewhere, the Crystal-Rich Volcaniclastic Breccia is barren and lacks ore-related hydrothermal alteration, indicating it was deposited after the ore-forming event. Furthermore, fragments of massive sulphides in rocks attributed to the uppermost Polymictic Volcaniclastic Breccia suggest that the deposit formed at shallow depths and was partially eroded before the deposition of the Crystal-Rich Volcaniclastic Breccia, probably in relationship with a fault scarp. These true massive sulphide boulders can be distinguished from the replacement pseudo-fragments by their irregular size and composition, irregularly oriented internal layering, neat and rounded edges, and lack of hydrothermal alteration of the host rocks. However, they are small in proportion and their stratigraphic location is dubious.

To our knowledge, there are few, if any, similar VMS deposits to those of the Macuchi Group. Although the location above felsic domes is a rather common feature in most major districts (e.g. the Hokuroko province, the Iberian Pyrite Belt, the Bergslagen district, and the Noranda camp), at none of these sites did the mineralization replace mafic glass-rich sequences. The mineralization is hosted either by shale, by pumice-rich rocks capping the domes, or as stratabound bodies between individual flows or volcaniclastic rocks. In this respect, the

Curipamba Group is rather unique, only sharing certain similarities with the broadly coeval deposits of Peru.

ORE-FORMING PROCESS

Most, if not all, massive sulphide deposits form when the deep, acidic, and reduced hydrothermal fluids carrying the metals mix with cold, alkaline, and oxidized, perhaps slightly modified, seawater. This process quickly destabilizes the metal-carrying chloride complexes and, if there is enough reduced sulphur available, precipitates the massive sulphides. The ore-forming process at Curipamba was probably equivalent to the hydrothermal fluids upflowing along the stockwork zone and mixing with seawater in the aquifer defined by the Polymictic Volcaniclastic Breccia. This induced the hydrothermal alteration and the irregular but stratabound replacement of selected breccia layers by the massive sulphides. An external aureole of barite suggests that the water within the aquifer was only slightly modified and oxidized seawater. The origin of the sulfur is unknown, but the evolution of the system suggests it did not derive from the biogenic reduction of seawater but was transported by hydrothermal fluids. Again, the presence of barite suggests that the sea bottom was oxic and not euxinic, which is where sulphate-reducing bacteria live.

ZONE REFINING

One of the most significant features of the El Domo deposit is well-marked lateral and vertical ore zoning in the massive sulphide lens, with a pyrite-Cu-rich stockwork, a lower pyrite-chalcopyrite zone, an upper Cu-Zn-Au-Ag zone, and a cap of barite ± sphalerite. This zoning is similar to that found elsewhere (Large 1977), and is interpreted as related with the maturation of the hydrothermal systems and the metal solubility. The early precipitation of sphalerite, galena, and barite takes place in the early stages of mineralization by rapid cooling in the fluid-mixing zone. Further input of hot hydrothermal fluids displaces the Zn-Pb-barite zone outwards by dissolution and still more distal reprecipitation of the Zn and Pb, which are replaced by chalcopyrite and pyrite, yielding a Cu core with a Zn-Pb external zone.

INVOLVEMENT OF MAGMATIC FLUIDS

Most volcanogenic massive sulphide deposits in spreading centres form by the circulation of heated seawater (Nehlig 1991). However, in intra- and back-arc basins, seawater can be accompanied by significant amounts of fluids exsolved from underlying crystallizing subvolcanic intrusions. These late fluids are abnormally enriched in Cu and Au as well as in other trace metals such as As, Te, Hg, and Sb (de Ronde 1995; Hannington et al. 1986; Sillitoe 1996), along with magmatic gas. Therefore, VMS deposits related with magmatic-

hydrothermal systems can be of greater economic interest than those related to seawater convection.

Along with the isotope geochemistry and the fluid inclusion data, the presence of high-sulphidation assemblages, including enargite, bornite, or hypogene covellite, and of argillic or advanced argillic assemblages, are criteria for defining these magmatic hydrothermal systems.

At La Plata, Chiaradia and Fontboté (2000) and Chiaradia et al. (2008) have described assemblages with bornite, digenite, and covellite that they interpret (along with the high Au contents) as indicative of formation in a magmatic-hydrothermal system. At El Domo, however, the criteria are not so straightforward. The assemblage includes iron-poor sphalerite, abundant bornite, and perhaps some enargite (uncommon minerals in seawater-recharged VMS systems), but a lack of covellite and chalcocite of hypogene origin. Furthermore, the hydrothermally altered rocks lack hypogene kaolinite, alunite, and jarosite. More detailed studies are needed to determine whether Curipamba is a high-sulphidation system.

A BOILING SYSTEM?

The reports of Franklin (2009) and Lavigne and McMonnies (2011) note that the El Domo system was boiling, at or near the seafloor, during ore deposition. Boiling would favour the separation of gold into the gaseous phase and its precipitation, as well as that of antimony, arsenic, and mercury, and could explain the high bromine contents observed in some of the chalcopyrite. However, our study has found no clear evidence of fluid boiling. The mechanism invoked by these reports is usually associated with advanced argillic alteration — not described at El Domo — and would imply the separation of this suite of metals from that of the base metals and barite.

GENETIC MODEL

Available geological data suggest that the El Domo deposit formed in somewhat similar conditions to those of many VMS deposits developing in active island-arc systems. As mentioned above, what is new and different at El Domo is the combination of a magmatic-hydrothermal system and the replacement of juvenile volcanoclastic rocks.

The Curipamba area includes volcanic and volcanoclastic mafic rocks of Paleocene–Eocene age (Macuchi Group) that both limit and fill a third-order basin. Thick units of volcanoclastic

rocks above the Lower Felsic Unit suggest that the mineralization formed synchronously with a topographic depression. The mineralized zone comprises areas of flat-lying strata bounded by steep NNE-SSW to NE-SW striking faults that define extensional structures within a major N-S trending kilometre-sized pull-apart structure (Figure 7.6). The ore-forming event was synchronous with widespread extension, which favoured bimodal magmatism, high heat flow, and basin compartmentalization synchronous with major erosion of the adjacent blocks. Some of the Polymictic Breccia fragments reflect a distal origin and probably come from those uplifted and eroded blocks.

The formation of these large basins could be related to the NE to E subduction of the Farallon-Nazca Plate beneath the South American Plate; here, the Macuchi arc sequence experienced clockwise rotation, which probably induced pulsatile dextral strike-slip movements along NNE-SSW faults (Buckle 2009). Although some of the volcanic and volcanoclastic rocks might well have been deposited in a subsiding caldera, there are no definitive arguments for its existence.

An increase in the heat flow and interaction in the middle to upper crust of the deep juvenile melts with a continental crust formed small batches of calc-alkaline melts that ascended through the strike-slip tensional structures along with larger amounts of more primitive, basalt to andesite, magmas. The number and volume of these dacite and rhyolite rocks is relatively small throughout the entire Macuchi arc, but they are invariably associated with the volcanogenic massive sulphide deposits, showing a direct link between the two.

Crystallization of the rhyodacite domes at sub-volcanic depths promoted fluid saturation and exsolution of magmatic-hydrothermal fluids that ascended overpressured along the tensional structures and promoted the formation of irregularly distributed hydrothermal breccias due to hydrofracturing. Cooling of these hot fluids promoted acidification and reaction with the host rocks at high fluid/rock ratios and induced the precipitation of quartz and sulphides in the veins and the widespread sericitic alteration in the Lower Felsic Unit. The formation of the breccia zones is not exclusive of submarine mounds; they can grow by the input of overpressured upflowing fluids that crack and seal the hydrothermally altered rocks.

Synchronously, the already crystallized upper part of the dome was covered by different mass flows, suggesting vigorous volcanic activity in the area synchronous with active faulting. The deposits covering the rhyodacite dome include mafic-dominated mass flow deposits as a result of the erosion of loose pyroclastic rocks (Polymictic Volcanoclastic Unit)

overlain by more acid, crystal-rich ones (Crystal-Rich Volcaniclastic Unit). While the former seems to represent a mass flow deposit related with a fault scarp, the latter seems to be several submarine (reworked?) pyroclastic flows with interbedded fine-grained sediments deposited between these flows. The emplacement of these mass flows was accompanied by the intrusion of shallow basaltic sills. In such an active system, it is very unlikely that exhalative massive sulphides could form and be preserved.

Upon reaching the contact of the rhyodacite with the overlying Polymictic Volcaniclastic Breccia, the hydraulic regime changed, and the hot and acid deep fluids carrying the metals and sulphur mixed with the alkaline, cool, oxidized seawater saturating the permeable, reactive glass-rich rocks of the Polymictic Volcaniclastic Breccia. This led to quick alkalinization and cooling, which produced the hydrothermal alteration and precipitation of the sulphides (Figure 8.1).

The main aquifer, that is, the contact between the two lithologies, was replaced by the major massive sulphide lens, whereas the less permeable rocks were irregularly replaced by the hydrothermal assemblages and ore. The system was controlled by an abundance of mafic glass and the more permeable rocks, which were probably the fine-grained volcaniclastic breccias despite the entire sequence being affected by the alteration. Upflowing hydrothermal fluids in the stratabound aquifer(s) gradually displaced seawater, promoting the growth of the orebody by fluid mixing and the replacement of the early low-temperature assemblages (marking the contact between the two fluids, barite, sphalerite and galena) by the high-temperature assemblage and precipitation at higher fluid/rock ratios, dominated by pyrite and chalcopyrite (hydrothermal refining).

The contact zone between these two ore assemblages is an area of major geochemical changes where most of the gold, arsenic, and silver precipitated. The massive sulphides are irregularly capped by a silica layer that likely reflects mixing of the exhausted deep fluids with cool seawater. The lateral zones of the orebody and stockwork zone, where heated seawater entered the system, were favoured sites for the precipitation of sulphide-poor anhydrite. The waning stages of the system also enhanced seawater intrusion into the hot rhyodacite, promoting widespread anhydrite precipitation, later replaced by gypsum. As Franklin (2009) has suggested, mapping the calcium sulphates should easily reflect the size and morphology of the hydrothermal system. The distribution of the Cu- and Zn-rich ores also reflects the location of the feeder zone. The fact that the eastern part of the orebody (below the andesite dome) has the higher Cu grades suggests that this was at least one of the feeder zones.

Both the hydrothermal fluids and the melts that produced the later andesite dome were probably channelized along the same NNE-SSW structures.

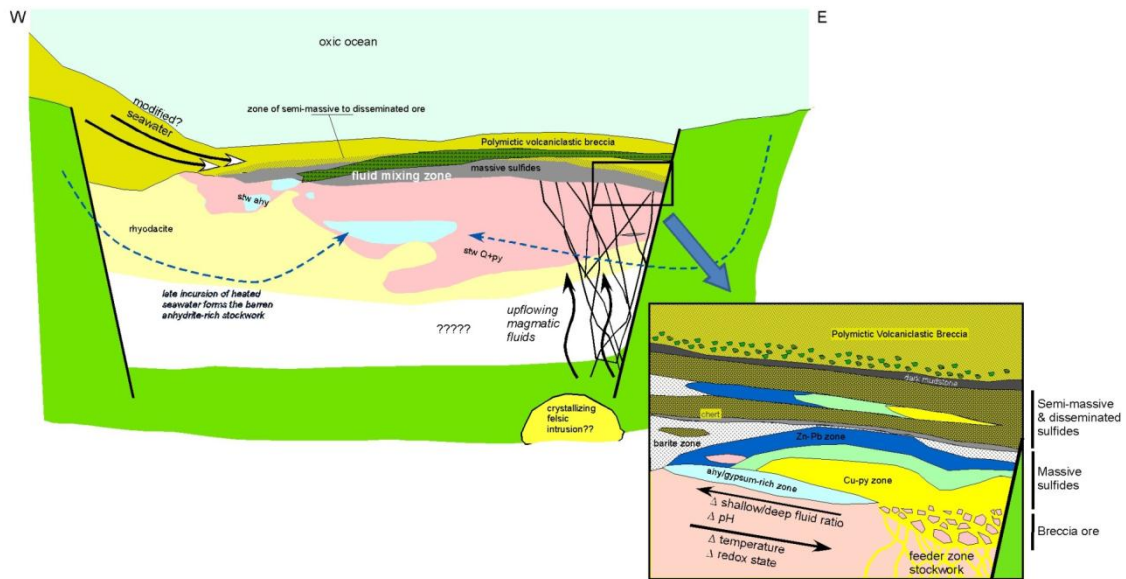


FIGURE 8.1 GENETIC MODEL FOR MASSIVE SULPHIDE AT CURIPAMBA. THE SKETCH SHOWS THE ZONE BEFORE INTRUSION OF THE LATE ANDESITE AND RHYOLITE.

The fact that the rhyodacite dome was covered by the volcanoclastic sediments before the ore deposition suggests that all these processes took place within a short time span, probably less than several thousand years. Although vigorous, the hydrothermal system also formed and finished rather quickly since the uppermost units of the Polymictic Breccia and the overlying Crystal-Rich Breccia Unit lack hydrothermal alteration. Fragments of massive sulphides (Vallejo 2013) that likely represent uplift and quick erosion on the seafloor near a fault scarp are also consistent with very rapid processes in the basin.

Overall, the system reflects high sulphidation-oxidation conditions, as defined by the presence of bornite and low-iron sphalerite and the absence of pyrrhotite accompanied by sulphates. However, these conditions are not as sulphur-rich as those found in high sulphidation systems, in which hypogene chalcocite and covellite are stable. The origin of the deep fluids is unknown, but the ore assemblage (with bornite and rich in As, Au, and Ag) suggests that they were deep magmatic-hydrothermal fluids separated from a crystallizing, deep subvolcanic intrusion that could well be an internal zone of this rhyodacitic dome that achieved fluid saturation and secondary boiling due to crystallization or (less likely) an independent deep intrusion.

The fact that the upper Polymictic Volcaniclastic Breccia and the Crystal-Rich Volcaniclastic Breccia show no or only subtle hydrothermal alteration suggests that the replaced rocks were very close to the seafloor and that the mineralization took place soon after its deposition. As mentioned above, no clear evidence of boiling has been found in this study. This, along with the deposition of the volcaniclastic rocks below seawater level, suggests that the mineralization took place at relatively deep water depths but only under some tens of metres of unconsolidated sediments. The sedimentary structures indicate deposition below storm wave base level and there is no evidence of pyroclastic ash flows that would suggest shallow-marine or subaerial volcanism. Furthermore, the lack of clear evidence of boiling of the hydrothermal fluids suggests that the fluids did not unmix — for the average salinities of magmatic-hydrothermal systems (ca. 10–15 wt% NaCl eq.) at temperatures of circa 300–350°C, this implies depths above 3 km. These figures are meant only as a guideline, and a fluid-inclusion study is needed to confirm these assumptions.

Later cooling of the system or (more likely) cessation of the magmatic-hydrothermal activity promoted the invasion of the system by heated seawater and precipitated large amounts of anhydrite within the most brittle rock, the Lower Felsic Unit. The distribution zones of the calcium sulphates mark the footwall contact of the VMS and the feeder zones.

Late tectonic activity has somewhat disturbed the orebody. The NNE-SSW and NE-SW fault systems that controlled the hydrothermal activity were partially reactivated and acted as channelways for late volcanic activity that led to the formation of late andesitic and rhyolitic (crypto-)domes. These intrusions recrystallized only small amounts of the massive sulphides, but apparently mechanically eroded a significant part of the orebody (Figure 7.5). Due to the contrasting brittle-ductile behaviour, the contact of these domes with the host rocks is the loci of late faulting.

The late intrusions of widespread epizonal granodiorite and tonalite probably formed synchronously with reactivation of these strike-slip faults during a second event that facilitated the emplacement of the intrusions. Late shearing along the NNE-SSW faults partially remobilized the mineralization and focused along the most hydrothermally altered rocks, including those with sericitic alteration or rich in anhydrite/gypsum; there are some detachment faults along sub-horizontal zones rich in calcium sulphates here. In fact, many of these structures are mineralized and host many of the Curipamba area prospects. Similar rocks have been described in the La Plata deposit, where a significant part of the ore occurs as fragments in the NNE-SSW Chimbo-Toachi shear zone (Chiaradia et al. 2008). However,

the rocks at Curipamba appear to be less deformed than at La Plata, where footwall rocks are foliated and the orebody is crosscut by several shear zones (Chiaradia et al. 2008).

MINERAL POTENTIAL

The potential for VMS deposits in Ecuador and specifically in the Curipamba area is high. It is an underexplored region hosting promising environments for the formation of Cu-Zn-Au volcanogenic massive sulphide deposits, including favourable rocks for the formation of large replacive mineralization.

The VMS deposits of Ecuador form part of a large, high-potential (and only recently recognized) belt that extends from Colombia to southern Peru (Sherlock and Logan 2000). Along these 2,000 km, there are abundant intra- and back-arc basins related with oblique tectonics of Cretaceous–Tertiary age that are the loci of several important VMS deposits. The best-known deposits include La Plata, Macuchi, Tambo Grande, Cerro Lindo, Perubar, María Teresa, and several small deposits in Colombia. Although there are not many deposits, they are large, and two of them, Tambo Grande (Winter et al. 2004) and Cerro Lindo, are world-class deposits. The location of these deposits is similar all along the belt. Except for Tambo Grande (interpreted as a mound with underlying replacement), they are found in the contact between rhyodacite domes and mafic volcanic rocks despite variations in the specific location and the style of mineralization from site to site. All these deposits seem to be located in a dominantly tholeiitic sequence in which there are pulses of a few calc-alkaline felsic rocks, with the change from felsic to mafic volcanism being the loci of the ore deposits. These deposits seem to be highly diachronous and range from middle Cretaceous to early Eocene in age. In the deposits of the Casma Group in Peru, the mineralization replaced glassy rhyodacite below impervious mafic rocks.

The Curipamba district shares all the features of the major camps, including the relationship with felsic domes, the abundance of (former) anhydrite in the system, and clear zonation. Furthermore, it appears to be hosted in the largest basin in the area. What makes the area different and interesting is the relationship with clastic and glassy, permeable and reactive, volcanic rocks. In addition, the location in a pull-apart structure in an overall compressive setting favoured channelization of the hydrothermal fluids through well-defined domains and prevented multiple small-scale venting. In fact, these settings are the most favourable for magmatic-hydrothermal activity and are the loci where the largest VMS deposits form (e.g., Iberian Pyrite Belt; Tornos 2006).

The relationship with a magmatic-hydrothermal system provides further interest as VMS deposits forming in relation with the exsolution of magmatic fluids are usually enriched in Cu and Au and can be among the largest and richest massive sulphide deposits (e.g. Eskay Creek and Green Creek).

The ore formation environment is also among the most productive ones, with the mineralization replacing volcanoclastic rocks, which can concentrate the mineralization (if enough sulphur was available) and inhibit further erosion, dispersion, and oxidation. Therefore, BISA agrees with Pratt (2008), Franklin (2009), and Buckle (2009) that there is potential for a giant or world-class deposit of the size of Tambo Grande.

Franklin (2009) has suggested an additional argument for the importance of the Curipamba district. He advocates that the 50–60 km separation between the Curipamba, La Plata, and Macuchi districts is the ideal range for the formation of large convective cells and the formation of large volcanogenic massive sulphide deposits, as has been recorded in the Abitibi Belt. However, this is not always true and the distance between giant deposits is much smaller in the Iberian Pyrite Belt and the Urals; in fact, they are usually clustered. However, comparing the geology of the Macuchi Formation with that of other well-explored camps, it appears that there is excellent potential for large VMS deposits in Ecuador. The presence, at least in the Macuchi Group, of suitable geochemical traps and clear evidence for the formation of magmatic hydrothermal systems in many exposed felsic domes are the best arguments for supporting such a hypothesis.

OTHER VMS DEPOSITS IN ECUADOR

The Macuchi Group hosts several VMS deposits. Apart from El Domo and others nearby, the most significant and best-studied mines are those of La Plata, Macuchi, and Patiño (Figure 7.1 and Figure 8.1). None of them is active, but significant exploration has been carried in recent years, especially in La Plata; although there are several other prospects nearby, no information is available. They have been interpreted as occurring at different levels of the Macuchi sequence (Chiaradia et al. 2008), but no specific studies on the deposit chronology have been performed. Although these deposits are not adjacent to the Curipamba Project, they can provide relevant information on the geological setting, mineralogy, and genesis of the El Domo deposit.

TABLE 8.1 GEOLOGICAL AND ECONOMIC DATA OF THE VMS DEPOSITS OF THE ECUADORIAN ANDES

Name	Geological setting	Size	History	References
Pilas, Cruzacta, Garumales	Cu-Zn-(Pb) stratabound mineralization in highly deformed mafic volcanic rocks and shale of Jurassic age.	Small prospects		Gonzalez (2001); Gonzalez et al. (2006)
La Plata	Stratabound massive sulphides in the contact between felsic and mafic volcanics. Sheared contact between rhyodacite dome and andesite.	0.9 Mt @ 5% Cu, 6.7% Zn, 0.8% Pb, 8 g/t Au, 88 g/t Ag	Historical mine. Mined in the 1970s	Chiaradia and Fontboté (2000, 2008)
Macuchi	Volcaniclastic glass-rich andesitic hyaloclastite.	3.9 Mt @ 0.59% Cu, 1.9 g/t Au, and 7.5 g/t Ag	Worked in the 1940s. Historic production from 1940–1946 of 435,000 tons at 11.7 g/t Au and 4.7% Cu	
Patiño	Most reports include it in Macuchi			
El Domo	Contact between rhyodacite dome and volcaniclastic mafic rocks.		No previous mining	This report

The **La Plata** deposit is located in the Western Cordillera Occidental, near Palo Quemado. It has been studied in detail by Tripodi et al. (2003), Chiaradia et al. (2008). The deposit lies 80 km north of El Domo. The orebody crops out and was known in historical times. Rediscovered in 1946 by Cotopaxi Exploration, the northern orebody was mined by Minera Toachi in the 1970s. The project has been owned by several companies undertaking major exploration that is currently continued by Sultana del Cóndor; this includes abundant drill holes, geophysics, and geochemistry. There are two major orebodies, the already mined northern Henry deposit and the La Plata deposit, where most recent exploration focuses.

The area is covered by thick soil and ash from recent volcanic activity. The La Plata deposit is located in the hinge and eastern limb of a vertical anticline plunging 30°E limited to the east by volcaniclastic rocks and to the west by dark shale. The footwall includes andesite likely overlain by a dacite dome including both coherent and hyaloclastic facies; devitrified facies are common. The orebody occurs as a stratabound lens of semi-massive and massive sulphides up to 10 m thick and less than 150 m in lateral extension. The assemblage

includes pyrite, chalcopyrite, low-iron sphalerite, bornite, and galena. There are trace amounts of tennantite and what Chiaradia et al. (2008) interpret as hypogene covellite and digenite. The gold occurs as free 5–50 µm grains (80–97% Au). The ore minerals are associated to quartz and barite. The deposit shows zonation with a Cu-enriched base overlain by a Zn-rich one, and Chiaradia et al. (2008) describe zonation opposite to that observed at El Domo, with early pyrite-chalcopyrite followed by the Zn-Pb assemblage and late barite. The orebody is enclosed in a hydrothermal aureole (tracked up to 100 m in the hanging wall) with an internal zone of quartz, sericite, and pyrite and an external one of propylitic alteration.

The mineralization is overlain by mudstone and a characteristic layer of red to purple, usually brecciated, hematitic jasper less than 10 m thick interpreted as an exhalite or as a silicified hyaloclastite. Regardless of its origin, the jasper level can be tracked laterally for more than 10 km and used as a guide level. It is overlain by coherent pillow lava basalt and underlain by in-situ and transported hyaloclastite of the same composition.

A key feature of La Plata is large N-S trending sub-vertical shear zones that crosscut the mineralization. These shear zones include fragments of massive sulphides enclosed in a mylonitic groundmass of chlorite and sericite, likely deformed hydrothermally altered dacite. These rocks show a significant increase in Au and local tectonic injection of the massive sulphides.

The system has been dismembered due to late sub-vertical faults. The regional metamorphism is low grade, and there is no noticeable modification of the primary assemblages.

The deposit's geochemistry (Chiaradia et al. 2008) shows that the reduced sulphur could be magmatic in origin or derived from the thermochemical reduction of seawater, whereas the Sr and the sulphur of the barite come from seawater, suggesting that fluid mixing was the ore-forming mechanism. The deposit shares many similarities with El Domo, including the ore assemblage, hydrothermal alteration and, especially, the location above a glassy felsic dome beneath mafic rocks. However, the main difference with El Domo is that at La Plata the mafic rocks and the underlying shale acted as a physical barrier to the hydrothermal fluids. Consequently, the mineralization is confined to the carapace of the dome whereas in El Domo it spread throughout the volcanoclastic sediments. Here, the dominant sulphate is

barite and anhydrite/gypsum has not been reported, suggesting a lower formation temperature.

The Macuchi mine lies 40 km N of Curipamba (in El Tingo, province of Cotopaxi). It includes eight different mineralized areas, two at Macuchi, La Esperanza, Mercedes, and Patiño prospects, and three ore outcrops (Minchoa 1–3). The mine (in the La Esperanza area) was in production between 1940 and 1946, extracting 0.57 Mt at 4.7% Cu, 11.5 g/t Au, and 68 g/t Ag. Largo Resources has quantified 3.9 Mt at 0.59% Cu, 1.9 g/t Au, and 7.5 g/t Ag. Nearby is the Patiño prospect (found by drilling), which shares many of the general area features. Several companies have worked in the area, but little information is available.

Despite being poorly known, the data of DGGM and Chiaradia et al. (2008) show that it is located within volcanoclastic glass-rich andesitic hyaloclastite trending north-south — there are no references to a felsic dome. The orebody includes a lens of semi-massive sulphides (up to 60% sulphides) 125 m long and 8 m thick with pyrite, chalcopyrite, bornite, tennantite and chalcocite, covellite, and digenite. It is not clear whether the latter are hypogene or supergene. The sulphide assemblage is accompanied by significant proportions of barite and quartz; the ore lens is enclosed in an aureole of quartz, sericite, pyrite, chlorite, and barite. The lens is underlain by a Cu-Au-bearing stockwork. There are also N-S trending late faults associated with chloritization.

No other VMS deposits (apart from the Macuchi Group) have been found in Ecuador except in the Cordillera Real (Gonzalez 2001; Gonzalez et al. 2006), where three mines (Pilas, Cruzacta, and Garumales) worked Zn-Cu-(Pb) massive sulphide deposits related to a Jurassic oceanic island arc associated to the earliest events of Andean accretion. The mineralization occurs as stratabound lenses within coherent basalt and volcanoclastic rocks of equivalent composition affected by pervasive quartz-sericite-pyrite alteration. These deposits are interpreted as being of the Besshi or Kuroko type but are located within the major Baños Shear Zone; sulphides and host-altered rocks show widespread evidence of ductile deformation.

9. EXPLORATION

All the information below on exploration in the Curipamba district and nearby areas is based on previous reports cited in Table 9.1. No exploration work has been done by BISA in the preparation of this report.

Modern exploration in the district began in 1991 when Rio Tinto completed a regional stream sediment survey. Since 2007, Salazar exploration has concentrated on the Curipamba South concessions. This block of concessions is further subdivided into the Naves Central and Sesmo Sur areas. The Naves Central area includes the anomalies of Sesmo, Caracol, most of El Domo area, and El Gallo. The Sesmo Sur area covers the Sesmo Sur and La Vaquera anomalies. Geological mapping, prospecting, and soil and stream sediment sampling were followed by geophysical surveys and diamond drilling (Table 9.1).

TABLE 9.1 SUMMARY OF EXPLORATION WORK, SALAZAR RESOURCES LTD. – CURIPAMBA PROJECT

Company	Year	Exploration Work	Description
RTZ Mining PLC Inc.	1991	Regional stream sediment survey	598 stream sediment samples. Cu anomalies found on northern part of property; scattered Au anomalies (21–200 ppb) in southern part of property
Newmont Mining Corporation	2006	BLEG stream sediment survey	225 BLEG samples. Identification of Cu-Au anomalies in northern area and Au-Ag-As-Hg-Mo in southern part of property
Salazar Resources Ltd	2007-2008	Geological reconnaissance, geochemical prospecting, geophysical surveys, and Phase I drilling	Naves Central: 17 line-km IP and Mag Sesmo Sur: 43 line-km IP and Mag Drilling: 51 DDH @ 10,003 m
Dr W. Pratt	2008-2009	Geological mapping and modelling	Geological modelling of the El Domo and Sesmo Sur deposits
Dr J. M. Franklin	2009	Geological reconnaissance and interpretation	
Salazar Resources Ltd	2009-2010	Phase II diamond drilling program	Drilling: 20 DDH @ 3,241.38 m
Scott Wilson RPA	2010	Technical Report on the Curipamba Project (NI 43-101)	Resources: Indicated 623,000 t @ 3.7% Cu, 0.41% Pb, 4.16% Zn, 3.9 g/t Au and 79.5 g/t Ag. Inferred: 2,499,000 t @ 3.24% Cu, 0.37% Pb, 4.28% Zn, 4.3 g/t Au, and 79.6 g/t Ag
Salazar Resources Ltd	2010	Phase III diamond drilling program	Drilling: 84 DDH @ 15,582.85 m
Roscoe Postle Associates Inc. (RPA)	2011	Technical Report on the Curipamba Project (NI 43-101)	Resources: Indicated: 5,530,000 t @ 2.4% Cu, 0.3% Pb, 2.5% Zn, 2.8 g/t Au, and 48.4 g/t Ag. Inferred: 1,460,000 t @ 1.9% Cu, 0.3% Pb, 2.8% Zn, 2.4 g/t Au, and 52.2 g/t Ag
Salazar Resources Ltd	2011-2012	Phase IV diamond drilling program	Drilling: 51 DDH @ 10,248.77 m
Buenaventura Ingenieros S.A. (BISA)	2013	Salazar commissioned BISA for an updated estimate of mineral resources in a NI 43-101 Technical Report, and for a lithological and mineralization 3D model	

The El Domo deposit is the largest but not the only deposit in the Curipamba area — many of the old prospects and anomalies described are currently included in El Domo (e.g. Gallo, Roble, Guayabillo, Roble Este, Roble 1, Cade, Cade Sur, Cade 1, and Caracol 1). Nearby,

there are other prospects of variable interest and abundant geophysical/geochemical anomalies studied in detail by Pratt (2009) (Sesmo Sur) and Buckle (2009). These prospects are grouped in Table 9.2 and their location shown in Figure 7.2 and Figure 9.1.

TABLE 9.2 CURIPAMBA PROSPECTS, OTHERS THAN THE EL DOMO

	Target	Mineralization	Style	Drill holes	Geochemistry	Geophysics
	Whole area			Rock and stream geochemical surveys		
Naves Central Area	El Domo	Cu-Au-Ag-(Zn-Pb)	Volcanogenic massive sulphide	167 drill holes	21 soil geochemistry profiles	21 km IP & magnetometry with significant chargeability and resistivity anomalies
	Sesmo	High Au and Ag. Minor Zn-Pb	Disseminated sulphides in a N55°E fault zone	1 drill hole?		
	Caracol	Zn-Cu-Pb-Au-Ag	Hydrothermal breccias			
Sesmo Sur Area	Sesmo Sur	Au-Ag	Stockwork zone underlying(?) a former VMS system	18 drill holes		76.15 km of magnetometry & 34.7 km of IP
	La Vaquera	Au-Ag-Cu	Silica cap + argillic alteration. Possible porphyry			
	El Zinc	Zn	Small replacement of Polymictic Volcaniclastic Breccia in a stockwork zone?			

Some of these prospects and anomalies (El Gallo) are located along the NNE-SSW faults controlling the location of the basin hosting the El Domo deposit and likely acted as feeder zones (Figure 7.3 and Figure 7.6). These faults have a complex history and include dykes, hydrothermal breccias, and clay-rich fault gauges with fragments of massive sulphide. Pratt (2008) proposed that these fragments and the clay/gypsum within the breccia are remobilized from the massive sulphides and the footwall.

The **Sesmo Sur** target, 6 km SSW of El Domo, is the largest zone with extensive hydrothermal alteration, within an area of 3x3 km; it was studied in detail by Pratt (2008). The Estrella prospect is the largest and best-studied outcrop. The main lithologic units recognized here also belong to the Macuchi island-arc sequence. From bottom to top, a volcanic sequence similar to El Domo has been recognized (Pratt 2008; Franklin 2010):

- a. A (crypto-)dome of autoclastic breccia intruded into andesite along a NE-SW structure. It is interpreted by Pratt (2008) as coeval with the Lower Felsic Unit at El Domo. Hydrothermal brecciation and alteration are widespread.
- b. Stratabound bodies of andesite with widespread brecciation and peperites indicating shallow intrusive to extrusive sub-aqueous emplacement. Hypothetically, it could be the lateral equivalent of the Polymictic Volcaniclastic Unit. Probably related to this unit are

some mafic volcanoclastic rocks described by (Franklin 2010). Likely related to this unit as well are some jasper boulders with sulphides found in the creeks.

- c. Dykes of vacuolar magnetite-rich basalt.
- d. Porphyry dykes of rhyodacite to dacite composition that crosscut the basalt and the andesite and could be equivalent to the late rhyolite at El Domo.
- e. Abundant dykes and epizonal stocks of quartz-diorite striking N50°E; these rocks are late in the sequence and interpreted as being apophysis of the Early to Mid-Miocene Echeandía Batholith.

The dome shows pervasive, widespread hydrothermal alteration that also seems to be controlled by the NNE-SSW structures. There are areas of strong silicification (\pm sericite) with disseminated sphalerite, chalcopyrite, and pyrite crosscut by irregular jigsaw and crackle hydrothermal breccia bodies, with fragments of the host volcanics and reworked fragments of altered rock in a quartz + sericite groundmass. These hydrothermal bodies have disseminated sulphides, clots, and veins of barite and the highest Au grades; the presence of banded textures typical of the epithermal environment indicates that mineralization took place close to the surface. The breccias are restricted to the zone of major hydrothermal alteration and include both jigsaw and crackle breccias. Low-temperature silica with disseminated sulphides occurs either as veins or cement of the hydrothermal breccias or replacing the groundmass of the volcanic breccias. The sulphides seem to be restricted to the upper part of the dome and the overlying volcanoclastic rocks. Pratt (2008) suggests there is vertical zonation where the deep veins are arranged in linear stockworks and have an illite-rich selvage, whereas the shallow ones are sinuous and banded, with barite and high sulphide contents.

Overall, Pratt (2008) and Franklin (2010) interpreted this system as the roots of a feeder or stockwork zone beneath a presumable massive sulphide. In fact, the Sesmo Sur zone lies at a significantly lower elevation than El Domo. While downward displacement would be theoretically possible, the model of these authors suggests that any likely VMS system capping these rocks would have been eroded away.

The zone seems to include other breccia bodies such as those described by Pratt (2008), a sub-horizontal breccia at least 10 m thick with dacite/rhyolite and massive sulphide clasts with pyrite + chalcocite. This breccia is of unknown origin but likely represents a tectonic-hydrothermal breccia similar to that at El Gallo.

Away from the mineralized zone, the rock shows only pervasive chloritization. The basalt sequence is particularly rich in epidote + magnetite + chlorite, likely a product of regional and/or burial metamorphism. These rocks also include some magnetite/hematite stockworks and rare magnetite-matrix breccias. The outcrops show systematic weathering, with only chalcocite and covellite remaining.

Soil, rock, and chip geochemistry has yielded interesting values of up to 58 g/t Au and up to 2,800 g/t Ag, suggesting that the zone is highly prospective. Systematic Induced Polarization (42 km) and magnetometric (55 km) geophysics (Figure 9.1) have mapped large zones of quartz-sericite-pyrite alteration and hydrothermal brecciation, which are clearly distinguishable from the nearby mafic volcanic rocks. However, the 18 drill cores have not shown any significant mineralization. Consequently, it seems that this interpreted stockwork zone is of little interest and efforts should focus on finding possible VMS deposits in depressed blocks or at higher elevations. In any case, the geophysics has delineated some interesting targets. At Sesmo Sur, 3,746 m of drilling in 18 holes has produced up to 12 m @ 2.25 g/t Au and 31 g/t Ag in DDH 1 and 15m @ 2.54 g/t Au and 50 g/t Ag in DDH 05.

Likely related to the quartz-diorite are some small veinlets with molybdenite in the deeper parts of some drill holes. They could be related to an independent and probably younger Cu-Au-Mo porphyry system.

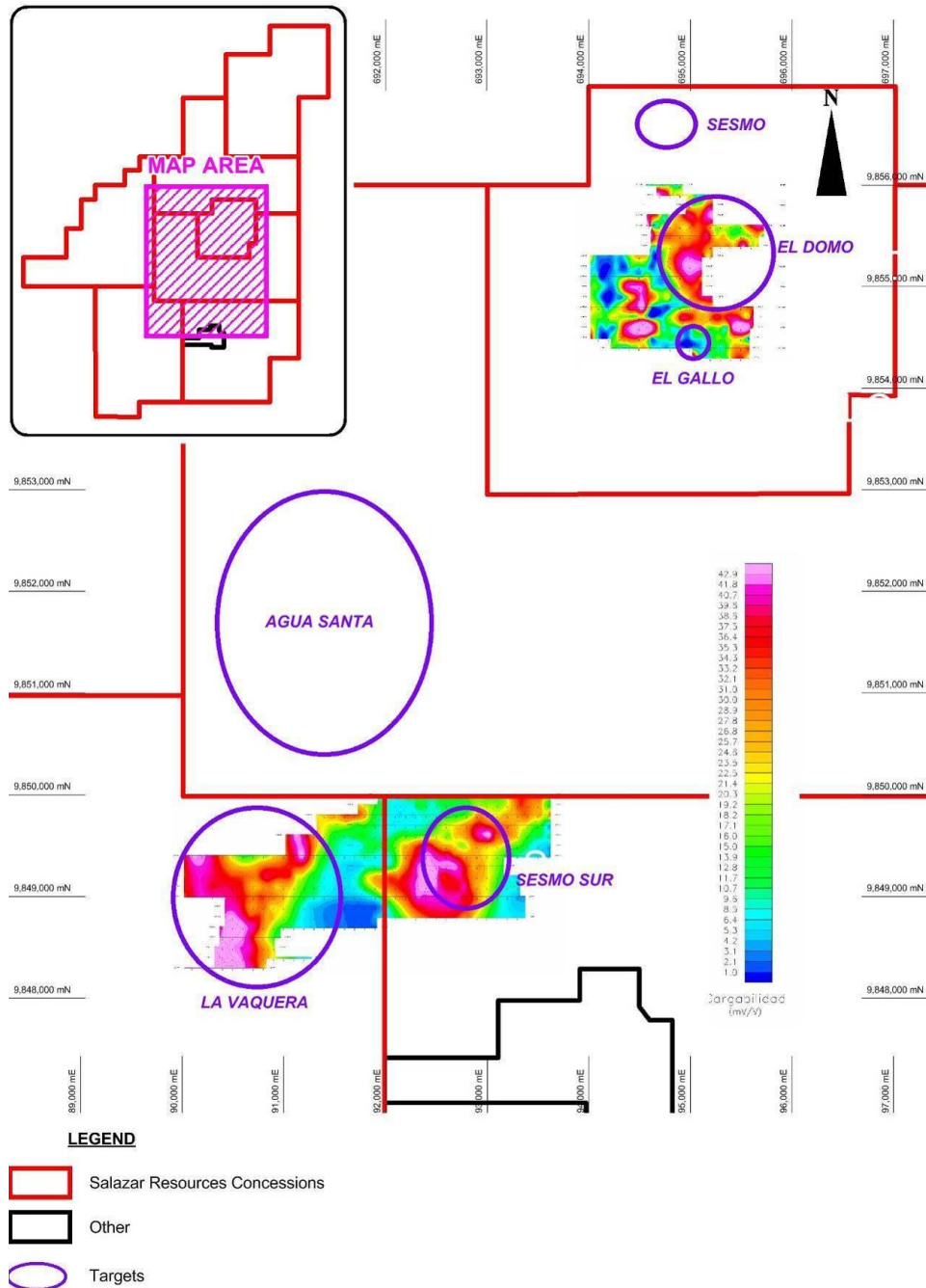


FIGURE 9.1 AREAS WHERE GEOPHYSICAL EXPLORATION HAS BEEN PERFORMED — IP ANOMALIES ARE SHOWN

These prospects are different from conventional VMS deposits, but they have economic potential as high grade–low tonnage deposits. However, and as has been discussed before, the area has potential for the discovery of large VMS deposits — the Curipamba area could host one or more deposits even larger than El Domo. More exploration is needed; in fact, only 17% of the Naves Central Zone has been explored in some detail. Currently, there are

eight untested geophysical anomalies around El Domo, five in the Sesmo Sur-La Vaquera Zone, and four in Barranco Colorado, Agua Santa, La Vaquera, and Coral.

EXPLORATION GUIDES

There are two main types of mineralization on the Curipamba Project. The volcanogenic massive sulphides enriched in Cu-Zn-Au and Ag form the most significant deposit, and a likely polymetallic epithermal mineralization. As described in Chapter 8, there is huge potential in the area and the whole Macuchi terrane for large orebodies of massive sulphides likely exceeding the size of El Domo. Hypothetically, there could also be mineralization related to porphyry copper-like prospects (Franklin 2009), but this seems to be an unattractive target since there appears to be an antithetic relationship between porphyry copper and VMS deposits (Sillitoe 1980); however, this situation could change if the porphyry deposits are interpreted as being genetically unrelated to the VMS systems. Mineralized fault zones at the contacts of the late andesite intrusions are also unattractive targets and it is unlikely they could form a sizeable orebody.

However, the discordant mineralization can include several different types of interesting mineralization that could carry significant amounts of gold (see Chapter 9.1). They comprise the feeder zones of the volcanogenic massive sulphides, the late remobilization of the massive sulphides, and (younger?) epithermal low sulphidation systems. The feeder zones of submarine magmatic-hydrothermal systems could form deposits as important as Pueblo Viejo (Russell et al. 1981) or Madneuli (Migineishvili 2000), both large deposits with high tonnage and economic Cu-Au grades. Discordant precious metal-bearing structure-controlled deposits that could be either the roots of the hydrothermal systems or a product of hydrothermal remobilization can also be economically important. There are reasonable possibilities of finding a small (1–3 Mt) high-grade gold orebody. Hypothetically, it could be similar to the Au-rich structures in the Henty mine in Tasmania (Halley and Roberts 1997; Callaghan 2001). Furthermore, there could be some interesting targets in the stockwork; similar rocks are sometimes enriched in gold despite low sulphide contents. Finally, the epithermal mineralization is typical of subaerial systems and has not been reported in submarine settings. Again, if they prove to be younger, they could be an attractive target for Au-Ag.

Existing information indicates that VMS exploration in Ecuador is in its early stages and most of the area is underexplored. Due to the lack of good, frequent exposures, most of the

deposits are assumed to be buried with only a minimal part exposed. There is plenty of room to hide lenses with volumes greater than 100 x 150 x 10 m near and far from the El Domo deposit. Therefore, the geological definition of targets must be a priority for later geophysical and geochemical studies.

As mentioned above, the main mineralization controls are the location in intra-arc N-S trending basins infilled with Macuchi Group rocks and with NNE-SSW and NE-SW structures. The mineralization always seems to be related to rhyodacitic domes. Consequently, the intersection of these structures with felsic domes should be a preferential target. Although the mineralization at El Domo occurs in the contact with polymictic mafic-rich glassy volcanoclastic units, this is not the only setting where it could form. Hypothetically, volcanogenic massive sulphides could also occur within the rhyodacitic domes, mostly in the glassy carapace or glass-rich flows below a sealing cap or as exhalative deposits in small basins with anoxic fine-grained sediments.

The size of the hydrothermal alteration zones as well as their characteristic mineralogy can be useful for exploration, as reported by Franklin (2009). The replacement of the rhyodacite by a quartz-sericite assemblage implies a drop in the Na₂O content and local Mg enrichment. The presence of anhydrite (an excellent marker of magmatic-hydrothermal systems) can be obscured by its high solubility and can only be useful in drill cores when associated with quartz-sericite assemblages.

Since most of the area is covered by rain forest or thick soil, it is unlikely that all the sub-superficial mineralization and related hydrothermal alteration can be localized by conventional field work. The general targets could well be tested via stream sediments (gold panning can be a very good way of finding deposits), but systematic stream sediment geochemistry is crucial for finding new deposits. Geophysical tests are also key techniques. However, the mineralization is poorly magnetic and the sphalerite is generally poor in iron. Negative magnetometric anomalies can be useful for defining hydrothermal systems and feeder zones. Helicopter-borne Versatile Time-Domain Electromagnetic (VTEM) and similar EM techniques can be useful to find Cu-pyrite-rich ores; targeting the sphalerite-rich zones can be trickier, but again VTEM has given good results in pyrite-poor orebodies. Ground EM and further drilling should be carried out in those areas with the best combination of geology and airborne anomalies.

OTHER DEPOSIT TYPES

Along with the VMS deposit of El Domo and the nearby prospects, the region adjacent to the Curipamba Project includes two other styles of mineralization (Table 9.3) that share features with the porphyry and epithermal styles of mineralization. However, these occurrences are poorly explored and therefore have an unknown but interesting potential. Pratt (2008) described a major granodiorite batholith southwest of the El Domo area that appears to have caused significant contact metamorphism of the host rocks. Sizeable bodies of coarse-grained diorite also occur within the project area, which Franklin (2009) interpreted as the possible subvolcanic roots of the mafic rocks and the sources of heat, metals, or fluids leading to the mineralization. However, and as discussed in the chapter on Regional Geology, they likely postdate the volcanic rocks. Therefore, the porphyry and epithermal deposits could be associated with an independent and younger subaerial magmatic-hydrothermal event unrelated to the VMS formation. The former would include the prospects of Chazo Juan, Telimbela, San Miguel, Torneado, and Yatubi-La Industrial, whereas Alluriquin, Norcay, and Salinas are more epithermal-like prospects. Both styles of mineralization need further studies for their characterization and exploration.

TABLE 9.3 PROSPECTS OTHER THAN VMS NEAR THE CURIPAMBA AREA

Project	Company	Comments
Telimbela (Cu-Mo Porphyry)	ENAMI	Discovered in 1977 by stream sediment geochemistry and geophysics. 8 drill holes crosscut Cu-rich quartz stockwork and hydrothermal breccia in subvolcanic (quartz)-diorite. Explored by Japanese Exploration Group, Ecuagold, and ENAMI. Large potential.
El Torneado (Balzapamba or Santa Lucia) Cu-Mo Porphyry	ENAMI	Cu and Mo anomalies discovered by DGGM and the Japanese Mission in the 1970s. Semi-massive orebody 500 m long and 30 m thick that could be a VMS deposit.
Chazo Juan (Cu-Mo Porphyry)	ENAMI	Cu and Mo anomalies discovered by DGGM and the Japanese Mission in the 1970s.
San Miguel (Cu-Mo Porphyry)	ENAMI	Mineralization and alteration related to copper-molybdenum porphyry with the potential of 500 Mt @ 0.6% Cu. Six large anomalies.
Yatubi-La Industria (Au-Cu Porphyry)	ENAMI	Tourmaline-rich hydrothermal breccias and quartz stockwork in an area of 10 x 5 km resembling a porphyry-like system. Sediment samples up to 0.5 g/t Au (British Mission and Newmont).
Alluriquin (Epithermal Gold Veins)	Junefield Resources Ecuador SA	Gold-rich epithermal veins 0.2–1.5 m thick in a system of at least 5 veins.
Salinas (Epithermal Ag- Au)	ENAMI	Epithermal breccias related to major silicification and acid leaching in an area of 1,000 x 600 metres. Rock sampling averages 0.42 g/t Au and 2.1 oz/t Ag and has high As-Sb-Hg-Ba tenors. Drilling has provided interesting Au-Ag values.
Parcatos		Epithermal breccias and veins rooted in a small porphyry copper with potassic and quartz-sericite alteration. Systematic drilling by RTZ (1990s).
Norcay	IAMGOLD	High-level low-dipping calcite- and Mn-rich epithermal gold swarm veins up to 6 m thick.
Estero Hondo		Alluvial gold deposit worked in the 1990s and now with informal mining. Exploited 60,000 ounces of Au.

10. DRILLING

Salazar completed four drilling campaigns at the Curipamba Project from 2007 to 2012, with 206 diamond drill holes totalling 39,192.64 m (Figure 10.1 and Table 12.1).

TABLE 10.1 DRILLING SUMMARY, SALAZAR RESOURCES LTD — CURIPAMBA PROJECT

Program	ID Drill Hole	No. Holes	Date	Drilled Targets	Metres
I	CURI-07-01 / CURI-08-51	51	2007–2008	Sesmo Sur, El Gallo, Roble 1, El Roble, Roble Este, Cade Sur, Cade 1, Cade, Caracol 1, El Domo	10,003.00
II	CURI-52 / CURI-71	20	2010	El Domo	3,241.38
III	CURI-72 / CURI-155	84	2010–2011	El Domo	15,699.51
IV	CURI-156 / CURI-206	51	2011–2012	El Domo	10,248.75
	TOTAL	206			39,192.64

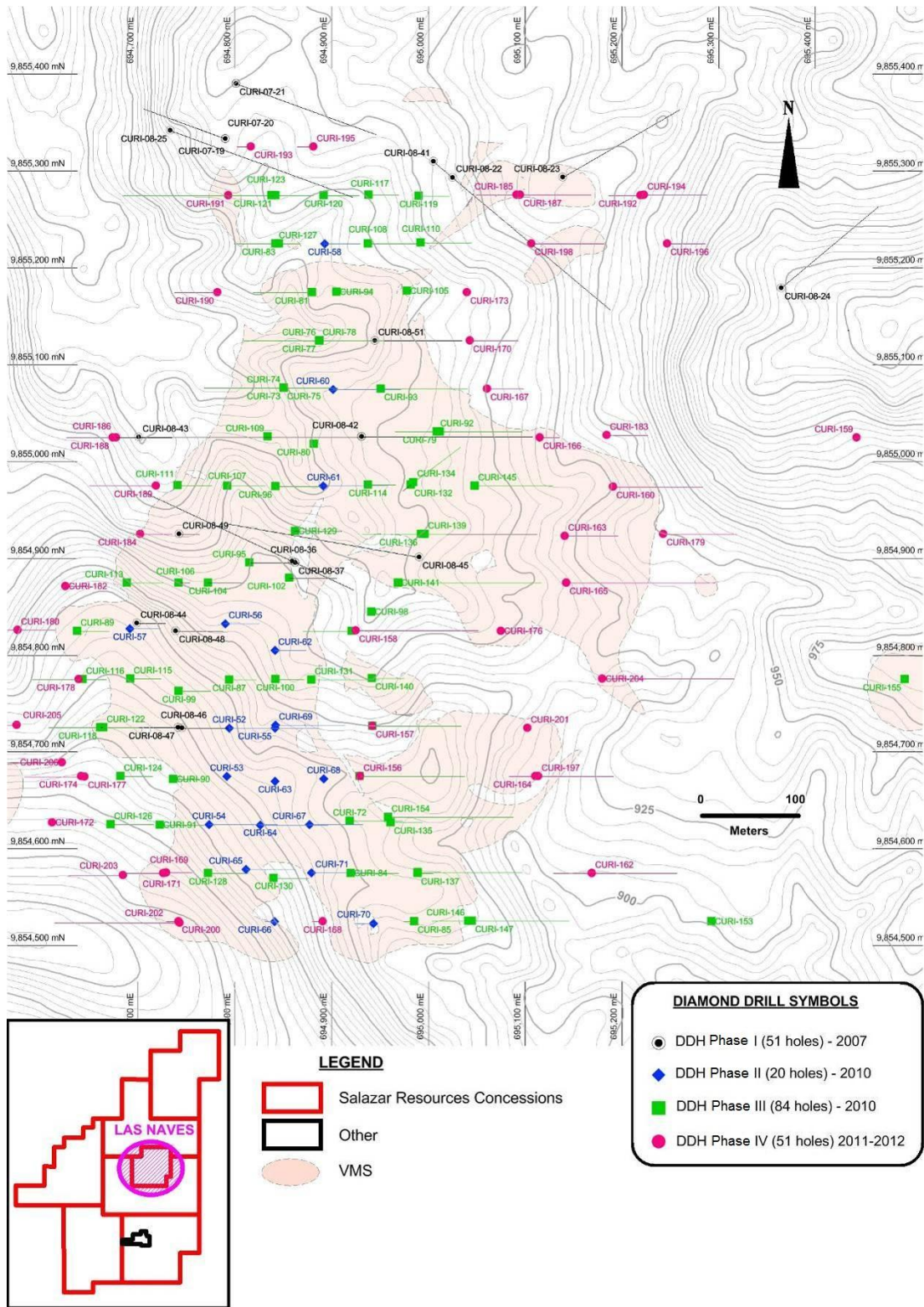


FIGURE 10.1 EL DOMO DRILLING MAP — LAS NAVES AREA

The **Phase I** drilling program at Curipamba began in late 2007 and was contracted to Kluane International Drilling and Perforadores Andesdrill S.A. Both companies used portable

hydraulic diamond drills (namely the Hydracore 2000 and 2004 model) with a depth capacity of 270 m for HQ core (63.5 mm diameter) and 450 m for NQ core (47.6 mm diameter). This initial drill program was completed in 2008 with 51 diamond drill holes (DDH) totalling 10,003 m (see Table 10.1 and Table 10.2). The drilling program tested 11 target areas: Sesmo Sur, El Gallo, El Roble, Roble 1, Roble Este, Cade, Cade 1, Cade Sur, Caracol 1, and El Domo (13 DDH).

TABLE 10.2 PHASE I DRILL HOLES, SALAZAR RESOURCES LTD — CURIPAMBA PROJECT

Prospect	Drill Hole ID	Easting	Northing	Elevation (m)	Azimuth (°)	Dip (°)	Depth (m)
Sesmo Sur	CURI-07-01	692775.45	9849299	412.316	270	-45	217.93
Sesmo Sur	CURI-07-02	692778.99	9849299	412.258	90	-45	141.73
Sesmo Sur	CURI-07-03	692762.03	9849397	405.549	270	-45	167.64
Sesmo Sur	CURI-07-04	692713.46	9849501	433.704	272.7	-46.9	214.88
Sesmo Sur	CURI-07-05	692665.20	9849501	450.273	273	-45	104.85
Sesmo Sur	CURI-07-06	692823.32	9849403	383.256	271.1	-47	208.48
Sesmo Sur	CURI-07-07	692908.36	9849300	436.781	270	-45	254.50
Sesmo Sur	CURI-07-08	692700.59	9849600	462.959	270	-45	185.62
Sesmo Sur	CURI-07-09	692764.51	9849395	406.111	180	-80	131.00
Sesmo Sur	CURI-07-10	692301.51	9849497	508.729	90	-50	295.96
Sesmo Sur	CURI-07-11	692303.97	9849393	485.911	90	-70	159.10
Sesmo Sur	CURI-07-12	692650.94	9849298	411.672	270	-50	272.79
Sesmo Sur	CURI-07-13	692683.79	9849700	506.446	270	-50	298.70
El Gallo	CURI-07-14	695001.35	9854459	928.911	50	-50	185.92
El Gallo	CURI-07-15	695013.28	9854496	930.657	140	-45	94.48
El Gallo	CURI-07-16	695024.03	9854489	924.089	230	-50	102.71
El Gallo	CURI-07-17	695034.13	9854469	922.348	320	-60	107.59
El Gallo	CURI-07-18	695009.76	9854527	939.623	230	-50	107.28
Roble 1	CURI-07-19	695047.96	9855708	908.12	290	-45	126.49
Roble 1	CURI-07-20	695047.65	9855708	908.12	290	-75	123.44
Roble 1	CURI-07-21	695059.81	9855765	902.70	110	-50	239.26
El Roble	CURI-08-22	695283.99	9855668	942.50	130	-50	330.70
El Roble	CURI-08-23	695398.18	9855670	956.75	60	-50	216.40
Roble Est	CURI-08-24	695623.19	9855554	992.75	50	-45	184.40
Roble 1	CURI-08-25	694992.74	9855717	937.23	110	-50	311.20
Sesmo Sur	CURI-07-26	692662.42	9849998	355.46	90	-50	140.50
Sesmo Sur	CURI-08-27	692895.20	9849501	371.78	90	-60	300.50
Sesmo Sur	CURI-08-28	692480.03	9849395	470.43	90	-70	326.70
Roble 1	CURI-08-29	695059.34	9855765	902.70	110	-75	214.27
Cade Sur	CURI-08-30	694654.14	9855120	814.07	120	-50	142.34
Sesmo Sur	CURI-08-31	692575.81	9849699	477.68	270	-50	181.65
Cade Sur	CURI-08-32	694683.24	9855078	819.65	130	-50	195.07
Sesmo Sur	CURI-08-33	692776.7	9849438	399.14	270	-50	143.55

Cade 1	CURI-08-34	694593.28	9855312	773.557	290	-50	110.94
Cade	CURI-08-35	694540.00	9855765	724.30	310	-55	201.16
El Domo	CURI-08-36	695120.08	9855271	948.41	115	-50	103.00
El Domo	CURI-08-37	695119.72	9855271	948.41	115	-75	114.30
Sesmo	CURI-08-38	694426.01	9856069	725.00	305	-50	205.74
El Domo	CURI-08-39	695116.24	9855272	949.06	295	-50	260.60
Caracol 1	CURI-08-40	695160.72	9855970	875.70	290	-50	245.36
El Roble	CURI-08-41	695263.24	9855685	950.70	130	-60	119.65
El Domo	CURI-08-42	695189.32	9855401	970.32	90	-55	308.00
El Domo	CURI-08-43	694959.67	9855400	915.29	90	-50	364.00
El Domo	CURI-08-44	694957.17	9855208	875.24	90	-50	45.20
El Domo	CURI-08-45	695246.95	9855276	975.94	280	-45	285.00
El Domo	CURI-08-46	695003.70	9855100	878.08	90	-60	209.70
El Domo	CURI-08-47	694999.98	9855100	877.19	270	-65	206.70
El Domo	CURI-08-48	694997.13	9855200	880.65	90	-75	188.70
El Domo	CURI-08-49	695000.74	9855300	904.11	90	-80	200.00
El Domo	CURI-08-50	695189.32	9855401	970.32	0	-90	200.00
El Domo	CURI-08-51	695203.60	9855500	974.63	90	-70	207.50
TOTAL PHASE							10,003
I							

The **Phase II** drilling program was carried out from June 4 to September 23 of 2010, with 20 drill holes completed in El Domo area for a total of 3,241.38 m (Table 10.1 and Table 10.3). This drilling aimed to investigate three areas: El Domo, Sesmo Sur, and La Vaquera. The drill hole data up to hole CURI-71 was the basis of the resource estimate completed by Scott Wilson RPA (Valliant et al. 2010).

TABLE 10.3 PHASE II DRILL HOLES, SALAZAR RESOURCES LTD — CURIPAMBA PROJECT

Drill Hole ID	Easting	Northing	Elevation (m)	Azimuth (°)	Dip (°)	Depth (m)
CURI-52	695052.55	9855099.98	895.24	90	-60	171.00
CURI-53	695049.95	9855050.14	896.02	0	-90	173.85
CURI-54	695031.87	9855000.30	887.92	90	-70	206.70
CURI-55	695100.12	9855099.99	910.41	90	-60	89.80
CURI-56	695049.22	9855207.48	905.13	90	-75	134.70
CURI-57	694949.90	9855202.47	871.65	90	-75	121.35
CURI-58	695151.21	9855600.08	941.4	90	-75	140.80
CURI-59	694752.66	9855895.37	958.93	90	-75	140.80
CURI-60	695160.06	9855449.92	960.82	90	-75	203.80
CURI-61	695150.00	9855350.00	903.19	90	-75	254.80
CURI-62	695099.95	9855179.96	910.65	90	-75	122.95
CURI-63	695100.03	9855045.03	904.99	0	-90	161.85
CURI-64	695084.97	9854999.99	891.08	90	-75	203.75

CURI-65	695069.91	9854953.98	906.81	90	-70	149.80
CURI-66	695099.59	9854900.04	925.09	270	-85	121.10
CURI-67	695135.25	9854999.94	936.4	90	-70	161.78
CURI-68	695149.99	9855049.80	910.44	0	-90	134.25
CURI-69	695100.22	9855102.60	937.79	90	-60	143.75
CURI-70	695200.00	9854900.00	910.37	270	-85	221.80
CURI-71	695137.50	9854950.00	895.24	90	-70	182.75
TOTAL PHASE						3,241.38
II						

The **Phase III** drilling was carried out from September 2010 to August 2011, with 84 drill holes totalling 15,699.51 m (Table 10.4). All of this drilling has been conducted exclusively in the El Domo area. This data was incorporated into the previous drilling database for the resource update completed by Roscoe Postle Associates Inc. (RPA) in their NI 43-101 Technical Report (Lavigne and McMonnies, 2011).

TABLE 10.4 PHASE III DRILL HOLES, SALAZAR RESOURCES LTD — CURIPAMBA PROJECT

Drill Hole ID	Easting	Northing	Elevation (m)	Azimuth (°)	Dip (°)	Depth (m)
CURI-72	695180.38	9855002.85	928.61	90	-70	158.75
CURI-73	695110.28	9855451.53	952.64	90	-70	161.90
CURI-74	695106.96	9855451.45	952.64	270	-85	150.00
CURI-75	695106.74	9855451.45	952.64	270	-60	164.75
CURI-76	695150.02	9855499.98	955.27	90	-70	195.60
CURI-77	695146.65	9855499.85	955.27	270	-85	128.80
CURI-78	695146.24	9855499.82	955.27	270	-55	135.90
CURI-79	695270.67	9855406.01	963.79	90	-65	200.75
CURI-80	695140.03	9855400.52	946.3	0	-90	171.00
CURI-81	695138.06	9855549.71	950.92	270	-90	182.85
CURI-82	695137.92	9855549.67	950.92	270	-65	143.70
CURI-83	695103.72	9855599.97	942.83	90	-80	124.05
CURI-84	695178.21	9854950.14	928.93	90	-70	144.25
CURI-85	695243.96	9854900.04	945.68	270	-85	132.00
CURI-86	695008.99	9854700.17	950.19	90	-80	224.70
CURI-87	695052.66	9855150.04	892.90	90	-75	107.95
CURI-88	695497.33	9854697.45	951.09	270	-75	191.90
CURI-89	694895.57	9855200.01	858.29	90	-75	128.95
CURI-90	694994.81	9855046.93	878.06	90	-75	99.00
CURI-91	694980.65	9854999.77	876.45	90	-70	134.95
CURI-92	695267.25	9855405.89	963.49	270	-80	248.85
CURI-93	695209.46	9855449.95	977.43	90	-70	260.80
CURI-94	695163.27	9855550.46	949.67	90	-75	134.95
CURI-95	695073.49	9855270.9	933.71	90	-75	197.80

CURI-96	695100.56	9855349.95	939.99	90	-75	179.95
CURI-97	695456.66	9854622.6	938.78	270	-75	170.95
CURI-98	695199.61	9855219.95	959.59	0	-90	251.80
CURI-99	695000.52	9855138.15	881.92	90	-75	125.95
CURI-100	695100.47	9855150.08	903.29	90	-75	113.95
CURI-101	694285.49	9854893.02	994.08	0	-90	227.80
CURI-102	695114.57	9855254.91	942.47	90	-75	188.80
CURI-103	695179.4	9855200.01	951.88	270	-80	293.80
CURI-104	695030.68	9855249.92	910.27	90	-75	140.80
CURI-105	695235.97	9855549.95	974.22	0	-90	224.90
CURI-106	695000.43	9855249.9	903.71	90	-85	134.95
CURI-107	695050.9	9855350.05	929.18	90	-75	149.95
CURI-108	695195.73	9855599.99	945.06	90	-75	216.05
CURI-109	695092.45	9855400.15	950.11	90	-90	155.80
CURI-110	695250.53	9855600.33	960.55	90	-75	200.95
CURI-111	695000.47	9855350.05	908.49	90	-75	137.95
CURI-112	695298.72	9855900.03	901.69	270	-78	155.35
CURI-113	694946.79	9855249.95	875.97	90	-75	143.95
CURI-114	695195.91	9855350.06	956.9	90	-75	110.75
CURI-115	694950.73	9855150.73	854.81	90	-75	122.95
CURI-116	694900.5	9855150.06	844.31	90	-75	94.25
CURI-117	695196.47	9855650.55	939.3	90	-75	120.00
CURI-118	694919.26	9855100.09	858.84	270	-65	125.95
CURI-119	695250.75	9855649.89	952.61	90	-75	121.75
CURI-120	695150.51	9855649.96	932.7	90	-75	140.90
CURI-121	695100.58	9855650.04	932.54	90	-75	149.90
CURI-122	694922.79	9855100.22	859.16	90	-75	140.95
CURI-123	695096.38	9855649.93	932.62	270	-50	239.40
CURI-124	694940.63	9855050.02	873.25	90	-70	95.95
CURI-125	695096.82	9855649.94	932.59	270	-70	119.95
CURI-126	694930.77	9855000.2	868.3	90	-70	128.95
CURI-127	695100.08	9855600.04	942.55	270	-60	84.80
CURI-128	695030.91	9854950.07	884.74	90	-70	119.95
CURI-129	695120.05	9855303.05	950.89	90	-75	185.95
CURI-130	695100.39	9854944.94	901.7	90	-75	137.95
CURI-131	695137.31	9855149.72	927.52	90	-75	269.80
CURI-132	695240.23	9855350.97	945.7	233	-87	191.95
CURI-133	695187.37	9855049.96	955.52	90	-85	270.00
CURI-134	695242.55	9855353.43	945.71	53	-72	198.00
CURI-135	695222.69	9855000.01	950.93	90	-80	185.95
CURI-136	695251.03	9855300.03	974.08	270	-75	236.80
CURI-137	695247.29	9854950.01	950.84	90	-85	180.00
CURI-138	695247.51	9854950.01	950.43	90	-60	215.80
CURI-139	695254.51	9855299.99	975.17	90	-85	257.80
CURI-140	695200.98	9855150.18	967.01	90	-82	243.80

CURI-141	695226.81	9855249.71	975.63	90	-90	309.00
CURI-142	695254.61	9855300.14	975.17	90	-65	274.30
CURI-143	695226.92	9855249.77	975.63	90	-75	332.80
CURI-144	695200.58	9855101.87	961.52	90	-90	303.00
CURI-145	695306.77	9855349.98	995.94	90	-90	251.80
CURI-146	695299.30	9854900.38	951.64	270	-80	218.95
CURI-147	695303.04	9854900.49	953.41	90	-60	200.80
CURI-148	695306.83	9855350.03	995.94	90	-70	235.95
CURI-149	695235.71	9854700.00	938.76	90	-75	248.90
CURI-150	695458.98	9854699.98	948.49	270	-75	215.90
CURI-151	695227.00	9855250.00	975.11	90	-55	257.00
CURI-152	695500.00	9854750.00	979.00	270	-75	398.50
CURI-153	695550.00	9854900.00	998.88	90	-90	257.95
CURI-154	695217.00	9855008.00	951.61	90	-60	257.85
CURI-155	695750.00	9855150.00	1070.07	90	-90	307.85
TOTAL PHASE						15,699.51
III						

The **Phase IV** drilling program was carried out from August 2011 to April 2012, with 51 new holes completed for a total of 10,248.77 m (Table 10.5). All of this drilling has been conducted in the El Domo area using one Hydracore 2000 and one 4000 portable hydraulic diamond drills. This new data has been incorporated into the existing drilling database.

TABLE 10.5 PHASE IV DRILL HOLES, SALAZAR RESOURCES LTD — CURIPAMBA PROJECT

Drill Hole ID	Easting	Northing	Elevation (m)	Azimuth (°)	Dip (°)	Depth (m)
CURI-156	695187.60	9855049.98	955.52	90	-65	255.40
CURI-157	695200.75	9855101.83	961.45	90	-70	266.90
CURI-158	695183.03	9855200.20	952.33	90	-65	299.85
CURI-159	695700.64	9855399.94	1052.54	90	-90	280.20
CURI-160	695451.00	9855349.96	1012.24	270	-90	270.00
CURI-161	695454.39	9855350.09	1012.24	90	-70	269.90
CURI-162	695427.31	9854949.86	1001.35	270	-80	230.00
CURI-163	695401.32	9855300.37	1016.13	90	-78.8	282.95
CURI-164	695368.92	9855049.96	1062.32	270	-85	311.80
CURI-165	695400.76	9855250.03	1043.56	90	-85	284.80
CURI-166	695375.67	9855399.88	997.74	90	-85	231.00
CURI-167	695319.50	9855450.38	990.91	90	-81.8	264.00
CURI-168	695149.43	9854899.93	924.06	270	-85	125.95
CURI-169	694987.61	9854950.17	872.45	90	-80	152.95
CURI-170	695301.14	9855500.13	1005.57	90	-80	288.00
CURI-171	694984.25	9854950.06	873.23	270	-71.3	137.95
CURI-172	694869.35	9855002.47	839.04	90	-70	134.80

CURI-173	695297.71	9855550.06	1000.51	90	-90	234.00
CURI-174	694899.79	9855049.78	863.6	90	-90	131.35
CURI-175	695400.93	9855250.03	1043.56	90	-60	308.75
CURI-176	695333.60	9855199.90	1057.43	90	-85	395.80
CURI-177	694903.16	9855049.69	864.87	270	-60	124.15
CURI-178	694896.95	9855149.99	843.95	270	-60	95.95
CURI-179	695501.00	9855300.02	1020.96	90	-75	292.35
CURI-180	694836.01	9855199.88	854.9	90	-75	149.95
CURI-181	694832.61	9855199.91	854.9	270	-55	94.55
CURI-182	694884.02	9855246.27	856.51	90	-75	91.45
CURI-183	695446.36	9855399.91	1026.93	90	-80	243.00
CURI-184	694960.90	9855299.92	884.42	90	-75	128.95
CURI-185	695349.42	9855650.11	972.19	270	-70	123.00
CURI-186	694935.64	9855399.94	911.56	90	-70	167.95
CURI-187	695352.86	9855650.19	971.43	90	-65	173.80
CURI-188	694932.08	9855399.91	911.6	270	-60	95.95
CURI-189	694976.85	9855349.92	902.25	270	-60	137.80
CURI-190	695040.51	9855549.92	938.46	270	-75	171.00
CURI-191	695051.21	9855649.85	923.23	270	-45	82.65
CURI-192	695477.58	9855650.18	963.3	270	-75	128.95
CURI-193	695074.99	9855700.02	915.28	270	-80	81.65
CURI-194	695481.26	9855650.24	964.64	90	-60	128.80
CURI-195	695139.11	9855699.88	925.64	270	-80	95.95
CURI-196	695505.39	9855599.84	991.05	90	-80	224.95
CURI-197	695368.92	9855049.96	1061.4	90	-75	299.80
CURI-198	695364.88	9855600.20	993.86	90	-70	218.95
CURI-199	695427.31	9854949.86	1001.37	90	-70	257.80
CURI-200	695000.00	9854900.00	881.41	270	-85	143.95
CURI-201	695358.00	9855100.00	1086.5	90	-90	343.15
CURI-202	695000.00	9854900.00	882.13	270	-45	182.75
CURI-203	694934.00	9854950.00	863.7	270	-70	164.95
CURI-204	695440.00	9855150.00	1104.16	90	-70	398.80
CURI-205	694833.00	9855103.00	845.36	270	-80	135.65
CURI-206	694881.50	9855064.00	862.45	270	-45	113.80
TOTAL PHASE						10,248.77
IV						

BISA updated the existing database with the 51 drill holes from Phase IV. The geological model and resource estimate performed by BISA include all the drill holes from the four drilling phases of the El Domo deposit (Table 10.6 and Table 10.7).

TABLE 10.6 DRILL HOLES USED ON THE RESOURCE ESTIMATE — BISA 2013

Phase	ID Drilling	Holes	Cumulative Metres
I	CURI-07-19 to CURI-08-51	22	4,556.41
II	CURI-52 to CURI-71	19	3,100.50
III	CURI-72 to CURI-155	76	13,865.50
IV	CURI-156 to CURI-206	51	10,248.75
TOTAL		168	31,771.16

TABLE 10.7 MINERALIZED INTERCEPTS FROM THE MAIN ORE ZONE IN EL DOMO — BISA 2013

Drill Hole	From (m)	To (m)	Copper (%)	Zinc (%)	Gold (g/t)	Silver (g/t)	Lead (%)
CURI-08-22	19.73	22.86	3.70	1.62	4.77	53.37	0.10
CURI-08-39	118.00	129.37	1.24	4.62	3.64	52.76	0.15
CURI-08-42	186.35	192.63	1.05	9.76	2.18	58.11	0.69
CURI-08-45	202.86	208.61	3.46	6.31	4.90	89.62	0.22
CURI-08-46	49.33	73.47	2.95	4.61	3.03	95.30	0.69
CURI-08-48	40.05	83.70	2.30	2.54	2.78	49.32	0.35
CURI-08-49	62.24	69.10	1.25	2.65	1.84	25.26	0.26
CURI-08-50	122.35	139.75	2.42	1.45	2.09	57.09	0.12
CURI-52	47.60	64.48	1.88	0.68	1.74	25.82	0.05
CURI-53	65.41	111.43	2.73	2.18	2.08	139.98	0.14
CURI-54	57.00	59.95	2.78	14.22	3.81	118.80	1.60
CURI-55	84.36	85.40	0.32	1.49	1.14	43.70	0.14
CURI-56	55.30	103.40	3.27	6.91	9.61	164.94	0.78
CURI-57	55.92	78.06	1.41	5.44	2.81	61.04	0.30
CURI-60	120.82	158.36	3.21	1.40	3.29	35.08	0.10
CURI-61	146.77	156.77	3.31	0.25	1.33	12.09	0.02
CURI-62	68.42	118.75	0.81	4.76	3.26	83.80	0.58
CURI-63	70.45	78.73	1.76	3.87	0.90	20.35	0.02
CURI-64	68.15	79.00	6.61	5.17	4.82	146.94	0.70
CURI-67	82.07	93.90	2.03	7.35	2.14	73.67	0.89
CURI-68	88.40	102.38	2.80	3.82	5.97	65.13	1.01
CURI-69	81.82	84.92	1.49	14.74	53.30	482.17	7.63
CURI-71	61.57	63.48	2.29	26.28	23.87	1252.71	5.69
CURI-72	111.00	116.16	1.69	3.88	1.43	58.43	0.22
CURI-73	100.00	115.36	2.24	0.37	0.90	13.17	0.04
CURI-74	91.20	96.56	0.68	4.23	3.98	31.44	0.33
CURI-75	105.17	107.29	0.10	0.32	0.37	4.90	0.04
CURI-76	124.38	145.67	0.64	0.45	0.36	12.12	0.03

CURI-77	85.54	96.07	9.16	8.75	11.04	141.42	0.55
CURI-78	103.00	104.75	0.32	0.73	0.72	12.69	0.11
CURI-79	159.77	161.07	0.06	0.17	0.49	11.38	0.08
CURI-80	97.10	122.10	1.33	0.27	1.08	11.04	0.07
CURI-81	84.25	89.55	2.58	2.88	2.42	51.47	0.21
CURI-82	104.00	109.18	1.77	16.93	4.06	114.40	0.68
CURI-83	96.60	98.80	0.02	0.27	3.00	79.14	0.12
CURI-84	81.35	85.75	1.21	3.55	0.99	47.02	0.13
CURI-85	83.30	85.41	0.89	0.63	0.40	23.14	0.26
CURI-87	45.40	67.56	6.09	1.25	2.54	29.48	0.08
CURI-89	40.58	43.06	0.03	0.41	0.75	24.38	0.05
CURI-90	46.53	47.90	0.50	5.64	4.40	355.59	1.45
CURI-91	58.27	60.22	1.74	4.49	3.81	60.59	1.85
CURI-92	152.06	155.78	0.47	0.50	1.23	14.27	0.04
CURI-93	187.67	189.12	0.43	2.56	5.30	134.10	0.41
CURI-94	82.60	100.77	0.94	3.42	3.12	70.91	0.41
CURI-95	109.85	117.62	1.44	0.10	0.90	9.65	0.01
CURI-96	105.27	117.72	0.72	0.44	1.16	18.25	0.07
CURI-99	54.74	76.25	4.90	1.56	6.91	46.20	0.14
CURI-100	43.35	82.30	0.78	0.66	1.11	18.19	0.05
CURI-102	144.93	146.95	0.46	1.51	2.44	26.59	0.03
CURI-104	62.42	74.95	4.62	1.96	5.18	39.73	0.08
CURI-105	147.60	148.48	10.30	3.76	2.05	157.00	0.86
CURI-106	64.18	93.33	6.43	1.80	4.86	40.29	0.12
CURI-107	86.82	94.43	0.21	0.42	1.33	12.01	0.10
CURI-109	107.63	124.26	1.06	2.54	1.33	23.20	0.03
CURI-111	47.50	50.76	2.19	3.54	0.76	17.81	0.01
CURI-113	36.75	76.96	1.27	10.61	15.43	352.49	4.37
CURI-115	34.50	45.00	3.94	4.30	4.86	162.71	0.68
CURI-122	54.54	56.48	1.48	27.41	12.92	348.41	3.34
CURI-123	65.10	77.10	3.88	28.48	12.36	426.49	1.77
CURI-127	68.03	69.00	0.04	0.25	0.30	20.20	0.05
CURI-128	57.00	58.67	1.14	8.52	12.00	868.00	2.39
CURI-129	150.40	152.35	1.14	2.29	0.99	26.41	0.22
CURI-131	165.66	166.45	2.59	32.50	7.53	250.00	3.06
CURI-132	125.20	145.10	1.54	0.54	0.89	12.48	0.03
CURI-133	156.63	163.84	0.41	0.87	0.90	16.20	0.05
CURI-134	137.00	145.00	0.36	0.55	1.08	10.51	0.05
CURI-135	133.07	143.37	1.29	6.55	5.86	173.24	1.07
CURI-136	193.25	194.50	2.02	0.93	1.20	29.80	0.02
CURI-137	103.87	110.90	5.89	19.16	4.68	119.83	0.65
CURI-139	176.78	183.40	1.26	0.11	0.92	12.04	0.02
CURI-141	221.68	222.90	1.49	2.88	1.04	38.67	0.73
CURI-142	180.85	237.43	1.18	0.05	0.54	6.83	0.01
CURI-143	201.08	204.80	1.48	9.00	4.49	102.13	0.53

CURI-145	182.35	187.41	1.45	1.07	0.96	16.54	0.32
CURI-146	80.60	82.22	0.00	0.01	0.00	0.14	0.00
CURI-148	164.14	180.46	2.42	0.41	1.31	6.79	0.01
CURI-151	201.52	219.00	2.77	3.00	0.94	25.15	0.01
CURI-154	160.55	162.60	0.26	1.61	0.42	10.20	0.47
CURI-155	72.82	194.60	0.04	0.30	0.80	16.25	0.09
CURI-156	180.56	185.27	4.79	0.54	1.38	108.51	0.04
CURI-157	187.70	188.45	1.20	6.90	5.01	126.40	0.86
CURI-160	161.90	173.37	5.42	0.39	0.80	16.05	0.03
CURI-163	175.22	191.73	4.17	1.91	1.16	10.79	0.02
CURI-164	261.82	270.80	6.09	1.36	0.49	20.03	0.01
CURI-165	207.40	218.18	1.53	0.16	0.72	7.53	0.01
CURI-166	165.98	168.87	1.73	1.46	0.85	9.45	0.01
CURI-169	56.95	61.36	4.56	13.89	7.16	246.41	2.00
CURI-171	61.65	62.74	4.09	11.76	4.86	135.80	1.03
CURI-175	287.40	290.75	0.14	2.99	0.21	4.35	0.01
CURI-176	260.80	265.45	0.74	1.17	0.60	3.92	0.01
CURI-184	54.00	75.62	0.63	6.26	2.92	64.60	0.69
CURI-185	92.85	95.95	2.21	4.33	3.09	57.82	0.31
CURI-187	89.35	95.70	0.75	4.54	4.53	58.05	0.46
CURI-198	138.60	142.10	6.50	9.19	4.62	137.15	0.34
CURI-200	56.00	59.95	1.58	11.29	6.45	159.49	1.06
CURI-201	289.60	291.10	1.52	3.64	0.98	80.82	0.37

11. SAMPLE PREPARATION, ANALYSIS AND SECURITY

In 2010 and 2011, RPA reviewed Salazar's procedures in the first three drilling phases. These procedures included handling core boxes and photographing them, logging cores, sample selection and marking, cutting cores with a power saw, sample bagging and sealing, and the chain of custody for transporting the samples to the laboratories of Inspectorate or ALS Global in Quito for preparation and subsequent analysis in Lima. RPA considered all the procedures to be acceptable and in accordance with international practices.

In April and July of 2013, BISA independently reviewed Salazar's operational procedures with the aid of Salazar geologists Francisco Soria (Exploration Manager) and Carlos Aguila (Senior Geologist). BISA verified that the cores from the diamond drilling are placed in duly tagged wooden boxes 1.20 x 0.34 m with four inside divisions. Wooden tags are also inscribed with the depth, start, and end of each interval. Each drill core is Quick Logged in the field, noting the lithological units, alteration, mineralization, and significant structures. The boxes are then sealed with wooden lids and transported by pick-up to the Salazar logging facility in Ventanas.

In the logging room, the boxes are opened and the cores prepared. The core length and position of the tags are checked, and they are photographed in groups of two boxes (Figure 11.1). The geotechnical logging is then performed, which records the percentage of RQD recovery, number of fractures per metre, and rock quality. A detailed core log is then filled in on the appropriate form, detailing the geological units, mineralization, type of alterations and intensity, and main structures.

The geologist decides which sections need to be sampled and marks them on the core and on the boxes; he also marks the centre cutting line on the drill core. Sampling intervals range from 0.5 m to 2 m, and samples are normally taken up to 10 m above the mineralization and 20 m below this zone. The core sample is then cut in half lengthwise with a diamond saw (Figure 11.2). One half is double-bagged in plastic and duly tagged, and the other half remains in the core box. The samples are weighed and sealed then grouped into batches of 7 to 10 units that are bagged and tagged with the project name, drill hole number, and sample codes.

A Salazar geologist accompanies the samples by pick-up from Ventanas to Quito for their analysis. The samples are received at the preparation laboratories of BSI Inspectorate or ALS Global. After preparation, sample pulps are sent by TNT Express courier to Inspectorate or ALS Global in Lima for analysis. BSI Inspectorate Services Peru S.A.C. is certified ISO 17025 and ISO 9001:2000. ALS Global is certified ISO/IEC 17025-2005 and ISO 9001:2008.



FIGURE 11.1 PHOTOGRAPHIC PROCEDURE FOR CORE BOXES



FIGURE 11.2 SAMPLE CUTTING WITH A DIAMOND SAW

At both laboratories, gold was analysed using fire assay (FA) with atomic absorption spectroscopy (AAS) after aqua regia digestion. The only difference lies in the weight of the sample analysed: 50 g for ALS Global and 30 g for Inspectorate. Silver and base metals (Cu, Pb, Zn) were determined at both laboratories with aqua regia digestion and ICP-AES (Inductively Coupled Plasma). Base metals greater than 1% and Ag >100 ppm were reanalyzed with AAS after aqua digestion. Some differences in sample preparation and analytical procedures used in both laboratories: sample weight, chemical reactives, digestion procedures, etc. have been reported by Lavigne and McMonnies (2011).

After the Phase III diamond drilling (September 2010 – August 2011), Salazar instituted a water-immersion procedure for in-situ determination of bulk density of lithological units and the various types of mineralization.

BISA has confirmed that Salazar has applied good practices in their handling and storage of core boxes, logging, sampling, and sample transport to the laboratories. The preparation and analysis procedures were also satisfactory. BISA did find some flaws in the organization and storage of coarse rejects and pulps at the Salazar facility in Quito. Salazar was informed of the flaws, and they were immediately corrected.

12. DATA VERIFICATION

Gustavo Calvo, P.Geo. (QP for the purposes of this report) and Fernando Tornos, PhD visited the Curipamba Project in April of 2013. During the site visit, they reviewed geological and geotechnical logging procedures, sampling, and bulk density measurements in the core samples. Sampling was conducted where Salazar personnel had succeeded in identifying evidence of mineralization, primarily related to the VMS unit. Several representative exploration drill holes in the mineral deposit were examined and compared with the logging records provided by Salazar in order to verify the lithology types, alterations, and mineralized sections. During a field inspection, several representative outcrops of the mineralization were visited and the coordinates, orientation, and inclination of some of the drill holes were verified.

The core sample storage area was inspected, and the core boxes were found to be in good condition, properly labelled and arranged in a suitable, dry and locked environment. BISA also inspected the storage facility in Quito, where the pulps and coarse rejects of samples from the four drilling campaigns are located; some minor observations were made regarding their order and arrangement, and Salazar immediately took corrective action.

The inspections by BISA did not reveal any important discrepancies and confirmed that Salazar's procedures are appropriate and comply with international standards.

BISA verified approximately 10% of the geochemical database for the 168 exploration drill holes (7,736 samples) completed in four consecutive drilling phases in the El Domo deposit and used in the geological modelling and resource estimation (Table 12.1). The input values were compared with the values reported in the assay certificates issued by the analytical laboratories ALS Global and Inspectorate. No significant differences were found, and errors were minimal and immediately corrected by Salazar. In summary, Salazar's methods conform with good practices used in the mining industry. BISA considers the database provided by Salazar to be sufficiently validated and supported to conduct a resource estimate of the El Domo deposit.

TABLE 12.1 SAMPLING AND ANALYTICAL LABS

Drilling Program	Analytical Lab	Samples	Core Length (m)
I	ALS Global	310	442.48
	Inspectorate	1,400	2,263.13
II	Inspectorate	761	1,008.34
	ALS Global	1,040	1,310.33
III	Inspectorate	2,325	2,824.03
	Inspectorate	1,900	2,639.78
Total		7,736	10,488.09

DATABASE VERIFICATION

The validation of the Salazar database included the files listed below:

Collar: The coordinates of the collars were checked, and it was found that, in many cases, they did not coincide with the topographic elevation from the photogrammetric map provided by Salazar. The elevation errors ranged from 0.32 m to 20.63 m above the topography and from 0.18 m to 40.76 m below it. Based on this, Salazar requested a new topographic survey of the El Domo drilling area using total station. This new survey (carried out by Aeromapa in July of 2013) covered 119 drill collars. With the new topographic base map thereby obtained, the coordinates of these 119 exploration drill holes were updated out of a total of 168 used in the geological modelling and resource calculation.

Survey: The data review confirmed that drill hole directional surveys were performed in only 49 of the 168 drill holes using a Reflex Maxibor II downhole tool. In general terms, the surveys reported variations in inclination of about 0° to 5°. Exploration drill hole CURI-93 showed a deviation of ~7°.

Assays: The review was conducted by a random extraction of 10% of the geochemical database (773 samples), which was then compared with the certificates from the ALS Global and Inspectorate laboratories. The seven elements considered to be of interest were used in this study: Cu (%), Zn (%), Au (g/t), Ag (g/t), Pb (%), Fe (%), and S (%).

The errors reported generally concerned the transcription of the data to Salazar's format and unit conversion (ppm and %). These errors were corrected by Salazar prior to using the database for modelling and estimating resources.

Lithology: BISA reviewed the lithological units used by Salazar in the 40 exploration drill holes, finding 16 different lithologic types and numerous discrepancies in the units mapped. In order to generate a simplified model of the deposit, BISA re-logged the 168 drill holes using the lithological logs, photographs of the drill core boxes, and the grades of the sampling intervals provided by Salazar. This work resulted in the definition of nine simplified units, which were verified and accepted by Salazar's geologists.

Recovery: BISA reviewed the core recovery's percentage from the 168 drill holes and found an average recovery of 93.9%; in the mineralized zone recovery reached 94.3%. However, 18 drill holes reported recoveries lower than 75% in some intervals when intersecting the mineralized zones (Table 12.2)

TABLE 12.2 DRILL HOLES WITH <75% CORE RECOVERY IN THE MINERALIZED ZONE

Drill Hole ID	From (m)	To (m)	Interval Length (m)	Recovery (%)	Total Mineralized Length in Drill Hole (m)
CURI-08-22	21.33	22.86	1.53	0	3.13
CURI-08-39	112.60	121.00	8.40	62	16.27
CURI-08-42	186.35	188.55	2.20	70	6.28
CURI-08-44	29.75	44.60	14.85	51	15.45
CURI-08-47	62.00	62.70	0.70	74	1.65
CURI-08-48	53.90	56.90	3.00	55	26.67
CURI-08-49	59.85	62.85	3.00	66	10
CURI-08-50	122.85	137.85	15.00	65	14.7
CURI-128	57.00	58.67	1.67	61	1.67
CURI-198	140.95	142.10	1.15	60	3.5
CURI-53	95.85	96.85	1.00	73	22.75
CURI-69	81.82	83.85	2.03	67	18.03
CURI-72	113.90	116.16	2.26	62	5.16
CURI-76	84.10	86.95	2.85	72	24.64
CURI-77	92.95	95.95	3.00	74	18.07
CURI-80	95.76	99.00	3.24	69	22.87
CURI-91	58.27	59.95	1.68	63	1.95
CURI-99	65.95	71.95	6.00	67	25.4

SALAZAR QUALITY ASSURANCE AND QUALITY CONTROL (QA/QC)

Quality Assurance (QA) involves certain tests to confirm that the analysis results have the expected precision and accuracy within the limits generally accepted for the type of sampling and analytical methods used. This ensures the reliability of the data used in the resource estimate.

Quality Control (QC) comprises the procedures used to ensure that an appropriate level of quality is maintained while collecting, preparing, and analysing the exploration samples. In general, QA/QC programs are designed to prevent or detect contamination and to enable quantification of reproducibility, precision, and analytical accuracy.

During the first two drilling phases, Salazar implemented a QA/QC program that included the use of standard samples, blanks, duplicates, and the re-analysis of samples with high levels of Au, Cu, and Zn. Beginning with Phase III, Salazar began inserting only standard and blank samples for QA/QC. The insertion rate for standard samples was one for every 10 or 15 samples and one blank for every 30 samples. The pulps from samples containing levels higher than 5 g/t Au, 5% Cu, or 5% Zn were re-analysed, and one sample out of every 10 was sent to an external laboratory for verification (the re-analyses were performed up to exploratory drill hole CURI-132).

RPA reviewed the results of Salazar's QA/QC program in its 2011 report and collected 10 independent samples for geochemical analysis. RPA recommended that Salazar's QA/QC program be modified to include the insertion of twin core samples and duplicates of the coarse rejects. RPA also recommended establishing a protocol for failed results and a formal system of reporting QA/QC results.

BISA reviewed Salazar's QA/QC program for Phase IV diamond drilling conducted in 2011 and 2012, which included 51 exploration drill holes (CURI-156 to CURI-206).

The QA/QC program conducted by Salazar for Phase IV includes only the insertion of standard samples and blanks, and does not include the use of twin core samples or duplicates of pulps and coarse rejects. Control re-analysis was not performed, and duplicate samples were not sent to an external laboratory as was done during the previous drilling

campaigns. BISA reviewed approximately 50% of the standards and 100% of the blanks used by Salazar during the Phase IV drilling.

CERTIFIED REFERENCE MATERIALS

The standard materials used by Salazar were prepared by WCM Minerals of Canada and do not meet the requirements for a Certified Reference Material (CRM) because they only report the values obtained through the round robin and the average value or best value, without consideration of the standard deviation of the population. The insertion rate was one standard for every nine samples, or a total of 142 standard samples (7.47% of 1,900 total samples). Table 12.3 indicates the standards utilized by Salazar and the samples inserted of each during the Phase IV drilling.

TABLE 12.3 REFERENCE MATERIALS EXPECTED VALUES AND RANGES

Standard	Au		Ag		Cu		Pb		Zn		Samples Submitted
	Mean (g/t)	SD (g/t)	Mean (g/t)	SD (g/t)	Mean (%)	SD (%)	Mean (%)	SD (%)	Mean (%)	SD (%)	
CU 121			33	1.131	0.97	0.02					8
CU 145			93	3.366	3.1	0.08					21
CU 152	1.62	0.069	27	0.622	1.16	0.028					21
CU 155	0.61	0.015	7	0.591	0.47	0.016					19
CU 163	4.35	0.129	99	2.366	1.06	0.017					19
CU 175	0.88	0.038	4	0.603	0.53	0.012					16
PB 130			82	2.194	0.25	0.003	0.73	0.077	1.44	0.138	20
PB 140			84	2.194	0.33	0.003	4.35	0.075	3.85	0.138	18

BISA selected CU-152, CU-163, PB-130, and PB-140 as reference materials, taking into account the number of analysed samples for each of them and the elements considered. In order to estimate the analytical accuracy of the Inspectorate laboratory, control diagrams were constructed using two statistical limits of $\pm 2SD$ (warning limit) and $\pm 3SD$ (failure limit) (see Table 12.4 and Table 12.5 for summaries of the results).

TABLE 12.4 REFERENCE MATERIALS CU-152 AND CU-16

Standard	Element	Unit	Samples	Outside $\pm 3SD$	Failures	Bias (%)
CU 152	Au	g/t	21		0	0
	Ag	g/t	21		0	0
	Cu	%	21		0	0
CU 163	Au	g/t	18		0	0
	Ag	g/t	18		0	0
	Cu	%	18		0	0

Table 12.4 shows that, of the 39 samples used (21 CU-152 samples and 18 CU-163 samples), none are outside of the $\pm 3SD$ line, and only a few of these are above the $\pm 2SD$ line because of the variable geochemical populations observed within WCM Minerals' certificates (Figure 12.1 and Figure 12.2).

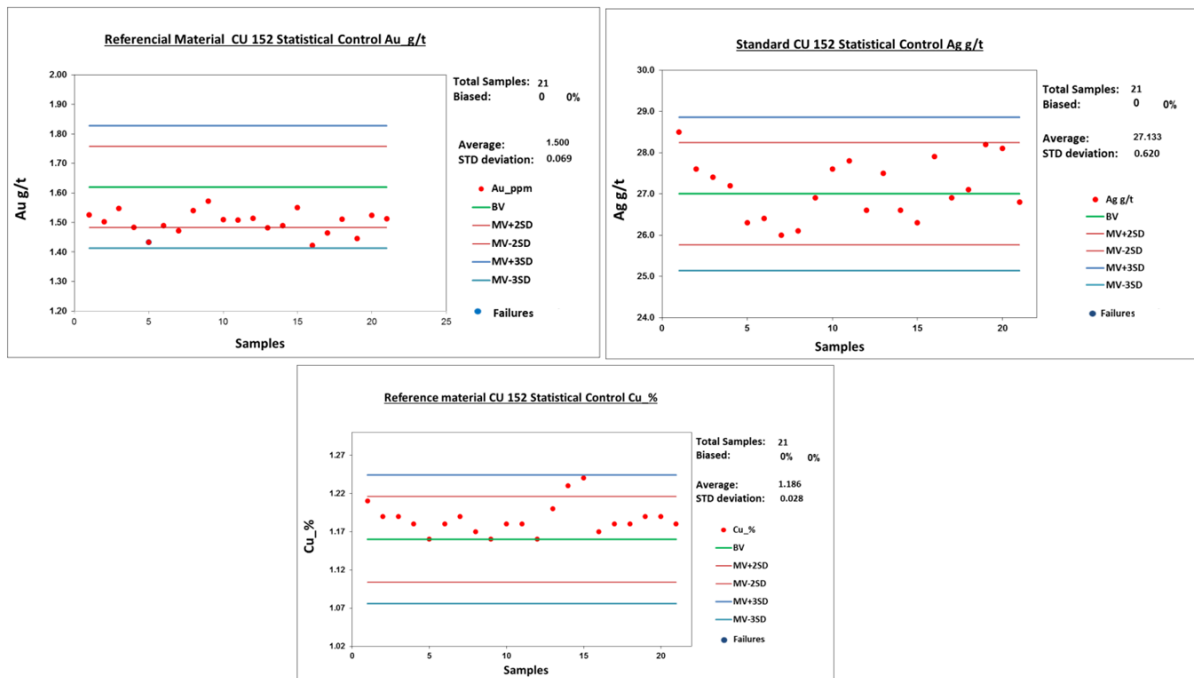


FIGURE 12.1 STATISTICAL CONTROL CHART FOR CU-152 FOR GOLD, SILVER, AND COPPER

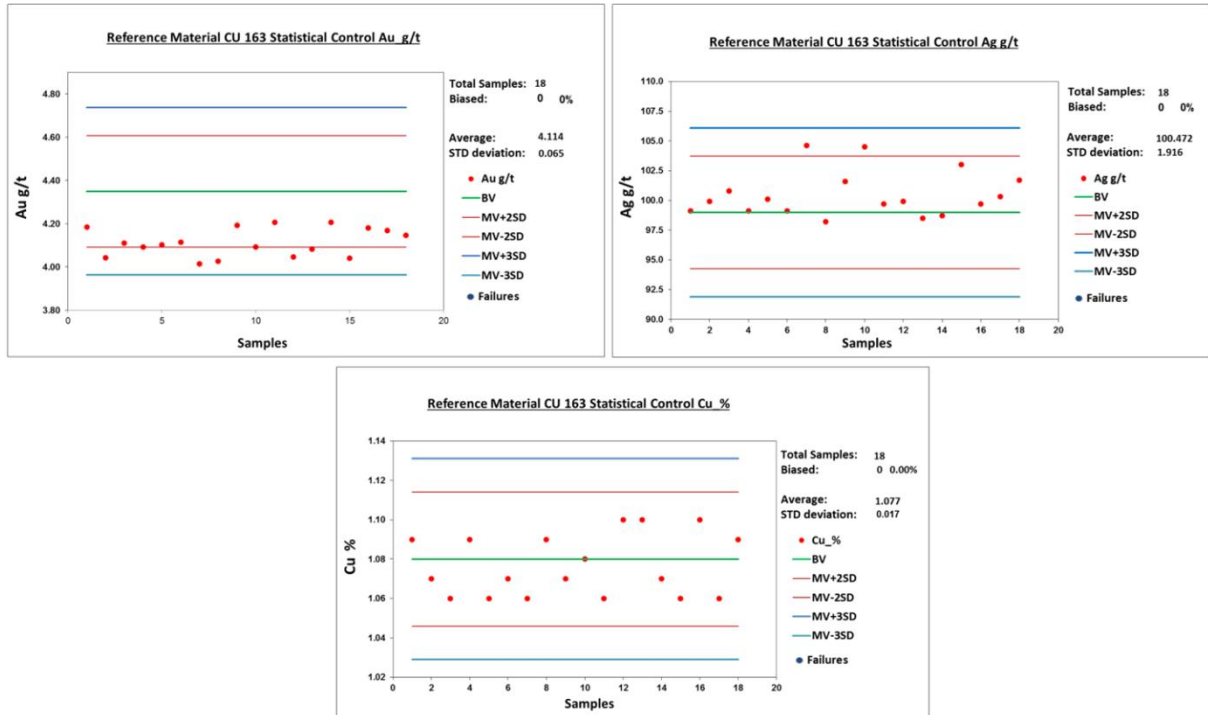


FIGURE 12.2 STATISTICAL CONTROL CHART FOR CU-163 FOR GOLD, SILVER, AND COPPER

TABLE 12.5 REFERENCE MATERIALS PB-130 AND PB-140

Standard	Element	Unit	Samples	Outside $\pm 3SD$	Failures	Bias (%)
PB 130	Ag	g/t	20		0	0
	Cu	%	20		0	0
	Pb	%	20		0	0
	Zn	%	20		0	0
PB 140	Ag	g/t	18		0	0
	Cu	%	18	8	8	44
	Pb	%	18	2	2	11
	Zn	%	18		0	0

Table 12.5 shows more failures for reference materials PB-130 and PB-140. This is particularly true for PB-140 and for Cu and Pb, with many samples even outside the $\pm 3SD$ line (Figure 12.3 and Figure 12.4).

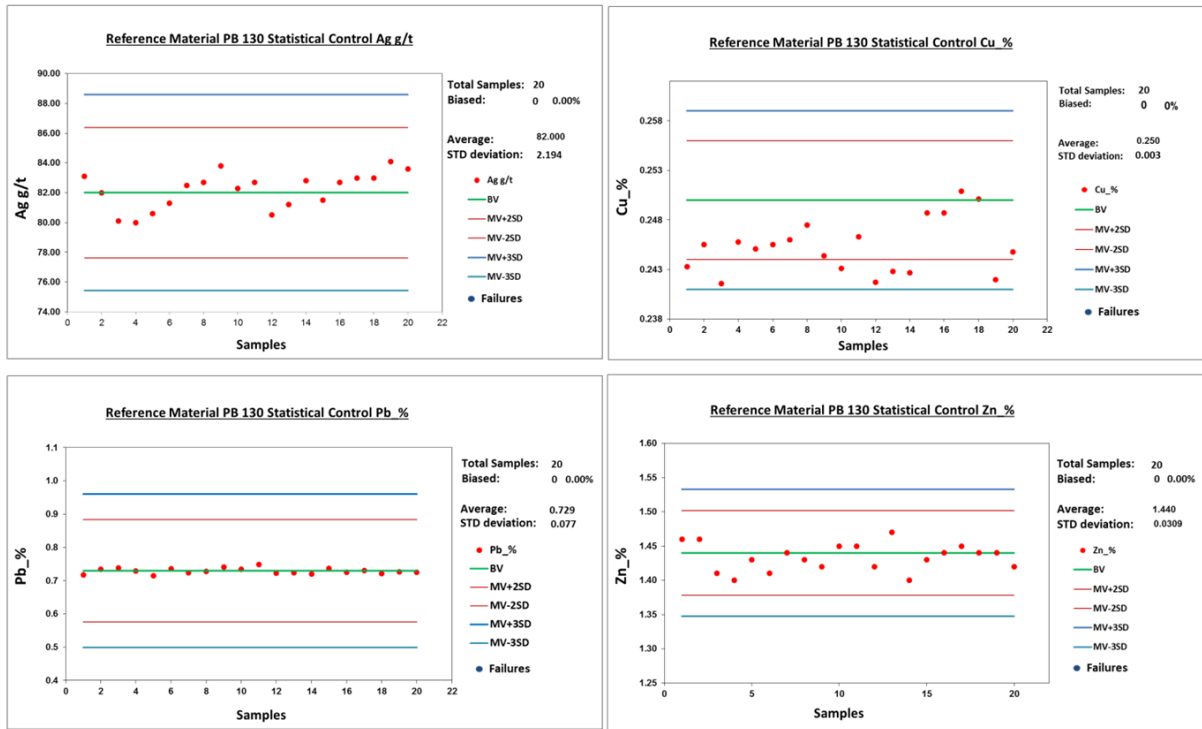


FIGURE 12.3 STATISTICAL CONTROL CHART FOR PB-130 FOR SILVER, COPPER, LEAD AND ZINC

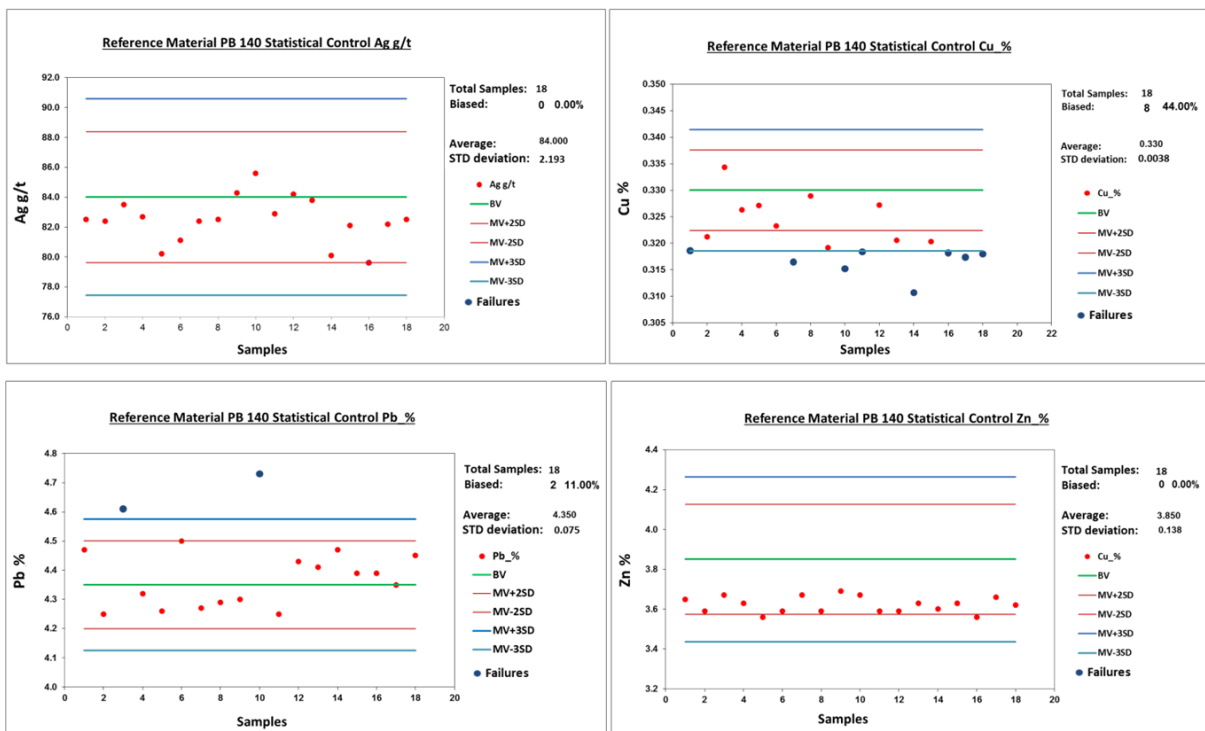


FIGURE 12.4 STATISTICAL CONTROL CHART FOR PB-140 FOR SILVER, COPPER, LEAD AND ZINC

BISA believes that the QA/QC analysis results for the standard samples contain a moderate number of failures. BISA recommends using duly certified reference materials prepared with mineral from the site itself for future geological sampling and/or drilling campaigns.

BLANK SAMPLES

Blank samples were submitted from two types of blanks: (1) Reference blank material BL115 purchased from WCM Minerals and (2) a BK blank standard prepared by Inspectorate Services (Peru). A BL115 assay was considered a failure if it returned a value greater than three times the detection limit of the assay method. A BK assay was considered a failure if the results were significantly higher than the certified means.

Salazar inserted 8 BL115 blank samples and 16 BK blank samples, not reporting any failure for the elements Au, Ag, and Pb. For Cu and Zn, all the samples had values over three times the lower detection limit (Table 12.6).

TABLE 12.6 BLANKS BL-115 AND BK SUMMARY

Element	Blanks (BL115 + BK)	Failures	% Failures
Au	24	0	0
Ag	24	0	0
Cu	24	24	100
Pb	24	0	0
Zn	24	24	100
TOTAL	120	48	

The high number of failed samples reported for Cu and Zn in both blanks (Figure 12.5 and Figure 12.6) is not a direct result of contamination during the sample preparation process, but is instead related to the high original Cu and Zn contents in the blanks used: 27 ppm Cu and 26 ppm Zn for BL 115, 97±8 ppm Cu and 46±8 ppm Zn for BK. Both values are well above Inspectorate's detection limits of 2 ppm for Cu and 5 ppm for Zn (Table 12.7).

TABLE 12.7 CU AND ZN ASSAYS FOR BLANKS BL115 AND BK — INSPECTORATE

BL 115			BK			BK		
ID Sample	Cu_ppm	Zn_ppm	ID Sample	Cu_ppm	Zn_ppm	ID Sample	Cu_ppm	Zn_ppm
169110	28	25	168420	101	47	169120	100	47
169250	29	25	168500	99	47	169260	102	45
169390	28	27	168660	99	44	169400	98	48
169530	30	25	168580	102	47	169540	100	50
169670	31	28	168740	98	47	169680	104	51
169810	29	30	168820	102	44	169820	105	51
169950	31	30	168900	99	41	169960	105	50
170090	31	33	168980	101	46	170100	109	53

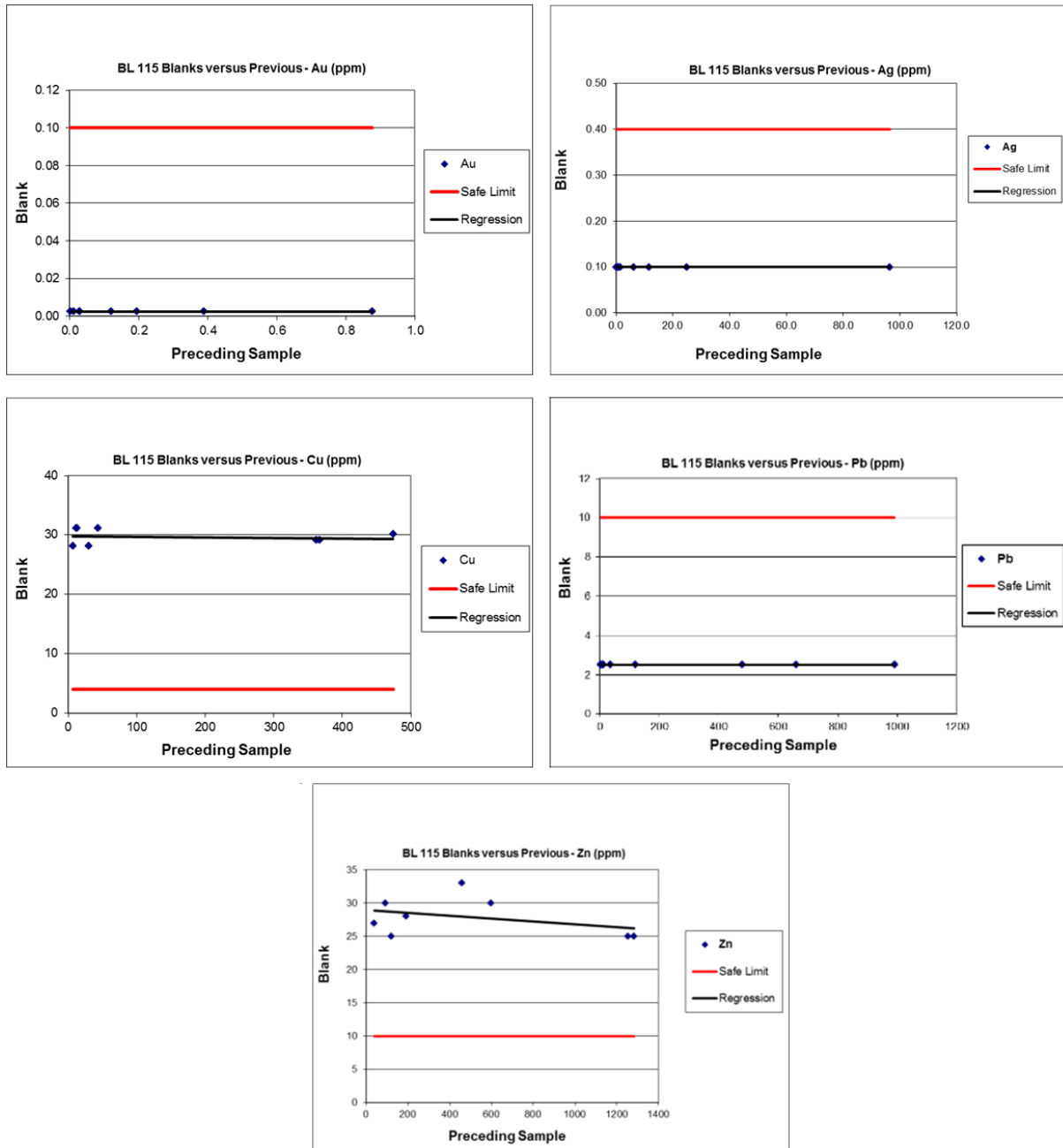


FIGURE 12.5 STATISTICAL CONTROL CHART FOR BLANK BL115

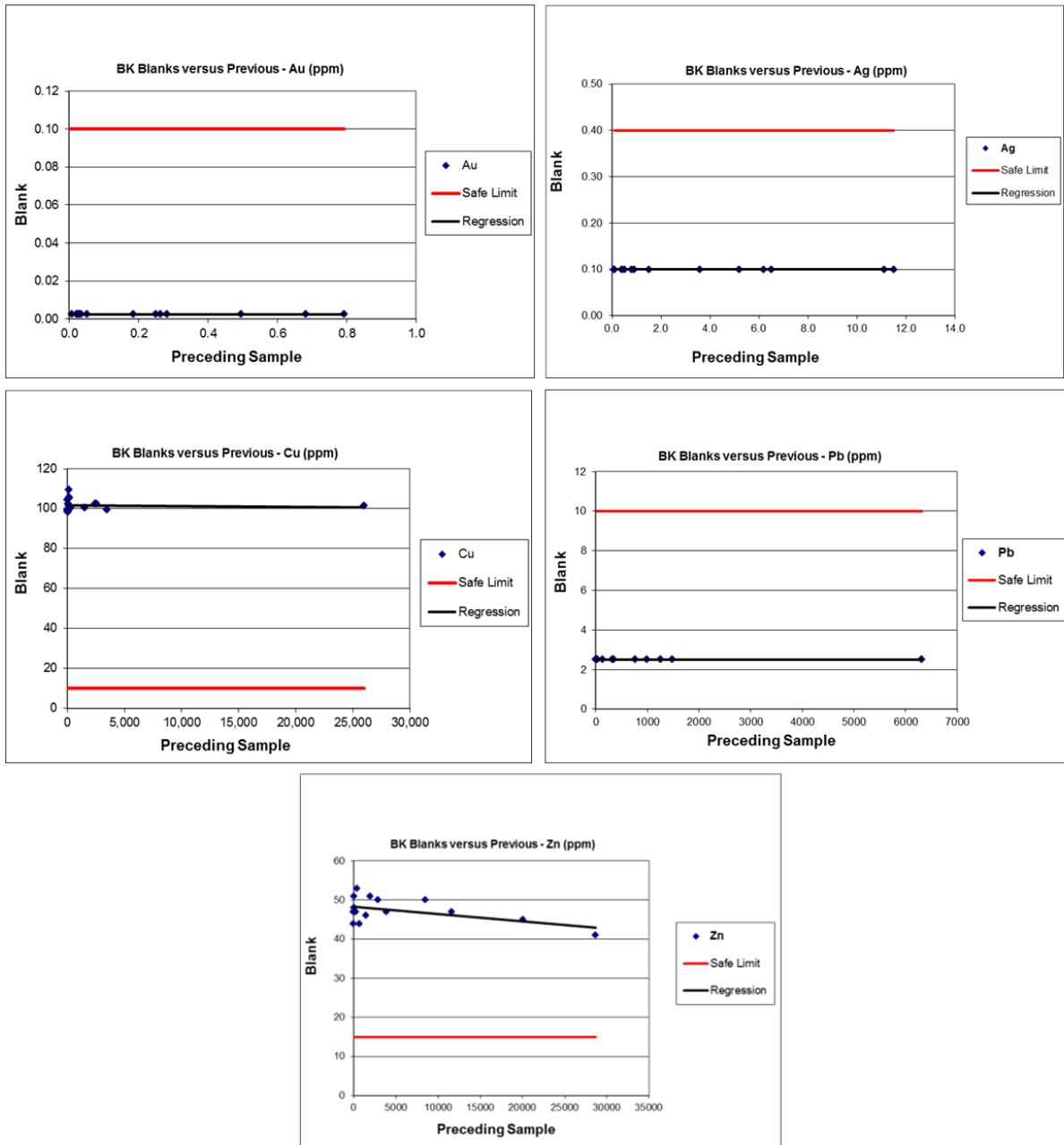


FIGURE 12.6 STATISTICAL CONTROL CHART FOR BLANK BK

BISA is of the opinion that the results from the statistical analysis of the blank samples are acceptable and do not evidence contamination. It is recommended that, in future, BK blanks not be used due to the elevated metal values reported. The blank materials to be used should have geochemical values close to the detection limits, particularly for Cu, Au, Zn, Ag, and Pb.

BISA VERIFICATION SAMPLING

During the visit to the project site in April of 2013, BISA undertook an initial re-sampling for verification (Verification Sampling 1), including 143 representative samples from the four Salazar drilling phases. This sampling included core twin samples, coarse rejects, and pulps. Also inserted were standard and blank samples provided by Salazar and pulp duplicates for internal and external controls (Table 12.9). The samples were prepared at the facilities of ALS Global in Quito and later analysed at ALS Global in Lima; Acme Labs was used as an external laboratory.

The results identified poor precision in the pulp duplicates used. To try to clarify this problem (previously detected by Lavigne and McMonnies, 2011), BISA carried out a second verification sampling round in July of 2013 (Verification Sampling 2), for which the pulps and coarse rejects of 50 samples representative of the four Salazar drilling campaigns were selected (Table 12.8), and 18 QA/QC samples (Internal duplicates, standards, and blanks) were inserted (Table 12.9).

TABLE 12.8 VERIFICATION SAMPLING 1 — BISA 2013

Drilling Program (Year)	Samples
I (2007–2008)	25
II (2010)	24
III (2010–2011)	63
IV (2011–2012)	31
TOTAL	143

TABLE 12.9 SAMPLE TYPE AND QUANTITY FOR VERIFICATION SAMPLINGS 1 AND 2

SAMPLE TYPE	VERIFICATION	VERIFICATION
	1	2
Core Twin Sample	49	
Coarse Reject	52	50
Pulp	41	50
Internal Duplicate	10	10
Standard	12	4
Blanks	11	4
External Duplicate	10	
TOTAL	185	118

43 samples were collected (approximately 2.3% of the total samples), representative of the four Salazar drilling campaigns over the period of 2007–2012 (see for details).

The selected samples include core twin samples, coarse reject samples, and pulp samples. Duplicate samples, certified standards (CU 152 and PB 140), and certified fine blanks (BK) were submitted, provided by Salazar (Table 12.10).

TABLE 12.10 VERIFICATION SAMPLING 1 BY TYPES — BISA 2013

Sample Type	Quantity
Twin (1/4 core)	49
Coarse Reject	52
Pulp	41
Duplicate	10
Standard	10
Blank	10
TOTAL	172

The samples were prepared at the facilities of ALS Global in Quito and later analysed at the ALS Global laboratory in Lima. The preparation and analysis methods are detailed in Table 12.11 and Table 12.12.

TABLE 12.11 PREPARATION METHODS — ALS GLOBAL

ALS Code	Description
LOG 24	Receipt of samples with no bar codes and selection of 1 in every 50 samples for QC testing.
PULP 32	Grinding of 1.5 kg of sample so that 85% passes through a 75 micron mesh (mesh #200)

TABLE 12.12 ANALYTICAL METHODS — ALS GLOBAL

ALS Code	Description
AA-Au 26	Fire Assay (FA) and AAS* analysis
ME-ICP 41	Aqua regia digestion and analysis of 35 elements using ICP-AES**
AA – 43 Ag, Cu, Pb, Zn	Aqua regia digestion and use of the gravimetric method and AAS for materials with elevated metal contents

*AAS: Atomic absorption spectroscopy

**ICP-AES Inductively coupled plasma atomic emission spectroscopy

As an external laboratory, the ACME Labs in Chile was used. Ten twin pulp and coarse reject samples were sent to this laboratory, accompanied by two standards (CU 152 and PB 140) and a fine blank (BK) (Table 12.13). The analytical methods are detailed in Table 12.14.

TABLE 12.13 EXTERNAL CONTROL SAMPLING — ACME LABS

Sample Type	Quantity
Pulp duplicate	10
Standard	2
Blank	1
TOTAL	13

TABLE 12.14 ANALYTICAL METHODS — ACME LABS

ALS Code	Description
G601+G610	Fire assay of 50 g of sample and AAS* analysis
ICP-ES Group 1D	0.5 g of sample digested in aqua regia and analysed for 34 elements using ICP-AES**

*AAS: Atomic absorption spectroscopy

**ICP-AES Inductively coupled plasma atomic emission spectroscopy

REFERENCE MATERIALS

Salazar provided BISA with two reference materials prepared by WCM Minerals of Canada:

- 1) Reference Material CU 152: 1.62±0.068 g/t Au, 27±0.622 g/t Ag, 1.16±0.028 % Cu.
- 2) Reference Material PB 140: 84±2.194 g/t Ag, 0.33±0.004 % Cu, 4.35±0.075 % Pb, 3.85±0.138 % Zn.

These were inserted by BISA in order to estimate the analytical accuracy of the primary and secondary laboratories.

BISA prepared statistical control charts using standard deviation (SD) limits of ±2SD and ±3SD (confidence intervals) for Au, Ag, Cu, Pb, and Zn.

REFERENCE MATERIAL CU 152

Five CU 152 samples were inserted in the batches sent to the primary laboratory (ALS Global), representing approximately one standard for every 18 samples; and one standard sample was sent in the shipment to the secondary laboratory (Acme Labs). The results are shown in Table 12.15 and Table 12.16.

TABLE 12.15 ANALYTICAL RESULTS FOR REFERENCE MATERIAL CU 152 — ALS GLOBAL

BISA Sample ID	Standard	Batch	Au-AA26 Au (ppm)	ME-ICP41 Ag (ppm)	Cu-AA46 Cu (%)
170425	CU 152	QU13096102	1.66	28.9	1.19
170475	CU 152	QU13096103	1.61	27.4	1.189
170532	CU 152	QU13096999	1.62	27.5	1.169
170579	CU 152	QU13097230	1.32	27.4	1.18
170596	CU 152	QU13096107	1.73	28.3	1.185

TABLE 12.16 ANALYTICAL RESULTS FOR REFERENCE MATERIAL CU 152 — ACME LABS

BISA Sample ID	Standard	Batch	G6-50 Au (ppm)	1D Ag (ppm)	8AR Cu (%)
170606	CU 152	LAA13000067	1,695	29,4	1,162

In the diagrams of Table 12.18, it can be seen that the Cu values are within the acceptable confidence intervals. However, Au and Ag show one and two failed values respectively, above the $\pm 3SD$ limit of the standard (Table 12.17), although the bias is magnified due to the small number of standard samples used.

TABLE 12.17 REFERENCE MATERIAL CU 152 — RESULTS SUMMARY

Standard	Element	Unit	Samples	Failures	Bias (%)
CU 152	Au	ppm	5	1	20
	Ag	ppm	5	1	20
	Cu	%	5	0	0

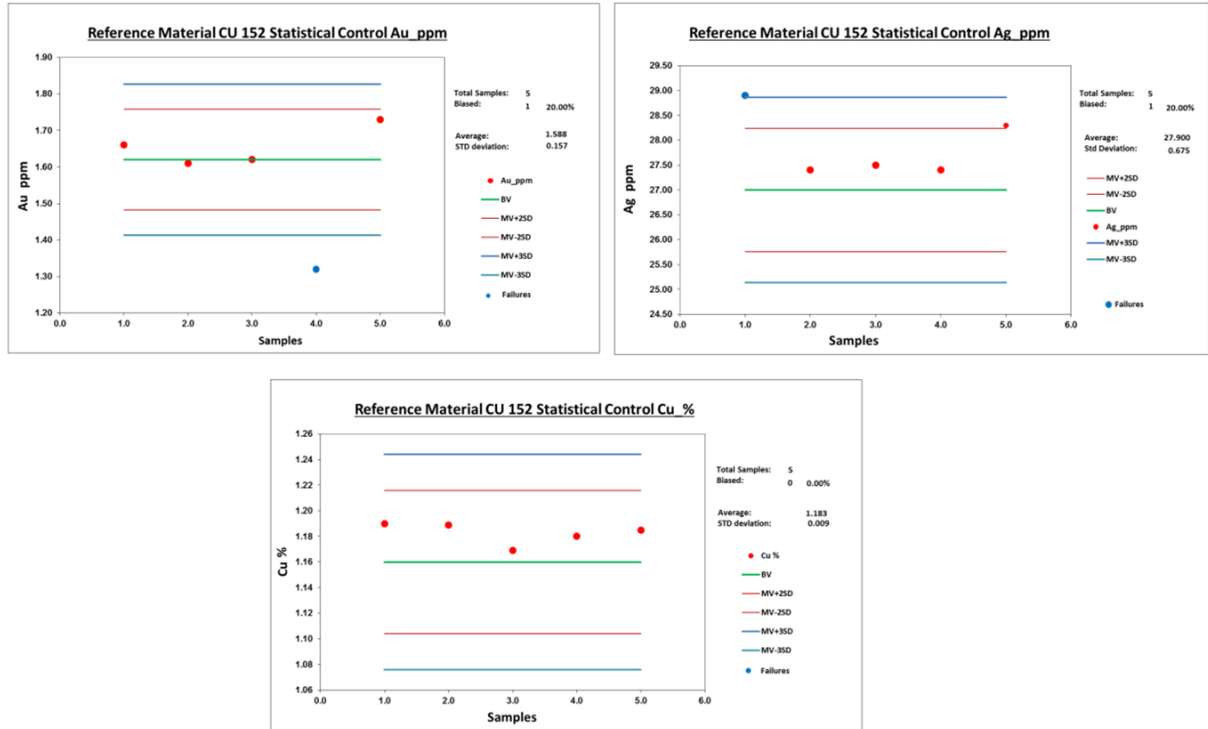


FIGURE 12.7 STATISTICAL CONTROL CHARTS FOR REFERENCE MATERIAL CU 152

REFERENCE MATERIAL PB 140

Five PB 140 samples were inserted in the batches sent to the primary laboratory (ALS Global), equivalent to approximately one reference for each 18 samples, and one PB 140 sample was sent in the batch to the secondary laboratory (Acme Labs). The results are shown in Table 12.18 and Table 12.19.

TABLE 12.18 ANALYTICAL RESULTS FOR REFERENCE MATERIAL PB 140 — ALS GLOBAL

BISA Sample ID	Standard	Batch	ME-ICP41 Ag (ppm)	ME-ICP41 Cu (ppm)	Pb-AA46 Cu (%)	Zn-AA46 Zn (%)
170451	PB 140	QU13096998	80,8	3190	4,27	3,86
170508	PB 140	QU13096104	84,3	3300	4,15	3,77
170560	PB 140	QU13096992	85,8	3320	4,21	3,89
170594	PB 140	QU13096106	83,7	3330	4,37	3,93
170600	PB 140	QU13096997	83,4	3100	4,17	3,84

TABLE 12.19 ANALYTICAL RESULTS FOR REFERENCE MATERIAL PB 140 — ACME LABS

BISA Sample ID	Standard	Batch	1D Ag (ppm)	1D Cu (ppm)	1D Pb (ppm)	8AR Zn (%)
170607	PB 140	LAA13000067	83	28,19	9737	3,81

In the diagrams in Figure 12.8, it can be seen that Ag, Zn, and Pb are within the acceptable confidence intervals, and for Cu two samples fall outside the $\pm 3SD$ limits (Table 12.20). As in the case of the standard CU 152, the small quantity of samples used (5) could magnify any bias.

TABLE 12.20 REFERENCE MATERIAL PB 140 — RESULTS SUMMARY

Standard	Element	Unit	Samples	Failures	Bias (%)
PB 140	Ag	ppm	5	0	0
	Cu	%	5	2	40
	Pb	%	5	0	0
	Zn	%	5	0	0

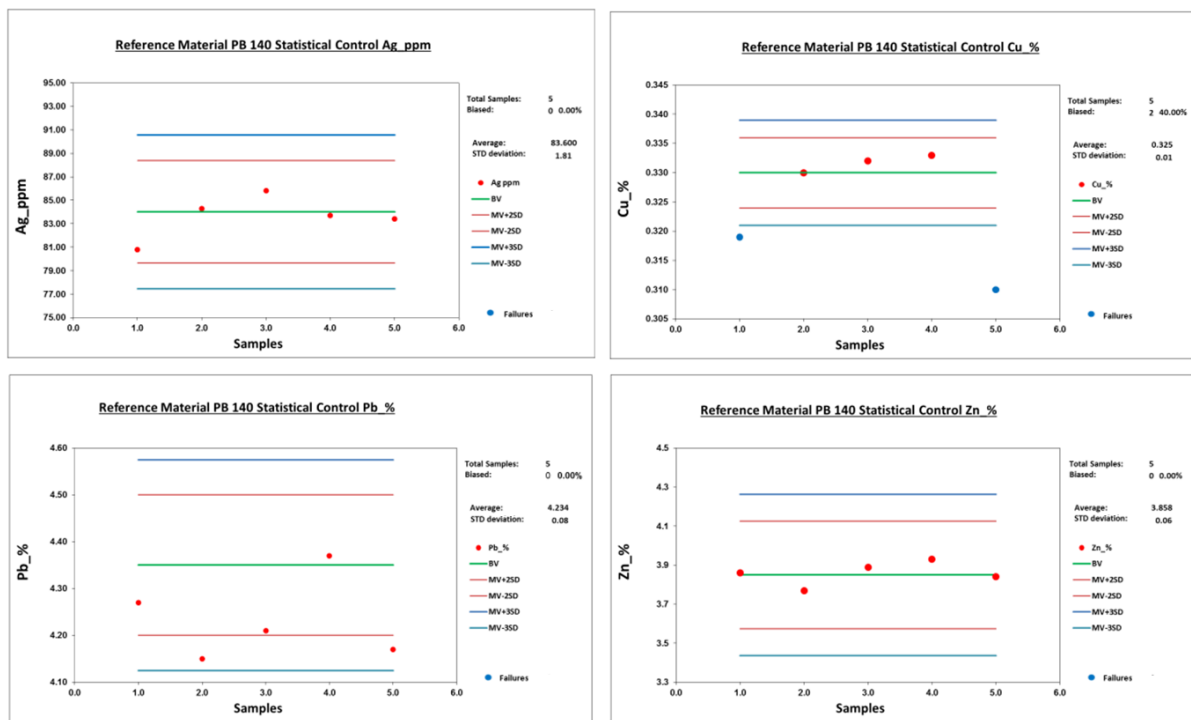


FIGURE 12.8 STATISTICAL CONTROL CHARTS FOR REFERENCE MATERIAL PB 140

TWIN SAMPLES

BISA collected 49 representative quarter-core twin samples of the four Salazar drilling campaigns in the El Domo deposit. The samples were obtained by cutting half of the drilling core kept by Salazar into two symmetrical parts using a power saw. These samples were used to estimate the geological variability (anisotropy) of the mineralization and also to identify possible errors introduced during sampling.

BISA prepared Max-Min scatter plots (hyperbolic method) for Au, Ag, Cu, Pb, and Zn using a relative error limit of $\pm 30\%$ in accordance with international practice (Figure 12.9). The pairs located above the red line are considered failures. A generally acceptable result is achieved when the number of rejects does not exceed 10% of the pairs used. In our case, the percentage of failed samples ranges from 8.3% for Zn to 28.6% for Pb (Table 12.21).

TABLE 12.21 TWIN SAMPLES SUMMARY

Sample Type	Element	Samples	Failures	Failures (%)
Twin	Au	49	10	20.4
	Ag	49	9	18.4
	Cu	49	14	28.6
	Pb	49	14	28.6
	Zn	49	10	20.4

The results, significantly higher than generally accepted limits, indicate a moderate natural variability/heterogeneity in the mineralization.

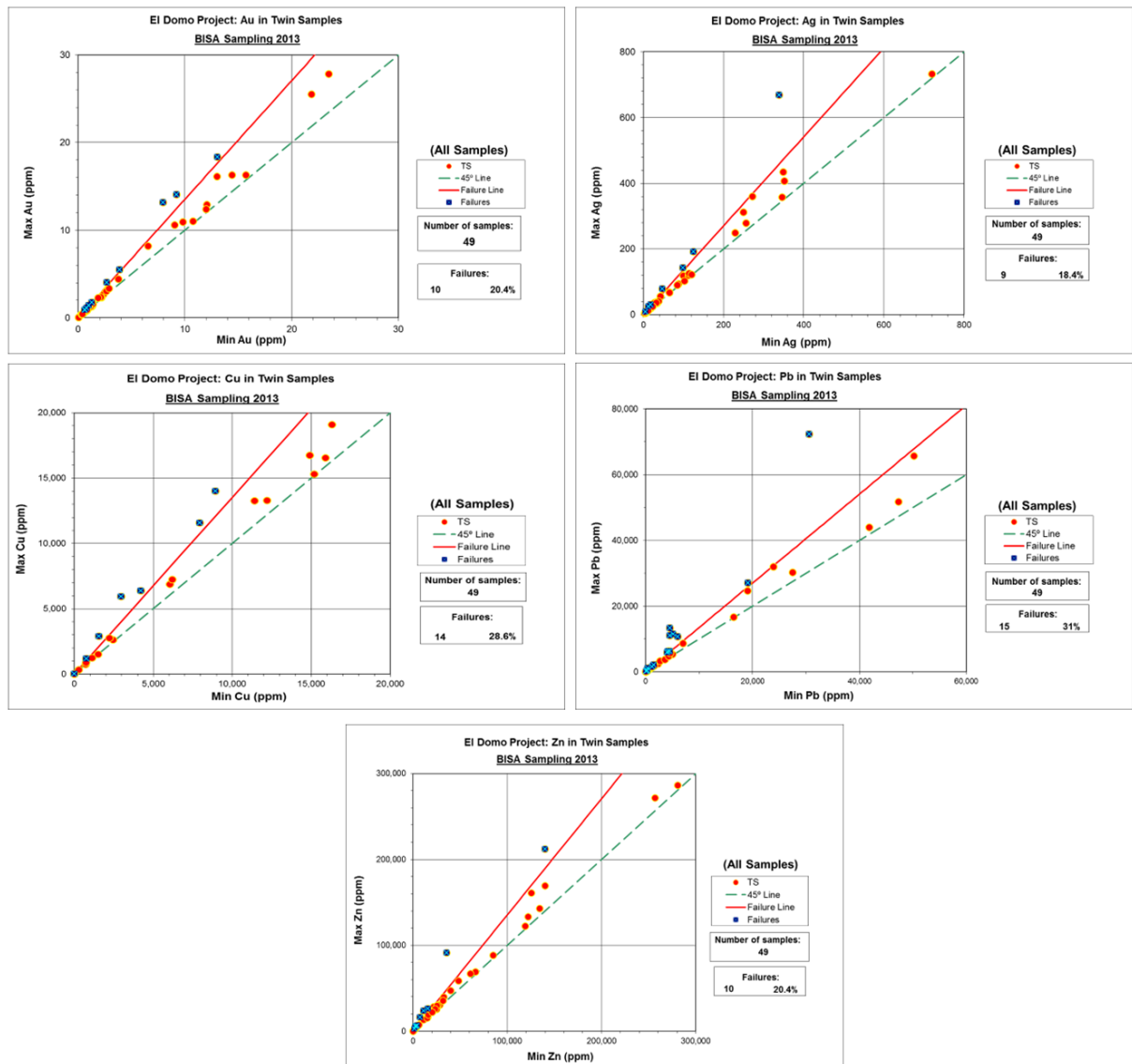


FIGURE 12.9 TWIN SAMPLES MAX-MIN CHARTS FOR GOLD, SILVER, COPPER, LEAD, AND ZINC

DUPLICATE SAMPLES

BISA selected 93 duplicate samples of coarse rejects and pulps, representative of the four drilling campaigns conducted by Salazar in El Domo (Table 12.22).

TABLE 12.22 DUPLICATE SAMPLES — BISA 2013

Sample Type	Quantity
Coarse Rejects	52
Pulp	41
TOTAL	93

COARSE REJECT DUPLICATES

These samples correspond to the rejects obtained at the crushing and splitting stage (material under 2 mm that passes through the No. #10 mesh) of the drilling cores in the ALS Global and Inspectorate laboratories. The coarse duplicates are used to identify any possible errors and contamination during sample splitting and grinding. Fifty-two stored samples were selected from the Salazar warehouses in the city of Quito. The samples were rebagged, tagged, and sent to the facilities of ALS Global in Quito for preparation.

BISA prepared Max-Min scatter plots for Au, Ag, Cu, Pb, and Zn using a relative error limit of $\pm 20\%$ (Figure 12.10). As in the previous case, the result is considered acceptable when the number of failed samples does not exceed 10% of the pairs used. The results indicate values below 10% for all the elements considered (Table 12.23) and therefore corroborate acceptable preparation, splitting, and sub-sampling practices, and adequate precision in the laboratories.

TABLE 12.23 COARSE REJECT DUPLICATE RESULTS

Sample Type	Element	Samples	Failures	Failures (%)
Coarse duplicate	Au	52	4	7.7
	Ag	52	2	3.8
	Cu	52	2	3.8
	Pb	52	4	7.7
	Zn	52	3	5.8

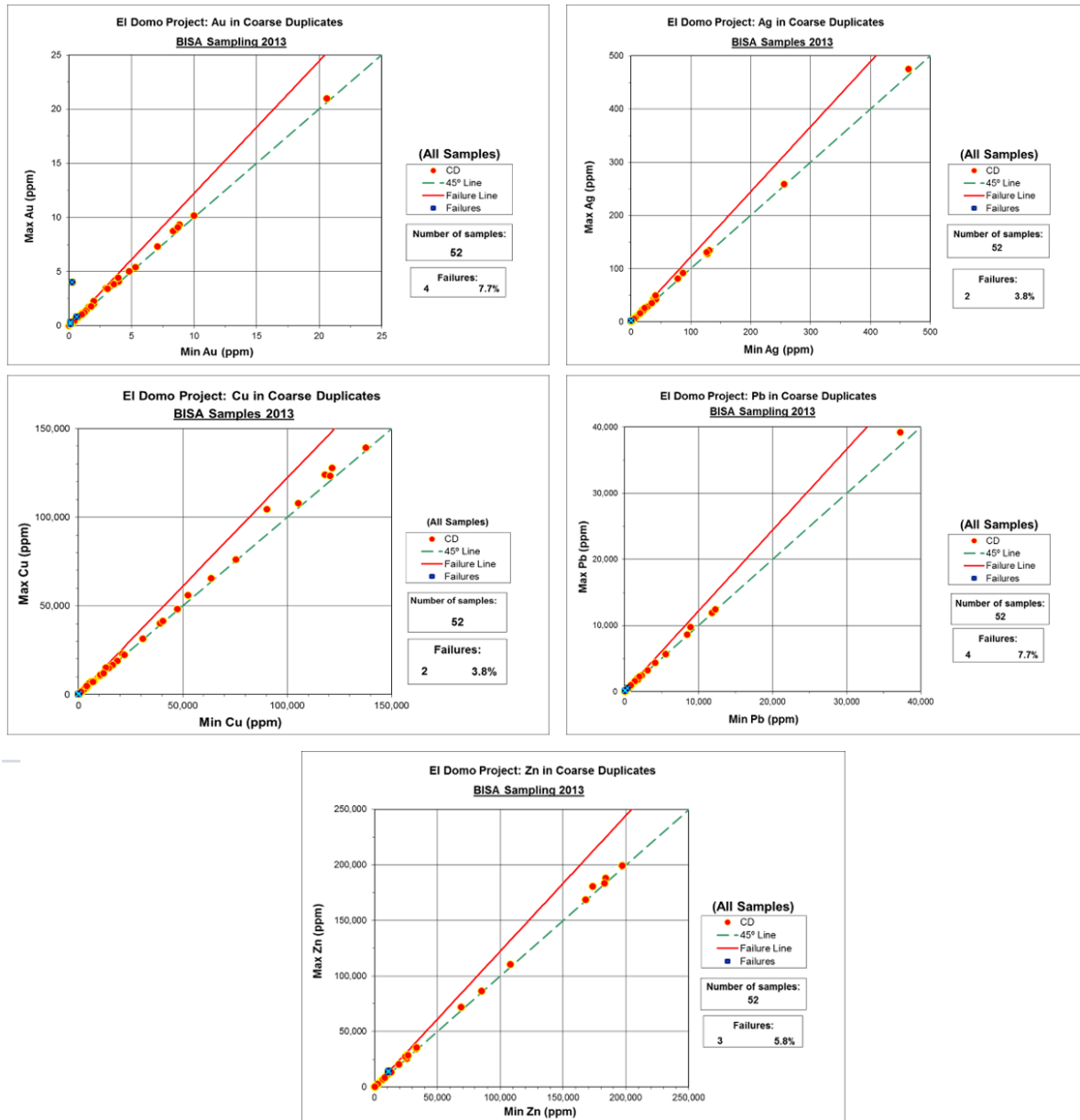


FIGURE 12.10 COARSE REJECT DUPLICATE MAX-MIN CHARTS FOR GOLD, SILVER, COPPER, LEAD, AND ZINC

PULP DUPLICATES

Pulp duplicates are generally used to evaluate a laboratory's analytical precision. In total, BISA analysed 41 representative pulp duplicate samples from the four diamond drilling campaigns undertaken by Salazar. Of these, 31 (75%) correspond to samples originally prepared and analysed by Inspectorate, and 10 (25%) to samples prepared and analysed by ALS Global.

The pulp samples were collected from the Salazar warehouses in Quito. These samples were obtained from the splitting of the original preserved pulps, which were prepared by grinding 1.5 kg of sample down to a grain size of less than 85% <75 microns (mesh No. #200) for the ALS Global laboratory, and grinding 300 g to 95% <106 microns (mesh No. #140) for the Inspectorate laboratory.

BISA has prepared hyperbolic Max-Min scatter plots for Au, Ag, Cu, Pb, and Zn using a relative error limit of $\pm 10\%$ (Figure 12.11). The statistical reports indicate, in all cases, that the number of failed samples is above the 10% tolerance limit (Table 12.24). This is particularly significant for Au (36.6%) and Pb (31.7%).

TABLE 12.24 PULP DUPLICATE RESULTS

Sample Type	Element	Samples	Failures	Failures (%)
Pulp duplicate	Au	41	15	36.6
	Ag	41	5	12.2
	Cu	41	7	17.1
	Pb	41	13	31.7
	Zn	41	6	14.6

It should be noted that most of the failures reported reflect samples with low metal values, near the lower analytical detection limit. In the case of Au, differences in mass for the samples analysed (30 g for Inspectorate and 50 g for ALS Global) could be the cause of failures. The segregation of sulphide particles in the stored pulp could also generate failures if they were not properly homogenized prior to extraction of the increase.

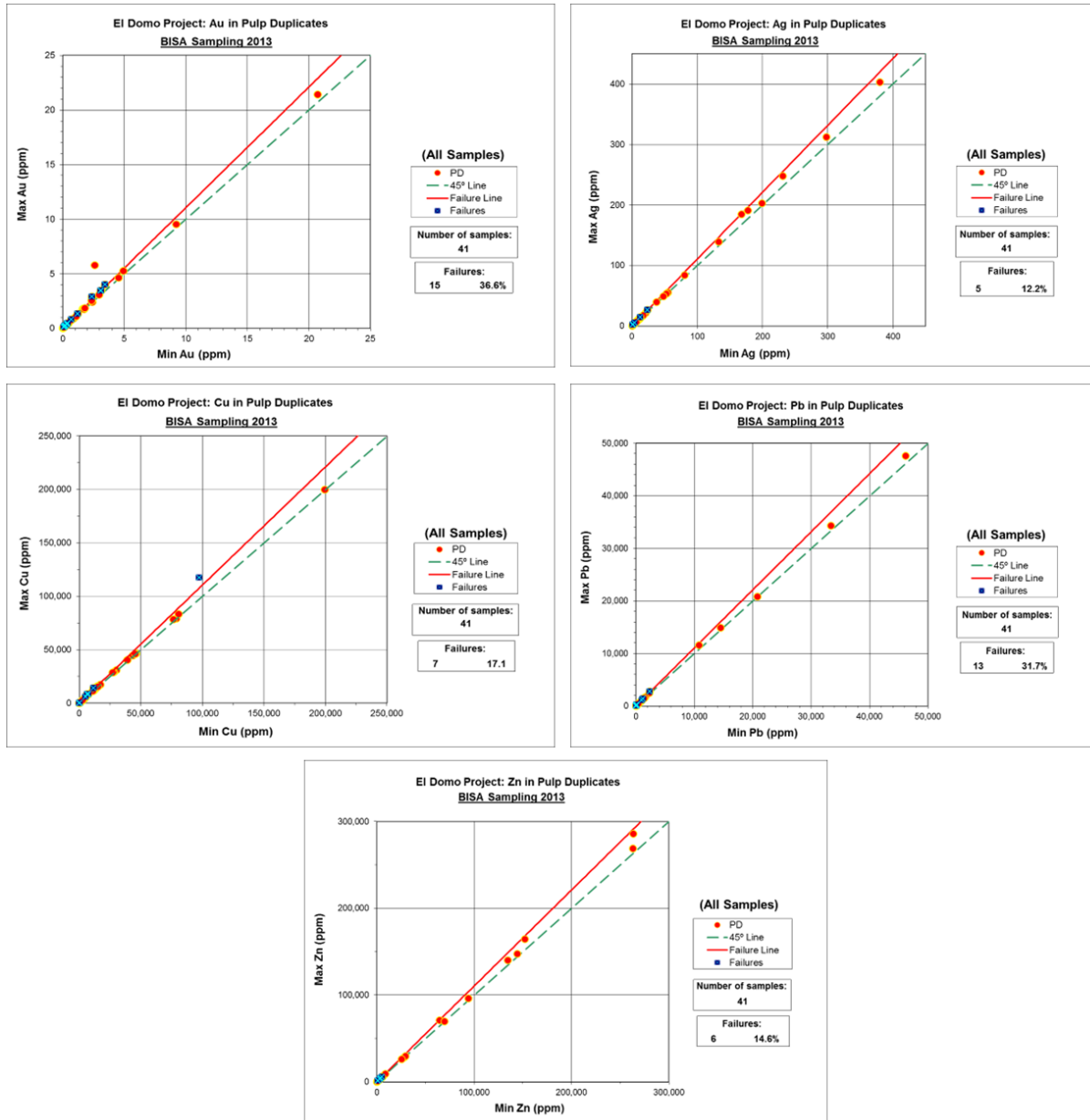


FIGURE 12.11 PULP DUPLICATES MAX-MIN CHARTS FOR GOLD, SILVER, COPPER, LEAD, AND ZINC

Table 12.25 shows the total duplicates analysed. The samples originally analysed at the Inspectorate laboratory showed a greater number of failures for Au and Pb, and to lesser extent Zn and Ag, all of which could indicate precision problems. The failures could also be due to differences in the analytical procedures and techniques at the two laboratories (particle size, digestion, weight of the increment analysed, instrumental, etc.). BISA recommend that a standard protocol should be implemented when using different labs on the same project.

TABLE 12.25 SUMMARY OF FAILED PULP DUPLICATE SAMPLES

Laboratory	Samples	%	Failures Au		Failures Ag		Failures Cu		Failures Pb		Failures Zn	
				%		%		%		%		%
ALS Global	10	24	2	13	0	0	2	29	0	0	0	0
Inspectorate	31	76	13	87	5	100	5	71	13	100	6	100
Total	41	100	15	100	5	100	7	100	13	100	6	100

BLANK SAMPLES

Salazar provided BISA with 11 fine blank samples (code BK) prepared by Inspectorate Services for use in the QA/QC program. Ten of these samples were inserted for controls for the ALS Global laboratory and one for a control for Acme Labs.

The blank pulps were usually inserted after heavily mineralized samples to verify whether contamination occurred during laboratory analyses. The analytical results of these blanks are shown in Table 12.26 and Table 12.27.

TABLE 12.26 BLANK SAMPLE RESULTS — ALS GLOBAL

Sample ID	Batch	Au-AA26	ME-ICP41	ME-ICP41	ME-ICP41	ME-ICP41
		Au (ppm)	Ag (ppm)	Cu (ppm)	Pb (ppm)	Zn (ppm)
170419	QU13096102	0,01	0,2	119	5	97
170456	QU13096102	0,01	0,2	148	5	67
170484	QU13096103	0,01	<0.2	100	2	51
170514	QU13096991	0,01	0,3	117	4	93
170526	QU13096105	0,01	0,2	100	2	52
170563	QU13097230	0,01	0,2	102	<2	52
170590	QU13097231	0,01	0,6	107	2	55
170591	QU13096106	0,01	<0.2	101	<2	53
170595	QU13096107	0,02	<0.2	101	2	52
170602	QU13097232	<0.01	0,2	101	2	51

TABLE 12.27 BLANK SAMPLE RESULTS — ACME GLOBAL

BISA Sample ID	Batch	G6-50	1D	1D	1D	1D
		Au (ppm)	Ag (ppm)	Cu (ppm)	Pb (ppm)	Zn (ppm)
170605	LAA13000067	0,007	<0.3	114	<3	59

The blank samples were evaluated in graphs with the blank values plotted on the Y axis and values for the previous samples plotted on the X axis (Figure 12.12). This type of graph clearly identifies and determines contamination patterns.

A blank sample is considered to have failed if the reported values are significantly higher at the corresponding lower limit of detection and lie above the safe line. In the case of elements with values above the respective detection limit, the sample is considered failed when the analysis reports results significantly higher than those of the certified blank. For Au, Ag, and Pb, the results were below the safe line, which is adequate, whereas for Cu and Zn some samples had values slightly above the certified blank values (97 ± 12 ppm Cu and 46 ± 8 ppm Zn). Nevertheless, the low values in both cases indicate there has been no significant contamination during the analytical process at ALS Global and Acme Labs.

In any case, though, the values for copper (97 ± 12 ppm Cu) and zinc (46 ± 8 ppm Zn) in the certified blanks are too high for a material of this type. In future, it is advisable that Salazar obtain materials with geochemical values for Cu and Zn close to the lower limits of detection.

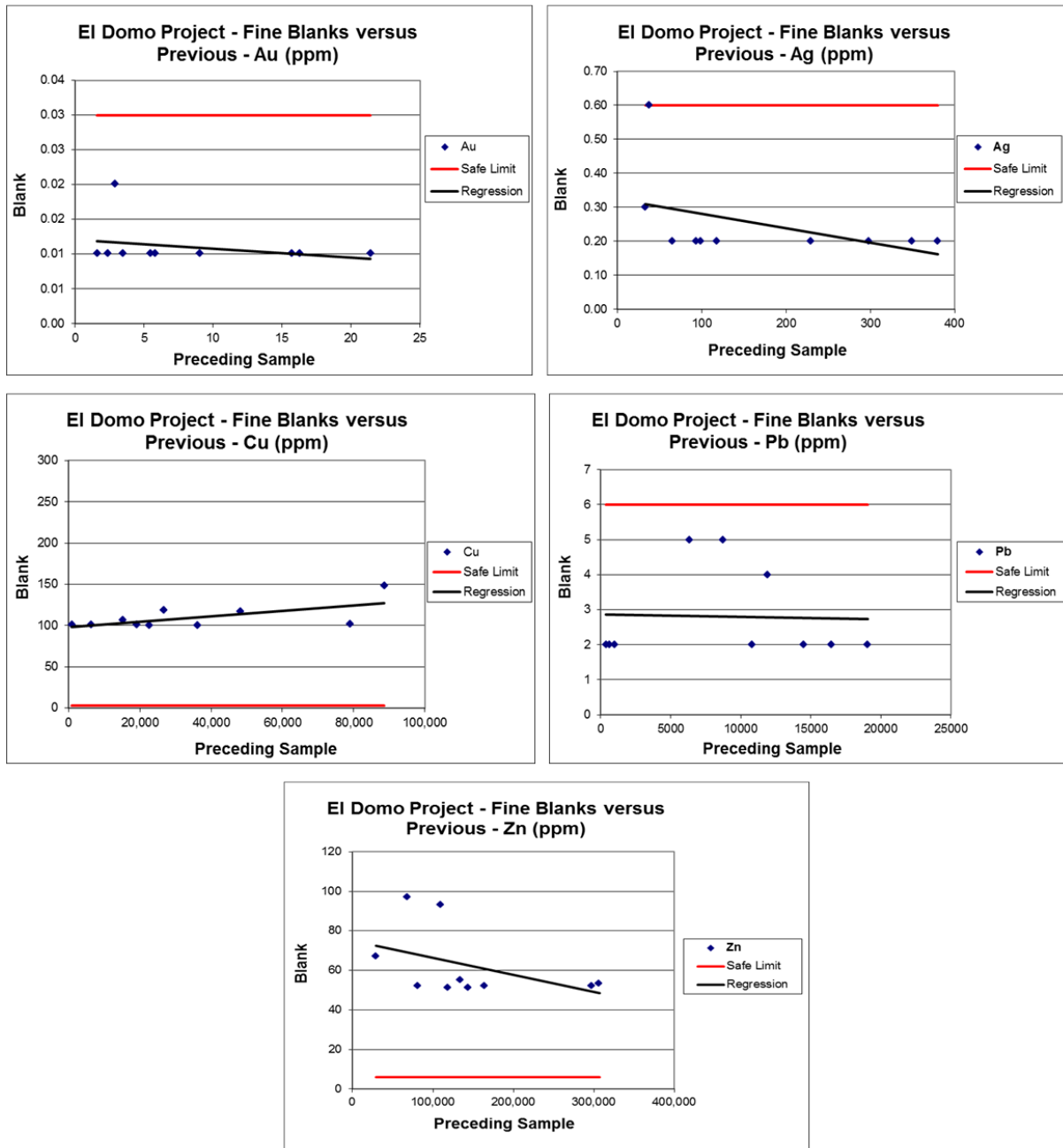


FIGURE 12.12 STATISTICAL CHARTS FOR BLANK BK

VERIFICATION SAMPLING 2

BISA conducted a second verification sampling in July of 2013 to determine possible causes for the failures reported in pulp duplicates analysed in the first sampling. To this end, BISA selected 50 representative samples, for which existing rejects and pulps were used. They were prepared and analysed in the ALS Global laboratory (100 analyses) using the same methods as in the previous sampling. To ensure sample representativeness, the analyses considered the four drilling campaigns conducted, the three mineral domains defined, and

the two analytical laboratories used (ALS Global and Inspectorate) (Table 12.28 and Table 12.29).

TABLE 12.28 SUMMARY OF VERIFICATION SAMPLING 2 — BISA 2013

Drilling program	Samples	%
I	13	28
II	5	11
III	20	43
IV	12	26
TOTAL	50	100

TABLE 12.29 SUMMARY OF SAMPLES BY ANALYTICAL LABORATORY

Laboratory	Samples	%
ALS Global	11	23
Inspectorate	36	77
Total	47	100

A total of 18 control samples (duplicates, blanks, and standards) were inserted (Table 12.30).

TABLE 12.30 QA/QC SAMPLE VERIFICATION SAMPLING 2

Type	Rejects	Pulps
Duplicate	5	5
Blank	2	2
Standard	2	2
Total	9	9

Three samples were discarded from this study due to the wide variations observed in the analytical results for Au, Ag, Cu, Pb, and Zn. These failures were attributed to improper labelling of samples 153933, 153877, and 153878 for drill CURI-08-22 from the first drilling campaign (Table 12.31). Therefore, only 47 samples were considered in this study.

TABLE 12.31 SAMPLES DISCARDED WITH ERRORS

HOLE ID	REJECTS								PULPS					
	Au-AA26 Au_ppm	ME-ICP41 Ag_ppm	ME-ICP41 Cu_ppm	ME-ICP41 Pb_ppm	ME-ICP41 Zn_ppm	Ag-AA46 Ag_ppm	Cu-AA46 Cu_%	Zn-AA46 Zn_%	Au-AA26 Au_ppm	ME-ICP41 Ag_ppm	ME-ICP41 Cu_ppm	ME-ICP41 Pb_ppm	ME-ICP41 Zn_ppm	Cu-AA46 Cu_%
CURI-08-22	1.5	>100	669	3920	6720	160			0.07	1	22	30	53	
CURI-08-22	5.43	76.9	>10000	2690	>10000		3.571	2.66	0.37	94.6	>10000	96	90	3.002
CURI-08-22	2.71	49	>10000	2280	>10000		1.792	1.925	0.09	1.7	778	59	119	

HOLE ID	Salazar	Au (g/t)	Ag (g/t)	Cu (ppm)	Pb (ppm)	Zn (ppm)	BISA
CURI-08-22	153933	1.616	142.1	601	3496	5569	2162
CURI-08-22	153877	5.5	75.8	35100	1371	24800	2163

SAMPLE PREPARATION AND ASSAY

Samples of rejects and pulps were selected by BISA and collected by Salazar personnel. The samples were prepared and analysed at ALS Global using the same parameters and protocols as in the first verification sampling. In this case, the pulps were mechanically homogenized using the HOM-01m method (mechanical homogenization of pulp or crushed materials) before extraction of the increase to prevent possible problems with sulphide segregation.

CERTIFIED REFERENCE MATERIALS

Salazar provided BISA with two reference materials (standards) prepared by WCM Minerals of Canada:

- 1) Reference material CU 145 for copper and silver, with the values: $3.01 \pm 0.038\%$ Cu and 93 ± 1.45 g/t Ag
- 2) Reference Material CU 163 for gold, silver, and copper with the values: 4.35 ± 0.069 g/t Au, 99 ± 1.48 g/t Ag, and $1.06 \pm 0.014\%$ Cu

Both reference materials were inserted in batches of pulps and rejects to estimate the laboratory's analytical accuracy.

BISA prepared statistical control charts for the elements Au, Ag, and Cu for CU 145 and CU 163 using confidence intervals of $\pm 2SD$ and $\pm 3SD$ (Figure 12.13 and Figure 12.14).

REFERENCE MATERIAL CU 145

One sample of standard CU 145 was inserted in the batch of coarse rejects and another in the batch of pulps sent to ALS Global. The analytical results for sample 1393 (corresponding to standard CU 145) did not match the certified values for Cu and Ag, evidently due to an insertion error (see Table 12.32 for results).

TABLE 12.32 ANALYTICAL RESULTS FOR REFERENCE MATERIAL CU 145

STANDARD	BISA	Batch	ME-ICP41	ME-ICP41
			Ag_ppm	Cu_ppm
CU 145	1393	LI13156075	156	640
CU 145	1743	LI13156075	93,5	30810

The values for Cu and Ag from the other standard sample (1743) are within the $\pm 2SD$ limits (Figure 12.13).

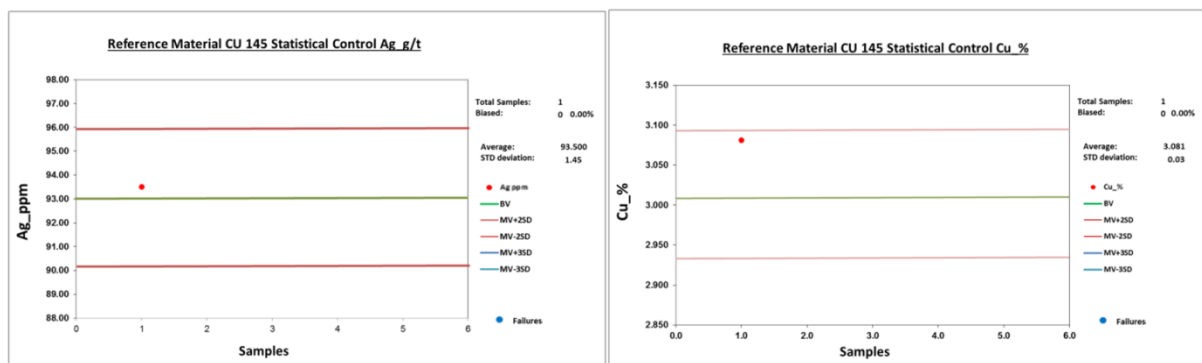


FIGURE 12.13 STATISTICAL CONTROL CHARTS FOR REFERENCE MATERIAL CU 145

REFERENCE MATERIAL CU 163

One sample of standard CU 163 was inserted in the batch of coarse rejects and another in the batch of pulps. The analytical results for Au, Ag, and Cu are reported in Table 12.33.

TABLE 12.33 ANALYTICAL RESULTS FOR REFERENCE MATERIAL CU 163

STANDARD	BISA	Batch	Au-AA26	ME-ICP41	ME-ICP41
			Au_ppm	Ag_ppm	Cu_ppm
CU 163	1593	LI13156075	4,82	98,1	10650
CU 163	1443	LI13156075	3,97	104	10680

BISA prepared statistical control charts for the elements Au, Ag, and Cu using the $\pm 2SD$ and $\pm 3SD$ as confidence intervals for the best value (Figure 12.14). The charts show that the Ag and Cu values are within acceptable limits, but Au gives one failure outside the $\pm 3SD$ limits (Table 12.34).

TABLE 12.34 REFERENCE MATERIAL COPPER 163 RESULTS SUMMARY

Standard	Element	Unit	Samples	Failures	Bias (%)
CU 163	Au	ppm	2	1	50
	Ag	ppm	2	0	0
	Cu	%	2	0	0

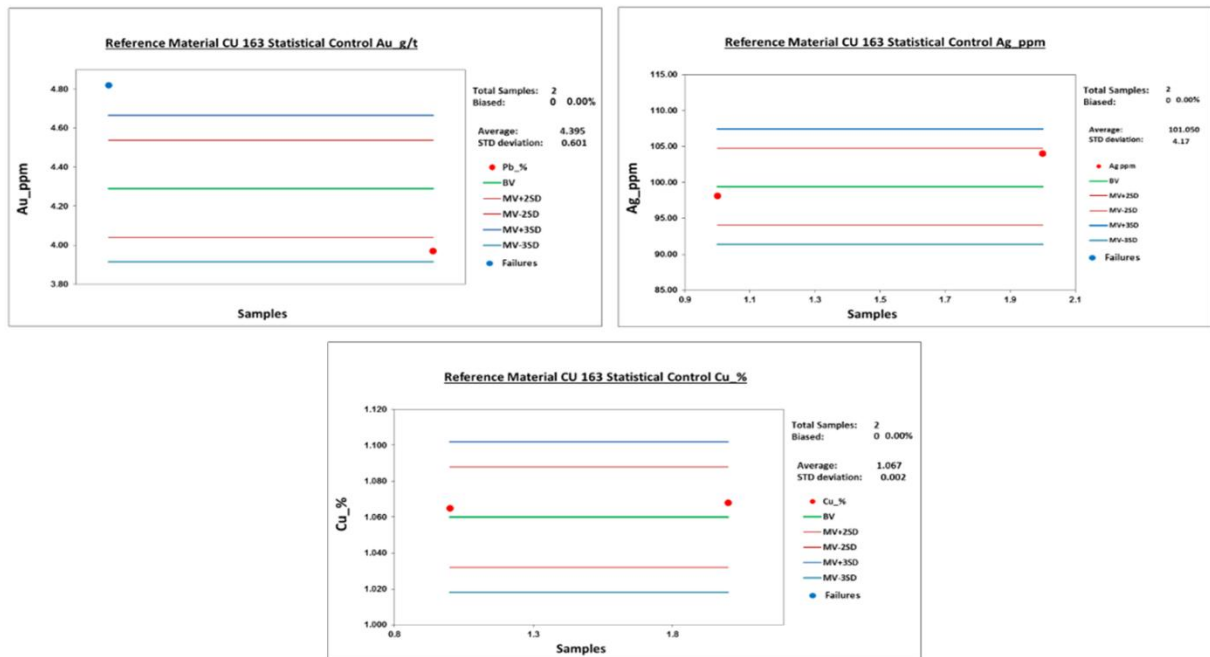


FIGURE 12.14 STATISTICAL CONTROL CHARTS FOR REFERENCE MATERIAL CU 163

Overall, the results are acceptable, but the small number of standard samples used does not allow us to provide any statistical validity to the failures reported.

COARSE REJECT DUPLICATES

BISA has selected a total of 47 samples of coarse rejects to compare the results with the originals reported by Salazar and with their corresponding pulps re-analysed by BISA to verify the precision of the primary laboratory and to evaluate possible errors or contamination arising during the mechanical preparation (splitting, sub-sampling, and pulverization).

The samples were prepared at the ALS laboratory in Quito using rejects for material with a particle size of <2 mm (85%) passing through a No. #10 mesh, generated in the crushing stage. These coarse rejects were stored in Salazar's warehouses in Quito.

BISA has prepared Max-Min scatter plots for the elements Au, Ag, Cu, Pb, and Zn using the relative error limit of $\pm 20\%$ (Figure 12.5). A result is considered acceptable when the number of failed samples does not exceed 10% of the pairs used.

All elements considered reported failures below the limit (10%) except zinc (12.8%). Based on these results, the test is deemed acceptable and largely validates Salazar's original results (Table 12.35).

TABLE 12.35 COARSE REJECT DUPLICATE RESULTS OF VERIFICATION SAMPLING 2

Sample Type	Element	Samples	Failures	Failures (%)
Coarse duplicate	Au	47	4	8.5
	Ag	47	3	6.4
	Cu	47	1	2.1
	Pb	47	4	8.5
	Zn	47	6	12.8

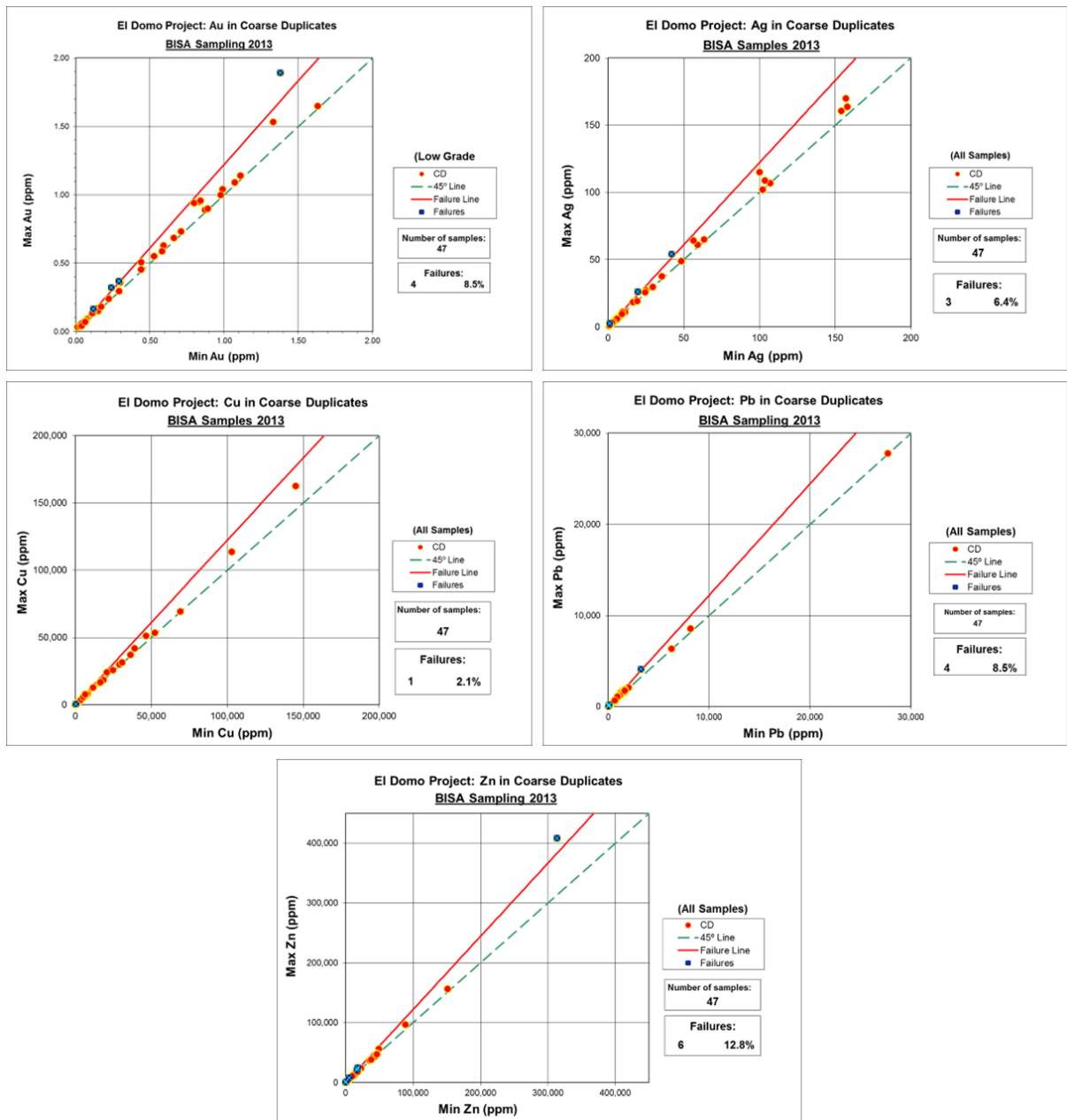


FIGURE 12.15 COARSE REJECT DUPLICATE MAX-MIN CHARTS FOR GOLD, SILVER, COPPER, LEAD, AND ZINC

It should be noted that most of the failures reported originate from samples with the lowest values, at times very near the lower detection limit. In the case of Zn, Pb, and Ag, a higher proportion of failures is noted in the samples originally analysed at the Inspectorate laboratory (Table 12.36).

TABLE 12.36 SUMMARY OF FAILED SAMPLES IN COARSE REJECT DUPLICATES

Laboratory	Samples	%	Au	%	Ag	%	Cu	%	Pb	%	Zn	%
ALS Global	11	23	1	25	1	33	0	0	0	0	1	17
Inspectorate	36	77	3	75	2	67	1	100	4	100	5	83
Total	47	100	4	100	3	100	1	100	4	100	6	100

PULP DUPLICATES

Pulp duplicates are generally used to evaluate a laboratory's analytical precision. In our case, differences in the amount of pulverized material and the particle size of the pulps prepared in the two laboratories introduces a certain degree of variability that could reasonably affect the precision of the analytical results reported.

A total of 47 representative samples of pulp duplicates from the four Salazar diamond drilling campaigns were analysed.

The pulps are pulverized material with 85% particle size at <75 microns (ASTM No. 200 mesh) in the case of ALS Global, and 95% at <106 microns (ASTM No. 140 mesh) in the case of Inspectorate. The amount originally pulverized varied according to the standard procedures at each laboratory: 1.5 kg at ALS Global and 0.3 kg at Inspectorate.

BISA has prepared Max-Min scatter plots for Au, Ag, Cu, Pb, and Zn using the relative error limit of $\pm 10\%$. As in the previous case, a result is considered acceptable when the number of failed samples does not exceed 10% of the total pairs used (Figure 12.16).

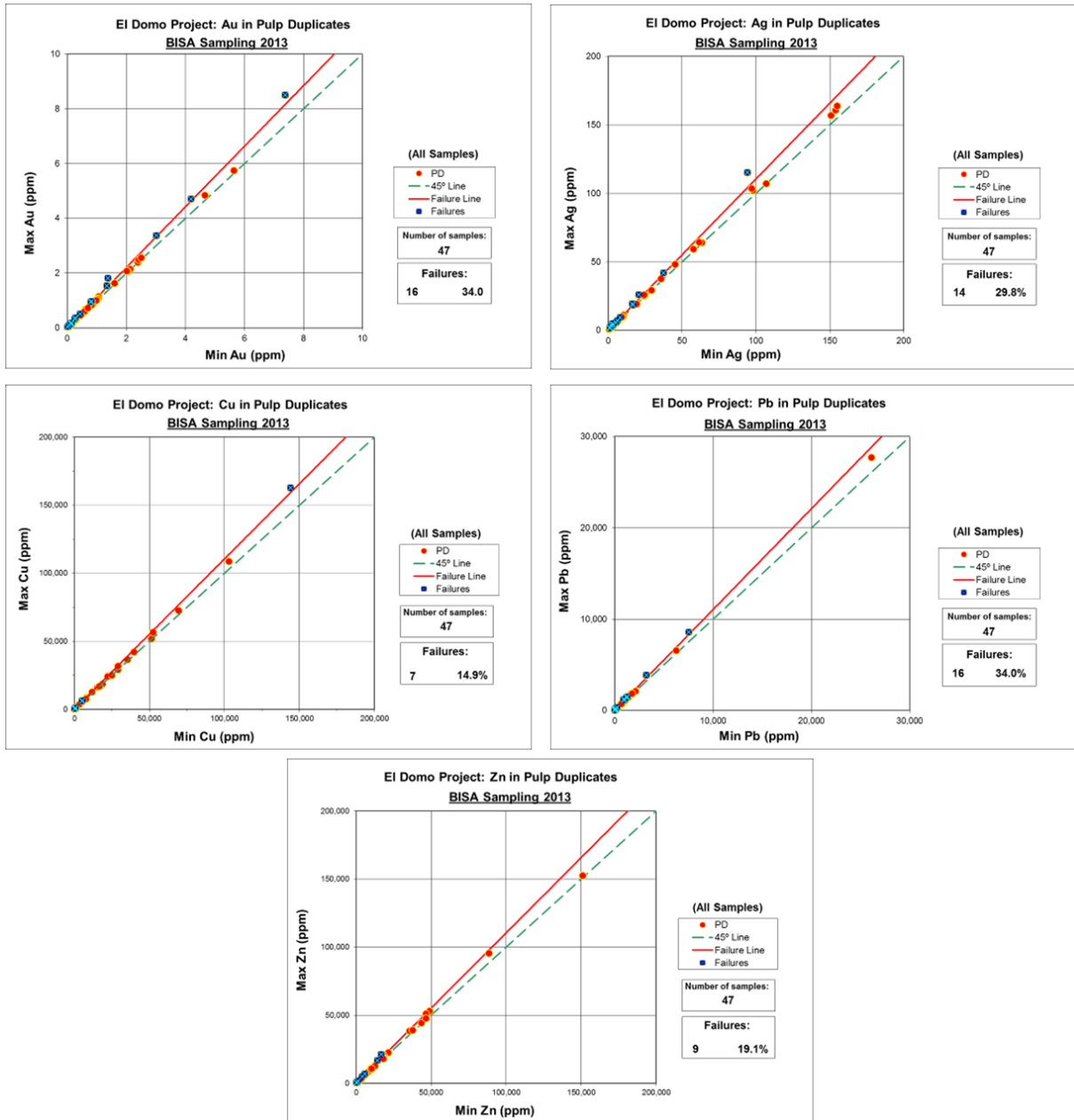


FIGURE 12.16 PULP DUPLICATE MAX-MIN CHARTS FOR GOLD, SILVER, COPPER, LEAD, AND ZINC

In all cases, the results show failed samples above the 10% level of tolerance (Table 12.37), particularly noteworthy for Au and Pb (both 34%), Ag (30%), and to a lesser extent for Cu (15%) and Zn (19%).

TABLE 12.37 SUMMARY OF FAILED SAMPLES - PULP DUPLICATES

Sample Type	Element	Samples	Failures	Failures (%)
Pulp duplicate	Au	47	16	34.0
	Ag	47	14	29.8
	Cu	47	7	14.9
	Pb	47	16	34.0
	Zn	47	9	19.1

As can be seen, a relatively higher proportion of failed samples are from Inspectorate, especially for Ag, Cu, and Zn (Table 12.38).

TABLE 12.38 SUMMARY OF FAILED SAMPLES BY LABORATORY - PULP DUPLICATES

Laboratory	Samples	%	Au	%	Ag	%	Cu	%	Pb	%	Zn	%
ALS Global	11	23	3	19	2	14	1	14	4	25	1	11
Inspectorate	36	77	13	81	12	86	6	86	12	75	8	89
Total	47	100	16	100	14	100	7	100	16	100	9	100

It should be pointed out that many of the failures correspond to samples with low metal contents close to the lower limits for analytical detection (especially for Cu, Pb, and Zn). In the deterministic models for Au, Cu, Pb, and Zn, BISA used the following threshold values for the envelopes: 0.2 g/t Au, 0.3% Cu, 0.8% Zn, and 0.05% Pb. Applying these values to the Max-Min plots, it can be seen that (with the exception of Au) many of the failures fall below the indicated thresholds for all the elements under consideration (i.e. Cu, Pb, and Zn) (Table 12.39).

TABLE 12.39 SUMMARY OF FAILED SAMPLES AS A FUNCTION OF THE THRESHOLDS USED FOR THE DETERMINISTIC MODEL

Cutoff	ALS Global	Inspectorate	Subtotal	Total
Au >= 0.2ppm	2	9	11	16
Au < 0.2ppm	1	4	5	
Cu >= 0.3%	1	2	3	7
Cu < 0.3%	0	4	4	
Pb >= 0.05%	3	4	7	16
Pb < 0.05%	1	8	9	
Zn >= 0.8%	1	2	3	9
Zn < 0.8%	0	6	6	

INTERNAL DUPLICATES

A total of 10 duplicate samples were inserted (5 for the coarse rejects and 5 for the pulps) to verify the precision of the ALS Global laboratory. Table 12.40 and Table 12.41 summarize the analytical results for the elements of interest.

TABLE 12.40 RESULTS FOR INTERNAL DUPLICATES OF COARSE REJECTS

BISA	PRIMARY SAMPLE					BISA	DUPLICATE SAMPLE				
	Au-AA26 Au_ppm	ME-ICP41 Ag_ppm	ME-ICP41 Cu_ppm	ME-ICP41 Pb_ppm	ME-ICP41 Zn_ppm		Au-AA26 Au_ppm	ME-ICP41 Ag_ppm	ME-ICP41 Cu_ppm	ME-ICP41 Pb_ppm	ME-ICP41 Zn_ppm
2158	0.9	17.5	6710	449	6360	2159	0.91	18.2	7080	493	6050
2196	1.65	109	30740	1880	408000	2164	1.64	108	31160	1930	393000
2169	0.29	8.3	331	1110	20100	2170	0.29	8.5	328	1030	19250
2179	0.99	5.8	18560	108	343	2180	0.97	5.7	18360	107	363
2190	1.33	154	69010	2020	96800	2191	1.39	156	72900	2150	102500

TABLE 12.41 RESULTS FOR INTERNAL DUPLICATES OF PULP SAMPLES

BISA	PRIMARY SAMPLE					BISA	DUPLICATE SAMPLE				
	Au-AA26 Au_ppm	ME-ICP41 Ag_ppm	ME-ICP41 Cu_ppm	ME-ICP41 Pb_ppm	ME-ICP41 Zn_ppm		Au-AA26 Au_ppm	ME-ICP41 Ag_ppm	ME-ICP41 Cu_ppm	ME-ICP41 Pb_ppm	ME-ICP41 Zn_ppm
2094	2.13	107	51900	635	43400	2103	2.29	106	50540	624	43000
2102	0.91	16.8	6440	418	5380	2108	0.88	17.2	6530	444	5410
2123	1	5.6	18500	107	355	2114	0.93	5.5	18080	105	346
2134	1.34	154	72440	2120	95500	2124	1.34	154	71210	2150	98100
2095	0.15	2	7760	45	505	2135	0.15	2	7980	51	501

BISA prepared Max-Min scatter plots for Au, Ag, Cu, Pb, and Zn using a relative error limit of $\pm 10\%$ (Figure 12.17 and Figure 12.18). For the duplicate pulps, none of the elements had failed samples except one for Pb. This test shows good analytical precision, confirming that the pulps were properly homogenized prior to extraction of the increment.

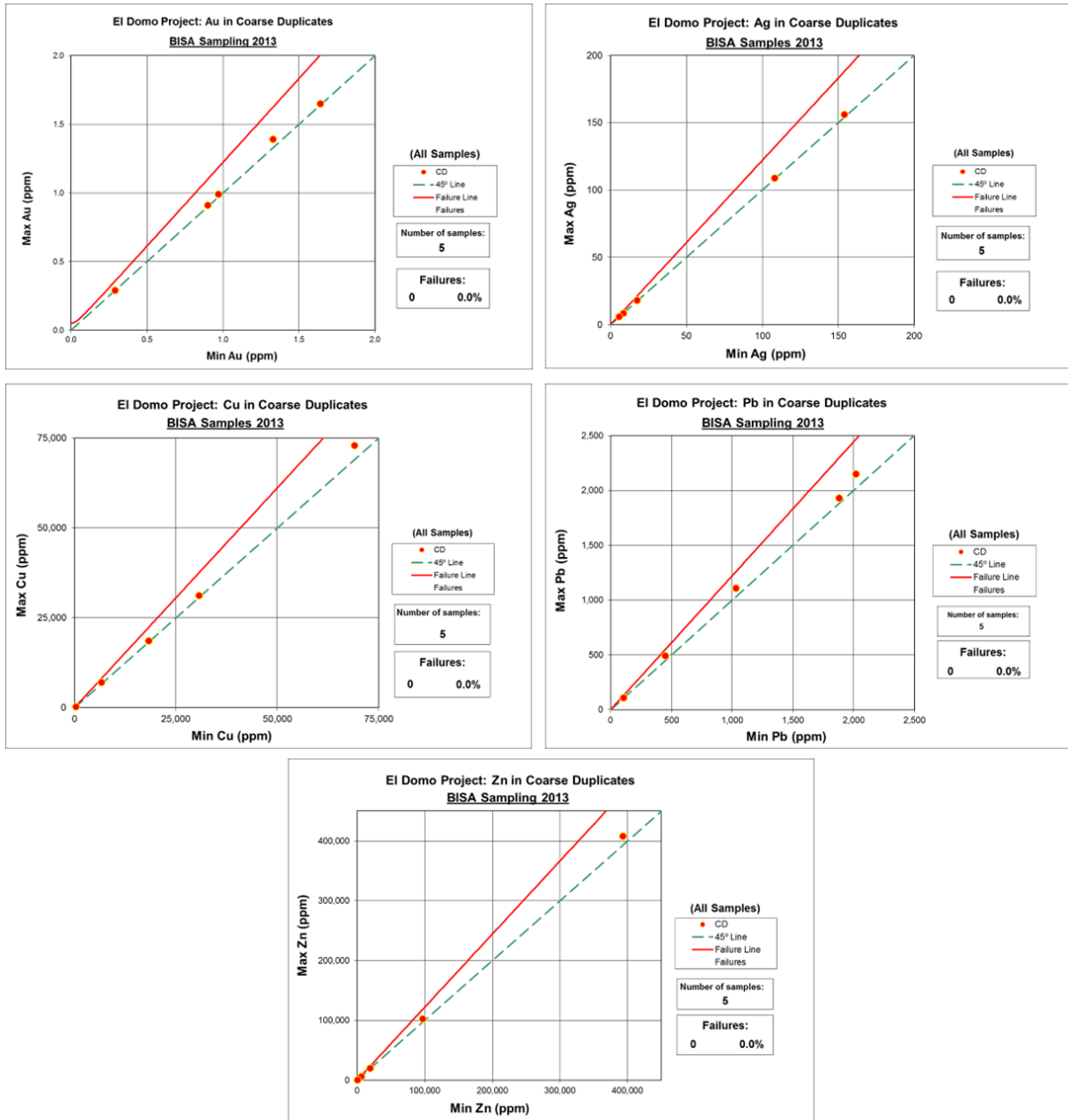


FIGURE 12.17 INTERNAL DUPLICATES OF COARSE REJECTS MAX-MIN CHART FOR GOLD, SILVER, COPPER, LEAD, AND ZINC

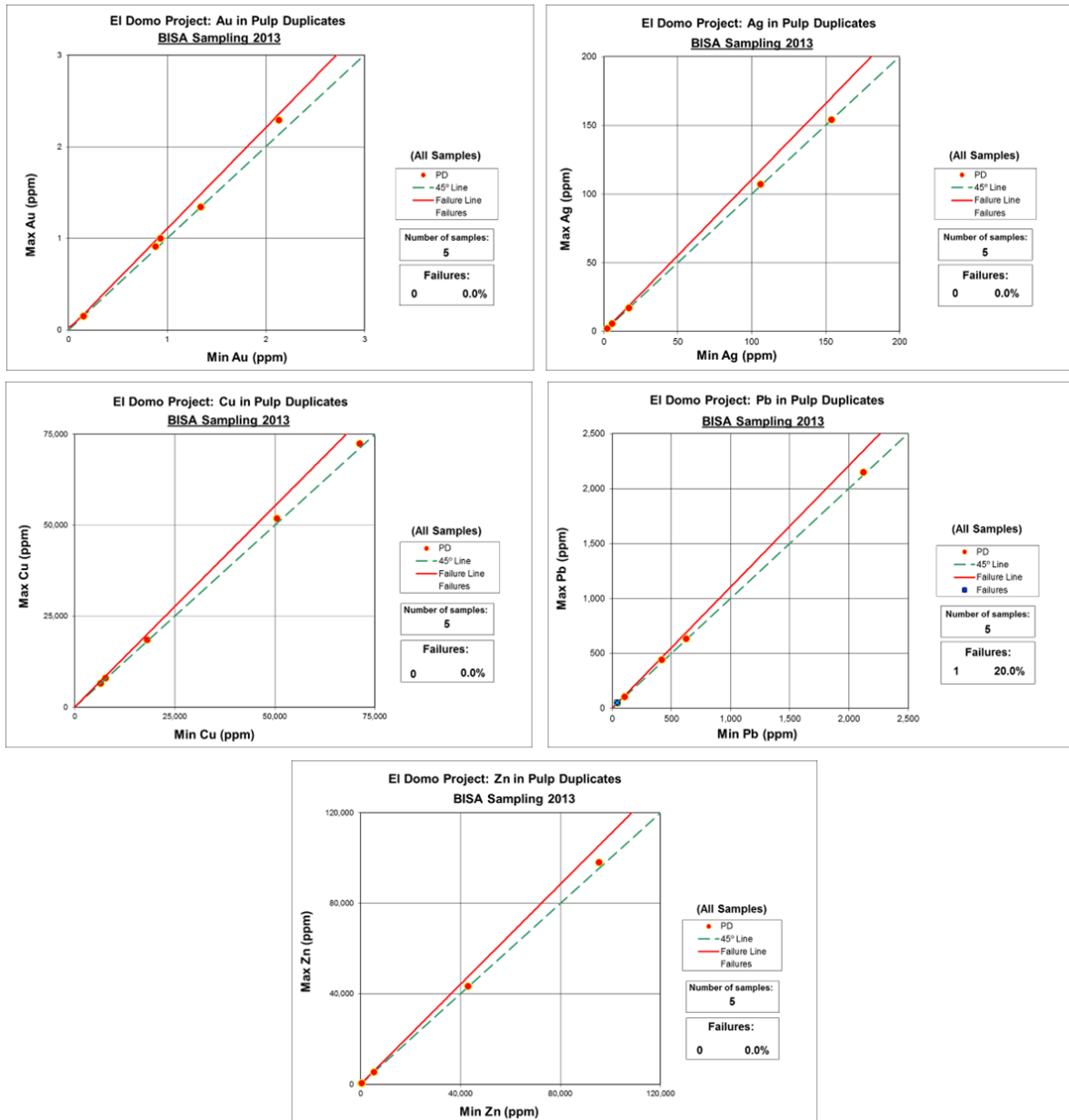


FIGURE 12.18 INTERNAL DUPLICATES OF PULP SAMPLES MAX-MIN CHART FOR GOLD, SILVER, COPPER, LEAD, AND ZINC

BLANK SAMPLES

As part of BISA's QA/QC system, BK standard fine blanks prepared by Inspectorate and provided by Salazar were inserted. These blanks are generally inserted just after heavily mineralized samples to detect possible contamination during the analytical procedure. A total of four blank samples were utilized, two inserted in the batch of coarse rejects and two in the batch of pulps. The results reported by ALS Global Lima are shown in Table 12.42.

TABLE 12.42 ANALYTICAL RESULTS FOR BLANK BK

REJECTS		Au-AA26	ME-ICP41	ME-ICP41	ME-ICP41	ME-ICP41
Code	Batch	Au_ppm	Ag_ppm	Cu_ppm	Pb_ppm	Zn_ppm
1543	LI13156075	0.01	<0.2	100	4	52
1793	LI13156075	<0.01	<0.2	100	3	51
PULPS		Au-AA26	ME-ICP41	ME-ICP41	ME-ICP41	ME-ICP41
Code	Batch	Au_ppm	Ag_ppm	Cu_ppm	Pb_ppm	Zn_ppm
1360	LI13156075	0.01	<0.2	99	3	51
1493	LI13156075	0.01	<0.2	107	3	53

The blank samples were evaluated by plotting the blanks (Y axis) against the previous sample (X axis) (see Figure 12.19). This type of graph enables a clear identification of potential contamination by a highly mineralized sample.

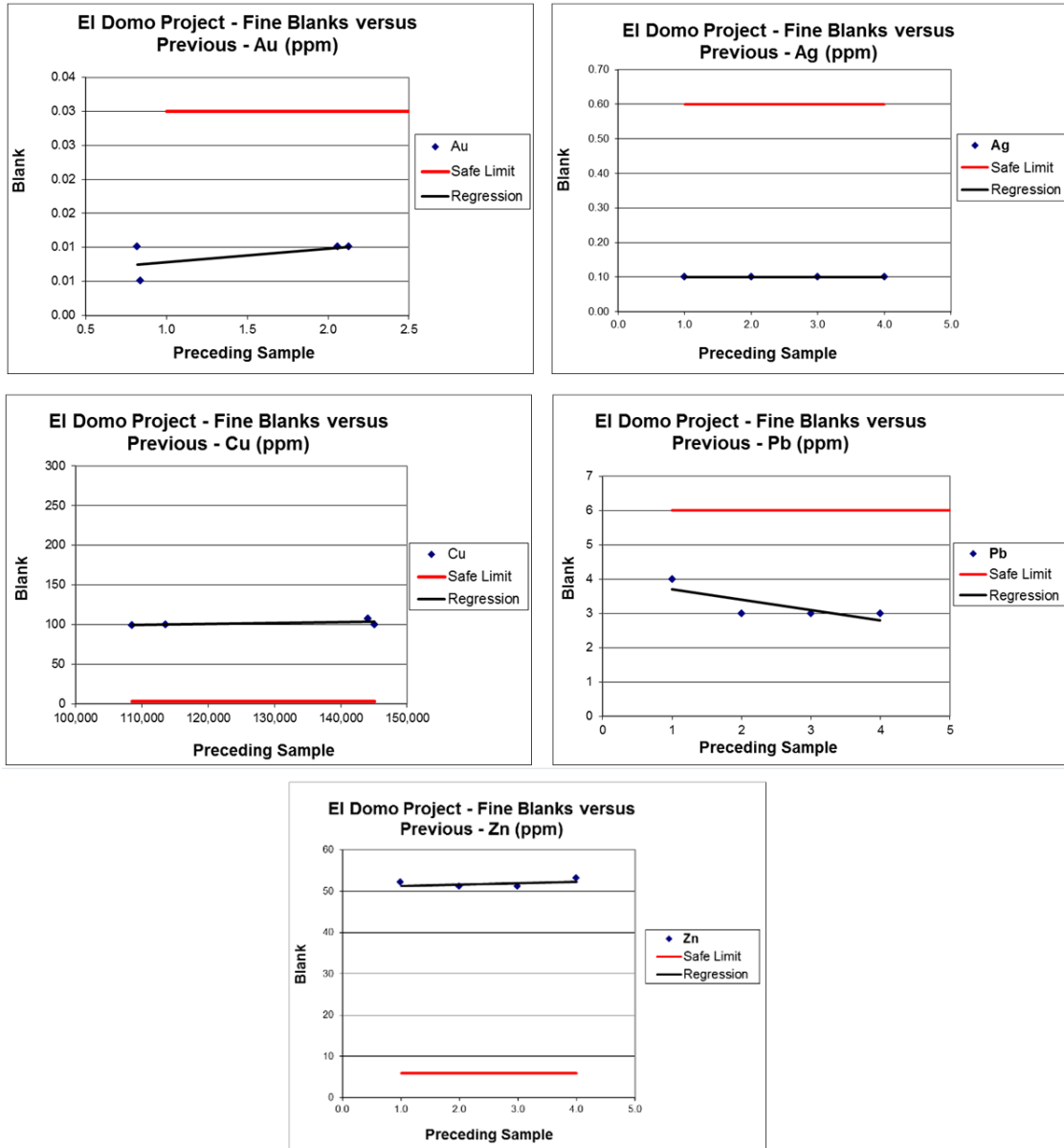


FIGURE 12.19 STATISTICAL CONTROL CHARTS FOR BLANK BK

A blank sample is considered to have failed if the analysed values are significantly higher than those reported on the corresponding certificate. These failed samples plot above the safe limit with a value three times the detection limit. Au, Ag, and Pb fall below the safe limit, which is ideal. In contrast, Cu and Zn lie above the safe limit because this blank's original contents in these elements are much higher than the lower detection limits of the analytical method used.

The low values reported for Au, Ag, and Pb indicate a lack of contamination in the analytical process of ALS Global laboratories. It was also concluded that this certified blank is not suitable because of its high Cu and Zn levels. Therefore, BISA recommends using blanks with metal levels near the detection limits used in the analytical laboratories.

13. MINERAL PROCESSING AND METALLURGICAL TESTING

BISA commissioned Transmin Metallurgical Consultants. (Lima, Peru) to design and supervise the metallurgical testwork. Transmin was also responsible for reviewing the metallurgical studies for the El Domo project in 2008 and 2010.

METALLURGICAL SAMPLES

The samples and composites were selected from the block model reported by Lavigne and McMonies in 2011.

Three metallurgical mineral types were initially defined by mutual accord between Salazar and BISA. These mineral types are based on the Cu/(Zn+Pb) ratio distribution as follows:

- Type 1: Zinc mineral: $Cu/(Zn+Pb) < 0.33$
- Type 2: Mixed Cu/Zn mineral: $0.33 \leq Cu/(Zn+Pb) \leq 3$
- Type 3: Copper mineral: $Cu/(Zn+Pb) > 3$

A total of 134 samples were selected by Transmin and extracted by Salazar from their drill-core warehouse in the city of Ventanas.

The criteria applied in the sample extraction for generating the three composites were:

- Cu/(Zn+Pb) metal ratio
- Spatial distribution
- Lithologies
- Geological zones
- Distribution of grades

Finally, the samples were grouped according to the Cu/(Zn + Pb) metal ratio and labelled as:

- Composite CPO-001: Zinc mineral: $Cu/(Zn+Pb) < 0.33$.
- Composite CPO-002: Mixed Cu/Zn mineral: $0.33 \leq Cu/(Zn+Pb) \leq 3$
- Composite CPO-003: Copper mineral: $Cu/(Zn+Pb) > 3$

REPRESENTATIVITY OF THE 2013 BLOCK MODEL

At the beginning of November 2013, BISA generated a new block model (2013 Block Model), making it necessary to check the representativity of the samples used. Figure 13.1 shows the distribution of tonnes and metal contents in Cu, Zn, and Pb for both block models (note slight differences between the two models).

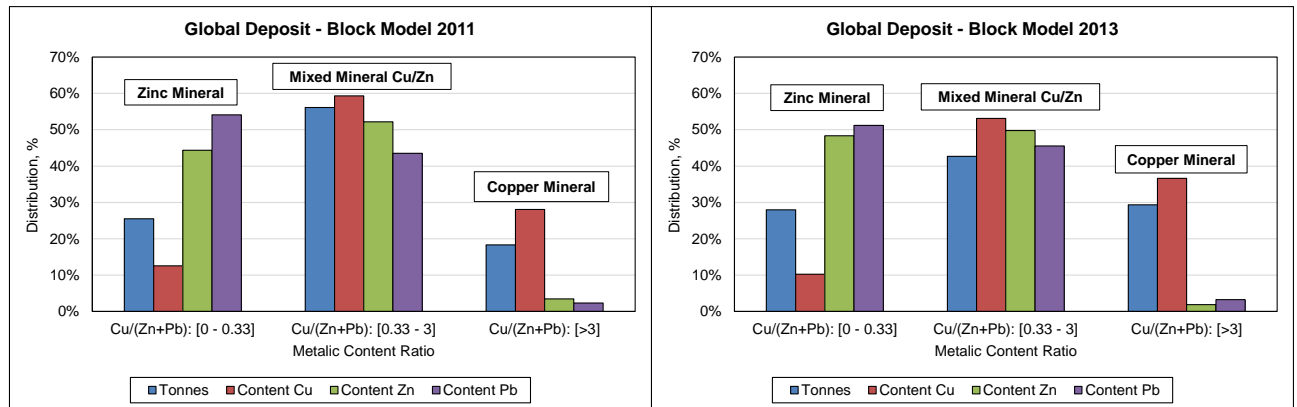
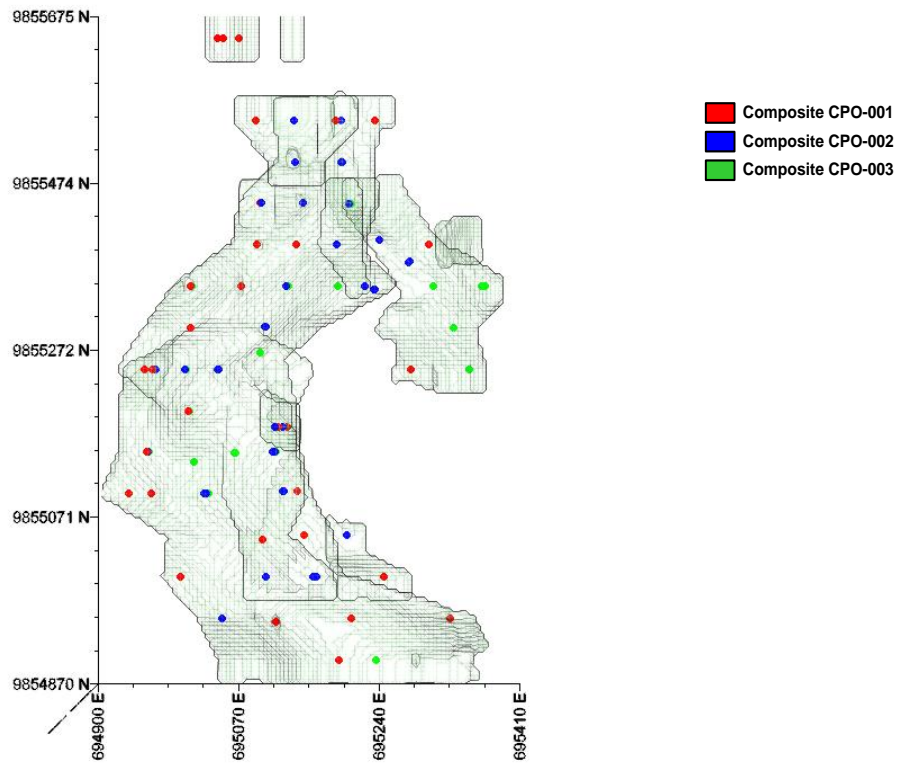


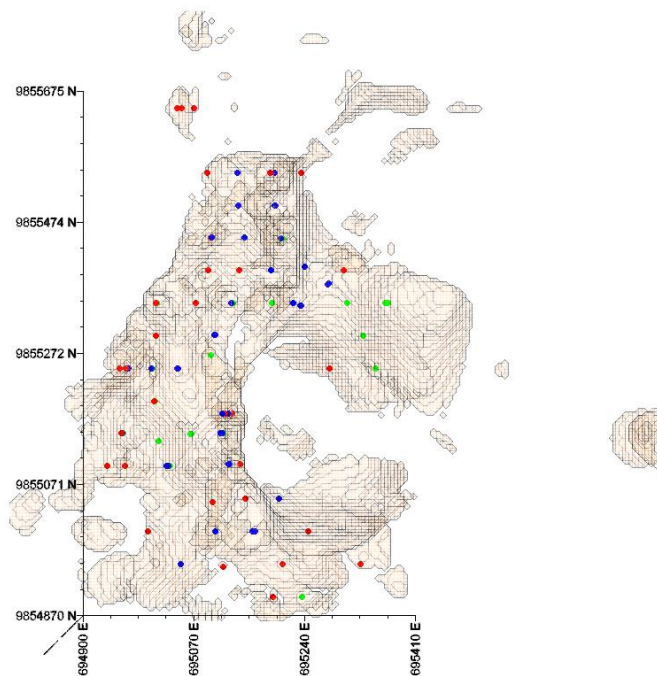
FIGURE 13.1 DISTRIBUTION OF TONNES AND METAL CONTENTS

- For copper, an increase in copper feed type tonnage and copper metal content was observed in the 2013 model compared to the 2011 model.
- For the mixed feed type, a decrease in tonnage and slight decreases in the metal contents for Cu and Zn were noted.
- For zinc feed type, slight differences in the tonnage and metal contents for Cu, Zn, and Pb were seen between the 2011 and the 2013 models.

Figure 13.2 shows a plan view of the 2011 and 2013 block models and the distribution of selected samples within the two models



PLAN VIEW — 2011 BLOCK MODEL



PLAN VIEW — 2013 BLOCK MODEL

FIGURE 13.2 COMPARISON OF 2011 AND 2013 BLOCK MODELS

Comments:

- There are zones in the 2013 Block Model that were not included in the sample selection.
- BISA's geological analysis of these new zones in the 2013 Block Model indicates that they are not substantially different with respect to oxidation or rock competence, and no differences were found with respect to contents in metals of interest.
- Consequently, for a PEA study, it would appear justifiable to assume that a similar recovery and concentrate grade will be obtained for the 2013 mineral resource samples as for those collected for the 2011 resource base.
- It is recommended that future studies include sample testing from the new zones to confirm their metallurgical performance.

METALLURGICAL TESTING

INSPECTORATE SAMPLES IN 2008

Three flotation tests were carried out on a master composite by Inspectorate Services Peru S.A.C. The master composite consisted of 21 samples from the core sample remains from three diamond drill holes in a mineralized zone of El Domo.

The results of the head assays reported 3.37% Cu, 1.32% Pb, 9.67% Zn, 190 g/t Ag, and 6.50 g/t Au (see the summary in Table 13.1).

TABLE 13.1 FLOTATION TEST RESULTS – INSPECTORATE 2008

Test	Grinding P80 (µm)	Products	Mass Pull (%)	Distribution (%)				
				Cu	Pb	Zn	Ag	Au
Test I	125	Conc. Ro + Scv Cu/Pb	22.5	32.7	53.8	31.8	33.0	28.6
Test II	125	Conc. Ro + Scv Cu/Pb	21.8	32.3	55.7	33.4	33.5	28.5
Test III	73	Conc. Ro + Scv Cu/Pb	30.8	63.0	80.3	57.6	50.2	44.7

- Reductions in grind size increased Cu, Ag, and Au recovery.
- Poor flotation selectivity is observed for copper and zinc.

G&T TESTS 2010

Flotation tests were performed by G&T Metallurgical Services Ltd (G&T) in 2010. Table 13.2 shows the head assays for the El Domo composites developed for the study.

TABLE 13.2 HEAD ASSAYS — G&T 2010

Sample ID	Head Assays								
	Cu (%)	Pb (%)	Zn (%)	Fe (%)	S (%)	Au (g/t)	Ag (g/t)	CuOx (%)	CuCN (%)
Master Composite 1	3.45	0.37	4.65	20.9	0.15	4.58	59.0	0.060	0.44
Master Composite 2	13.6	0.11	1.17	32.3	35.6	7.86	66.0	0.090	0.36
Master Composite 3	2.38	2.65	12.5	12.3	23.4	3.57	174	0.001	0.24

Flotation tests focused on Master Composite 1, and the following parameters were examined:

- Primary grind sizes
- Re grind sizes
- Types of reagents and dosages
- Flotation schemes

The best results for the copper circuit came from the KM2738-17 cleaner test, which yielded a recovery of 72% Cu and a grade of 27% Cu for the final concentrate.

Two locked cycle tests were conducted to evaluate the performance of the zinc circuit. The best results for zinc were obtained in locked cycle test KM2738-20, which yielded a recovery of 57% Zn and a grade of 49% Zn for the zinc concentrate.

While the tests achieved satisfactory grades of zinc and copper concentrates, recoveries were low. The mineralogy shows that the copper concentrate contains high amounts of sphalerite, which was caused by associations between zinc and copper minerals.

SGS LABORATORY TESTS 2013

The tests were performed on three composites with the aim of developing a robust, efficient flotation scheme for all mineral types in El Domo (see Table 13.3 for head assays of the composites formed).

TABLE 13.3 CHEMICAL ANALYSIS OF HEAD COMPOSITES

Composite ID	Classification Study 2013	Head Assays													
		Cu (%)	Zn (%)	Pb (%)	Au (g/t)	Ag (g/t)	Fe (%)	PbOx (%)	ZnOx (%)	Cu_SS (%)	Cu_CN (%)	Cu_R (%)	S _{Sulfato} (%)	S _{Sulfuro} (%)	S _{Native} (%)
CPO-001	Zinc Mineral	0.84	5.11	0.40	3.26	89.4	4.80	0.21	0.12	0.03	0.17	0.59	1.34	7.30	-
CPO-002	Mixed Mineral Cu / Zn	2.15	2.18	0.13	2.17	44.4	12.6	0.08	0.06	0.04	0.14	1.84	1.30	15.1	-
CPO-003	Copper Mineral	3.78	0.41	0.03	2.02	19.6	22.4	0.02	0.02	0.14	0.32	3.26	1.60	30.4	-

The following parameters were examined during the testing program:

- Grind sizes
- Effect of the solids concentration in the flotation on reducing interference from clays

- Types of reagents for pyrite depression and reduction of insoluble entrainment to concentrate
- Regrind effect
- Flotation schemes

In preliminary tests, it was noted that the flotation froths were overloaded with gangue. Tests were conducted to evaluate alternatives to resolve this phenomenon. The use of lime to adjust the flotation pH was noted to cause the activation of gangue minerals, impairing the selective flotation of valuable minerals.

Consequently, a bulk sulphide flotation stage at low pH and coarse grinding was successfully implemented. Thus, the gangue minerals were rejected, enabling the use of fine milling and lime to achieve selective flotation of a bulk concentrate. This same method was necessary for the three composites studied.

COMPOSITE CPO-001 (ZINC FEED TYPE)

After implementing the bulk flotation system for the rougher stage, the use of the following schemes was evaluated for the separation of copper and zinc:

- Float the zinc and depress the copper
- Float the copper and depress the zinc

It was found that it was better to float the copper and depress the zinc. Two additional tests were carried out to confirm the results, one with metabisulphite to depress iron and another without metabisulphite (Table 12.5). Better results were obtained in the flotation test without metabisulphite (Table 12.6).

TABLE 13.4 CPO-001 – REAGENTS AND DOSAGES

Stage	Reagents Added (g/t)								Cal (Kg/t)	pH	Time (minutes)		
	3894	404	Z-11	CuSO ₄	MIBC	Activated Carbon	MT 4130	ZnSO ₄ /Na ₂ S ₅ O ₂			Grind	Cond.	Flotation
Grind	-	-	-	-	-	-	-	-	-	-	6.21	-	-
Cond-1	12.4	5.20	80.0	300	3.00	-	5.60	-	-	4.75	-	8.00	-
Sulphide Flot.	-	-	-	-	-	-	-	-	-	4.76	-	-	10.0
Cond-2	-	-	-	-	-	-	-	-	-	4.70	-	25.0	-
Cond-3	6.20	-	19.0	190	9.00	-	5.60	-	-	4.75	-	5.00	-
Rougher Flot.	-	-	-	-	-	-	-	-	2.80	11.5	-	-	7.00
Regrind	-	-	-	-	-	-	-	-	-	-	5.00	-	-
Scavenger Flot.	6.20	-	-	-	3.00	-	-	-	0.80	11.5	-	-	3.00
Regrind	-	-	-	-	-	-	-	-	-	-	15.0	-	-
Cond-4	12.4	-	10.0	100	6.00	-	-	-	0.80	-	-	-	-
Bulk Cleaner 1	-	-	-	-	-	-	-	-	0.40	11.5	-	-	8.00
Bulk Cleaner 2	-	-	-	-	3.00	-	-	-	-	11.5	-	-	6.00
Cond-5	-	-	-	-	-	500	-	-	-	9.50	-	5.00	-
Cond-6	6.20	-	-	-	6.00	-	-	1,000	-	9.50	-	3.00	-
Cleaner 1 Flot.	-	-	-	-	-	-	-	-	-	8.50	-	-	4.00
Cleaner 2 Flot.	-	-	-	-	-	-	-	1,000	-	8.50	-	-	3.50
Total	43.4	5.20	109	590	30.0	500	11.2	2,000	4.80		26.2	46.0	41.5

Figure 13.3 shows the scheme for the treatment of composite CPO-001.

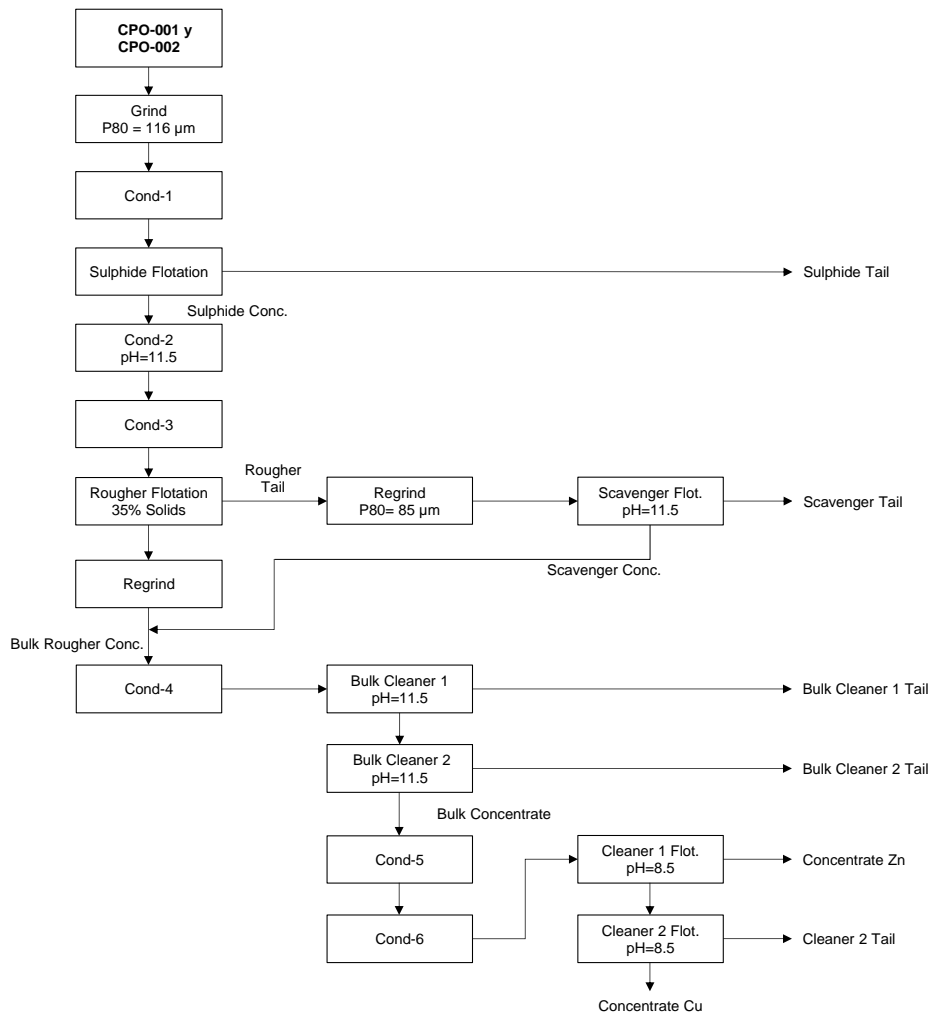


FIGURE 13.3 TESTS DIAGRAM FOR COMPOSITES CPO-001 AND CPO-002

Table 13.5 shows the better results obtained for composite CPO-001.

TABLE 13.5 CPO-001 – RESULTS OF FLOTATION TEST

Products	Weight (%)	Assays						Distribution					
		Au (g/t)	Ag (g/t)	Cu (%)	Fe (%)	Zn (%)	Pb (%)	Au (%)	Ag (%)	Cu (%)	Fe (%)	Zn (%)	Pb (%)
Concentrate Cu	1.93	12.0	558	16.3	16.0	28.7	10.5	7.11	13.3	38.0	5.72	11.0	48.4
Cleaner 2 Tail	1.34	11.3	490	8.40	4.48	52.3	2.40	4.63	8.09	13.5	1.11	13.9	7.65
Cleaner 1 Tail (Conc. Zn)	7.01	17.0	484	3.40	10.5	49.6	1.44	36.6	41.8	28.7	13.6	68.9	24.0
Bulk Concentrate	10.3	15.3	499	6.48	10.7	46.0	3.27	48.3	63.1	80.2	20.5	93.7	80.0
Bulk Cleaner 2 Tail	1.32	21.2	414	2.06	37.7	2.26	0.94	8.58	6.73	3.28	9.22	0.59	2.95
Bulk Cleaner 1 Tail	7.43	11.6	183	0.76	29.9	1.17	0.28	26.3	16.7	6.80	41.1	1.72	4.95
Bulk Rougher Conc.	19.0	14.3	369	3.94	20.1	25.5	1.94	83.2	86.6	90.3	70.8	96.0	87.9
Scavenger Tail	4.79	0.90	21.9	0.49	2.07	0.56	0.09	1.32	1.29	2.83	1.84	0.53	1.04
Sulphide Concentrate	23.8	11.6	300	3.25	16.5	20.5	1.57	84.5	87.9	93.1	72.6	96.6	89.0
Sulphide Tail	76.2	0.66	12.9	0.08	1.94	0.23	0.06	15.5	12.1	6.90	27.4	3.44	11.0
Final Tail	81.0	0.68	13.5	0.10	1.95	0.25	0.06	16.8	13.4	9.72	29.2	3.97	12.1
Head Calculated	100	3.26	81.2	0.83	5.40	5.05	0.42	100	100	100	100	100	100
Head Assay		3.26	89.4	0.84	4.83	5.11	0.40						

- All test results show low Cu recoveries and low grades in the final copper concentrates.
- The Cu/Zn separation conducted during the cleaner stages show a recovery of 69% Zn, and an average grade of 49% Zn in the final Zn concentrate.
- Results show that the addition of a regrind stage and an increase to pH 11.5 in the flotation in the bulk cleaner stage significantly diminished recovery from 71% Fe in the bulk rougher concentrate to 21% Fe recovery in the bulk concentrate.

Composite CPO-002 (Mixed Cu/Zn Feed Type)

After implementing the bulk flotation system for the rougher stage, the following schemes for the separation of copper and zinc were evaluated:

- Float the zinc and depress the copper
- Float the copper and depress the zinc

Based on the results, it was determined that it was better to float the copper and depress the zinc. Two additional tests were carried out to confirm the results, one with the use of metabisulphite to depress iron and another without metabisulphite (Table 13.6). Better results were obtained in the flotation test without metabisulphite (see Table 13.7).

TABLE 13.6 CPO-002 – REAGENTS AND DOSAGES

Stage	Reagents Added (g/t)							Cal (Kg/t)	pH	Time (minutes)		
	3894	404	Z-11	CuSO ₄	MIBC	Activated Carbon	ZnSO ₄ / Na ₂ S ₅ O ₂			Grind	Cond.	Flotation
Grind	-	-	-	-	-	-	-	-	-	7.21	-	-
Cond-1	6.20	5.20	50.0	100	3.00	-	-	-	4.75	-	8.00	-
Sulphide Flot.	-	-	-	-	-	-	-	-	4.76	-	-	10.0
Cond-2	-	-	-	-	-	-	-	-	4.70	-	25.0	-
Cond-3	12.4	-	8.00	-	3.00	-	-	-	4.75	-	5.00	-
Rougher Flot.	-	-	-	-	-	-	-	2.60	11.5	-	-	8.00
Regrind	-	-	-	-	-	-	-	-	-	10.0	10.0	-
Scavenger Flot.	6.20	-	-	-	3.00	-	-	0.70	11.5	-	-	3.00
Regrind	-	-	-	-	-	-	-	-	-	10.0	10.0	-
Bulk Cleaner 1	12.4	-	-	100	3.00	-	-	0.40	11.5	-	-	6.00
Bulk Cleaner 2	6.20	-	-	-	-	-	-	-	11.5	-	-	5.00
Cond-4	-	-	-	-	-	500	-	-	9.50	-	15.0	-
Cond-5	6.20	-	-	-	-	-	1,000	-	9.50	-	3.00	-
Cleaner 1 Flot.	-	-	-	-	-	-	1,000	-	8.50	-	-	7.00
Cleaner 2 Flot.	6.20	-	-	-	-	-	-	-	8.50	-	-	6.00
Total	55.8	5.20	58.0	200	12.0	500	2,000	3.70	-	27.2	76.0	45.0

Figure 13.3 shows the scheme developed for the treatment of composite CPO-002. Table 13.7 shows the better results obtained for composite CPO-002.

TABLE 13.7 CPO-002 – RESULTS OF FLOTATION TEST

Products	Weight (%)	Assays						Distribution					
		Au (g/t)	Ag (g/t)	Cu (%)	Fe (%)	Zn (%)	Pb (%)	Au (%)	Ag (%)	Cu (%)	Fe (%)	Zn (%)	Pb (%)
Concentrate Cu	7.50	9.99	219	21.2	25.1	11.9	0.86	32.9	38.3	74.5	15.2	41.2	44.6
Cleaner 2 Tail	0.42	8.56	119	1.95	31.3	9.74	0.31	1.57	1.16	0.38	1.05	1.87	0.90
Concentrate Zn	7.14	6.81	170	5.07	31.5	14.6	0.46	21.3	28.3	17.0	18.1	47.8	22.6
Bulk Concentrate	15.1	8.45	193	13.0	28.3	13.1	0.65	55.8	67.8	91.9	34.3	90.9	68.1
Bulk Cleaner 2 Tail	1.68	2.58	55.2	0.87	40.6	0.32	0.12	1.91	2.17	0.69	5.50	0.25	1.38
Bulk Cleaner 1 Tail	12.5	3.50	35.5	0.40	35.6	0.20	0.08	19.1	10.3	2.34	35.7	1.15	6.91
Bulk Rougher Conc.	29.2	6.00	118	6.93	32.1	6.87	0.38	76.8	80.2	94.9	75.5	92.3	76.4
Scavenger Tail	21.7	0.90	23.9	0.27	10.0	0.48	0.08	8.57	12.1	2.73	17.5	4.80	12.0
Sulphide Concentrate	50.9	3.82	77.8	4.09	22.7	4.14	0.25	85.4	92.4	97.6	93.0	97.1	88.5
Sulphide Tail	49.1	0.68	6.67	0.10	1.77	0.13	0.03	14.6	7.64	2.40	6.99	2.94	11.5
Final Tail	70.8	0.75	12.0	0.15	4.31	0.24	0.05	23.2	19.8	5.12	24.5	7.73	23.6
Head Calculated	100	2.28	42.9	2.13	12.4	2.17	0.14	100	100	100	100	100	100
Head Assay		2.17	44.9	2.15	12.6	2.18	0.13						

- Significant Zn recovery is observed in the Cu concentrate. These results could be caused by one or both of the following phenomena:
 - A mineralogical association at a submicroscopic level that inhibits Cu-Zn separation.
 - The use of copper sulphate during the bulk sulphide flotation stage, leading to overactivation of the zinc minerals, which would not be efficiently depressed during the cleaner flotation stage.
- A zinc cleaning stage was added to improve the quality of the zinc concentrate.

- Results show that the addition of a regrind stage and an increase to pH 11.5 in the flotation in the bulk cleaner stage significantly diminishes recovery from 76% Fe in the bulk rougher concentrate to 34% Fe recovery in the bulk concentrate.

Composite CPO-003 (Copper Feed Zone)

After using a range of flotation methods to maximize the production of Cu concentrate from the minerals in composite CPO-003, the system for the treatment of the copper feed type consists of:

- A bulk flotation stage to remove clays and silicates
- A pyrite elimination stage
- Three cleaning stages to obtain the final copper concentrate

Table 13.8 shows the conditions and reagents employed for the flotation test.

TABLE 13.8 CPO-003 – REAGENTS AND DOSAGES

Stage	Reagents Added (g/t)					Cal (Kg/t)	pH	Time, minutes		
	3894	404	Z-11	Metabisulphite	MIBC			Grind	Cond.	Flotation
Grind	-	-	-	-	-	-	5.19	7.21	-	-
Cond-1	6.20	5.20	50.0	-	3.00	-	5.09	-	8.00	-
Sulphide Flot.	-	-	-	-	-	-	5.00	-	-	7.00
Cond-2	-	-	-	-	-	2.10	11.1	-	25.0	-
Cond-3	6.20	5.20	8.00	500	3.00	-	11.0	-	5.00	-
Rougher Flot.	-	-	-	-	-	-	11.5	-	-	8.00
Regrind	-	-	-	-	-	-	-	5.00	-	-
Scavenger Flot.	3.10	-	1.00	500	-	0.60	11.2	-	-	3.00
Regrind	-	-	-	-	-	-	-	7.00	-	-
Cleaner 1 Flot.	3.10	-	-	200	-	0.40	11.5	-	-	6.00
Cleaner 2 Flot.	-	-	-	100	-	0.20	11.5	-	-	5.00
Cleaner 3 Flot.	-	-	-	-	-	-	11.5	-	-	4.00
Total	18.6	10.4	59.0	1,300	6.00	3.30	-	19.2	38.0	33.0

Figure 13.4 shows the system for the treatment of composite CPO-003.

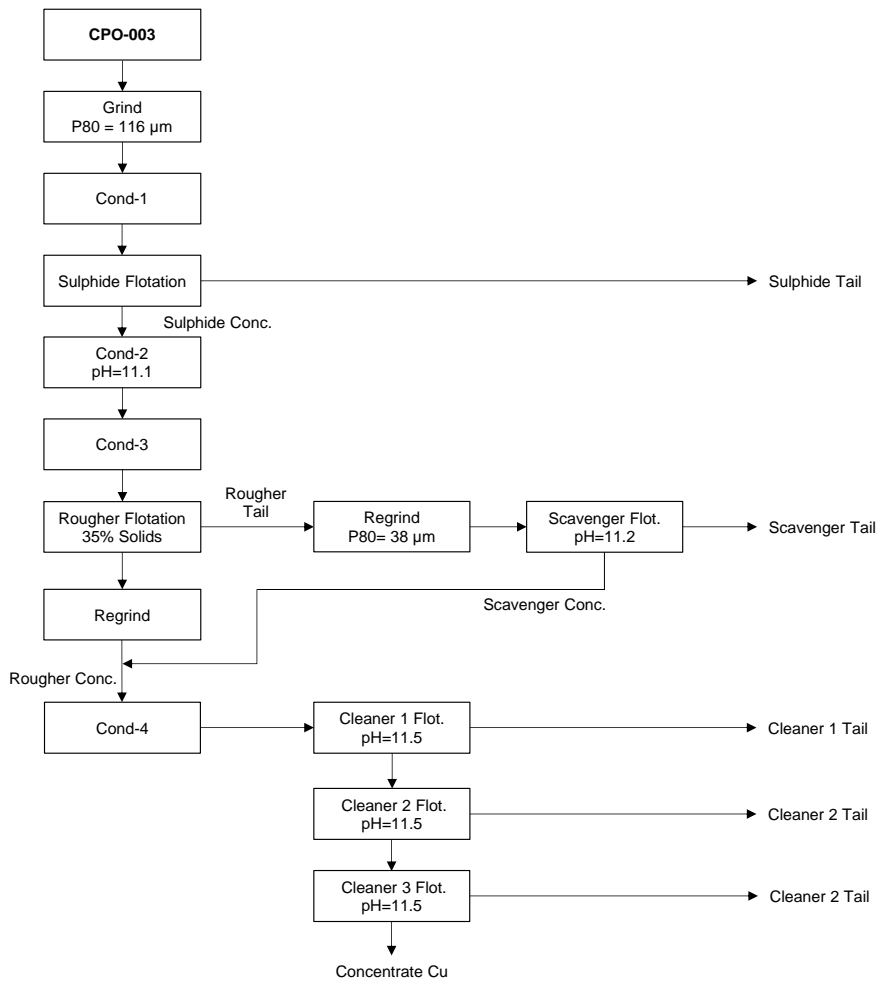


FIGURE 13.4 TESTS DIAGRAM FOR COMPOSITE CPO-003

Table 13.9 shows the better results obtained for composite CPO-003.

TABLE 13.9 CPO-003 – RESULTS OF FLOTATION TEST

Products	Weight (%)	Assays						Distribution					
		Au (g/t)	Ag (g/t)	Cu (%)	Fe (%)	Zn (%)	Pb (%)	Au (%)	Ag (%)	Cu (%)	Fe (%)	Zn (%)	Pb (%)
Concentrate Cu	13.9	3.69	53.1	24.2	33.4	2.34	0.094	24.4	39.7	89.7	17.9	80.9	43.4
Cleaner 3 Tail	1.56	4.33	36.2	2.60	35.0	0.16	0.034	3.22	3.03	1.08	2.11	0.62	1.76
Cleaner 2 Tail	3.25	3.79	30.3	1.90	41.3	0.11	0.031	5.87	5.29	1.65	5.18	0.89	3.35
Cleaner 1 Tail	6.94	3.09	22.5	0.75	42.7	0.10	0.033	10.2	8.39	1.39	11.4	1.73	7.62
Rougher Concentrate	25.6	3.58	40.9	13.7	37.0	1.32	0.066	43.7	56.4	93.8	36.6	84.1	56.2
Scavenger Tail	38.7	2.28	13.3	0.28	39.8	0.10	0.019	42.1	27.7	2.87	59.5	9.63	24.6
Sulphide Concentrate	64.3	2.80	24.3	5.63	38.7	0.59	0.038	85.8	84.1	96.7	96.1	93.8	80.7
Sulphide Tail	35.7	0.83	8.29	0.35	2.80	0.07	0.016	14.2	15.9	3.34	3.87	6.23	19.3
Final Tail	74.4	1.59	10.9	0.31	22.0	0.09	0.018	56.3	43.6	6.21	63.4	15.9	43.8
Head Calculated	100	2.10	18.6	3.75	25.9	0.40	0.030	100	100	100	100	100	100
Head Assay		2.22	19.6	3.78	26.2	0.41	0.030						

- The flotation system and the conditions applied were sufficient to produce a copper concentrate with satisfactory grades and recoveries.
- Recovery of 89.7% Cu and 24% Cu grade were obtained.
- Despite the high zinc recovery in the copper concentrate, the zinc grade was below typical penalizable thresholds due to the low head assay of zinc.
- Adding a regrind stage and increasing the pH to 11.5 during the rougher stage reduced recovery from 96% Fe in the sulphide concentrate to 37% Fe recovery in the rougher concentrate.

Table 13.10 shows the results of the chemical analyses of the main elements and contaminants of the copper and zinc concentrates.

TABLE 13.10 CHEMICAL ANALYSES OF COPPER AND ZINC CONCENTRATES

Element	Unit	CPO - 001		CPO - 002		CPO - 003
		Conc. Cu	Conc. Zn	Conc. Cu	Conc. Zn	Conc. Cu
Au	g/t	12.6	17.0	9.49	6.71	3.40
Cu	%	16.0	3.38	21.2	5.07	24.0
Fe	%	16.0	10.2	25.1	31.5	32.2
Pb	%	10.2	1.45	0.86	0.46	0.09
Zn	%	29.2	48.7	11.9	14.6	2.30
Ag	g/t	560	482	217	166	53.1
As	ppm	2,328	4,386	2,710	4,009	1,717
Bi	ppm	108	96.0	75.0	217	288
Cd	ppm	1,577	2,440	565	712	106
Sb	ppm	791	2,763	799	933	230

The assays found the presence of potentially penalizable elements such as arsenic, antimony, bismuth, and cadmium.

RESULTS

Based on the results from the 2013 flotation testing program, an estimate was made of the recoveries and grades of the Cu and Zn concentrates that would be produced in an efficiently operated industrial plant, with ore similar to the composites studied.

TABLE 13.11 METALLURGICAL BALANCE PROJECTION – RECOVERIES AND GRADES

Composite ID	Products	Weight (%)	Assays					Distribution				
			Cu (%)	Zn (%)	Pb (%)	Au (g/t)	Ag (g/t)	Cu (%)	Zn (%)	Pb (%)	Au (%)	Ag (%)
CPO-001 Zinc Mineral	Concentrate Cu	2.46	19.7	17.0	1.31	8.18	748	58.2	8.24	7.67	6.16	22.6
	Concentrate Pb	0.61	17.7	17.0	47.3	21.8	1,995	6.47	0.92	69.0	4.11	15.1
	Concentrate Zn	9.49	1.73	45.5	0.31	14.0	286	19.7	85.4	6.90	40.8	33.4
	Final Tail	87.4	0.15	0.31	0.08	1.83	26.9	15.5	5.39	16.4	49.0	28.9
	Head Calculated	100	0.89	5.11	0.42	3.26	81.2	100	100	100	100	100
CPO-002 Mixed Mineral Cu / Zn	Concentrate Cu	7.62	21.0	8.51	0.94	8.77	230	75.0	29.8	49.6	29.3	40.8
	Concentrate Zn	2.59	6.28	42.0	0.86	19.4	371	7.62	50.0	15.4	22.0	22.4
	Final Tail	89.8	0.41	0.49	0.06	1.24	17.6	17.4	20.2	35.0	48.7	36.8
	Head Calculated	100	2.13	2.17	0.14	2.28	42.9	100	100	100	100	100
CPO-003 Copper Mineral	Concentrate Cu	13.9	24.2	2.34	0.09	3.69	53.1	89.7	80.9	43.4	24.4	39.7
	Final Tail	86.1	0.45	0.09	0.02	1.84	13.0	10.3	19.1	56.6	75.6	60.3
	Head Calculated	100	3.75	0.40	0.03	2.10	18.6	100	100	100	100	100

Results of the 2013 tests were used as a basis for the simulation models. The performance of different flotation systems was simulated where there was insufficient test data available. For CPO-001, the system in Figure 13.3 was modified. A Zn-cleaning stage and a Cu-Pb separation stage were added. The aim of the changes was to estimate recoveries for acceptable grades for the Cu and Zn concentrates and to evaluate the potential of producing a lead concentrate.

For composite CPO-002, a Cu-cleaning stage and two Zn-cleaning stages were added. The aim was to project the copper recovery in the Cu concentrate and project a Zn concentrate with a grade of over 42% Zn.

The results shown in Table 13.9 were used directly for the metallurgical projection of composite CPO-003.

14. MINERAL RESOURCES ESTIMATE

GENERAL STATEMENT

The current Mineral Resource estimate for the El Domo deposit was prepared by BISA and supervised by Gustavo Calvo, P. Geo. (Table 14.1). The Mineral Resource estimate is based on 168 diamond drill holes from four drilling campaigns undertaken by Salazar from 2007 to 2012. The geological interpretation of the deposit was based on the geological sections delivered by Salazar. A Net Smelter Return (NSR) cutoff value of US\$30 per tonne has been used.

Four geological units have been considered for mineral resource reporting: volcanogenic massive sulphides (VMS); polymictic volcanoclastic breccia with massive sulphide clasts (GRAINSTONE); quartz-pyrite stockwork and breccias (BRECCIA); and anhydrite-gypsum stockwork (GYPSUM). More details on the geological features of these units are found in Chapter 7.

TABLE 14.1 EL DOMO MINERAL RESOURCE ESTIMATE - DECEMBER 15, 2013

Unit	Category	Tonnes (Mt)	Copper (%)	Zinc (%)	Lead (%)	Gold (g/t)	Silver (g/t)
VMS	Indicated	5.468	2.52	3.27	0.30	3.23	59.19
Grainstone	Indicated	0.216	0.92	1.01	0.12	1.09	27.91
Breccia	Indicated	0.345	0.49	1.33	0.13	0.76	26.91
Gypsum	Indicated	0.051	0.94	0.39	0.03	0.34	7.40
Total Indicated		6.080	2.33	3.06	0.28	2.99	55.81
VMS	Inferred	3.093	1.75	2.59	0.19	2.38	49.45
Grainstone	Inferred	0.170	0.96	0.69	0.10	1.00	19.24
Breccia	Inferred	0.370	0.53	0.83	0.07	0.78	24.89
Gypsum	Inferred	0.249	1.13	0.26	0.01	0.27	4.80
Total Inferred		3.882	1.56	2.19	0.16	2.03	42.92

NOTE:

- CIM definitions were followed for mineral resources
- The Mineral Resource Estimate is based on 3D geological modelling of the volcanogenic massive sulphide deposit (VMS). Four mineralized units with an NSR cutoff of US\$30 per tonne were considered as mineral resource
- Metal prices used are US\$2.95/lb Cu, US\$0.91/lb Zn, US\$0.91/lb Pb, US\$1,200/oz Au, and US\$20.00/oz Ag
- Metallurgical recovery factors assumed were based on three mineral types defined by the metal ratio Cu/(Zn+Pb):
 - Zinc Mineral (Cu/(Pb+Zn)<0.3): 15% Cu, 90% Zn, 40% Pb, 50% Au, and 65% Ag
 - Mixed Cu/Zn Mineral (0.3≤Cu/(Pb+Zn)≤3.0): 75% Cu, 50% Zn, 0% Pb, 55% Au, and 65% Ag
 - Copper Mineral (Cu/(Pb+Zn)>3.0): 90% Cu, 0% Zn, 0% Pb, 30% Au, and 40% Ag
- Common industry values for smelter terms were assumed
- Bulk density was estimated based on specific gravity determinations for each lithological unit

Values of one percent grade for copper, zinc, and lead, of one gram grade for gold, and of one ounce for silver were calculated based on assumed metal prices, metallurgical recovery factors, and common smelter terms. These values support the NSR calculation and are summarized in Table 14.2.

TABLE 14.2 METAL UNIT VALUES FOR NSR CALCULATION

Metal	Unit	Zinc Mineral	Mixed Cu/Zn Mineral	Copper Mineral
		Cu/(Zn+Pb) < 0.33	Cu/(Zn+Pb): 0.33-3.0	Cu/(Zn+Pb): > 3.0
		Value	Value	Value
Cu	US\$/ 1%	4.7	31.5	44.6
Zn	US\$/ 1%	8.8	3.9	0.0
Pb	US\$/ 1%	3.7	0.0	0.0
Au	US\$/ 1g	13.7	15.6	7.1
Ag	US\$/ 1oz	9.0	9.0	3.2

DATABASE

The El Domo database consists of 5 csv (comma-separated value) files that contain the following information: drill hole header locations (collar.csv), drill hole directional surveys (survey.csv), geochemical assays of core samples (assay.csv), lithology logs (litología.csv), and core recovery logs (recuperacion.csv). This database includes a total of 168 diamond drill holes, but only 163 of these holes have been used in the resource estimation. These drill holes are the result of four drilling campaigns undertaken by Salazar from 2007 to 2012 (Table 14.3).

Table 14.4 shows the number of drill holes and drilled metres used in resource estimation updates from 2010 to 2013.

TABLE 14.3 SUMMARY OF DRILLING CAMPAIGNS AT EL DOMO

Phase	ID Drilling	Holes	Cumulative Metres
I	CURI-07-19 to CURI-08-51	22	4,556.41
II	CURI-52 to CURI-71	19	3,100.50
III	CURI-72 to CURI-155	76	13,865.50
IV	CURI-156 to CURI-206	51	10,248.75
TOTAL		168	31,771.16

TABLE 14.4 DRILL HOLES USED IN THE RESOURCE DECLARATIONS FOR EL DOMO

Resource Declaration	Resource Estimation	Drilled Metres	Drill Holes	Reference
October, 2010	September, 2010	3,336.80	18	--
November, 2011	September, 2011	13,924.10	78	Includes up to drill hole Curi-155.
December, 2013	November, 2013	31,771.16	168	Includes drill holes from the year 2007 to drill hole Curi-206

Collar: This file contains 168 drill hole collar locations, and includes the 119 drill hole collars staked out by Aeromapa in July of 2013. The locations are in the coordinate system PSAD 1956 - UTM, Zone 17 S.

Survey: Contains directional surveys for 168 drill holes: 42 drill holes with surveys taken every 3 m with a Reflex Maxibor II; 7 drill holes from the first drilling campaign with surveys taken every 50 m by the Kluane company; and 119 drill holes with a single inclination measurement taken at the drill hole collar.

Assay: Contains 7,736 geochemical samples from the 163 drill holes sampled by Salazar. The data include the assays for: Cu, Zn and Pb in percentage (%), and Au and Ag in grams per tonne (g/t). The values of the analytical results with "less" or "less than" signs ("-" or "<"), which correspond to values below the lower detection limits, have been replaced by one half of that value.

Lithology: Contains the nine lithological codes established by BISA.

Recovery: Contains the core recovery percentage from the 168 drill holes. Drill holes: CURI-08-22, CURI-08-39, CURI-08-44, CURI-08-49 and CURI-08-50 reported low core recovery (<70%) when intersecting the massive sulphides.

DENSITY

Salazar has generated 1,140 specific gravity (SG) determinations in sub-samples from the diamond drilling cores. The specific gravity tests were conducted using a paraffin method with immersion in water for samples of approximately 10 cm in size.

BISA has verified in situ the method and procedures used by Salazar and concludes that SG data are locally representative for units where the tests were performed, but not for the full

sample intervals where these subsamples are located. BISA recommends that Salazar make the effort to obtain SG measurements of the complete geochemical sampling intervals for refining the deposit density model.

HISTORICAL MODELS

Modelling work and resource estimation have been conducted in El Domo since 2010. The first resource estimate was carried out based on the interpretation of 18 drill holes that intersected the mineralized zone (VMS); these resources were classified under the categories of indicated and inferred. This work was performed in September of 2010 by Scott Wilson Roscoe Postle Associates Inc. (Scott Wilson RPA). The resource was estimated using a cutoff value of US\$50 NSR (Table 14.5).

In 2011, Roscoe Postle Associates Inc. (Lavigne and McMonies) conducted a resource update on El Domo supported by 78 drill holes and using the same cutoff value (US\$50 NSR), but assuming, in this case, different economic parameters to those employed in 2010 (Table 14.5).

TABLE 14.5 MINERAL RESOURCE ESTIMATE BY RPA IN 2010 AND 2011

Year	NSR Cutoff (US\$)	Category	Tonnes (millions)	Cu (%)	Zn (%)	Au g/t	Ag g/t	Pb (%)
2010	50	Indicated	0.623	3.70	4.16	3.00	98.00	0.41
		Inferred	2.499	3.24	4.28	4.30	79.50	0.37
2011	50	Indicated	5.530	2.40	2.50	2.80	48.40	0.30
		Inferred	1.460	1.90	2.80	2.40	52.20	0.30

GEOLOGICAL MODEL

The geological model for El Domo was generated from a regular 50x50 metre drill hole grid. The geological interpretation was carried out using Leapfrog Mining 3D (v2.5) application. Leapfrog Mining 3D (Leapfrog) is an application for implicit, quick, dynamic and accurate 3D modelling of geological units. It utilizes radial-basis interpolation for logged intervals and performs Boolean operations to generate mutually exclusive solids. It should be noted that, in addition to constructing 3D solids, Leapfrog enables the visualization of sections in any direction.

BISA verified the lithological coding used to ensure its consistency (Chapter 12). Generally, the BISA 3D lithological model is consistent with the sections delivered by Salazar.

LITHOLOGICAL MODEL

The lithological model constructed by BISA confirms the main properties identified by the Salazar drill holes. Nine lithological units have been defined (see Table 7.2). For modelling, mutually exclusive solids were generated for all the lithological units identified in drill holes, considering the temporal relationship with the mineralization. Therefore, the modelling parameters defined for each of these units consider the length of the lithology intervals used for point compositing in Leapfrog as well as the minimum allowable interval in the modelled units and the precision required to define its contacts (Table 14.6).

TABLE 14.6 PARAMETERS USED IN THE LITHOLOGICAL MODELLING

Lithological Unit	Abbreviation	Compositing Length (m)	Minimum Length of Accepted Range (% Compositing Length)	Accuracy of Contacts (+/- m)
Cover	COB	NA	NA	NA
Andesite	AND	8	50	0
Basalt	B	6	50	0
Tuffs	T	2	50	0
Grainstone	GR	2	50	0
Volcanogenic Massive Sulphides	VMS	2	50	0
Breccia	BXH	2	50	0
Gypsum	GY	2	50	0
Rhyolite	RHY	2	50	0

Figure 14.1 and Figure 14.2 show various N-S and E-W and plan view sections of the El Domo lithological model.

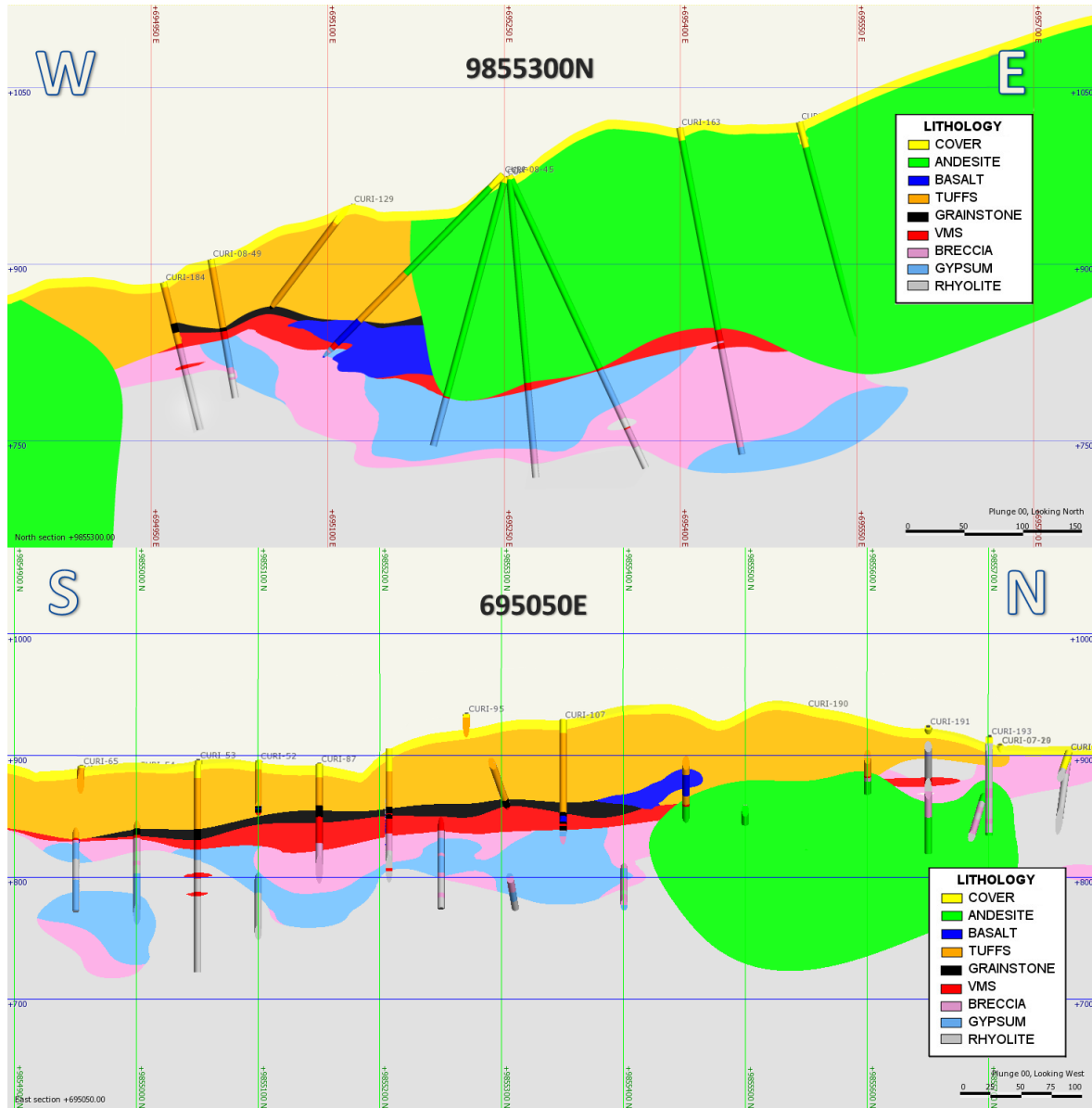


FIGURE 14.1 LITHOLOGICAL MODEL IN SECTION 9588300N AND SECTION 695050E

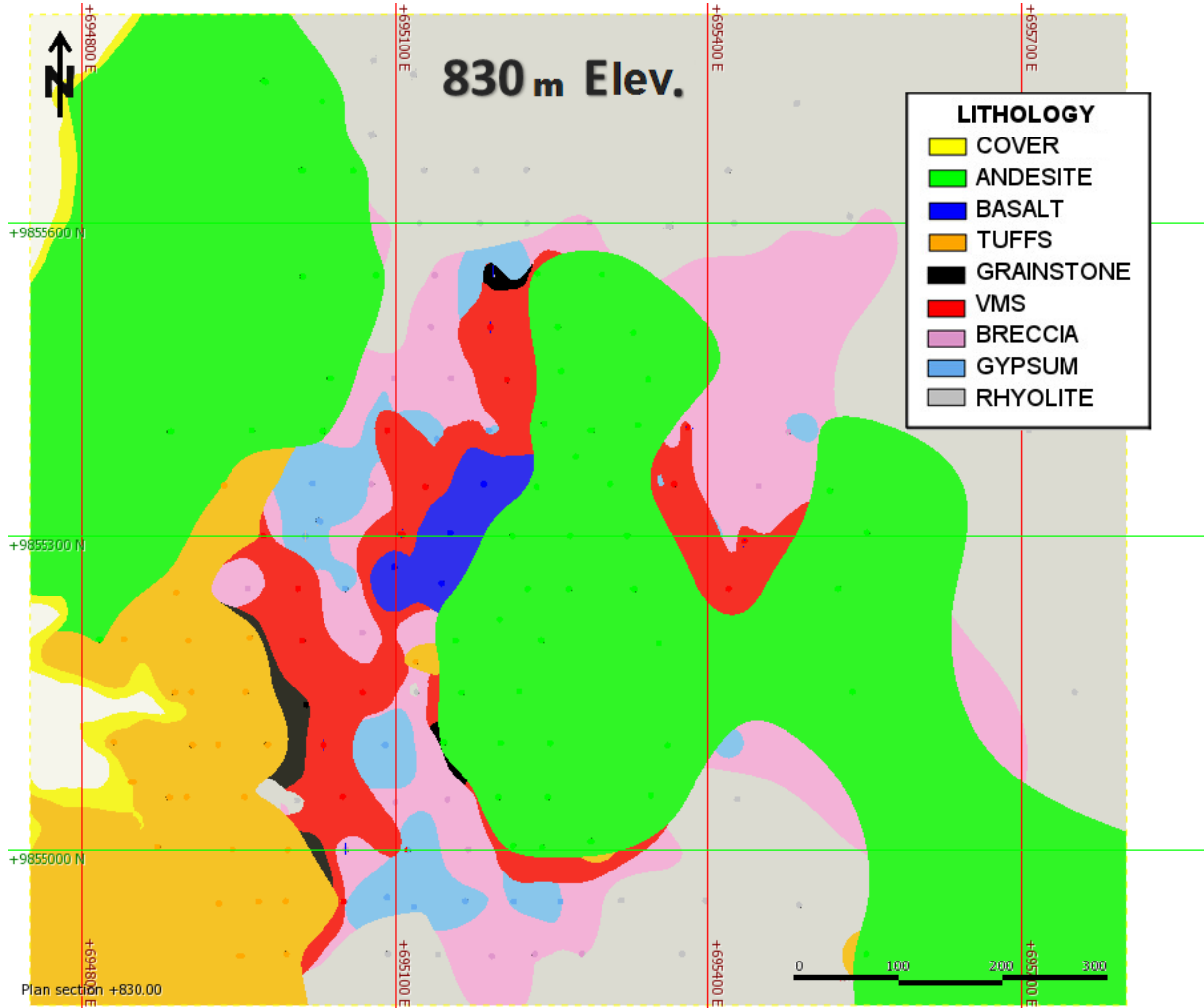


FIGURE 14.2 LITHOLOGICAL MODEL IN PLAN VIEW AT THE 830 M LEVEL

VALIDATION OF THE LITHOLOGICAL MODEL

The lithological model was validated by visually inspecting the correspondence between the coded lithological intervals in the drill holes compared with the solid of the modelled unit. This visual inspection was carried out in various directions: north-south, east-west, and by levels. Figure 14.3 illustrates the 3D model generated for the VMS unit, where the mineralized intercepts are highlighted.

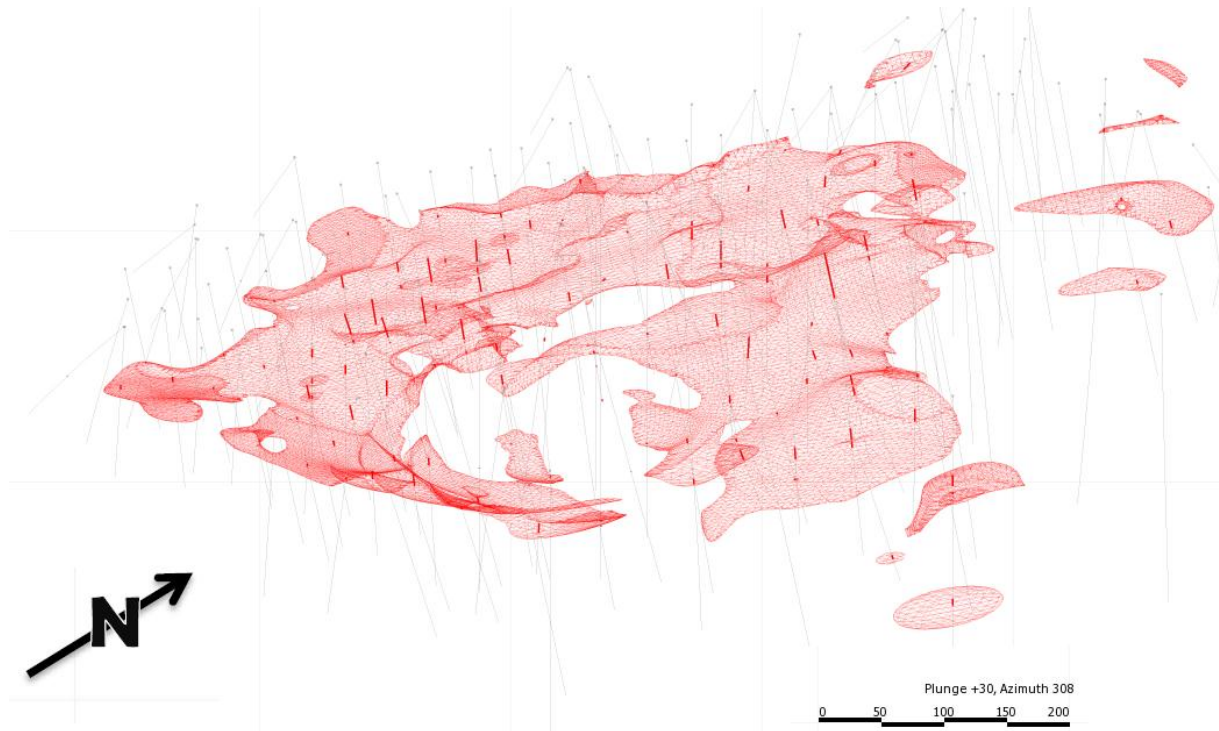


FIGURE 14.3 3D VIEW OF THE VMS SOLID WITH THE MINERALIZED INTERSECTS

In addition to the visual inspection, the lithological model was also validated by reviewing the correspondence of the coded lithological intervals with the flagged intervals within the solids. The flagging process was performed with the Vulcan software using the Flag Samples tool. The comparison was carried out between the codes stored in the LITON and LITO variables, which contain the codes for the lithological units of the original coding and the codes stored based on the flagging. The flagging process was performed using a straight composite database (compositing method in Vulcan software). Table 14.7 shows the results of the analysis of the correspondence between the lithologies recorded in the drill holes and the interpretation (Lithological Model).

TABLE 14.7 CORRESPONDENCE BETWEEN MODELLED AND LOGGED LITHOLOGICAL UNITS

Lithological Unit	Code	Modelled	Logged	Correspondence (m)	Correspondence (%)
		Total (m)	Total (m)		
Cover	-1	159.70	189.21	150.79	79.69%
Andesite	70	297.20	291.28	287.78	98.80%
Basalt	30	100.27	111.38	97.67	87.69%
Tuffs	60	659.68	630.08	622.48	98.79%
Grainstone	40	327.79	342.63	321.87	93.94%
VMS	20	797.83	788.42	770.07	97.67%
Breccia	21	3,070.84	3,038.96	3,025.31	99.55%
Gypsum	22	1,599.97	1,614.30	1,583.69	98.10%
Rhyolite	10	3,295.03	3,302.05	3,281.49	99.38%
Total		10,308.31	10,308.31	10,141.15	98.38%

DETERMINISTIC MODEL

BISA conducted deterministic modelling of Cu, Zn, Au, and Pb (the remaining metals were not modelled at this time). BISA recommends evaluating the suitability of also modelling deterministic solids for Ag.

Geological criteria were used for the construction of deterministic solids, and the Cu, Zn, Au, and Pb grades were visually inspected in the drill holes to identify the mineralized zones. The mineralization was studied in the VMS unit and the related mineralized units (Grainstone, Breccia, and Gypsum).

In addition, the grade distributions of metals in normal probability plots were reviewed to verify the thresholds identified during the visual inspection of the elements considered. The selected values are considered appropriate to differentiate high- and low-grade zones.

DETERMINISTIC MODEL FOR CU

The deterministic model for Cu is based on a visual review and interpretation of the Cu grades in the drill holes and a review of its distribution in a normal probability plot.

The Cu distribution was reviewed with available samples from the VMS unit. The VMS unit was chosen for review because its drill cores have been fully sampled and analysed. Figure 14.4 shows the normal probability plot used to verify the threshold defining the mineralized zone. The deterministic model for Cu grades was generated with Leapfrog. The solids were constructed using Boolean operations between solids generated for the lithological model and solids generated from selections of grades over the threshold of 0.3% Cu. Figure 14.5 illustrates the methodology used to construct the deterministic model for Cu via an inspection

of grades in the drill holes, where 0.3% Cu defines the threshold of the mineralized envelope. Figure 14.6 shows section 9855350N, where the deterministic model for copper and related mineralized units can be seen. Finally, the deterministic domain for Cu has been termed DOMCU.

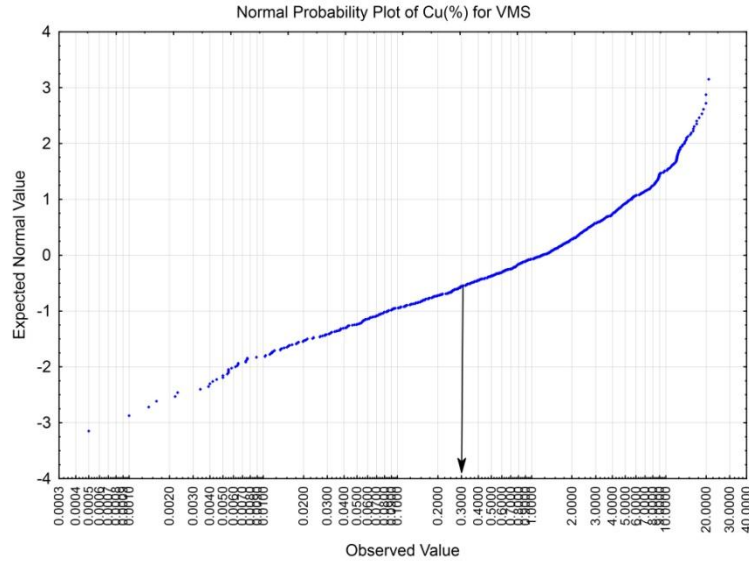


FIGURE 14.4 NORMAL PROBABILITY PLOT FOR CU (%) IN THE VMS UNIT

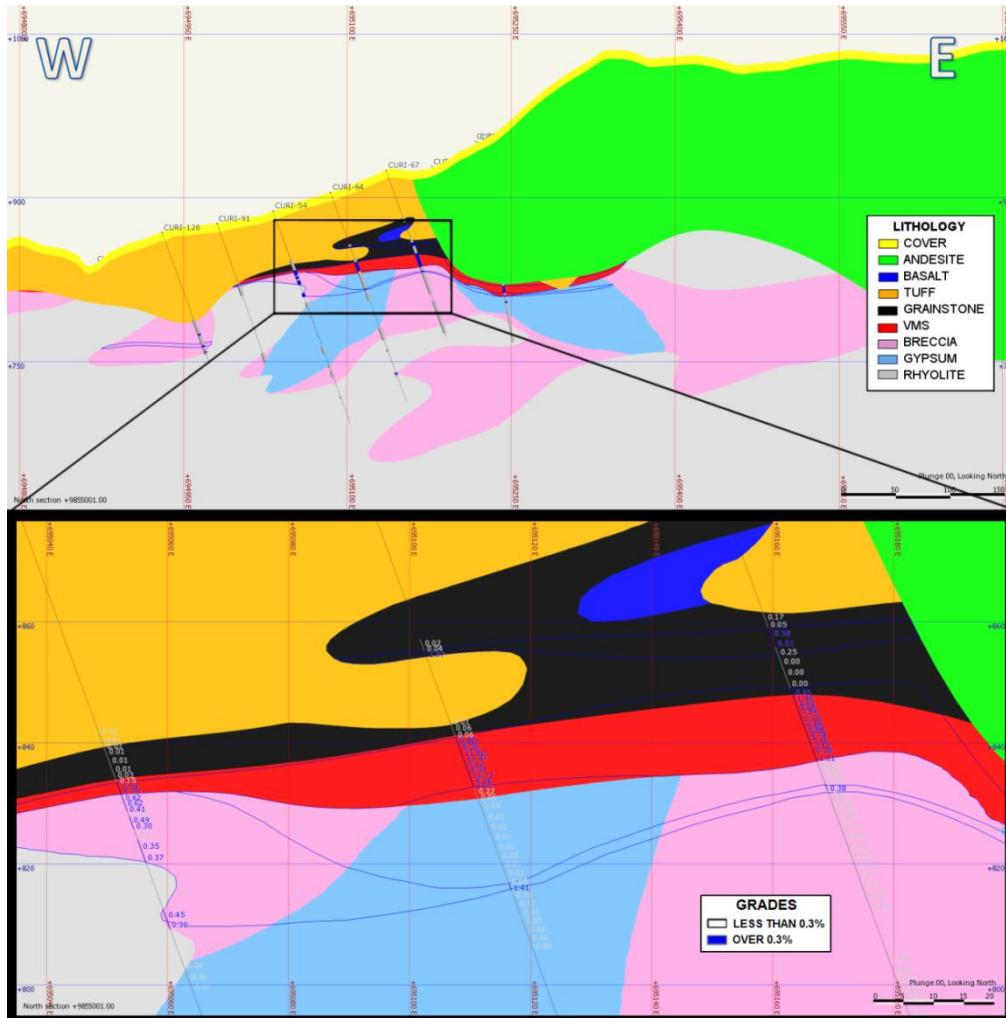


FIGURE 14.5 GENERATION OF THE DETERMINISTIC MODEL FOR CU (%) WITH A 0.3% CU THRESHOLD

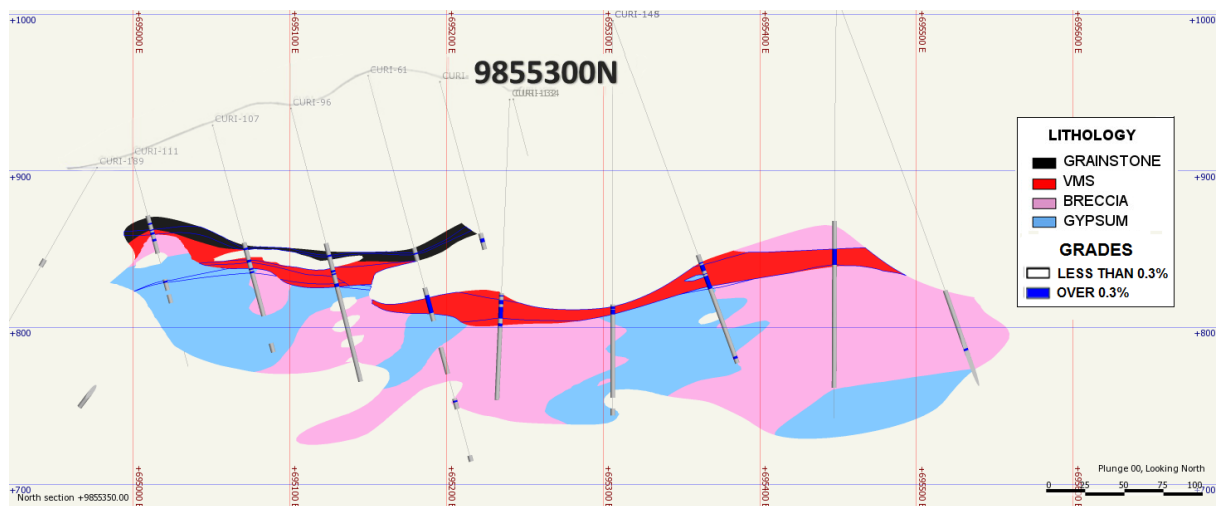


FIGURE 14.6 DETERMINISTIC MODEL FOR CU IN SECTION 9855300N

DETERMINISTIC MODELS FOR ZN, AU, AND PB

The deterministic models for Zn, Au, and Pb were constructed using the same methodology as for Cu. Figure 14.7 shows the deterministic models for Zn, Au, and Pb in section 9855300N as well as the normal probability plots used to verify the selected thresholds. In these cases, the thresholds used were 0.3 % Zn, 0.2 g/t Au, and 0.05% Pb. The codes for the deterministic models are DOMZN for Zn, DOMAU for Au, and DOMPb for Pb.

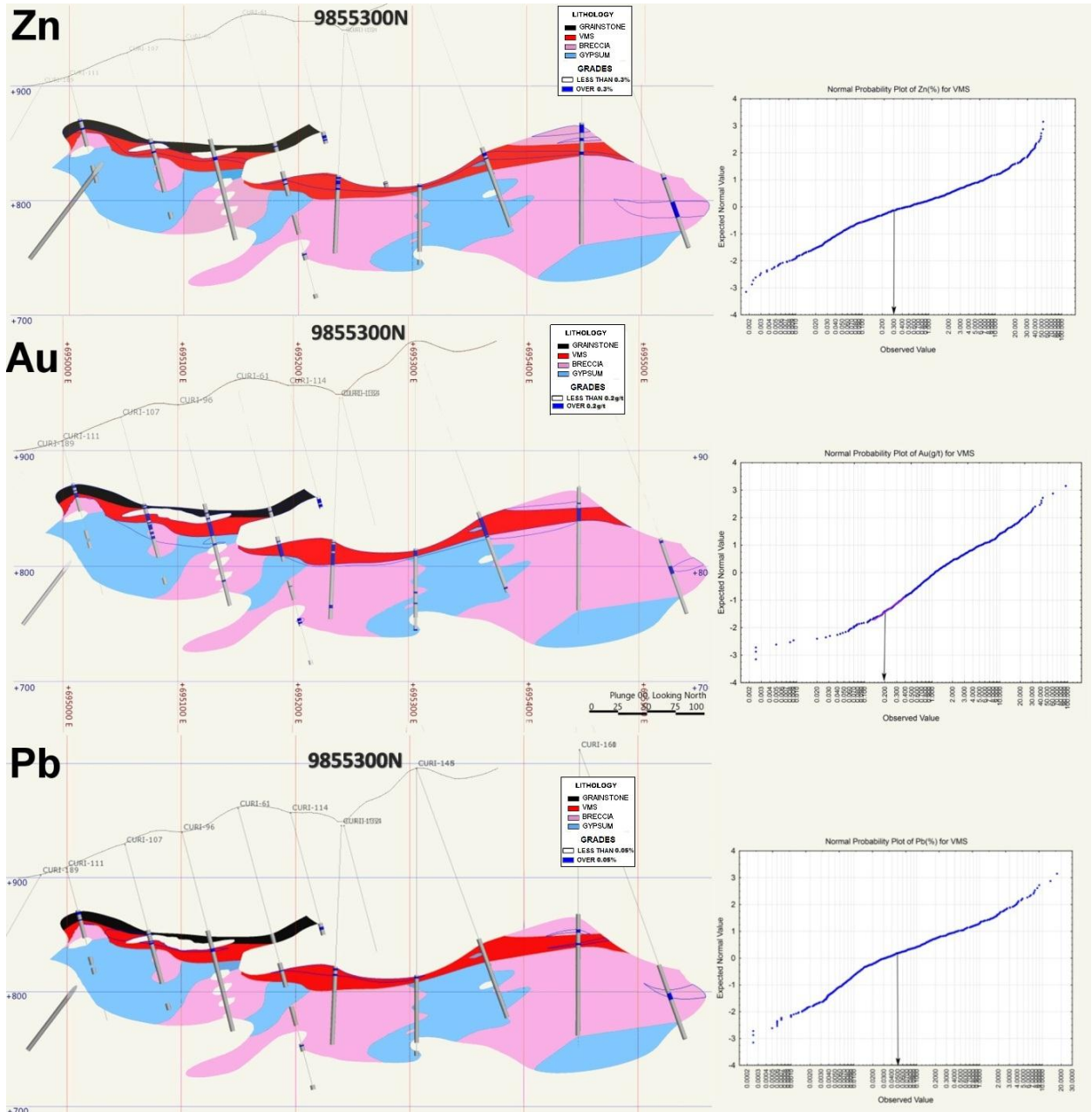


FIGURE 14.7 DETERMINISTIC MODELS AND NORMAL PROBABILITY PLOTS FOR ZN, AU, AND PB

STRUCTURAL DOMAINS

Two domains have been established to account for the Eastern Sector (site of El Domo hill) and the Western Sector, where most of the deposit is located (Figure 14.8). The faulted contact between the andesitic dome and the upper volcanoclastic unit is the limit of the two domains. In the Eastern Sector, the VMS unit lies at a greater depth and below the andesitic dome, and the Grainstone unit is absent. The difference in the competence of the wall rock in both domains is also notable. In the Eastern Sector, the predominant rock is andesite, a very competent rock, whereas the Western Sector is dominated by volcanoclastic sequences generally overprinted by argillic and, to a lesser extent, sericitic alteration. The term for the structural domains is DOM.

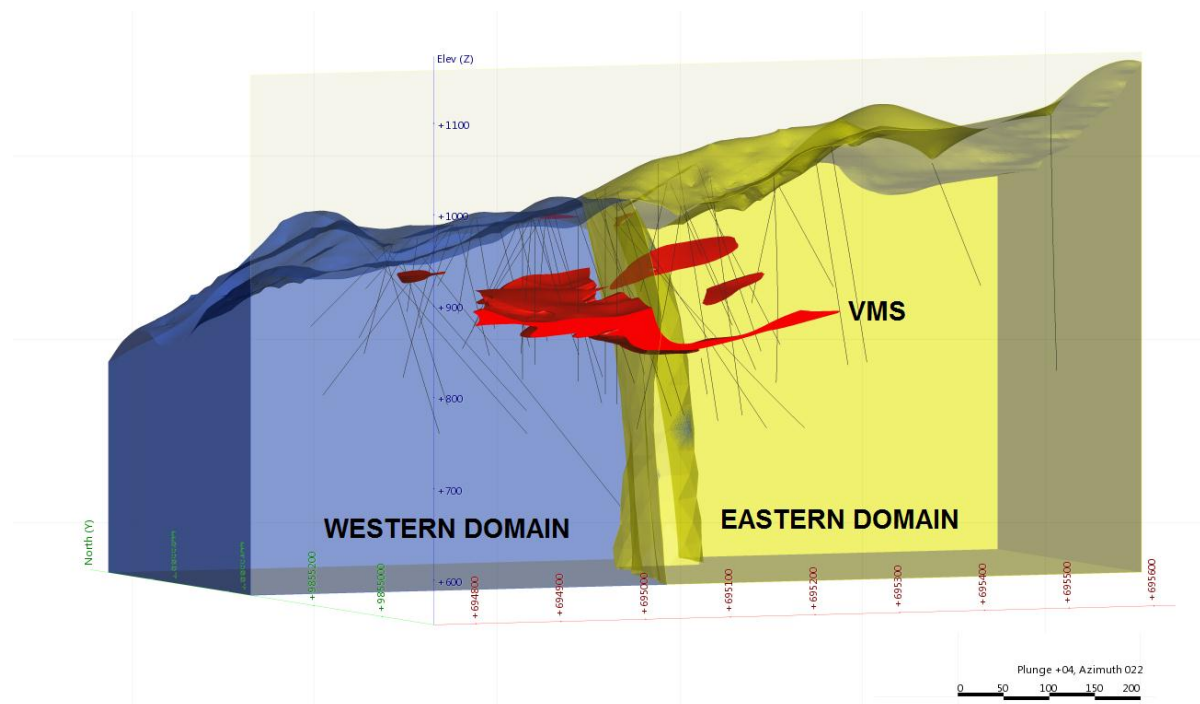


FIGURE 14.8 CROSS-SECTION OF EL DOMO SHOWING TWO STRUCTURAL DOMAINS

EXPLORATORY DATA ANALYSIS

BISA completed the Exploratory Data Analysis (EDA) for Cu, Zn, Pb, Au, and Ag using the available samples and taking into account the geological variables in the deposit. The EDA includes univariate statistics to assess all the lithological units modelled, the deterministic domains for each element, and the structural domains. This allows the definition of groups from these domains for estimation purposes.

With the aim of defining common characteristics associated with the individual mineralizations of Cu, Zn, Pb, Au, and Ag, groupings were generated based on domains

taking into consideration geological and statistical criteria (termed Geological Units – GU). An EDA was also conducted for the specific gravity samples reviewed based only on the lithological units and the structural domains.

Prior to completing the EDA, a general procedure was conducted to prepare the drill hole data. It includes straight compositing into Vulcan software. Then the resulting composites were flagged with the solids from the geological domains with the Flag Samples procedure. Table 14.8, Table 14.9, Table 14.10, Table 14.11, and Table 14.12 show the GUs defined for the Cu, Zn, Pb, Au, and Ag. The most important GUs are related to the VMS and Grainstone units.

TABLE 14.8 ESTIMATION DOMAINS DEFINED FOR COPPER (%)

GUCU	LITHOLOGY	DOMCU	DOM	# Samples	Average	Std. Dev.	Minimum	Maximum
1	VMS	High Cu	East/West	616	3.52	3.93	0.0119	20.90
2	VMS	Low Cu	East/West	201	0.26	0.82	0.0005	7.65
3	GRAINSTONE	High Cu	East/West	76	1.17	1.54	0.0138	8.01
4	GRAINSTONE	Low Cu	East/West	271	0.13	0.51	0.0005	6.37
	BASALT	High/Low Cu	East/West					
5	BRECCIA	High Cu	East/West	179	0.68	0.92	0.0028	8.10
	GYPSUM	High Cu	East/West					
6	BRECCIA	Low Cu	East	2,078	0.03	0.13	0.0001	2.12
	GYPSUM	Low Cu	East/West					
7	BRECCIA	Low Cu	West	1,356	0.06	0.19	0.0001	2.84
8	RHYOLITE	High/Low Cu	East	866	0.01	0.04	0.0001	0.49
9	RHYOLITE	High/Low Cu	West	1,351	0.02	0.08	0.0001	1.42
10	TUFFS	High/Low Cu	East/West	449	0.01	0.06	0.0001	0.86
11	ANDESITE	High/Low Cu	East/West	208	0.03	0.25	0.0001	3.04
12	COVER	High/Low Cu	East/West	85	0.01	0.01	0.0002	0.03

TABLE 14.9 ESTIMATION DOMAINS DEFINED FOR ZINC (%)

GUZN	LITHOLOGY	DOMZN	DOM	# Samples	Average	Std. Dev.	Minimum	Maximum
1	VMS	High Zn	East	118	4.62	7.49	0.0200	40.50
2	VMS	High Zn	West	375	6.81	10.51	0.0271	52.75
3	VMS	Low Zn	East	121	0.16	0.42	0.0022	3.50
4	VMS BASALT	Low Zn High/Low Zn	West East/West	275	0.28	1.56	0.0018	24.87
5	GRAINSTONE BRECCIA	High Zn High Zn	East/West West	639	1.24	2.20	0.0222	33.55
6	GRAINSTONE	Low Zn	East/West	170	0.15	0.58	0.0036	6.85
7	BRECCIA GYPSUM	High Zn High Zn	East East/West	259	0.75	0.80	0.0030	8.25
8	BRECCIA	Low Zn	East	778	0.04	0.09	0.0003	0.70
9	BRECCIA	Low Zn	West	963	0.10	0.83	0.0002	20.30
10	GYPSUM RHYOLITE	Low Zn High/Low Zn	East/West East	1,945	0.04	0.15	0.0001	2.65
11	RHYOLITE	High/Low Zn	West	1,351	0.08	0.23	0.0001	2.62
12	TUFFS	High/Low Zn	East	39	0.04	0.07	0.0027	0.36
13	TUFFS ANDESITE	High/Low Zn High/Low Zn	West East/West	618	0.04	0.17	0.0031	3.45
14	COVER	High/Low Zn	East/West	85	0.02	0.02	0.0039	0.16

TABLE 14.10 ESTIMATION DOMAINS DEFINED FOR LEAD (%)

GUPB	LITHOLOGY	DOMPB	DOMZN	# Samples	Average	Std. Dev.	Minimum	Maximum
1	VMS	High Pb	High/Low Zn	416	0.75	1.64	0.0013	17.20
2	VMS	Low Pb	High/Low Zn	401	0.01	0.01	0.0003	0.12
3	GRAINSTONE	High Pb	High/Low Zn	88	0.21	0.40	0.0037	3.43
4	GRAINSTONE	Low Pb	High/Low Zn	187	0.03	0.07	0.0001	0.76
5	BRECCIA	High Pb	High/Low Zn	600	0.16	0.38	0.0003	5.17
6	BRECCIA	Low Pb	Low Zn	311	0.03	0.06	0.0003	0.88
7	BRECCIA	Low Pb	Low Zn	1,531	0.01	0.02	0.0002	0.53
8	BASALT	High/Low Pb	High/Low Zn	72	0.02	0.04	0.0001	0.19
9	GYPSUM RHYOLITE	High/Low Pb High/Low Pb	High/Low Zn High/Low Zn	3,388	0.01	0.03	0.0001	0.61
10	TUFFS ANDESITE	High/Low Pb High/Low Pb	High/Low Zn High/Low Zn	657	0.00	0.02	0.0001	0.32
11	COVER	High/Low Pb	High/Low Zn	85	0.00	0.01	0.0003	0.05

TABLE 14.11 ESTIMATION DOMAINS DEFINED FOR GOLD (G/T)

GUAU	LITHOLOGY	DOMAU	DOM	# Samples	Average	Std. Dev.	Minimum	Maximum
1	VMS	High/Low Au	East	239	1.54	2.36	0.0025	19.70
2	VMS	High/Low Au	West	578	4.08	7.68	0.0025	94.00
3	GRAINSTONE	High Au	East/West	207	1.04	1.40	0.0100	9.22
4	GRAINSTONE	Low Au	East/West	68	0.04	0.04	0.0025	0.18
5	BRECCIA	Alto Au	East/West	717	0.62	1.82	0.0100	43.00
6	BRECCIA	Low Au	East/West	1,725	0.08	0.21	0.0025	7.66
7	BASALT	High/Low Au	East/West	72	0.20	0.40	0.0025	2.39
8	GYPSUM	High Au	East/West	88	0.33	0.29	0.0025	1.76
	GYPSUM	Low Au	East/West					
9	RHYOLITE	High/Low Au	East/West	3,339	0.05	0.14	0.0025	5.60
	TUFFS	High/Low Au	East					
10	TUFFS	High/Low Au	West	410	0.04	0.09	0.0025	1.09
11	ANDESITE	High/Low Au	East/West	208	0.04	0.21	0.0025	2.71
12	COVER	High/Low Au	East/West	85	0.01	0.03	0.0025	0.21

TABLE 14.12 ESTIMATION DOMAINS DEFINED FOR SILVER (G/T)

GUAG	LITHOLOGY	DOMCU	DOMZN	DOMAU	# Samples	Average	Std. Dev.	Minimum	Maximum
1	VMS	High Cu	High Zn	High/Low Au	406	118.91	197.20	1.30	1836.00
2	VMS	High Cu	Low Zn	High/Low Au	210	15.00	57.77	0.10	834.00
3	VMS	Low Cu	High Zn	High/Low Au	87	63.15	238.75	0.90	2160.00
4	VMS	Low Cu	Low Zn	High/Low Au	520	12.41	25.57	0.10	244.40
	BRECCIA	High/Low Cu	Low Zn	High Au					
5	GRAINSTONE	High/Low Cu	High Zn	High/Low Au	105	30.97	42.66	0.50	272.50
6	GRAINSTONE	High/Low Cu	Low Zn	High/Low Au	242	4.37	7.96	0.10	51.10
	BASALT	High/Low Cu	High/Low Zn	High/Low Au					
7	BRECCIA	High/Low Cu	High Zn	High Au	311	26.25	59.57	0.40	736.00
8	BRECCIA	High/Low Cu	High Zn	Low Au	390	4.62	10.15	0.10	126.90
9	BRECCIA	High/Low Cu	Low Zn	Low Au	1,335	2.03	14.54	0.10	510.00
10	TUFFS	High/Low Cu	High/Low Zn	High/Low Au	449	1.11	6.62	0.10	114.90
11	ANDESITE	High/Low Cu	High/Low Zn	High/Low Au	208	1.02	5.51	0.10	66.50
12	RHYOLITE	High/Low Cu	High/Low Zn	High/Low Au	3,388	1.26	3.91	0.10	118.30
	GYPSUM	High/Low Cu	High/Low Zn	High/Low Au					
13	COVER	High/Low Cu	High/Low Zn	High/Low Au	85	1.28	4.06	0.10	32.70

SPECIFIC GRAVITY REVIEW

The specific gravity (SG), assumed as representative in-situ bulk density, was reviewed using the same methodology as for the metallic elements (i.e. geological and statistical criteria). Unlike the metals, these geological units (GU) were generated based on lithological units and structural domains.

The methodology to estimate the bulk density is based on their distribution analysis for each of the lithologies. Ten GUs were defined with this aim. The preliminary stage included

assessing the selection of representative samples in order to discard outliers. Threshold values were two or three standard deviations depending on the GU.

Table 14.13 shows the specific gravity GUs based on available samples and applied thresholds. Note that GUs 1, 2, 7, 8, and 9 have an adequate number of specific gravity samples. In these GUs, the specific gravity values are the estimates, whereas in the other cases, the values are averaged.

TABLE 14.13 ESTIMATION DOMAINS DEFINED FOR SPECIFIC GRAVITY

GUD	LITHOLOGY	DOM	# Samples	Average	Std. Dev.	Minimum	Maximum	Lower Threshold	Upper Threshold
1	VMS	East	101	3.45	0.57	2.07	4.55	-2 σ	+2 σ
2	VMS	West	212	3.72	0.50	2.41	4.65	-2 σ	+2 σ
3	GRAINSTONE	East/West	67	2.82	0.36	2.40	3.92	NA	NA
4	BASALT	East/West	4	2.70	0.28	2.45	3.08	NA	NA
5	ANDESITE	East/West	4	2.89	0.76	2.39	4.03	NA	NA
6	COVER	East/West	0	0.00	0.00	0.00	0.00	NA	NA
7	RHYOLITE GYPSUM	East/West East/West	277	2.61	0.29	1.72	3.94	-3 σ	+3 σ
8	BRECCIA	East	190	2.78	0.35	2.00	4.45	-2 σ	+2 σ
9	BRECCIA	West	238	2.75	0.38	1.84	4.21	-2 σ	+2 σ
10	TUFFS	East/West	47	2.48	0.21	2.10	3.48	NA	NA

σ : Standard Deviation

Figure 14.9 shows the probabilistic diagram of specific gravity for the various GUs considered.

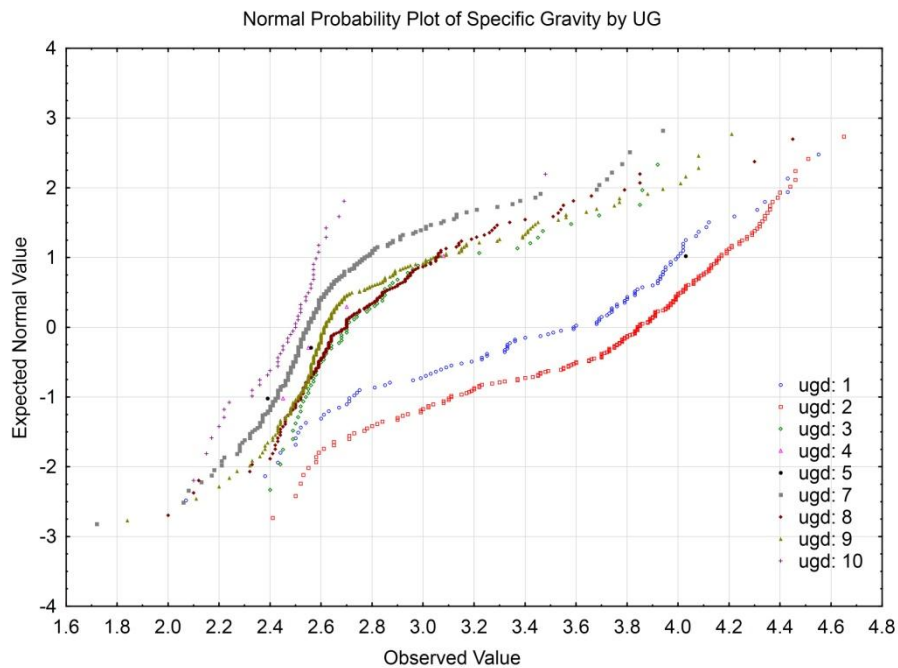


FIGURE 14.9 PROBABILISTIC DIAGRAM OF SPECIFIC GRAVITY BY ESTIMATION DOMAINS

COMPOSITING

Compositing was done using the available samples, which have been standardized to 1.25 m in length, which represents half the assumed block height of 2.5 metres. Composites with a length of less than 0.5 m have been discarded for the interpolation. This exercise was carried out in Vulcan software with the run-length compositing procedure honouring the Geological Units for each metal and bulk density.

TREATMENT OF HIGH GRADES

The methodology applied for the treatment of outliers in the El Domo deposit includes two different techniques depending on the type of situation: (1) capping extreme values and (2) limiting extreme values in a given region (“High Yield Limit Field” in Vulcan Software). Probabilistic diagrams have been used for this purpose as they are a very effective graphic tool for the study of data distribution and the detection of outliers. Tonnage/grade curves are another way to estimate whether it is appropriate to use a capped distribution.

Figure 14.10, Figure 14.11, and Figure 14.13 summarize the analyses performed on GU01 for Cu, Zn, Pb, Au, and Ag run-length composites.

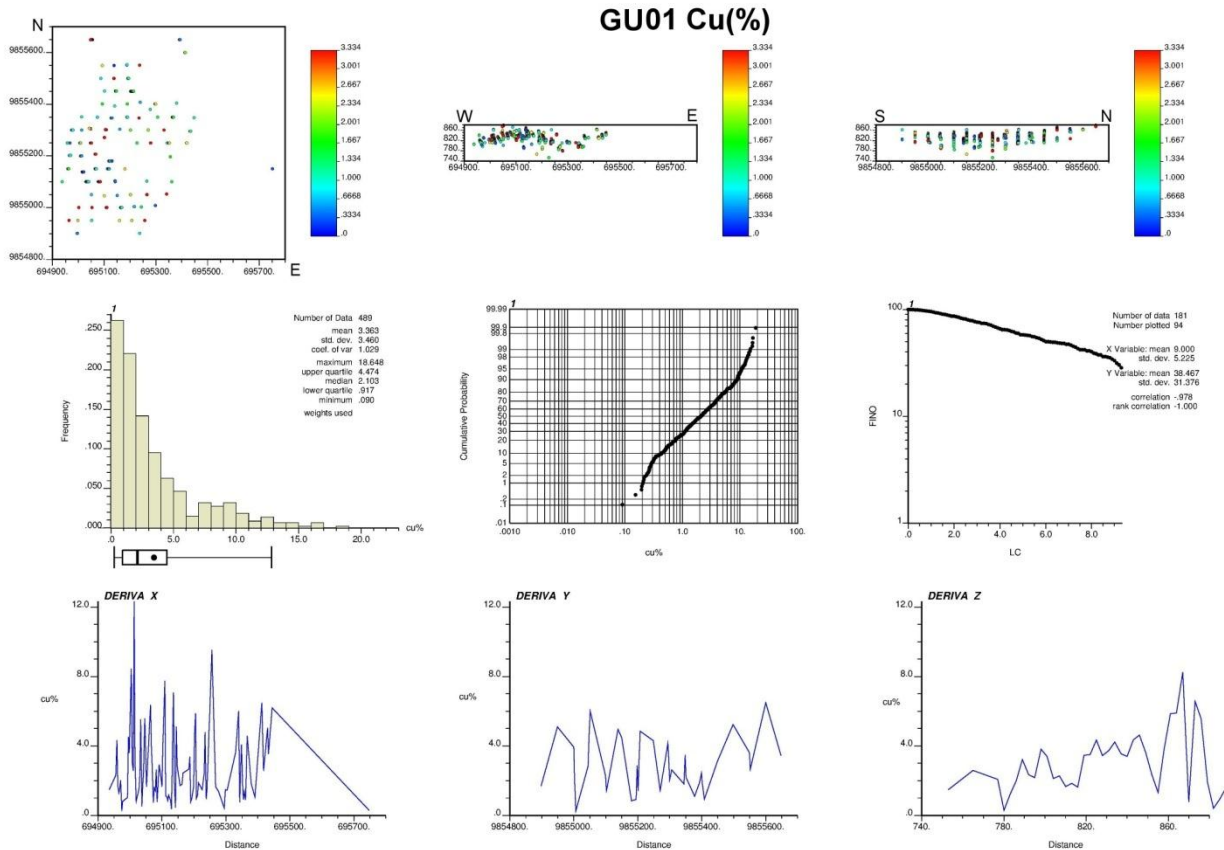


FIGURE 14.10 ANALYSIS OF RUN-LENGTH COMPOSITES FOR CU GU01

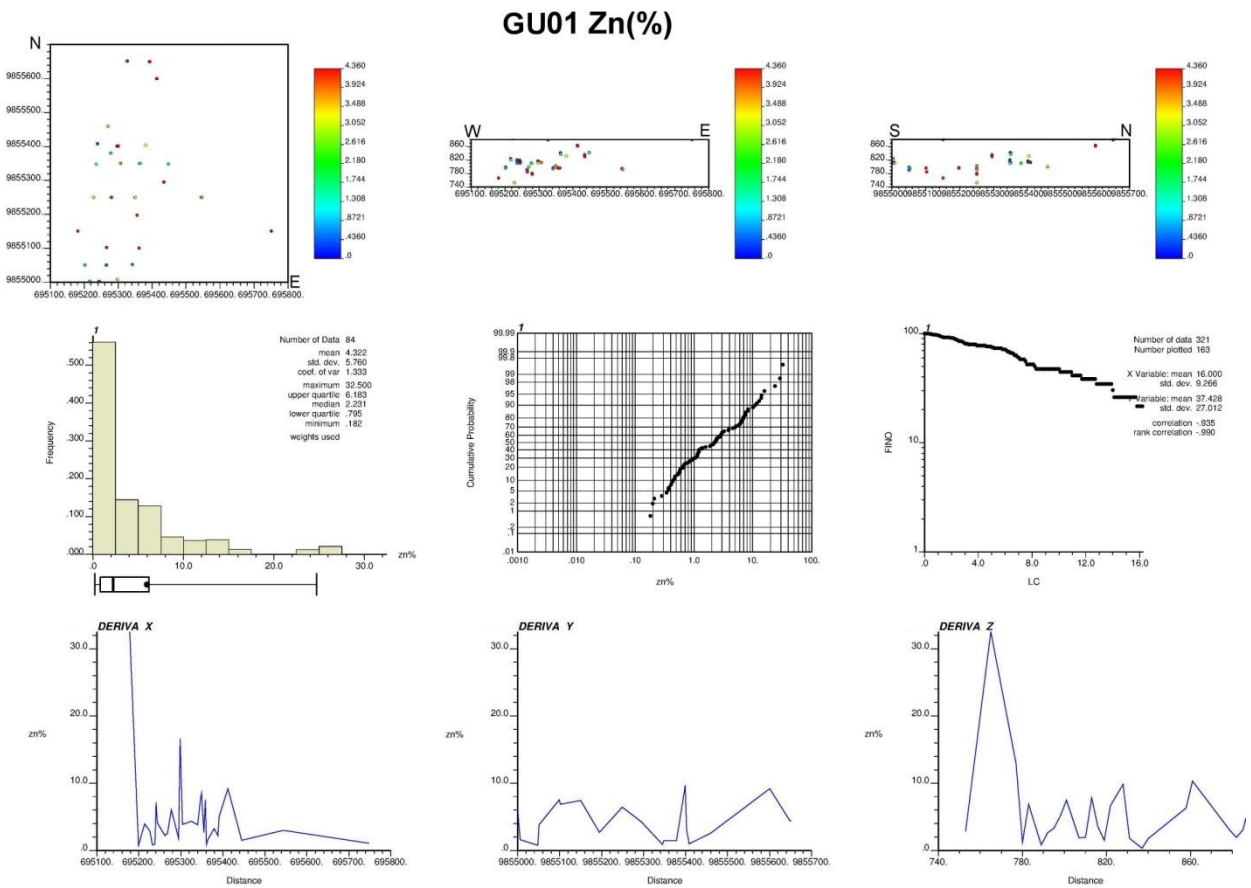


FIGURE 14.11 ANALYSIS OF RUN-LENGTH COMPOSITES FOR ZN GU01

GU01 Pb(%)

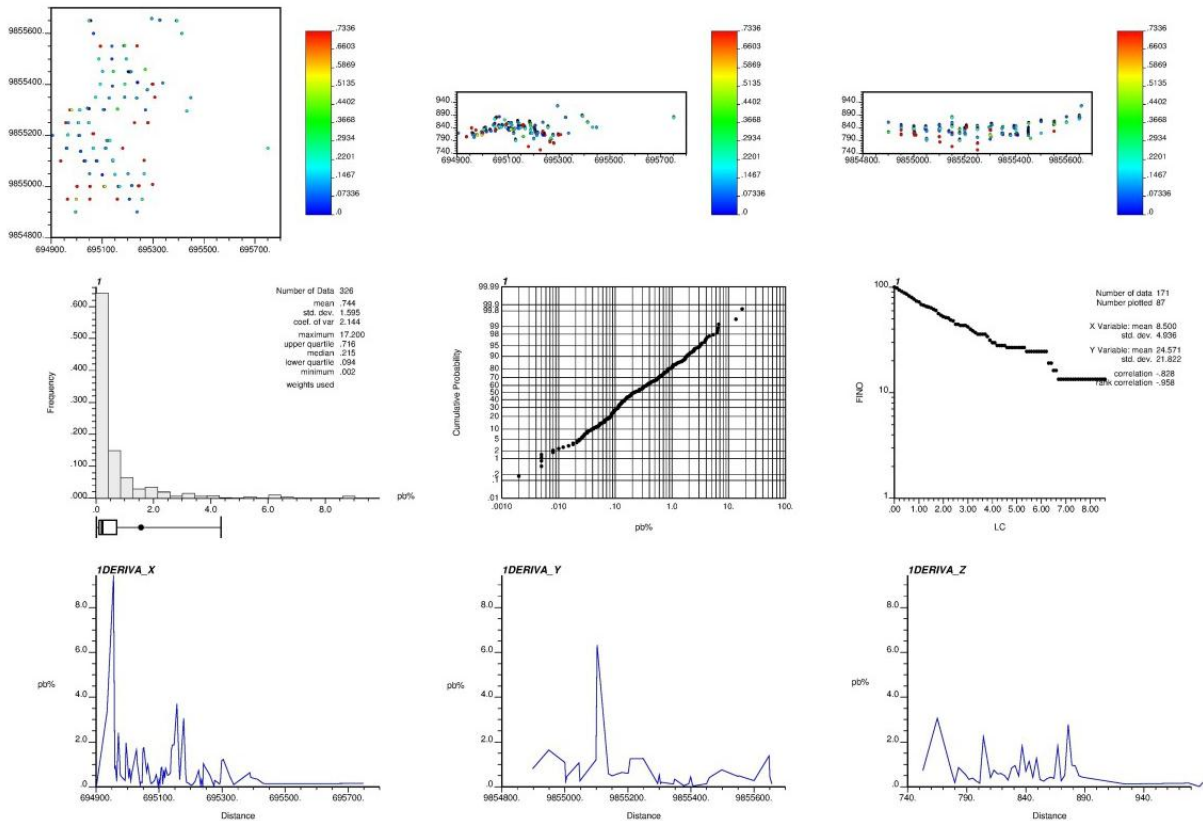


FIGURE 14.12 ANALYSIS OF RUN-LENGTH COMPOSITES FOR PB GU01

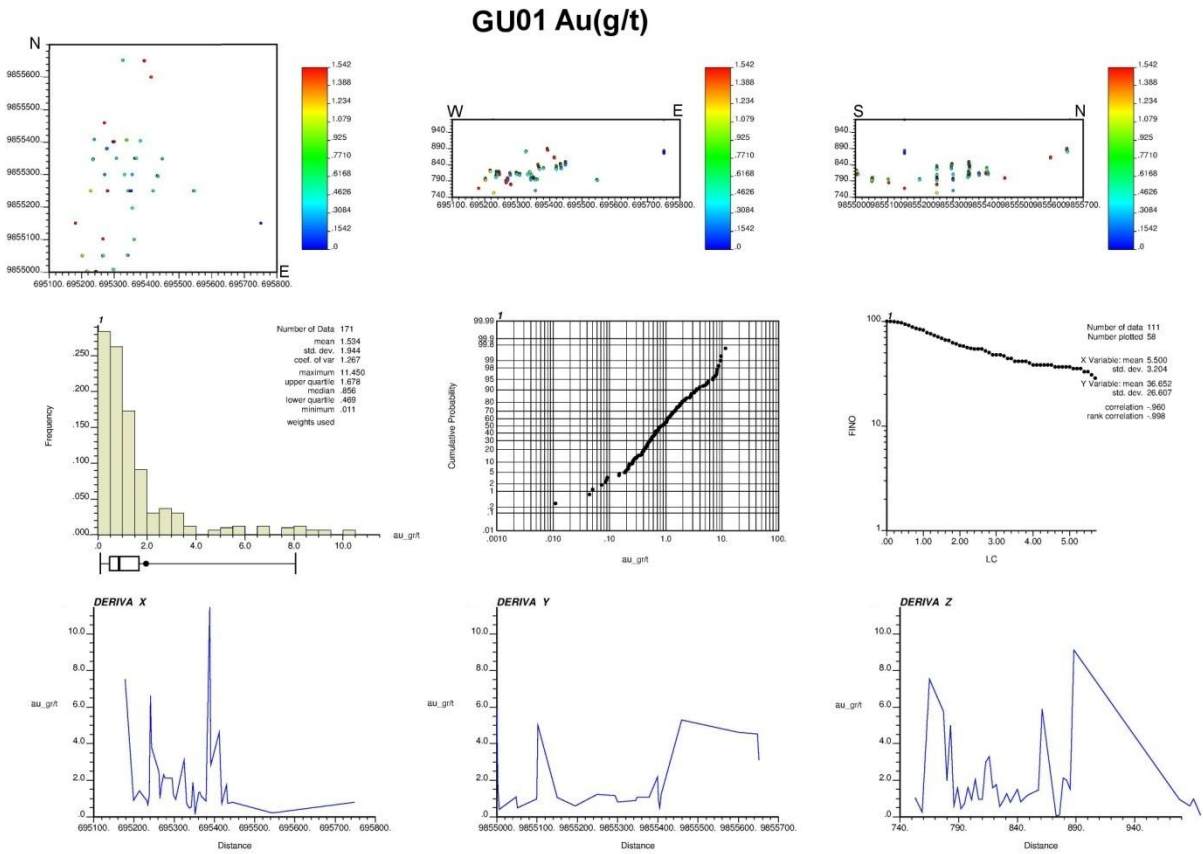


FIGURE 14.13 ANALYSIS OF RUN-LENGTH COMPOSITES FOR AU GU01

GU01 Ag(g/t)

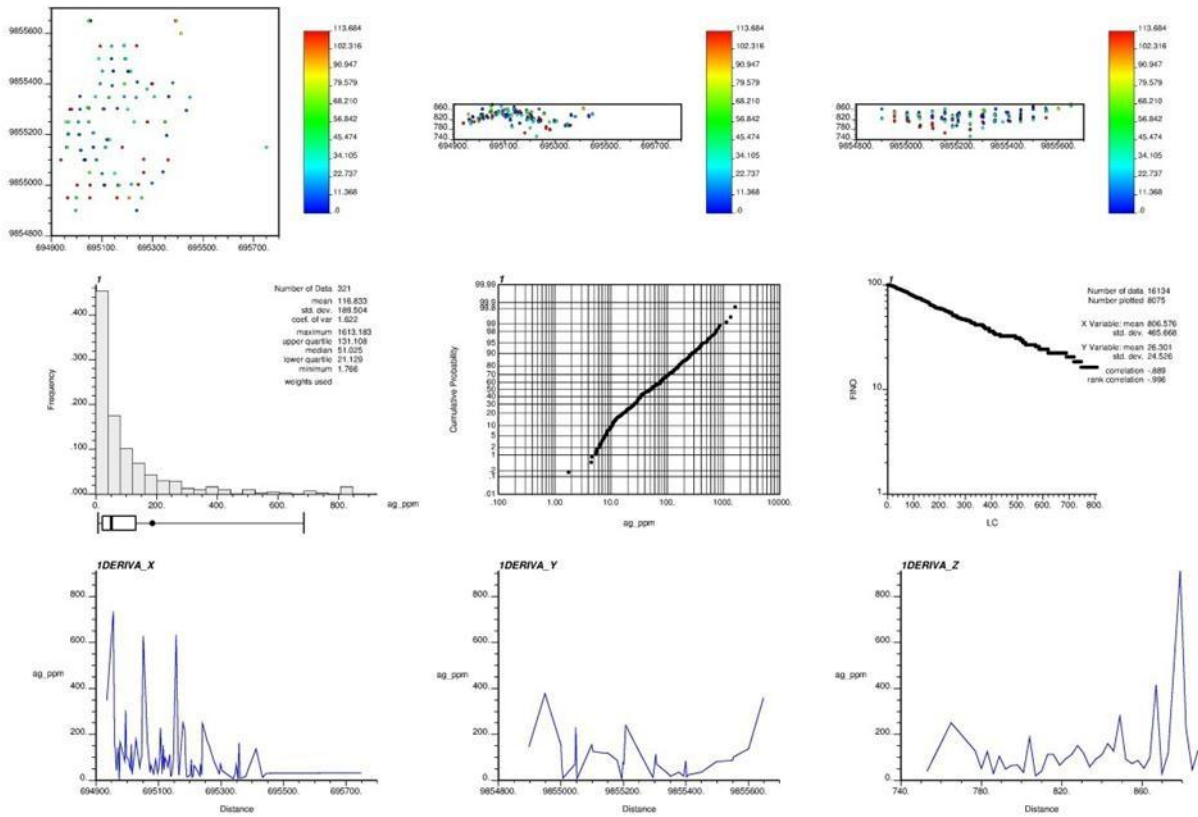


FIGURE 14.14 ANALYSIS OF RUN-LENGTH COMPOSITES FOR AG GU01

VARIOGRAPHY

The spatial continuity of the grades for Cu, Zn, Au, Ag, and Pb in the deposit was reviewed using a reverse correlogram standardized to the unit, termed the “correlograma” for the purposes of this study. SAGE2001 was used to calculate the correlograms. Although a correlogram is generally a function that decreases with distance, it tends to zero as the distance increases. SAGE2001 uses the following corrections worth mentioning:

$$\gamma(h) = 1 - \frac{1}{N(h)} \sum_{i=1}^{N(h)} \frac{(Z_i Z_{i+h} - m_{-h} m_{+h})}{\sigma_{-h} \sigma_{+h}}$$

h = Vectoral separation or distance

Z_i = Value of a sample in position i

Z_{i+h} = Value of a sample in position i , at a distance h

σ_{i+h} = Standard deviation Z_i at a distance h

m_{+h} = Measurement of the tails between walls of samples separated by a vector distance h

The correlograms were calculated with the parameters shown in Table 14.14. The correlogram was modelled using 13 experimental directions adjusted to a three-dimensional ellipsoidal model defined for the experimental points in all directions, using two spherical structures.

Correlograms were calculated for all the GU metals (Cu, Zn, Pb, Au, and Ag) that have an adequate number of run-length composites. It should be noted that, in general, the ranges obtained with the correlograms are short in the vertical direction, and with a variable nugget effect. Figure 14.15 shows an example of the correlogram for the Cu GU02 in the direction Azimuth 90° and Dip 0°. The resulting variographic parameters are summarized in the interpolation plans.

BISA recommends further study of the trends and anisotropies identified to verify the ranges and variability of metals in the deposit as the investigation progresses.

TABLE 14.14 PARAMETERS FOR CALCULATION OF EXPERIMENTAL CORRELOGRAMS

Lag (m)	Max. No. Of Lags	Direction of Increase		Band Width		Tolerance	
		Azimuth (°)	Dip (°)	Vertical (m)	Horizontal (m)	% of Lag	Angular (°)
50	10	90	30	25	40	50	30

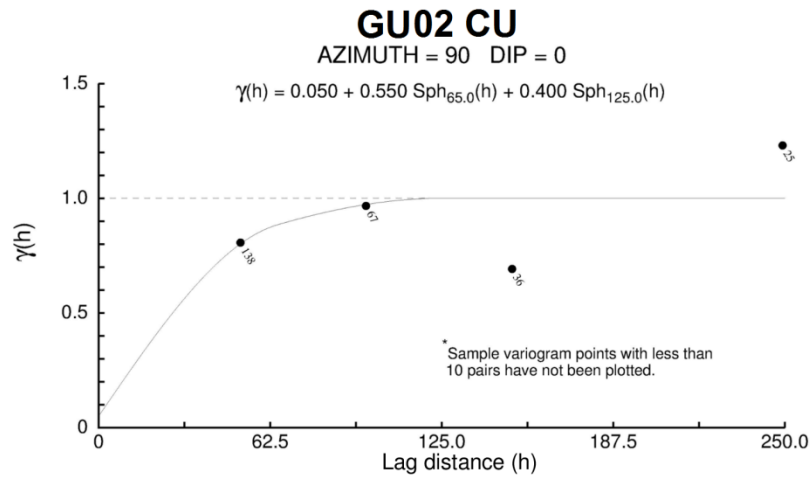


FIGURE 14.15 CORRELOGRAM OF CU GU02 IN THE AZIMUTH 90° AND DIP 0°

BLOCK MODEL

The block model was constructed in Vulcan (version 8.0.2) as a sub-cell type block model that includes the lithological units, deterministic domains for metals, and the structural domains based on geological interpretations made in the 3D modelling. It also contains the variables needed to estimate the metals considered in this study. The dimensions of the sub-cell type model vary from 2.5 x 2.5 x 2.5 m to 5 x 5 x 2.5 m. The regular block model where the estimates were re-blocked has a block size of 5 m (east) x 5 m (north) x 2.5 m (elevation).

Estimates were calculated in the sub-cell type block model for each GU of the metals considered, which were then re-blocked into the regular block model as a volume-weighted average for metals. Furthermore, the categorical variables, such as lithological units, deterministic domains, structural domains, geological units, and resource category, were re-blocked into the regular block model considering the majority percentage within each regular block. Table 14.15 shows the geometry and orientation of the two models defined in the UTM PSAD 56 coordinate system.

TABLE 14.15 LIMITS OF BLOCK MODELS

	Sub-Cell Type Block Model	Regular Block Model
Minimum Coordinate East (m)	694,750	694,750
Maximum Coordinate East (m)	695,800	695,800
Minimum Coordinate North (m)	9,854,850	9,854,850
Maximum Coordinate North (m)	9,855,800	9,855,800
Minimum Elevation (m)	550	550
Maximum Elevation (m)	1150	1150
Bearing (°)	90	90
Dip (°)	0	0
Plunge (°)	0	0

INTERNAL DILUTION

The block model considers the internal dilution of the geological contacts, using the sub-cell type block model, which is standardized to a regular-sized block model using a volume-weighted average for metals. Similarly, the codes associated with the lithological units, deterministic domains, structural domains, and so on, were standardized. This was done taking into account the majority percentage of each domain and/or unit within a regular block. The height of the blocks used in El Domo is 2.5 metres based on the criteria of geological continuity established mainly in the VMS unit, while taking into account the dimensions of equipment that might be used in a mining operation.

ESTIMATION PARAMETERS

The interpolation methodology for estimating Cu, Zn, Pb, Au, Ag, and bulk density were Ordinary Kriging (OK) and Inverse Distance weighted (IDW) to the power of 2 and/or 3. The estimation was carried out separately for each GU, considering the aforementioned metals and specific gravity, using their respective correlogram models as appropriate.

Search distances and anisotropies are derived from the spatial correlation in each GU. Generally, the estimation in each GU has been made in three passes, so called due to the strategy of increasing searches used in each one. Therefore, the estimation is sequential, with an appropriate adjustment for the first passes, as well as a good correlation between adjacent composites and the block to be estimated. The blocks not estimated during the three passes were assigned an average metal value for the corresponding GU, setting this as the fourth pass. It should be noted that, in the GU for the coverage of the different metals, they have been assigned a default value. In addition, The GU12 for Zn was assigned an averaged value.

Regarding the interpolation parameters, it should be noted that the search radii are flattened ellipsoids with the shortest distance in the Z axis. The search radii have been adjusted for each GU. Concerning the search by octants, the minimum and maximum number of composites per octant, the minimum number of octants with composites required to estimate a block to ensure good spatial coherence, and the influence of all the directions have all been defined for each pass as appropriate. In addition, the use of the maximum number of composites per drill hole, the minimum number of composites, and the maximum number of composites for the interpolation for each pass are summarized in interpolation planes for each metal, where the parameters are set for the three passes for each GU. Table 14.16, Table 14.17, Table 14.18, Table 14.19, Table 14.20, and Table 14.21 summarize the interpolation planes for Cu, Zn, Pb, Au, Ag, and SG.

In addition, hard contacts have been assumed in estimating each GU due to the strong contrast in the high grades for the VMS relative to the other units. BISA recommends that a contact analysis be conducted in future for all units, particularly for the GUs for the Breccia and Gypsum units.

To limit the extreme values, the High Yield Limit Field was used in the various GUs on each pass as applicable. Capping of extreme values has also been applied in the interpolation planes depending on the estimated GU.

Finally, a discretization has been used on blocks of 3x3x2 nodes, which is considered reasonable for the size of the blocks and the composites used. Specific gravity was estimated using interpolation only in GUs 1, 2, 7, 8, and 9; for the remaining GUs, an average specific gravity was assigned.

TABLE 14.16 INTERPOLATION PLAN FOR COPPER (%)

Metal	Geological Unit	PASS	Interpolator	Search Ranges Major Axis/Semi-Major Axis/Minor Axis (m)	Rotation (Bearing / Plunge / Dip) (°)	Variographic Parameters											Discretization (x/y/z)	Min. No. Comp.	Max. No. Comp.	Max. No. Comp. per Drift Hole	Capping		High Yield		
						C0	1st St.	C1	Rotation (Bearing / Plunge / Dip) (°)	Ranges (E.M.A / E.S-M / E.M.E)	2nd St.	C2	Rotation (Bearing / Plunge / Dip) (°)	Ranges (E.M.A / E.S-M / E.M.E)	Lower	Upper					Limit	Major Axis/Semi-Major Axis/Minor Axis (m)			
Cu(%)	1	1	OK	60/20/10	0/0/0	0.280	SPH	0.520	0/0/30	30/7/8	SPH	0.200	0/0/30	60/100/10	3/3/2	5	9	2	3	1	2	0.00	16.29	12.00	2.5/2.5/2.5
Cu(%)		2	OK	100/40/15	0/0/0	0.280	SPH	0.520	0/0/30	30/7/8	SPH	0.200	0/0/30	60/100/10	3/3/2	4	9	3	3	1	3	0.00	16.29	12.00	25/10/2.5
Cu(%)		3	OK	150/60/20	0/0/0	0.280	SPH	0.520	0/0/30	30/7/8	SPH	0.200	0/0/30	60/100/10	3/3/2	4	12	3	2	1	3	0.00	16.29	12.00	20/10/5
Cu(%)	2	1	OK	70/180/9	0/0/0	0.050	SPH	0.550	0/0/0	35/65/2.5	SPH	0.400	0/0/0	60/125/6	3/3/2	4	9	2	3	1	3	0.00	5.30	3.10	10/15/2.5
Cu(%)		2	OK	110/180/15	0/0/0	0.050	SPH	0.550	0/0/0	35/65/2.5	SPH	0.400	0/0/0	60/125/6	3/3/2	4	16	3	3	1	3	0.00	5.30	100	10/10/5
Cu(%)		3	OK	150/220/20	0/0/0	0.050	SPH	0.550	0/0/0	35/65/2.5	SPH	0.400	0/0/0	60/125/6	3/3/2	3	12	2	3	1	3	0.00	5.30	0.35	2.5/2.5/2.5
Cu(%)	3	1	OK	35/35/8	0/0/0	0.300	SPH	0.300	0/0/0	8/8/1	SPH	0.400	0/0/0	65/30/2	3/3/2	4	12	3	3	1	3	0.00	5.30	-	-
Cu(%)		2	OK	55/55/12	0/0/0	0.300	SPH	0.300	0/0/0	8/8/1	SPH	0.400	0/0/0	65/30/2	3/3/2	4	12	3	3	1	3	0.00	5.30	-	-
Cu(%)		3	OK	80/80/15	0/0/0	0.300	SPH	0.300	0/0/0	8/8/1	SPH	0.400	0/0/0	65/30/2	3/3/2	4	12	3	3	1	3	0.00	5.30	3.78	10/10/2.5
Cu(%)	4	1	OK	25/40/4	0/0/0	0.400	SPH	0.100	0/0/-30	15/30/3	SPH	0.500	0/0/-30	60/80/4	3/3/2	4	9	3	3	1	2	0.00	3.55	127	5/5/2.5
Cu(%)		2	OK	50/80/6	0/0/0	0.400	SPH	0.100	0/0/-30	15/30/3	SPH	0.500	0/0/-30	60/80/4	3/3/2	4	12	3	3	1	3	0.00	3.55	127	5/5/2.5
Cu(%)		3	OK	80/120/8	0/0/0	0.400	SPH	0.100	0/0/-30	15/30/3	SPH	0.500	0/0/-30	60/80/4	3/3/2	3	12	3	2	1	3	0.00	3.55	0.40	5/5/2.5
Cu(%)	5	1	OK	45/20/10	0/0/0	0.050	SPH	0.350	0/0/12	30/10/5	SPH	0.600	0/0/12	75/35/11	3/3/2	4	9	3	3	1	3	0.00	7.45	4.40	15/15/2.5
Cu(%)		2	OK	80/40/15	0/0/0	0.050	SPH	0.350	0/0/12	30/10/5	SPH	0.600	0/0/12	75/35/11	3/3/2	4	12	3	3	1	2	0.00	7.45	4.40	15/15/5
Cu(%)		3	OK	120/60/20	0/0/0	0.050	SPH	0.350	0/0/12	30/10/5	SPH	0.600	0/0/12	75/35/11	3/3/2	3	12	3	2	1	2	0.00	7.45	199	10/10/2.5
Cu(%)	6	1	OK	20/20/10	0/0/0	0.350	SPH	0.400	0/0/0	12/15/3	SPH	0.250	0/0/0	28/40/13	3/3/2	4	9	3	3	1	3	0.00	1.19	0.97	5/5/2.5
Cu(%)		2	OK	40/40/15	0/0/0	0.350	SPH	0.400	0/0/0	12/15/3	SPH	0.250	0/0/0	28/40/13	3/3/2	4	12	3	3	1	3	0.00	1.19	0.70	5/5/2.5
Cu(%)		3	OK	60/60/20	0/0/0	0.350	SPH	0.400	0/0/0	12/15/3	SPH	0.250	0/0/0	28/40/13	3/3/2	3	12	3	2	1	3	0.00	1.19	0.26	5/5/2.5
Cu(%)	7	1	OK	30/30/10	0/0/0	0.050	SPH	0.500	0/0/30	19/15/2.5	SPH	0.450	0/0/30	70/70/4	3/3/2	4	9	3	3	1	3	0.00	2.00	2.00	5/5/2.5
Cu(%)		2	OK	60/60/20	0/0/0	0.050	SPH	0.500	0/0/30	19/15/2.5	SPH	0.450	0/0/30	70/70/4	3/3/2	4	12	3	3	1	3	0.00	2.00	130	5/5/2.5
Cu(%)		3	OK	100/100/30	0/0/0	0.050	SPH	0.500	0/0/30	19/15/2.5	SPH	0.450	0/0/30	70/70/4	3/3/2	3	12	3	2	1	3	0.00	2.00	0.81	5/5/2.5
Cu(%)	8	1	OK	40/20/10	0/0/0	0.050	SPH	0.550	0/0/-25	25/10/3	SPH	0.400	0/0/-25	50/30/13	3/3/2	4	9	3	3	1	3	0.00	0.27	0.20	10/10/2.5
Cu(%)		2	OK	80/40/20	0/0/0	0.050	SPH	0.550	0/0/-25	25/10/3	SPH	0.400	0/0/-25	50/30/13	3/3/2	4	12	3	3	1	3	0.00	0.27	0.15	10/10/2.5
Cu(%)		3	OK	120/70/30	0/0/0	0.050	SPH	0.550	0/0/-25	25/10/3	SPH	0.400	0/0/-25	50/30/13	3/3/2	4	12	3	3	1	3	0.00	0.27	0.15	10/10/2.5
Cu(%)	9	1	OK	25/40/10	0/0/0	0.150	SPH	0.600	0/0/0	15/25/4	SPH	0.250	0/0/0	80/70/22	3/3/2	4	9	3	3	1	3	0.00	0.50	0.40	10/10/2.5
Cu(%)		2	OK	50/60/12	0/0/0	0.150	SPH	0.600	0/0/0	15/25/4	SPH	0.250	0/0/0	80/70/22	3/3/2	4	12	3	3	1	3	0.00	0.50	0.25	10/10/2.5
Cu(%)		3	OK	100/90/24	0/0/0	0.150	SPH	0.600	0/0/0	15/25/4	SPH	0.250	0/0/0	80/70/22	3/3/2	3	12	3	3	1	3	0.00	0.50	0.25	10/10/2.5
Cu(%)	10	1	OK	40/40/10	0/0/0	0.050	SPH	0.250	0/0/0	25/25/5	SPH	0.700	0/0/0	50/50/9	3/3/2	4	9	3	3	1	3	0.00	0.90	0.10	10/10/2.5
Cu(%)		2	OK	80/80/20	0/0/0	0.050	SPH	0.250	0/0/0	25/25/5	SPH	0.700	0/0/0	50/50/9	3/3/2	4	12	3	3	1	3	0.00	0.90	0.10	10/10/2.5
Cu(%)		3	OK	120/20/25	0/0/0	0.050	SPH	0.250	0/0/0	25/25/5	SPH	0.700	0/0/0	50/50/9	3/3/2	3	12	3	3	1	3	0.00	0.90	0.07	10/10/2.5
Cu(%)	11	1	OK	120/10/10	0/0/0	0.450	SPH	0.400	0/0/10	100/2/2	SPH	0.150	0/0/10	100/8/14	3/3/2	4	9	3	3	1	3	0.00	0.75	0.75	5/5/2.5
Cu(%)		2	OK	240/20/20	0/0/0	0.450	SPH	0.400	0/0/10	100/2/2	SPH	0.150	0/0/10	100/8/14	3/3/2	4	12	3	3	1	3	0.00	0.75	0.75	5/5/2.5
Cu(%)		3	OK	300/30/30	0/0/0	0.450	SPH	0.400	0/0/10	100/2/2	SPH	0.150	0/0/10	100/8/14	3/3/2	3	12	3	2	1	3	0.00	0.75	0.20	5/5/2.5

TABLE 14.17 INTERPOLATION PLAN FOR ZINC (%)

Metal	Geological Unit	PASS	Interpolator	Search Ranges Major Axis/Semi-Major Axis/Minor Axis (m)	Rotation (Bearing / Plunge / Dip) (°)	Variographic Parameters							Discretization (x/y/z)	Min. No. Comp. Max. No. Comp. Max. No. Comp. per	Mln. No. with Comp.	Mln. No. Comp. per	Max. Comp. per Drill Hole	Capping		High Yield					
						C0	1st St.	C1	Rotation (Bearing / Plunge / Dip) (°)	Ranges (E.M.A / E.S-M / E.ME)	2nd St.	C2						Rotation (Bearing / Plunge / Dip) (°)	Ranges (E.M.A / E.S-M / E.ME)	Lower	Upper	Limit	Major Axis/Semi-Major Axis/Minor Axis (m)		
Zn(%)	1	1	OK	45/25/10	0/0/0	0.050	SPH	0.650	0/0/0	40/20/2	SPH	0.300	0/0/0	88/50/4	3/3/2	5	9	3	3	1	3	0.00	29.09	29.00	5/5/2.5
Zn(%)		2	OK	80/50/15	0/0/0	0.050	SPH	0.650	0/0/0	40/20/2	SPH	0.300	0/0/0	88/50/4	3/3/2	4	9	3	3	1	2	0.00	29.09	29.09	5/5/2.5
Zn(%)		3	OK	120/90/20	0/0/0	0.050	SPH	0.650	0/0/0	40/20/2	SPH	0.300	0/0/0	88/50/4	3/3/2	4	12	3	3	1	2	0.00	29.09	29.09	5/5/2.5
Zn(%)	2	1	OK	70/50/10	0/0/0	0.057	SPH	0.500	0/0/0	52/34/3	SPH	0.443	0/0/0	72/34/6	3/3/2	6	9	3	3	2	2	0.00	50.00	-	-
Zn(%)		2	OK	100/75/15	0/0/0	0.057	SPH	0.500	0/0/0	52/34/3	SPH	0.443	0/0/0	72/34/6	3/3/2	9	12	3	3	1	2	0.00	50.00	-	-
Zn(%)		3	OK	140/100/20	0/0/0	0.057	SPH	0.500	0/0/0	52/34/3	SPH	0.443	0/0/0	72/34/6	3/3/2	9	12	3	3	1	3	0.00	50.00	-	-
Zn(%)	3	1	OK	25/25/10	0/0/0	0.050	SPH	0.300	0/0/0	40/35/15	SPH	0.650	0/0/0	60/45/15	3/3/2	4	9	3	3	1	2	0.00	0.90	0.90	10/10/2.5
Zn(%)		2	OK	30/30/15	0/0/0	0.050	SPH	0.300	0/0/0	40/35/15	SPH	0.650	0/0/0	60/45/15	3/3/2	4	12	3	3	1	2	0.00	0.90	-	-
Zn(%)		3	OK	60/60/20	0/0/0	0.050	SPH	0.300	0/0/0	40/35/15	SPH	0.650	0/0/0	60/45/15	3/3/2	3	12	3	2	1	2	0.00	0.90	-	-
Zn(%)	4	1	OK	25/40/4	0/0/0	0.010	SPH	0.600	0/0/2	50/95/4.6	SPH	0.390	0/0/2	50/130/5.1	3/3/2	4	9	3	3	1	3	0.00	2.45	-	-
Zn(%)		2	OK	50/80/6	0/0/0	0.010	SPH	0.600	0/0/2	50/95/4.6	SPH	0.390	0/0/2	50/130/5.1	3/3/2	4	12	3	3	1	3	0.00	2.45	-	-
Zn(%)		3	OK	80/120/8	0/0/0	0.010	SPH	0.600	0/0/2	50/95/4.6	SPH	0.390	0/0/2	50/130/5.1	3/3/2	3	12	3	2	1	2	0.00	2.45	-	-
Zn(%)	5	1	OK	45/20/10	0/0/0	0.300	SPH	0.450	0/0/25	17.5/14/2.5	SPH	0.250	0/0/25	100/75/9.5	3/3/2	4	9	3	3	1	3	0.00	7.58	6.87	10/10/2.5
Zn(%)		2	OK	80/40/15	0/0/0	0.300	SPH	0.450	0/0/25	17.5/14/2.5	SPH	0.250	0/0/25	100/75/9.5	3/3/2	4	12	3	3	1	3	0.00	7.58	6.87	10/10/2.5
Zn(%)		3	OK	120/60/20	0/0/0	0.300	SPH	0.450	0/0/25	17.5/14/2.5	SPH	0.250	0/0/25	100/75/9.5	3/3/2	3	12	3	2	1	3	0.00	7.58	5.68	10/10/2.5
Zn(%)	6	1	OK	10/10/5	0/0/0	0.600	SPH	0.250	0/0/0	27/4/2	SPH	0.50	0/0/0	63/8/3	3/3/2	4	9	3	3	1	3	0.00	165	-	-
Zn(%)		2	OK	40/40/15	0/0/0	0.600	SPH	0.250	0/0/0	27/4/2	SPH	0.50	0/0/0	63/8/3	3/3/2	4	12	3	3	1	3	0.00	165	-	-
Zn(%)		3	OK	45/45/25	0/0/0	0.600	SPH	0.250	0/0/0	27/4/2	SPH	0.50	0/0/0	63/8/3	3/3/2	3	12	3	2	1	3	0.00	165	-	-
Zn(%)	7	1	OK	120/100/8	0/0/0	0.050	SPH	0.600	0/0/60	100/60/2	SPH	0.350	0/0/0	110/110/5	3/3/2	4	9	3	3	1	2	0.00	3.56	3.25	5/5/2.5
Zn(%)		2	OK	200/180/10	0/0/0	0.050	SPH	0.600	0/0/60	100/60/2	SPH	0.350	0/0/0	110/110/5	3/3/2	4	12	3	3	1	3	0.00	3.56	2.79	5/5/2.5
Zn(%)		3	OK	300/250/15	0/0/0	0.050	SPH	0.600	0/0/60	100/60/2	SPH	0.350	0/0/0	110/110/5	3/3/2	3	12	3	2	1	3	0.00	3.56	2.27	5/5/2.5
Zn(%)	8	1	OK	70/80/10	0/0/0	0.100	SPH	0.250	0/0/0	50/60/3	SPH	0.650	0/60/0	70/90/12	3/3/2	4	9	3	3	1	3	0.00	0.51	0.45	10/10/2.5
Zn(%)		2	OK	140/160/20	0/0/0	0.100	SPH	0.250	0/0/0	50/60/3	SPH	0.650	0/60/0	70/90/12	3/3/2	4	12	3	3	1	3	0.00	0.51	0.29	10/10/2.5
Zn(%)		3	OK	200/250/30	0/0/0	0.100	SPH	0.250	0/0/0	50/60/3	SPH	0.650	0/60/0	70/90/12	3/3/2	3	12	3	2	1	3	0.00	0.51	0.20	10/10/2.5
Zn(%)	9	1	OK	120/50/5	0/0/0	0.300	SPH	0.450	0/0/25	17.5/14/2.5	SPH	0.250	0/0/25	100/75/9.5	3/3/2	3	12	3	3	1	3	0.00	5.80	123	10/10/2.5
Zn(%)		2	OK	40/40/20	0/0/0	0.300	SPH	0.450	0/0/25	17.5/14/2.5	SPH	0.250	0/0/25	100/75/9.5	3/3/2	4	12	3	3	1	3	0.00	5.80	0.40	10/10/2.5
Zn(%)		3	OK	60/60/30	0/0/0	0.300	SPH	0.450	0/0/25	17.5/14/2.5	SPH	0.250	0/0/25	100/75/9.5	3/3/2	3	12	3	2	1	2	0.00	5.80	0.23	10/10/2.5
Zn(%)	10	1	OK	70/50/10	0/0/0	0.100	SPH	0.500	0/0/30	65/45/3.5	SPH	0.400	0/0/30	100/20/40	3/3/2	4	9	3	3	1	3	0.00	127	100	10/10/2.5
Zn(%)		2	OK	100/90/20	0/0/0	0.100	SPH	0.500	0/0/30	65/45/3.5	SPH	0.400	0/0/30	100/20/40	3/3/2	4	12	3	3	1	3	0.00	127	0.55	10/10/2.5
Zn(%)		3	OK	150/130/30	0/0/0	0.100	SPH	0.500	0/0/30	65/45/3.5	SPH	0.400	0/0/30	100/20/40	3/3/2	3	12	3	2	1	3	0.00	127	0.30	10/10/2.5
Zn(%)	11	1	OK	50/50/10	0/0/0	0.010	SPH	0.500	0/0/0	35/35/4	SPH	0.490	0/0/0	50/110/27	3/3/2	4	9	3	3	1	3	0.00	2.08	100	5/5/2.5
Zn(%)		2	OK	100/100/20	0/0/0	0.010	SPH	0.500	0/0/0	35/35/4	SPH	0.490	0/0/0	50/110/27	3/3/2	4	12	3	3	1	3	0.00	2.08	0.70	5/5/2.5
Zn(%)		3	OK	150/150/30	0/0/0	0.010	SPH	0.500	0/0/0	35/35/4	SPH	0.490	0/0/0	50/110/27	3/3/2	3	12	3	2	1	3	0.00	2.08	0.40	5/5/2.5
Zn(%)	13	1	OK	70/40/10	0/0/0	0.620	SPH	0.280	0/0/0	60/25/8	SPH	0.100	0/0/0	62/60/9	3/3/2	4	9	3	3	1	3	0.00	100	0.50	10/10/2.5
Zn(%)		2	OK	120/70/30	0/0/0	0.620	SPH	0.280	0/0/0	60/25/8	SPH	0.100	0/0/0	62/60/9	3/3/2	4	12	3	3	1	3	0.00	100	-	-
Zn(%)		3	OK	200/100/40	0/0/0	0.620	SPH	0.280	0/0/0	60/25/8	SPH	0.100	0/0/0	62/60/9	3/3/2	3	12	3	2	1	3	0.00	100	-	-

TABLE 14.18 INTERPOLATION PLAN FOR LEAD (%)

Metal	Geological Unit	PASS	Interpolator	Search Ranges	Rotation (Bearing / Plunge / Dip) (°)	Variographic Parameters								Power IDW	Diacretization (x/y/z)	Min. No. Comp.	Max. No. Comp.	Max. No. Comp. per Oct.	Min. No. Oct. with Comp.	Min. No. Comp. per Oct.	Max. Comp. per Drill Hole	Capping		High Yield	
						Major Axis/ Semi-Major Axis/Minor Axis (m)	C0	1st St.	C1	Rotation (Bearing / Plunge / Dip) (°)	Ranges (E.M.A / E.S.M / E.M.E)	2nd St.	C2									Rotation (Bearing / Plunge / Dip) (°)	Ranges (E.M.A / E.S.M / E.M.E)	Lower	Upper
Fb(%)	1	OK	100/25/5	0/0/0	0.050	SPH	0.500	0/0/-40	100/4/1.5	SPH	0.450	0/0/40	150/20/3.5	--	3/3/2	3	12	3	3	1	2	0.00	6.64	6.40	20/20/2.5
Fb(%)	2	OK	125/50/7.5	0/0/0	0.050	SPH	0.500	0/0/-40	100/4/1.5	SPH	0.450	0/0/40	150/20/3.5	--	3/3/2	3	9	3	3	1	2	0.00	6.64	6.40	25/25/2.5
Fb(%)	3	OK	175/80/10	0/0/0	0.050	SPH	0.500	0/0/-40	100/4/1.5	SPH	0.450	0/0/40	150/20/3.5	--	3/3/2	3	12	3	3	1	2	0.00	6.64	6.40	15/15/2.5
Fb(%)	4	OK	200/140/20	0/0/0	0.050	SPH	0.500	0/0/-40	100/4/1.5	SPH	0.450	0/0/40	150/20/3.5	--	3/3/2	3	12	3	3	1	2	0.00	6.64	6.40	15/15/2.5
Fb(%)	1	OK	50/62/10	0/0/0	0.050	SPH	0.450	0/0/0	43/65/2	SPH	0.500	0/0/60	70/7.5/8	--	3/3/2	3	6	3	3	1	2	--	--	0.03	5/5/2.5
Fb(%)	2	OK	80/100/15	0/0/0	0.050	SPH	0.450	0/0/0	43/65/2	SPH	0.500	0/0/60	70/7.5/8	--	3/3/2	3	9	2	3	1	2	--	--	0.03	5/5/2.5
Fb(%)	3	OK	100/120/20	0/0/0	0.050	SPH	0.450	0/0/0	43/65/2	SPH	0.500	0/0/60	70/7.5/8	--	3/3/2	3	12	3	3	1	2	--	--	0.03	5/5/2.5
Fb(%)	1	IDW	80/80/8	0/0/0	--	--	--	--	--	--	--	--	--	2	3/3/2	4	9	3	3	1	2	--	--	--	--
Fb(%)	2	IDW	100/100/12	0/0/0	--	--	--	--	--	--	--	--	--	2	3/3/2	3	9	3	3	1	2	--	--	--	--
Fb(%)	3	IDW	50/120/30	0/0/0	--	--	--	--	--	--	--	--	--	2	3/3/2	3	12	3	2	1	2	--	--	--	--
Fb(%)	1	IDW	15/75/10	0/0/0	--	--	--	--	--	--	--	--	--	2	3/3/2	3	12	0	1	1	2	0.00	0.31	--	--
Fb(%)	2	IDW	20/120/12	0/0/0	--	--	--	--	--	--	--	--	--	2	3/3/2	3	9	0	1	1	2	0.00	0.00	--	--
Fb(%)	3	IDW	40/200/20	0/0/0	--	--	--	--	--	--	--	--	--	2	3/3/2	3	9	0	3	1	2	0.00	0.31	--	--
Fb(%)	1	OK	30/40/10	0/0/0	0.350	SPH	0.250	0/0/0	20/30/3	SPH	0.400	0/88/-7	18/120/13	--	3/3/2	3	9	3	3	1	2	0.00	0.90	--	--
Fb(%)	2	OK	50/70/16	0/0/0	0.350	SPH	0.250	0/0/0	20/30/3	SPH	0.400	0/88/-7	18/120/13	--	3/3/2	3	9	3	3	1	3	0.00	0.90	0.71	5/5/2.5
Fb(%)	3	OK	60/80/20	0/0/0	0.350	SPH	0.250	0/0/0	20/30/3	SPH	0.400	0/88/-7	18/120/13	--	3/3/2	3	9	3	3	1	3	0.00	0.90	0.71	5/5/2.5
Fb(%)	1	OK	65/25/10	0/0/0	0.350	SPH	0.380	0/0/-60	28/2/2.3	SPH	0.270	0/0/-60	10/28/7.5	--	3/3/2	3	9	3	1	1	2	0.00	0.17	--	--
Fb(%)	2	OK	90/40/15	0/0/0	0.350	SPH	0.380	0/0/-60	28/2/2.3	SPH	0.270	0/0/-60	10/28/7.5	--	3/3/2	3	9	3	1	1	2	0.00	0.17	--	--
Fb(%)	3	OK	180/100/30	0/0/0	0.350	SPH	0.380	0/0/-60	28/2/2.3	SPH	0.270	0/0/-60	10/28/7.5	--	3/3/2	3	12	3	3	1	2	0.00	0.17	--	--
Fb(%)	1	OK	40/40/10	0/0/0	0.180	SPH	0.550	0/0/-60	100/20/2	SPH	0.270	0/0/-60	150/40/30	--	3/3/2	3	9	3	3	1	2	--	--	0.10	5/5/2.5
Fb(%)	2	OK	60/60/15	0/0/0	0.180	SPH	0.550	0/0/-60	100/20/2	SPH	0.270	0/0/-60	150/40/30	--	3/3/2	3	9	3	3	1	3	--	--	0.10	5/5/2.5
Fb(%)	3	OK	80/80/20	0/0/0	0.180	SPH	0.550	0/0/-60	100/20/2	SPH	0.270	0/0/-60	150/40/30	--	3/3/2	3	9	3	3	1	2	--	--	--	--
Fb(%)	1	IDW	60/60/15	0/0/0	--	--	--	--	--	--	--	--	--	2	3/3/2	3	12	3	3	1	2	--	--	--	--
Fb(%)	2	IDW	80/80/20	0/0/0	--	--	--	--	--	--	--	--	--	2	3/3/2	3	12	3	3	1	2	0.00	0.08	--	--
Fb(%)	3	IDW	200/200/80	0/0/0	--	--	--	--	--	--	--	--	--	2	3/3/2	3	12	3	3	1	2	0.00	0.07	--	--
Fb(%)	1	OK	40/40/20	0/0/0	0.100	SPH	0.300	0/60/0	3/100/4	SPH	0.600	0/60/0	25/88/11	--	3/3/2	3	12	3	3	1	3	0.00	15.80	1.23	10/10/2.5
Fb(%)	2	OK	50/50/22	0/0/0	0.100	SPH	0.300	0/60/0	3/100/4	SPH	0.600	0/60/0	25/88/11	--	3/3/2	4	12	3	3	1	2	0.00	15.80	0.40	10/10/2.5
Fb(%)	3	OK	60/60/30	0/0/0	0.100	SPH	0.300	0/60/0	3/100/4	SPH	0.600	0/60/0	25/88/11	--	3/3/2	3	12	3	2	1	2	0.00	15.80	0.23	10/10/2.5
Fb(%)	1	OK	75/120/10	0/0/0	0.050	SPH	0.800	0/0/21	30/100/3	SPH	0.150	0/0/21	90/100/3	--	3/3/2	3	12	3	3	1	2	--	--	--	--
Fb(%)	2	OK	100/200/15	0/0/0	0.050	SPH	0.800	0/0/21	30/100/3	SPH	0.150	0/0/21	90/100/3	--	3/3/2	3	12	3	3	1	2	--	--	--	--
Fb(%)	3	OK	150/300/20	0/0/0	0.050	SPH	0.800	0/0/21	30/100/3	SPH	0.150	0/0/21	90/100/3	--	3/3/2	3	12	3	3	1	2	--	--	--	--

TABLE 14.19 INTERPOLATION PLAN FOR GOLD (G/T)

Metal	Geological Unit	PASS	Interpolator	Search Ranges Major Axis/ Semi-Major Axis/ Minor Axis (m)	Rotation (Bearing / Plunge / Dip) (°)	Variographic Parameters							Power/DW	Discretization (x/y/z)	Min. No. Comp.	Max. No. Comp.	Max. No. Comp. per Oct.	Min. No. Oct. with Comp.	Min. No. Comp. per Oct.	Max. Comp. per Drill Hole	Capping		High Yield			
						C0	1st St.	C1	Rotation (Bearing / Plunge / Dip) (°)	Ranges (E.M.A / E.S-M / E.M.E)	2nd St.	C2									Rotation (Bearing / Plunge / Dip) (°)	Ranges (E.M.A / E.S-M / E.M.E)	Lower	Upper	Limit	Major Axis/ Semi-Major Axis/ Minor Axis (m)
Au(gr/t)	1	OK	50/30/10	0/0/0	0.05	SPH	0.65	0/0/30	25/10/5	SPH	0.30	0/0/30	65/40/11	--	3/3/2	4	9	3	2	1	3	0.00	10.00	10.00	15/15/2.5	
Au(gr/t)	1	2	OK	90/50/15	0/0/0	0.05	SPH	0.65	0/0/30	25/10/5	SPH	0.30	0/0/30	65/40/11	--	3/3/2	4	12	3	2	1	3	0.00	10.00	10.00	15/15/2.5
Au(gr/t)	3	OK	120/70/20	0/0/0	0.05	SPH	0.65	0/0/30	25/10/5	SPH	0.30	0/0/30	65/40/11	--	3/3/2	4	12	3	3	1	3	0.00	10.00	8.65	5/5/2.5	
Au(gr/t)	1	OK	35/15/8	0/0/0	0.05	SPH	0.65	0/0/30	25/10/5	SPH	0.30	0/0/30	65/40/11	--	3/3/2	4	9	3	3	1	3	0.00	37.53	33.43	5/5/2.5	
Au(gr/t)	2	2	OK	70/30/12	0/0/0	0.05	SPH	0.65	0/0/30	25/10/5	SPH	0.30	0/0/30	65/40/11	--	3/3/2	4	9	3	3	1	3	0.00	37.53	33.43	5/5/2.5
Au(gr/t)	3	OK	110/50/16	0/0/0	0.05	SPH	0.65	0/0/30	25/10/5	SPH	0.30	0/0/30	65/40/11	--	3/3/2	3	12	3	3	1	3	0.00	37.53	28.27	10/10/2.5	
Au(gr/t)	1	OK	50/40/10	0/0/0	0.15	SPH	0.35	-90/0/0	25/4/3	SPH	0.50	-90/0/0	95/12/5	--	3/3/2	5	9	2	3	1	2	0.00	6.83	6.83	15/5/2.5	
Au(gr/t)	3	2	OK	100/70/15	0/0/0	0.15	SPH	0.35	-90/0/0	25/4/3	SPH	0.50	-90/0/0	95/12/5	--	3/3/2	4	9	2	3	1	3	0.00	6.83	6.83	5/5/2.5
Au(gr/t)	3	OK	140/110/20	0/0/0	0.15	SPH	0.35	-90/0/0	25/4/3	SPH	0.50	-90/0/0	95/12/5	--	3/3/2	3	12	3	2	1	3	0.00	6.83	4.83	10/10/2.5	
Au(gr/t)	1	OK	35/20/10	0/0/0	0.15	SPH	0.35	-90/0/0	25/4/3	SPH	0.50	-90/0/0	95/12/5	--	3/3/2	4	9	3	3	1	3	0.00	0.18	0.12	5/5/2.5	
Au(gr/t)	4	2	OK	70/30/15	0/0/0	0.15	SPH	0.35	-90/0/0	25/4/3	SPH	0.50	-90/0/0	95/12/5	--	3/3/2	4	12	3	3	1	3	0.00	0.18	0.12	5/5/2.5
Au(gr/t)	3	OK	140/50/20	0/0/0	0.15	SPH	0.35	-90/0/0	25/4/3	SPH	0.50	-90/0/0	95/12/5	--	3/3/2	3	12	3	2	1	3	0.00	0.18	0.11	5/5/2.5	
Au(gr/t)	1	OK	50/25/5	0/0/0	0.05	SPH	0.60	-90/0/0	20/11/2	SPH	0.35	-90/0/0	60/75/9	--	3/3/2	4	9	3	3	1	3	0.00	8.70	6.80	20/20/5	
Au(gr/t)	5	2	OK	70/40/10	0/0/0	0.05	SPH	0.60	-90/0/0	20/11/2	SPH	0.35	-90/0/0	60/75/9	--	3/3/2	4	12	3	3	1	2	0.00	8.70	6.80	20/20/5
Au(gr/t)	3	OK	100/70/15	0/0/0	0.05	SPH	0.60	-90/0/0	20/11/2	SPH	0.35	-90/0/0	60/75/9	--	3/3/2	3	12	3	2	1	3	0.00	8.70	4.00	10/10/5	
Au(gr/t)	1	OK	45/70/4	0/0/0	0.35	SPH	0.45	0/0/0	35/55/2	SPH	0.20	0/0/0	75/90/11	--	3/3/2	4	9	3	3	1	3	0.00	2.70	0.66	5/5/2.5	
Au(gr/t)	6	2	OK	90/100/10	0/0/0	0.35	SPH	0.45	0/0/0	35/55/2	SPH	0.20	0/0/0	75/90/11	--	3/3/2	4	12	3	3	1	3	0.00	2.70	0.48	5/5/2.5
Au(gr/t)	3	OK	150/160/20	0/0/0	0.35	SPH	0.45	0/0/0	35/55/2	SPH	0.20	0/0/0	75/90/11	--	3/3/2	3	12	3	2	1	3	0.00	2.70	0.31	5/5/2.5	
Au(gr/t)	1	DW	50/50/5	0/0/0	--	--	--	--	--	--	--	--	--	3	3/3/2	4	9	0	1	1	3	0.00	0.99	0.99	10/10/5	
Au(gr/t)	7	2	DW	100/100/10	0/0/0	--	--	--	--	--	--	--	--	3	3/3/2	3	12	0	1	1	2	0.00	0.99	0.93	5/5/2.5	
Au(gr/t)	3	DW	150/150/20	0/0/0	--	--	--	--	--	--	--	--	--	3	3/3/2	3	12	0	1	1	3	0.00	0.99	0.50	5/5/2.5	
Au(gr/t)	1	OK	50/70/10	0/0/0	0.20	SPH	0.40	0/0/0	35/55/3	SPH	0.40	0/0/0	60/70/23	--	3/3/2	4	9	3	3	1	3	0.00	1.18	1.18	20/20/5	
Au(gr/t)	8	2	OK	90/120/20	0/0/0	0.20	SPH	0.40	0/0/0	35/55/3	SPH	0.40	0/0/0	60/70/23	--	3/3/2	4	12	3	3	1	3	0.00	1.18	1.18	10/10/2.5
Au(gr/t)	3	OK	140/200/30	0/0/0	0.20	SPH	0.40	0/0/0	35/55/3	SPH	0.40	0/0/0	60/70/23	--	3/3/2	3	12	3	2	1	3	0.00	1.18	0.91	10/10/2.5	
Au(gr/t)	1	OK	45/70/10	0/0/0	0.20	SPH	0.40	0/0/0	35/55/3	SPH	0.40	0/0/0	60/70/23	--	3/3/2	4	9	3	3	1	3	0.00	1.11	1.11	5/5/2.5	
Au(gr/t)	9	2	OK	80/120/20	0/0/0	0.20	SPH	0.40	0/0/0	35/55/3	SPH	0.40	0/0/0	60/70/23	--	3/3/2	4	12	3	3	1	3	0.00	1.11	0.82	5/5/2.5
Au(gr/t)	3	OK	140/180/30	0/0/0	0.20	SPH	0.40	0/0/0	35/55/3	SPH	0.40	0/0/0	60/70/23	--	3/3/2	4	12	3	3	1	3	0.00	1.11	0.30	10/10/2.5	
Au(gr/t)	1	OK	50/40/10	0/0/0	0.05	SPH	0.50	0/0/25	35/22/3	SPH	0.45	0/0/25	90/80/8	--	3/3/2	4	9	3	3	1	3	0.00	0.42	0.42	10/10/5	
Au(gr/t)	10	2	OK	90/60/10	0/0/0	0.05	SPH	0.50	0/0/25	35/22/3	SPH	0.45	0/0/25	90/80/8	--	3/3/2	4	12	3	3	1	3	0.00	0.42	0.42	5/5/2.5
Au(gr/t)	3	OK	140/100/15	0/0/0	0.05	SPH	0.50	0/0/25	35/22/3	SPH	0.45	0/0/25	90/80/8	--	3/3/2	3	12	3	2	1	3	0.00	0.42	0.20	5/5/2.5	
Au(gr/t)	1	DW	55/40/10	0/0/0	--	--	--	--	--	--	--	--	--	3	3/3/2	4	9	0	1	1	3	0.00	0.56	0.56	5/5/2.5	
Au(gr/t)	11	2	DW	100/60/30	0/0/0	--	--	--	--	--	--	--	--	3	3/3/2	4	12	0	1	1	3	0.00	0.56	0.51	5/5/2.5	
Au(gr/t)	3	DW	200/120/50	0/0/0	--	--	--	--	--	--	--	--	--	3	3/3/2	3	12	0	1	1	2	0.00	0.56	0.36	5/5/2.5	

TABLE 14.20 INTERPOLATION PLAN FOR SILVER (G/T)

Metal	Geological Unit	PASS	Interpolator	Search Ranges Major Axis/ Semi-Major Axis/ Minor Axis (m)	Rotation (Bearing / Plunge / Dip) (°)	Variographic Parameters							Power DW	Discretization (x/y/z)	Min. No. Comp.	Max. No. Comp.	Max. No. Comp. per Oct.	Min. No. Oct. with Comp.	Min. No. Comp. per Oct.	Max. Comp. per Drill Hole	Capping		High Yield			
						C0	1st SL	C1	Rotation (Bearing / Plunge / Dip) (°)	Ranges (E.M.A / E.S.M / E.M.E)	2nd SL	C2									Rotation (Bearing / Plunge / Dip) (°)	Ranges (E.M.A / E.S.M / E.M.E)	Lower	Upper	Limit	Major Axis/ Semi-Major Axis/ Minor Axis (m)
Ag(grf)	1	1	ID	80/20/10	0/0/0	--	--	--	--	--	--	--	2	3/3/2	3	6	0	1	1	2	0.00	1500.00	--	--		
Ag(grf)		2	ID	100/30/15	0/0/0	--	--	--	--	--	--	--	2	3/3/2	3	12	0	1	1	2	0.00	1500.00	--	--		
Ag(grf)		3	ID	120/40/20	0/0/0	--	--	--	--	--	--	--	2	3/3/2	3	12	0	1	1	2	0.00	1500.00	--	--		
Ag(grf)	2	1	ID	80/30/10	0/0/0	--	--	--	--	--	--	--	2	3/3/2	3	6	3	3	1	2	0.00	43.70	--	--		
Ag(grf)		2	ID	100/45/15	0/0/0	--	--	--	--	--	--	--	2	3/3/2	4	9	0	1	1	2	0.00	43.70	--	--		
Ag(grf)		3	ID	160/90/20	0/0/0	--	--	--	--	--	--	--	2	3/3/2	3	9	3	3	1	2	0.00	43.70	--	--		
Ag(grf)	3	1	ID	130/70/15	0/0/0	--	--	--	--	--	--	--	2	3/3/2	3	9	0	1	1	2	0.00	302.10	--	--		
Ag(grf)		2	ID	160/80/20	0/0/0	--	--	--	--	--	--	--	2	3/3/2	3	9	0	1	1	2	0.00	302.10	--	--		
Ag(grf)		3	ID	200/120/25	0/0/0	--	--	--	--	--	--	--	2	3/3/2	3	9	0	1	1	2	0.00	302.10	--	--		
Ag(grf)	4	1	ID	60/60/5	0/0/0	--	--	--	--	--	--	--	3	3/3/2	3	5	0	3	1	2	0.00	96.40	--	--		
Ag(grf)		2	ID	90/90/10	0/0/0	--	--	--	--	--	--	--	3	3/3/2	3	7	0	1	1	2	0.00	96.40	--	--		
Ag(grf)		3	ID	120/120/15	0/0/0	--	--	--	--	--	--	--	3	3/3/2	3	9	0	1	1	2	0.00	96.40	--	--		
Ag(grf)	5	1	ID	80/40/7.5	0/0/0	--	--	--	--	--	--	--	2	3/3/2	3	9	2	3	1	2	0.00	121.60	--	--		
Ag(grf)		2	ID	100/50/15	0/0/0	--	--	--	--	--	--	--	2	3/3/2	3	9	3	3	1	2	0.00	121.60	92.10	2.5/2.5/2.5		
Ag(grf)		3	ID	120/70/20	0/0/0	--	--	--	--	--	--	--	2	3/3/2	3	12	3	3	1	2	0.00	121.60	75.10	5/5/5		
Ag(grf)	6	1	ID	60/40/7.5	0/0/0	--	--	--	--	--	--	--	2	3/3/2	5	9	0	3	1	2	0.00	29.80	--	--		
Ag(grf)		2	ID	80/60/15	0/0/0	--	--	--	--	--	--	--	2	3/3/2	5	12	0	3	1	2	0.00	29.80	--	--		
Ag(grf)		3	ID	110/90/20	0/0/0	--	--	--	--	--	--	--	2	3/3/2	3	12	3	3	1	2	0.00	29.80	--	--		
Ag(grf)	7	1	OK	80/55/10	0/0/0	0.373	SPH	0.400	0/0/10	95/90/2.2	SPH	0.227	0/10/10	90/90/9	--	3/3/2	3	6	3	3	1	2	0.00	168.32	160.00	5/5/2.5
Ag(grf)		2	OK	110/85/15	0/0/0	0.373	SPH	0.400	0/0/10	95/90/2.2	SPH	0.227	0/10/10	90/90/9	--	3/3/2	3	9	3	3	1	2	0.00	168.32	160.00	5/5/2.5
Ag(grf)		3	OK	140/115/20	0/0/0	0.373	SPH	0.400	0/0/10	95/90/2.2	SPH	0.227	0/10/10	90/90/9	--	3/3/2	3	9	3	3	1	2	0.00	168.32	160.00	5/5/2.5
Ag(grf)	8	1	ID	120/80/10	0/0/0	--	--	--	--	--	--	--	2	3/3/2	5	9	0	1	1	2	0.00	59.10	--	--		
Ag(grf)		2	ID	165/125/15	0/0/0	--	--	--	--	--	--	--	2	3/3/2	7	9	0	1	1	2	0.00	59.10	--	--		
Ag(grf)		3	ID	220/160/20	0/0/0	--	--	--	--	--	--	--	2	3/3/2	5	9	0	1	1	2	0.00	59.10	--	--		
Ag(grf)	9	1	OK	60/100/10	0/0/0	0.350	SPH	0.380	0/12/-8	20/90/11	SPH	0.270	0/-12/0	25/125/17	--	3/3/2	3	6	3	3	1	2	0.00	27.10	--	--
Ag(grf)		2	OK	90/130/15	0/0/0	0.350	SPH	0.380	0/12/-8	20/90/11	SPH	0.270	0/-12/0	25/125/17	--	3/3/2	5	9	3	3	1	2	0.00	27.10	25.00	2.5/2.5/2.5
Ag(grf)		3	OK	150/200/20	0/0/0	0.350	SPH	0.380	0/12/-8	20/90/11	SPH	0.270	0/-12/0	25/125/17	--	3/3/2	3	9	3	3	1	2	0.00	27.10	23.00	15/15/2.5
Ag(grf)	10	1	ID	80/40/5	0/0/0	--	--	--	--	--	--	--	2	3/3/2	3	6	0	1	1	2	0.00	12.20	--	--		
Ag(grf)		2	ID	120/60/7.5	0/0/0	--	--	--	--	--	--	--	2	3/3/2	3	9	0	1	1	2	0.00	12.20	--	--		
Ag(grf)		3	ID	160/80/10	0/0/0	--	--	--	--	--	--	--	2	3/3/2	3	12	0	1	1	2	0.00	12.20	--	--		
Ag(grf)	11	1	ID	120/80/15	0/0/0	--	--	--	--	--	--	--	2	3/3/2	4	6	3	3	1	2	0.00	5.40	--	--		
Ag(grf)		2	ID	220/110/20	0/0/0	--	--	--	--	--	--	--	2	3/3/2	3	9	3	3	1	2	0.00	5.40	4.00	5/5/2.5		
Ag(grf)		3	ID	280/160/20	0/0/0	--	--	--	--	--	--	--	2	3/3/2	3	9	3	3	1	2	0.00	5.40	2.30	5/5/2.5		
Ag(grf)	12	1	OK	80/50/10	0/0/0	0.350	SPH	0.520	0/-30/-9	50/30/10	SPH	0.130	0/0/0	60/50/55	--	3/3/2	3	9	3	3	1	2	0.00	45.00	--	--
Ag(grf)		2	OK	160/100/20	0/0/0	0.350	SPH	0.520	0/-30/-9	50/30/10	SPH	0.130	0/0/0	60/50/55	--	3/3/2	3	12	3	3	1	2	0.00	45.00	--	--
Ag(grf)		3	OK	240/150/30	0/0/0	0.350	SPH	0.520	0/-30/-9	50/30/10	SPH	0.130	0/0/0	60/50/55	--	3/3/2	3	12	3	3	1	2	0.00	45.00	--	--

TABLE 14.21 INTERPOLATION PLAN FOR SPECIFIC GRAVITY

Metal	Geological Unit	PASS	Interpolator	Search Ranges Major Axis / Semi-Major Axis / Minor Axis (m)	Rotation (Bearing / Plunge / Dip) (°)	Variographic Parameters										Discretization (m/y/z)	Min. No. Comp.	Max. No. Comp.	Max. No. Comp. per Oct.	Min. No. Oct. with Comp.	Min. No. Comp. per Oct.	Max. Comp. per Drill Hole	Capping		High Yield	
						C0	1st St.	C1	Rotation (Bearing / Plunge / Dip) (°)	Ranges (E.M.A / E.S.M / E.M.E)	2nd St.	C2	Rotation (Bearing / Plunge / Dip) (°)	Ranges (E.M.A / E.S.M / E.M.E)	Lower								Upper	Limit	Major Axis / Semi-Major Axis / Minor Axis (m)	
SG		1	OK	90/25/3	0/0/0	0.300	SFH	0.300	0/0/0	85/20/1.5	SFH	0.400	0/0/0	125/40/10	3/3/2	4	9	0	3	1	2	2.32	4.58	--	--	
SG	1	2	OK	180/50/6	0/0/0	0.300	SFH	0.300	0/0/0	85/20/1.5	SFH	0.400	0/0/0	125/40/10	3/3/2	4	12	0	1	1	2	2.32	4.58	4.12	5/5/5	
SG		3	OK	270/75/9	0/0/0	0.300	SFH	0.300	0/0/0	85/20/1.5	SFH	0.400	0/0/0	125/40/10	3/3/2	3	12	0	1	1	3	2.32	4.58	4.12	10/10/5	
SG		1	OK	20/30/20	0/0/0	0.670	SFH	0.100	0/0/0	15/30/15	SFH	0.230	0/0/0	50/120/30	3/3/2	4	9	0	1	1	2	2.72	4.72	--	--	
SG	2	2	OK	40/50/40	0/0/0	0.670	SFH	0.100	0/0/0	15/30/15	SFH	0.230	0/0/0	50/120/30	3/3/2	4	12	0	3	2	2	2.72	4.72	4.46	5/5/2.5	
SG		3	OK	60/80/45	0/0/0	0.670	SFH	0.100	0/0/0	15/30/15	SFH	0.230	0/0/0	50/120/30	3/3/2	3	9	2	3	1	3	2.72	4.72	4.35	5/5/2.5	
SG		1	OK	50/30/10	0/0/0	0.580	SFH	0.120	0/0/-30	40/22/9	SFH	0.300	0/0/-30	103/78/12	3/3/2	7	12	0	1	1	3	1.75	3.47	--	--	
SG	7	2	OK	100/45/20	0/0/0	0.580	SFH	0.120	0/0/-30	40/22/9	SFH	0.300	0/0/-30	103/78/12	3/3/2	4	12	0	1	1	2	1.75	3.47	--	--	
SG		3	OK	150/90/30	0/0/0	0.580	SFH	0.120	0/0/-30	40/22/9	SFH	0.300	0/0/-30	103/78/12	3/3/2	3	12	0	1	1	4	1.75	3.47	--	--	
SG		1	OK	50/30/15	0/0/0	0.580	SFH	0.120	0/0/-30	40/22/9	SFH	0.300	0/0/-30	103/78/12	3/3/2	7	12	0	1	1	2	2.32	3.83	--	--	
SG	8	2	OK	100/60/30	0/0/0	0.580	SFH	0.120	0/0/-30	40/22/9	SFH	0.300	0/0/-30	103/78/12	3/3/2	7	12	2	3	1	2	2.32	3.83	--	--	
SG		3	OK	150/90/45	0/0/0	0.580	SFH	0.120	0/0/-30	40/22/9	SFH	0.300	0/0/-30	103/78/12	3/3/2	3	12	0	1	1	2	2.32	3.83	--	--	
SG		1	OK	30/15/6	0/0/0	0.350	SFH	0.120	0/0/30	20/10/4	SFH	0.530	0/0/30	65/250/8	3/3/2	4	9	0	1	1	2	2.00	3.50	--	--	
SG	9	2	OK	60/30/12	0/0/0	0.350	SFH	0.120	0/0/30	20/10/4	SFH	0.530	0/0/30	65/250/8	3/3/2	4	9	0	1	1	2	2.00	3.50	--	--	
SG		3	OK	90/45/18	0/0/0	0.350	SFH	0.120	0/0/30	20/10/4	SFH	0.530	0/0/30	65/250/8	3/3/2	3	9	0	1	1	2	2.00	3.50	--	--	

BLOCK MODEL VALIDATION

A wide range of validation tools has been used on an ongoing basis during the interpolation of the different metals in each GU.

GRAPHIC VALIDATION OF THE BLOCK MODEL

A visual inspection of the final block model was carried out to verify the following:

- Consistency of the estimated block model based on the interpolation plan and the neighbouring composites available.
- The blocks that were not estimated until the third interpolation pass are those that do not meet the criteria for the estimation plan and for composite availability.
- Appropriate spatial allocation of the GUs for the metals and bulk density in composites and blocks.

Figure 14.16 through Figure 14.21 show section 9588300N at the 830 m level with estimates of Cu, Zn, and Au.

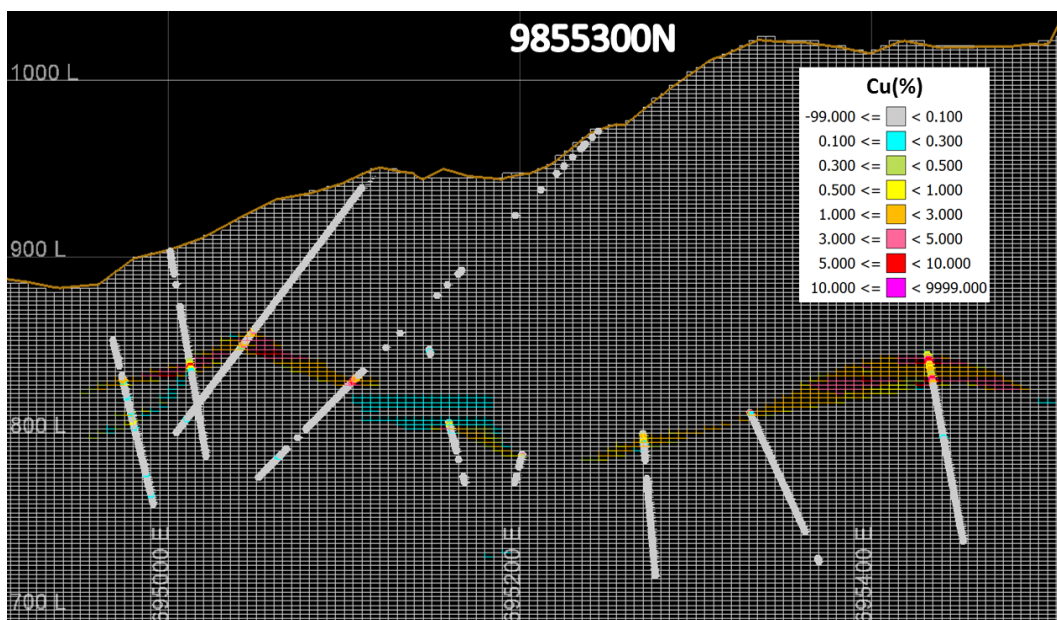


FIGURE 14.16 ESTIMATES OF COPPER (%) IN SECTION 9588300N, HIGHLIGHTING THE VMS UNIT

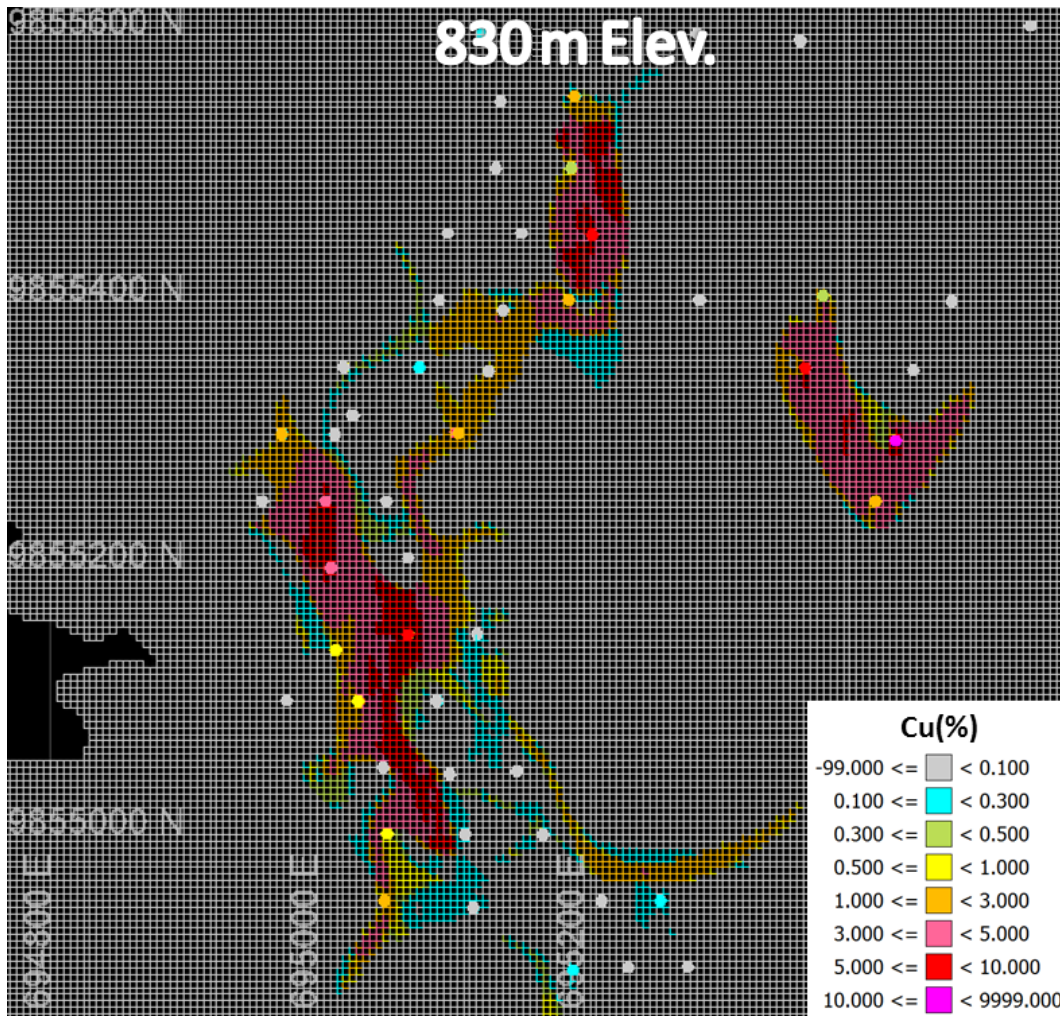


FIGURE 14.17 ESTIMATES FOR COPPER (%) IN SECTION 830 M, HIGHLIGHTING THE VMS UNIT

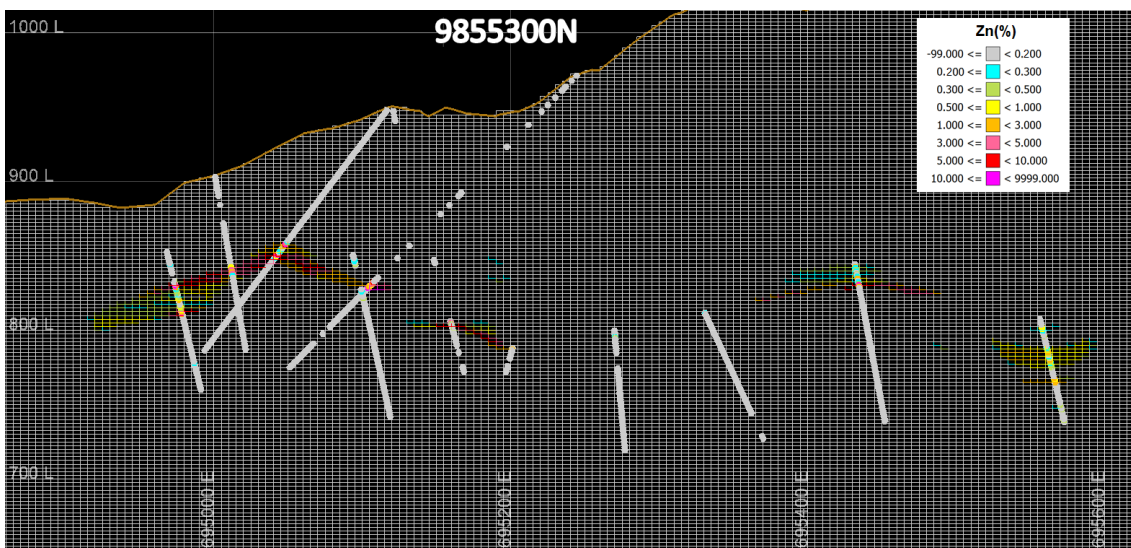


FIGURE 14.18 ESTIMATES FOR ZINC (%) IN SECTION 9588300N, HIGHLIGHTING THE VMS UNIT

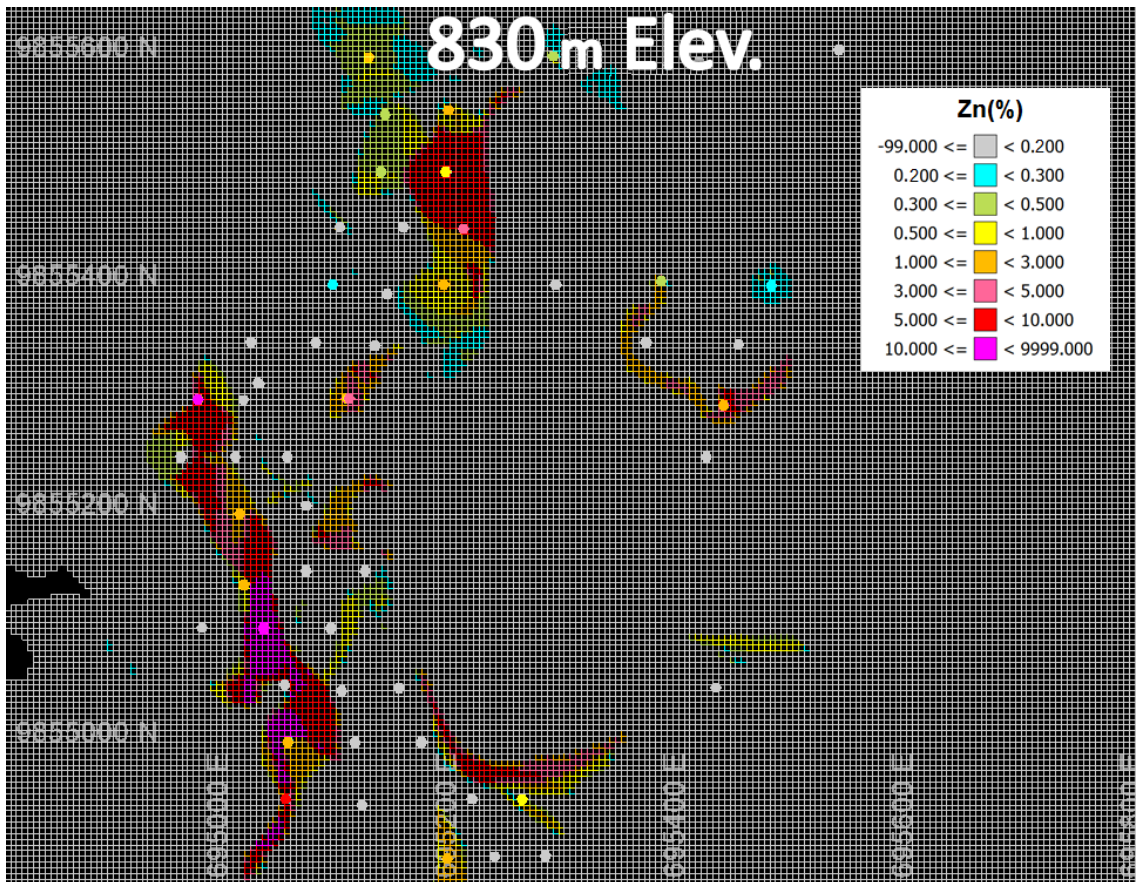


FIGURE 14.19 ESTIMATES FOR ZINC (%) AT LEVEL 830 M, HIGHLIGHTING THE VMS UNIT

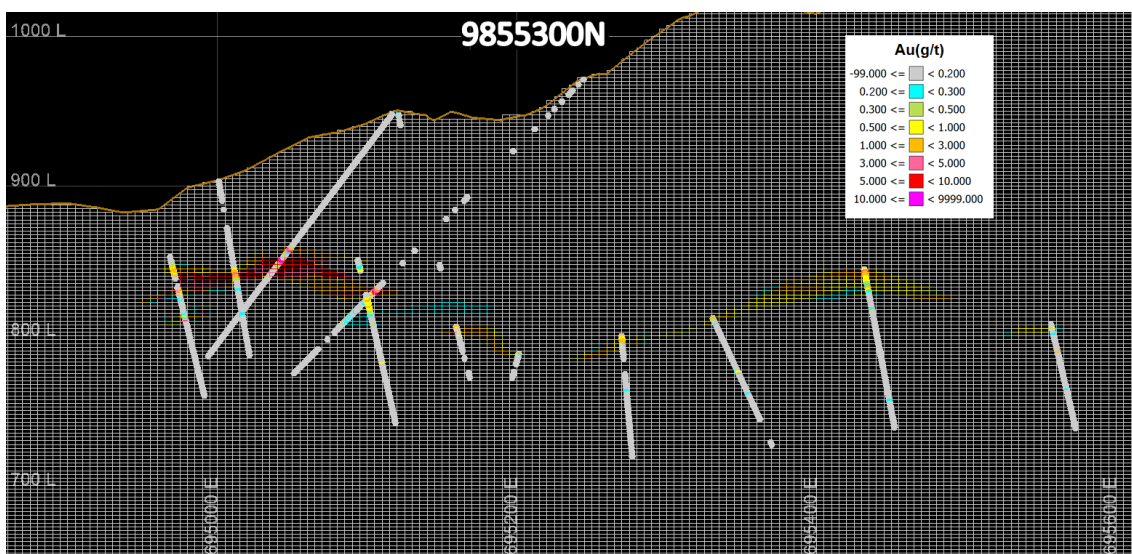


FIGURE 14.20 ESTIMATES OF GOLD (G/T) IN SECTION 9588300N, HIGHLIGHTING THE VMS UNIT

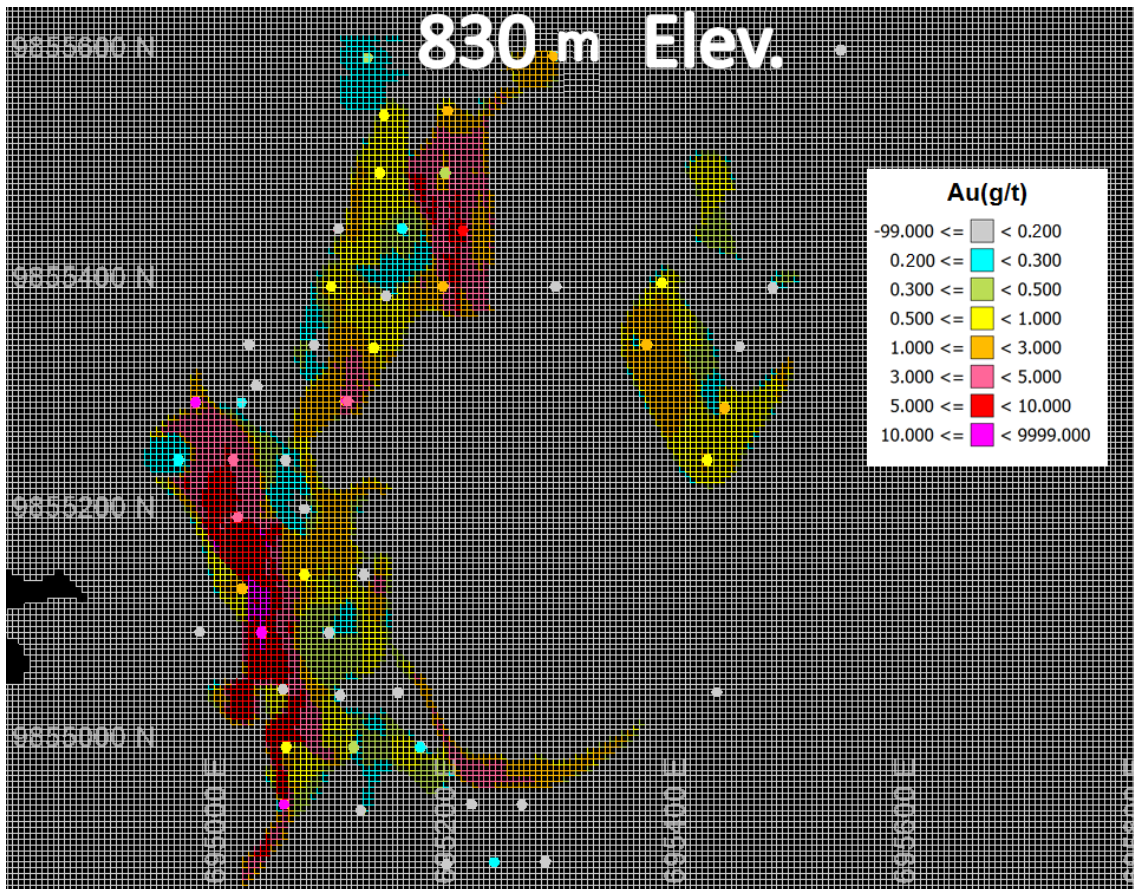


FIGURE 14.21 ESTIMATES OF GOLD (G/T) AT LEVEL 830 M, HIGHLIGHTING THE VMS UNIT

COMPARISON OF COMPOSITES AND POPULATION ESTIMATE

During the validation of the interpolation, basic statistics were performed between the estimates and the composites for each GU for the metals. It should be noted that some GUs have only a small number of composites.

DRIFT ANALYSIS

A drift analysis was developed for the estimated models to detect any possible local bias. Drift plots have been generated to identify local bias in the south-north and west-east directions and in elevation. The distance used for the drift analysis was 5 m for the south-north and west-east directions and 2.5 m for elevation. This revision was implemented for each GU in the three passes.

Figure 14.22 to Figure 14.26 show the validation schemes used for the Cu, Zn, and Au of GU01.

GU01CU

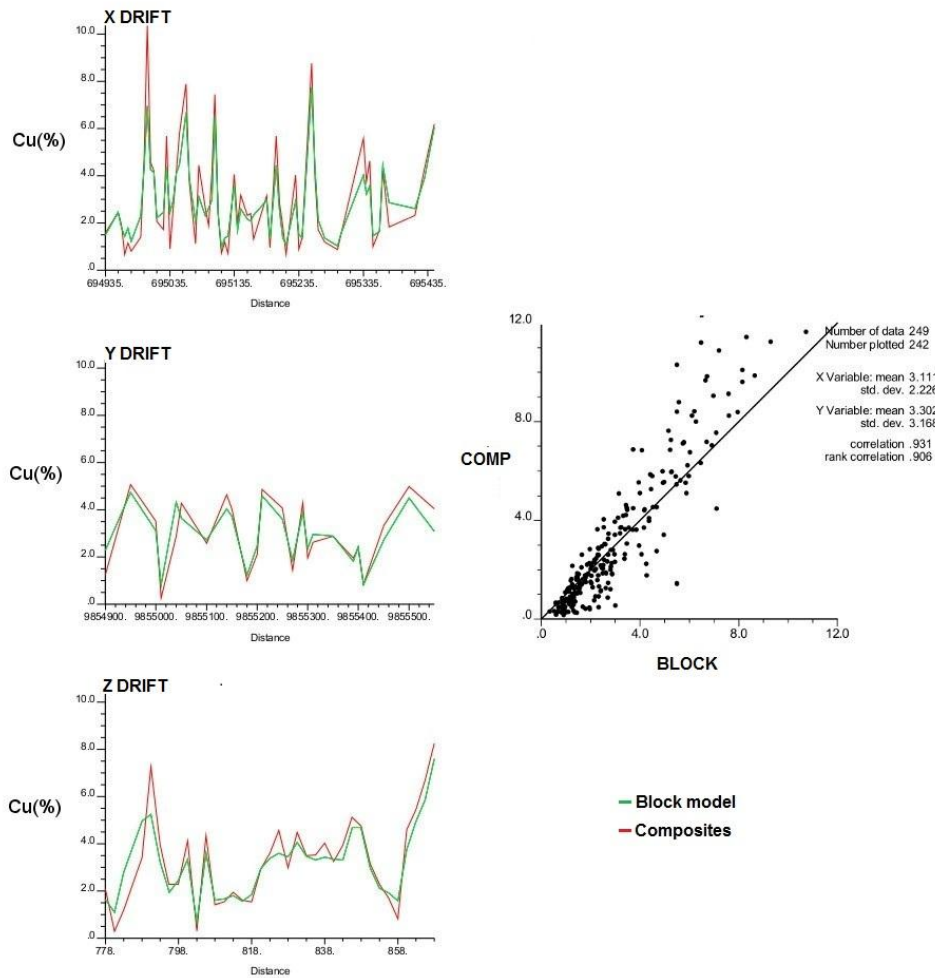


FIGURE 14.22 VALIDATION OUTLINE FOR GU01CU

GU01ZN

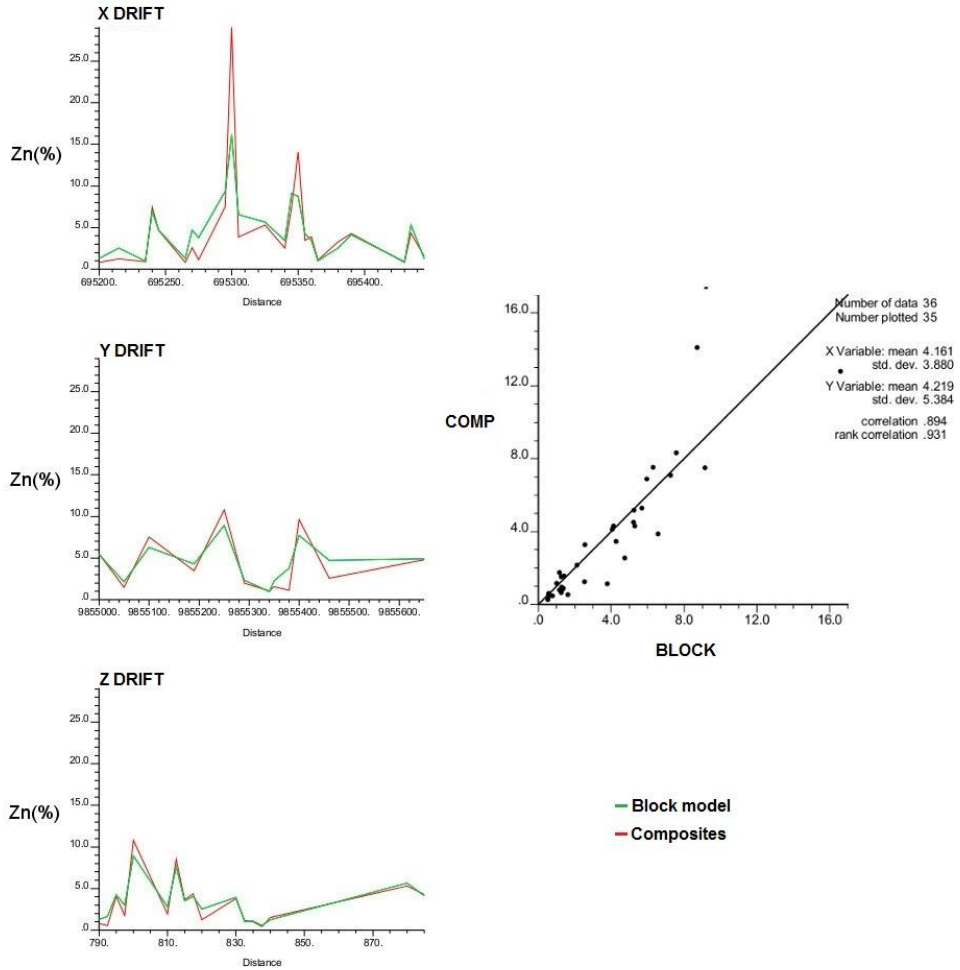


FIGURE 14.23 VALIDATION OUTLINE FOR GU01ZN

GU01PB

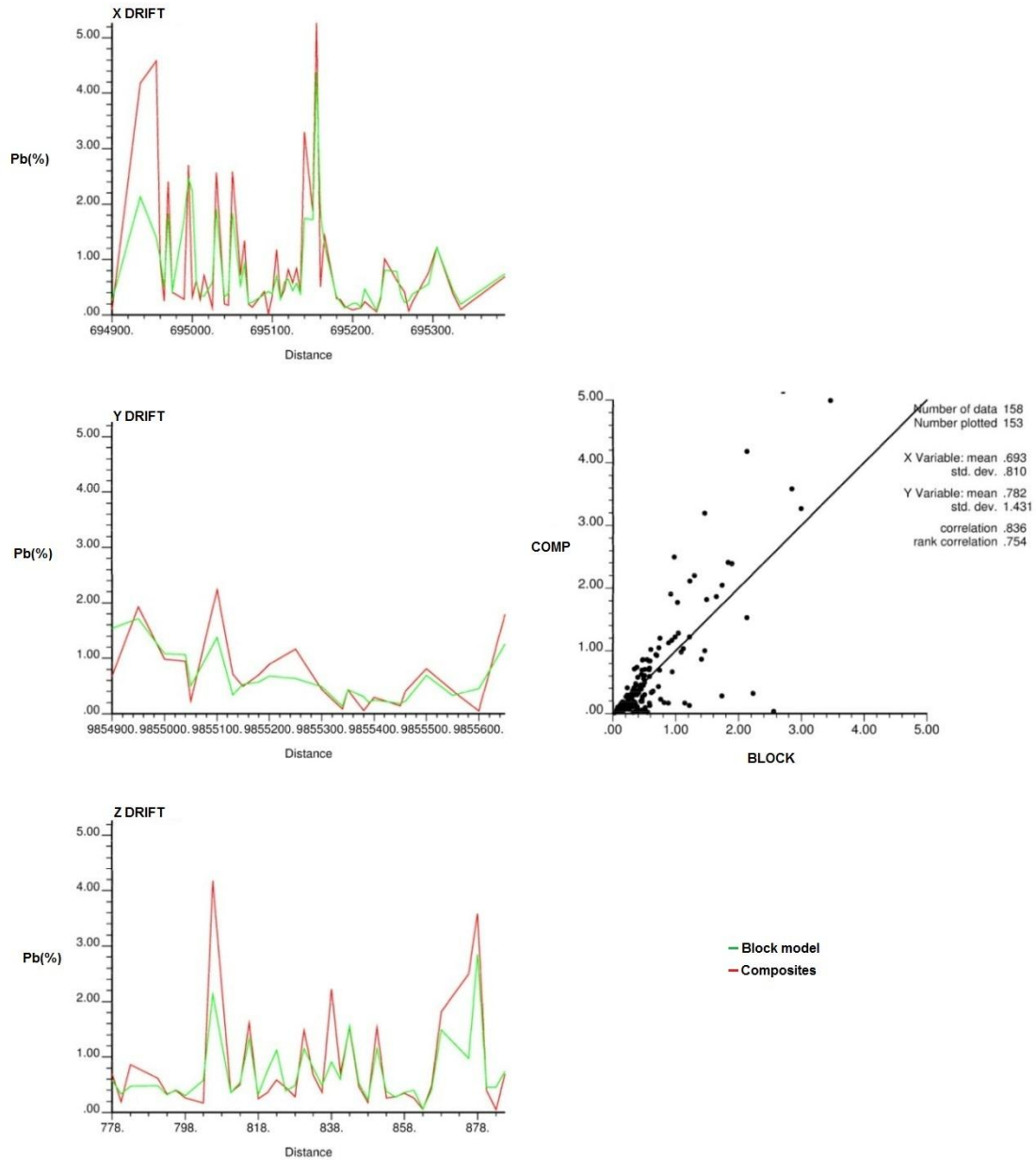


FIGURE 14.24 VALIDATION OUTLINE FOR GU01PB

GU01AU

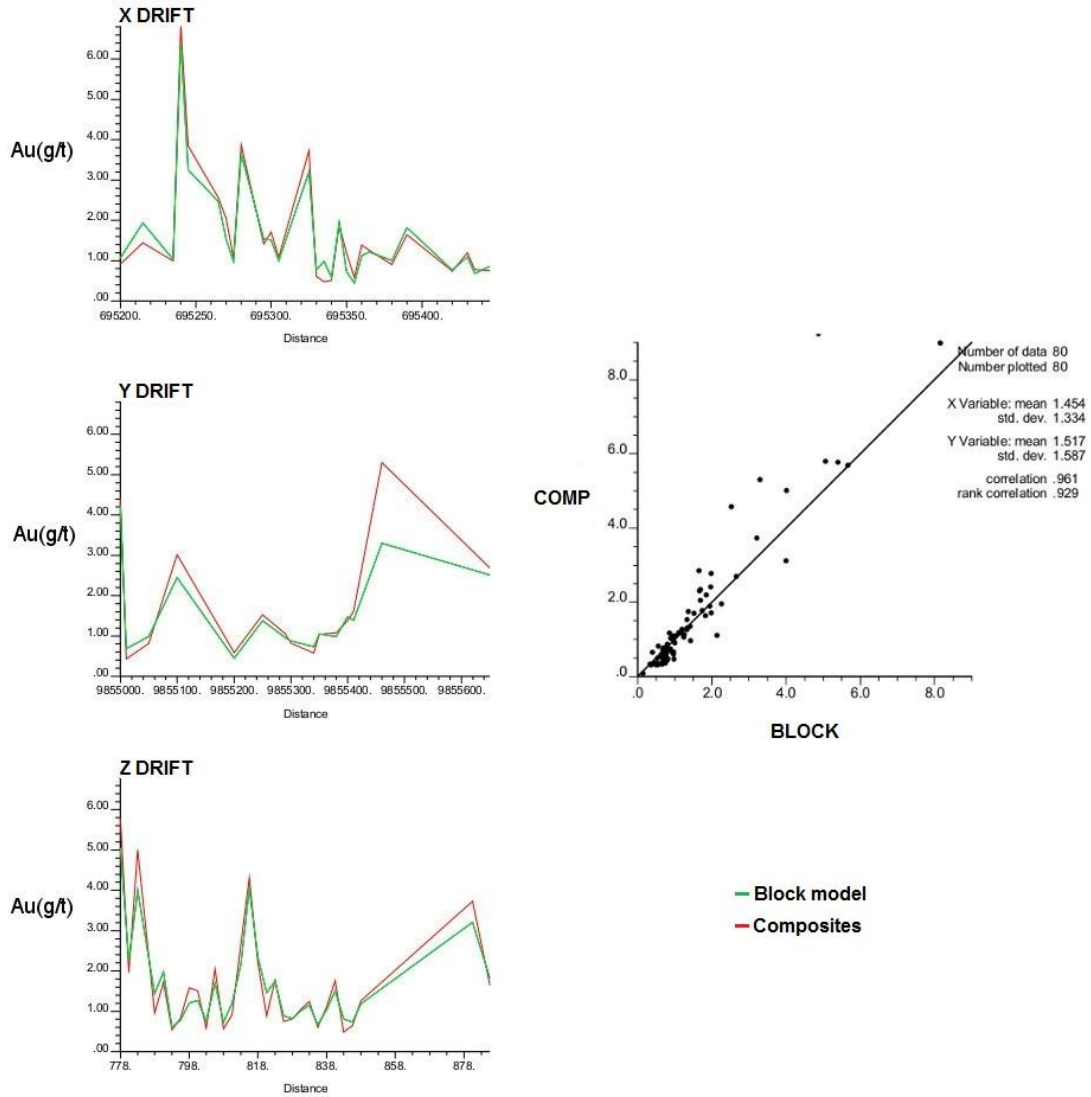


FIGURE 14.25 VALIDATION OUTLINE FOR GUAU01

GU01AG

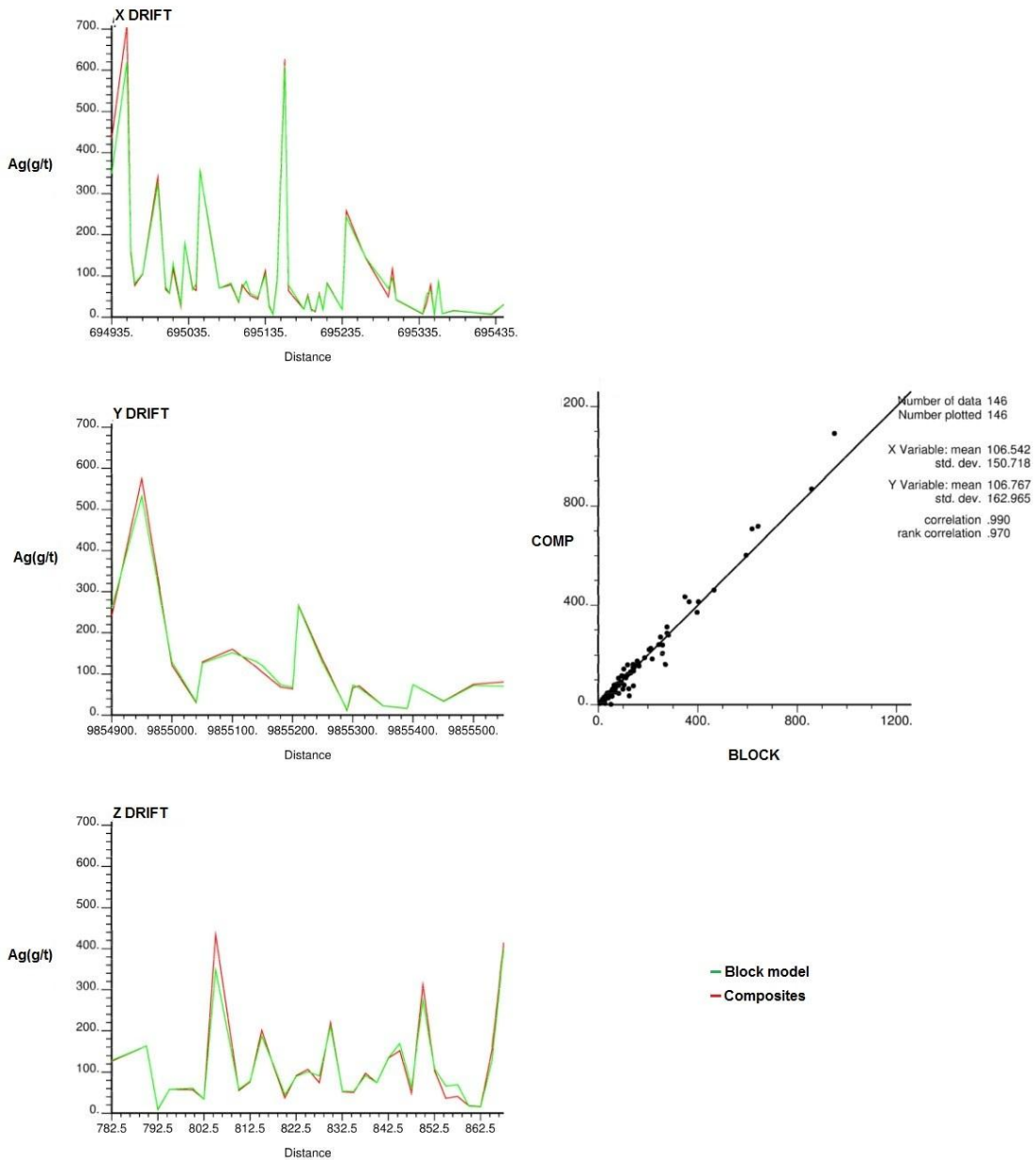


FIGURE 14.26 VALIDATION OUTLINE FOR GUAG01

ASUMPTIONS USED IN RESOURCE MODELLING

The assumptions used for the resource model are listed below:

- BISA has conducted analyses to define the criteria for calculation of the NSR value (Table 14.2).
- The regular block size assumed in the estimation is 5 x 5 x 2.5 m taking into account the geometry and dimensions of the mineralization and considering the characteristics of the mining equipment and the scale of future mining production.
- The geological (lithological) model is consistent with the drilling information and representative of the nature and characteristics of a volcanogenic massive sulphide deposit (VMS).

MINERAL RESOURCE ESTIMATE AND CLASSIFICATION

MINERAL RESOURCE ESTIMATION

The resource estimate is based on an NSR cutoff value of US\$30 per tonne. The NSR was calculated based on the following assumptions: metal prices, metallurgical recovery factors, and common industry values for smelter terms. Four mineralized units have been considered for mineral resource reporting.: Volcanogenic massive sulphides (VMS), polymictic volcanoclastic breccia with massive sulphide clasts (Grainstone), stockwork quartz-pyrite (Breccia), and stockwork anhydrite-gypsum (Gypsum). In accordance with the mineral resource classification methodology, they have been classified into two categories: indicated and inferred. No measured resources have been established for any of the four reported units.

TABLE 14.22 EL DOMO MINERAL RESOURCE ESTIMATE - DECEMBER 15, 2013

Lithology Unit	Category	Tonnes (Mt)	Copper (%)	Zinc (%)	Lead (%)	Gold (g/t)	Silver (g/t)
VMS	Indicated	5.468	2.52	3.27	0.30	3.23	59.19
Grainstone	Indicated	0.216	0.92	1.01	0.12	1.09	27.91
Breccia	Indicated	0.345	0.49	1.33	0.13	0.76	26.91
Gypsum	Indicated	0.051	0.94	0.39	0.03	0.34	7.40
Total Indicated		6.080	2.33	3.06	0.28	2.99	55.81
VMS	Inferred	3.093	1.75	2.59	0.19	2.38	49.45
Grainstone	Inferred	0.170	0.96	0.69	0.10	1.00	19.24
Breccia	Inferred	0.370	0.53	0.83	0.07	0.78	24.89
Gypsum	Inferred	0.249	1.13	0.26	0.01	0.27	4.80
Total Inferred		3.882	1.56	2.19	0.16	2.03	42.92

NOTE:

- CIM definitions were followed for mineral resources
- The Mineral Resource Estimate is based on 3D geological modelling of the volcanogenic massive sulphide deposit (VMS). Four mineralized units with an NSR cutoff of US\$30 per tonne were considered as mineral resource
- Metal prices used are US\$2.95/lb Cu, US\$0.91/lb Zn, US\$0.91/lb Pb, US\$1,200/oz Au, and US\$20.00/oz Ag
- Metallurgical recovery factors assumed were based on three mineral types defined by the metal ratio Cu/(Zn+Pb):
 - Zinc Mineral (Cu/(Pb+Zn)<0.3): 15% Cu, 90% Zn, 40% Pb, 50% Au, and 65% Ag
 - Mixed Cu/Zn Mineral (0.3≤Cu/(Pb+Zn)≤3.0): 75% Cu, 50% Zn, 0% Pb, 55% Au, and 65% Ag
 - Copper Mineral (Cu/(Pb+Zn)>3.0): 90% Cu, 0% Zn, 0% Pb, 30% Au, and 40% Ag
- Common industry values for smelter terms were assumed
- Bulk density was estimated based on specific gravity determinations for each lithological unit

RESOURCE CLASSIFICATION METHODOLOGY

The method for resource classification is based on the geological knowledge of the deposit and the assumption of the spatial continuity of Cu and Zn. The geological controls and geostatistics used in the interpolation of the metal grades in the sub-cell type block model, produced various confidence levels as a function of the spatial configuration of the composites used for estimating a block. For each individual block, a number of parameters were recorded:

- (1) The interpolation pass in which the block was estimated
- (2) The number of drill holes with composites that contributed to the block interpolation
- (3) The total number of composites used in the block interpolation
- (4) The average weighted distance (by interpolation weights) for the composites used

The resource classification has been undertaken considering the four mineralized units (VMS, Grainstone, Breccia, and Gypsum) and three copper and three zinc domains defined by interpolation parameters for Cu and Zn. The resources have been classified into the two categories of: indicated and inferred; no measured resources have been established for any of the four reported units.

For the **VMS** and **Grainstone**, the Cu and Zn domains have been established as given below.

Cu Domains

-Cu Domain 1

- Blocks estimated during the first Cu interpolation pass, using at least three different drill holes and an average weighted distance from the block centroid to the composites of less than 7.5 metres.

-Cu Domain 2

- Blocks estimated during the first Cu interpolation pass, using at least three different drill holes and an average weighted distance from the block centroid to the composites of more than 7.5 metres.
- Blocks estimated during the first Cu interpolation pass, using at least two drill holes were also included in the Cu Domain 2.
- Finally, blocks estimated during the second Cu interpolation pass, using at least two different drill holes and an average weighted distance from the block centroid to the composites of less than 60 metres.

-Cu Domain 3

- Blocks not previously included within Cu Domain 1 or Domain 2 have been classified as Cu Domain 3.

Zn Domains

-Zn Domain 1

- Blocks estimated during the first interpolation pass for Zn, using at least three different drill holes and an average weighted distance from the block centroid to the composites of less than 20 metres.

-Zn Domain 2

- Blocks estimated during the first Zn interpolation pass, using at least three different drill holes and an average weighted distance from the block centroid to the composites of more than 20 metres.
- Blocks estimated during the first Zn interpolation pass using at least two drill holes have also been included in Zn Domain 2.
- Finally, blocks estimated during the second Zn interpolation pass, using at least two different drill holes and an average weighted distance from the block centroid to the composites of less than 72 metres.

-Zn Domain 3

- Blocks not previously included within Zn Domain 1 or Domain 2 have been classified as Zn Domain 3.

Finally, the Cu and Zn domains were incorporated into a matrix used to categorize the resources in the VMS and Grainstone units. (Figure 14.27)

		Cu Domains		
		Domain 1	Domain 2	Domain 3
Zn Domains	Domain 1	Measured Resources	Indicated Resources	Indicated Resources
	Domain 2	Indicated Resources	Indicated Resources	Indicated Resources
	Domain 3	Indicated Resources	Indicated Resources	Inferred Resources

	Measured Resources
	Indicated Resources
	Inferred Resources

FIGURE 14.27 RESOURCE CLASSIFICATION MATRIX FOR THE VMS AND GRAINSTONE

In the **Breccia** and **Gypsum** units, the criteria for defining the Cu and Zn domains are as given below.

Cu Domains

-Cu Domain 1

- Blocks estimated during the first Cu interpolation pass, using at least three different drill holes and an average weighted distance from the block centroid to the composites of less than 17 metres.

-Cu Domain 2

- Blocks estimated during the first Cu interpolation pass, using at least three different drill holes and an average weighted distance from the block centroid to the composites of more than 17 metres.
- Blocks estimated during the first Cu interpolation pass, using at least two drill holes, were also included in the Cu Domain 2.
- Finally, blocks estimated during the second Cu interpolation pass, using at least two different drill holes and an average weighted distance from the block centroid to the composites of less than 75 metres.

-Cu Domain 3

- Blocks not previously included within Cu Domain 1 or Domain 2 have been classified as Cu Domain 3.

Zn Domains

-Zn Domain 1

Blocks estimated during the first interpolation pass for Zn, using at least three different drill holes and an average weighted distance from the block centroid to the composites of less than 34 metres.

-Zn Domain 2

- Blocks estimated during the first Zn interpolation pass, using at least three different drill holes and an average weighted distance from the block centroid to the composites of more than 34 metres.

- Blocks estimated during the first Zn interpolation pass using at least two different drill holes have also been included in Zn Domain 2.
- Finally, blocks estimated during the second Zn interpolation pass, using at least two different drill holes and an average weighted distance from the block centroid to the composites of less than 110 metres.

-Zn Domain 3

- Blocks not previously included within Zn Domain 1 or Domain 2 have been classified as Zn Domain 3.

In the Breccia and Gypsum units, the spatial continuity of the mineralization is more constrained, and therefore the resource categorization has been more restrictive (Figure 14.28).

		Cu Domains		
		Domain 1	Domain 2	Domain 3
Zn Domains	Domain 1	Measured Resources	Indicated Resources	Indicated Resources
	Domain 2	Indicated Resources	Indicated Resources	Inferred Resources
	Domain 3	Indicated Resources	Inferred Resources	Inferred Resources

	Measured Resources
	Indicated Resources
	Inferred Resources

FIGURE 14.28 RESOURCE CLASSIFICATION MATRIX FOR THE BRECCIA AND GYPSUM

Once the categories of mineral resource estimates in the sub-cell type block model had been established, the category codes were standardized in a regular block model taking into account the majority percentage. The blocks at the edges and at the contacts between the four mineralized units were not classified in this process. These blocks were removed and their category determined by the predominant category in their adjacent blocks. Figure 14.29 shows the resource classification of the four mineralized units with an NSR cutoff value of US\$30 per tonne in plan view.

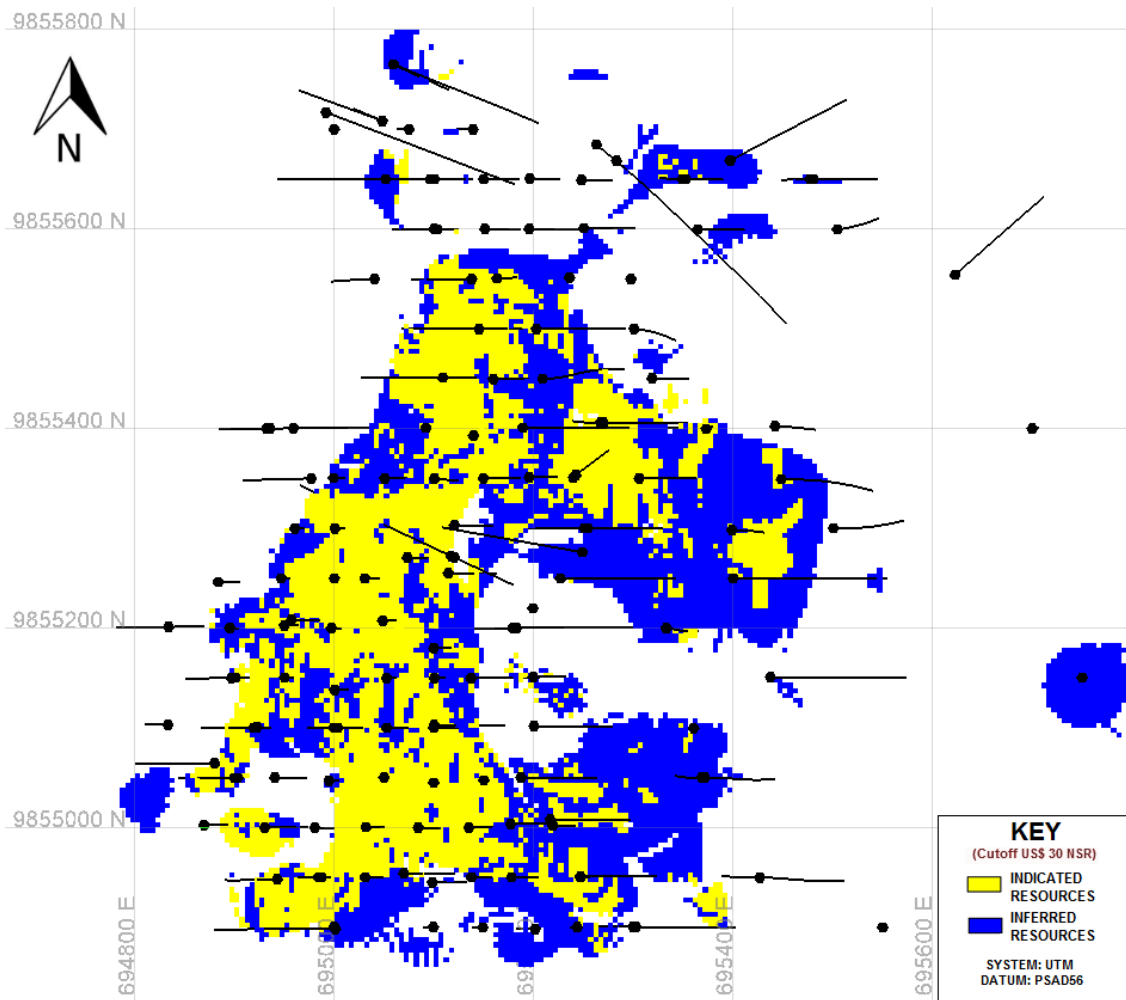


FIGURE 14.29 RESOURCE CLASSIFICATION IN PLAN VIEW

Figure 14.30 shows a comparative graph of the resource estimates in the declarations from 2010 to date.

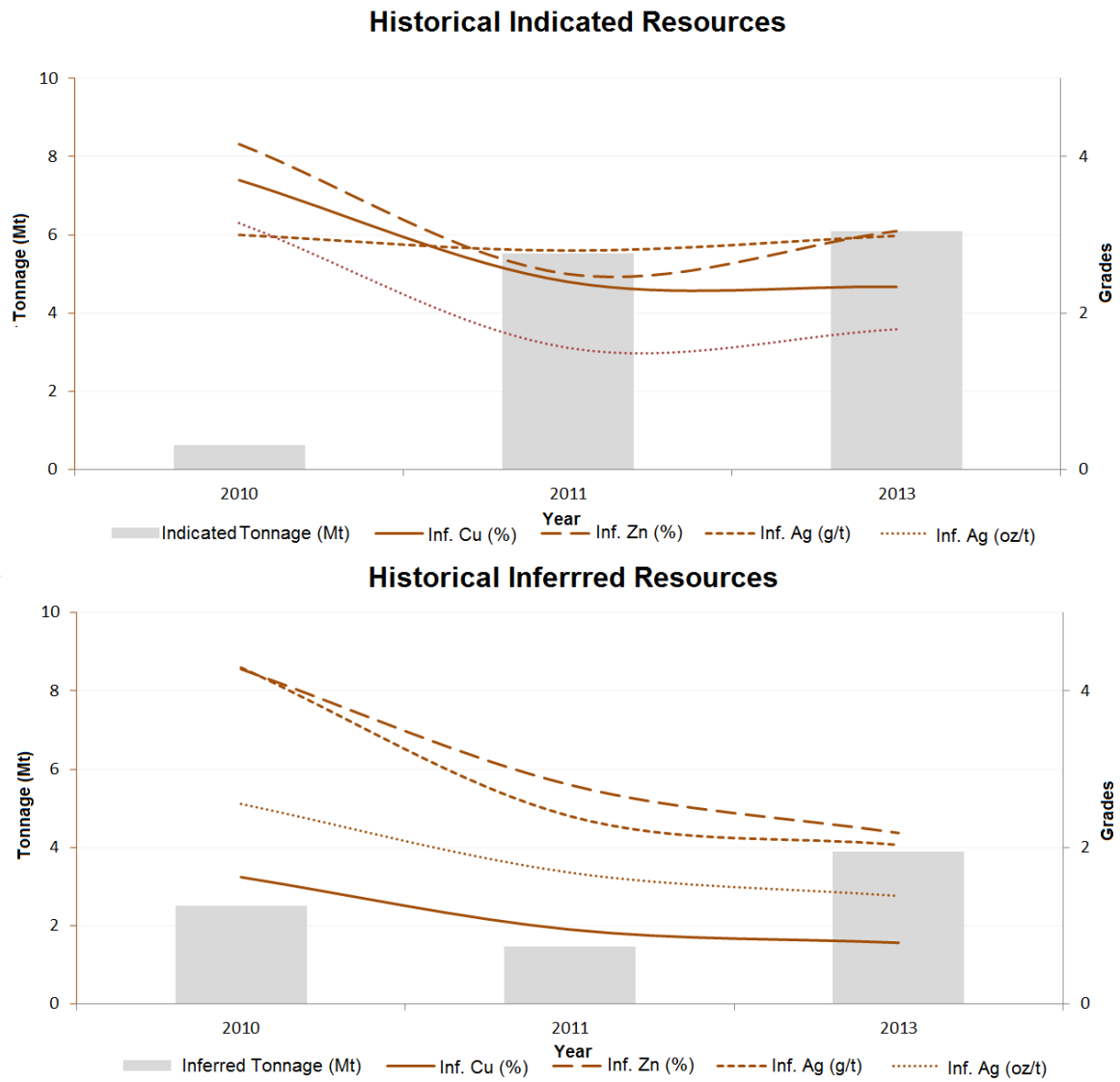


FIGURE 14.30 MINERAL RESOURCES ESTIMATES FROM 2010 TO 2013

GRADE-TONNAGE CURVES

The Grade-Tonnage curves for the indicated and inferred resources of the mineralized units: VMS, Grainstone, Breccia, and Gypsum are shown in Figure 14.31.

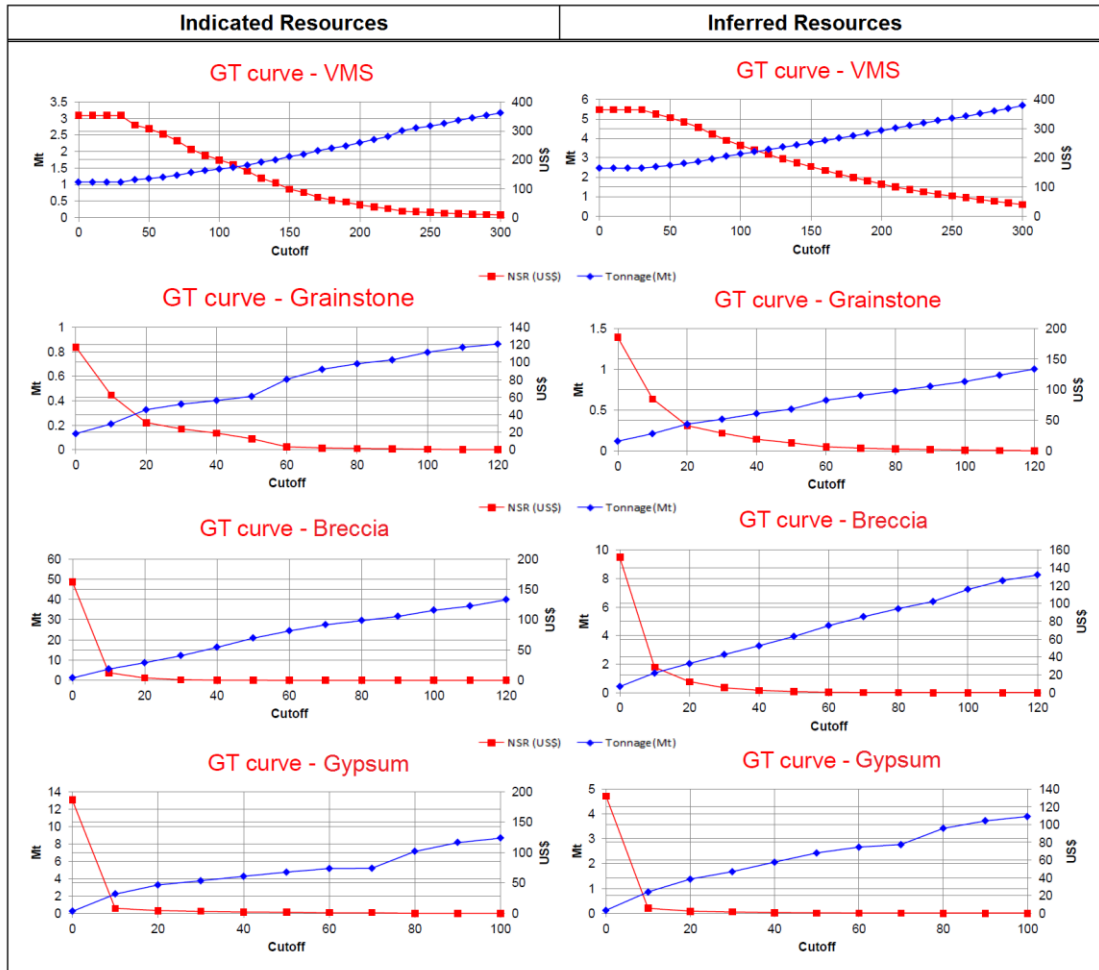


FIGURE 14.31 GRADE-TONNAGE CURVES FOR THE MINERALIZED UNITS - EL DOMO DEPOSIT

15. MINERAL RESERVE ESTIMATE

This section is not applicable

16. MINING METHODS

Because two geological structural domains have been established at the El Domo deposit, the mine development has been divided into two sectors and extraction by various mining methods was analysed for each. Extraction will begin with the open pit method and continue later with underground mining. The economic and financial assessment takes into account a nine-year lifespan for the surface mining with a production of 2,000 tpd, followed by a five-year lifespan underground mining with a production of 1,000 tpd, for a total of 14 years of mining.

OPEN PIT

The El Domo VMS deposit has two structural domains: the Eastern sector, which contains the deepest mineralized zone, below the Andesite unit, and the Western sector, which encompasses the mineralized zone underneath the tuff unit. The latter unit is mostly composed of incompetent rocks, and will be mined by open pit methods. First the topsoil will be removed, and then the overburden, and finally the ore will be extracted. Drilling and blasting first, and then shovels and trucks will be used for loading and hauling the ore and overburden.

OPEN PIT OPTIMIZATION

The optimized pit was generated from a theoretical cone with no access ramps or benches. The objective is to find a cone with the optimal utility value (benefit-cost) that complies with the mining, geotechnical, metallurgical, legal, and environmental restrictions. This pit shell was generated using the Lerchs Grossmann algorithm in the MineSight Economic Planner software, which, for each block of ore, weighs the ore value and the cost of extracting the block to obtain saleable products. In other words, this algorithm determines whether or not each block is economical. The optimization process was performed using the block model developed by BISA.

The block model was developed with 5 m x 5 m x 2.5 m blocks and exported to the MineSight Economic Planner, where such parameters as slopes of the pit walls, process recovery (provided by Salazar Resources), mining costs, and processing costs (calculated by BISA) were assigned to resources and to blocks for optimization purposes.

OPTIMIZATION PARAMETERS

The MineSight Economic Planner requires parameters such as the price of the metal, recovery, mining costs, and processing costs to determine the optimal economic cone. The relevant factors and costs for the optimization are presented in Table 16.1, Table 16.2, and Table 16.3.

The mineralization is classified into three different types of concentrate according to the metallurgical characteristics defined by the Cu/(Pb + Zn) ratio: Zinc Mineral, Mixed Cu/Zn Mineral, and Copper Mineral. The values of one percent grade for copper, zinc, and lead, of one gram grade for gold, and of one ounce for silver (Metal Unit Values) were determined by BISA based on assumed metal prices, metallurgical recovery factors and common smelter terms, and are summarized in Table 16.1.

TABLE 16.1 MINING BLOCK PARAMETERS

Block Value Parameters		
Metal Price		
	Unit	Value
Lead	\$/t	2000
Zinc	\$/t	2000
Copper	\$/t	6500
Silver	\$/oz	20
Gold	\$/oz	1200
Process recovery by Mineral Types		
Zinc Mineral: Cu/(Zn+Pb)<0.33		
Pb conc	Pb Recov	40%
	Pb grade	40%
Zn conc	Zn recov	90%
	Zn grade	50%
Cu conc	Cu recov	15%
	Cu grade	18%
Ag Recov	In Pb	10%
	In Cu	15%
	In Zn	40%
Au Recov	In Pb	5%
	In Cu	10%
	In Zn	35%
Mixed Cu/Zn Mineral: 0.33≤Cu/(Zn+Pb)≤3.0		
Pb conc	Pb Recov	0%
	Pb grade	0%
Zn conc	Zn recov	50%
	Zn grade	42%
Cu conc	Cu recov	75%
	Cu grade	21%
Ag Recov	In Pb	0%
	In Cu	40%
	In Zn	25%
Au Recov	In Pb	0%
	In Cu	30%
	In Zn	25%
Copper Mineral: Cu/(Zn+Pb)>3.0		
Pb conc	Pb Recov	0%
	Pb grade	0%
Zn conc	Zn recov	0%
	Zn grade	0%
Cu conc	Cu recov	90%
	Cu grade	21%
Ag Recov	In Pb	0%
	In Cu	40%
	In Zn	0%
Au Recov	In Pb	0%
	In Cu	30%
	In Zn	0%
Metal Unit Values		
Zinc Mineral: Cu/(Zn+Pb)<0.33		
Pb US\$/1%		3.7
Zn US\$/1%		8.8
Cu US\$/1%		4.7
Ag US\$/1 Oz		9.0
Au US\$/1 g		13.7
Mixed Cu/Zn Mineral: 0.33≤Cu/(Zn+Pb)≤3.0		
Pb US\$/1%		-
Zn US\$/1%		3.9
Cu US\$/1%		31.5
Ag US\$/1 Oz		9.0
Au US\$/1 g		15.6
Copper Mineral: Cu/(zn+pb)>3.0		
Pb US\$/1%		-
Zn US\$/1%		-
Cu US\$/1%		44.6
Ag US\$/1 Oz		3.2
Au US\$/1 g		7.1

TABLE 16.2 MINING BLOCK COST PARAMETERS

Mining Cost Parameters		
	Unit	Value
Mine Cost Overburden	\$/t material	2.75
Mine Cost Ore	\$/t material	2.75
Ore and Overburden Haulage per Bench	\$/bench	0.02
Ore Processing Cost	\$/t ore	20
GG & AA	\$/t	5

TABLE 16.3 MINING BLOCK DESIGN PARAMETERS

Mining Design Parameters		
Slope Angle		
	Unit	Value
COVER	(°)	43
RHYOLITE	(°)	46
VMS	(°)	43
BRECCIA	(°)	43
GYPSUM	(°)	43
BASALT	(°)	43
GRAINSTONE	(°)	43
TUFFS	(°)	46
ANDESITE	(°)	55

OPTIMIZATION RESULTS

The results of the optimization give the optimal cone (Table 16.4 and Figure 16.1). It results in 6,391,916 tonnes of mineral and 48,450,723 tonnes of waste rock with a stripping ratio (SR) of 7.58.

TABLE 16.4 OPTIMIZATION RESULTS

Mineral Type	Mineral (t)	Cu (%)	Zn (%)	Au (g/t)	Pb (g/t)	Ag (g/t)	Waste Rock (t)	Stripping Ratio
Cu/(Zn+Pb)<0.33	1,917,744	0.77	4.96	3.54	0.46	74.67	14,536,500	
0.33≤Cu/(Zb+Pb)≤3.0	2,914,408	2.82	3.47	3.55	0.28	73.89	22,091,213	
Cu/(zn+pb)>3.0	1,559,764	2.48	0.20	1.93	0.03	11.13	11,823,011	
Total	6,391,916	2.13	3.12	3.15	0.27	58.81	48,450,723	7.58

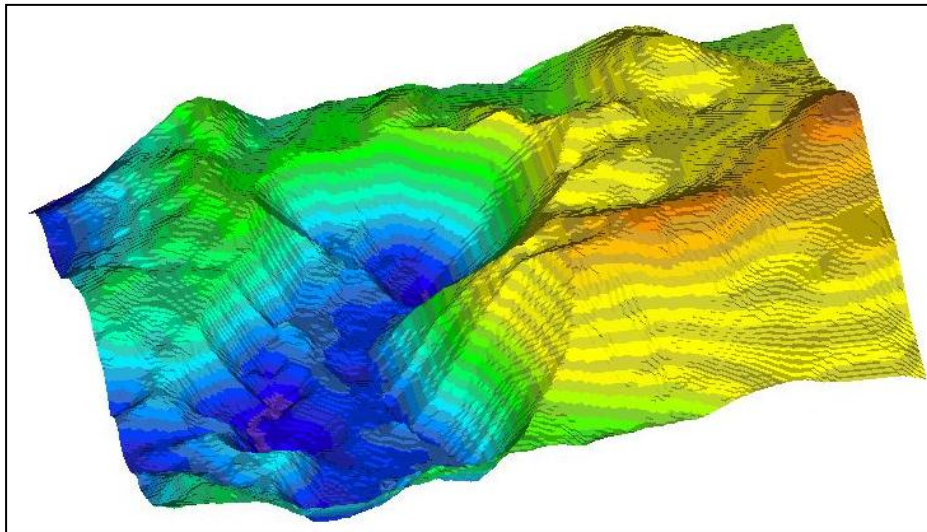


FIGURE 16.1 OPEN PIT OPTIMAL CONE

Based on this initial result, BISA performed a set of iterations to optimize the mine plan and maximize profitability. Sensitivity analysis was undertaken by varying the metal prices in order to compare the economic performance (NPV) of each of these alternatives and thus obtain an optimal cone that would be the base case on which to anchor the conceptual study. The metal prices used for the sensitivity analysis are shown in Table 16.5, and their results are given in Table 16.6.

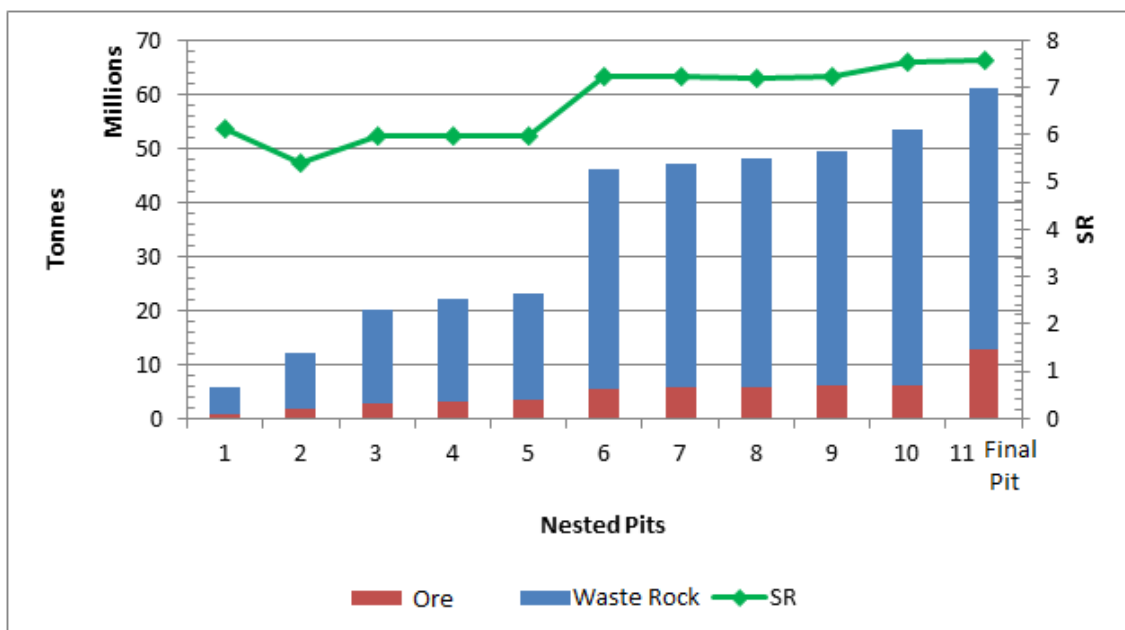
TABLE 16.5 METAL PRICES FOR SENSITIVITY ANALYSIS

Price	Pb	Zn	Cu	Ag	Au
	\$/t	\$/t	\$/t	\$/oz	\$/oz
1	1,000	1,000	1,800	9	400
2	1,100	1,100	2,270	10	480
3	1,200	1,200	2,740	11	560
4	1,300	1,300	3,210	12	640
5	1,400	1,400	3,680	13	720
6	1,500	1,500	4,150	14	800
7	1,600	1,600	4,620	15	880
8	1,700	1,700	5,090	16	960
9	1,800	1,800	5,560	17	1,040
10	1,900	1,900	6,030	18	1,120
11 - Final Pit	2,000	2,000	6,500	20	1,200

TABLE 16.6 SENSITIVITY ANALYSIS

Pit	Mineral (t)	Cu (%)	Zn (%)	Au (g/t)	Pb (%)	Ag (g/t)	Waste Rock (t)	Stripping Ratio (SR)
1	823,160	3.33	4.71	6.01	0.50	110.78	5,054,202	6.14
2	1,888,219	3.28	3.98	4.69	0.41	99.82	10,177,500	5.39
3	2,870,204	2.99	3.95	4.20	0.44	94.67	17,163,820	5.98
4	3,175,068	2.87	3.83	4.07	0.42	89.24	18,923,405	5.96
5	3,326,053	2.80	3.76	3.99	0.41	86.82	19,823,276	5.96
6	5,615,688	2.27	3.21	3.37	0.29	63.48	40,545,267	7.22
7	5,741,796	2.25	3.18	3.34	0.29	62.54	41,455,767	7.22
8	5,842,280	2.23	3.15	3.31	0.29	61.87	42,122,839	7.21
9	5,988,109	2.20	3.13	3.26	0.28	61.16	43,413,790	7.25
10	6,262,886	2.15	3.13	3.19	0.28	59.49	47,222,160	7.54
11 - Final Pit	6,391,916	2.13	3.12	3.15	0.27	58.81	48,450,723	7.58

As shown in Table 16.6, a higher production rate of mineral diminishes the copper grade and increases the stripping ratio, consequently increasing the amount of waste rock. Figure 16.2 gives a graphic depiction of the results.


FIGURE 16.2 SENSITIVITY OF OPEN PIT OPTIMIZATION

Following the optimization, Cone 11 was selected as the base case for this study.

OPEN PIT DESIGN

The final pit design was founded on the base case cone. The geometric, operational, and geotechnical variables as well as the inclusion of a ramp, the bench height, and the presence of berms were taken into account.

The design parameters are listed in Table 16.7. The width of the ramp is 12 m, including the safety berms, which enables safe operation for 40-tonne trucks. The final 3D open pit design is shown in Figure 16.3, and the plan view is given in Figure 16.4.

TABLE 16.7 OPEN PIT DESIGN PARAMETERS

Design Parameters			
		Unit	Value
Bench height		m	6
Benches before berms		n	1
Maximum ramp gradient		%	10
Ramp width		m	12
Total final slope			
	COVER	(°)	43
	RHYOLITE	(°)	46
	VMS	(°)	43
	BRECCIA	(°)	43
	GYPSUM	(°)	43
	BASALT	(°)	43
	GRAINSTONE	(°)	43
	TUFFS	(°)	46
	ANDESITE	(°)	55
Bench Slope			
	COVER	(°)	60
	RHYOLITE	(°)	60
	VMS	(°)	50
	BRECCIA	(°)	50
	GYPSUM	(°)	50
	BASALT	(°)	60
	GRAINSTONE	(°)	50
	TUFFS	(°)	60
	ANDESITE	(°)	60

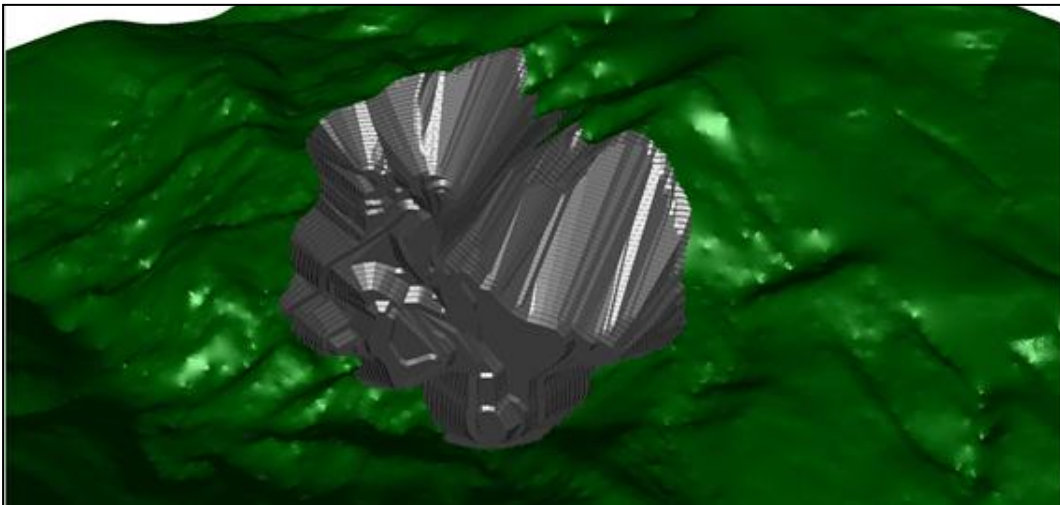


FIGURE 16.3 3D OPEN PIT VIEW



FIGURE 16.4 PIT DESIGN IN PLAN VIEW

OPERATIVE CUTOFF GRADES

An operative cutoff of 1% Cu (equivalent) has been used for open pit mining purposes which is approximately US\$ 30 NSR.

RESOURCES WITH MINING POTENTIAL

BISA calculated the resources with mining potential that serve as a basis for the production plan. In this plan, the resources (indicated + inferred) can be classified as copper mineral 1,483,593 tonnes; zinc mineral 1,880,788 tonnes and mixed Cu/Zn mineral 2,864,219 tonnes, for a total of 6,228,600 tonnes of mineral and 46,205,000 tonnes of waste rock (see).

DILUTION AND LOSSES

For this preliminary stage, BISA considered 5% mining losses and 5% ore dilution, which is permitted for this stage.

MINE PLAN

The production plan was designed to extract 2,000 tpd, approximately 700,000 tpy. At this rate of production, the mine life is nine (9) years, and one (1) year of pre-production (stripping). This plan complies with the new Ecuadorian mining regulations.

Table 16.9 shows the mine plan with the total production from the three metallurgical mineral types as well as the waste rock generated during the 10 years of open pit operation. shows the production plan for ore sent to the processing plant. Figure 16.5 is a graphic presentation of ore production by type.

STOCKPILE

For the first four years, the low-grade ore will be mined and stored in a stockpile close to the processing plant, which will be further processed during the last five years of mining operation. This stockpile will be made of materials other than the VMS.

TABLE 16.8 BASE CASE — RESOURCES WITH MINING POTENTIAL

MINERAL TYPE	LITHOLOGY	ORE (t)	CU (%)	ZN (%)	AU (g/t)	PB (%)	AG g/t	FE (%)	S (%)	NSR (\$/t)	WASTE ROCK (t)
Zinc Mineral	RHYOLITE	12,410	0.128	2.120	1.697	0.140	28.912	6.477	8.320	51.385	
	VMS	1,555,150	0.872	5.554	3.933	0.519	80.283	10.818	15.567	132.009	
	BRECCIA	71,841	0.380	2.427	0.601	0.141	30.806	3.446	5.317	40.808	
	GYPSUM	3,382	0.254	1.788	1.109	0.072	17.277	4.543	13.680	37.400	
	BASALT	6,416	0.184	1.576	1.034	0.120	19.255	7.039	5.393	34.922	
	GRAINSTONE	219,854	0.130	1.333	1.352	0.147	30.580	5.992	5.436	40.236	
	TUFFS	8,665	0.325	2.274	1.349	0.172	49.261	5.189	4.562	54.882	
	ANDESITE	3,070	0.130	1.516	1.088	0.221	9.182	4.883	4.323	32.360	
	TOTAL	1,880,788	0.753	4.878	3.456	0.454	71.764	9.859	13.805	116.259	
Mixed Cu/Zn Mineral	RHYOLITE	9,387	1.165	1.539	1.679	0.017	37.173	8.287	11.079	79.696	
	VMS	2,418,124	3.194	3.914	4.023	0.321	80.871	14.630	21.526	202.160	
	BRECCIA	88,524	0.740	1.055	0.461	0.084	21.107	4.720	6.344	40.774	
	GYPSUM	8,963	1.005	1.150	0.648	0.031	12.033	4.854	13.310	49.793	
	BASALT	19,021	0.555	0.685	0.919	0.052	18.788	7.521	5.186	39.933	
	GRAINSTONE	315,151	0.836	0.932	1.056	0.111	26.791	5.869	4.831	54.225	
	TUFFS	2,833	0.653	1.399	1.420	0.128	63.051	6.217	6.065	66.483	
	ANDESITE	2,216	0.725	1.203	0.618	0.036	15.904	5.586	5.171	41.817	
	TOTAL	2,864,219	2.828	3.466	3.545	0.287	73.083	13.237	19.022	179.150	
Copper Mineral	RHYOLITE	920	1.366	0.079	1.812	0.150	8.351	8.455	11.575	74.643	
	VMS	1,219,882	2.841	0.226	2.171	0.027	12.225	21.857	32.382	143.377	
	BRECCIA	113,112	0.951	0.075	0.373	0.013	7.848	7.267	8.117	45.862	
	GYPSUM	21,357	0.930	0.074	0.374	0.008	2.465	4.374	16.651	44.399	
	BASALT	6,966	0.658	0.083	0.728	0.019	4.406	8.002	6.589	34.979	
	GRAINSTONE	121,002	0.848	0.090	0.781	0.036	3.629	4.511	1.811	43.718	
	TUFFS	0	0.000	0.000	0.000	0.000	0.000	0.000	0.000	0.000	
	ANDESITE	354	0.560	0.093	1.014	0.033	4.519	7.073	7.764	32.667	
	TOTAL	1,483,593	2.496	0.201	1.898	0.027	11.035	18.975	27.621	125.946	
Grand Total		6,228,600	2.1222	3.1143	3.1257	0.2754	57.9051	13.5839	19.4949	147.4870	46,205,000

TABLE 16.9 DILUTED MINING PLAN

Diluted production plan	Year	-A 1	Y1	Y2	Y3	Y4	Y5	Y6	Y7	Y8	Y9	Preprod	Producción	Grand
Mine to plant ore	Months	12	12	12	12	12	12	12	12	12	12	TOTAL	TOTAL	TOTAL
Total mine production														
Copper Mineral	t		179,550	179,550	179,550	179,550	139,650	139,650	139,650	129,675	12,269		1,279,094	1,279,094
Cu	%		4.00	3.72	3.08	2.07	2.06	2.06	1.90	1.82	1.43		2.66	2.66
Zn	%		0.31	0.20	0.25	0.16	0.19	0.17	0.17	0.17	0.17		0.21	0.21
Pb	%		0.03	0.02	0.02	0.01	0.04	0.04	0.03	0.03	0.03		0.03	0.03
Au	g/t		3.30	2.57	1.83	1.68	1.79	1.79	1.75	1.75	1.43		2.09	2.09
Ag	g/t		16.59	10.74	11.58	8.90	11.06	11.06	11.45	11.48	11.38		11.65	11.65
Fe	%		23.14	23.16	21.50	19.98	19.72	19.72	19.12	18.88	17.07		20.79	20.79
S	%		37.35	37.13	32.89	31.01	26.28	26.28	25.50	24.46	22.56		30.64	30.64
Mixed Mineral Cu/Zn	t		319,200	319,200	319,200	319,200	269,325	269,325	269,325	219,450	143,441		2,447,666	2,447,666
Cu	%		4.14	3.91	3.60	3.51	2.49	2.31	2.31	1.93	1.74		3.04	3.04
Zn	%		4.84	4.55	4.15	4.44	3.23	2.92	2.92	2.73	2.42		3.73	3.73
Pb	%		0.50	0.44	0.35	0.47	0.22	0.13	0.13	0.13	0.13		0.30	0.30
Au	g/t		6.65	5.59	4.13	3.11	2.84	2.91	2.91	2.42	1.93		3.82	3.82
Ag	g/t		118.79	118.66	118.48	83.88	54.48	45.14	45.14	38.60	35.45		78.82	78.82
Fe	%		13.74	13.73	13.71	13.91	14.81	14.03	14.03	14.11	13.25		13.94	13.94
S	%		23.09	21.92	20.31	20.50	20.87	19.40	19.40	19.48	17.86		20.55	20.55
Zinc Mineral	t		199,500	199,500	199,500	199,500	159,600	159,600	159,600	169,575	61,646		1,508,021	1,508,021
Cu	%		1.46	1.63	1.21	0.50	0.41	0.41	0.43	0.71	0.54		0.87	0.87
Zn	%		8.02	7.98	6.88	4.12	3.72	3.72	3.71	4.63	4.16		5.44	5.44
Pb	%		0.88	1.10	0.98	0.27	0.16	0.16	0.17	0.28	0.24		0.52	0.52
Au	g/t		6.19	5.66	5.47	3.06	2.73	2.73	2.59	2.37	2.36		3.91	3.91
Ag	g/t		168.15	185.92	135.73	34.44	25.93	25.93	25.11	33.20	28.72		82.41	82.41
Fe	%		9.55	7.98	8.66	11.17	11.38	11.38	11.45	11.39	11.01		10.29	10.29
S	%		17.77	14.24	14.59	14.87	14.80	14.80	14.78	14.16	13.97		14.99	14.99
Total ore	t	-	698,250	698,250	698,250	698,250	568,575	568,575	568,575	518,700	217,355	-	5,234,780	5,234,780
StockPile	t						129,675	129,675	129,675	179,550	409,673		978,248	978,248
Cu	%						0.87	0.58	0.63	0.60	0.62		0.64	0.64
Zn	%						0.87	0.70	0.70	1.09	1.04		0.93	0.93
Pb	%						0.88	0.92	0.82	0.59	1.08		0.91	0.91
Au	g/t						0.07	0.07	0.07	0.07	0.11		0.09	0.09
Ag	g/t						25.61	16.08	15.86	19.59	27.27		22.65	22.65
Fe	%						6.05	5.85	5.75	4.78	5.44		5.50	5.50
S	%						6.43	5.40	5.76	5.76	4.79		5.40	5.40
Total StockPile	t	-	-	-	-	-	129,675	129,675	129,675	179,550	409,673	-	978,248	978,248
Production plan mine to plant	t		698,250	698,250	698,250	698,250	698,250	698,250	698,250	698,250	627,029	-	6,213,029	6,213,029
Cu	%		3.34	3.21	2.78	2.28	1.63	1.51	1.27	1.27	0.88		2.06	2.06
Zn	%		4.58	4.41	3.93	3.25	2.30	2.14	2.14	2.29	1.65		2.98	2.98
Pb	%		0.49	0.52	0.44	0.30	0.29	0.27	0.25	0.27	0.76		0.39	0.39
Au	g/t		5.66	4.83	3.92	2.73	2.09	2.12	2.09	1.68	0.77		2.90	2.90
Ag	g/t		106.61	110.13	95.92	50.47	33.91	28.53	28.38	27.36	28.98		57.02	57.02
Fe	%		14.96	14.51	14.27	14.69	13.38	13.04	12.92	11.94	8.00		13.14	13.14
S	%		25.23	23.64	21.91	21.59	17.88	17.12	17.03	15.58	9.03		18.89	18.89
Overburden	t	5,000,000	5,702,000	5,702,000	5,702,000	5,702,000	5,701,750	4,301,750	4,301,750	3,001,750	1,105,572	5,000,000	41,220,572	46,220,572
Stripping ratio	t/t		8.17	8.17	8.17	8.17	8.17	6.16	6.16	4.30	1.76		6.63	7.44

TABLE 16.10 MINERAL PRODUCTION PLAN FOR PROCESSING

Diluted mining plan	Year	-Y1	Y1	Y2	Y3	Y4	Y5	Y6	Y7	Y8	Y9	Pre-prod	Production	Grand
	Months	12	12	12	12	12	12	12	12	12	12			
Diluted Cooper Mineral production	t		179,550	179,550	179,550	179,550	139,650	139,650	139,650	129,675	12,269		1,279,094	1,279,094
Cu	%		4.00	3.72	3.08	2.07	2.06	2.06	1.90	1.82	1.43		2.66	2.66
Zn	%		0.31	0.20	0.25	0.16	0.19	0.19	0.17	0.17	0.17		0.21	0.21
Pb	%		0.03	0.02	0.02	0.01	0.04	0.04	0.03	0.03	0.03		0.03	0.03
Au	g/t		3.30	2.57	1.83	1.68	1.79	1.79	1.78	1.75	1.43		2.09	2.09
Ag	g/t		16.59	10.74	11.58	8.90	11.06	11.06	11.45	11.48	11.38		11.65	11.65
Fe	%		23.14	23.16	21.50	19.98	19.72	19.72	19.12	18.88	17.07		20.79	20.79
S	%		37.35	37.13	32.89	31.01	26.28	26.28	25.50	24.46	22.56		30.64	30.64
Diluted Mixed Cu/Zn Mineral production	t		319,200	319,200	319,200	319,200	269,325	269,325	269,325	219,450	143,441		2,447,666	2,447,666
Cu	%		4.14	3.91	3.60	3.51	2.49	2.31	2.31	1.93	1.74		3.04	3.04
Zn	%		4.84	4.55	4.15	4.44	3.23	2.92	2.92	2.73	2.42		3.73	3.73
Pb	%		0.50	0.44	0.35	0.47	0.22	0.13	0.13	0.13	0.13		0.30	0.30
Au	g/t		6.65	5.59	4.13	3.11	2.84	2.91	2.91	2.42	1.93		3.82	3.82
Ag	g/t		118.79	118.66	118.48	83.88	54.48	45.14	45.14	38.60	35.45		78.82	78.82
Fe	%		13.74	13.73	13.71	13.91	14.81	14.03	14.03	14.11	13.25		13.94	13.94
S	%		23.09	21.92	20.31	20.50	20.87	19.40	19.40	19.48	17.86		20.55	20.55
Diluted Zinc Mineral production	t		199,500.0	199,500.0	199,500.0	199,500.0	159,600.0	159,600.0	159,600.0	169,575.0	61,645.5		1,508,021	1,508,021
Cu	%		1.46	1.63	1.21	0.50	0.41	0.41	0.43	0.71	0.54		0.87	0.87
Zn	%		8.02	7.98	6.88	4.12	3.72	3.72	3.71	4.63	4.16		5.44	5.44
Pb	%		0.88	1.10	0.98	0.27	0.16	0.16	0.17	0.28	0.24		0.52	0.52
Au	g/t		6.19	5.66	5.47	3.06	2.73	2.73	2.59	2.37	2.36		3.91	3.91
Ag	g/t		168.15	185.92	135.73	34.44	25.93	25.93	25.11	33.20	28.72		82.41	82.41
Fe	%		9.55	7.98	8.66	11.17	11.38	11.38	11.45	11.39	11.01		10.29	10.29
S	%		17.77	14.24	14.59	14.87	14.80	14.80	14.78	14.16	13.97		14.99	14.99
Diluted stockpile material	t		99,750	99,750	99,750	99,750	129,675	129,675	129,675	179,550	10,673		978,248	978,248
Cu	%		0.52	0.66	0.65	0.65	0.87	0.58	0.63	0.60	0.58		0.64	0.64
Zn	%		0.95	1.20	1.10	0.92	0.87	0.67	0.70	1.09	1.08		0.93	0.93
Pb	%		1.14	1.15	1.09	1.00	0.88	0.92	0.82	0.59	0.49		0.91	0.91
Au	g/t		0.14	0.12	0.11	0.09	0.07	0.07	0.07	0.07	0.06		0.09	0.09
Ag	g/t		24.84	31.82	29.02	24.31	25.61	16.08	15.86	19.59	18.93		22.65	22.65
Fe	%		5.00	5.54	5.60	5.72	6.05	5.85	5.75	4.78	4.50		5.50	5.50
S	%		4.89	4.89	4.61	4.67	6.43	5.40	5.76	5.76	5.86		5.40	5.40
Total ore production	t		798,000	798,000	798,000	798,000	698,250	698,250	698,250	698,250	228,029		6,213,029	6,213,029
Diluted waste rock production	t	5,000,000	5,702,000	5,702,000	5,702,000	5,702,000	5,701,750	4,301,750	4,301,750	3,001,750	1,105,572	5,000,000	41,220,572	46,220,572
Stripping ratio	t/t		7.15	7.15	7.15	7.15	8.17	6.16	6.16	4.30	4.85		6.63	7.44

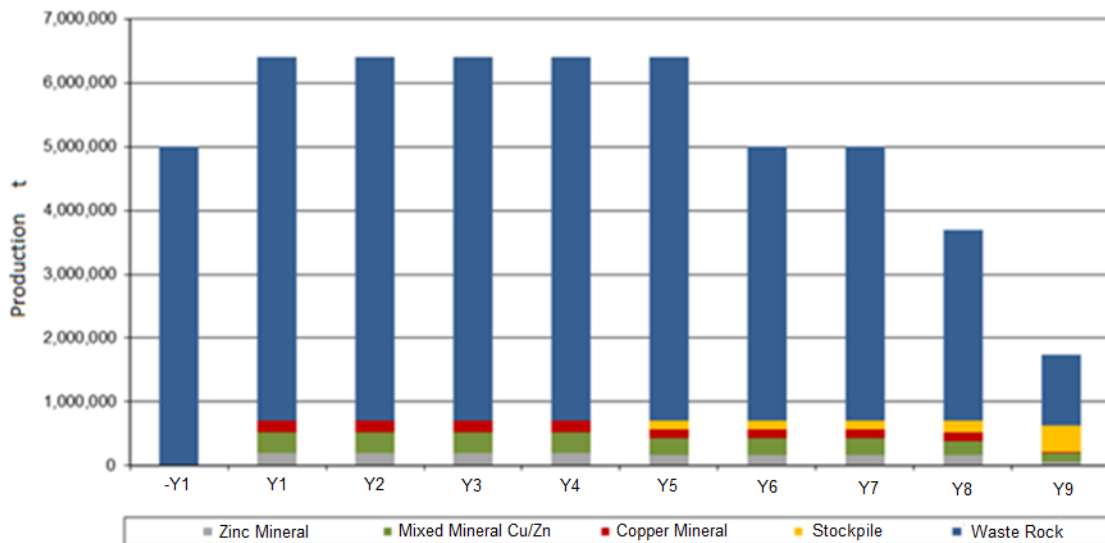


FIGURE 16.5 ANNUAL MINING PLAN

EQUIPMENT LIST

The requirements for mining equipment were based on annual mining production, estimated effective operating time (uptime), and the productivity of the equipment. The size and type of equipment are consistent with the project scope:

- Initial work and construction of access roads to the mine and crusher, stockpile, and waste rock dump
- First year of stripping (pre-production)
- Transport of ore or waste rock to the plant, stockpile, and waste rock dump
- Maintenance of open pit working areas, internal and external access roads, etc
- Waste rock dumps and stockpile
- Construction of infrastructure

A summary of the proposed equipment is detailed in Table 16.11.

TABLE 16.11 MINING EQUIPMENT FLEET

YEAR	-Y1	Y1	Y2	Y3	Y4	Y5	Y6	Y7	Y8	Y9
Main Equipment										
Ore trucks - Volvo FMX84R - 20 m ³		2	2	2	2	2	2	2	1	1
Ore excavators - CAT 365 - 3.8 m ³		1	1	1	1	1	1	1	1	1
Overburden trucks - Volvo FMX84R -20 m ³	7	8	8	8	8	8	9	7	6	3
Overburden excavator - CAT 365- 3.8 m ³	2	2	2	2	2	2	2	2	2	1
Drills - ROC L8 - 4 1/2"	1	2	2	2	2	2	2	2	1	1
Front end loader - 966 CAT - 3.6 m ³	2	2	2	2	2	2	2	2	1	1
Bulldozer - D8R - 11.8 m ³	2	2	2	2	2	2	2	2	2	1
Grader - CAT 140H - 3.7m ³	1	1	1	1	1	1	1	1	1	1
Water tanker - 15900 - 15 m ³	2	2	2	2	2	2	2	2	2	2
Auxilliary Equipment										
Service truck	1	1	1	1	1	1	1	1	1	1
Production truck - anfo+emulsion - 13.5 t	1	1	1	1	1	1	1	1	1	1
Bobcat - 1.7 m ³	1	1	1	1	1	1	1	1	1	1
Pick-up 4x4 Domo	2	4	4	4	4	4	4	4	4	2
Pick-up 4x4 Contractor	5	5	5	5	5	5	5	5	5	5
Pick-up 4x4 Sampling	0	1	1	1	1	1	1	1	1	1
Personnel bus	1	2	2	2	2	2	2	2	1	1
Pump	0	1	1	1	1	1	1	1	1	1
Lighting	6	7	7	7	7	7	7	7	7	4
Total	34	45	45	45	45	45	46	44	39	29

DRILLING AND BLASTING

The drilling equipment considered is the ROC L8 (sized in accordance with the properties of the ore and the waste rock), which is capable of drilling holes of up to 4½" in diameter. 20% of overdrilling will be applied to the final height of each bench extracted.

LOADING AND TRANSPORT

Blasted material will be loaded with CAT365 excavators and hauled with Volvo FMX84R trucks with a 20 m³ capacity.

DESIGN OF WASTE ROCK DUMP

The waste rock dump lies south of the open pit (see Table 16.12 for the design parameters).

TABLE 16.12 WASTE ROCK DUMP DESIGN PARAMETERS

Design Parameters	Unit	Amount
Dry waste rock density	t/m ³	1.8
Overall slope		1.5H:1V
Maximum waste dump elevation	masl	920
Waste dump removal area of influence	ha	75.44
Volume of waste dump	Mm ³	33.01
Volume of containment dyke	m ³	18,800
Waste rock weight	Mt	59.42

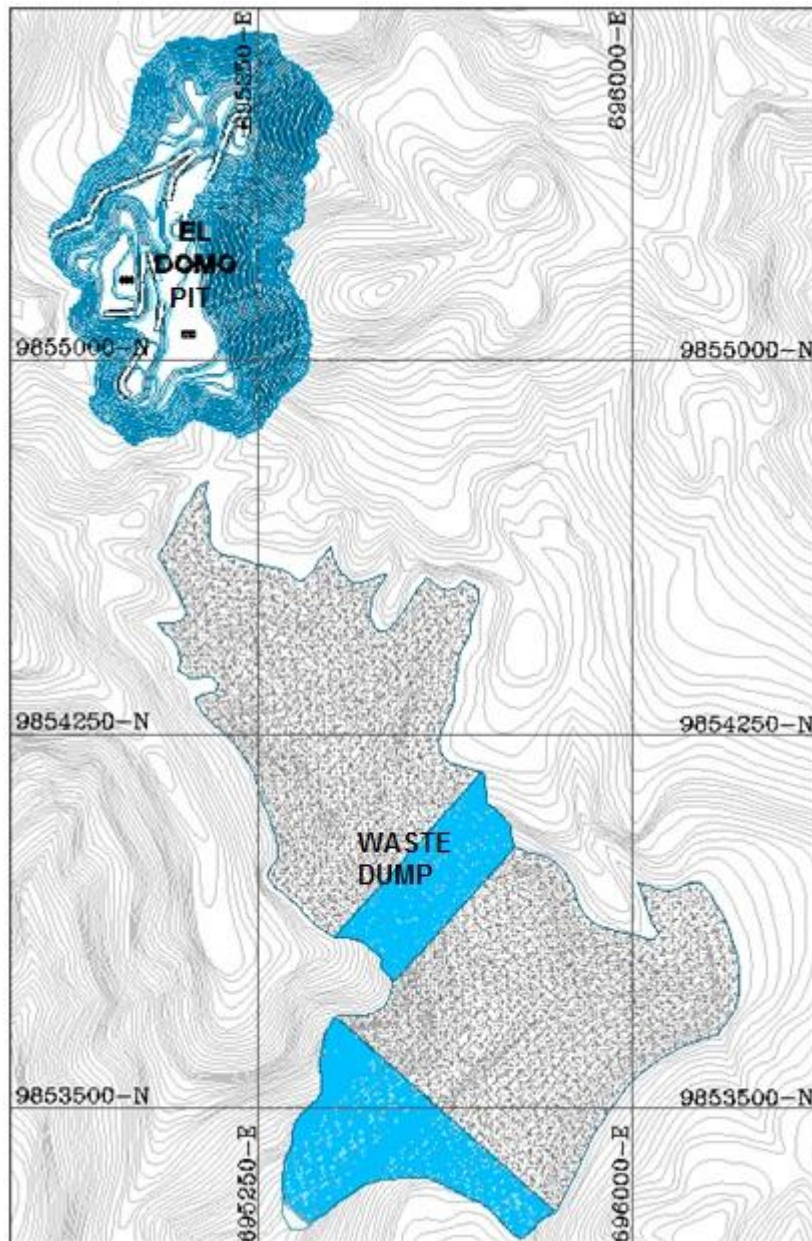


FIGURE 16.6 WASTE ROCK DUMP FINAL BOUNDARY

The cost estimate considers a sub-drainage system that discharges seepage water to a seepage collection pond. Surface drainage includes the installation of collection channels on the perimeter of the waste rock dumps, and crest channels to capture rainwater, thus minimizing water entry into the waste rock dumps. The construction of a containment dyke is also considered in the design.

MINING EQUIPMENT UPTIME

Mine operation system consists of 2 shifts per day and 350 effective operating days per year. A shift is assumed to be 12 hours and includes:

- 1 hour non-operational delays (shift change, lunch hours)
- 3 hours operational delays (equipment maintenance, shutdowns, and other unplanned delays)

The net productive operating time is 952 min/day or 5,556 hours/year. Table 16.13 shows the distribution of planned hours and uptime hours used in calculating productivity and equipment requirements.

TABLE 16.13 UPTIME PER DAY

Description	Unit	Quantity
Scheduled time per shift	min	720
Travel time/shift change/blasting	min	20
Equipment inspection	min	10
Lunch/breaks	min	40
Fuelling, lubrication, and servicing	min	15
Net uptime scheduled	min	635
Work efficiency (45 min of productive time per hour measured)		0.75
Net uptime per shift	min	476
Work days per year	day	350
Shifts per day		2
Hours/shift	h	12
Net uptime per day	min	952.5
Net uptime per year	h	5,556

The mechanical availability and use of loading and hauling equipment are estimated at 85% and 88%, respectively. Therefore, net usage will be on the order of 75%.

ANCILLARY MINE FACILITIES

Mine services include the following activities and equipment for:

- Maintenance of roads and dumps
- Power
- Lighting

The mine will be in operation 24 hours per day except during blasting. Adequate lighting will be required during the night shifts for drilling, loading, and hauling activities as well as for the access and haul roads.

The proposed ancillary equipment consists of:

- Front end loader
- Bulldozer
- Grader
- Water tanker
- Service truck
- Production truck
- Bobcat
- 4x4 Pick-up
- Personnel bus
- Floodlights

The ancillary equipment, such as front end loaders, should serve as support equipment for the excavators. The bulldozers are necessary for dump maintenance and road development. Graders and water tankers will be used for road construction and maintenance. Fuel tanks must be available for the mining equipment in each sector.

MINING CONTRACTOR

Salazar has indicated that the future mining operation will be run by a contractor, which they will supervise. This is a standard procedure worldwide. The contract will be fully inclusive, with the contractor providing the appropriate personnel, mining equipment, support facilities, and infrastructure to achieve the mining objectives.

The contractor's field of operation shall include the following items:

- Mobilization/Demobilization
- Drilling and blasting
- Loading and hauling
- Mine services

Loading and hauling includes the cost of facilities, among which are the gas stations, fuel tanks, truck maintenance, and other items related to loading and hauling processes. These costs should also include road construction and maintenance. The mining equipment investment and operating costs are included in the contractor's operating costs.

UNDERGROUND MINE

The eastern mineral deposit (Eastern Sector) is about 250 metres below the surface, extending from 910 masl to 750 masl. This deposit has two main lenses and several secondary lenses, which have been grouped into four main orebodies (see Figure 16.7).

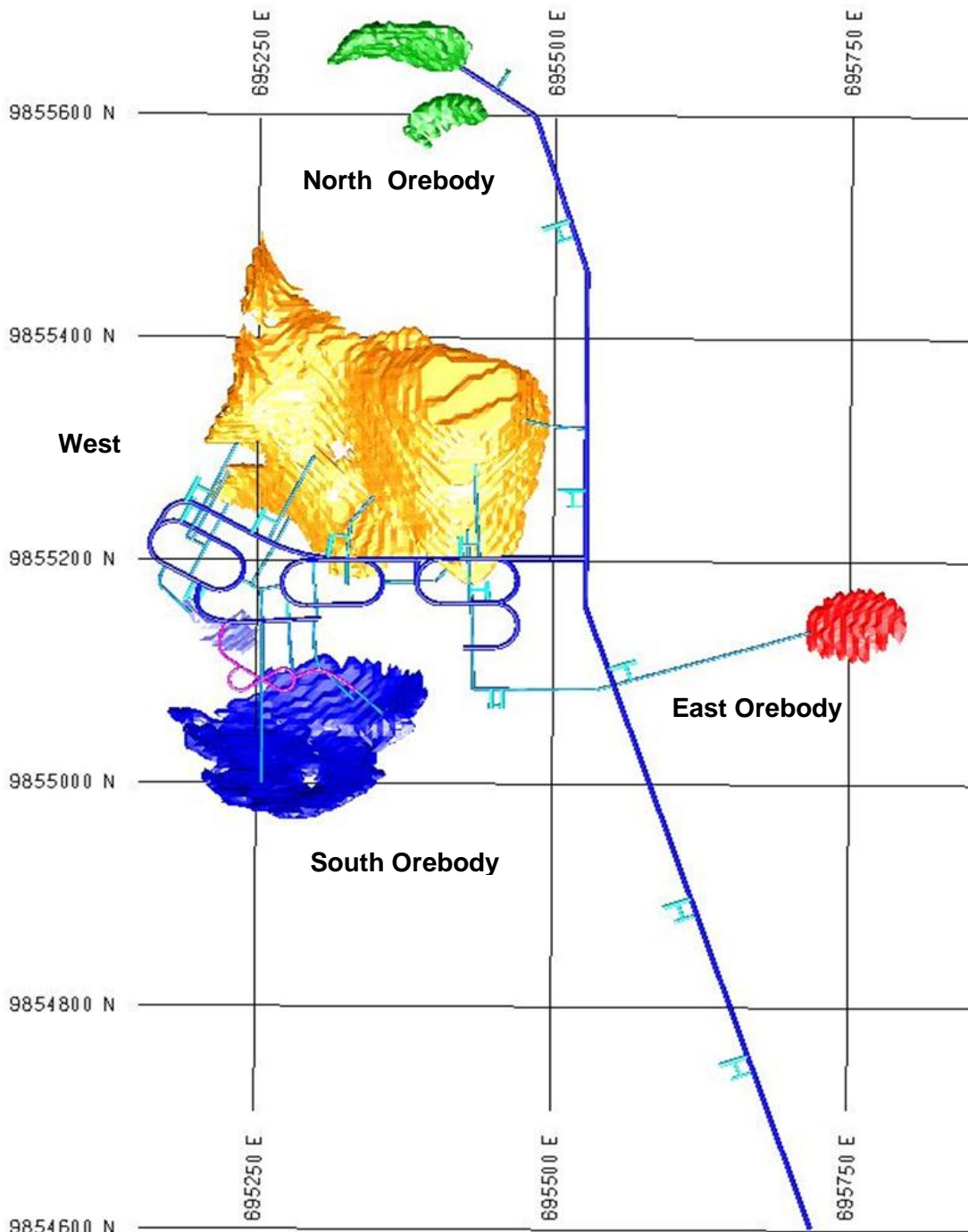


FIGURE 16.7 UNDERGROUND MINERALIZED LENSES

The chamber-and-pillar method is suggested for mining this deposit below the andesite unit. The method involves opening a gallery the length of the ore lens, off which multiple production areas or chambers will be opened, leaving intact areas to serve as pillars to bear the vertical load and thus prevent collapse of the crown. For this project, pillar sizes were estimated at 4.0 x 4.0 metres. Since the use of pillars involves more ore loss than other methods, the pillars should be located in lower-grade areas as much as possible.

MINERAL RESOURCES ANALYSIS

The mineral resource analysis for underground mining used an NSR (Net Smelter Return) cutoff of US\$40 per tonne, considering the solid resulting from using this restriction in the block model. To calculate the NSR value, BISA has taken into account the same Metal Unit Values of one percent grade for copper, zinc, and lead, of one gram grade for gold, and of one ounce for silver assumed for the open pit analysis (Tabla 16.1)

The total mineral resources (indicated + inferred) were divided into three mineral types according to the Cu/(Zn+Pb) ratio: zinc mineral (Cu/(Zn+Pb):[0-0.3>), mixed Cu/Zn mineral (Cu/(Zn+Pb): [0.3-3]), and copper mineral (Cu/(Zn+Pb):>3). These types reported totals of 2,064,787 tonnes of mineral with an average NSR of 127.37 US\$/t. Table 16.14 shows resource details for each mineral type.

TABLE 16.14 RESOURCES BY MINERAL TYPE

Mineral Type	Tonnage (t)	NSR (\$/t)	Cu (%)	Zn (%)	Au (g/t)	Pb (g/t)	Ag (g/t)	Fe (%)	S (%)
Cooper Mineral	1,042,241	140.03	2.96	0.16	0.97	0.03	9.68	16.67	23
Mixed Cu/Zn Mineral	744,739	122.62	2.32	2.65	1.4	0.12	59.5	14.17	20.06
Zinc Mineral	277,807	92.59	0.77	4.39	2.04	0.34	72.98	11.05	16.9
Overall Total	2,064,787	127.37	2.44	1.63	1.27	0.1	36.17	15.01	21.12

All resources were sorted by accessibility, and resources in isolated zones between the main orebodies (primarily north and west) were considered inaccessible.

DESIGN PARAMETERS AND CRITERIA

The underground mineral resource comprises several orebodies of variable dip (mainly 0°–20°). The mineralized lenses lie beneath the andesite dome, which has good geomechanical properties, therefore favouring optimal use of the chamber-and-pillar method. In addition, since this method is highly versatile, it can be adapted to the areas where the orebody dips more steeply.

The mine design plans for a main ramp (cross-section of 4.8 m x 5.3 m), with a gradient of -12% on straight sections and -10% on curves (with a curve radius of 20 m).

For secondary ramps, the gradient is +15% with a cross-section of 3.0 x 3.0 m, dimensions suitable only for scoops and jumbos.

The gallery design plans for a cross-section of 3.0 x 3.0 m. Subsequently, these works will be scaled by 1 m on each drift wall to reach a final cross-section of 5.0 x 3.0 metres. This will create a pillar width of 4 m, as shown in Figure 14.8**.

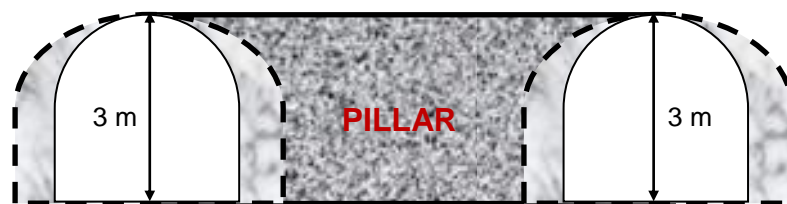


FIGURE 16.8 CHAMBERS AND PILLARS — CROSS SECTION

Table 16.15 shows the advance rates per heading according to the mining schedule.

TABLE 16.15 UNDERGROUND DEVELOPMENT — ADVANCE RATES

Activity	Rate
Main ramp (4.5x4.8)	120 m/month
Secondary ramp (3x3)	90 m/month
Exploratory cross-cut (4.5X4.8)	120 m/month
Cross-cut (3x3)	120 m/month
Gallery (3x3)	100 m/month
Shaft RB (Ø 3m)	160 m/month
Ore cleaning	2,970 t/month
Backfill	350 m ³ /day

MINE DESIGN AND DEVELOPMENT

The following conditions were taken as requirements for the mine design: design outside the lower-grade lithologies, such as gypsum and breccia, and preferred development in andesite. BISA has proposed three topographic points for the mine entrance and also requested design of an exploratory level above the central orebodies. Consequently, the point at 950 m was chosen for the main mine entrance. From this entrance, BISA designed a main ramp over 2 km long that forks at the 879-m elevation, which allows deepening for mining and opening the exploratory cross-cut, which will extend to the farthest orebody to facilitate its mining.

The main ramp is 4.5 x 4.8 m in cross-section and descends at a gradient of -12%. It is located on the central axis relative to the orebodies and has a favourable lithology for mining. Cross-cuts will be dug out from the ramp to access the orebodies. From the cross-cuts, drifts with a gradient of -15% will be opened, from which mining the orebody, level by level, with the chamber-and-pillar method will follow. This will basically consist of a main gallery central to the orebody, from which chambers will be opened and pillars left to serve as weight-bearing columns for the host rock.

Access to the first orebody begins 500 m from the start of the ramp, at elevation 890 m, via a cross-cut, from which the orebody will be mined by drifts and galleries.

At a depth of 790 m from the main ramp, a cross-cut will be opened to mine the south orebody through another ramp. This secondary ramp will have a cross-section of 3.0 x 3.0 m, therefore only allowing entry to scoops and jumbos.

Six shafts have been designed for ventilation, services, and auxiliary or secondary personnel exits. The design includes details such as draw points (also serving as safety bays) and sumps.

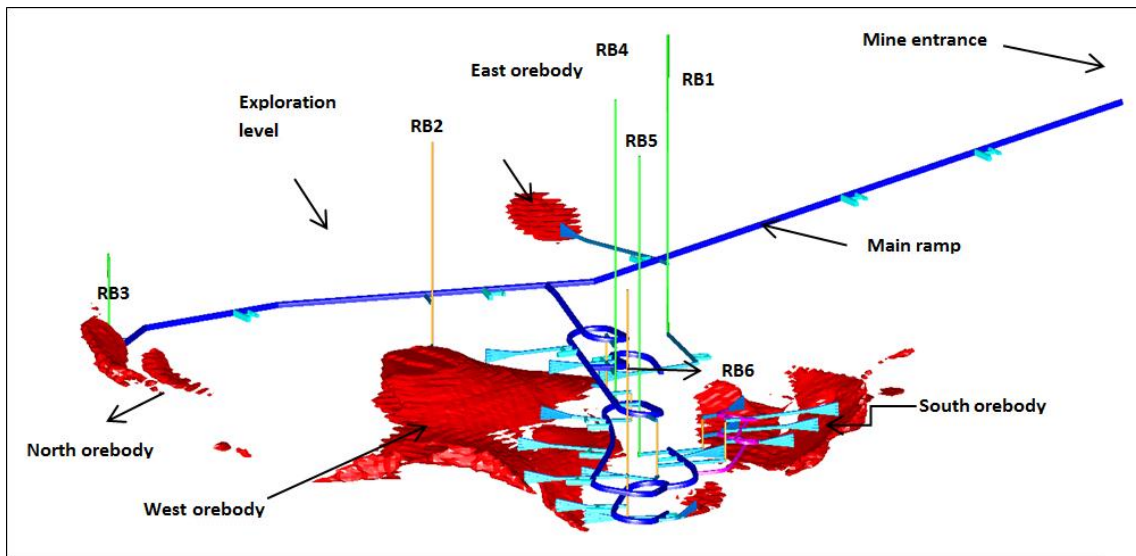


FIGURE 16.9 UNDERGROUND MINE DESIGN

RESOURCES WITH MINING POTENTIAL

BISA calculated the resources with underground mining potential that serve as a basis for the production plan. First, the inaccessible mineral resources were subtracted since the solid produced with an NSR of over US\$40 per tonne gave isolated structures. This represents 2.6% of the total resource volume.

Then the available resources were recalculated using a recovery rate of 80% with the applied method, which involves leaving natural pillars for support. A total of 1,608,100 tonnes of resources was obtained with grades of 2.41% Cu and 1.59% Zn.

TABLE 16.16 UNDERGROUND RESOURCES WITH MINING POTENTIAL

Mineral Type	Tonnes (t)	Cu (%)	Zn (%)	Pb (%)	Ag (g/t)	Au (g/t)	Fe (%)
Copper Mineral	828,972	2.87	0.16	0.02	9.51	0.95	16.42
Mixed Cu/Zn Mineral	569,180	2.32	2.65	0.11	58.27	1.39	14.24
Zinc Mineral	209,947	0.79	4.40	0.33	73.11	2.03	11.13
Total	1,608,100	2.41	1.59	0.09	35.07	1.25	14.96

UNDERGROUND DEVELOPMENT PROGRAM

A detailed underground development program was prepared based on the production requirements, resulting in 8,971 metres, which includes horizontal and vertical development. A summary of the total length by work type is shown in Table 16.17.

TABLE 16.17 UNDERGROUND DEVELOPMENT PROGRAM

Material	Type of Development	Type of Work	Y9	Y10	Y11	Y12	Y13	Y14	Total
Waste rock	Horizontal development	Crosscut	880	867	106	64	69	70	2,056
		Ramp (-)	1,475	1,068					2,543
		Ramp(+)		206	114				320
		Crosscut Pivot	30	203	90	60	90	60	533
	Vertical development	Shaft		226	7				233
		Raise Bore	576	565					1,141
	Subtotal		2,355	2,141	220	64	69	70	6,826
Ore	Horizontal	Gallery	60	482	485	501	271	346	2,145
	Subtotal		60	482	485	501	271	346	2,145
Total			2,445	2,826	795	625	430	476	8,971

UNDERGROUND PRODUCTION PROGRAM

The production program was designed to mine 1,000 tpd, within the range of medium-scale underground mining legislation in Ecuador. The program was designed considering the mineral types and production advances and stoping.

TABLE 16.18 UNDERGROUND PRODUCTION PROGRAM BY MINERAL TYPE

Mineral Type	Variables	Units	Y9	Y10	Y11	Y12	Y13	Y14	Total
Zinc Mineral	Ton	t	1,902	39,640	34,154	31,026	96,724	25,031	228,477
	Cu	%	0.32	0.49	0.87	0.6	0.74	0.75	0.69
	Zn	%	3.38	3.28	3.34	3.54	4.13	4.73	3.84
	Pb	%	0.48	0.33	0.13	0.13	0.36	0.32	0.29
	Ag	g/t	35.07	48.08	62.32	44.51	82.18	46.53	63.88
	Au	g/t	1.37	1.31	1.34	1.27	2.34	1.57	1.77
	Fe	%	11.3	11	9.98	10.78	8.56	10.41	9.72
Mixed Cu/Zn Mineral	Ton	t	1,652	107,231	141,077	164,010	130,749	74,984	619,703
	Cu	%	1.91	2.07	2.37	1.96	1.84	1.79	2.03
	Zn	%	2.18	2.63	2.38	1.97	2.47	2.19	2.31
	Pb	%	0.41	0.22	0.07	0.04	0.08	0.1	0.09
	Ag	g/t	58.83	59.85	57.56	45.74	46.44	44.39	50.89
	Au	g/t	1.3	1.14	1.22	1.17	1.28	1.26	1.21
	Fe	%	11.79	11.29	13.79	12.36	12.25	12.03	12.44
Cooper Mineral	Ton	t	357	120,619	216,804	196,939	165,270	203,034	903,023
	Cu	%	1.75	2.55	2.37	2.09	2.01	3.42	2.50
	Zn	%	0.14	0.1	0.11	0.15	0.13	0.17	0.13
	Pb	%	0.04	0.02	0.01	0.02	0.02	0.04	0.02
	Ag	g/t	13.66	8.24	8.39	8.11	7.95	8.7	8.30
	Au	g/t	1.29	0.87	0.82	0.76	0.78	0.91	0.83
	Fe	%	18.55	15.78	14.62	12.88	13.79	14.97	14.32

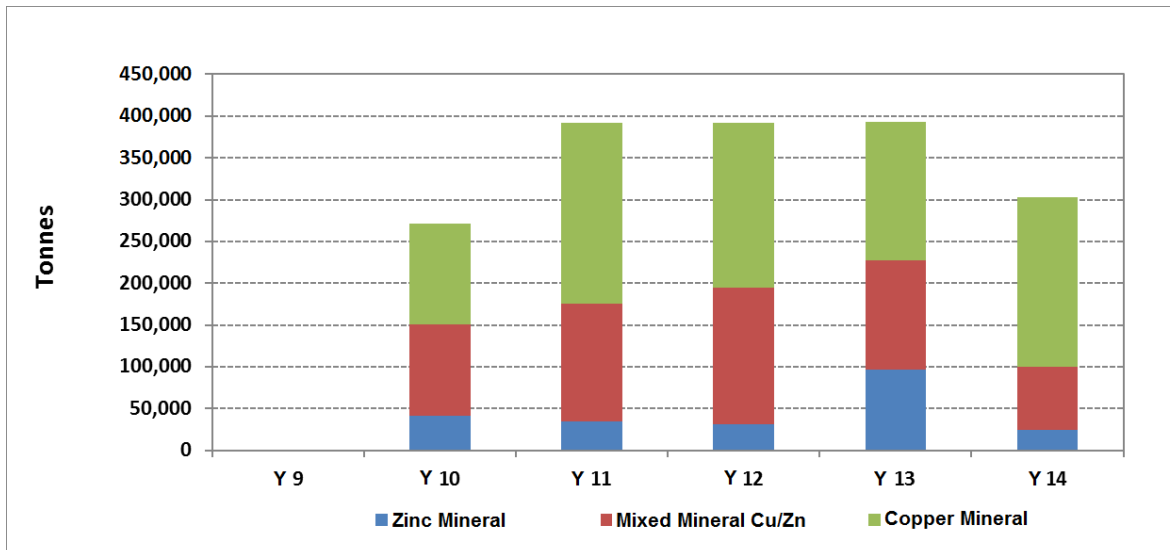


FIGURE 16.10 UNDERGROUND PRODUCTION PROGRAM BY MINERAL TYPE

TABLE 16.19 UNDERGROUND PRODUCTION PROGRAM

Type of Work	Variables	Units	Y9	Y10	Y11	Y12	Y13	Y14
Stoping	Ton	t	2,294	255,045	378,530	376,547	384,854	293,552
	Cu	%	1.07	2.1	2.28	1.94	1.63	2.87
	Zn	%	2.46	1.57	1.21	1.16	1.88	1.05
	Pb	%	0.39	0.14	0.04	0.03	0.12	0.08
	Ag	g/t	41.17	34.44	31.1	26.58	38.11	20.98
	Au	g/t	1.27	1.05	1.03	0.97	1.31	1.07
	Fe	%	11.6	13.5	14.1	12.6	11.9	14.1
Development Work	Ton	t	1,619	12,445	13,505	15,429	7,888	9,497
	Cu	%	1.19	1.21	1.16	1.53	2.15	0.63
	Zn	%	2.74	1.84	1.25	1.67	2.8	1.1
	Pb	%	0.44	0.2	0.01	0.07	0.21	0.08
	Ag	g/t	45.96	42.88	21.77	30.57	84.73	10.64
	Au	g/t	1.42	0.86	0.56	1.02	2.33	0.49
	Fe	%	13	7.7	7.7	11.1	16.5	5.2
Total Underground Production	Ton	t	3,912	267,490	392,035	391,976	392,742	303,049
	Cu	%	1.12	2.06	2.24	1.92	1.64	2.8
	Zn	%	2.58	1.59	1.21	1.18	1.9	1.05
	Pb	%	0.41	0.15	0.04	0.04	0.12	0.08
	Ag	g/t	43.15	34.83	30.78	26.73	39.04	20.65
	Au	g/t	1.33	1.04	1.01	0.97	1.33	1.05
	Fe	%	12.2	13.3	13.9	12.5	12	13.9

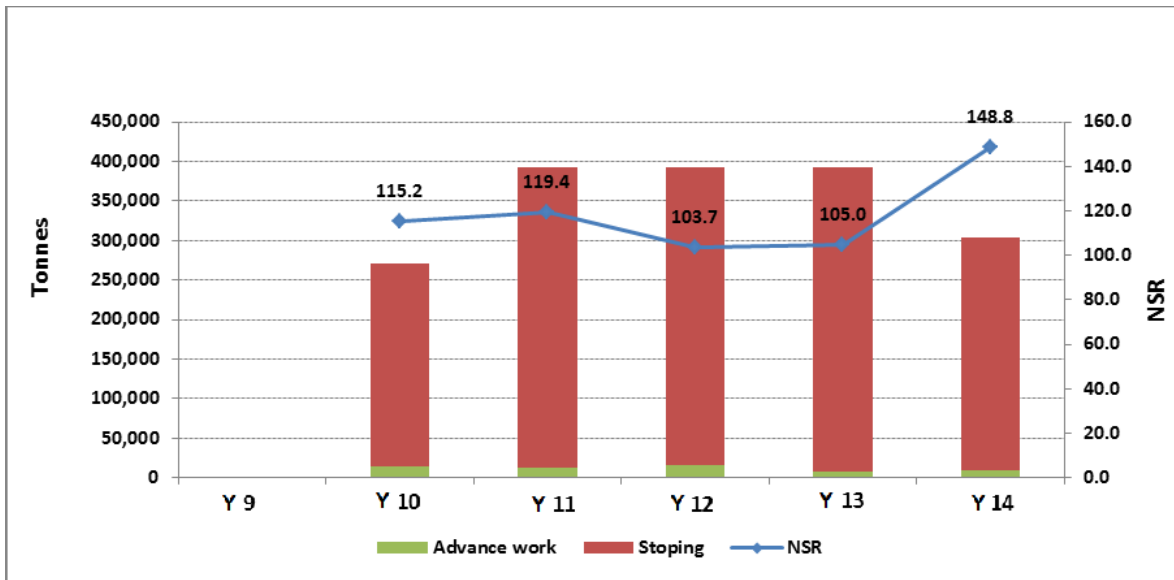


FIGURE 16.11 UNDERGROUND PRODUCTION PROGRAM BY TYPE OF WORK

LIST OF EQUIPMENT

The requirements and replacement of mine equipment are based on annual mine production, development and preparation programs, and on the productivity and availability of the equipment required. The size and type of equipment are in accordance with the working dimensions (see Table 16.20). The mining equipment will be used for the following activities:

- Preparation work: Building mine access points and a portal to the mine area, a crusher, a stockpile, and a waste rock dump.
- Pre-production for the first year and then operation and development.
- Development and production work: Drilling, ventilation, support, haulage, and personnel transport.
- Ore transport to the plant or stockpile and waste rock transport to the dump.
- Maintenance of internal and external access roads.

TABLE 16.20 UNDERGROUND MINE EQUIPMENT FLEET

Responsibility		Equipment	Y8	Y9	Y10	Y11	Y12	Y13	Y14
		Pick-up 4 x 4	2	4	4	4	4	4	4
		Fans		0	1	2	2	2	2
		Stationary pumps		0	2	2	2	2	2
		Submersible pumps		1	2	2	2	2	2
Contractor	Main	Jumbo Boomer 281		2	3	3	3	3	3
		Scooptram 4 yd ³		2	4	4	4	4	4
		Truck Volvo FMX 84r 15 m ³	1	2	4	4	4	4	3
	Auxiliary	Jackleg drill		4	6	6	6	6	6
		Aliva 246		1	1	1	1	1	1
		Boltec 235		1	1	1	1	1	1
		Personnel transport bus		1	1	1	1	1	1
		Service truck		1	1	1	1	1	1
		Compressor		1	1	1	1	1	1
		Water tanker		1	1	1	1	1	1
Pick-up 4x4		2	2	2	2	2	2		

UNDERGROUND MINING OPERATIONS

DRILLING AND BLASTING

The development and production drilling equipment consists of a Boomer 281 that will drill at a diameter of 51 mm and 14 feet in length for 4.8 x 5.3 m sections and 12 feet in length for 3.0 x 3.0 m sections. This equipment has been selected based on characteristics such as the ore type, waste rock, and working dimensions. In addition, the ventilation shafts will be raised with Raise Borer equipment with a diameter of 3 m, and the service shafts will be drilled conventionally.

Emulsion will be used as the blasting agent and carmax as a blasting accessory. Pre-split blasting will be used for greater control over the roof crown in order to reduce damage to the rock mass blasted out. This will decrease the exposure time of staff and equipment during preparation and reinforcement work.

REINFORCEMENT

A Boltec bolter will be used for reinforcement with rock bolts and mesh, shotcrete reinforcement will use an Aliva wet-mix shotcreting machine, and poor-quality rock will be

shored with formwork. Additional geotechnical studies will be needed to expand on the reinforcement requirements.

LOADING AND HAULING

Blasted material will be hauled in 4 yd³ Scooptrams from the production works to the stacking chambers and then loaded into 15 m³ dump trucks. The dump trucks will be loaded in the stacking chambers, which will be located along the ramp and at the exit to production works. From these points, the material will be hauled to the processing plant or the waste rock dump.

BACKFILL

The project considers the construction of a surface plant for paste backfill to supply the mine. The paste backfill will be pumped from the surface to the production workings by pipes.

The paste plant will have a capacity of 350 m³/d, which will be used to backfill the empty spaces produced by the operation, thus preventing the collapse of adjacent workings and, in turn, allowing the orebody to be mined upwards in steeply dipping zones.

MINING

Mining of the orebodies will be carried out by the chamber-and-pillar method with ascending backfill. As can be seen in Figure 16.9, the production zone is divided into four orebodies: North, West, South, and East. This method is suitable due to the layout of the orebodies in a nearly horizontal plane as a result of their geomechanical properties.

To mine the North, West, and East orebodies, crosscuts will be made from the base of the main ramp towards the orebodies, from which drifts will be opened to reach the base of the mineralized zones (see Figure 16.9).

When the drifts reach the base of the orebodies, main galleries will be opened around them for lateral workings opposite the direction of dip. These will in turn be connected with each other by workings parallel to the main gallery. Due to the slight dip of the structure, the ore does not flow by gravity. Consequently, it will have to be hauled to the stacking chambers so it can be loaded onto dump trucks and hauled to the processing plant.

Figure 16.14 shows each crosscut with its respective drift assigned to each mining area, represented in distinctive colours.

Once each zone has been mined, paste backfill will be used to stabilize the surrounding rock and continue mining higher levels. The pillars created in the lower levels will continue up through successive levels, thereby increasing the stability of the host rock.

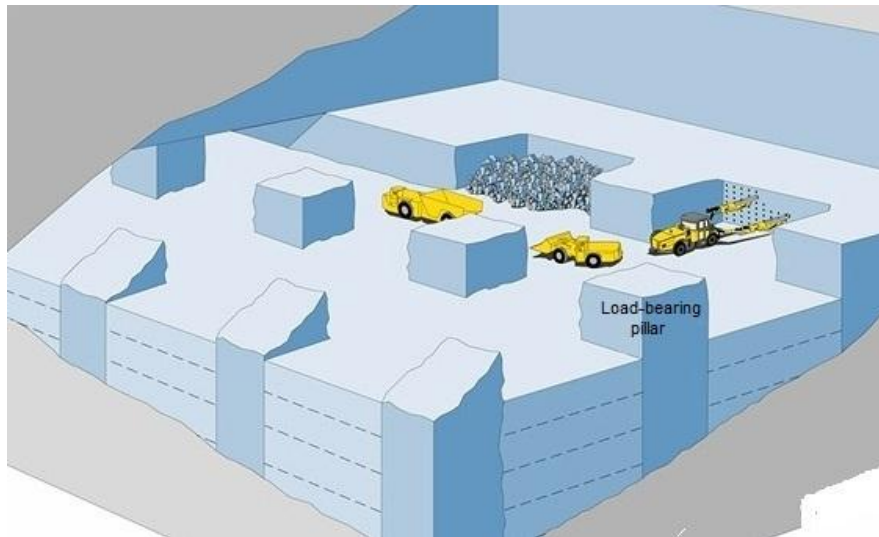


FIGURE 16.12 CHAMBER-AND-PILLAR MINING METHOD LAYOUT

In the South orebody, the main ramp will reach to 750 m and be used solely for extraction. A secondary ramp will start from this level (cross-section of 3.0 x 3.0 m), designed to access the South orebody by scoops, jumbos, and personnel. The orebody will be mined by the chamber-and-pillar method with ascending backfill, the same as for the North, East, and West orebodies. The scoops will haul muck to the orepasses remuck bays on the ramp, which reach down to the extraction level. The ore is then hauled by dump trucks.

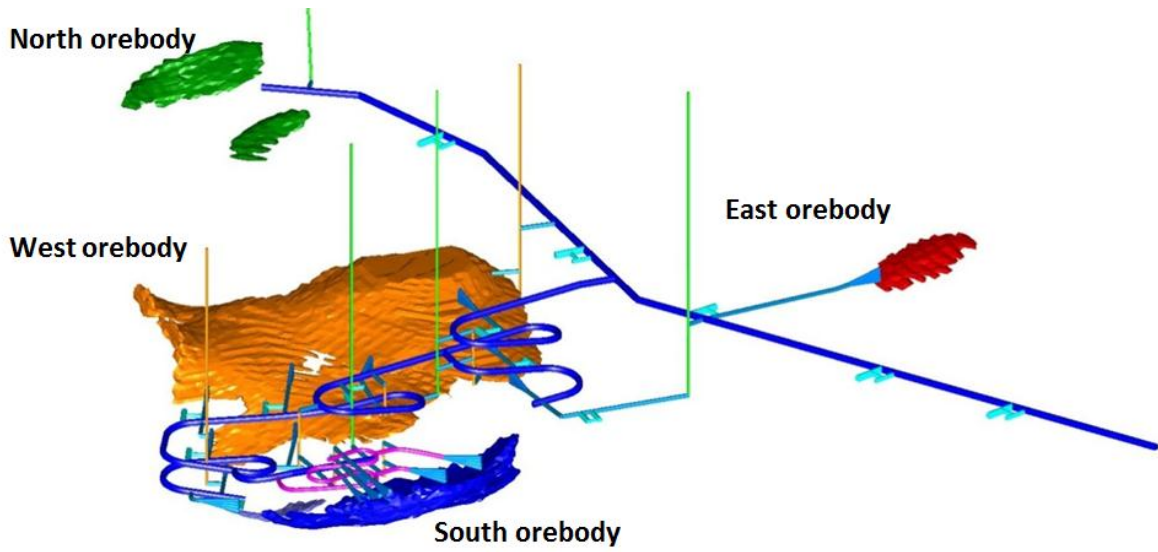


FIGURE 16.13 UNDERGROUND MINING AREAS

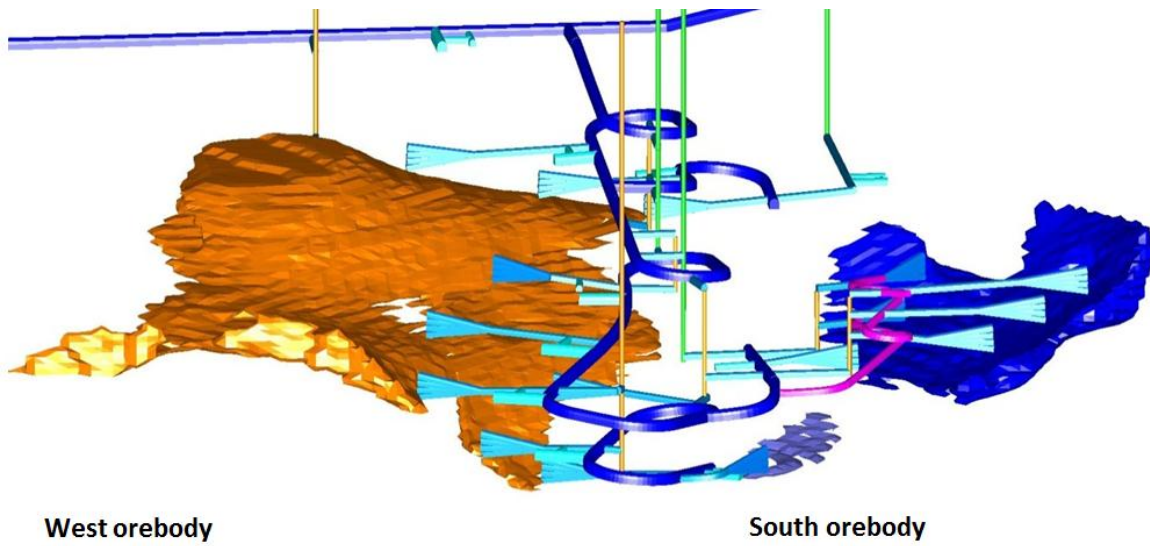


FIGURE 16.14 CENTRAL AND SOUTHERN UNDERGROUND MINING ZONES

UNDERGROUND MINE INFRASTRUCTURE

The project facilities will be built in several stages in accordance with the mine's development plan. The installations to build at the start of the project will optimize the mining works as well as the proper course of environmental activities.

TABLE 16.21 UNDERGROUND INFRASTRUCTURE

Infrastructure

Preliminary activities building the entrance platform and mine entrance
Access to raise on the surface
Concrete slab for Raise Bore
Electrical substations inside mine
Paste backfill plant
Equipment Maintenance and Heavy Equipment Workshop inside mine
Lamp room
Mine dining rooms
Magazine
Explosives accessory magazine
Electrical installations inside mine
Mine services installations
EPCM (Engineering, Procurement, Construction, and Management)

WASTE ROCK DUMP

The waste rock dump is described in the open pit chapter. The same waste dump will be used for a waste rock production of 270,904 tonnes for the life of the underground mine.

MINE SERVICES

VENTILATION

BISA's experience dictates that a production of 1,000 tpd would need 270,000 cfm of fresh air pumped into it. Air simulations with the Ventsim application showed that the mine's resistance is approximately $0.04217 \text{ N s}^2/\text{m}^8$. Consequently, nearly 150 kW of power is needed for the mine's main ventilation.

MAINTENANCE

For maintenance a workshop has been considered inside the mine with the necessary facilities for this type of work. This would provide good equipment availability for the operation.

ANCILLARY SERVICES

Mine ancillary services consider a piping network for the appropriate distribution of drilling water and compressed air. A piping network is also envisaged for pumping water out of the mine.

17. RECOVERY METHODS

Based on the results of the metallurgical tests reported in Chapter 13, a possible scenario for processing the ore from the El Domo deposit has been outlined. This process selection is preliminary and may be subject to change based on the results of future metallurgical studies as the project progresses. The results of metallurgical tests indicate that conventional flotation technology can be used to treat the ore from El Domo. The flowsheet includes a coarse primary grind, bulk sulphide flotation, flotation of a rougher bulk Cu/Zn concentrate, concentrate regrinding, and selective Cu/Zn flotation.

The preliminary process selection considers the following stages:

- A circuit of crushing, grinding, and classification that would include an intermediate stockpile to feed the grinding and classification circuit. Due to clay in the ores, only a primary crusher would be used to avoid problems entailed in the transport of fine, wet material. The grinding circuit would be made up of a SAG or rod mill, a ball mill, and a nest of cyclones.
- The product from grinding and classification would be sent to the Cu/Zn flotation plant, which would consist of a sulphide flotation circuit, a rougher bulk Cu/Zn flotation circuit, a regrinding circuit, a Cu/Zn bulk cleaner circuit, and a Cu/Zn separation circuit.
- The tailings from the sulphide flotation and the rougher bulk tailings would each be sent to a different thickener and then to their final locations. The copper and zinc concentrates would be sent to different thickeners and filter presses, stored, and then transported to third-party smelters as final concentrates.

The inclusion of a copper-lead separation circuit for ores containing a high lead head grade should be studied in the next phase of testwork.

A simplified process flow diagram is shown in Figure 17.1.

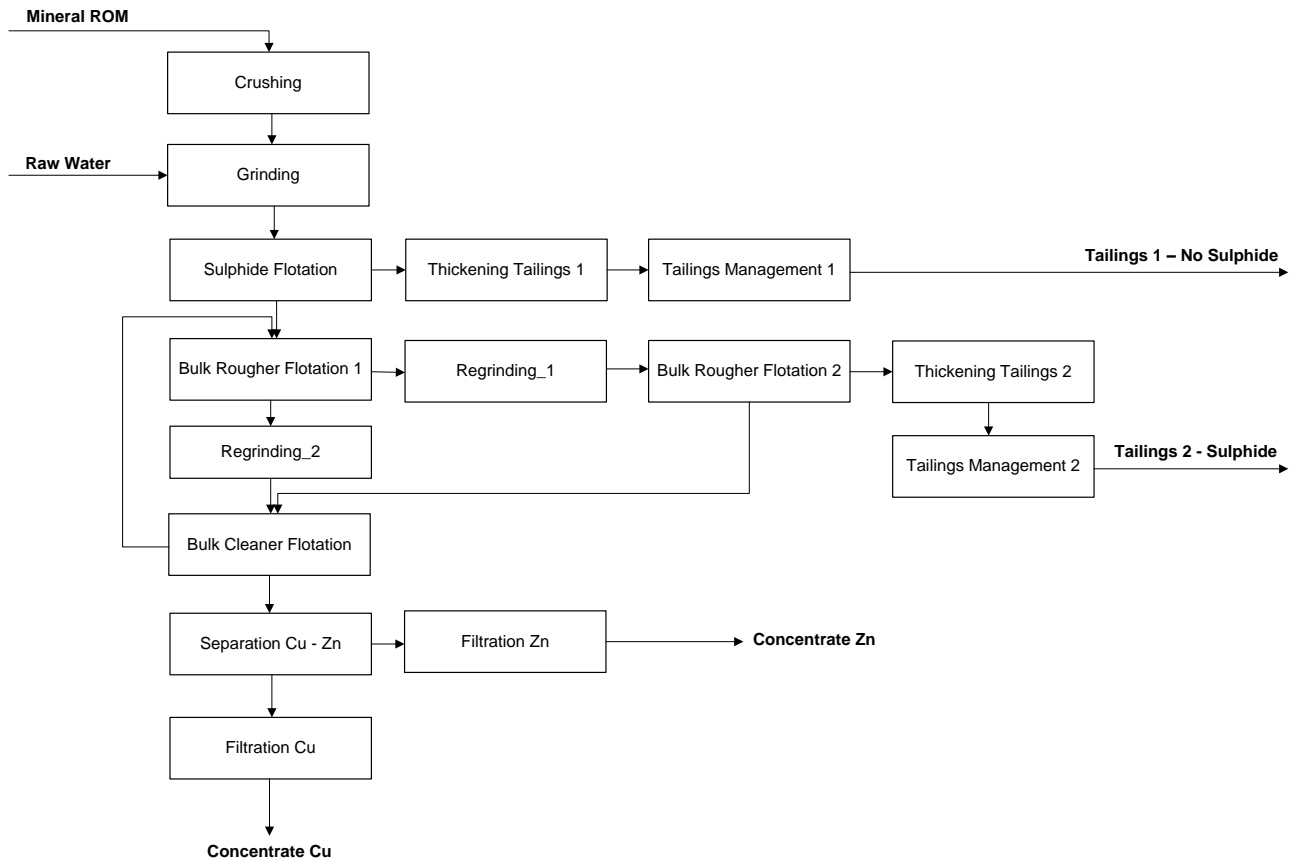


FIGURE 17.1 PROCESS FLOW DIAGRAM

18. PROJECT INFRASTRUCTURE

As part of the PEA (Preliminary Economic Assessment), BISA designed alternative layouts for the surface structures of the El Domo deposit, which included: tailings dams, waste rock dumps, a topsoil deposit, a processing plant platform, a facilities platform, a water supply system, a tailings driving system, an electrical supply system, and alternative road access to the mine.

To evaluate the surface structures at this stage, a production of 2,000 tpd has been considered. BISA conducted a reconnaissance evaluation of the area, taking into account the terrain morphology, the basin and/or stream structure and its topographical features, the existence of borrow materials, surface water runoff, and geological-geotechnical hazards.

GENERAL CHARACTERIZATION OF ALTERNATIVES

DESIGN CRITERIA

Design criteria refers to the preliminary operational data taken into account for the geometry and layout of the tailings dams, waste rock dumps, topsoil deposit, facilities platform, processing plant platform, and accessibility to the mining area.

The most important parameters considered are:

Average tailings production	2,000 tpd
Estimated tailings production	10 Mt
Estimated waste rock	30 Mt
Specific gravity of ore	3.7
Type of tailings	Pulp
Type of dam	Granular and rip rap
Upstream and downstream slope	1.5H:1V – 2.0H:1V
Potentially acidic tailings	Yes
Impermeabilization of tailings dam	Simple textured geomembrane

Overall slope of waste rock dump	2.5H:1V
Drainage and sub-drainage system	Yes
Infiltration-collection pond	Yes
Overall slope of topsoil dump	5.0H:1V
Monitoring pond	Yes
Access roads — driving surface width	6 m
Access roads — maximum gradient	12%
Access roads — turning radius	30 m
Land area for facilities	1.95 ha
Land area for processing plant (includes expansion)	4.0 ha

LOCATION OF ALTERNATIVE SURFACE STRUCTURES

The design comprises seven (7) tailings dams alternatives, five (5) alternative waste rock dumps, two (2) topsoil deposit alternatives, three (3) alternatives for the processing plant, and four (4) facility alternatives (Figure 18.1).

The mineral deposit and the surface structures are mostly in the Las Naves Canton, with the exception of tailings dam alternatives 2A, 2B, and 2C, which are located in the Echeandía Canton.

The locations of the assessed alternatives close to the project site are between 900 and 1,000 masl, whereas alternatives 2A, 2B, and 2C are 350 to 400 masl.

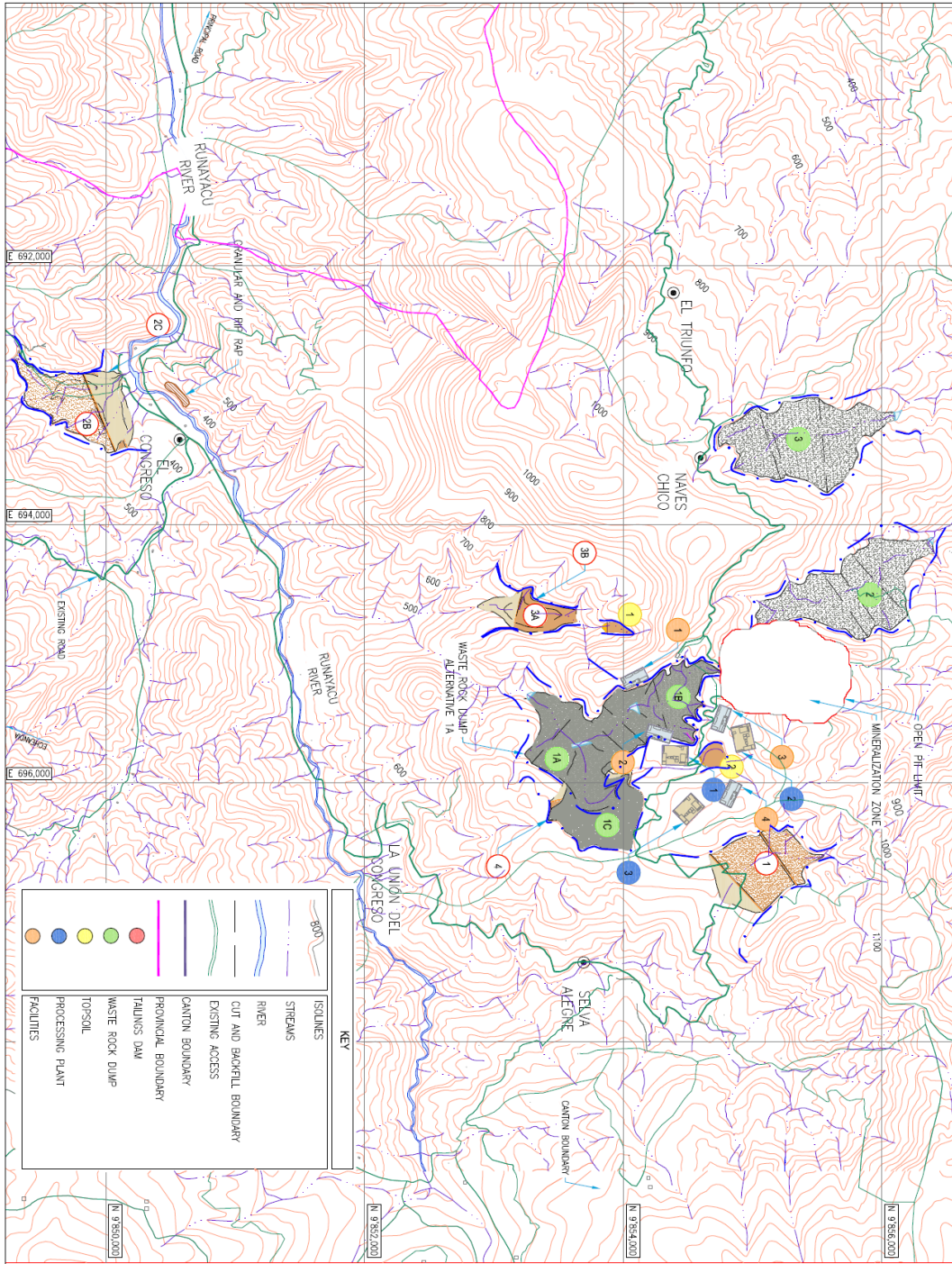


FIGURE 18.1 ALTERNATIVE LOCATIONS OF MAIN STRUCTURES

HYDROLOGICAL EVALUATION

The hydrological study has examined the physiography of the watershed and its hydro-meteorological regime. The analyses were based on pluviometric information provided by the client and distributed by INAMHI-Ecuador (National Institute for Meteorology and Hydrology). This study can be found in the technical report by BISA, Hydrological Study IT-1122MI0001A-000-00-001.

LOCATIONS OF TAILINGS DAM ALTERNATIVES

Seven (7) alternative locations for tailings dams have been considered. For the purposes of this exercise, an operation of 360 days a year and an average tailings production of 2,000 tpd have been considered.

Table 18.1 shows the geometric data and estimated volumes for the alternative tailings dams.

TABLE 18.1 SIZE AND VOLUME OF TAILINGS DAMS ALTERNATIVES

DESCRIPTION	TAILINGS DAMS ALTERNATIVES									
	1		2A	2B	2C		3A	3B		4
	Initial stage	Final stage			Initial stage	Final stage		Initial stage	Final stage	
Maximum height of dam (m)	30	76	49	68	19	52	60	40	62	100
Tailings discharge slope	1%									
Length of dam 01 (m)	171	608	290	642	447		279	208		635
Length of dam 02 (m)	308	500								
Highest point of dam (masl)	925	970	395	403	370	370	700	685	708	925
Dam slope	1.50H:1.0V and 2.0H:1.0V									
Crest width (m)	8.00 m									
Basin excavation in the tailings dam for extracting dam-filling material (Mm ³)	0.32	0.28	0.09	0.55	0.03		0.14	0.06		1.23
Volume of dam 01 (Mm ³)	0.32	3.02	0.47	2.75	0.15		0.71	0.29		6.13
Volume of dam 02 (Mm ³)	0.27	0.99								
Tailings dam 01 area of influence (ha)	6.34	19.12	10.34	28.05	10.00	22.71	8.16	4.44	9.41	24.84
Tailings dam 02 area of influence (ha)	0.79	8.18								
Volume of tailings dam 01 (Mm ³)	0.98	6.46	1.74	6.56	0.34	6.83	1.59	0.59	3.02	8.08
Volume of tailings dam 02 (Mm ³)	0.28	2.03								
Weight of tailings (Mt)	2.03	13.58	2.79	10.50	0.55	10.93	2.55	0.94	4.83	12.93
Lifetime (years)	281	18.66	3.88	14.58	0.76	15.18	3,54	1.30	6.71	17.96
Efficiency ratio (vol. tailings/dam)	2.15	2.12	3.75	2.39			2.24			1.32

Mm³: Million cubic metres, Mt: Million metric tons, ha: hectares, masl: metres above sea level

ALTERNATIVE LOCATIONS FOR WASTE ROCK DUMPS

Five (5) alternative locations for waste rock dumps have been planned, considering a production of 16.67 Mm³. BISA recommends alternative 1A from a technical point of view. Table 18.2 shows the geometric characteristics and the estimated volumes for the alternative waste rock dumps.

TABLE 18.2 VOLUME AND GEOMETRY OF WASTE ROCK DUMPS ALTERNATIVES

DESCRIPTION	WASTE ROCK DUMPS ALTERNATIVES				
	1A	1B	1C	2	3
Highest point of waste rock dump (masl)	920	920	920	850	895
Overall slope	2.5H:1.0V				
Waste rock dump area of influence (ha)	75.44	20.91	36.97	55.73	58.70
Volume of waste rock dump (Mm ³)	33.01	5.35	11.27	24.98	25.29
Containment dyke volume (m ³)	18,800	21,385	35,250	12,925	16,450
Waste rock weight (Mt)	59.42	9.63	20.29	44.96	45.52

Mm³: Million cubic metres, Mt: Million metric tons, ha: hectares, masl: metres above sea level

ALTERNATIVES FOR TOPSOIL DEPOSITS

Two (2) alternative locations have been planned for accumulation of the topsoil generated from the stripping for tailings dams, waste rock dumps, plant platforms, and facilities platforms. Table 18.3 shows the geometric data and estimated volumes for the alternative topsoil deposits.

TABLE 18.3 VOLUME AND GEOMETRY OF TOPSOIL DEPOSIT ALTERNATIVES

DESCRIPTION	TOPSOIL DEPOSIT ALTERNATIVES	
	1	2
Maximum height of deposit (masl)	780	940
Overall slope	1.5H:1.0V	
Volume of dam or containment dyke (Mm ³)	0.022	0.003
Area of influence of topsoil (ha)	0.970	2.800
Volume of topsoil (Mm ³)	0.765	2.036
Weight of topsoil (Mt)	0.918	2.443

ALTERNATIVES FOR THE LOCATION OF FACILITIES

BISA has assessed four (4) alternatives for the location of facilities. In each alternative, considerations include a training room, a general storage area, changing rooms, offices, dining room, kitchen, automotive workshop, electrical workshop, vehicle parking and internal vehicle circulation, as well as additional space to expand the facilities. BISA recommends Alternative 3. Table 18.4 shows the reference areas used to assess each alternative.

TABLE 18.4 PARAMETERS FOR THE ASSESSMENT OF LOCATION OF FACILITIES

Proposed Areas		
Name of Module	Proposed Land Area (m ²)	Proposed Built-Up Area (m ²)
Training Room Module	340.00	340.00
General Storage Module	1600.00	1,020.00
Changing Room Module	500.00	500.00
Office Module	920.00	920.00
Kitchen-Dining Module	1,000.00	1,000.00
Automotive Workshop Module	3,400.00	1,280.00
Electrical Workshop Module	900.00	265.00
Vehicle Parking and Internal Circulation	7,150.00	-----
Area for Expanding Facilities	3,690.00	-----
Total Areas	19,500.00	5,325.00

ALTERNATIVE LOCATIONS FOR TAILINGS DAMS

BISA has considered three (3) alternative processing plant locations. Table 18.5 shows the reference areas used to assess each alternative.

TABLE 18.5 PARAMETERS FOR ASSESSING LOCATION OF THE PROCESSING PLANT

Proposed Areas		
Name of Module	Proposed Land Area (m ²)	Proposed Built-Up Area (m ²)
Coarse Hopper and Primary Crusher	20.00	20.00
Secondary Crusher	260.00	260.00
Fines Hoppers	225.00	225.00
Grinding	460.00	460.00
Flotation	370.00	370.00
Filters	65.00	65.00
Thickeners	320.00	320.00
Sample Preparation and Metallurgical Laboratory	480.00	480.00
Chemical Analysis Laboratory	120.00	120.00
Reagent Store	80.00	80.00
Fuel Station	330.00	330.00
Mechanical workshop	120.00	120.00
Electrical Workshop	80.00	80.00
Plant Warehouse	80.00	80.00
Plant Offices	80.00	80.00
Truck Scales 1	120.00	120.00
Truck Scales 2	120.00	120.00
Substation and Main Electrical Room	750.00	750.00
Mine Ore Area	1,800.00	-----
Concentrate Yard	2,400.00	-----
Vehicle Parking and Internal Circulation	4,350.00	-----
Processing Plant Expansion Area to 2000 TPD	17,370.00	-----
Total Areas	30,000.00	4,080.00

ELECTRICAL POWER SUPPLY

A 33 kV overhead power line has been considered for supplying power to the new processing plant and its respective facilities, with a starting point at the Echeandía Electrical Substation (Table 18.6 shows the estimated power demand.)

TABLE 18.6 ESTIMATED ELECTRICAL POWER PEAK DEMAND

Description	Estimated Load (kW)
Processing Plant at 2,000 tpd and its facilities	3000
Pumping stations	500
Pithead	2000
Total	5500

This power demand has been estimated on the basis of rates recorded in similar projects and historical data from similar processing plants.

WATER SUPPLY

The capacity of the water supply is based on the daily production of the processing plant, which will be 2,000 tpd. Thus, the estimated unit consumption taking into account water recycling is 1.2 m³/t, which is equivalent to a water consumption of 2,400 m³/day (100 m³/h). The alternative solutions were developed taking into account this consumption figure.

The proposed system uses the Runayacu River as a water source. From the uptake point, the water is stored and then re-pumped to the water tank platform at 1,030 masl, from whence it supplies the processing plant and facilities with water.

COMPONENTS SYSTEM

The planned system comprises the following components and structures: uptake, sand trap, storage reservoir, HDPE pressure pipes, re-pumping stations, and a tank area (comprising a drinking water treatment plant (DWTP), drinking water storage tank, and a freshwater storage tank).

SOLID WASTE LANDFILL

Two location alternatives are planned for the domestic solid waste landfill. The final site will depend on the definitive location of the processing plant and facilities as well as on the results of pertinent studies required for the landfill engineering works.

Domestic Wastewater Treatment Plant (WWTP)

The domestic wastewater treatment plant (WWTP) has three alternative locations, with the final sitting depending on the site of the facilities building and the processing plant.

ROAD ACCESS

Sections evaluated for road access to the mine are shown in Table 18.7 and Figure 18.2.

TABLE 18.7 PARAMETERS FOR EVALUATING ACCESS ALTERNATIVES

Alternative	Length (km)	Road Type	Width of Roadway (m)
Las Naves - Naves Chico	11.00	Paved	6.0
Naves Chico - Mine	2.76	Gravel	6.0
Mine - El Congreso	13.80	Gravel	6.0
El Congreso - Echeandía	12.00	Gravel	6.0
El Congreso - Main Roadway	13.60	Gravel	6.0
Echeandía - Main Roadway	12.21	Gravel	6.0

* The roads are planned with an extra 1.0 m for the drainage ditch.

Sections evaluated for roadway access to the mine (mineralized zone) are shown in Figure 18.2, indicating the length, width, and road type.

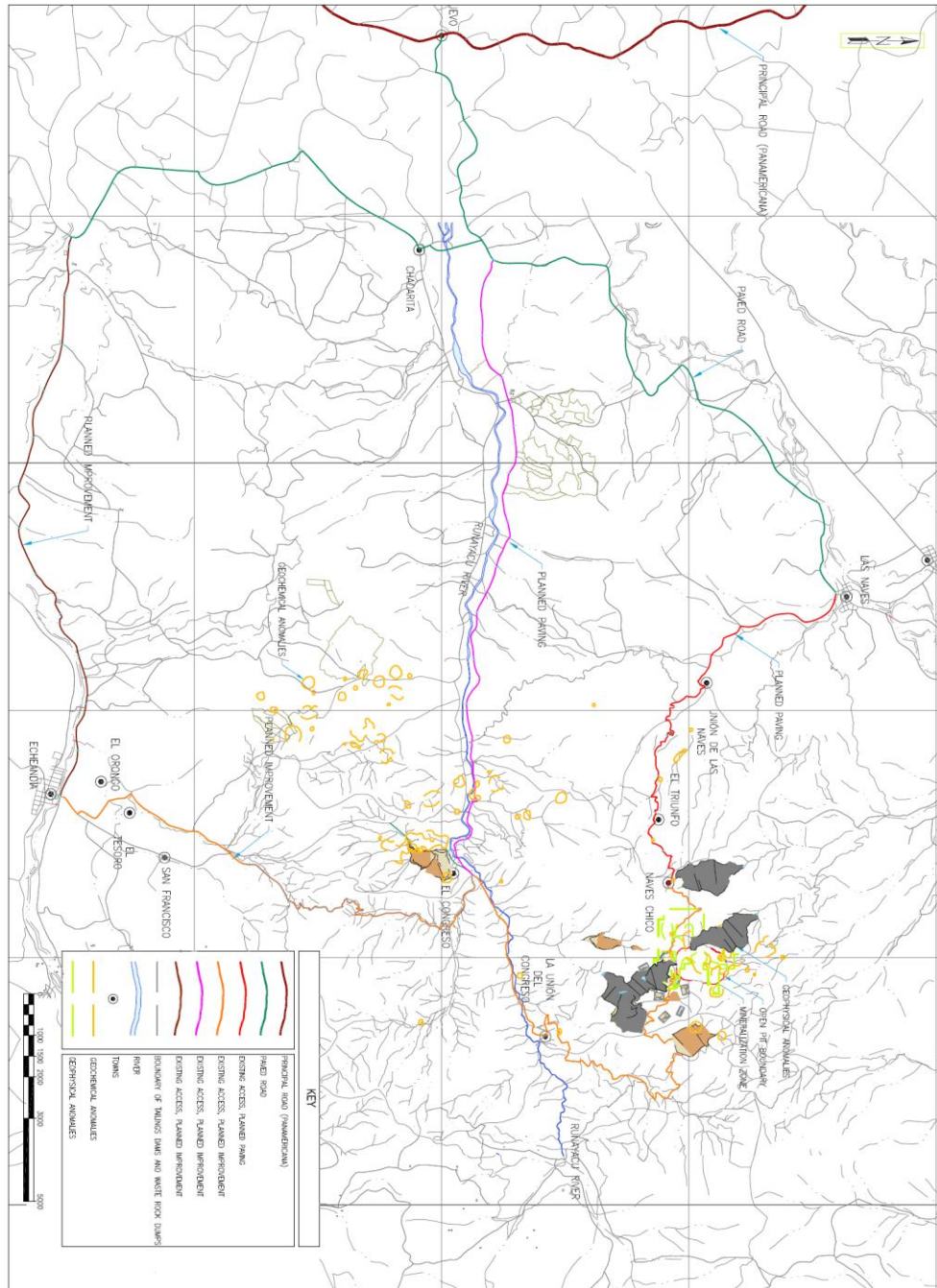


FIGURE 18.2 PROJECT ACCESS ROADS

ASSUMPTIONS

BISA has worked with the topography generated from Salazar's photographic mosaic, which is assumed to have a good approximation for this level of conceptual study. The topography is superimposed with the map used for the mineral resource estimate. BISA recommends a topographic survey of the entire project area, particularly of spots slated for infrastructure.

19. MARKET STUDIES AND CONTRACTS

This section is not applicable.

20. ENVIRONMENTAL STUDIES, PERMITTING, AND SOCIAL OR COMMUNITY IMPACT

This section is not applicable

21. CAPITAL AND OPERATING COSTS

ESTIMATE OF OPERATING AND CAPITAL EXPENDITURES

BISA has developed a conceptual estimate of the costs associated with the project development and operation. First, the costs for the open pit are analysed and then the same items are presented for the underground mining.

CONTINGENCIES

BISA has considered a 25% contingency for capital costs and a 20% contingency for operating costs, in accordance with industry standards.

OPEN PIT OPERATION

OPEN PIT PRE-PRODUCTION AND SUSTAINING CAPITAL COSTS (CAPEX)

The pre-production capital investment and sustaining capital costs (CAPEX) are differentiated by the start time of mining operations, and the beginning of ore delivery to the processing plant (Table 21.1).

TABLE 21.1 PRE-PRODUCTION INVESTMENT AND SUSTAINING CAPITAL EXPENDITURES

CAPEX	No Contingency			25% Contingency		
	Pre-production	Sustaining	Total	Pre-production	Sustaining	Total
Mine	15,611,109	443,292	16,054,401	19,513,886	554,115	20,068,001
Processing plant	35,112,000	0	35,112,000	43,890,000	0	43,890,000
Infrastructure	30,504,633	70,615,720	101,120,353	38,130,792	88,269,650	126,400,442
Others	7,000,000	13,600,000	20,600,000	8,750,000	17,000,000	25,750,000
Total (US\$)	88,227,742	84,659,012	172,886,754	110,284,678	105,823,765	216,108,443

OPEN PIT OPERATING COSTS

Operating costs (OPEX) during the first nine years of the life of mine amount to about US\$303.8 million for an estimated production rate of 2,000 tpd.

Operating costs include the mining costs for contractors, supervision, maintenance, consumables, general expenses, and processing costs. The mine operating costs were estimated based on cost rating on similar projects. The cost summary can be seen in Table 21.2 and in Figure 21.1.

TABLE 21.2 OPEN PIT OPERATING COSTS (2,000 TPD)

Operating Costs	No Contingency	25% Contingency
Mine	151,753,347	182,104,016
Processing	77,662,856	93,195,428
Administration	12,943,809	15,532,571
Others	10,853,389	13,024,067
Total (US\$)	253,213,401	303,856,082

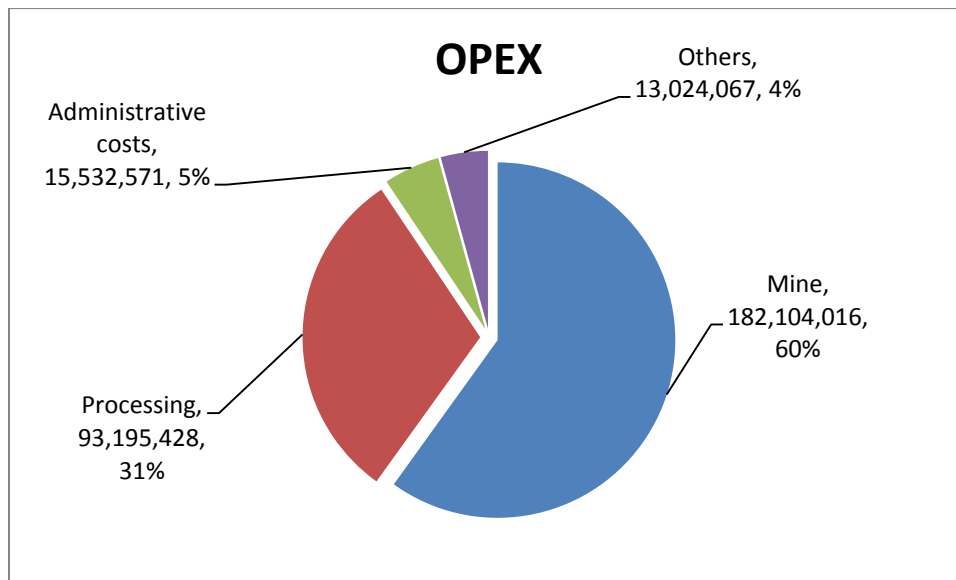


FIGURE 21.1 OPEN PIT — DISTRIBUTION OF OPERATING COSTS

UNDERGROUND OPERATION

UNDERGROUND PRE-PRODUCTION AND SUSTAINING CAPITAL COSTS

The estimated capital costs (CAPEX) take into account the likely scenario of underground production (1,000 tpd) in which the mineral will be processed at the existing plant used for the surface mining production. Therefore, a plant investment has not been considered for the capital cost estimate for underground mining.

The pre-production capital investment and sustaining capital costs are differentiated by the start time of mining operations, and the beginning of ore delivery to the processing plant (Table 21.3).

TABLE 21.3 UNDERGROUND PRE-PRODUCTION INVESTMENT AND SUSTAINING CAPITAL COSTS

CAPEX	No Contingency			25% Contingency		
	Pre-production	Sustaining	Total	Pre-production	Sustaining	Total
Mine	9,466,167	2,401,480	11,867,647	11,832,708	3,001,850	14,834,558
Others	3,200,000	450,000	3,650,000	4,000,000	562,500	4,562,500
Total (US\$)	12,666,167	2,851,480	15,517,647	15,832,708	3,564,350	19,397,058

UNDERGROUND OPERATING COSTS

Operating costs (OPEX) during the first five years of the life of the underground mine amount to about US\$49.7 million for an estimated production rate of 1,000 tpd.

Operating costs include the mining costs for contractors, supervision, maintenance, consumables, general expenses, and processing costs. The mine operating costs were estimated based on cost rating on similar projects. The cost summary can be seen in Table 21.4 and in Figure 21.2.

TABLE 21.4 UNDERGROUND OPERATING COSTS (1,000 TPD)

Operating Costs	No Contingency	25% Contingency
Mine	55,902,884	67,083,461
Processing	21,890,054	26,268,065
Administration	3,648,342	4,378,011
Total (US\$)	81,441,280	97,729,537

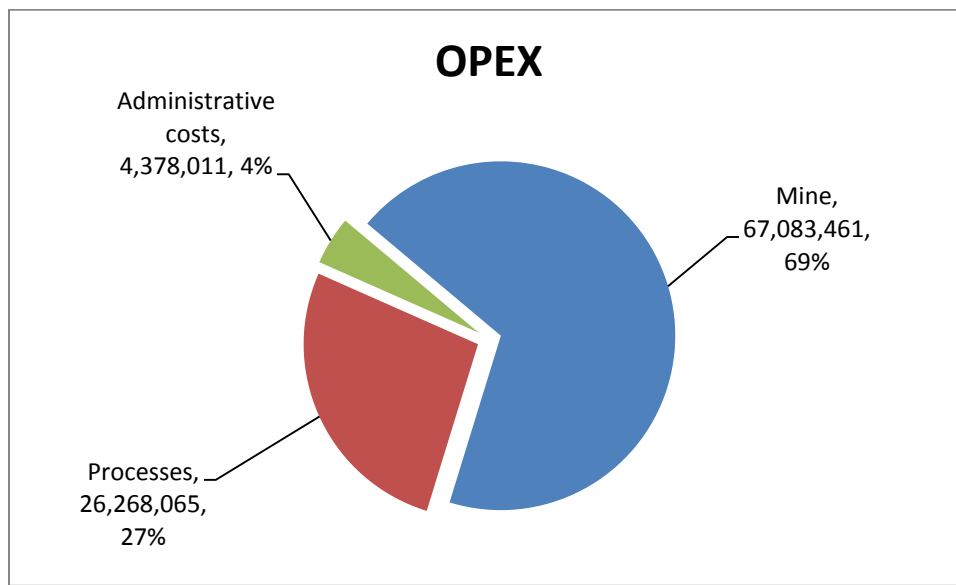


FIGURE 21.2 UNDERGROUND — DISTRIBUTION OF OPERATING COSTS

22. ECONOMIC ANALYSIS

BISA has developed a financial assessment for the El Domo deposit within the Curipamba Project. In this assessment, values of one percent grade for copper, zinc, and lead, of one gram grade for gold, and of one ounce for silver used for NSR calculation were obtained from the final calculated metallurgical recovery factors (Table 22.1).

TABLE 22.1 METAL UNIT VALUES USED FOR NSR CALCULATION

		Mineral Type			
Cu/(Zn+Pb)<0.33		0.33<Cu/(Zb+Pb)<3.0		Cu/(zn+pb)>3.0	
Pb US\$/1%	8.0	Pb US\$/1%	-	Pb US\$/1%	-
Zn US\$/1%	7.5	Zn US\$/1%	4.0	Zn US\$/1%	-
Cu US\$/1%	21.1	Cu US\$/1%	33.7	Cu US\$/1%	48.9
Ag US\$/1 oz	9.9	Ag US\$/1 oz	9.3	Ag US\$/1 oz	3.6
Au US\$/1 g	13.4	Au US\$/1 g	14.8	Au US\$/1 g	5.9

REVENUE ASSUMPTIONS

The revenue assumptions are based on the following metal prices provided by Salazar:

- Copper – 3.06 US\$/lb
- Zinc – 0.86 US\$/lb
- Lead – 0.95 US\$/lb
- Gold – 1,200 US\$/oz
- Silver – 20 US\$/oz

Estimated charges for smelting treatment and charges for refining of the copper, zinc, and lead concentrate are shown in Table 22.2, Table 22.3, and Table 22.4.

TABLE 22.2 SMELTING TREATMENT AND CHARGES FOR REFINING COPPER

Cu Concentrate			
Payables			
Minimum Cu deduction			1%
Payable Cu			96.5%
Minimum Ag deduction	g/t		30
Payable Ag			95%
Minimum Au deduction	oz/t		1.5
Payable Au			95%
Treatment cost (CIF Korea/Japan)			
Base	US\$/t		90
Price scaler	US\$/t		4750
			0%
Refining cost			
Cu	US\$/t		9.00
Ag	US\$/t		1.00
Au	US\$/t		10.00
Penalties			
Limit of free As + Sb			0.5%
AS+Sb penalty (for each % exceeding the limit)	US\$/t		25
Limit of free Bi			0.10%
Bi penalty (for each % exceeding the limit)	US\$/t		150
Pb+Zn limit			4%
PB+Zn penalty (for each % exceeding the limit)	US\$/t		2
Losses			0.20%
Fleet			
Inside mine - Port	US\$/t		30
Terminal handling tariff	US\$/t		15
Shipping fleet	US\$/t		53

TABLE 22.3 SMELTING TREATMENT AND CHARGES FOR REFINING ZINC

Zn Concentrate			
Payables			
	Minimum deduction Zn		8%
	Payable Zn		85%
	Minimum deduction Ag	oz/t	3
	Payable Ag		70%
	Minimum deduction Au	oz/t	1.25
	Payable Au		70%
Treatment cost (CIF Korea/Japan)			
	Base	US\$/t	200
	Price scaler	US\$/t	1950
			15%
Penalties			
	Limit of free Fe		9%
	Fe penalty (for each % it exceeds the limit)	US\$/t	1.5
	Limit of free Cd		0.40%
	Cd penalty (for each % it exceeds the limit)	US\$/t	15
	Losses		0.20%
Fleet			
	Interior mine - Port	US\$/t	30
	Terminal handling tariff	US\$/t	15
	Shipping fleet	US\$/t	53

TABLE 22.4 SMELTING TREATMENT AND CHARGES FOR REFINING LEAD

Pb Concentrate			
Payables			
Minimum Pb deduction			3%
Payable Pb			95.0%
Minimum Ag deduction	gr/t		1
Payable Ag			95%
Minimum Au deduction	oz/t		1.5
Payable Au			95%
Treatment costs (CIF Korea/Japan)			
		US\$/t	250
Base		US\$/t	2000
Price scaler			15%
Refining costs			
Ag		US\$/t	1.00
Au		US\$/t	10.00
Penalties			
Free As limit			0.8%
As penalty (for each % exceeding the limit)	US\$/t		12.5
Free Sb limit			0.80%
Sb penalty (for each % exceeding the limit)	US\$/t		13
Losses			0.20%
Flete			
Inside mine - Port		US\$/t	30
Terminal loading tariff		US\$/t	15
Shipping fleet		US\$/t	53

DEPRECIATION

The depreciation rates for CAPEX items have been considered in the following ranges according to the Ecuadorian regulations:

- Any mobile equipment will be depreciated at a rate of 20% per year
- All fixed equipment, including conveyor belts, electrical and automated equipment, as well as capitalized costs for the prior extraction of waste rock, and for owner's costs (additional studies) during the pre-production phase are depreciated at a rate of 10% per year.

All equipment installation, including civil and structural architecture and installation of the work, including piping, will depreciate at a rate of 5% per year.

In cases of obsolescence, intensive utilization, accelerated deterioration, or other duly justified reasons, the Director General of Revenue (Ecuadorian authority) may authorize depreciations using annual percentages higher than those specified, which shall be set in the resolution enacted for that purpose.

Clearly, with the given regime, several individual CAPEX items have not been appropriately handled in terms of their exact depreciation rate. However, the overall estimate of depreciation amounts over the long term has a narrow margin for the purposes of this study. A more detailed account of appropriate depreciation rates for the different CAPEX items shall require consultation with the Ecuadorian authorities (in this case the Director General of Revenue).

TAXES AND OTHER EXPENSES

Ecuadorian law provides for the application of royalties to net revenue, which will be 4% in this case, which is in the range for medium-scale mining production. In addition, value added tax (VAT/IVA: *Impuesto al valor agregado* in Spanish) must also be applied, which is on the order of 12% of gross revenue less royalties. These earnings are subject to income tax, which is 22%. Additionally, there is a profit-sharing scheme involving workers and the state, which in the case of medium-scale mining is 5% and 10% respectively.

DISCOUNT RATE

The discount factor assumed by BISA was 10%, which was considered with a fair value basis to reflect current interest rates and discount rates used in other mining projects in Latin America.

FINANCING SCHEME

BISA has not assumed any financing scheme or financing costs at this evaluation stage.

PARAMETERS OF FINANCIAL ANALYSIS

Operating costs will reach US\$401 million over 14 years of production. All expenses prior to the start of production will be capitalized. These expenses will generate an accumulated depreciation of US\$235 million.

The project will be subject to payment of taxes from the first year of production forward. It is also assumed that the company royalties must be paid from the first year of production forward.

The utilities participation scheme of workers and the Ecuadorian state is considered an extraordinary expense element, which is paid only when the Earnings Before Interests and Taxes (EBIT) is positive. This participation scheme will reach a maximum of US\$13.7 million during the second year of operation. Therefore, this issue has an important impact on the project's financial performance.

PROFIT AND LOSSES STATEMENT

The profit and losses statement for the project includes one year of pre-production for the open pit and 14 years of production, of which nine years will be open pit production, following by five years of underground mine production.

Annual revenues range from US\$31M in year 10 to US\$ 179 M in year 1 (Figure 22.1 and Figure 22.2).

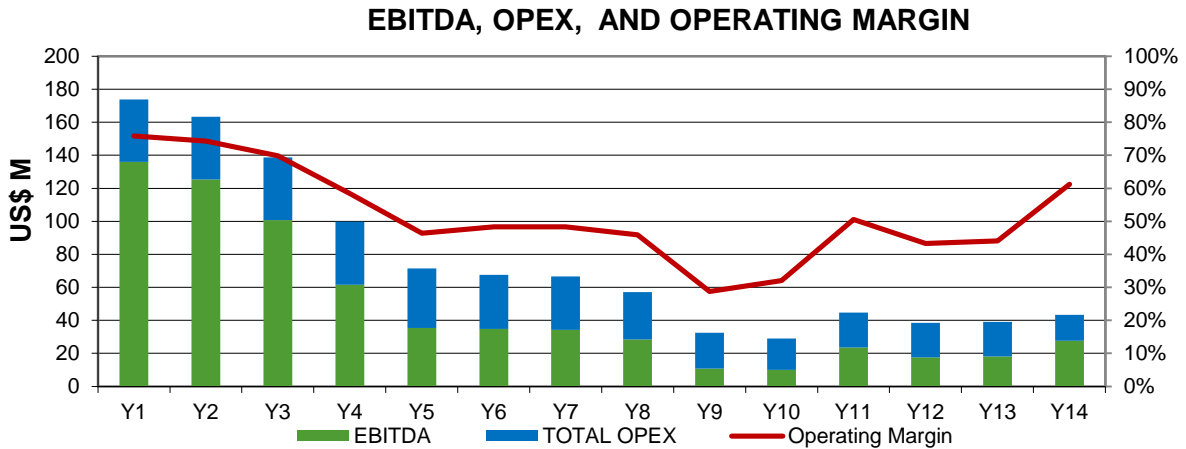


FIGURE 22.1 LIFE OF THE PROJECT EBITDA, OPEX, AND OPERATING MARGIN

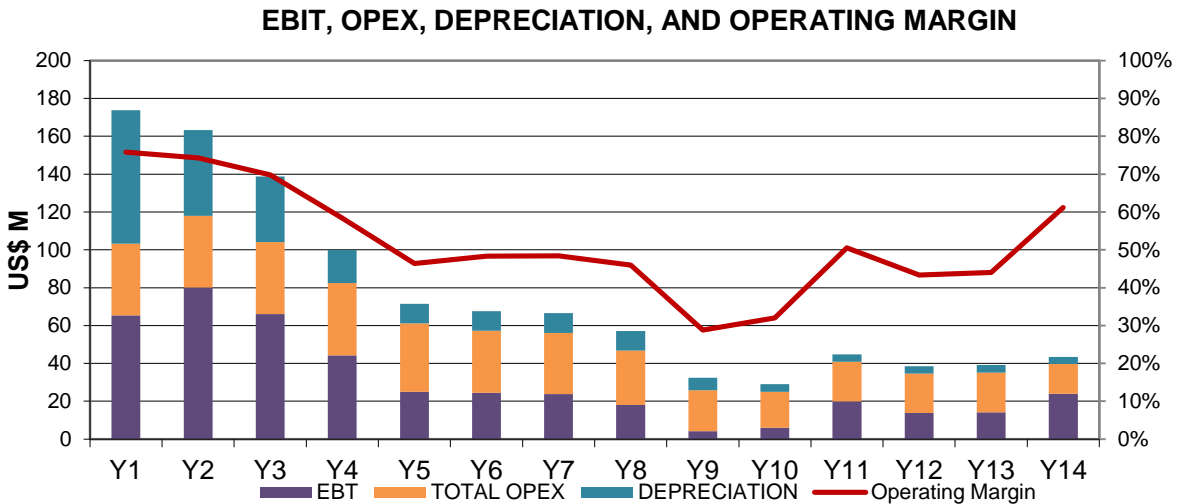


FIGURE 22.2 LIFE OF THE PROJECT OPEX, DEPRECIATION, AND PRE-TAX PROFITS

CASH FLOW AND FINANCIAL INDICATORS

The cash flow analysis considers scenarios before and after taxation (including the calculation of taxes on dividends). The financial indicators used in the analysis include Net Present Value (NPV), Internal Rate of Return (IRR), and the Payback Period (PP) (Figure 22.3).

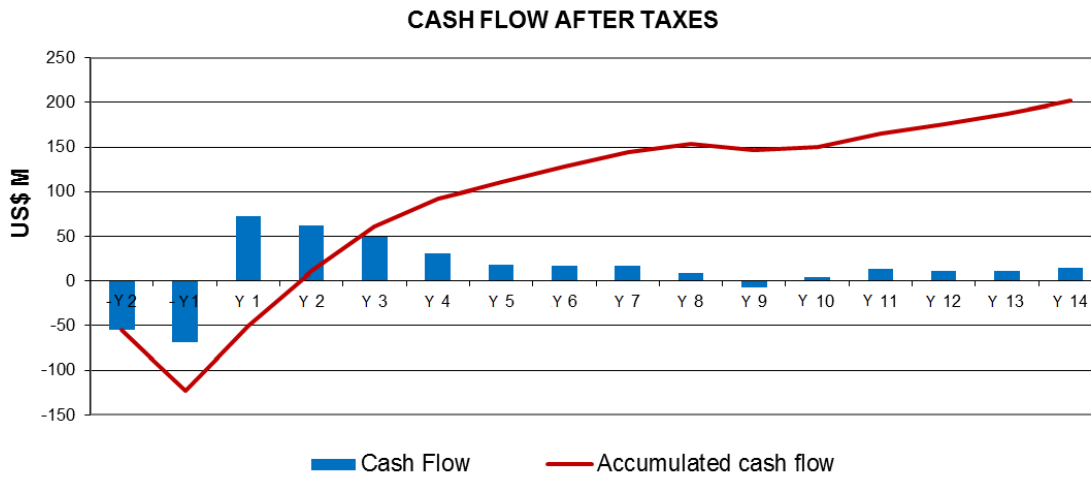


FIGURE 22.3 CASH FLOW AFTER TAXES

- Total Cash Flow: US\$202.6 million
- Net Present Value (10% Discount Rate): US\$86.72 million
- Internal Rate of Return: 30%
- Payback Period: 2 years

TABLE 22.5 PROFIT AND LOSSES STATEMENT

Calculation of Costs of Conceptual Study – Economic Assessment																					
	ARO	-Y2	-Y1	Y1	Y2	Y3	Y4	Y5	Y6	Y7	Y8	Y9	Y10	Y11	Y12	Y13	Y14	Initial	Producción	Total	
CASH FLOW																					
SUPERFICIAL NSR																					
Copper Ore	US\$			38,947,991	35,571,812	29,192,293	20,113,398	15,733,329	15,733,329	14,636,786	13,022,452	980,025							183,931,414	183,931,414	
Complex Ore	US\$			93,421,747	85,558,674	74,736,013	66,097,503	41,782,280	39,350,446	27,018,901	15,385,983								482,701,992	482,701,992	
Zinc Ore	US\$			46,875,071	47,577,431	40,281,821	19,101,471	13,245,095	13,245,095	12,955,393	16,027,800	5,274,086							214,583,263	214,583,263	
Stock Ore	US\$			0	0	0	0	5,412,880	3,759,374	3,933,913	5,624,474	15,577,275							34,307,916	34,307,916	
UNDERGROUND NSR																					
Stopping Production	US\$												30,192,997	45,997,691	39,262,573	39,992,929	44,702,961		200,149,151	200,149,151	
Production of Progress	US\$												1,084,153	819,881	1,392,503	1,230,818	377,300		4,904,654	4,904,654	
TOTAL NSR	US\$			179,244,810	168,707,917	144,210,127	105,312,371	76,173,584	72,088,244	70,876,538	61,693,627	37,217,369	31,277,149	46,817,572	40,655,076	41,223,746	45,080,261		1,120,578,390	1,120,578,390	
SUPERFICIAL OPEX																					
Open Pit Mining	US\$			24,030,680	24,073,200	24,194,295	24,470,601	22,347,848	19,188,572	18,624,544	15,345,958	9,828,318							182,104,016	182,104,016	
Open Pit Processing	US\$			10,473,750	10,473,750	10,473,750	10,473,750	10,473,750	10,473,750	10,473,750	10,473,750	9,405,428							93,195,428	93,195,428	
GG&AA Open Pit	US\$			1,745,625	1,745,625	1,745,625	1,745,625	1,745,625	1,745,625	1,745,625	1,745,625	1,567,571							15,532,571	15,532,571	
Other Costs	US\$			1,612,247	1,614,019	1,619,064	1,630,577	1,542,129	1,410,493	1,386,991	1,250,384	958,163							13,024,067	13,024,067	
UNDERGROUND OPEX																					
Underground Mining	US\$												14,273,823	14,149,997	14,061,421	14,082,917	10,515,303		67,083,461	67,083,461	
Underground Processing	US\$												4,071,037	5,880,521	5,879,637	5,891,134	4,545,736		26,268,065	26,268,065	
GG&AA Underground	US\$												678,506	980,087	979,939	981,856	757,623		4,378,011	4,378,011	
TOTAL OPEX	US\$			37,862,302	37,906,594	38,032,734	38,320,553	36,109,352	32,818,439	32,230,911	28,815,716	21,759,480	19,023,419	21,010,641	20,921,033	20,955,942	15,818,696		401,585,619	401,585,619	
IVA																					
Value Added Tax (VAT) Surface	US\$	5,910,246	7,323,916	5,428,772	5,442,564	5,464,070	5,472,764	4,740,411	4,433,880	4,358,540	4,040,222	2,711,483						13,234,161	42,092,705	55,326,866	
Value Added Tax (VAT) Underground	US\$												504,313	2,035,209	2,233,994	2,142,127	2,126,804	2,120,793	1,664,519	12,827,758	
Value Added Tax (VAT)	US\$	5,910,246	7,323,916	5,428,772	5,442,564	5,464,070	5,472,764	4,740,411	4,433,880	4,358,540	4,544,535	4,746,693	2,233,994	2,142,127	2,126,804	2,120,793	1,664,519		54,920,463	68,154,624	
EBITDA																					
EBITDA	US\$	-5,910,246	-7,323,916	135,953,736	125,358,759	100,713,323	61,519,054	35,323,821	34,835,924	34,287,087	28,333,376	10,711,196	10,019,737	23,664,803	17,607,240	18,147,012	27,597,046	-13,234,161	664,072,114	650,837,952	
PROFIT BEFORE DEPRECIATION																					
DEPRECIATION SURFACE	US\$			38,139,851	26,913,482	26,929,382	26,960,944	22,531,561	18,719,559	18,772,162	18,756,262	18,385,238							216,108,442	216,108,442	
DEPRECIATION UNDERGROUND	US\$												4,007,064	3,829,223	3,888,848	3,951,785	3,720,139		19,397,058	19,397,058	
DEPRECIATION	US\$			38,139,851	26,913,482	26,929,382	26,960,944	22,531,561	18,719,559	18,772,162	18,756,262	18,385,238	4,007,064	3,829,223	3,888,848	3,951,785	3,720,139		235,505,501	235,505,501	
EBIT																					
EBIT	US\$	-5,910,246	-7,323,916	97,813,885	98,445,276	73,783,940	34,558,110	12,792,260	16,116,365	15,514,925	9,577,114	-7,674,042	6,012,673	19,835,581	13,718,392	14,195,227	23,876,907	-13,234,161	428,566,613	415,332,451	
OTHER COSTS																					
Royalties Surface	US\$	0	0	7,169,792	6,748,317	5,768,405	4,212,495	3,046,943	2,883,530	2,835,062	2,467,745	1,488,695							36,620,983	36,620,983	
Royalties Underground	US\$												1,251,086	1,872,703	1,626,203	1,648,950	1,803,210		8,202,152	8,202,152	
Royalties	US\$	0	0	7,169,792	6,748,317	5,768,405	4,212,495	3,046,943	2,883,530	2,835,062	2,467,745	1,488,695	1,251,086	1,872,703	1,626,203	1,648,950	1,803,210		44,823,136	44,823,136	
EBT																					
EBT	US\$	-5,910,246	-7,323,916	90,644,093	91,696,959	68,015,535	30,345,616	9,745,316	13,232,835	12,679,864	7,109,369	-9,162,737	4,761,587	17,962,878	12,092,189	12,546,277	22,073,697	-13,234,161	314,306,850	301,072,689	
PROFIT SHARING																					
State	US\$	0	0	9,289,192	11,003,635	8,161,864	3,641,474	1,169,438	1,587,940	1,521,584	853,124	0	476,159	1,796,288	1,209,219	1,254,628	2,207,370		44,171,914	44,171,914	
Employees	US\$	0	0	2,322,298	2,750,909	2,040,466	910,368	292,359	396,985	380,396	213,281	0	238,079	898,144	604,609	627,314	1,103,685		12,778,894	12,778,894	
TOTAL PROFITS	US\$			11,611,490	13,754,544	10,202,330	4,551,842	1,461,797	1,984,925	1,901,980	1,066,405	0	714,238	2,694,432	1,813,828	1,881,942	3,311,055		56,950,808	56,950,808	
TAXES																					
Revenue Tax	US\$	0	0	17,387,173	17,147,331	12,718,905	5,674,630	1,822,374	2,474,540	2,371,135	1,329,452	0	890,417	3,359,058	2,261,239	2,346,154	4,127,781		73,910,189	73,910,189	
PROFIT AFTER TAXES	US\$	0	0	17,387,173	17,147,331	12,718,905	5,674,630	1,822,374	2,474,540	2,371,135	1,329,452	0	890,417	3,359,058	2,261,239	2,346,154	4,127,781		73,910,189	73,910,189	
NET EARNINGS AFTER TAXES																					
Net Earnings After Sharing and Taxes	US\$	-5,910,246	-7,323,916	61,645,430	60,795,084	45,094,300	20,119,143	6,461,145	8,773,370	8,406,750	4,713,511	-9,162,737	3,156,932	11,909,388	8,017,121	8,318,181	14,634,861	-13,234,161	252,882,480	239,648,318	
SOVEREIGN TAX																					
Sovereign Tax	US\$			12,194,455	11,237,988	7,262,603	950,095	0	0	0	0	0	0	1,580,402	549,234	630,716	2,660,368		37,065,860	37,065,860	
Net Earnings After Total Taxes	US\$	-5,910,246	-7,323,916	49,450,976	49,557,096	37,831,697	19,169,048	6,461,145	8,773,370	8,406,750	4,713,511	-9,162,737	3,156,932	10,328,986	7,467,887	7,687,466	11,974,493	-13,234,161	215,816,620	202,582,458	
OPERATING CASH FLOW																					
Operating Cash Flow	US\$	-5,910,246	-7,323,916	87,590,827	76,470,579	64,761,079	46,129,992	28,992,706	27,492,929	27,178,912	23,469,773	9,222,501	7,163,996	14,158,209	11,356,735	11,639,251	15,694,632	-13,234,161	451,322,120	438,087,959	
CAPEX SURFACE																					
Mining	US\$	354,500	19,159,386		79,500	157,808		79,500	157,808		79,500								19,513,886	554,115	20,068,001
Processing	US\$	21,945,000	21,945,000																43,890,000	0	43,890,000
Infrastructure	US\$	18,202,547	19,928,245	13,240,447	13,240,447	13,240,447	13,240,447	8,826,965	8,826,965	8,826,965	8,826,965							38,130,792	88,269,650	126,400,442	
Others	US\$	8,750,000		1,500,000	1,500,000	1,500,000	1,500,000	1,500,000	1,500,000	1,500,000	1,500,000	5,000,000							17,000,000	8,750,000	25,750,000
CAPEX UNDERGROUND																					
Mining	US\$											202,609	11,630,099	2,650,725	178,875	125,875	46,375		14,834,558	14,834,558	
Processing	US\$																		0	0	
Infrastructure	US\$																		0	0	
Others	US\$												4,000,000						562,500	4,562,500	
TOTAL OPEX	US\$	49,252,047	61,032,631	14,740,447	14,819,947	14,898,255	14,740,447	10,406,465	10,484,772	10,326,965	14,609,074	16,630,099	2,650,725	178,875	125,875	46,375	562,500		110,284,677	125,220,823	235,505,501
Cash Flow after CAPEX																					
Cash Flow	US\$	-55,162,292	-68,356,546	72,850,379	61,650,631	49,862,824	31,389,544	18,586,241													

SENSITIVITY ANALYSIS

The sensitivity analysis was performed to estimate the variability of the project economics by changing certain key parameters.

Figure 22.4 shows the sensitivity of NPV to changes in revenue (metal prices). It is clear in the figure that fluctuations in metal prices are the most critical factor in NPV and IRR.

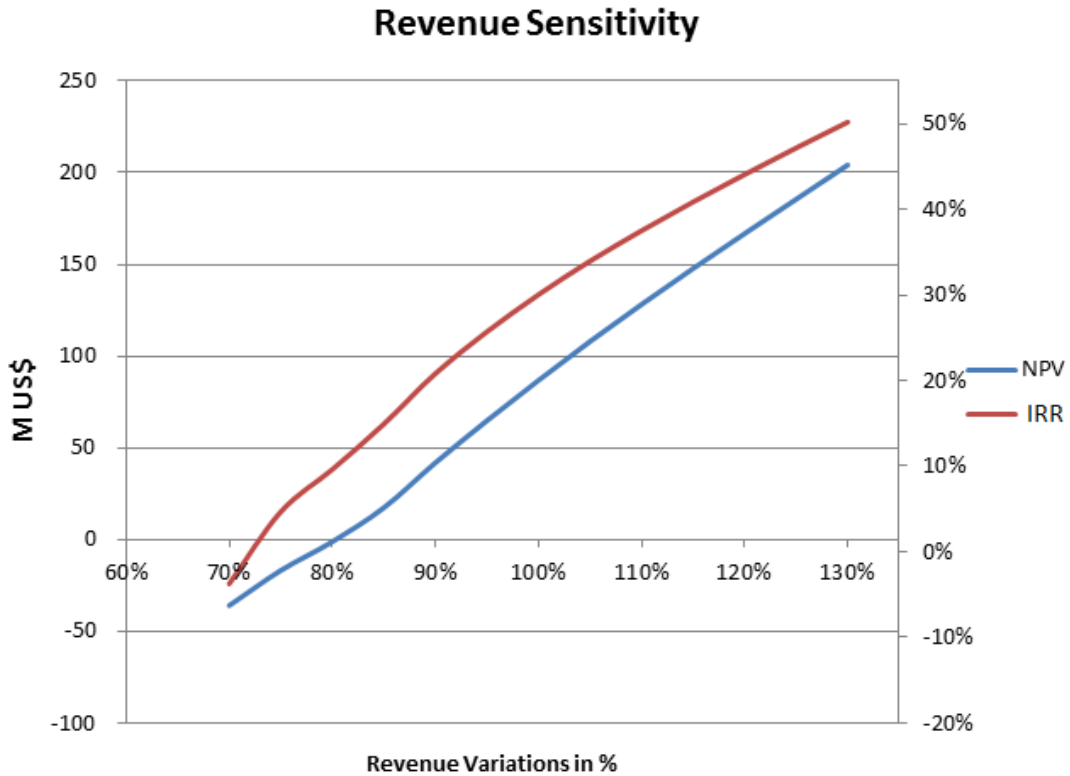


FIGURE 22.4 PROJECT SENSITIVITY TO METAL PRICES

Figure 22.5 shows the sensitivity of the project economics to three important parameters: revenue, operating costs (OPEX), and pre-tax capital costs (CAPEX). These figures show again that the project is most sensitive to metal prices.

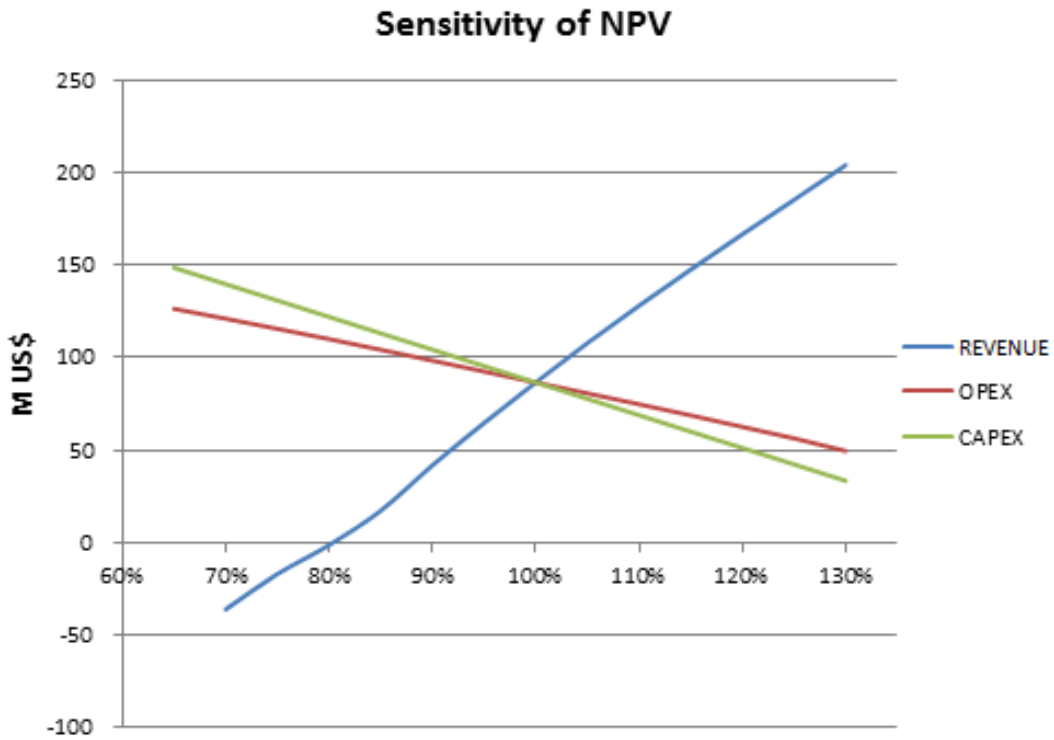


FIGURE 22.5 SENSITIVITY OF NPV TO REVENUE, OPEX AND CAPEX

Table 22.6 details project sensitivity of NPV, CF, and IRR to variations in OPEX and CAPEX

TABLE 22.6 RANGE OF SENSITIVITY OF ECONOMIC PARAMETERS

	Sensitivity of NPV (US\$)		Sensitivity of CF (US\$)		Sensitivity of IRR (%)	
	OPEX	CAPEX	OPEX	CAPEX	OPEX	CAPEX
65%	127	149	280	285	36%	54%
70%	121	140	270	273	35%	50%
75%	116	131	259	261	35%	46%
80%	110	122	248	250	34%	42%
85%	104	113	237	238	33%	39%
90%	99	104	226	226	32%	36%
95%	93	96	214	214	31%	33%
100%	87	87	203	203	30%	30%
105%	81	78	191	191	29%	27%
110%	75	69	180	179	28%	25%
115%	69	60	168	167	27%	23%
120%	63	51	156	155	26%	21%
125%	56	42	143	144	25%	19%
130%	50	34	130	132	23%	17%

23. ADJACENT PROPERTIES

This section is not applicable

24. OTHER RELEVANT DATA AND INFORMATION

This section is not applicable

25. INTERPRETATION AND CONCLUSIONS

BISA offers the following conclusions and recommendations:

- The El Domo deposit is the largest known Au-rich, Cu-Zn-Ag-Pb volcanogenic massive sulphide (VMS) deposit emplaced within the Macuchi Terrane, a juvenile island magmatic arc of Paleocene–Eocene age. It formed in an intra-magmatic arc third-order basin in a setting similar to that of other Andean deposits. Somewhat similar global equivalents are the bimodal-felsic deposits of the Hokuroko basin (Japan) and the VMS deposits of Tasmania.
- The massive sulphide mineralization occurs in the Macuchi Formation as stratabound orebodies, mainly in the contact between a rhyodacitic dome and the overlying mafic, glass-rich, mass flows. The overlying rocks host semi-massive to disseminated mineralization. The mineralization is replacive on both the glassy carapace of the rhyodacite and the volcanoclastic rocks. This replacement took place only a few metres below the seafloor.
- The massive polymetallic sulphides consist primarily of pyrite, sphalerite, chalcopyrite, and less abundant galena, bornite, and tennantite; silver is concentrated in discrete phases such as stromeyerite and proustite.
- The orebody has marked lateral and vertical zoning with a lower Cu-rich zone and an external Zn-Pb-barite zone. The copper-rich zone replaced the external zone, with most of the gold and silver concentrated along this replacement zone.
- The area has good exploration potential for VMS deposits. The optimal target should be the contact of the rhyodacite domes with mafic, glass-rich rocks, or the outer carapace of domes capped by massive andesite-basalt.
- BISA believes that the procedures and protocols used by Salazar for its drilling, logging, sampling, preparation, and sample analysis program comply with international practices in the mining industry.
- The independent QA/QC verification carried out by BISA concludes that the duplicates of coarse rejects from preparation demonstrate acceptable precision and reproducibility of the original results. In contrast, the pulp duplicate precision is relatively low, with failures of over 10% for all the elements analysed (especially Au, Pb, and Cu) in both the ALS Global and Inspectorate laboratories.
- The blank samples used are adequate for Au, Ag, and Pb, but in the case of Cu and Zn, the values are much higher than the lower analytical limits of detection established in the laboratories used by Salazar.

- The metallurgical tests indicate that the recovery of pay metals to concentrates by froth flotation of feed from the El Domo deposit is technically feasible.
- It may be possible to improve Cu-Zn separation. Mineralogical results indicate that significant amounts of free sphalerite are present in the copper concentrate. This means that the selectivity of copper and zinc separation may be improved, compared to the results of the first phase of testing reported in the PEA.
- Mineral Resources were estimated based on a 3D geological interpretation for a VMS deposit; four mineralized units have been considered for mineral resource estimation (VMS, Grainstone, Breccia, and Gypsum). The cutoff value applied is US\$30 NSR per tonne.
- Indicated Mineral Resources have been estimated at 6.080 million tonnes at an average grade of 2.33% Cu, 3.06% Zn, 0.28% Pb, 2.99 g/t Au, and 55.81 g/t Ag, containing 312.95 million pounds Cu, 409.56 million pounds Zn, 37.76 million pounds Pb, 584,457 ounces Au, and 10.91 million ounces Ag. The current Indicated Mineral Resource estimate shows the following increases relative to the 2011 Indicated Resource estimate: a 7% increase in contained copper, a 34.4% increase in contained zinc, a 17.4% increase in contained gold, and a 26.8% increase in contained silver.
- The Inferred Mineral Resource is 3.882 million tonnes at an average grade of 1.56% Cu, 2.19% Zn, 0.16% Pb, 2.03 g/t Au, and 42.92 g/t Ag, containing 133.46 million pounds Cu, 187.39 million pounds Zn, 13.96 million pounds Pb, 253,607 ounces Au, and 5.36 million ounces Ag. The current Inferred Mineral Resource estimate shows the following increases compared to the 2011 Indicated Resource estimate: a 118.1% increase in contained copper, a 108.0% increase in contained zinc, a 125.2% increase in contained gold, and a 118.7% increase in contained silver.
- Two structural domains have been established in the El Domo deposit: the Eastern Sector (El Domo hill) and the Western Sector, where most of the deposit is located. In the Eastern Sector, the VMS lenses lie at a greater depth underneath the andesitic dome. The eastern continuity of the lenses needs to be confirmed by a drilling program.
- The mining methods study considers two scenarios: open pit mining for the western domain of the deposit and underground mining for the eastern domain.
- The economic and financial assessment considers a total 14-year life of mine: nine years of surface mining, with production of 2,000 tpd, followed by five years of underground mining with a production of 1,000 tpd.

- The mining production, considering the mine plans for both scenarios (open pit and underground) and the reported metallurgical ore types, are: zinc mineral type 1.74 Mt; mixed mineral Cu/Zn type 3.00 Mt; and copper mineral type 2.18 Mt. The mining scenario also includes 46 Mt of waste rock and 0.98 Mt of low-grade material.
- A preliminary evaluation of infrastructure alternatives have been carried out: seven alternatives for tailings dams, five areas for the waste rock dumps, two deposits for topsoil, three alternative locations for the processing plant, four alternatives for facilities, three alternatives for the water adduction line, two alternatives for the water pipeline, five alternatives for the tailings transport system, three alternatives for the power supply system, and three alternatives for access to the mine. No major drawbacks are noted, and some work will have to be done to ensure the services required for the project.
- The preliminary estimates of pre-production capital investment total US\$110.3 million, an amount consistent with the current costs of mining and construction equipment. Operating through a mining contractor has been considered; this option reduces CAPEX but increases the operating cost. The mode of operation will be analysed in more detail in the pre-feasibility stage.
- The after-taxes financial evaluation of the project gives the following results:
 - Net Present Value (10% discount rate): US\$86.72 million
 - Internal Rate of Return: 30%
 - Payback Period: 2 years

26. RECOMMENDATIONS

BISA proposes the following recommendations:

- A systematic directional survey location program should be implemented for all future drilling.
- To provide consistency in the methods, one laboratory of the two currently used should be used as the primary laboratory for all analyses, and that the second laboratory should be used for external checking of the assays.
- The QA/QC program should be modified to include: establishment of a protocol for non-compliant results and a formal reporting system for QA/QC results; insertion of twin samples, coarse and fine duplicates, certified standards, and blanks in future programs; use of certified reference materials representative of the deposit; and preparation of adequate blanks.
- In future, the original stored pulp samples should not be used due to the low precision reported in the QA/QC programs of RPA and BISA. Any verification or validation must be done with existing samples of coarse rejects.
- Improving storage conditions of the reject samples in Quito, Ecuador. The samples should be stored in an orderly fashion, in a suitable environment.
- A detailed petrographic and mineragraphic study is strongly recommended to support metallurgical testing and aid in defining geometallurgical domains.
- Future exploration should focus on zones of mafic volcanoclastic flows with evidence of underlying felsic volcanics. Stream sediment geochemistry is crucial for finding new anomalies. Geophysical surveys are also key techniques. However, the mineralization is poorly magnetic and the sphalerite is generally poor in iron. Negative magnetometric anomalies may be useful for defining hydrothermal systems and feeder zones. Helicopter-borne Versatile Time-Domain Electromagnetic (VTEM) and similar EM techniques can be useful to find Cu-pyrite-rich ores; targeting the sphalerite-rich zones can be trickier, but again VTEM has given good results in pyrite-poor orebodies. Ground EM and further drilling should be carried out in areas with the best combination of geology and airborne anomalies.
- Additional metallurgical testing should be carried out to optimize the process performance for the selective recovery of Cu, Zn, and Pb and to reduce reagent consumption.
- Geo-metallurgical mapping should be performed to identify areas with high clay contents that may interfere with the recovery processes.

- Study the use of specific reagents for Au and Ag to increase their recovery to the copper concentrate.
- Study the use of a Cu/Pb separation train to clean the copper concentrate and produce a lead concentrate as another commercial product.
- Closed-cycle flotation tests are needed in order to confirm the recoveries and grades obtained.
- Conduct flotation tests with water drawn from the project's area of influence to assess its effect on the recovery of Cu and Zn.
- Salazar should acquire systematic SG measurements of full sample lengths from all lithology units, thus providing direct information relating density to grade.
- Salazar should continue the investigation and interpretation of grade directional trends and further variography evaluation.
- An infill drilling program should be completed to upgrade the start-pit resources to the measured category as a requirement for the pre-feasibility.
A drilling program to define the nature and continuity of the VMS mineralization under the El Domo andesite is also recommended.
- It is advisable to promptly undertake a topographic survey of the project area, with greater accuracy in areas required for the facilities.
- Hydrological and geotechnical studies should be undertaken in areas slated for the pits, waste dumps, processing plant, and in general in all areas requiring heavy structures. The geotechnical investigation is a priority in order to define the pit profiles and volumes of mineral and waste material that must be removed.
- In the next project stage, the technical options identified in this conceptual study should be analysed in greater detail. Trade-off studies should be developed in the prefeasibility stage to set the basis for a subsequent feasibility study.
- Although the financial projection results are positive, the high cost of pre-stripping presents a significant outlay and risk. Therefore, the underground alternative could be reconsidered. The pit profiles are provisional and may change, as there are no geotechnical studies available. The pre-stripping volumes could vary, changing the economic and financial parameters presented in this report.
- A pre-feasibility stage work program should consist of several studies that include: infill drilling, additional metallurgical testing, resource model update and reserve estimates, processing plant engineering, infrastructure and project engineering. The work program and estimated budget for a prefeasibility study are summarized in Table 26.1.

TABLE 26.1 PROPOSED PROGRAM AND BUDGET

Pre-Feasibility Program	Proposed Cost US\$
Project Management	200,000
Staff relocation	20,000
Communications- telephone/fax/radio/hardware/software	15,000
Community Engagement	170,000
Environmental compliance	160,000
Land Acquisition	800,000
Mining Concessions	500,000
Road Maintenance	20,000
Transportation - Vehicles	50,000
Shipping - Couriers, Freight	20,000
Field Costs	500,000
Underground Development (300m)	600,000
GEOLOGY	
Geological Model Update	20,000
Structural Study	30,000
Ore mineralogy	35,000
QA/QC Program	10,000
Resource Model Update	95,000
Infill Diamond Drilling	
Drilling 6,055m@150US\$/m	908,250
Logging and Sampling	185,000
Supplies and Core Boxes	55,000
Preparation and Assaying 4,000 Samples	280,000
MINING	
Geotechnical / Geomechanical Evaluation	300,000
Open Pit Studies	120,000
METALLURGICAL TESTING AND PROCESS	
Metallurgical and process studies	500,000
INFRASTRUCTURE	
Geotechnical and Hydrogeological Studies	420,000
ECONOMIC EVALUATION	
Financial Study	40,000
<hr/>	
Sub-total	6,053,250
Contingencies - 10%	605,325
Total	6,658,575

27. REFERENCES

- Aguirre L, Atherton MP (1987) Low-grade metamorphism and geotectonic setting of the Macuchi Formation, Western Cordillera of Ecuador. *Journal of Metamorphic Geology* 5:473-494. doi: 10.1111/j.1525-1314.1987.tb00397.x.
- Barrie CT, Hannington MD (1999) Classification of volcanic-associated massive sulfide deposits based on host rock composition In: Barrie CT, Hannington MD (eds) *Volcanic-associated massive sulfide deposits; processes and examples in modern and ancient settings*. Society Economic Geologists, pp. 2–12.
- Barrie CT, Ludden JN, Green TH (1993) Geochemistry of volcanic rocks associated with Cu-Zn and Ni-Cu deposits in the Abitibi subprovince. *Economic Geology* 88:1341-1358.
- Beate B (2007) Geological report of the Curipamba Project.
- BGS-CODIGEM (1993) Mapa tectono metalogénico del Ecuador, escala 1:1.000.000.
- Buckle J (2009) Technical Report on the Curipamba Project, Bolívar Province, Central-West Ecuador Internal Report, Salazar Resources, Pp. 294.
- Callaghan T (2001) Geology and host rock alteration of the Henty and Mount Julia gold deposits, Western Tasmania. *Economic Geology* 96:1073–1088.
- Chiaradia M, Fontboté L (2000) Gold-rich vhms deposits of the Western Cordillera of Ecuador: Mineralogy, lead isotope and metal contents In: Sherlock R, M.A.V. L (eds) *VMS deposits of Latin America*. Geol.Assoc.Canada Spec.Publ., 2 pp 333–339.
- Chiaradia M, Fontboté L (2001) Radiogenic lead signatures in Au-rich volcanic-hosted massive sulfide ores and associated volcanic rocks of the Early Tertiary Macuchi Island arc (Western Cordillera of Ecuador). *Economic Geology* 96:1361–1378.
- Chiaradia M, Tripodi D, Fontboté L, Reza B (2008) Geologic Setting, Mineralogy, and Geochemistry of the Early Tertiary Au-Rich Volcanic-Hosted Massive Sulfide Deposit of La Plata, Western Cordillera, Ecuador. *Economic Geology* 103:161–183. doi: 10.2113/gsecongeo.103.1.161.
- de Ronde CEJ (1995) Fluid chemistry and isotopic characteristics of seafloor hydrothermal systems and associated VMS deposits: potential for magmatic contribution In: Thompson JFH (ed) *Magmas, fluids and ore deposits*, pp. 479–509.
- Dunham RJ (1962) Classification of carbonate rocks according to depositional texture In: Ham WE (ed) *Classification of carbonate rocks*, pp. 108–121.
- Egüez A (1986) Evolution Cenozoique de la Cordillere Occidentale septentrionale d'Equateur (0°15' S - 01°10'S), les mineralisations associeetes. UPMC, Paris, pp. 116.
- Franklin JM (2009) Observations on the Curipamba Massive Sulfide District Ecuador Salazar Resources, Internal Report, pp. 57.

- Franklin JM (2010) Report from Office and Field Visit, November 8-11, 2010 Curipamba Project, Salazar Resources Internal Report, Salazar Resources, pp. 31.
- Franklin JM, Gibson HL, Jonasson IR, Galley AG (2005) Volcanogenic Massive Sulfide Deposits In: Hedenquist JW, Thompson JFH, Goldfarb RJ, Richards JP (eds) Economic Geology - One hundredth anniversary Volume. Society of Economic Geologists, Littleton, pp. 523–560.
- Franklin JM, Sangster DM, Lydon JW (1981) Volcanic associated massive sulfide deposits In: Skinner BJ (ed) Economic Geology 75th Anniversary Volume. Society Economic Geologists, pp. 485–627.
- Gonzalez Clavijo E (2001) VHMS in the Eastern Cordillera of the Ecuadorian Andes? In: Tornos F, Pascual E, Saez R, Hidalgo R (eds) GEODE Workshop "Massive sulphide deposits in the Iberian Pyrite Belt: New advances and comparison with equivalent systems". Aracena, pp. 21–22.
- Gonzalez Clavijo E, Ortiz C, Figueroa J (2006) Sulfuros masivos volcanogénicos de la Cordillera Real del Ecuador. Minería Ecuatoriana.
- Halley SW, Roberts RH (1997) Henty: A shallow-water gold-rich volcanogenic massive sulfide deposit in Western Tasmania. Economic Geology 92:438-447.
- Hannington MD, Peter JM, Scott SD (1986) Gold in sea floor polymetallic sulfide deposits. Economic Geology 81:1867–1883.
- Herrington RJ, Maslennikov VV, Spiro B, Zaykov VV, Little CTS (1998) Ancient vent chimney structures in the Silurian massive sulfides of the Urals In: Mills RA, Harrison K (eds) Modern Ocean Floor Processes and the Geological Record. Geological Society London Special Publication, pp. 241–257.
- Hughes RA, Pilatasig LF (2002) Cretaceous and Tertiary terrane accretion in the Cordillera Occidental of the Andes of Ecuador. Tectonophysics 345:29-48. doi: [http://dx.doi.org/10.1016/S0040-1951\(01\)00205-0](http://dx.doi.org/10.1016/S0040-1951(01)00205-0).
- Kerr AC, Aspden JA, Tarney J, Pilatasig LF (2002) The nature and provenance of accreted oceanic terranes in western Ecuador: geochemical and tectonic constraints. Journal of the Geological Society 159:577–594. doi: 10.1144/0016-764901-151.
- Large RR (1977) Chemical evolution and zonation of massive sulfide deposits in volcanic terrains. Economic Geology 72:549–572.
- Large RR (1992) Australian volcanic-hosted massive sulfide deposits: Features, styles and genetic models. Economic Geology 87:471–510.
- Large RR, Blundell DLe (2000) Database on Global VMS districts. CODES-GEODE, Hobart.
- Large RR, McPhie J, Gemmell JB, Herrmann W, Davidson GJ (2001) The spectrum of ore deposit types, volcanic environments, alteration halos and related exploration vectors

- in submarine volcanic successions: Some examples from Australia. *Economic Geology* 96:913-938.
- Lavigne J, McMonnies E (2011) Technical Report on the Curipamba Project, Ecuador NI 43-101 Report In: Inc. RPA (ed) Internal Report, Salazar Resources, pp. 166.
- Litherland M, Aspden JA (1992) Terrane-boundary reactivation: A control on the evolution of the Northern Andes. *Journal of South American Earth Sciences* 5:71–76. doi: [http://dx.doi.org/10.1016/0895-9811\(92\)90060-C](http://dx.doi.org/10.1016/0895-9811(92)90060-C).
- Luzieux LDA, Heller F, Spikings R, Vallejo CF, Winkler W (2006) Origin and Cretaceous tectonic history of the coastal Ecuadorian forearc between 1°N and 3°S: Paleomagnetic, radiometric and fossil evidence. *Earth and Planetary Science Letters* 249:400-414. doi: <http://dx.doi.org/10.1016/j.epsl.2006.07.008>.
- Lydon JW (1988a) Volcanogenic massive sulphide deposits: I. A descriptive model In: Roberts RG, Sheanan PA (eds) *Ore deposit models*, pp. 14–56.
- Lydon JW (1988b) Volcanogenic massive sulphide deposits: II. Genetic models In: Roberts RG, Sheanan PA (eds) *Ore deposit models*, Geoscience Canada, reprint series 3, pp. 43–65.
- Lydon JW (1996) Characteristics of volcanogenic massive sulphide deposits: Interpretations in terms of hydrothermal convection systems and magmatic hydrothermal systems. *Boletín Geológico Minero* 107, 3–4, 15–64.
- Mayor JN (2010) Some observations on the geological structure at El Domo-Las Naves, Bolívar Province, Ecuador Salazar Resources Internal Report, pp. 4.
- McCourt WJ, Duque P, Pilatasig LF (1997) Geology of the Western Cordillera of Ecuador between 1-2°S Proyecto de Desarrollo Minero y Control Ambiental, Programa de Información Cartográfica y Geológica, CODIGEM-BGS, Report 3.
- Migineishvili R (2000) Formation of a volcanic hosted massive sulfide deposit in a shallow water setting: The Madneuli Cu-Au deposit, Georgia *Volcanic Environments and Massive Sulfide Deposits*. CODES Special Publication 3rd International Conference, Hobart, pp. 123–125.
- Nehlig P (1991) Salinity of oceanic hydrothermal fluids: A fluid inclusion study. *Earth Planetary Science Letters* 102: 310–325.
- Peter JM, Goodfellow WD (1996) Mineralogy, bulk and rare earth element geochemistry of massive sulphide associated hydrothermal sediments of the Brunswick Horizon, Bathurst Mining Camp, New Brunswick. *Canadian Journal Earth Sciences* 33:252–283.
- Pratt W (2008) Las Naves Project, Bolívar, Ecuador. Specilized Geological Mapping Ltd, pp 42.

- Pratt W (2009) Sesmo Sur Project, Ecuador. Specilized Geological Mapping Ltd, pp 27.
- Ramos VA (2009) Anatomy and global context of the Andes: Main geologic features and the Andean orogenic cycle In: Kay SM, Ramos VA, Dickinson WR (eds) Backbone of the Americas: Shallow subduction, plateau uplift, and ridge and Terrane collision. Geological Society of America, bulletin 204, pp. 31–65.
- Reynaud Cd, Jaillard Ãt, Lapierre H, Mamberti M, Mascle GH (1999) Oceanic plateau and island arcs of southwestern Ecuador: Their place in the geodynamic evolution of northwestern South America. *Tectonophysics* 307:235-254. doi: [http://dx.doi.org/10.1016/S0040-1951\(99\)00099-2](http://dx.doi.org/10.1016/S0040-1951(99)00099-2).
- Russell N, Seaward M, Rivera J, McCurdy K, Kesler SE, Cumming GL, Sutter JF (1981) Geology and geochemistry of the Pueblo Viejo gold-silver deposit and its host Los Ranchos Formation, Dominican Republic. *Transactions Institution Mining Metallurgy* 90:b153-b162.
- Schandl VS (2009) Petrographic and mineralogical study of the Curipamba Project, Central West Ecuador Internal Report, Salazar Resources. pp 78.
- Sherlock R, Logan MAV (eds) (2000) VMS Deposits of Latin America. Geological Association of Canada.
- Sillitoe RH (1980) Are porphyry copper and Kuroko type massive sulfide deposits incompatible? *Geology* 8, 11–14.
- Sillitoe RH (1999) VMS and porphyry copper deposits: Products of discrete tectonomagmatic settings En: *Mineral deposits: Processes to Processing*, Stanley et al, eds, Balkema, 7–10.
- Sillitoe RH, Hannington, M. D., Thompson, J. F. (1996) High sulfidation deposits in the volcanogenic massive sulfide environment. *Economic Geology* 91–1, 204–212.
- Spikings RA, Winkler W, Hughes RA, Handler R (2005) Thermochronology of allochthonous terranes in Ecuador: Unravelling the accretionary and post-accretionary history of the Northern Andes. *Tectonophysics* 399:195-220. doi: <http://dx.doi.org/10.1016/j.tecto.2004.12.023>.
- Spikings RA, Winkler W, Seward D, Handler R (2001) Along-strike variations in the thermal and tectonic response of the continental Ecuadorian Andes to the collision with heterogeneous oceanic crust. *Earth and Planetary Science Letters* 186:57–73. doi: [http://dx.doi.org/10.1016/S0012-821X\(01\)00225-4](http://dx.doi.org/10.1016/S0012-821X(01)00225-4).
- Spry PG, Peter JM, Slack JF (2000) Meta-exhalites as exploration guides to ore In: Spry PG, Marshall B, Vokes FM (eds) *Metamorphosed and Metamorphogenic Ore Deposits Reviews in Economic Geology*, 11, pp. 163–201.

- Tesalina SG, Maslennikov VV, Surin NT (1998) Aleksandrinka Cu-Zn massive sulphide deposit (east Magnitogorsk paleoisland arc, Ural). IMIN, Miass.
- Tripodi D, Fontboté, L., Chiaradia, M. (2003) Geologic setting, mineralogy and geochemistry of the Early tertiary Au-rich volcanic-hosted massive sulfide deposit of La Plata (Western Cordillera, Ecuador) In: Eliopoulos, DG, et al (eds), Mineral Exploration and Sustainable Development, Millpress Rotterdam, 199–202.
- Tornos F (2006) Environment of formation and styles of volcanogenic massive sulfides: The Iberian Pyrite Belt. *Ore Geology Reviews* 28:259–307.
- Tornos F, Peter JM, Allen RL, Conde C (in press) Controls on the sitting and style of volcanogenic massive sulphide deposits. *Ore Geology Reviews*.
- Vallejo C (2007) Evolution of the Western Cordillera in the Andes of Ecuador (Late Cretaceous-Paleogene). ETH Zurich, pp. 215.
- Vallejo C (2013) Stratigraphy and geological setting of El Domo VMS deposit within the Eocene Macuchi submarine arc, Central Ecuador Salazar Resources, Internal Report, pp. 21.
- Vallejo C, Spikings RA, Luzieux L, Winkler W, Chew D, Page L (2006) The early interaction between the Caribbean Plateau and the NW South American Plate. *Terra Nova* 18:264–269. doi: 10.1111/j.1365-3121.2006.00688.x.
- Vallejo C, Winkler W, Spikings R, Luzieux LDA, Heller F, Bussy F (2009) Mode and timing of terrane accretion in the forearc of the Andes in Ecuador In: Kay SM, Ramos VA, Dickinson WR (eds) Backbone of the Americas: Shallow subduction, plateau uplift, and ridge and Terrane collision. Geological Society of America, bulletin 204, pp. 197–216.
- Valliant W, Peltz P, Cook B (2010) Technical Report on the Curipamba Project, Central Ecuador NI 43-101 Report, Scott Wilson Roscoe Postle Associates INBc
- Winter LS, Tosdal RM, Mortensen JK, Franklin JM (2004) Volcanic Stratigraphy and Geochronology of the Cretaceous Lancones Basin, Northwestern Peru: Position and Timing of Giant VMS Deposits. *Economic Geology* 105:713–742.

28. DATE AND SIGNATURE PAGE

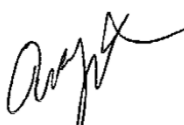
This report titled “Curipamba Project – El Domo Deposit Preliminary Economic Assessment, Central Ecuador” and dated March 21, 2014, was prepared and signed by following authors;

Dated at Lima, Peru
March 21, 2014



Gustavo Calvo Martin, M.Sc.A., P.Geol

Dated at Lima, Peru
March 21, 2014



Adam Johnston, B. Eng, FAusIMM

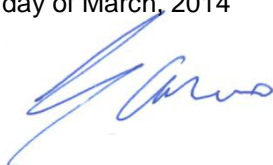
29. CERTIFICATE OF QUALIFIED PERSON

GUSTAVO CALVO MARTIN

I, Gustavo Calvo Martin, M.Sc.A., P.Geo., as an author of this report entitled "Curipamba Project – El Domo Deposit Preliminary Economic Assessment, Central Ecuador" prepared for Salazar Resources Ltd. and dated March 21, 2014, do hereby certify that: I am the Director of Geology with Buenaventura Ingenieros, S.A. of Larrabure y Unanue 146, Lima 1, Peru.

1. I graduated from the Universidad Complutense of Madrid in 1988 with a B.Sc. degree in Geology and from McGill University in 1991 with a M.Sc.A. in Mineral Exploration.
2. I am registered as a Professional Geoscientist in the Province of British Columbia (Reg. # 173072). I have worked as an exploration geologist for a total of 25 years since my graduation. My relevant experience for the purpose of this Technical Report is:
 - Design and implementation of base metals and precious metals exploration programs in the Andean Cordillera, including management of advanced exploration and resource delineation drilling programs.
 - Project evaluation/valuation and Mineral Resource Estimates for copper and gold projects in Peru, Ecuador, Colombia, Bolivia, Central America, China, Kazakhstan, PNG, Spain.
3. I have read the definition of "qualified person" set out in National Instrument 43-101 (NI 43-101) and certify that by reason of my education, affiliation with a professional association (as defined in NI 43-101) and past relevant work experience, I fulfill the requirements to be a "qualified person" for the purposes of NI 43-101.
4. I visited the Project on April 22 to 27, 2013.
5. I am responsible for the preparation of Sections 2 to 12, 14 to 16 and 18 to 26 of the Technical Report and contributed to Sections 1, 25, and 26.
6. I am independent of the Issuer applying the test set out in Section 1.5 of NI 43-101.
7. I have had no prior involvement with the property that is the subject of the Technical Report.
8. I have read NI 43-101, and the Technical Report has been prepared in compliance with NI 43-101 and Form 43-101F1.
9. To the best of my knowledge, information, and belief, the Technical Report contains all scientific and technical information that is required to be disclosed to make the technical report not misleading.

Dated this 21st day of March, 2014



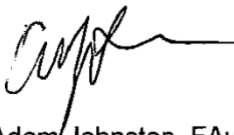

Gustavo Calvo Martin, M.Sc.A., P.Geo.

ADAM JOHNSTON

I, Adam Johnston, B. Eng (Minerals Engineering), FAusIMM (CP Metallurgy), as an author of this report entitled "Curipamba Project – El Domo Deposit Preliminary Economic Assessment, Central Ecuador" prepared for Salazar Resources Ltd. and dated March 21, 2014, do hereby certify that:

1. I am the Chief Metallurgist with Transmin MC E.I.R.L. of La Perricholi 110, San Isidro, Lima 27, Peru.
2. I am a graduate of Curtin University, Australia in 1995 with a B.Eng. degree in Minerals (Extractive Metallurgy).
3. I am registered as a Chartered Professional with the Australian Institute of Mining and Metallurgy. I have worked as a metallurgist for a total of 18 years since my graduation. My experience for the purpose of the Technical Report is in the metallurgical testing of base metal and precious metal ores.
4. I have read the definition of "qualified person" set out in National Instrument 43-101 (NI 43-101) and certify that by reason of my education, affiliation with a professional association (as defined in NI 43-101) and past relevant work experience, I fulfill the requirements to be a "qualified person" for the purposes of NI 43-101.
5. I have not visited the Project.
6. I am responsible for preparation of Section 13 and 17 of the Technical Report.
7. I am independent of the Issuer applying the test set out in Section 1.5 of NI 43-101.
8. I have had no prior involvement with the property that is the subject of the Technical Report.
9. I have read NI 43-101, and the Technical Report has been prepared in compliance with NI 43-101 and Form 43-101F1.
10. To the best of my knowledge, information, and belief, the Technical Report contains all scientific and technical information that is required to be disclosed to make the technical report not misleading.

Dated this 21st day of March, 2014



Adam Johnston, FAusIMM (CP Metallurgy)

30. APPENDIX 1

PHOTOGRAPHS



1. Coherent almost aphyric rhyodacite of the Lower Felsic Unit showing flow banding. DH 12-196 m.



2. Coherent aphyric rhyodacite with widespread devitrification, showing local spherulitic textures. DDH 11-106 m.



3. Irregularly devitrified rhyodacite with sparse phenocrysts of quartz and feldspar. DDH 11-187 m.



4. In situ hyaloclastic rhyodacite showing remnants of flow banding. DDH 11-106 m.



5. Hyaloclastic rhyodacite, with the devitrification highlighting the curvilinear fragments. DDH 11-123 m.



6. Anhydrite-rich stockwork crosscutting the hyaloclastic rhyodacite of the Lower Felsic Unit. DDH 10-64 m.



7. Lower Felsic Unit: hyaloclastite of rhyodacitic composition with sometimes banded in situ fragments highlighted by hydrothermal quartz - sericite alteration. DDH 11-106 m.



8. Hyaloclastite with the ground mass replaced by sericite, quartz and pyrite, something that highlights the fragments. DDH 11-106 m.



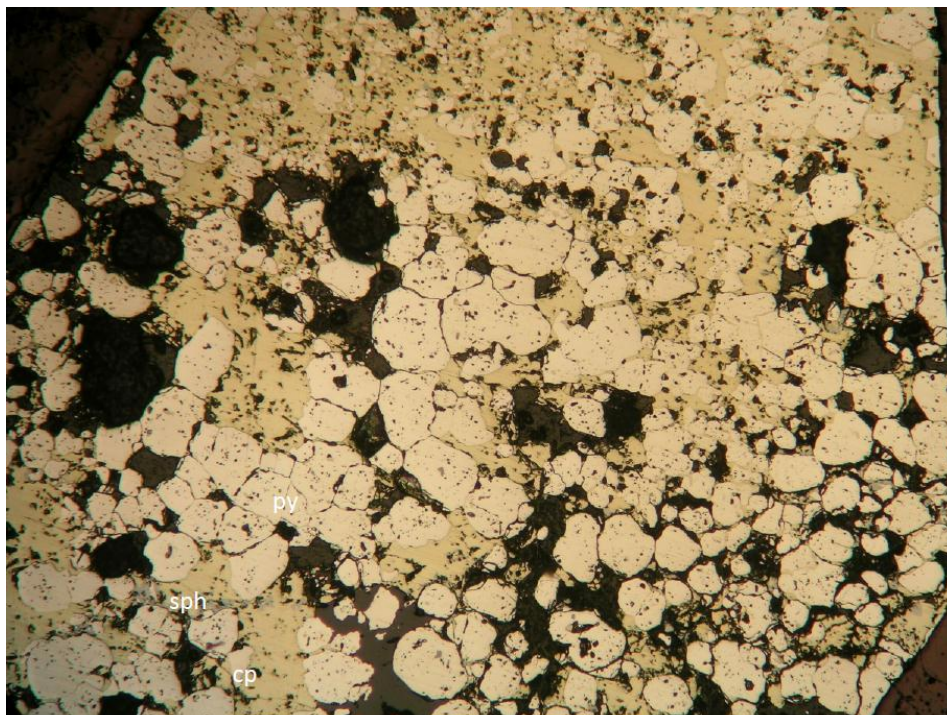
9. Rhyodacite replaced by a texturally destructive assemblage of quartz, sericite and pyrite in the stockwork zone. DDH 106-18 m.



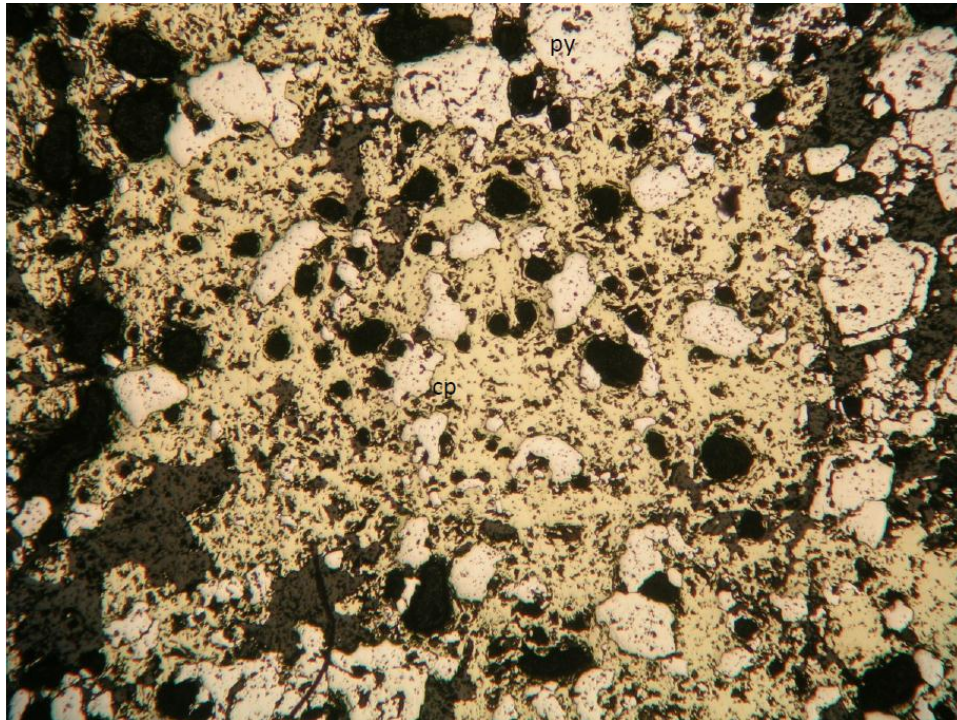
10. Hyaloclastite in rhyodacite with an early quartz - sericite - pyrite alteration and later anhydrite - rich veins. DDH 106-21 m.



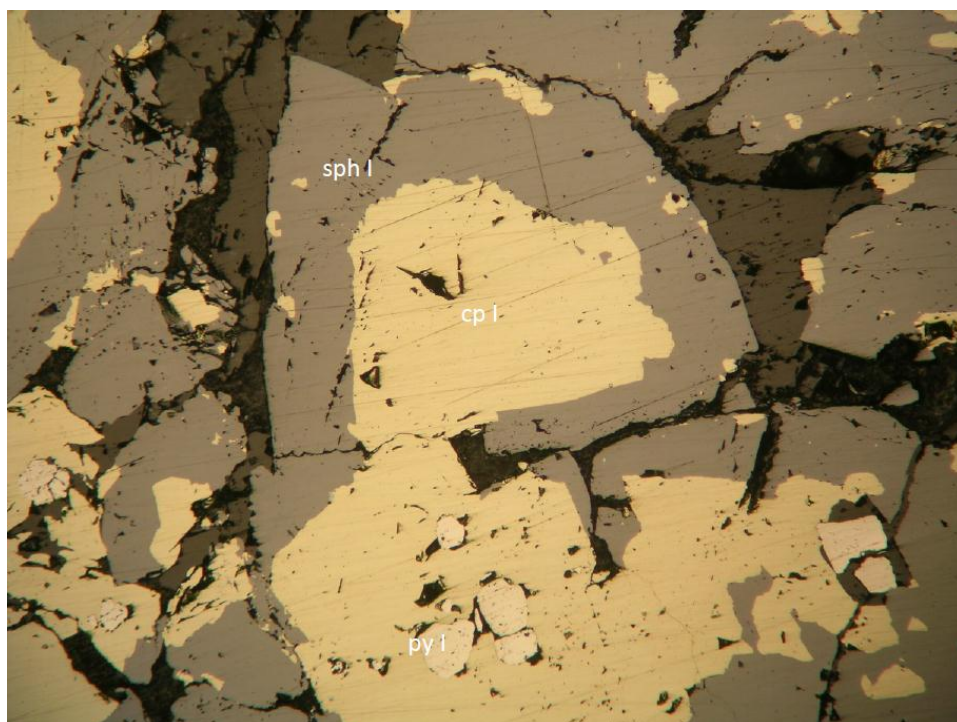
11. Rhyodacite pervasively replaced by a quartz-sericite-pyrite-(chlorite) alteration and crosscut by anhydrite-rich veins. DDH 10-64 m.



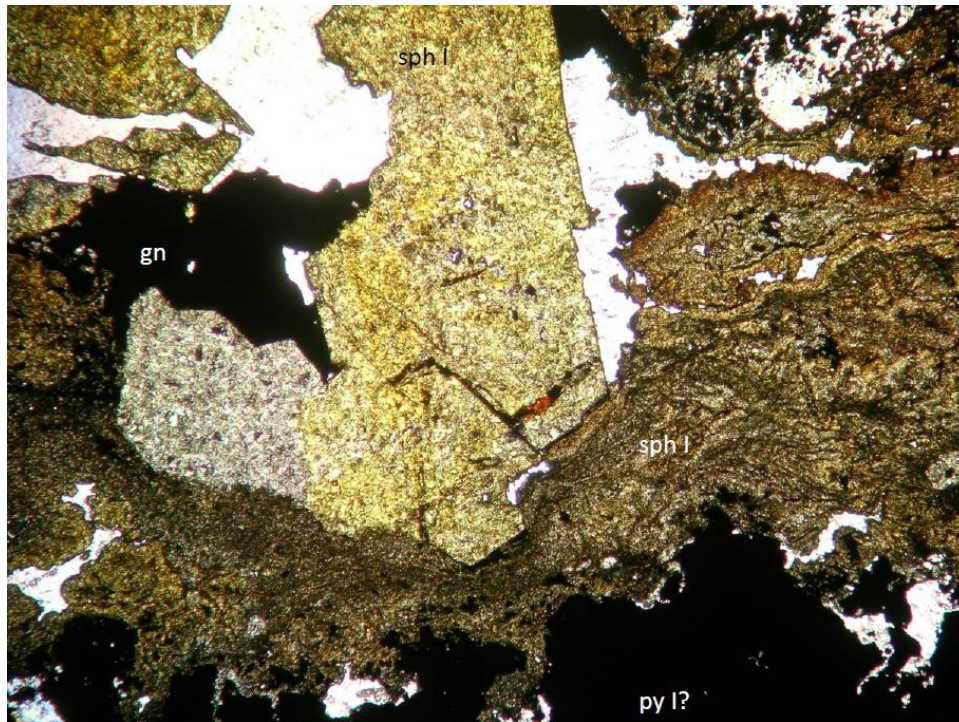
12. DOM - 25 (DDH 68 98 m). Mineralization of the Assemblage A. Early pyrite (py I) in rounded and porous subeuhedral crystals cemented by chalcopyrite (cp I) and scarce sphalerite (sph). Dimensions photograph: 0.8x0.6 mm. Reflected light.



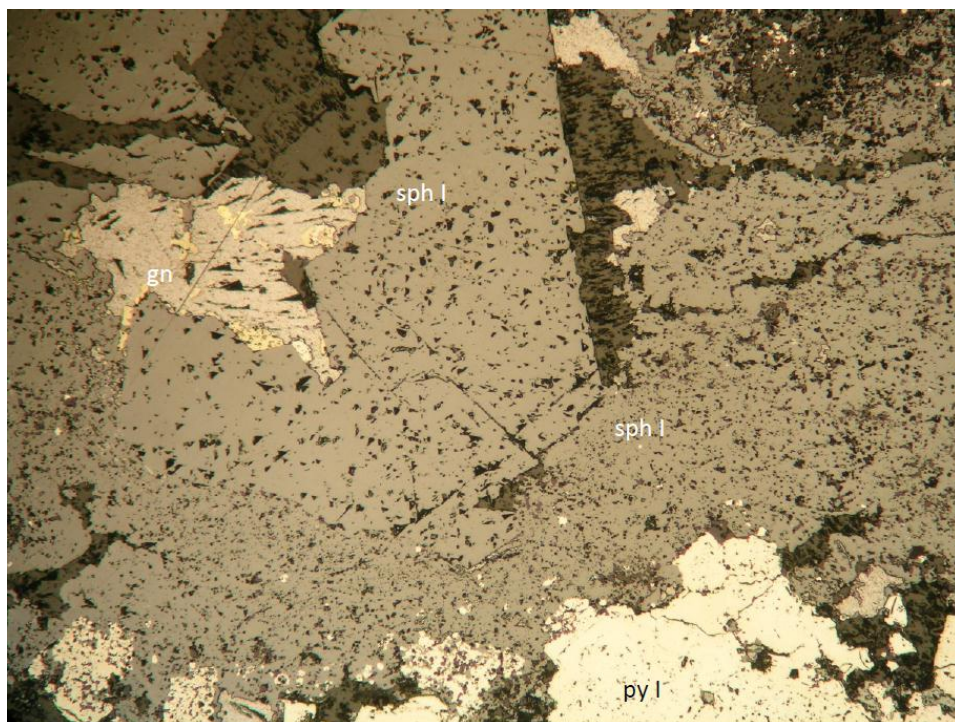
13. DOM - 68 (DDH 56 71 m). Assemblage A. Remnants of anhedral pyrite I corroded and replaced by chalcopyrite I. Dimensions photograph: 1.5x1.13 mm. Reflected light.



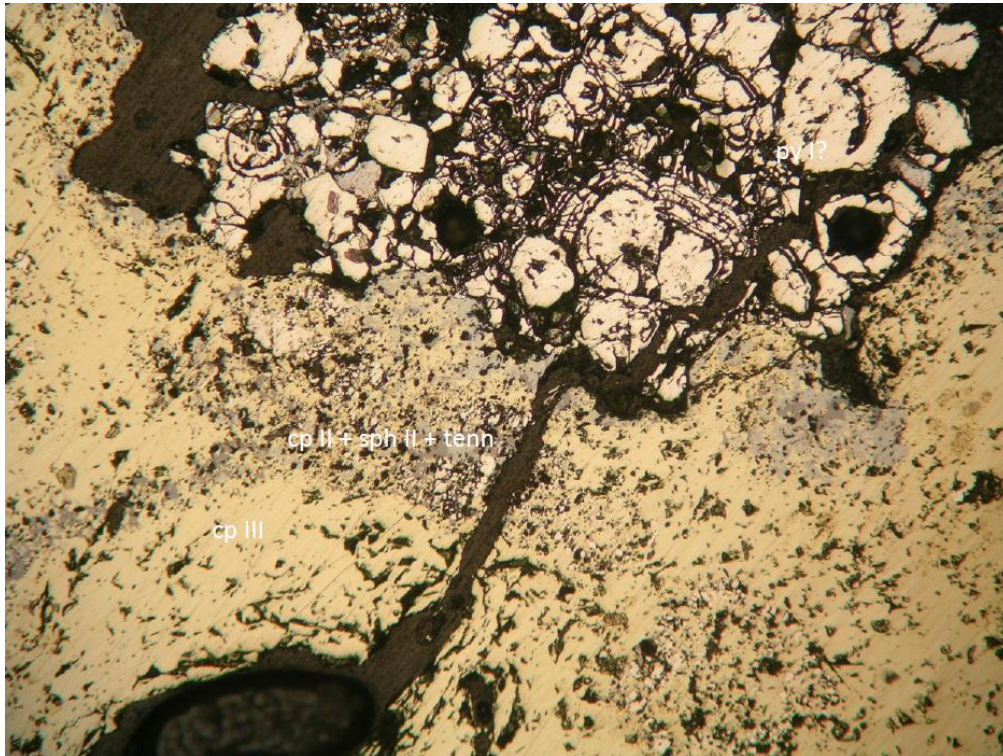
14. DOM - 28 (DDH 123 77.2 m). Assemblage A replaced by Assemblage B. Chalcopyrite I with remnants of anhedral pyrite I replaced by Fe - poor sphalerite (sphalerite I). Dimensions photograph: 0.8x0.6 mm. Reflected light.



15. DOM - 28 (DDH 123 77.1 m). Assemblage B. Coarse grained Fe - poor sphalerite associated with barite replaced by also Fe - poor but fine grained sphalerite with galena, pyrite I and chalcopyrite I. Dimensions photograph: 0.8x0.6 mm. Transmitted light.



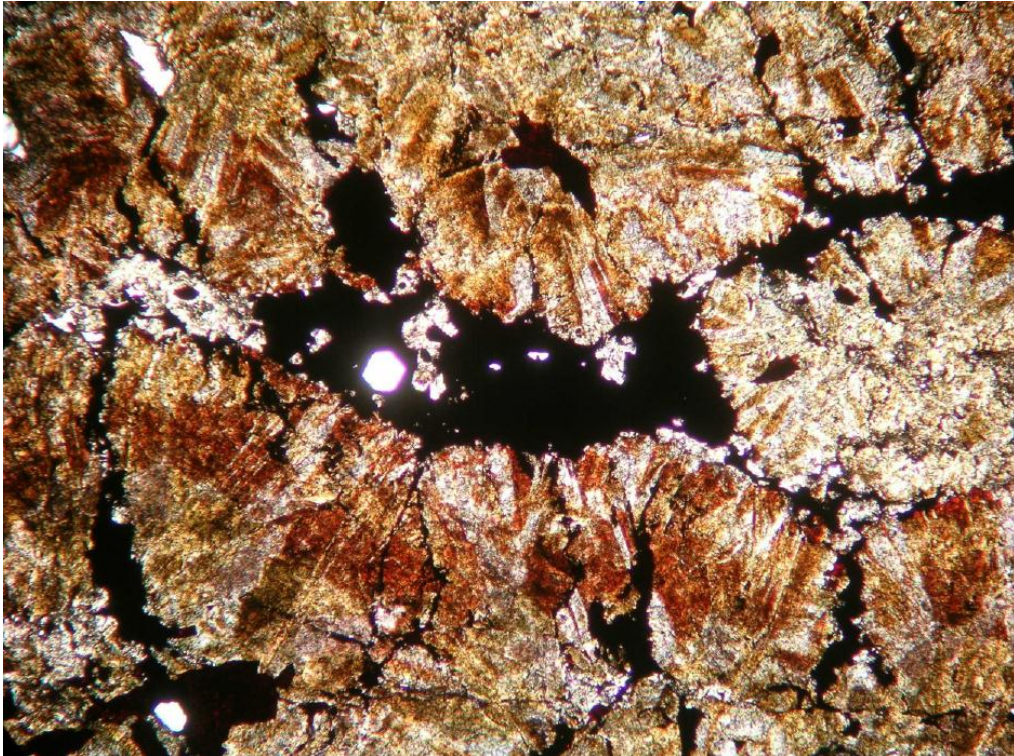
16. DOM - 28. Idem, reflected light.



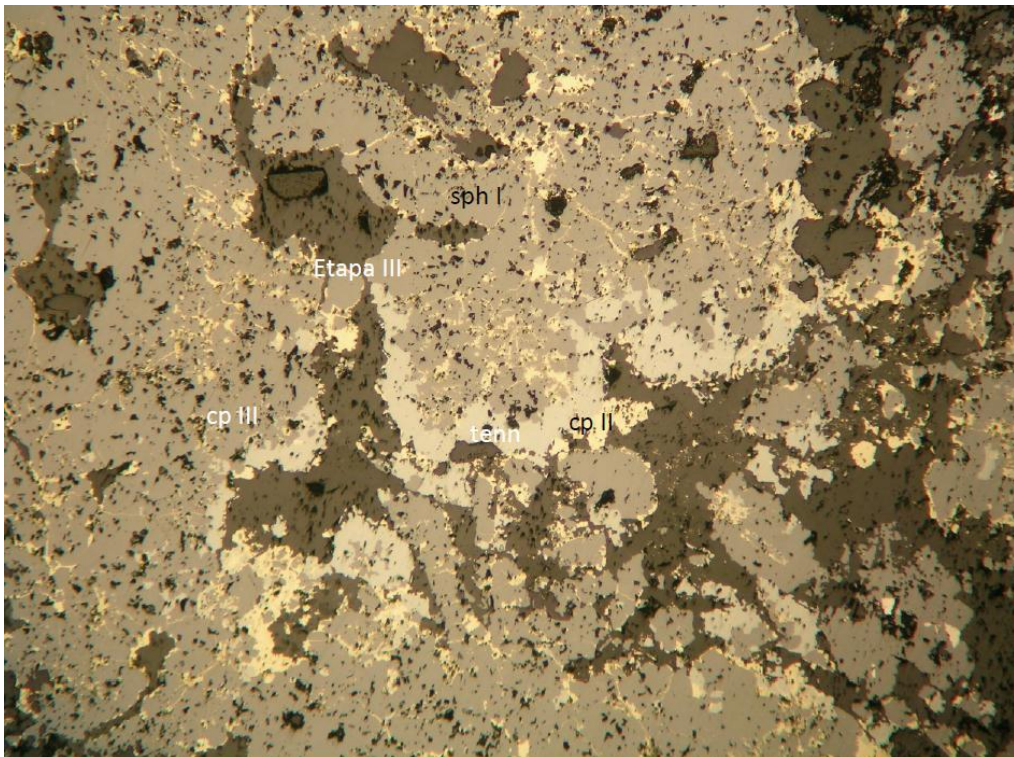
17. DOM - 6a. Pyrite I in coarse grained aggregates replaced by chalcopyrite II - sphalerite II - tennantite (Assemblage C) and massive chalcopyrite III (Assemblage D1). Dimensions photograph: 0.8x0.6 mm. Reflected light



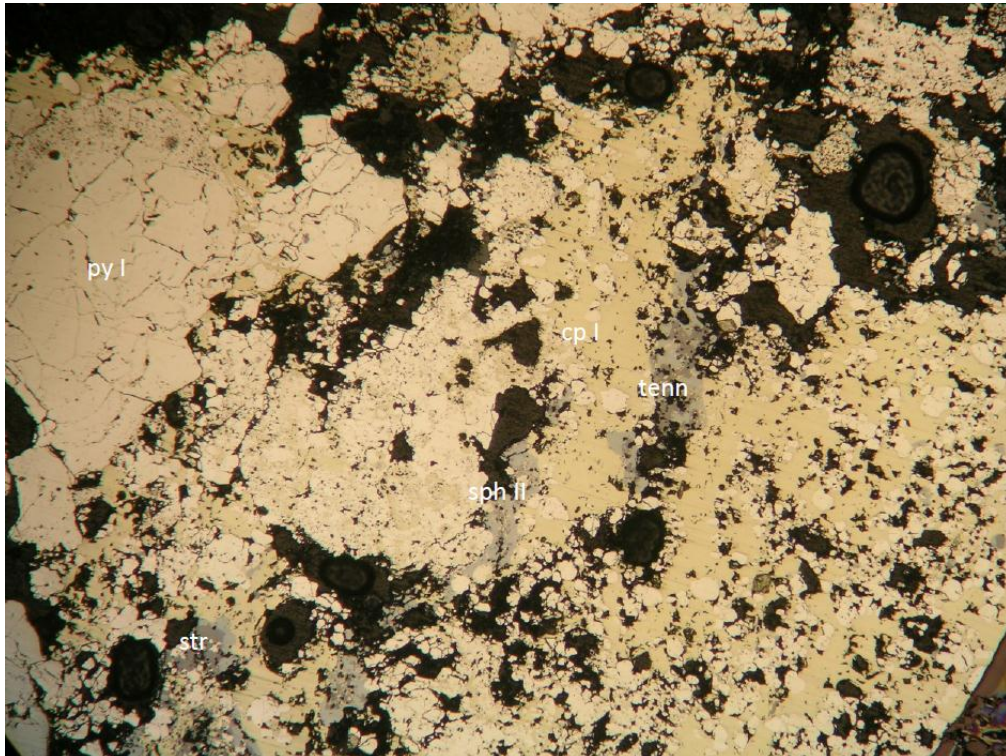
18. DOM - 4 (DDH 106 49.9 m). Fe - rich sphalerite II with later replacement of chalcopyrite II, galena and tennantite (Assemblage C). Dimensions photograph: 0.8x0.6 mm. Reflected light.



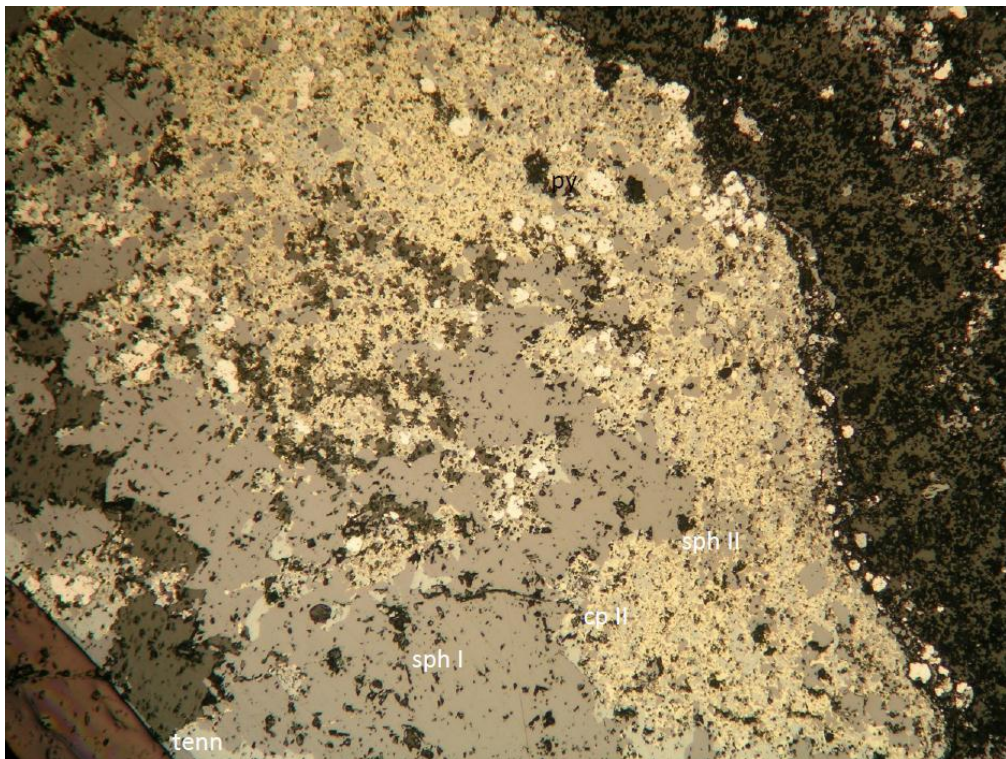
19. DOM - 4. Idem, transmitted light.



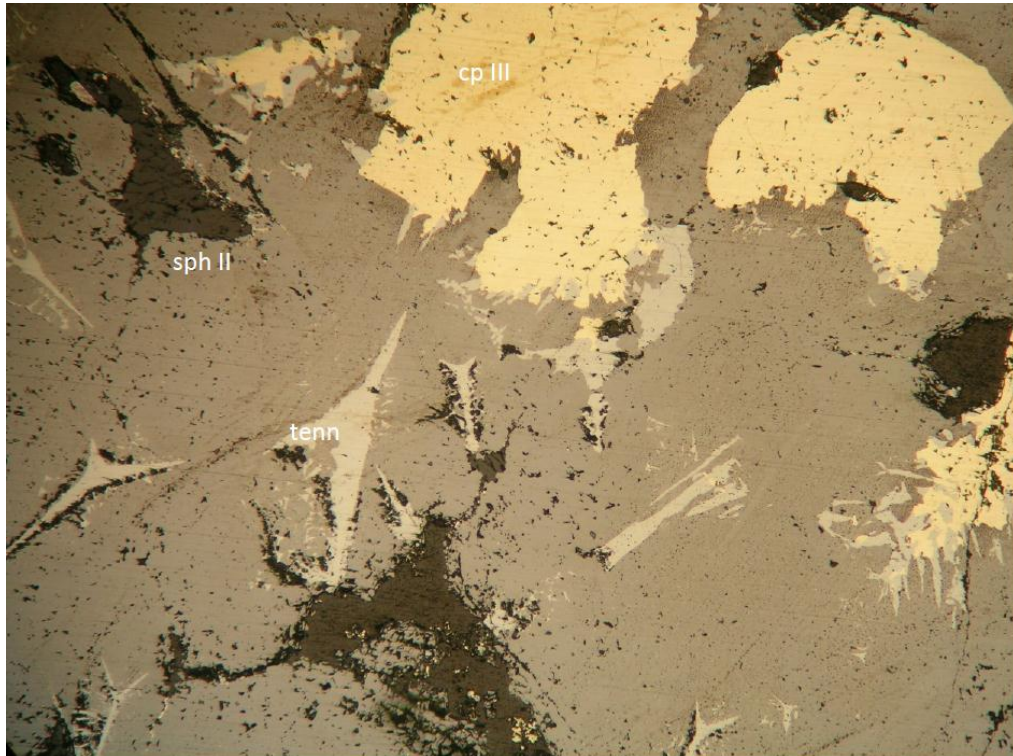
19. DOM - 21 (DDH 68 88.4 m). Sphalerite I replaced along fractures by chalcopyrite II and tennantite (Assemblage C). Dimensions photograph: 0.8x0.6 mm. Reflected light.



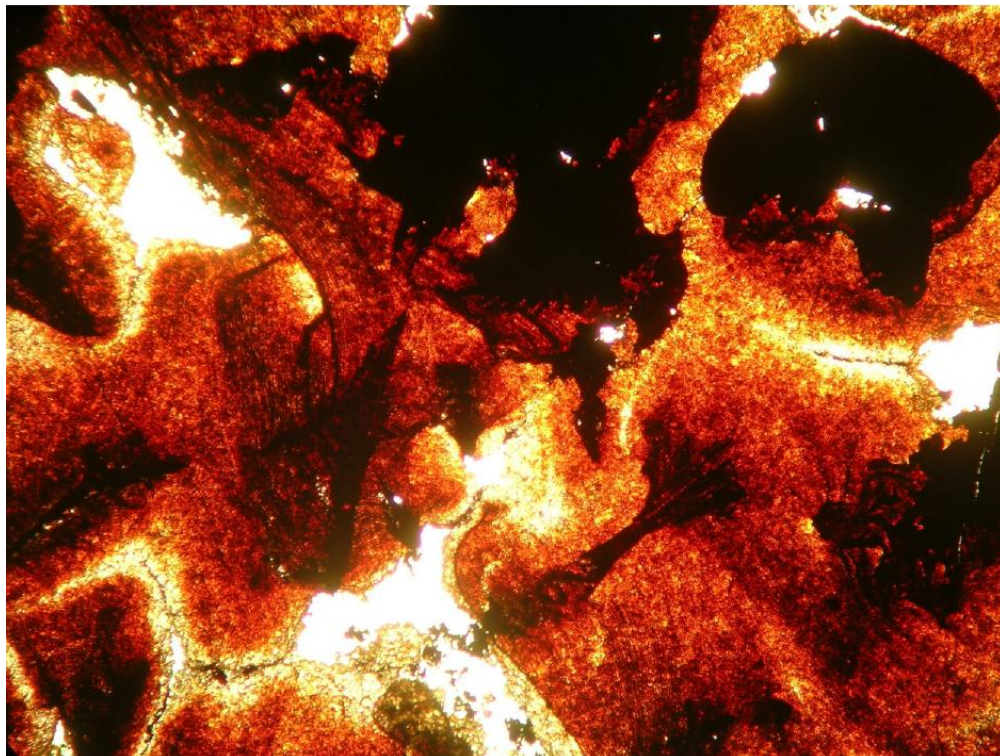
20. DOM - 6a. Pyrite I in coarse grained aggregates replaced by chalcopyrite I (Assemblage A) and sphalerite II - tennantite - stromeyerite (Assemblage C). Dimensions photograph: 0.8x0.6 mm. Reflected light.



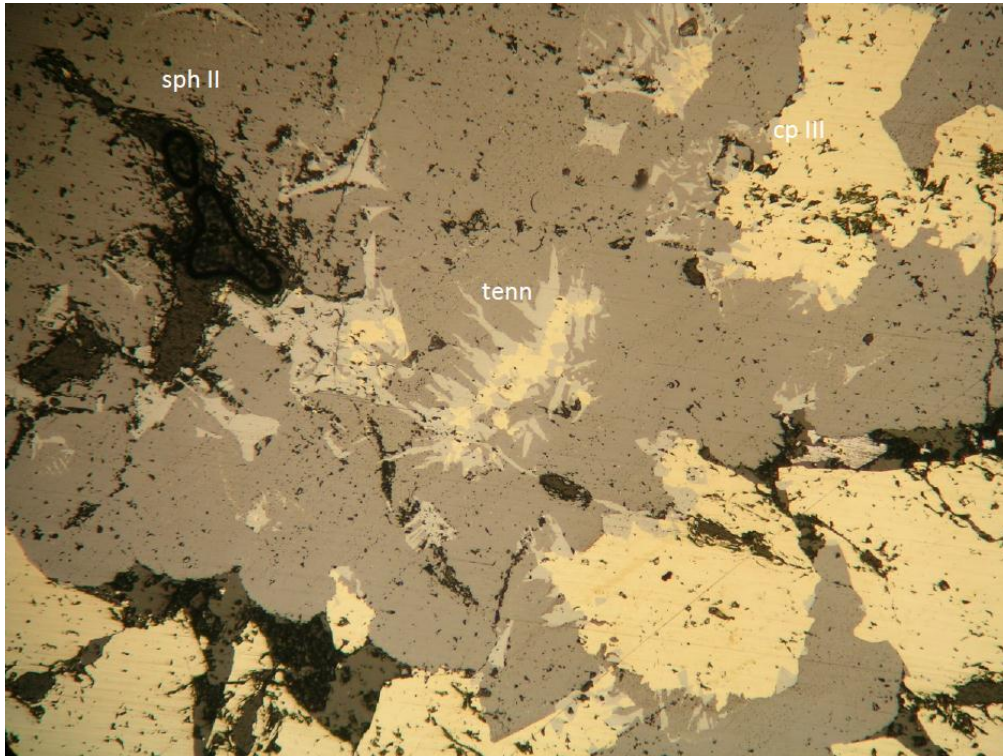
21. DOM - 22 (DDH 68 92 m). Sphalerite I (Assemblage B) replaced by sphalerite II, chalcopyrite II, pyrite and tennantite (Assemblage C). Dimensions photograph: 0.8x0.6 mm. Reflected light.



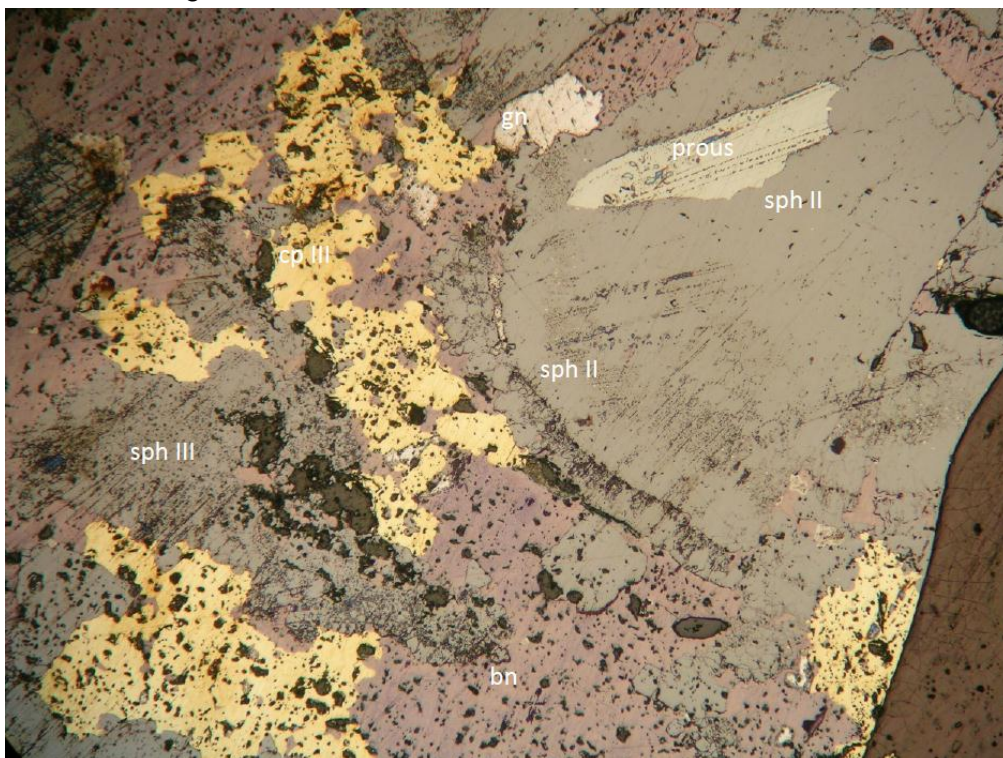
22. DOM - 27 (DDH 123 69.3 m). Sphalerite II coexisting con tennantite (Assemblage C) replaced by chalcopyrite III massive of the Assemblage D1. Dimensions photograph: 0.8x0.6 mm. Reflected light.



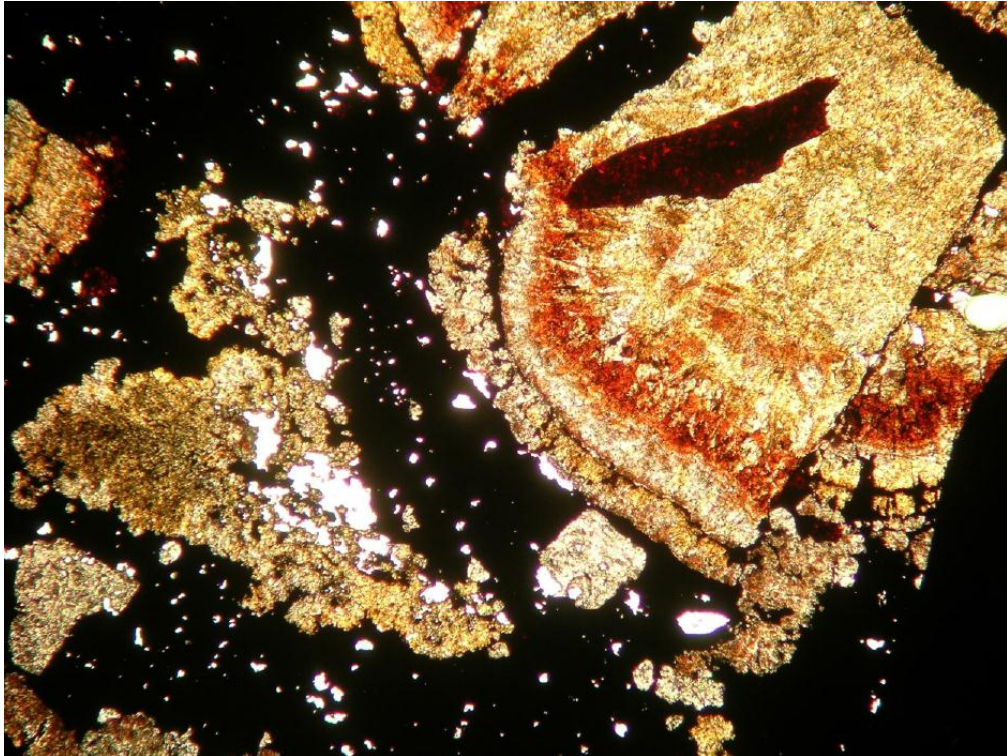
23. DOM - 27. Idem, reflected light.



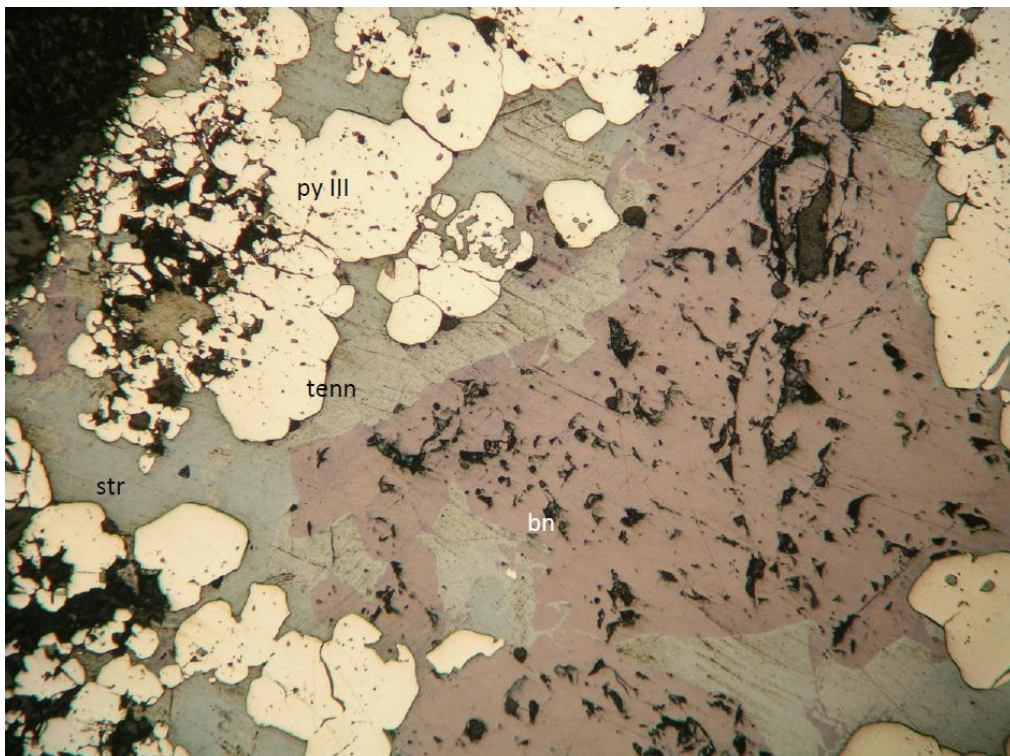
24. DOM - 27 (DDH 123 69.3 m). Sphalerite II associated with tennantite (Asociation C) and replaced by chalcopyrite III (Association D1). Dimensions photograph: 0.8x0.6 mm. Reflected light.



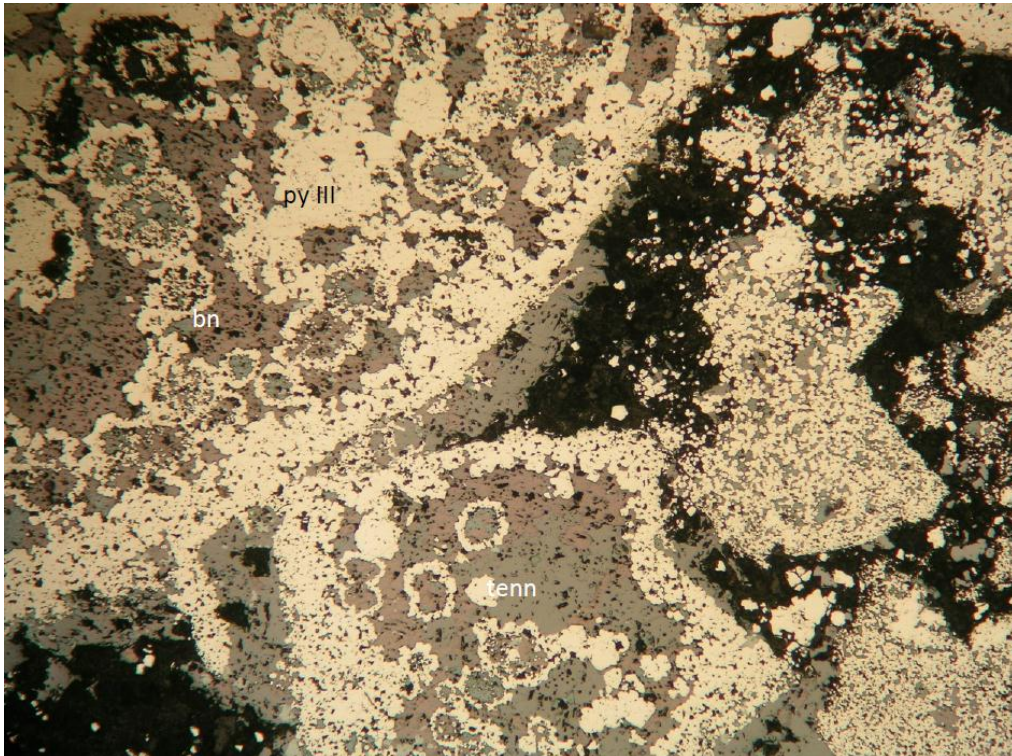
25. DOM - 4 (DDH 106 49.9 m). Sphalerite I (Association B) replaced by sphalerite II and proustitite (Association C) and later by bornite - chalcopyrite III - sphalerite III - tennantite (Association D). Dimensions photograph: 0.8x0.6 mm. Reflected light.



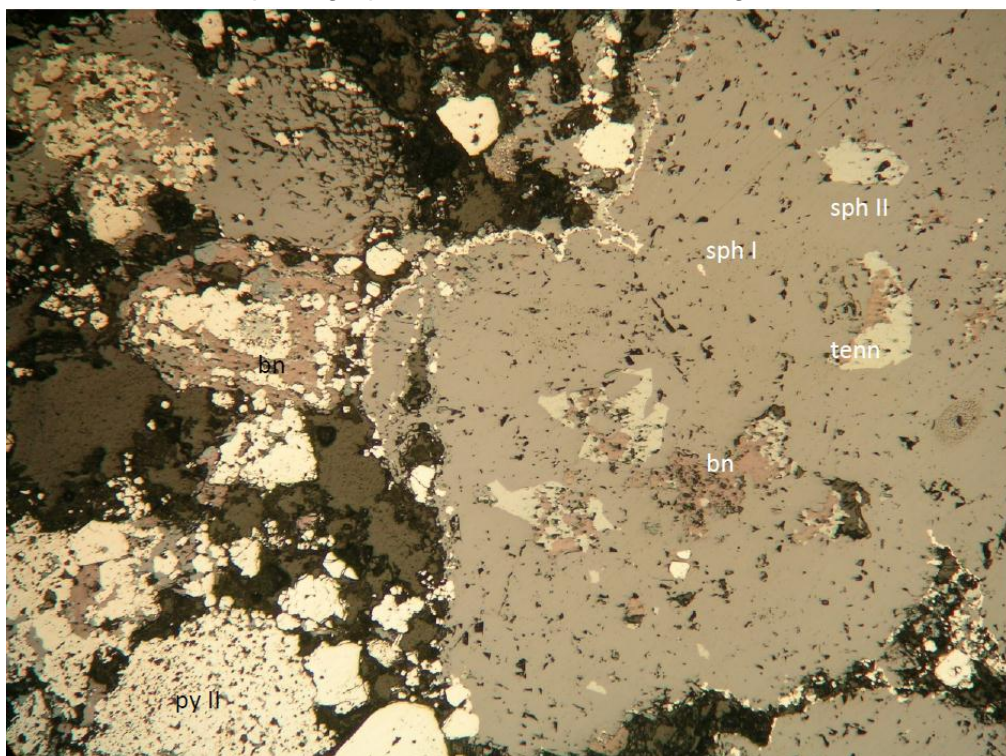
26. DOM - 4. Idem, transmitted light.



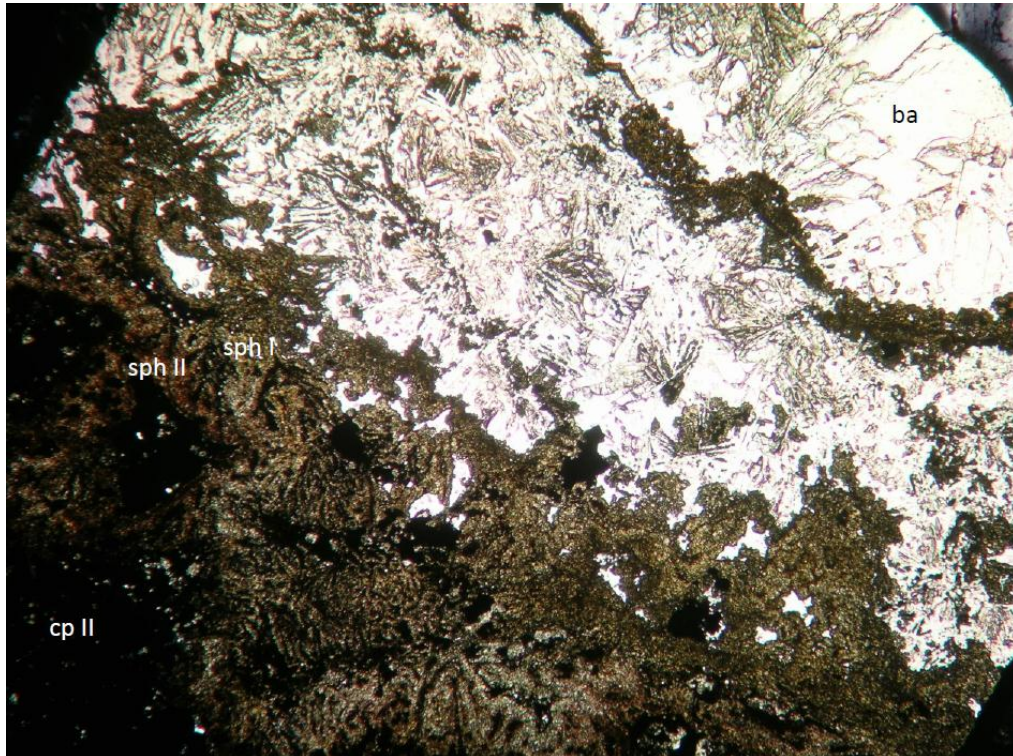
27. DOM - 67 (DDH 161 262.1 m). Typical assemblage of the Assemblage D. Bornite intergrown with tennantite, stromeyerite and pyrite II. Dimensions photograph: 0.8x0.6 mm. Reflected light.



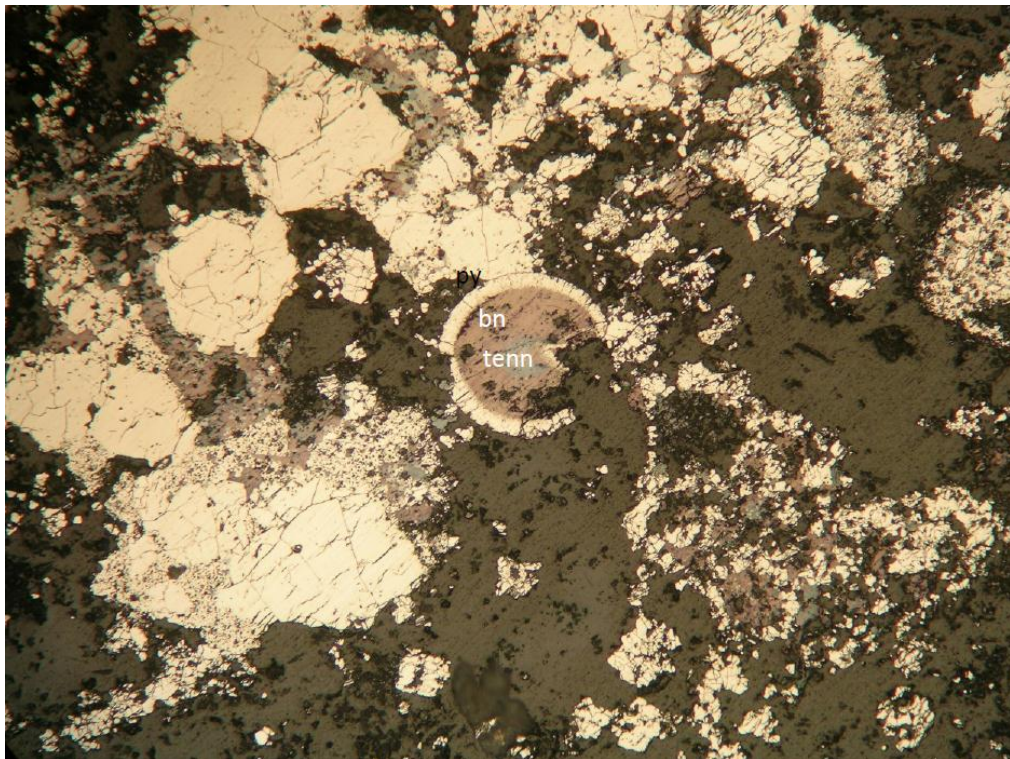
28. DOM - 70 (DDH 73 58 m). Bornite - tennantite of the Assemblage D replaced by late pyrite II. Dimensions photograph: 0.8x0.6 mm. Reflected light.



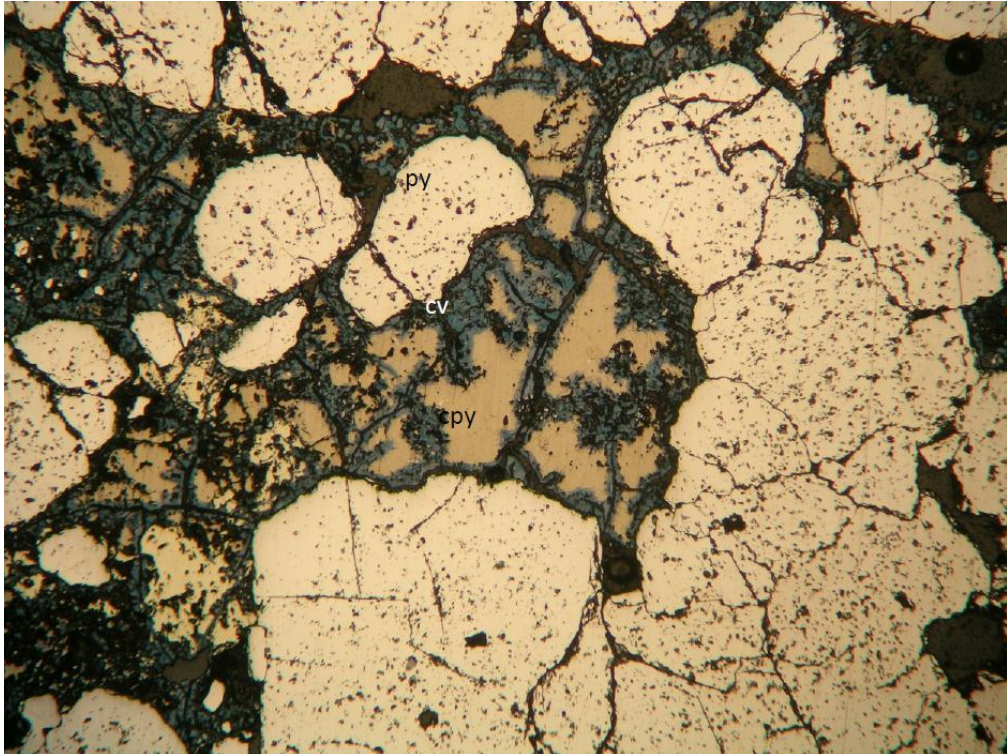
29. DOM - 70 (DDH 73 58 m). Sphalerite I (Association B) replaced by sphalerite II with stromeyerite (Association C) and later bornite - tennantite - pyrite II (Association D). Dimensions photograph: 0.8x0.6 mm. Reflected light.



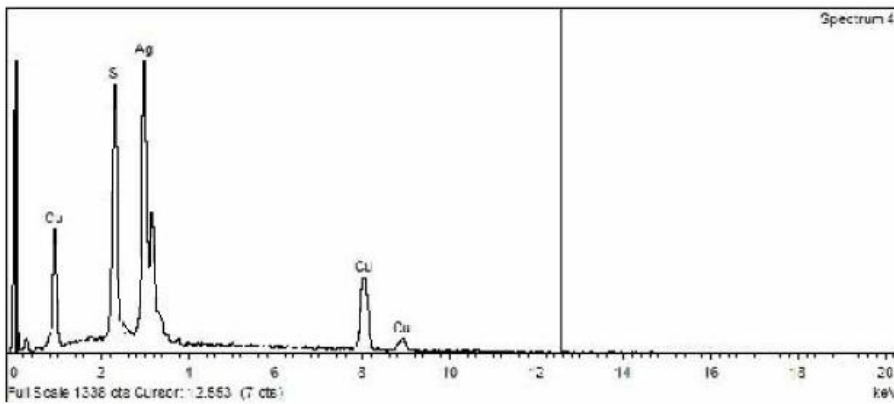
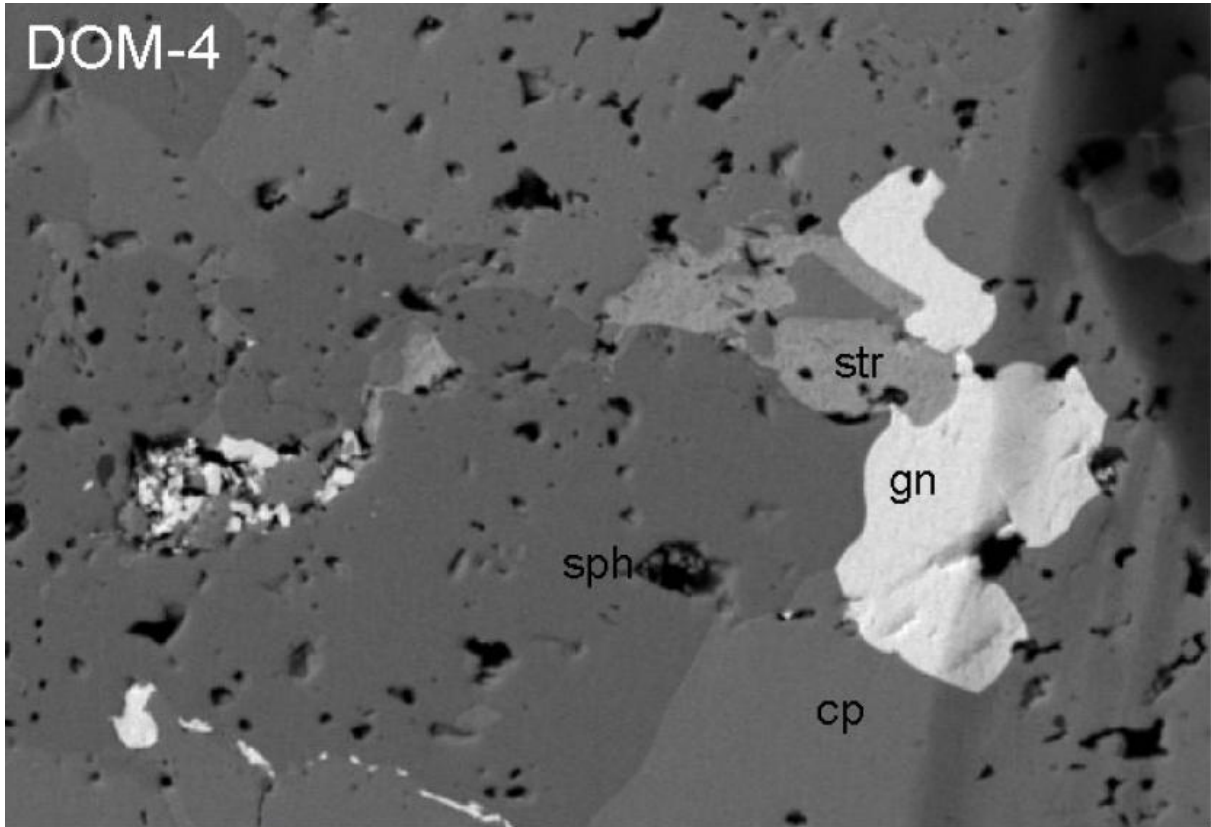
30. DOM - 23 (DDH 68 92.4 m). Sphalerite I replaced by sphalerite II, chalcopyrite and tennantite adjacent to barite. Dimensions photograph: 0.8x0.6 mm. Reflected light.



31. DOM - 70 (DDH 73 58 m). Possible hydrothermal conduit in the Assemblage D with infilling of bornite and tennantite and an edge of pyrite. Dimensions photograph: 0.8x0.6 mm. Reflected light.



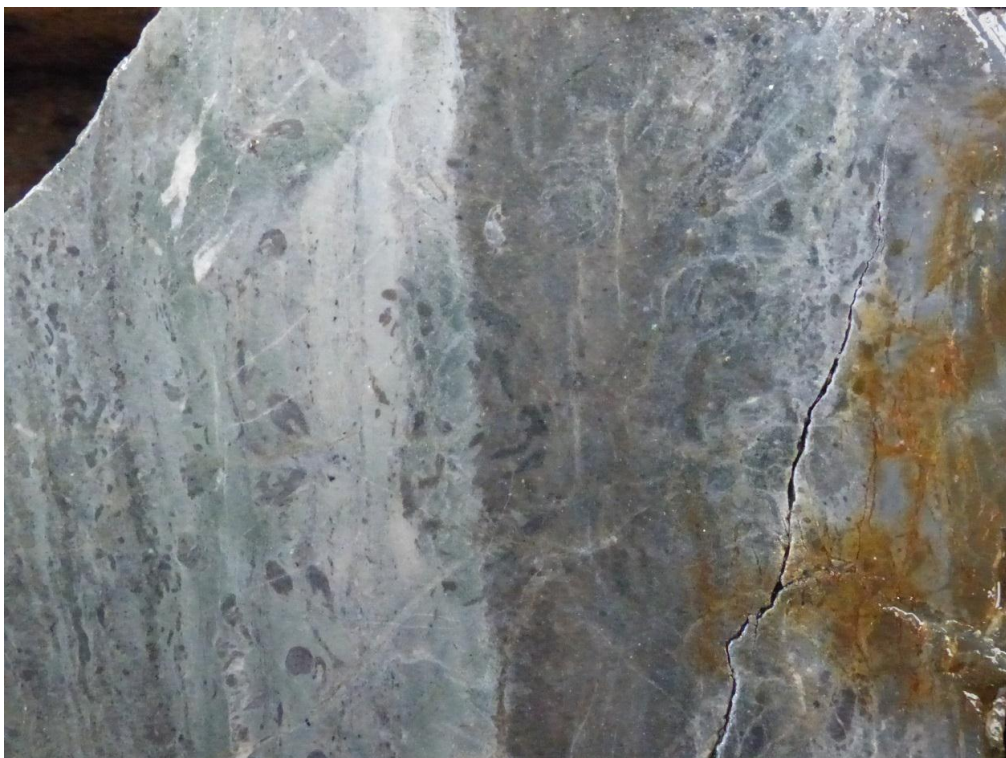
32. DOM - 72. Pyrite - chalcopyrite of the Assemblage A with supergene alteration to covellite (Assemblage E). Outcrop sample. Dimensions photograph: 0.8x0.6 mm. Reflected light.



33. DOM - 4. Early Fe - poor sphalerite and galena replaced by chalcopyrite and stromeyerite.



34. Upper contact of the massive sulphides with the Polymictic Volcaniclastic Breccia via a 40 cm thick band of fine grained grey silica. DDH 11-106, 78 m.



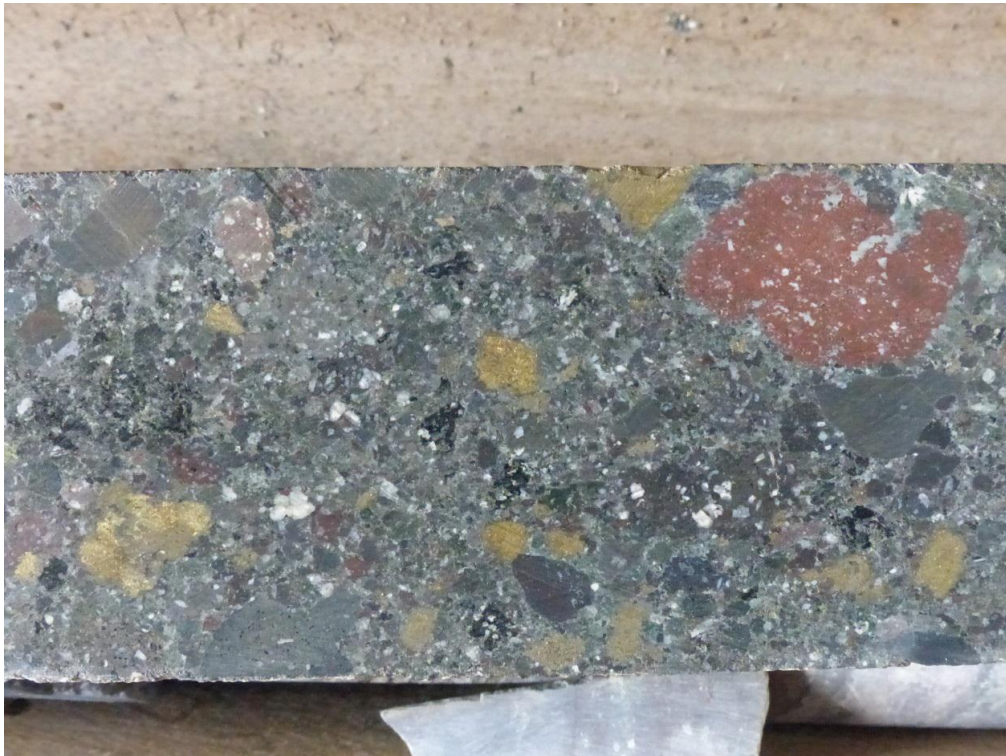
35. Detail of the zone of silica - rich rocks capping the massive sulfide lens. The silica - rich rock shows a delicate banding and partially replaced fragments inherited from the host rock. DDH 10-64m.



36. Polymictic Volcaniclastic Breccia with fragments of andesite and dacite in an heterogeneous groundmass showing only crude banding. DDH 10-64m.



37. Fine - grained polymictic volcaniclastic breccia with local grading and crude banding. DDH 10-64m.



38. Polymictic Volcaniclastic Breccia directly overlying the massive sulfides with heterometric fragments of volcanic rock and an irregular replacement by sulfides. DDH 10-64m.



39. Mineralization replacing the Polymictic Volcaniclastic Breccia with presumable fluid conditions infilled with sphalerite and lined with chalcopyrite. DDH 11-122, 69.3m.



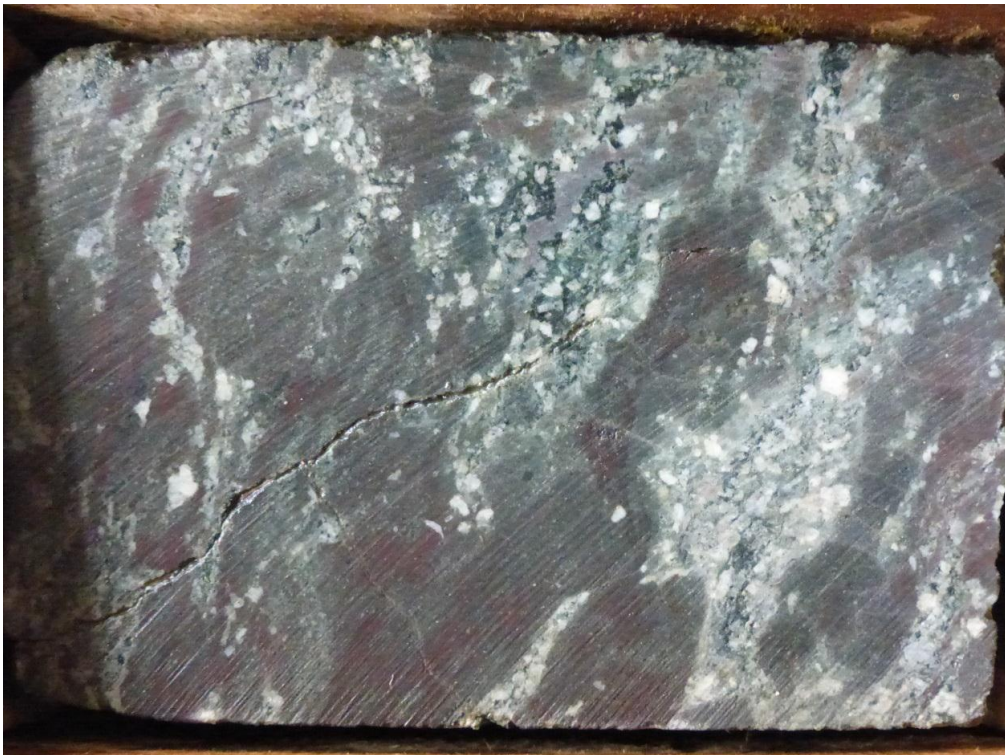
40. Coarse - grained layer of Polymictic Volcaniclastic Breccia irregularly replaced by sulfides and capped by massive pyrite below a fine grained layer that likely acted as a barrier to the hydrothermal fluids. DDH 10-64-.



41. Polymictic Volcaniclastic Breccia with major hydrothermal alteration of the glass to smectite, illite and quartz. DDH 11-106, 15m.



42. Vesicular basalt that delineates the upper part of the subvolcanic sill. DDH 10-68m.



43. Crystal - rich fragments of likely pumice intermixed with versicolor mudstone, likely representing ripped - out soft clasts in the base of a mass flow. Crystal - rich Volcaniclastic Breccia. DDH 10-64m.



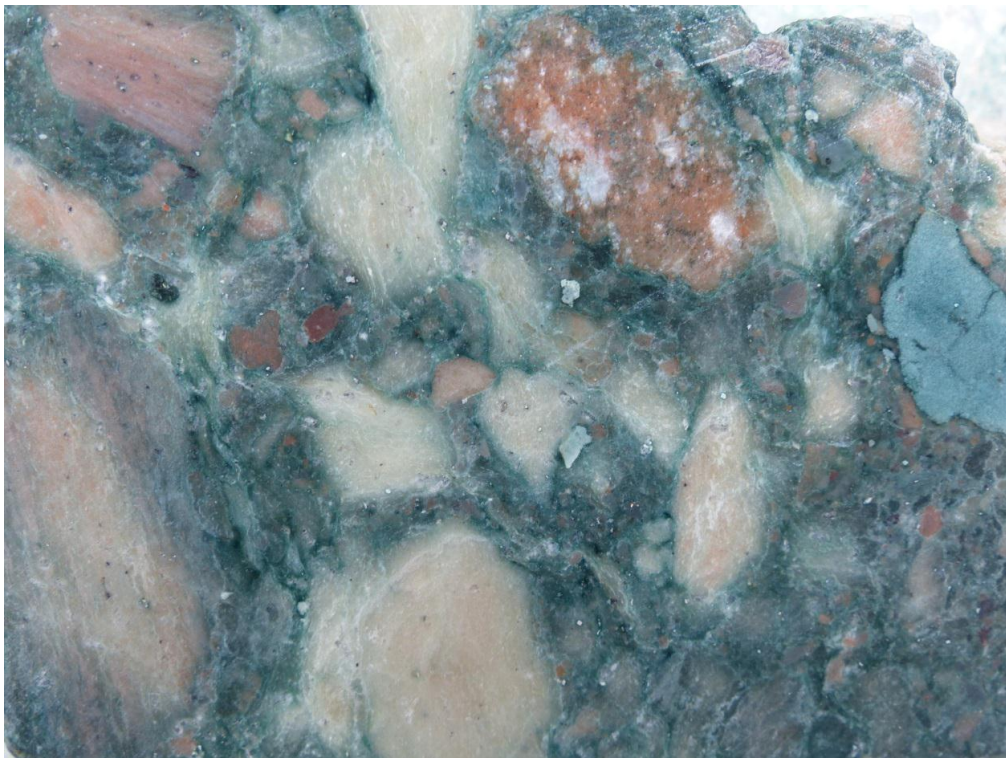
44. Contact between two mass flow units of the Crystal - rich Volcaniclastic Breccia separated by red mudstone. DDH 10-64m. Note the irregular contacts due to ripening and the presence of water - saturated sediments.



45. Crystal - rich Volcaniclastic Breccia showing the abundance of broken plagioclase phenocrysts in what is interpreted as a compacted vesicular (pumice) non welded rock. DDH 10-64m.



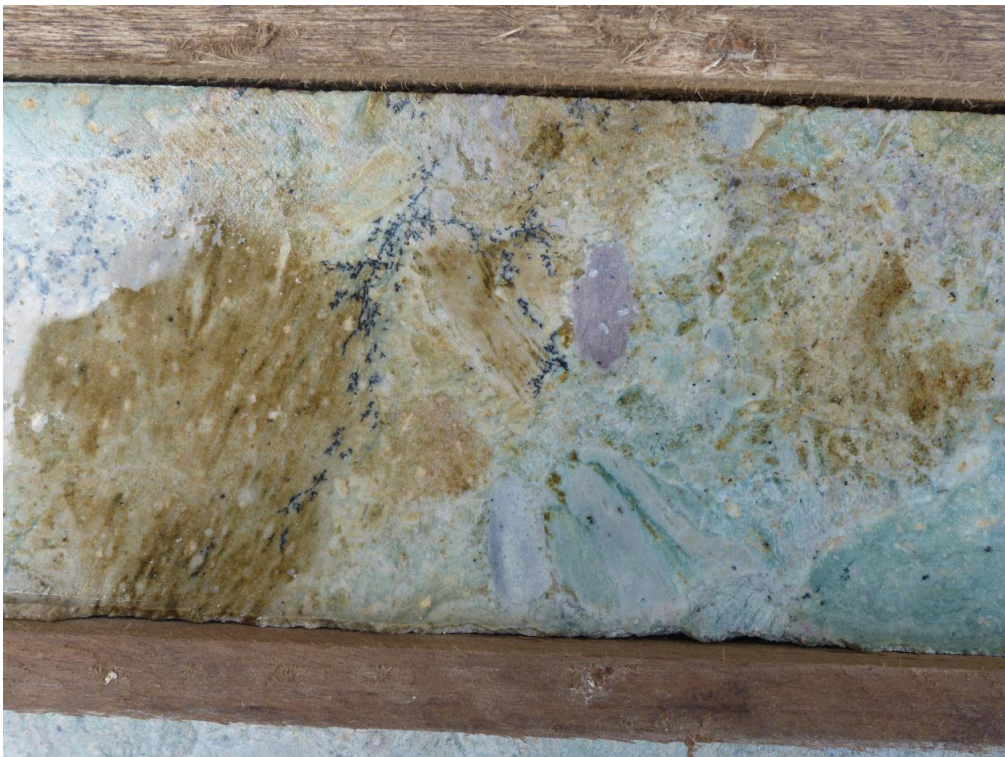
46. Breccia interbedded in the Crystal - rich Polymictic Breccia with cm - sized fragments of aphyric rhyolite and likely related to the late rhyolite domes. This rock is similar to that described as the “grainstone” in the deposit. DDH 11-106m.



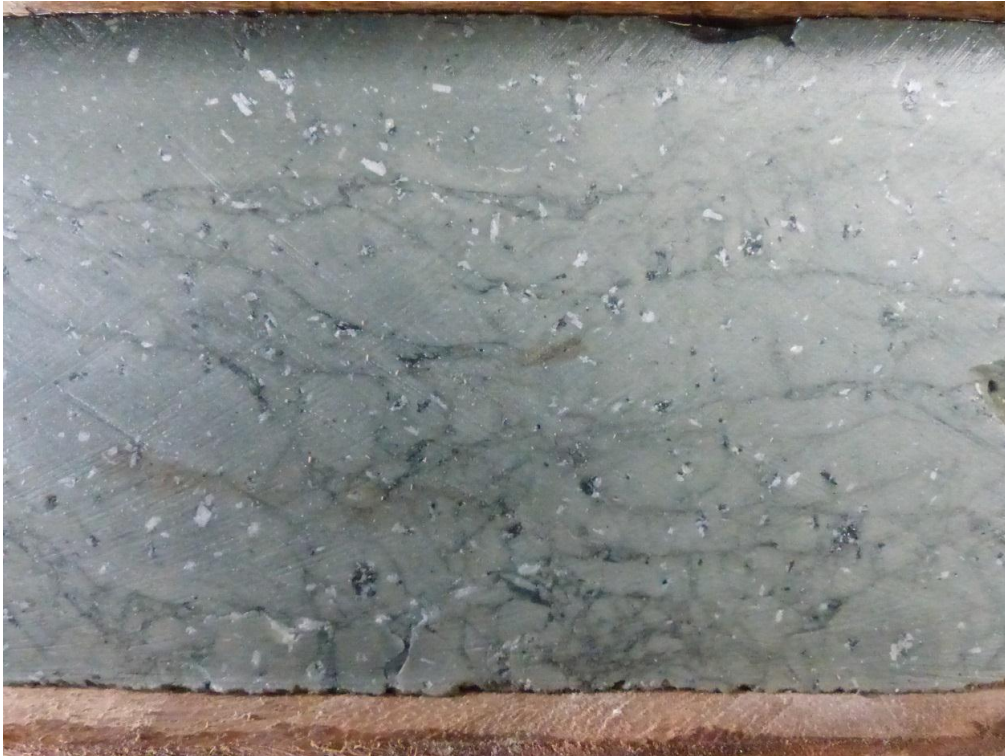
47. Transported hyaloclastite of aphyric rhyolite of the possible late domes lateral to the deposit. DDH 7-15m.



48. In situ hyaloclastite of rhyolite from the late post - ore domes. DDH 11-187m.



49. Transported hyaloclastite related to the late rhyolite dome with texturally different clasts including one of pumice - but of similar composition. DDH 7-15m.



50. Porphyritic coherent andesite of the “El Domo” . DDH 11-106m.